

CRC Report No. DP-07-16-1

**Identification of Potential Parameters
Causing Corrosion of Metallic
Components in Diesel Fuel
Underground Storage Tanks**

Final Report

July 2021



COORDINATING RESEARCH COUNCIL, INC.

5755 NORTH POINT PARKWAY • SUITE 265 • ALPHARETTA, GA 30022

The Coordinating Research Council, Inc. (CRC) is a non-profit corporation supported by the petroleum and automotive equipment industries. CRC operates through the committees made up of technical experts from industry and government who voluntarily participate. The four main areas of research within CRC are: air pollution (atmospheric and engineering studies); aviation fuels, lubricants, and equipment performance; heavy-duty vehicle fuels, lubricants, and equipment performance (e.g., diesel trucks); and light-duty vehicle fuels, lubricants, and equipment performance (e.g., passenger cars). CRC's function is to provide the mechanism for joint research conducted by the two industries that will help in determining the optimum combination of petroleum products and automotive equipment. CRC's work is limited to research that is mutually beneficial to the two industries involved. The final results of the research conducted by, or under the auspices of, CRC are available to the public.

LEGAL NOTICE

This report was prepared by Battelle and Frederick J. Passman, PhD as an account of work sponsored by the Coordinating Research Council (CRC). Neither the CRC, members of the CRC, Battelle, nor any person acting on their behalf: (1) makes any warranty, express or implied, with respect to the use of any information, apparatus, method, or process disclosed in this report, or (2) assumes any liabilities with respect to use of, inability to use, or damages resulting from the use or inability to use, any information, apparatus, method, or process disclosed in this report. In formulating and approving reports, the appropriate committee of the Coordinating Research Council, Inc. has not investigated or considered patents which may apply to the subject matter. Prospective users of the report are responsible for protecting themselves against liability for infringement of patents.

(Page intentionally left blank)

Identification of Potential Parameters Causing Corrosion of Metallic Components in Diesel Fuel Underground Storage Tanks

Final Report

Battelle does not engage in research for advertising, sales promotion, or endorsement of our clients' interests including raising investment capital or recommending investments decisions, or other publicity purposes, or for any use in litigation.

Battelle endeavors at all times to produce work of the highest quality, consistent with our contract commitments. However, because of the research and/or experimental nature of this work the client undertakes the sole responsibility for the consequence of any use or misuse of, or inability to use, any information, apparatus, process or result obtained from Battelle, and Battelle, its employees, officers, or Trustees have no legal liability for the accuracy, adequacy, or efficacy thereof.

(Page intentionally left blank)

TABLE OF CONTENTS

1 CONTENTS

1	Contents	vi
	List of Figures	ix
	List of Tables	xi
	Acronyms and Abbreviations	xiv
	Executive Summary	xix
1	Introduction	1
1.1	Background	1
1.2	Problem Definition	2
1.3	Project Organization	3
1.4	Project Objectives	3
2	Experimental Methods	3
2.1	Experimental Design	3
2.2	Fuel Additive Partition Coefficient Determination	4
2.3	Corrosion Coupon Preparation	6
2.3.1	Steel Coupons	6
2.3.2	Fiber-Reinforced Polymer Coupons	7
2.4	Microbiological Challenge Population Development	7
2.4.1	Challenge Population Sources	7
2.4.2	Primary Microcosms	7
2.4.3	Secondary Microcosms	8
2.5	Test Microcosm Preparation	8
2.5.1	Fuels	8
2.5.2	Additives	8
2.5.3	Test Microcosm Assembly	9
2.6	Observations and testing	10
2.6.1	Periodic Observations	10
2.6.2	Gross Observations	11
2.6.3	Microcosm Sampling	13
2.6.4	Chemistry Testing – Gas Chromatography-Mass Spectrometry	15
2.6.5	Corrosion Testing	16
2.6.6	Microbiological Testing	17

2.7	Statistical Analysis.....	20
2.7.3	Logistic Regression Analysis	20
2.7.4	Analysis of Variance	20
2.7.5	Stepwise Regression Analysis	20
3	Results and Discussion	22
3.1	Test Plan Development.....	22
3.2	STOCK Fuel Chemistry.....	25
3.3	Partition coefficient testing.....	25
3.4	Statistical Analysis.....	29
3.4.1	Background	29
3.4.2	Tier 1 - Stepwise Ordinal Logistic Regression for Aqueous-Fuel Interface	29
3.4.3	Tier 2 - Stepwise Regression of Corrosion Rating Changes between T_0 and T_{6wk} .	37
3.4.4	Tier 3 -Semi-quantitative Analysis of Microcosms Containing Steel Coupons that Exhibited High Corrosion Severity	41
3.5	Microcosm Gross Observations.....	45
3.5.1	Conceptual Overview	45
3.5.2	Observations	45
3.6	Corrosion.....	50
3.6.1	Coupon Corrosion Ratings	50
3.6.2	General Corrosion Rate – Coupon Weight Loss	51
3.6.3	Corrosion Morphology and Elemental Composition	54
3.7	Microbiology.....	75
3.7.1	Overview	75
3.7.2	Adenosine Triphosphate	75
3.7.3	Microscopy	84
3.7.4	Genomics	86
3.8	Chemistry.....	96
3.8.1	Sulfur Concentration	96
3.8.2	Vapor-phase Low Molecular Weight Organic Acids	96
3.8.3	Aqueous-phase Low Molecular Weight Organic Acids	96
3.8.4	Aqueous-phase alcohols	100
3.8.5	Surfactant	101
3.9	Results Summary.....	110
3.9.1	Microcosm Design	110
3.9.2	Fractional-factorial Test Plan	110

3.9.3	Relationships between Controlled Variables and Corrosion	110
3.9.4	Relationships between Controlled Variables and Gross Observations	111
3.9.5	Relationships among Uncontrolled Variables	111
4	Lessons Learned	113
4.1	Test Plan and Microcosm Design	113
4.1.3	Fuel preparation	114
4.2	Analysis.....	115
4.2.1	Subset Selection	115
4.2.2	Corrosion Ratings	115
4.2.3	Microbiology	115
4.2.4	Data Interpretation	116
5	Conclusions	117
5.1	Primary factors affecting corrosivity in fuel microcosms.....	117
5.2	Independent variable Interactions.....	117
6	Recommendations	117
6.1	Microcosm Design	117
6.2	Specimen Collection	118
6.3	Independent Factor Selection.....	118
6.4	Test plan design	118
6.5	Dependent variables.....	119
7	References	120
8	Glossary	126

APPENDICES

APPENDIX A Microcosm Test Condition Matrix

APPENDIX B LC-MS Test Method Parameters

APPENDIX C Statistical Data Analysis

APPENDIX D Statistical Data Analysis – Ln-transformed data

APPENDIX E Gross Observations of Microcosms

APPENDIX F Coupon Observations

APPENDIX G GCR Data

APPENDIX H cATP Data

APPENDIX I Microscopy Data Whole

APPENDIX J Genomic Data

APPENDIX K Chemical Analyses

ATTACHMENT 1 Passman *et al.* [48]

LIST OF FIGURES

Figure 1. Partitioning experiment with 99:1 fuel to water ratio, after 24h.	5
Figure 2. Coupons used in test microcosms – a) Low carbon steel coupon (face view); b) FRP coupon (face view); c) FRP coupon (side view).....	7
Figure 3. Partial view of test microcosm array – Right: LSD microcosms; Left ULSD microcosms.	10
Figure 4. Test microcosm set-up – a) schematic showing coupon and acid indicator array; b) water-free (two-phase), ULSD microcosm at week 1; c) water-containing (three-phase) ULSD microcosm at week 2.	10
Figure 5. Corrosion coupons from microcosm 101 at week 12 – suspended from stand used to photograph coupons.	12
Figure 6. Week 12, microcosm bottom-view images – a) microcosm 59 (B5 LSD over aqueous-phase); b) microcosm 55 (B0 LSD over aqueous-phase).	13
Figure 7. Positioning of Dräger tube in three-phase microcosm – a) Dräger tube in microcosm 114 showing inlet positioned approximately 3 cm above fuel-aqueous-phase interface; b) close-up view of Dräger tube.	15
Figure 8. Flow diagram part 1 – observation-based testing – gross observations.	26
Figure 9. Flow diagram part 2 – observation-based testing – physical, chemical, and microbiological tests.	27
Figure 10. Flow diagram part 3 – observation-based testing – additional physical, chemical, and microbiological tests.	27
Figure 11. $P_{CR=5}$ (vertical axis) versus exposure period (weeks) – from Appendix C, page C-59.	33
Figure 12. Relationship between CI and $P_{CR\geq 3}$ with and without CI-treatment.	33
Figure 13. Corrosion coupons – a) through f): Microcosm 1, coupon 1-2, at weeks 1, 2, 3, 4, 6, and 12; g) through l) Microcosm 4, coupon 4-2, at weeks 1, 2, 3, 4, 6, and 12.	37
Figure 14. Impact of CI on $\Delta CR \text{ week}^{-1}$ – from Appendix D, page D-6.	40
Figure 15. Comparison of weekly CR_{avg} between CI-treated and CI-untreated microcosms – from Appendix D, page D-6.	40
Figure 16. CI-microbial challenge interaction effect – a) microbially challenged microcosms; b) unchallenged microcosms (from Appendix D, page D-7).	40
Figure 17. CR rating frequencies by week – a) aqueous-phase exposure; b) aqueous-fuel interface exposure.	44
Figure 18. Microcosm gross observations – a) through c) microcosm 1 at T_{wk3} , T_{wk6} , and W_{wk12} (all $RS_{GO} = 0$); d) through f) microcosm 3 at T_{wk3} , T_{wk6} , and W_{wk12} (all $RS_{GO} = 5$); g) microcosm 1, bottom view at T_{wk12} ; h) microcosm 3, bottom view at T_{wk12}	46
Figure 19. Microcosm 19 corrosion coupons with CR provided.	51
Figure 20. EDS basics – a) x-ray emission lines; b) example of EDS spectrograph.	60
Figure 21. Optical micrograph of microcosm #35 specimen with annotated regions of interest.	61
Figure 22. Microcosm #35 – a) SEM micrograph of aqueous-phase corrosion product; b) overall EDS data; c) spot scan (1) EDS data (area $\approx 0.14 \text{ mm}^2$).	61
Figure 23. Microcosm #35 – a) SEM micrograph of aqueous-fuel interface corrosion product; b) overall EDS data, c) spot scan (1) EDS data (area $\approx 0.26 \text{ mm}^2$).	61
Figure 24. Microcosm #35 – a) SEM micrograph of fuel-phase corrosion product; b), overall EDS data; c) spot scan (1) EDS data (area $\approx 0.07 \text{ mm}^2$).	62
Figure 25. Optical micrograph of microcosm #40 specimen.	62
Figure 26. Microcosm #40 – a) SEM micrograph of aqueous-phase corrosion product; b) overall EDS data; c) spot scan (1) EDS data.	63
Figure 27. Microcosm #40 – a): SEM micrograph of aqueous-fuel interface corrosion product; b) overall EDS data – no heterogeneity observed.	63

Figure 28. Microcosm #40 – a) SEM micrograph of fuel-phase corrosion product; b) overall EDS data; c) spot scan (1) EDS data.	63
Figure 29. Optical micrograph of microcosm #77 specimen.	65
Figure 30. Microcosm #77 – a) SEM Micrograph of aqueous-phase corrosion product; b) overall EDS data; c) spot scan (1) EDS data.	65
Figure 31. Microcosm #77 – a) SEM micrograph of aqueous-fuel interface corrosion product; b) overall EDS data; c) spot scan (1) EDS data.	65
Figure 32. Microcosm #77 – a) SEM micrograph of fuel-phase corrosion product; b) overall EDS data; c) spot scan (1) EDS data.	66
Figure 33. Optical micrograph of microcosm #85 specimen.	67
Figure 34. Microcosm #85 – a) SEM micrograph of aqueous-phase corrosion product; b) overall EDS data – no heterogeneity observed.	67
Figure 35. Microcosm #85 – a) SEM micrograph of aqueous-fuel interface corrosion product; b) overall EDS data – no heterogeneity observed.	67
Figure 36. Microcosm #85 – a) SEM micrograph of fuel-phase corrosion product; b) overall EDS data – no heterogeneity observed.	68
Figure 37. Optical micrograph of microcosm #100 specimen.	68
Figure 38. Microcosm #100 – a) SEM micrograph of aqueous-phase corrosion product; b) overall EDS data; c) spot scan (1) EDS data.	69
Figure 39. Microcosm #100 – a) SEM micrograph of aqueous-fuel interface corrosion product; b) overall EDS data – no heterogeneity observed.	69
Figure 40. Microcosm #100 – a) SEM micrograph of fuel-phase corrosion product; b) overall EDS data; c) spot scan (1) EDS elemental data.	69
Figure 41. Optical micrograph of microcosm #105 specimen.	70
Figure 42. Microcosm #105 – a) SEM micrograph of aqueous-phase corrosion product; b) overall EDS data; c) spot scan (1) EDS data.	70
Figure 43. Microcosm #105 – a) SEM micrograph of aqueous-fuel interface corrosion product; b) overall EDS data; c) spot scan (1) EDS data.	71
Figure 44. Microcosm #105 – a) SEM micrograph of fuel-phase corrosion product; b) overall EDS data; c) spot scan (1) EDS data.	71
Figure 45. Microcosm #105 – a) SEM micrograph of vapor-phase corrosion product (inset - ~310 mm ² area around hole through which monofilament from which coupon hung was threaded); b) overall EDS data; c) spot scan (1) EDS data.	71
Figure 46. Optical micrograph of microcosm #109 specimen.	72
Figure 47. Microcosm #109 – a) SEM micrograph of aqueous-phase corrosion product; b) overall EDS data; c) spot scan (1) EDS data.	72
Figure 48. Microcosm #109 – a) SEM micrograph of aqueous-fuel interface corrosion product; b) overall EDS data; c) spot scan (1) EDS data.	72
Figure 49. Microcosm #109 – a) SEM micrograph of fuel-phase corrosion product; b) overall EDS data; c) spot scan (1) EDS data.	73
Figure 50. Microcosm #109 – a) SEM micrograph of fuel-phase (~2 cm to 3 cm above fuel-water interface) corrosion product (inset – unmeasured area near coupon edge); b) overall EDS data; c) spot scan (1) EDS data.	73
Figure 51. Log ₁₀ [cATP] ([cATP] ± s) versus time (weeks) between T ₀ and T _{wk9} (black line – intentionally challenged; blue line – unchallenged).	78
Figure 52. Planktonic ATP-bioburden profile in fuel over aqueous-phase microcosm. Averages and ranges are for 20 microcosms.	80
Figure 53. Sessile ATP-bioburden profile on low-carbon steel corrosion coupons in fuel over aqueous-phase microcosms. Averages and ranges are for 18 microcosms.	81
Figure 54. Primary morphological features used to classify molds.	84
Figure 55. Taxonomic tree of fungal taxa detected in test microcosms.	85

Figure 56. Illustrative microscopic images of fungal growth from microcosms #56 and #61.....	86
Figure 57. Krona plot for microcosm 40, illustrating significance of each ring.	90
Figure 58. Venn diagram illustrating differences among the three microbial populations recovered from microcosms.	95
Figure 59. Venn diagrams of taxonomic profile similarities between replicate specimens – a) microcosm 45; b) microcosm 81.	95
Figure 60. Acetic acid Dräger tube -a) schematic from manufacturer’s instruction sheet; b) simulation of color change when acetic acid concentration is ~7 ppmv (mg m^{-1}) in sampled air.	96
Figure 61. Relationship between aqueous-phase and interface corrosion coupon corrosion ratings and [LMOA] – ♦ - CR_{AQ} ; ° - CR_{I}	100
Figure 62. Surfactants – a) schematic of surfactant molecule showing polar head and nonpolar tail; b) schematic of invert-emulsion micelle showing polar heads encapsulating water droplet and nonpolar tails extending into the medium (i.e., fuel); c) schematic of invert emulsion micelles dispersed in fuel; d) photo of 10 mL each fuel and water – left: before shaking; right: 24h after shaking (note stability of invert emulsion).	102

Figure I.1 Microscopic Images of Selected Microcosm Samples.

Figure J.1 Krona Plot of Metagenomic Sequencing Results of Microcosms #3 and #4.

Figure J.2 Krona Plot of Metagenomic Sequencing Results of Microcosms #21 and #28.

Figure J.3 Krona Plot of Metagenomic Sequencing Results of Microcosms #32 and #36.

Figure J.4 Krona Plot of Metagenomic Sequencing Results of Microcosms #40.

Figure J.5 Krona Plot of Metagenomic Sequencing Results of Microcosms #45A and #45B.

Figure J.6 Krona Plot of Metagenomic Sequencing Results of Microcosms #46 and #47.

Figure J.7 Krona Plot of Metagenomic Sequencing Results of Microcosms #48 and #56.

Figure J.8 Krona Plot of Metagenomic Sequencing Results of Microcosms #57 and #78.

Figure J.9 Krona Plot of Metagenomic Sequencing Results of Microcosms #81A and #81B.

Figure J.10 Krona Plot of Metagenomic Sequencing Results of Microcosms #102 and #110.

Figure J.11 Krona Plot of Metagenomic Sequencing Results of Microcosms #126 and #127.

LIST OF TABLES

Table 1. Fractional factorial test plan – number of microcosms containing each controlled factor.	5
Table 2. Partition coefficient determination test plan.	6
Table 3. Additive and contaminant concentrations in test fuels.	9
Table 4. Test microcosm gross observation parameters and risk scores.....	11
Table 5. Microcosms Tested for All Parameters at T_0	14
Table 6. Summary of Analytical Methods and Sampling Frequency by Sample Type.....	14
Table 7. Fractional Factorial Test Plan – Controlled Variables in 128 Microcosms.	21
Table 8. Fuel and Fuel Additive Partition Test Results – Impact of LSD to Water Ratios on Aqueous-Phase Conductivity ($\mu\text{S cm}^{-1}$) All values are averages \pm standard deviations.	28
Table 9. Two-way ANOVA – Five additive treatments x two fuel to water ratios – summary statistics (sums, averages and variances are conductivities in $\mu\text{S cm}^{-1}$).	28
Table 10. Two-way ANOVA – Five additive treatments x two fuel to water ratios – ANOVA.	29
Table 11. Relationships between independent variables and CR – 12-week microcosm study.	31
Table 12. Summary ANOVA statistics, stepwise regression – aqueous-fuel interface 12-week microcosm study at $T_{12\text{wk}}$ and throughout 12-week exposure period.	32
Table 13. Relationships between independent and dependent variables – 12-week microcosm study.	34

Table 14. Summary ANOVA statistics, stepwise regression between independent and dependent variables – 12-week microcosm study.	35
Table 15. ANOVA, F-test summary statistics for week to week $\Delta CR dt^{-1}$ between T_{wk1} and T_{wk6}	38
Table 16. Effect of microbial challenge on CR between weeks 1 and 4 – summary statistics. Values are $CR_{AVG \pm s}$	39
Table 17. Effect of microbial challenge on CR between weeks 1 and 4 – ANOVA summary.	39
Table 18. Tier 3 statistical analysis - corrosion rating scenarios.	43
Table 19. Gross observation, overall risk scores (RS_{GO}) for microcosms at weeks 3, 4, 6, 9, and 12.	47
Table 20. Relationship between microcosm gross observation risk scores (RS_{GO}) and corrosion ratings (CR).	49
Table 21. Relationship between microcosm gross observation and [ATP]-based risk scores (RS_{GO} and RS_{ATP} , respectively).	50
Table 22. Test condition profiles in microcosms with greatest and least ($GCR \pm s$).	52
Table 23. Test condition profiles in microcosms with greatest and least GCR_{max}	53
Table 24. Correlation coefficients among dependent variables – [ATP], CGR_{Std} and CR.	54
Table 25. Corrosion product analysis microcosm subset – independent variable profiles. ^a	54
Table 26. Corrosion product analysis microcosm subset –dependent variable profiles.	55
Table 27. Corrosion deposit elemental analysis by EDS. All values are in wt. %.....	56
Table 28. Corrosion deposit elemental profile correlation coefficients ($ r _{crit [5 df; \alpha = 0.05]} = 0.75$). Significant correlation coefficients are highlighted in bold font.	58
Table 30. ATP-bioburdens in ULSD UST bottoms-water samples.	76
Table 31. ATP-bioburdens in aqueous-phases of 1° and 2° microcosms.	76
Table 36. Controlled variable profiles of challenged and unchallenged microcosms with aqueous-phase $[cATP]_{min}$ and $[cATP]_{max}$ at T_{wk12}	79
Table 37. ATP-bioburden correlation coefficients between planktonic and sessile populations in different microcosm phases.	81
Table 38. ANOVA Summary effect of controlled variables on T_{wk12} aqueous-phase [cATP].	82
Table 344. Population diversity differences between challenged and unchallenged microcosms ($F_{crit[1,19; \alpha = 0.05]} = 4.38$).	89

Table A.1 Fractional factorial fuel corrosivity test plan – microcosm details.

Table E.1 Gross observations of 128-jars set up in the microcosm study.

Table F.1 Zonal observations in coupon samples 1-3 in the microcosm test.

Table G.1 Cumulative average GCR data per microcosm.

Table G.2 Cumulative Maximum GCR Data per Microcosm. Microcosm # are Rank Ordered and Color-Coded Dependent on the Severity of Mass Loss (Red – highest, Green – Lowest).

Table H.1 cATP data for microcosm samples collected on days 0 and 30.

Table H.2 cATP data for microcosm samples collected on day 67.

Table H.3 cATP data for microcosm samples collected on day 120.

Table H.1 Microscopy – specimen descriptions and interpretive notes.

Table I.1 Microscopy – specimen descriptions and interpretive notes.

Table J.1 Genomic profile UST Bottoms-water Sample I by Whole Genome Sequencing Analysis.

Table J.2 Genomic profile UST Bottoms-water Sample II by Whole Genome Sequencing Analysis.

Table J.3 Microbial Diversity in Microcosm # 3 Sample.

Table J.4 Microbial Diversity in Microcosm # 4 Sample.

Table J.5 Microbial Diversity in Microcosm # 21 Sample.

Table J.6 Microbial Diversity in Microcosm # 21 Sample.

Table J.7 Microbial Diversity in Microcosm # 28 Sample.

Table J.8 Microbial Diversity in Microcosm # 32 Sample.

Table J.9 Microbial Diversity in Microcosm # 36 Sample.
Table J.10 Microbial Diversity in Microcosm # 40 Sample.
Table J.11 Microbial Diversity in Microcosm # 45A Sample.
Table J.12 Microbial Diversity in Microcosm # 45B Sample.
Table J.13 Microbial Diversity in Microcosm # 46 Sample.
Table J.14 Microbial Diversity in Microcosm # 47 Sample.
Table J.15 Microbial Diversity in Microcosm # 48 Sample.
Table J.16 Microbial Diversity in Microcosm # 56 Sample.
Table J.17 Microbial Diversity in Microcosm # 57 Sample.
Table J.18 Microbial Diversity in Microcosm #78 Sample.
Table J.19 Microbial Diversity in Microcosm #81A Sample.
Table J.20 Microbial Diversity in Microcosm #81B Sample.
Table J.21 Microbial Diversity in Microcosm #102 Sample.
Table J.22 Microbial Diversity in Microcosm #110 Sample.
Table J.23 Microbial Diversity in Microcosm #126 Sample.
Table J.24 Microbial Diversity in Microcosm #127 Sample.

ACRONYMS AND ABBREVIATIONS

[A]	additive concentration
ACC	American Chemical Council
ANOVA	analysis of variance
AST	aboveground storage tank
ATP	adenosine triphosphate
BDL	below detection limit
BLAST	Basic Local Alignment Search Tool
bp	base pair
BX	biodiesel blend, where X is the vol % FAME in diesel fuel
C	carbon
CA	conductivity additive
cATP	cell-bound ATP (cellular ATP)
CDFA	Clean Diesel Fuel Alliance
CFI	cold flow improver
CI	corrosion inhibitor
CRC	Coordinating Research Council, Inc.
CR _X	corrosion coupon corrosion rating on, where X is the substance with which the coupon surface is in contact. For example, CR _I is the corrosion rating at the fuel-aqueous-phase interface and CR _{AQ} is the rating on coupon surfaces in the aqueous-phase.
C _X	number of carbon atoms in a molecule
DNA	deoxyribonucleic acid
DPG	Diesel Performance Group
DQO	data quality objective
DSA TM	Deposit & Surface Analysis
E	evenness
EDS	energy dispersive spectroscopy
E _H	Shannon's equitability
EPA	U.S. Environmental Protection Agency
EX	ethanol blend, where X is the vol % ethanol in gasoline
FAME	fatty acid methyl ester

FATG	Fuel Additive Technology Group
FCP	fuel corrosivity panel
Fe	iron
FRP	fiber reinforced polymer
FTPI	Fiberglass Tank and Pipe Institute
GC	gas chromatography
GC-FID	gas chromatography – flame ionization detector
GC-MS	gas chromatography – mass spectrometry
GCR	general corrosion rate
GLY	glycerin
GNP	gross national product
H	Shannon-Wiener diversity index
HSD	high sulfur diesel
ITS	internal transcribed spacer
K	potassium
LSD	low sulfur diesel
LMOA	low molecular weight organic acids
LMW	low molecular weight
LMWA	low molecular weight acids
MAL	mono-acid, lubricity
MIC	microbiologically influenced corrosion
MS	mass spectrometry
NACE	National Association of Corrosion Engineers
NaCl	sodium chloride
NBB	National Biodiesel Board
NCH	Nationwide Children’s Hospital
NGS	next generation sequencing
OTU	operational taxonomic unit
OUST	Office of Underground Storage Tanks
P	phosphorous
PCR	polymerase chain reaction

p_i	proportion of total sample represented by an individual species (OTU)
ppm	part per million
PTFE	polytetrafluoroethylene
QAPP	Quality Assurance Project Plan
QC	quality control
qPCR	quantitative PCR
RLU	relative light unit
RNA	ribonucleic acid
RS _{GO}	gross observation based risk score
S	sulfur; also, species (OTU) richness
SEM	scanning electron microscopy
SME	subject matter expert
SOP	standard operating procedure
STI	Steel Tank Institute
STP	submersible turbine pump
tATP	total ATP
TDS	total dissolved solids
T _{wk X}	Test interval – week after which microcosms were started, where X is the week number.
ULSD	ultra-low-sulfur diesel
UST	underground storage tank
UV	ultraviolet
w	weight (mass) fraction as %
WGS	Whole Genome Sequencing
XRD	X-ray diffraction

ACKNOWLEDGEMENTS

This report represents the results and conclusions from an effort between scientists and engineers represented by the Coordinating Research Council, Inc. (CRC) Diesel Performance Group (DPG) DP-07-16-1 Project Panel. and the Battelle Memorial Institute (Columbus, OH). The members of the FCP include representatives from industry associations, equipment manufacturers, fuel vendors, and service/contractor organizations. This project was funded by the CRC with the goal of determining the actual relationship between the presence of different diesel fuel grades and common contaminants, and fuel system component corrosion.

Battelle Technical Team

James, Ryan, PhD (PM)	Gemler, Bryan	Koebel, David
Cafmeyer, Jeff	Gregg, Anne	Kucharzyk, Kate, PhD (PI)
Eastwood, Stephanie, PhD	Hill, Amy	Triplett, Cheryl, PhD
Garbark, Dan	James, Joshua, PhD	

CRC Project DP-07-16-1 Panel Membership:

Bera, Tushar	Shell	Lax, David	API
Beu, Paul	WaWa	Lewis, Russ	Marathon Petroleum
Broughton, Shawn	Marathon Petroleum	Long, Rick	PEI
Chapman, Rick	Fuel Quality Consultants	Martinez, Jo	Chevron
Eckstrom, John C	BP	McNutt, Ryan	Sigma
Eichberger, John	Fuels Institute	Moriarty, Kristi	NREL
English, Edward W	FQS Inc.	Mukkada, Nick	Chevron
Fenwick, Scott	Biodiesel Board	Passman, Fred	Consultant
Golisz, Suzanne R.	ExxonMobil	Pollock, Steve	Steel Tank
Gunter, Garry	Phillips 66	Raney-Pablo, Beth	Ford
Haerer, Ryan	US EPA	Renkes, Bob	Fiberglass Tank and Pipe
Hernandez, Sandra	Chevron	Ryzyi, Sheila (S.M.)	Ford
Hove, Jeff	Fuels Institute	Searles, Prentiss	API
Howell, Steve	Marc IV	Spiker, Keith	QuikTrip
Huang, Chung-Hsuan	Cummins	Sutton, Tia	EMA
Kass, Mike	Oak Ridge National Lab		

(Page intentionally left blank)

EXECUTIVE SUMMARY

A considerable amount of anecdotal evidence indicated that since 2007, the incidence of corrosion-related, diesel fuel underground storage tank (UST) component failures has increased substantially. Two previous studies were inconclusive, but both postulated that the primary factors contributing to UST system corrosion were diesel fuel sulfur content, free-water, microbial contamination, and presence of ethanol. Both previous studies used data obtained from a limited number of retail and fleet fueling sites.

The CRC Fuel Corrosivity Panel sponsored a laboratory study recognizing that the cost of conducting a third survey of several hundred UST would be no more conclusive than the previous two field efforts. The ultimate test plan was a fractional-factorial design that included eleven independent (controlled) variables: water, sulfur concentration (low-sulfur – LSD – versus ultra-low-sulfur – ULSD – diesel fuel), biodiesel (soy-based, fatty acid methyl ester – FAME), glycerin, ethanol, microbial contamination, common fuel additives (cold flow improver - CFI, conductivity additive – CA, corrosion inhibitor – CI, and a mono-acid lubricity additive – MAL), and fiber-reinforced polymer (FRP). Several dependent (uncontrolled) variables were observed [microcosm gross appearance (RS_{GO}), corrosion coupon corrosion ratings (CR), general corrosion ratings (GCR), adenosine triphosphate bioburdens ([cATP]), taxonomic profiles of contaminant populations, and low molecular weight organic acid (LMOA concentrations)]. The test plan was designed to determine whether one or more of the dependent variables – CR, in particular – covaried with one or more of the independent variables. It was not designed to test causes and effects.

The most severe corrosion was observed at the aqueous-fuel interface (CR_I) in microcosms that contained fuel over an aqueous-phase. Substantial CR_I was visible within a week (T_{wk1}) into the exposure period. Water was the only controlled variable that correlated unequivocally with CR – both CR_I (interface corrosion ratings) and CR_{AQ} (aqueous-phase corrosion ratings). The greatest rate of CR change – particularly CR_I – ($\Delta CR dt^{-1}$) was observed during the first four weeks of testing (T_{wk0} to T_{wk4}). At T_{wk12} CR_I was generally greater than CR_{AQ} (CR on surfaces exposed to microcosms' aqueous-phase). In contrast to CR_I and CR_{AQ} , CR_F (fuel-phase surface CR) and CR_V (vapor-phase surface CR) generally remained unchanged between T_{wk0} and T_{wk12} .

Unequivocal determination of the relationship between microbial contamination and CR was thwarted by the proliferation of an indigenous (most likely fuel-borne) population in unchallenged microcosms. By week 9 of the study (T_{wk9}) [cATP] in the unchallenged microcosms were indistinguishable from those in the challenged ones. Notwithstanding the comparable bioburdens in challenged and unchallenged microcosms, the rate at which CRs increased between weeks 2 and 6 was generally greater in intentionally challenged microcosms. This suggested that microbes from UST in which corrosion had been observed were more aggressive than those transported as fuel contaminants.

None of the other independent variables correlated consistently with any of the dependent variables. Particularly noteworthy were the absence of consistently significant correlations between fuel grade, or FAME, ethanol, or glycerin presence and corrosion. By some of the statistical analyses, corrosion in ULSD microcosms was less than that in LSD ones. Similarly, corrosion ratings in FAME-containing microcosms tended to be less than in FAME-free ones. Where ethanol correlated significantly with corrosion, the direction of that relationship varied depending on interactions with other controlled variables. Moreover, there was no significant correlation between the presence of ethanol and LMOA concentration. However, among the ten microcosms tested for LMOA, the three in which the acetic acid concentration was $>3,000$ mg mL⁻¹ had all been dosed with ethanol. The test results suggested that both abiotic and biotic processes contributed to the oxidation of ethanol to acetic acid. Neither fuel grade nor the presence of FAME seemed to influence acetic acid production. These results illustrate the need for further research to better understand how acetic acid accumulates in fuel systems.

One avoidable challenge was the fact that during the study, sub-sets of microcosms were selected for additional testing. However, there was little overlap among subsets – for example, different microcosms were tested for LMOA than those tested ATP-bioburdens. Consequently, it was not possible to assess correlations between ATP-bioburdens and either water-separability properties or LMOA concentrations.

The research tested for the presence, type, and volume of microbial populations (i.e., taxonomic profiles) and found that they varied widely. The taxonomic profiles among tested microcosms were surprisingly varied. There was little similarity between T_{wk12} microbial populations and the challenge inoculum population. Also, there was no correlation between the number of different types of microbes detected and ATP-bioburdens. Thus, no conclusions could be drawn regarding the relationships between the types of microbes present and CR values. These observations indicate the need for more metagenomic testing in fuel systems.

This was the first CRC-sponsored fuel microcosm study of such magnitude. In the course of completing the study a number of crucial lessons were learned. All laboratory test systems are based on assumptions made during the test design effort. These assumptions enable laboratory simulation of field conditions. Although some relevant assumptions – such as fuel additive partitioning into the aqueous-phase – were tested, others – such as $\Delta CR dt^{-1}$ – were not (see Section 4). In future studies, more care should be taken to articulate assumptions and to test them before launching full-scale testing.

The first four weeks of exposure represent a dynamic period of ATP-bioburden increase ($\Delta[cATP] dt^{-1}$) and $\Delta CR dt^{-1}$. In future studies, observations and testing should be performed weekly during the first month.

The results from this 12-week study confirmed that the presence of free-water was essential to corrosion. The data also suggested that microbiologically influenced corrosions – including biogenic oxidation of ethanol to acetic acid - were important corrosion mechanisms. Based on the results of this study, future studies should focus on the relationships between microbial contamination, FAME, ethanol, and water as factors contributing to diesel fuel system component corrosion.

1 INTRODUCTION

1.1 BACKGROUND

Corrosion is the deterioration of a material, usually a metal, that results from a chemical or electrochemical reaction with its environment [1]. It occurs in systems constructed from metals and other engineered materials. Ubiquitous, corrosion affects all sectors of the economy. A 2013 NACE International -sponsored study [2] estimated the global cost of corrosion to be \$2.5 trillion (U.S.). Based on a 2018 estimate of global gross national product (GNP) of \$135 trillion (U.S.) [3], corrosion costs consume approximately 2 % of the global GNP. Perhaps more significantly, the NACE-sponsored report estimated that the cost of corrosion in the U.S. petroleum sector in 2013 was \$7 billion (U.S.). This estimate included pipeline and terminal corrosion costs but did not breakout fuel retail and fleet dispensing operations as a separate category. Consequently, the cost impact of fueling facility corrosion remains unquantified.

Reports of corrosion-related issues in underground storage tank (UST) equipment, dispensers, and epoxy-coated vehicle metal fuel tanks [4] at commercial retail outlets and private bulk fleet storage facilities used to handle diesel fuel are not new. However, the apparent frequency of such reports began to increase starting in 2007, and seem to have increased substantially since 2010 [5]. Anecdotal reports suggest that accelerated corrosion is also affecting metal equipment, such as riser pipes, dispenser filters, tanks, meters or pumps in USTs storing diesel fuel [6,7]. It remains to be determined whether increased reporting reflects increased incidence, awareness, or a combination of the two.

The reported issues include fuel storage tank and fuel dispensing system component corrosion. Several hypotheses have been developed to explain these corrosion failures. One theory is that the increased frequency of corrosion reports coincided with changes to the diesel fuel specifications in 40 CFR 80 Subpart 1, requiring a transition from low sulfur diesel (LSD – sulfur concentration $<500 \mu\text{g g}^{-1}$) to ultra-low sulfur diesel (ULSD – sulfur concentration $\leq 15 \mu\text{g g}^{-1}$) for all on-highway use [7]. Another theory postulates that the increased use of biodiesel-blended ULSD – ULSD containing biodiesel blend stock at $\geq 5 \%$ by volume – is responsible for the apparent increased incidence of corrosion in ULSD fuel systems. Around the same time as the diesel fuel changes, the Energy Policy Act of 2005 and the Energy Independence and Security Act of 2007 [8] resulted in greater use of biodiesel and ethanol in the US fuel supply. Biodiesel blend-stocks are varied but are most commonly fatty acid methyl esters (FAMEs) produced from soy or rapeseed oil. Other FAME sources include an increasing variety of vegetable oils and animal fats. Biodiesel blends are designated with the letter “B” followed by the nominal FAME concentration in the product. Thus, B5 ULSD is ULSD in which the FAME’s volume fraction is 5 %. Although the oxidative stability and bioresistance of different FAMEs are affected by their chemical properties and varies widely among FAME blend-stocks, there is no requirement to report the FAME’s source in biodiesel fuels.

Increased reports of fuel system corrosion are not limited to ULSD systems. Gasoline retailers have also reported an apparent increase of corrosion incidents. In the U.S., nearly all on-highway, spark-ignition fuel (i.e., gasoline) is now E10 (gasoline containing ethanol at a nominal volume percentage = 10 %). Ethanol is also the primary component of Flex fuel (E85 – gasoline blended with ethanol volume percentage at 51% to 83% [9]). As with ULSD systems, there is no unequivocal proof that the apparent correlation between the change in fuel chemistry and increased incident reports actually reflects increased incidence of corrosion. Passman [11] noted that reports of fuel biodeterioration and fuel system corrosion date back to the late 19th century. Previous diesel corrosion research has identified ethanol presence in diesel fuel systems and suggested it should be included with other variables investigated as potentially contributing factors to diesel corrosion.

During the past two decades, fuel chemistry changes are only one of several watershed changes that have occurred within the petroleum sector. During the late 1990s, the ratio of shell capacity (total fuel terminal

storage capacity) to fuel consumption has decreased by approximately 10 % annually [10]. This meant that fuel remained in terminal tanks for shorter periods and, consequently, contaminants had less time to settle out of product before it is transferred to tankers for delivery to retail and fleet fueling sites. Concurrently, ownership of pipelines and terminals has generally moved from vertically integrated petroleum companies to third-party operators [10]. Cradle to grave product stewardship was largely replaced by a network of fungible systems in which product that meets grade specifications can be comingled as it moves through the midstream sector. Traces of contaminants that are below detection limits (BDL) in product samples can accumulate as product moves from refineries to retail and fleet dispensing systems. As the use of ULSD increases, mid-grade gasoline tanks are being converted to ULSD service. Some industry stakeholders have reported that switch-loading – using a given tanker compartment to carry different fuel grades on successive runs – has become a means for cross-contamination that can cause fuel corrosivity issues [6]. As dispensing equipment becomes more sophisticated, tolerances between moving parts have become tighter. Consequently, increased corrosion reporting could reflect the earlier impact a given level of corrosion has on system operation. Alternatively, the increased educational outreach efforts conducted by ASTM, CRC, NACE, Steel Tank Institute, U.S. EPA, and other organizations, might just be increasing operator awareness. Increased awareness can be the primary cause for increased corrosion incident reporting.

The Clean Diesel Fuel Alliance (CDFA) [6] and U.S. Environmental Protection Agency (EPA) Office of Underground Storage Tanks (OUST) [7] have each conducted field surveys investigating these corrosion phenomena – sampling and analyzing water, fuel, and vapor layers from USTs. The CDFA work also evaluated corrosion products from tanks and metallic equipment [6]. Neither investigation yielded conclusive evidence of the corrosion mechanism(s) involved. However, the combination of study results and industry field experience suggested that microbiologically influenced corrosion (MIC) was a leading mechanism of corrosion in diesel USTs [6]. The CDFA report hypothesized that low molecular weight organic acid (LMOA – organic acids with one – C₁ – to six – C₆ – carbon atoms) production was the primary MIC mechanism. It is well known that *LMOA* can contribute to ferrous metal corrosion. The CDFA study suggested that fuel and fuel additive molecules, FAME, and glycerol (present as a trace contaminant in FAME) provided the nutrition that supported microbial growth in fuel systems. Microbial use of these chemistries has been known for more than 100 years [11]. Both the CDFA [6] and U.S. EPA [7] reports included the hypothesis, among others, that the blending of FAME into ULSD contributed to the increased incidence of UST and dispensing corrosion. However, as for other possible mechanisms summarized in this section, a direct relationship between biodiesel blends and fuel corrosivity has not been proven.

Although it is not certain whether the increased number of corrosion reports reflects the increased frequency of moderate to heavy corrosion in fuel systems, there is tremendous value in gaining a better understanding of the actual relationship between the presence of different diesel fuel grades and common contaminants, and fuel system component corrosion. This provided the impetus for the current study.

1.2 PROBLEM DEFINITION

Based on the results of the aforementioned CDFA [6] and U.S. EPA [7] studies, the Coordinating Research Council, Inc. (CRC) Diesel Performance Group (DPG) Fuel Corrosion Panel (FCP) agreed that further work should be based on the assumption that increased reports of corrosion issues reflected increased incidence of corrosion problems in retail and fleet fueling systems. After initially debating the relative merits of a third field survey, the FCP members agreed that the most appropriate next step would be a laboratory test. Through the course of a nearly two-year planning process, members of the DPG identified 11 factors that seemed most likely to directly or through interactions contribute to accelerated fuel system component corrosion. The list of factors included those well known to influence corrosion (for example water and microbial contamination), those widely believed to be responsible for increased corrosion incidence (for example, reduction in sulfur concentration and introduction of FAME), and additives that have been introduced to improve fuel stability, lubricity, and other performance properties. The factors included in the final test plan were:

- Diesel sulfur content (i.e., ULSD vs. LSD)
- Presence of biodiesel at 5% in the fuel
- Presence of lubricity additive
- Presence of conductivity additive
- Presence of cold flow improver (CFI)
- Presence of corrosion inhibitor
- Presence of fiber reinforced polymer (FRP) material
- Presence of free water
- Presence of a microbial population
- Presence of glycerin
- Presence of ethanol

A full factorial test plan design would have been impractical requiring 2,048 microcosms). The DPG designed a modified factorial design. The final test plan – 128 microcosm jars – was designed to identify the primary factors and factor interactions contributing to increased fuel corrosivity. As detailed below, each microcosm had either two (fuel and head-space – vapor phases) or three phases (aqueous, fuel, and vapor). The test period was determined based on historical observations of the time between new equipment installation and first reports of component corrosion.

1.3 PROJECT ORGANIZATION

Battelle conducted this project with technical oversight provided by the FCP. The members of the FCP include representatives from industry associations, equipment manufacturers, fuel vendors, and service/contractor organizations. Nominally, Battelle conducted the research specified in the Quality Assurance Project Plan (QAPP) according to the CRC process and technical guidance. Deviations from the QAPP are summarized in the Methods section.

1.4 PROJECT OBJECTIVES

The primary objective of this project was to determine how the 11 selected factors affected ferrous metal corrosion either directly or through interactions among two or more factors. A secondary objective was to use the results to identify appropriate additional laboratory and field studies to further test the conclusions drawn from this study.

2 EXPERIMENTAL METHODS

2.1 EXPERIMENTAL DESIGN

Working under the assumption that the increased number of fuel system corrosion incidents reported reflect the actual increased number of corrosion-related operational issues, the CRC FCP identified 11 factors likely to be responsible for the increased incidence of corrosion. The panel also determined that lab-scale testing was the most appropriate means of assessing how these factors contributed to fuel corrosivity. A complete evaluation of the direct and interaction effects of the eleven factors would have included 2^{11} (2,048) test jars. Recognizing the impracticality of such a large test plan, the FCP developed a fractional factorial experimental design. The final design included 128 test jars (*microcosms*). Table 1 provides a summary of the plan and Appendix A Table A.1 details the contents of each microcosm.

The 11 factors listed in Table 1 were *controlled* (or *independent*) variables – each either included or excluded per the test plan design. To assess the impact of the controlled variables on corrosivity, a number

of parameters were observed or measured during the course of a 12-week period. These *uncontrolled* (or *dependent*) variables are described in the subsections to follow.

2.2 FUEL ADDITIVE PARTITION COEFFICIENT DETERMINATION

The partition coefficients of corrosion inhibitor (CI), conductivity additive (CA), cold flow improver (CFI) and mono-acid lubricity additive (MAL) were tested to determine the impact of fuel to water ratios. Figure 1 shows the 1 L separatory funnel array used to test partition coefficients. Table 2 summarizes the test plan. Partitioning into the aqueous-phase was measured as conductivity (in μS) and reported as total dissolved solids – TDS (in mg L^{-1}). Additive partitioning into the aqueous phase was determined for two fuel to water ratios: 99:1 (simulating the ratio commonly found in fuel storage tanks) and 70:30 (a practical ratio for use in 2 L microcosms). For the 99:1 ratio tests, 990 mL fuel and 10 mL of aqueous phase solution were used. For the 70:30 tests, the fuel and aqueous-phase volumes were 70 mL and 30 mL, respectively. The aqueous phase was a synthetic bottoms-water – deionized water augmented with NaCl ($w = 5\%$), ethanol (10,000 ppmv), and glycerin (5,000 ppmv). After additized fuel and aqueous solutions were added to a separatory funnel, the funnel was shaken for 30 sec and then allowed to settle for 24h before the aqueous phase was drained off and tested for conductivity (mS cm^{-1}). Triplicate separatory funnels were used for each additive and fuel to water ratio listed in Table 2. ULSD was used for all partition coefficient testing.

Table 1. Fractional factorial test plan – number of microcosms containing each controlled factor.

Factor	# Microcosms ^a
Water ^b	106
Sulfur [S] – LSD ^c	64
FAME (volume fraction 5 %)	64
Ethanol (1,000 ppmv) ^d	51
Glycerin ^d	51
Microbial challenge ^d	55
Mono-acid lubricity additive	67
Cold flow improver	63
Corrosion inhibitor	62
Conductivity additive	66
FRP ^e coupon	63

Notes:

- a) Microcosms were 2L glass jars.
- b) 700 mL – see 2.4.2.
- c) [S] – Sulfur concentration, LSD ($[S] = 274 \text{ mg L}^{-1}$) or ULSD ($[S] = 5 \text{ mg L}^{-1}$)
- d) Not added to microcosms that did not contain an aqueous-phase.
- e) FRP – fiber-reinforced polymer.



Figure 1. Partitioning experiment with 99:1 fuel to water ratio, after 24h.

Table 2. Partition coefficient determination test plan.

Additive	[A] ^a	Fuel:Water
Fully additized ^b	413	99:1
		70:30
Cold flow improver	200	99:1
		70:30
Conductivity additive	3	99:1
		70:30
Corrosion inhibitor	10	99:1
		70:30
Mono-acid lubricity additive	200	99:1
		70:30

Notes:

- a) [A] – additive concentration in mg L⁻¹.
- b) Fully additized fuel included cold flow improver, conductivity additive, corrosion inhibitor, and mono-acid lubricity additive.

2.3 CORROSION COUPON PREPARATION

2.3.1 Steel Coupons

All steel coupons used in test microcosms were produced from 1/8 inch (0.125 in; 0.318 cm) thick, grade 1018, low carbon steel bar (#8910K394, McMaster-Carr, Aurora, OH). The bar stock was segmented into 7 in x 0.75 in (17.8 cm x 1.9 cm) coupons with a 0.08 in (0.2 cm) hole drilled 0.11 in (0.3 cm) at one end for hanging in the microcosms (Figure 2). The carbon steel coupons were prepared for exposure in accordance with ASTM G1-03e1 Standard Practice for Preparing, Cleaning, and Evaluating Corrosion Test Specimens [12]. The initial cleaning procedure included degreasing the coupon with isopropanol and handling with nitrile gloves. Each coupon was visually inspected, photographed, and weighed prior to exposure to the test conditions.

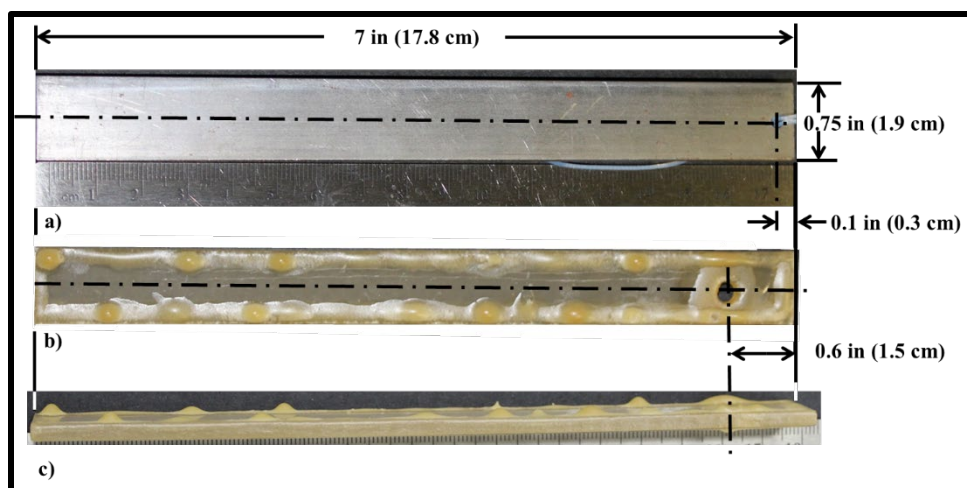


Figure 2. Coupons used in test microcosms – a) Low carbon steel coupon (face view); b) FRP coupon (face view); c) FRP coupon (side view).

2.3.2 Fiber-Reinforced Polymer Coupons

Fiber-reinforced polymer (FRP) coupons were provided by a member of the Fiberglass Tank and Pipe Institute (FTPI). The composition of the FRP coupons was compliant with ASTM C581-15 Standard Practice for Determining Chemical Resistance of Thermosetting Resins Using in Glass-Fiber Reinforced Structures Intended for Liquid Service [13]. This ASTM standard recognizes that FRP is not homogenous, and that edge effects or exterior resins may confound testing results.

The standard specifies that the test coupons be specially prepared using only the resins that encounter the liquid. The FRP coupon dimensions were similar to those of the steel coupons, except that the hole was 0.16 in (0.4 cm) dia and it was drilled 0.6 in (1.5 cm) from the end of the coupon.

2.4 MICROBIOLOGICAL CHALLENGE POPULATION DEVELOPMENT

2.4.1 Challenge Population Sources

2.4.1.1 Bottom samples were collected in accordance with ASTM D7464-14 [14] from two ULSD UST known or suspected to have high microbial contamination bioburdens. Immediately after collection, samples were labelled and stored at 4 °C (39 °F) and then shipped via overnight delivery to Battelle’s Columbus OH laboratories.

2.4.1.2 Upon receipt, 5 mL specimens from each UST sample were tested for adenosine triphosphate (ATP) bioburden per ASTM D7687-17 [15].

2.4.1.3 An additional specimen was removed from each sample with cellular ATP concentration ([cATP]) $\geq 10,000 \text{ pg mL}^{-1}$ ($\geq 4 \text{Log}_{10} \text{ pg mL}^{-1}$). This specimen was processed for genomic testing (see Section 2.6.6.2)

2.4.2 Primary Microcosms

2.4.2.1 Two primary microcosms were prepared by adding 500 mL LSD to 100 mL Bushnell-Hass mineral salts medium [18].

2.4.2.2 Microcosms were inoculated with approximately 20 mL of bottom-water (2.4.1.1) and incubated in the dark at room temperature ($20 \pm 1 \text{ }^\circ\text{C}$; $68 \pm 2 \text{ }^\circ\text{F}$).

2.4.2.3 The aqueous-phase of each microcosm was tested weekly for ATP-bioburden by ASTM Method D7687 [15].

2.4.2.4 Primary microcosms were ready for inoculum transfer when the aqueous-phase's [cATP] $\geq 10,000$ pg mL⁻¹ ($\geq \text{Log}_{10}$ pg mL⁻¹). The [cATP] was the lower threshold for high-bioburden bottoms-water.

2.4.3 Secondary Microcosms

2.4.3.1 Secondary microcosms were prepared in the same manner as primary microcosms (2.4.2).

2.4.3.2 Duplicate LSD microcosms were inoculated with 10 mL of primary microcosm, high-bioburden, aqueous-phase fluid.

2.4.3.3 The aqueous-phase of each microcosm was tested weekly for ATP-bioburden by ASTM Method D7687 [15].

2.4.3.4 Secondary microcosm, aqueous-phase populations were ready for use in test microcosms when their [cATP] $\geq 10,000$ pg mL⁻¹ ($\geq \text{Log}_{10}$ pg mL⁻¹)

2.4.3.5 Before the test program began, secondary microcosm specimens were collected and processed for genomic testing (see Section 2.6.6.2 Genomic Testing).

2.5 TEST MICROCOSM PREPARATION

2.5.1 Fuels

2.5.1.1 Two fuel grades – LSD and ULSD, were provided by Chevron and clay treated by Southwest Research Institute, before receipt at Battelle.

2.5.1.1.1 The fuels were tested for sulfur concentration by one of the following ASTM methods: D4294 [19], D5453 [20], or D7039 [21].

2.5.1.1.2 The fuels were also tested for water concentration per ASTM D6304 [22].

2.5.1.2 Soy-derived, fatty acid methyl ester (B100 FAME) was provided by the National Biodiesel Board (NBB).

2.5.2 Additives

2.5.2.1 Other than B100, all additives listed in Table 1 were obtained through the coordination of the American Chemistry Council (ACC) Fuel Additive Technology Group (FATG). Table 3 summarizes the in-fuel concentrations of each of the contaminants or additives (other than FAME and water) in the microcosms to which they were added.

Table 3. Additive and contaminant concentrations in test fuels.

Substance	mg L⁻¹
Ethanol	10,000
Glycerin	5,000
CFI ^a	200
MLA ^b	200
CI ^c	9±1 ^d
CA ^e	2.5±0.5 ^d

Notes:

- a) CFI – cold flow improver.
- b) MLA – mono-acid lubricity additive.
- c) CI – corrosion inhibitor.
- d) 9±1 and 2.5±0.5 reflect pipetter precision limitations.
- e) CA – conductivity additive.

The cold flow improver (CFI) was ethylene vinyl acetate. The mono-acid lubricity additive (MAL) was a proprietary carboxylic acid. The corrosion inhibitor (CI) was dodecylsuccinic anhydride, and the conductivity additive (CA) polysulfonic acid. Neither Battelle nor the FCP members were informed of any proprietary information regarding the additives used.

2.5.3 Test Microcosm Assembly

- 2.5.3.1 Based on the determination that the fuel to water ratio did not affect fuel-additive partitioning into the aqueous-phase as described in Section 3.3, 2L, wide-mouthed, glass jars were used as the test microcosms.
- 2.5.3.2 Sufficient volumes of LSD and ULSD were additized with one or more of the additives/contaminants to provide a sufficient volume of fuel to dispense into the appropriate test microcosms per Appendix A. First, fuels were blended with B100 FAME to prepare B5 LSD and B5 ULSD. Appropriate volumes of B0 and B5 fuels were then spiked with glycerin, ethanol, or both. Larger volumes of these fuels were split before being dosed with additional additives.
- 2.5.3.3 Per the Appendix A test plan matrix, 1,300 mL of fuel was dispensed into each of 128 microcosms (Figure 3).
- 2.5.3.4 Sterile Bushnell-Haas mineral salts medium (2.4.2.1) was prepared (80L), then 500 mL of the medium was dispensed into each of 106 microcosms designated to include an aqueous-phase.
- 2.5.3.5 A 10 mL volume of secondary microcosm aqueous-phase cell suspension ($[cATP] \geq 4\text{Log}_{10} \text{ pg mL}^{-1}$) was then added to each of the 55 microcosms designated to be microbially contaminated – designated as intentionally challenged microcosms below.
- 2.5.3.6 Polytetrafluoroethylene (PTFE) monofilament was used to hang six steel corrosion coupons (2.3.1) from the top of each microcosm. As depicted in Figure 4, coupons were hung to ensure two-phase (Figure 4b – vapor and fuel) or three-phase (Figure 4c – vapor, fuel, and aqueous) exposure. To facilitate corrosion observations, an identification label was placed on each coupon’s suspension cord. Coupons were spaced to minimize the risk of contact between coupons. The length of each coupon’s monofilament was adjusted to ensure that the coupon was exposed to all phases but did not contact the jar’s bottom.
- 2.5.3.7 Similarly, monofilament was used to hang an FRP coupon (2.3.2) in designated microcosms.

- 2.5.3.8 Passive low molecular weight acid (LMWA) samplers (SKC Acetic Acid Diffusion Tube, Dräger No. 8101071, Eighty-Four, PA) were also suspended in each microcosm.
- 2.5.3.9 To accommodate the logistics of setting up 128 microcosm jars, jars were divided into two groups, with half of the jars prepared on each of two days. Microcosm groupings are listed in Appendix A, Table A.1, Column B.
- 2.5.3.10 After test initiation, jars were placed into one of several fume hoods for incubation at room temperature.
- 2.5.3.11 Exposure to light (both artificial and natural) was minimized during the 12-week test period. The hood sash remained covered and lowered, except during weekly collection or data recording efforts. Although temperature and humidity were not evaluated as part of this study, they were recorded weekly.



Figure 3. Partial view of test microcosm array – Right: LSD microcosms; Left ULSD microcosms.

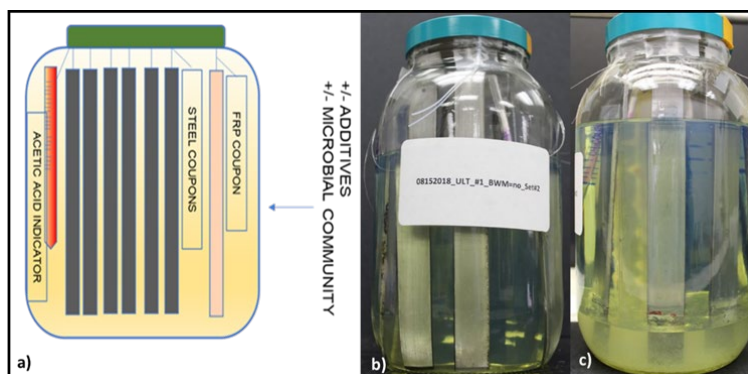


Figure 4. Test microcosm set-up – a) schematic showing coupon and acid indicator array; b) water-free (two-phase), ULSD microcosm at week 1; c) water-containing (three-phase) ULSD microcosm at week 2.

2.6 OBSERVATIONS AND TESTING

2.6.1 Periodic Observations

- 2.6.1.1 Microcosms were removed from the fume hoods and photographed at T_{wk2} , T_{wk3} , T_{wk4} , T_{wk6} , T_{wk9} , and T_{wk12} (where T is time and wk is week). Periodically, gross observations were recorded (2.6.2.1). Each week, corrosion coupons were observed (2.6.2.2)

2.6.2 Gross Observations

2.6.2.1 Test microcosms were observed for visible changes at T_{wk3}, T_{wk4}, T_{wk6}, T_{wk9}, and T_{wk12}. Table 4 lists the parameters included in microcosm gross observations. As depicted in Table 4, a net risk factor (low: 1, moderate: 3, or high: 5) was computed from the individual parameter risk scores.

Table 4. Test microcosm gross observation parameters and risk scores.

PARAMETER	CRITERION	SCORE	PARAMETER	CRITERION	SCORE
<i>Fuel phase</i>			<i>Water phase</i>		
Haze	ASTM ^a < 2	1	Turbidity	Water-white	0
	ASTM 2 to 3	2		Translucent	2
	ASTM > 3	3		Opaque	4
Color	ASTM ^b < 2	1	Color	ASTM ^b < 2	1
	ASTM 2 to 5	2		ASTM 2 to 5	2
	ASTM > 5	3		ASTM > 5	3
Invert emulsion (rag layer)			Sediment (bottom coverage)	< 25%	1
	Present	No		0	25 % to 75 %
		Yes	3	> 75 %	3
Thickness	No rag layer	0	Odor	None (fuel volatiles only)	1
	< 1 mm	1		Sulfide	3
	1 to 3 mm	2		Ammonia	5
	> 3 mm	3		Risk Rating Summary	
Stalactites/stalagmites	No rag layer	0	Risk score sums:	Min.	10
	No	2		Max.	40
	Yes	5			
Consistency	No rag layer	0	Sums converted to	10 to 15	1
	Easily disaggregated	1	Gross Observation Risk	16 to 25	3
	Difficult to disperse	2	Score	> 25	5
	Membranous pellicle	5			
Adheres to glass	No rag layer	0		Subtotal for rag layer >	5
	No	1	Overrides: ^c	10	
	Yes	3		Subtotal for odor > 1	5

Notes:

- ASTM D4176 [23]
- ASTM D1500 [24]
- Overrides – regardless of other gross observation risk scores, if the *rag layer* subtotal > 10 or the odor subtotal > 1, then the gross observation score = 5.

2.6.2.2 Corrosion Coupons were observed periodically for percent surface coverage by corrosion deposits.

2.6.2.2.1 For inspection, the coupon array was removed from the microcosm and hung from a support stand (Figure 5). The support stand was disinfected with isopropanol (90 % vol) before each coupon array was hung.

2.6.2.2.2 In an attempt to minimize the impact of light and shading on photographic images (Section 2.6.2.3), for each photo documentation session, the cameras and specimen set up in accordance with a standardized set-up plan. Each photograph captured three designated replicate coupons so that for each array, a time course of corrosion development could be captured.

2.6.2.2.3 As illustrated in Figure 5, the face of each coupon was rated at each of five positions, based on the liquid phase with which the coupon was in contact:

- Aqueous-phase
- Fuel-aqueous-phase interface (invert emulsion zone)
- Fuel-phase
- Fuel-vapor-phase interface
- Vapor-phase

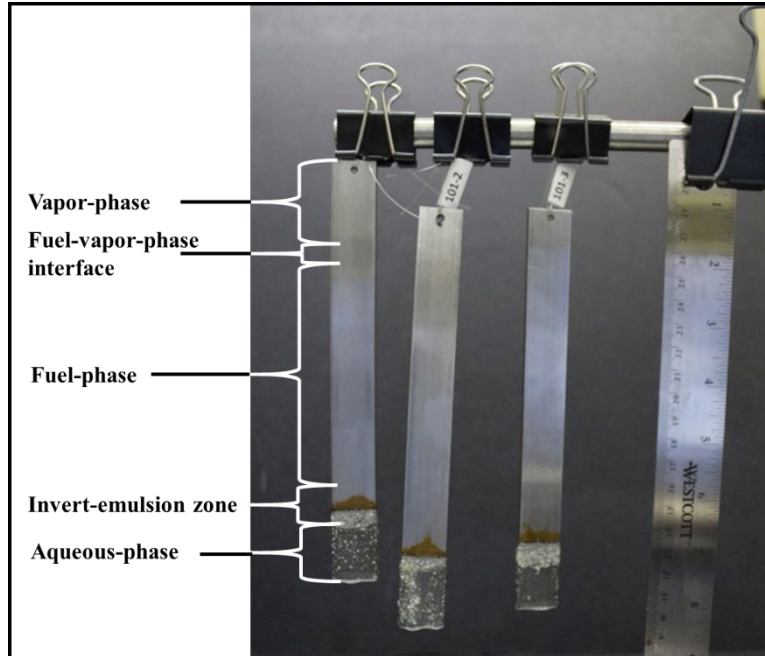


Figure 5. Corrosion coupons from microcosm 101 at week 12 – suspended from stand used to photograph coupons.

Observation zones are noted to left.

2.6.2.2.4 Each zone of the coupon was scored in accordance with NACE TM0172-2001 [25], where coupon corrosion ratings A through E represented the percentage of corrosion coverage on each coupon:

- A = 0 %
- B+ = 0 % to 5 %
- B = 5 % to 25 %
- C = 25 % to 50 %
- D = 50 % to 75 %
- E = >75 %

For computational purposes, the lettered attribute scores were transformed to ordinal values (A=1, B=2, C=3, D=4, and E=5).

2.6.2.3 Photography – as indicated under 2.6.2.2.1, corrosion coupons were removed from microcosms and photographed at intervals during the study period. At weeks 2, 3, 4, 6, 9 and 12 each microcosm was removed from the fume hood to a photo station. Throughout the study, nominally identical conditions (lighting, distance between camera and jar, and camera settings) were maintained so that photographic images of actual changes within each microcosm were not affected by external variables. To record sediment accumulation on microcosm bottoms, at week 12, jars were placed on supports and photographed from underneath (Figure 6).

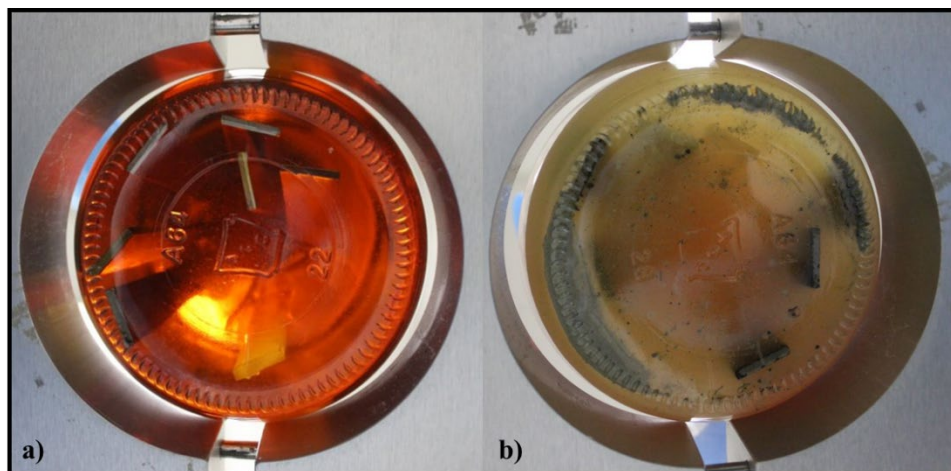


Figure 6. Week 12, microcosm bottom-view images – a) microcosm 59 (B5 LSD over aqueous-phase); b) microcosm 55 (B0 LSD over aqueous-phase).

2.6.3 Microcosm Sampling

2.6.3.1 Fuel, aqueous, or both types of samples were collected from selected microcosms at T_0 (Table 5) and subsequently per the schedule summarized in Table 6. All sampling was performed in a chemical fume hood.

2.6.3.2 Volumetric pipets were used to draw samples from tested microcosms. When drawing samples, precautions were taken to minimize disturbances to the liquid layers.

2.6.3.3 An estimated 50 mL of water and 150 mL of fuel was sampled from selected microcosms exhibiting progressed corrosion [i.e., NACE TM0172 ratings (CR) ≥ 4 at the fuel-aqueous-phase interface] at weeks 4, 9, and 12 (T_{wk4} , T_{wk9} , and T_{wk12}).

2.6.3.4 The vapor-phase of each microcosm was sampled continuously using passive samplers (SKC Acetic Acid Diffusion Tube, Dräger No. 8101071, Eighty-Four, PA). The Dräger tubes were designed to detect low molecular weight (C_2 to C_6) organic acid (LMOA) formation colorimetrically – with an increasing volume of the tube’s contents changing color from pink to yellow as LMOA were absorbed. The Dräger tubes were graduated to indicate [LMOA] across a range of 0.5 mg L^{-1} to 100 mg mL^{-1} based on an 8h exposure period. Had LMOA been detected, the concentration reading on the tube would have been divided by the interval between observations (7-days). Additionally, positive test results would have triggered vapor-phase sample collection and analysts (2.6.4).

2.6.3.5 Dräger tube placement in the microcosms was in accordance with the manufacturer’s recommendation. As shown in in Figure 7, a Dräger tube was placed with its top immersed into the fuel-phase to trap LMOA migrating from the fuel-corrosion coupon interface.

Table 5. Microcosms Tested for All Parameters at T₀

Jar ^a	Sulfur	Biodiesel	Microbes	Glycerin	EtOH	Lubricity	CFI	CI	CA	H ₂ O	FRP
1	LSDF	5%	yes	no	no	yes	no	no	no	yes	no
34	ULSD	none	no	yes	yes	no	no	no	no	yes	yes
38	LSDF	none	no	yes	no	yes	yes	yes	yes	yes	no
71	ULSD	none	yes	no	no	yes	yes	yes	no	yes	no
96	ULSD	5%	yes	no	yes	no	yes	no	no	yes	no
109	LSDF	none	yes	yes	yes	yes	yes	no	yes	yes	yes

Note: a) Jar numbers are from Appendix A, Table A.1.

Table 6. Summary of Analytical Methods and Sampling Frequency by Sample Type

Parameter	Test Method	Frequency ^a
<i>Fuel Phase</i>		
cATP Concentration	ASTM D7687 ^b	Start, Week 4, 9, 12 (Only IF CR ≥ 4)
C2-C6 organic acids, other unexpected compounds	GC/MS (In-house method)	Week 4, 9, 12 (Only IF CR ≥ 4)
<i>Water Phase</i>		
cATP Concentration	ASTM D7687 ^b	Week 4, 9, 12 (Only IF CR ≥ 4)
C2-C6 organic acids,	GC/MS (In-house method)	Week 4, 9, 12 (Only IF CR ≥ 4)
Surfactants (phase separability)	ASTM D7261 ^c and D7451 ^d	Week 12
<i>Vapor Phase</i>		
Low molecular weight acids	Passive sampler (up to 100 ppm) or GC method	Passive sampler did not indicate presence throughout testing. ^e

Notes:

- a) At T_{wk18} corrosion coupons were pulled for scanning electron microscopy, energy dispersive x-ray analysis, and general corrosion rate measurements. Additionally, 26 aqueous-phase specimens were collected for ATP-bioburden testing.
- b) ASTM D7687 [15]
- c) ASTM D7261 [16]. Per D7261, the type of filter used depended on whether B0 or B5 fuel was tested.
- d) ASTM D7451 [17]
- e) The positioning of passive sampler in the fuel layer of the microcosms as well as the regular opening of the microcosm may have prevented accurate indication of volatile acid presence.



Figure 7. Positioning of Dräger tube in three-phase microcosm – a) Dräger tube in microcosm 114 showing inlet positioned approximately 3 cm above fuel-aqueous-phase interface; b) close-up view of Dräger tube.

2.6.4 Chemistry Testing – Gas Chromatography-Mass Spectrometry

2.6.4.1 A modified Marathon gas chromatography-mass spectrometry (GC-MS) protocol was used (Appendix B):

2.6.4.1.1 Approximately 0.5 μL of the aqueous samples were injected at a 30:1 split ratio into a Model 6890 Agilent GC System connected to a Model 5973 Mass Selective Detector.

2.6.4.1.2 Injection port temperature was 150 $^{\circ}\text{C}$. The column was a HP-5MS (cross linked 5% di-phenyl-95%-dimethyl siloxane), 25 mm x 30 mm 0.25 μm .

2.6.4.1.3 ChemStation for GC (Agilent Technologies) was used for instrument control and data acquisition and analysis.

2.6.4.1.4 The temperature program was a 2-minute initial hold with a 10 $^{\circ}\text{C min}^{-1}$ linear ramp from 30 to 325 $^{\circ}\text{C}$, concluding with a 5-minute hold time at 325 $^{\circ}\text{C}$.

2.6.4.1.5 An initial solvent delay of 0.5 minutes was included to protect the detector.

2.6.4.1.6 The volumetric flow rate was 1.1 mL min^{-1} . [26]

2.6.4.1.7 Fuel samples were injected onto the same column; however, the temperature program included a 2-minute hold time with a 7 $^{\circ}\text{C min}^{-1}$ linear ramp from 30 to 325 $^{\circ}\text{C}$, and ended with a 5-minute hold time at 325 $^{\circ}\text{C}$ with no solvent delay.

2.6.4.1.8 For both fuel and aqueous-phase specimens, a reference standard solution (AccuStandard, New Haven, CT) was used for instrument calibration. The reference solution contained: acetic acid, propanoic acid, 2-methyl propanoic acid, butanoic acid, 3-methyl butanoic acid, pentanoic acid, 4-methyl pentanoic acid, hexanoic acid, and heptanoic acid. Volatile acid calibration standard mixtures were diluted from the stock standard mixture (10 mM). For aqueous-phase testing, seven concentrations of methanol and ethanol were prepared to produce a calibration curve that spanned the range of concentrations expected to be present in test specimens. Glycerol was diluted with water to span a range of concentrations for quantification in aqueous samples (0.265 mg mL⁻¹ to 34 mg mL⁻¹).

2.6.5 Corrosion Testing

2.6.5.1 Weight Loss

2.6.5.1.1 Weight loss testing was performed on triplicate coupons after 18-weeks exposure.

2.6.5.1.2 Triplicate steel coupons (2.3.1) were removed from each microcosm.

2.6.5.1.3 Surface organic and inorganic deposits were removed mechanically, using a non-metallic bristle brush.

2.6.5.1.4 Coupons were then cleaned and de-scaled in accordance with ASTM G1 [12] and weighed on a microbalance accurate to ±0.1 g.

2.6.5.1.5 Generalized corrosion rates (GCRs) – in mpy (mils y⁻¹) – were determined as described by Andrade and Alonso [27]. After net weight loss was determined per Equation 1, GCR was computed per Equation 2.

$$\Delta M = M_{18} - M_0 \quad (1)$$

Where:

M = mass (mg)

M₀ = mass (mg) before exposure

M₁₈ = mass (mg) after exposure

$$GCR = (K * \Delta M) / (A * t * D) \quad (2)$$

Where:

K = unit-based constant from ASTM G1 [11]

ΔM = change in mass (g) from equation 1

A = coupon surface area (cm²) – A_{coupon} = 33.87 cm².

t = exposure period (h) – 12 weeks @ 168h week⁻¹ = 2,016h = 0.23 y.

D = density of material in mg cm⁻³ (for coupons used, D = 7.86 x 10³ mg cm⁻³)

2.6.5.1.6 Using equation 2, GCR per coupon was reported to the nearest 0.1 mpy.

2.6.5.1.7 Average (\overline{GCR}) ± standard deviation (s) was computed for each set of triplicate coupons.

2.6.5.2 Microscopy

2.6.5.2.1 After de-scaling, the cleaned coupon surfaces were inspected for obvious pitting. Example pitting attacks were photo documented using a low magnification stereoscope.

2.6.5.2.2 A subset of microcosms was selected for examination by scanning electron microscopy (SEM) and energy dispersive spectroscopy (EDS) for further material analysis of the corrosion product. Selection of coupons for examination by SEM and EDS was done under the guidance of FCP members.

- To accommodate SEM chamber space limitations, a 4 cm to 5 cm corrosion coupon section was cut so that portions of aqueous-phase, aqueous-fuel interface, and fuel-phase contact zones were included in the observed subsection. A liquid-cooled abrasive saw was used to remove portions of the coupon on either side of this subsection.
- Low-power magnification (20x to 100x), light microscopy was used to observe corrosion deposit morphology.
- SEM was used to obtain higher magnification imagery. To prepare specimens for SEM, coupon sections were dried in a vacuum oven and then vacuum coated with gold. Surface corrosion products were analyzed by EDS. Multiple SEM fields were tested by EDS when corrosion product appeared to be heterogeneous.

2.6.6 Microbiological Testing

2.6.6.1 Adenosine Triphosphate

2.6.6.1.1 Planktonic ATP-bioburdens (i.e., ATP associated with microbial cells floating in the fuel, interface, and aqueous zones) were determined by the ASTM D7687 [15] test method. Results were reported as [cATP] in pg mL^{-1} . Specimens from the aqueous-phase (~2 cm above the jar's bottom) of all four-phase microcosms (vapor, fuel, invert-emulsion, aqueous phases) and from ~2 cm above the bottom of selected two-phase microcosms (vapor and fuel phases) were collected and tested. Fuel and interface specimens from a sub-set of four-phase microcosms were also collected and tested.

2.6.6.1.2 Sessile ATP-bioburdens (i.e., ATP associated with biofilms that had developed on microcosm surfaces) were assayed using the Deposit and Surface Analysis test kit (DSA™ – DSA is a trademark of LuminUltra Technologies, Ltd., Fredericton, NB, Canada). Surface swab samples (1 cm^2) were collected from corrosion coupons at the bottom, invert emulsion zone, ~2 cm above the invert emulsion zone and the vapor-phase zone of selected coupons. Coupons were selected for DSA testing based on their gross appearance. Several microcosms had apparent biofilm development on their glass walls. These were also tested by the DSA method. Sessile ATP-bioburdens were reported as [tATP] in pg cm^{-2} , where tATP is *total ATP* (the ATP contained within intact cells plus the ATP that is either cell-free – dissolved – or bound to cell fragments). Sessile ATP-bioburden testing was not part of the project's test plan, but was added as an extracurricular parameter, tested only at T_{wk12}.

2.6.6.1.3 Both ASTM D7687 and DSA measurements were performed using test kits and equipment provided by the LuminUltra Technologies, Ltd., Fredericton, NB, Canada.

2.6.6.2 Genomic Testing

2.6.6.2.1 Deoxyribonucleic acid (DNA) extraction

2.6.6.2.1.1 Specimens from selected microcosms were collected in separate 15-mL sterile conical tubes.

2.6.6.2.1.2 DNA was extracted from solid mass samples (i.e., bottom water sediment and fungal mats) by the Ultraclean® Mega Soil DNA Isolation Kit (MO BIO Laboratories, Inc., Carlsbad, CA). The manufacturers protocol – modified for sediment extraction (Battelle Standard Operating Procedure [SOP]) – was used.

2.6.6.2.1.3 DNA was extracted from filtered fuel and water samples, by the Meta-G-Nome™ DNA Isolation Kit (Epicentre, Madison, WI). The manufacturer's protocol for direct extraction from biomass captured on nitrocellulose filters was followed.

2.6.6.2.1.4 Post-extraction cleanup for all samples was performed using OneStep™ polymerase chain reaction (PCR) Inhibitor Removal Kit (Zymo Research Corp., Irvine, CA).

2.6.6.2.1.5 Purified DNA samples were analyzed with an ultraviolet (UV) absorbance (NanoDrop™ 200 spectrophotometer, Thermo Scientific, Waltham, MA), Qubit® dsDNA HS Assay Kit, and SYBR® Gold Nucleic Acid Gel Stain according to the manufacturer's protocols (Invitrogen/LifeTechnologies, Grand Island, NY).

2.6.6.2.2 Sequencing

2.6.6.2.2.1 Numerically coded aliquots of approximately 0.5 µg to 1 µg DNA per sample were used to create sequencing libraries.

2.6.6.2.2.2 First, genomic DNA was fragmented using a Covaris™ S220 Sonicator (Covaris, Inc., Woburn, MA) to approximately 300 base pairs (bps).

2.6.6.2.2.3 Fragmented DNA was used to synthesize indexed sequencing libraries using the TruSeq DNA Sample Prep Kit V2 (Illumina, Inc., San Diego, CA), according to the manufacturer's recommended protocol.

2.6.6.2.2.4 Cluster generation was performed on the cBOT using the TruSeq PE Cluster Kit v3 – cBot – HS (Illumina).

2.6.6.2.2.5 Libraries were sequenced with an Illumina HiSeq 2000 at Nationwide Children's Hospital (NCH) Biomedical Genomics Core (Columbus, OH) using the TruSeq SBS Kit v3 reagents (Illumina) for paired end sequencing with read lengths of 100 bps (200 cycles).

2.6.6.2.2.6 Primary analysis (image analysis and base calling) was performed using HiSeq Control Software version 1.5.15.1 and Real Time Analysis version 1.13.48.

2.6.6.2.2.7 Secondary analysis (demultiplexing) was performed using Illumina CASAVA Software v1.6 on the NCH computer cluster. Sequence data (.fastq files) and QC reports for library construction were delivered to Battelle via an external hard drive.

2.6.6.2.3 16S rRNA and Internal Transcribed Splicer (ITS) Analysis

2.6.6.2.3.1 DNA extracts with less than suitable yields of material for sequencing were also subjected to PCR amplification to detect bacterial DNA.

2.6.6.2.3.2 Primers for 16S sequencing were: Forward (341F): 5'- CCTACGGGNBGCASCAG-3'; and Reverse (850R): 5'- GGACTACNVGGGTATCTAATCC-3, and for ITS sequencing: Forward: 5'- CTTGGTCATTTAGAGGAAGTAA-3'; Reverse: 5'- GCTGCGTTCTTCATCGATGC-3' were used with Phusion High fidelity DNA polymerase (New England BioLabs, Ipswich, MA) [28].

2.6.6.2.3.3 The thermal cycling parameters were: 98°C for 30 s, 35 cycles of 98 °C for 10 s, 56 °C for 30 s and 72 °C for 60 s, followed by 72°C for 5 minutes in a PTC-200 thermal cycler (Bio-Rad, Hercules, CA).

2.6.6.2.4 Bioinformatics

2.6.6.2.4.1 Sequencing data were received on an external hard drive from the laboratory. The hard drive contained the raw *fastq* files in *gzipped* format. These files were transferred to the Battelle High Performance Computing System for analysis.

2.6.6.2.4.2 Raw files were unzipped and then merged using the bioinformatic command line paired read merging tool, FLASH1 v.1.2.11. Before running the reads through the Basic Local Alignment Search Tool (BLAST), a filter was applied to the merged reads to remove low quality reads using the fastq quality filter of the FASTX Toolkit2.

2.6.6.2.4.3 All reads that did not pass the fastq quality filter were excluded from further analysis. A plot of the quality for each sample was created using the fastq quality boxplot graph shell script, also part of the FASTX Toolkit. These plots allowed a visual inspection of the average quality for each sample after merging and filtering. All samples were of acceptable quality to move on to BLAST analysis.

2.6.6.2.4.4 The merged and quality filtered reads were sent through BLAST v.2.6.0, to identify the organisms in each sample.

- The 16S samples were analyzed through BLAST using the NCBI 16S database v. June 11, 2017.
- The ITS samples were analyzed through BLAST using the UNITE3 fungal ITS database v. January 12, 2017.
- Post BLAST, additional filtering was used to remove false identifications and low-quality identifications. BLAST results were filtered to remove all results with less than 97% identity over less than 80% of the read length.
- Following this filter, a filter was applied that is designed to remove false positive identifications.
- False positive identifications are defined as hits that comprise less than 0.01 percent of the identifications in the results. False positive hits have too few reads identified as belonging to a given organism to be considered strong identifications.

2.6.6.2.4.5 Two scripts from KronaTools4 were used to get both the TaxID of all filtered BLAST results (reported in an .xlsx spreadsheet) and to generate an interactive Krona plot for relative abundance visualization of the results. The ktClassifyBLAST script gathers the TaxID for all results when the -s flag (summary) is used. The ktImportBLAST script organizes all of the results into a single, interactive plot and exploration of results.

2.6.6.2.4.6 For each organism identified at greater than 0.1% of the sample, a quick search through the scientific literature was performed to determine origin or bioactivity for the identified organisms. The R programming and statistical analysis language was used to create heat maps to compare sample community composition in a plot.

2.6.6.2.5 Diversity Analysis

2.6.6.2.5.1 The Shannon-Wiener Index (H) [29], for determining microbial diversity was calculated using Equation 3:

$$H = -\sum_{i=1}^S p_i \ln p_i \quad (3)$$

Where:

- p_i = proportion of total sample represented by an individual species (S – operational taxonomic units – OTU – genetic sequence that is determined [probability ≥ 95 %] to be unique) i_i , and
- S = number of species in the sample = species richness

2.6.6.2.5.2 *Evenness* – the observed diversity index relative to the theoretically possible diversity – was computed as Shannon’s Equitability (E_H) per Equation 4. E_H values range between 0 and 1, with 1 being complete evenness/diversity. As the number of detected OTU decreases, H approaches 0.

$$E_H = H/\ln S \quad (4)$$

2.7 STATISTICAL ANALYSIS

2.7.1 All statistical analyses were performed using JMP® Statistical Discovery software (JMP® is a registered trademark of SAS, Cary, NC). Because most of the corrosion occurred at the aqueous-fuel interface, corrosion ratings at the aqueous-fuel interface were the primary data used for statistical analysis. When appropriate, statistical computations were supplemented with graphical representations.

2.7.2 Descriptive statistics (mean and standard deviation) were calculated and presented for each test condition.

2.7.3 Logistic Regression Analysis

2.7.3.1 The test plan was designed to assess whether one or more of the 11 independent variables (water-presence, ethanol, etc.) had a statistically significant impact on corrosivity in the test microcosms, individually or through interaction effects. Moreover, except for microbiological and chemical data, observations were ordinal (also referred to as *categorical* or *attribute score*). They were reported as whole numbers derived from categorical ranges (see 2.6.2.1). Consequently, ordinal logistic regression was used to predict an ordinal dependent variable given one or more independent variables.

2.7.4 Analysis of Variance

2.7.4.1 Analysis of variance (ANOVA) was used to supplement the logistic regression analysis results and assess primary and two-factor interaction effects on corrosion rates as computed from the weekly fuel-aqueous interface corrosion scores. Table 7 summarizes the 11 main and 52 two-way interactions analyzed.

2.7.4.2 Dependent variables included in the ANOVA were: coupon weight loss, coupon total corrosion severity rating, and microcosm total risk scores. Total ratings values were natural-log (i.e., \log_e or \ln , where $e = 2.718$) transformed to satisfy the normality of error terms or the constant variance assumption of the ANOVA method.

2.7.5 Stepwise Regression Analysis

2.7.5.1 Stepwise regression analysis was used to identify statistically significant 2-factor interaction effects. Those 2-factor interaction effects with P-values < 0.05 were defined as statistically significant and are included in the final model. If $P = 0.05$, there is a 95 % probability that the null hypothesis was wrong – i.e., that conclude that the interaction effect was significant.

Table 7. Fractional Factorial Test Plan – Controlled Variables in 128 Microcosms.

Main Effects	Interaction Effects			
Sulfur	Sulfur*Biodiesel	Biodiesel*Mircobes	Mircobes*Glycerin	Glycerin*Ethanol
Biodiesel	Sulfur*Mircobes	Biodiesel*Glycerin	Mircobes*Ethanol	Glycerin*MAL Additive
Water	Sulfur*Glycerin	Biodiesel*Ethanol	Mircobes*MAL Additive	Glycerin*CFI Additive
Glycerin	Sulfur*Ethanol	Biodiesel*MAL Additive	Mircobes*CFI Additive	Glycerin*Corrosion Inhibitor
Ethanol	Sulfur*MAL Additive	Biodiesel*CFI Additive	Mircobes*Corrosion Inhibitor	Glycerin*Conductivity Additive
Mircobes	Sulfur*CFI Additive	Biodiesel*Corrosion Inhibitor	Mircobes*Conductivity Additive	Glycerin*FRP Material
MAL Additive	Sulfur*Corrosion Inhibitor	Biodiesel*Conductivity Additive	Mircobes*FRP Material	CFI Additive*Corrosion Inhibitor
CFI Additive	Sulfur*Conductivity Additive	Biodiesel*Water	MAL Additive*CFI Additive	CFI Additive*Conductivity Additive
Corrosion Inhibitor	Sulfur*Water	Biodiesel*FRP Material	MAL Additive*Corrosion Inhibitor	CFI Additive*Water
Conductivity Additive	Sulfur*FRP Material	Corrosion Inhibitor*Conductivity Additive	MAL Additive*Conductivity Additive	CFI Additive*FRP Material
FRP Material	Conductivity Additive*Water	Corrosion Inhibitor*Water	MAL Additive*Water	Ethanol*MAL Additive
	Conductivity Additive*FRP Material	Corrosion Inhibitor*FRP Material	MAL Additive*FRP Material	Ethanol*CFI Additive
	Water*FRP Material	Ethanol*Conductivity Additive	Ethanol*FRP Material	Ethanol*Corrosion Inhibitor

3 RESULTS AND DISCUSSION

3.1 TEST PLAN DEVELOPMENT

3.1.1 The details of the test plan design are provided in Section 2.1. This section discusses the rationale.

3.1.2 After reviewing Investigation Of Corrosion-Influencing Factors In Underground Storage Tanks With Diesel Service [7], CRC's FCP members considered alternative strategies for improving the industry's understanding of what was generally perceived to have been a spike in the frequency with which corrosion damage affected diesel fuel dispensing systems. Alternatives included a variety of survey designs to better quantify the extent of the problem. One of the barriers to the planning effort was the absence of any cost-impact data. A 2014 NACE report [30] estimated that in the U.S. the annual direct cost due to metallic corrosion was \$276 billion. The report indicated that the cost to the transportation sector was \$29.9 billion annually. However, the NACE report made no mention of corrosion costs borne by the fuel retail and fleet operations sector. None of the FCP members were aware of any analysis of the cost impact of corrosion in diesel fuel dispensing systems. FCP members were aware of operating and environmental risk of corroding diesel systems and engines. Quantitative cost analyses had yet to be developed, so this effort was pursued without such estimation in an effort to proactively help to address this issue. The FCP set about building this effort based on the contributions and findings from the two previous national efforts, while identifying key challenges and opportunities to address them and knowledge gaps in this research approach. Consequently, there was no basis for estimating the potential return on investment on any effort towards reducing the corrosion risk in these systems. Moreover, lessons learned from the two previous survey studies [6, 7] included recognition of the limitations of including too few sites. The panel members agreed that to address this issue, a representative number of UST would need to be included in a future survey design. Equations for determining the required samples size are offered in most statistics textbooks [31]. For a statistically significant survey – one from which the results would be $\geq 95\%$ likely to reflect reality – at least 500 UST would need to be inspected and tested. Based on the logistic challenges a survey this large would present, the FCP determined that a laboratory study would be more appropriate.

- 3.1.3 The first step in designing a laboratory study is to identify the most relevant independent variables. Water and microbial contamination are two variables well known to contribute to fuel system corrosion [32]. As reviewed in the *Introduction* (Section 1.1) implementation of 40 CFR § 80 [33] included the reduction of the sulfur concentration in on-highway diesel fuel $\leq 15 \text{ mg L}^{-1}$. There has been considerable speculation that the move from LSD ($[\text{S}] \leq 500 \text{ mg L}^{-1}$) to ULSD ($[\text{S}] \leq 15 \text{ mg L}^{-1}$) contributed to diesel fuel becoming more corrosive. Moreover, the use of biodiesel has increased substantially since the implementation of Renewable Fuel Standard – part of the Energy Policy Act of 2005 [34]. Glycerin is a byproduct of FAME production [35] and potential contaminant of B100 biodiesel blend stock. Increased hydrotreating to remove sulfur for ULSD, also removes nitrogen and oxygen from petroleum-derived diesel blendstocks, converts olefins to paraffins, and can reduce the overall concentration of aromatic compounds, depending upon the severity of the hydrotreating. Removal of these heteroatoms and conversion/removal of some compounds from ULSD means modern diesel fuel will have decreased lubricity and less conductivity but exhibit better thermal oxidation stability and improved corrosivity associated with reactive sulfur compounds as compared to LSDF. Petroleum-derived ULSD typically contains lubricity improvers, conductivity additives, water-related corrosion inhibitors, and cold flow improvers. Biodiesel contains antioxidant to improve stability and prevent the formation of byproducts. When added to petroleum diesel at 1% or greater, biodiesel will typically improve lubricity of the finished product to the point that additional lubricity additive is not required. Evidence of ethanol –introduced via switchloading, or vapor recovery system crossover between tanks containing different fuel grades – was reported in the 2012 Battelle study [6]. That same study hypothesized that *Acetobacter* spp. recovered from UST samples might have been metabolizing the ethanol to acetic acid. Finally, there has been speculation that ULSD and biodiesel blends can react with the polymer components or additives of FRP. Given that there are numerous combinations of fiber types and polymers used in the manufacturing of FRP USTs, it was recognized that the results from microcosms containing FRP coupons could not be extrapolated to apply generally to all FRP material deployed in the field. The 11 variables listed in Table 1 were selected to assess whether any of them individually (main effects) or through interactions among two or more of them (interaction effects) contributed to increased fuel corrosivity.
- 3.1.4 After identifying the controlled (independent) variables, the next step was to determine the complexity of the test plan. Full factorial experimental designs are based on three primary considerations:
- 3.1.4.1 Number of independent variables – discussed above.
- 3.1.4.2 Number of levels (i.e., concentrations) for each independent variable – for example, a test design could have included various concentrations of dissolved water, ethanol, glycerin, etc. The FCP agreed to focus on two levels – present or absent – for each independent variable. Without replication, an 11 variable x 2 level test plan would have required more than 2,000 test jars (see 2.1).
- 3.1.4.3 Number of replicates – to differentiate between inherent differences (variability) among systems (microcosms) that are nominally identical (same fuel grade, additives, and contaminants) and differences caused by the presence or absence of a given independent variable, replicates are needed. The appropriate number of replicates is based on the inherent variability of the parameters to be observed or tested. Had duplicate microcosms be included in the test plan, more than 4,000 test jars would have been needed.

- 3.1.4.4 The FCP members agreed that the study's focus should be on identifying major variables that contributed to fuel corrosivity. Consequently, a fractional-factorial test plan was developed. Fractional-factorial design is based on the sparsity-of-effects principle (i.e., only main effects – for example [S] and two-way interaction affects are relevant). For this study, it was the assumption that the sparsity-of-effects principle applied apropos of understanding increased corrosion aggressiveness in fuel systems. The 128-microcosm test plan was finalized based on these considerations (the number of microcosms is computed from the number of levels – 2 – and the number of factors minus the number of times the full matrix has been fractioned – i.e., $\frac{1}{2} \rightarrow 2^{11-1}$, $\frac{1}{4} \rightarrow 2^{11-2}$, $\frac{1}{8} \rightarrow 2^{11-3}$, and $\frac{1}{16} \rightarrow 2^{11-4} = 2^7 = 128$).
- 3.1.5 In the test plan, ethanol and glycerin was only added to microcosms containing water. The reason was that both ethanol and glycerin are water soluble and thought to accumulate in bottoms water even though they are present in only trace quantities in fuel. During fuel delivery into an underground storage tank, the water bottoms gets disturbed and mixed with fuel. This results in trace ethanol and glycerin present in fuel being extracted into the water bottoms and accumulating over time. This is consistent with results of previous studies which observed measurable quantities of ethanol and glycerin in bottoms water although they were not measurable in fuel ([6] and [7]).
- 3.1.6 At this point, the contents of the test plan microcosms had been defined, and the next step was to determine microcosm size. Hydrocarbons are non-polar, but many fuel additives have some polarity (a partial ionic charge) that gives them some solubility in water. To simulate field conditions, fuel over water testing is typically performed with 99 parts fuel over 1-part water. To maintain this ratio and have sufficient water to allow for water specimen collection during the test period, each microcosm would need to be > 100 L (26 gal) – 99 L fuel over 1 L water. The logistics of handling 128 100 L microcosms would have been challenging. However, there was concern that varying from the 99:1 fuel to water ratio would affect polar molecule partitioning from the fuel into the underlying water and introduce a bias to the test results. If the fuel to water ratio did not affect partitioning smaller microcosms could be used. Consequently, partitioning was investigated per Section 2.2.
- 3.1.7 The initial alloy choice for corrosion coupons was A36 steel. The Steel Tank Institute (STI) provided a sheet 10-gauge (0.123 in; 0.312 cm thick) A36 steel. However, scale on the sheet and warping that occurred during the in-house machining process to fabricate coupons from the sheet, rendered the material unsuitable for the purposes of this project. Pre-cut, 1018 grade, low carbon steel coupons proved to be a satisfactory alternative.
- 3.1.8 Once the test conditions had been determined, it was necessary to identify the parameters to be monitored. The parameters described in Section 2.6 were selected because they were expected to provide the most useful information about the relationships between the independent and dependent variables. More detailed explanations of the rationale for choosing each dependent variable will be provided in Sections 3.5 through 3.8.
- 3.1.9 Given that the focus was accelerated corrosion, the test period was set for 12-weeks. Based on Passman's experience [37] an option for extending the test period was included in case there were no visible changes in the microcosms by week 12 (T_{wk12}).

3.1.10 The cost of running all of the desired tests on a weekly basis would have been prohibitive. To balance the need for data against the analytical costs, a plan was developed for criteria driven testing. Figures 8, 9, and 10 are flow diagrams that were to have been used to determine which tests were to have been performed prior to T_{wk12} . Microcosm gross observations (2.6.2.1) and coupon corrosion ratings (2.6.2.2) were to be reported weekly. Additional tests included water separability and surfactant production (ASTM D7451 [17], analysis for LMOA (2.6.4), pH, acidity, and ATP-bioburden. Although weekly microcosm and coupon gross observations were performed, the additional tests prescribed in Figures 8 through 10 were not performed because of delays in recording CR data as discussing in Section 4.2.2.

3.2 STOCK FUEL CHEMISTRY

3.2.1 Analysis of the stock fuels' sulfur and water concentrations showed that the LSD contained $274 \mu\text{g g}^{-1}$ sulfur and 50 mg kg^{-1} water. The ULSD contained $5 \mu\text{g g}^{-1}$ sulfur and 74 mg kg^{-1} water.

3.3 PARTITION COEFFICIENT TESTING

3.3.1 Within fuel distribution systems, polar organic compounds are known to partition from the fuel phase into the aqueous phase. Passman (unpublished) has observed that historically TDS in diesel fuel system bottoms-waters typically ranged from 150 mg L^{-1} to 250 mg L^{-1} (234 mS cm^{-1} to 312 mS cm^{-1}) but since the late 1990's TDS in the g L^{-1} ($\geq 1,560 \text{ mS cm}^{-1}$) range had become common. During CRC FCP meetings, Passman speculated that the order of magnitude TDS increase was due to additive partitioning. As noted in 3.1.6, it was hypothesized that the fuel to water ratio would affect additive and contaminant partitioning from the fuel to water phase. This would, in turn, affect corrosivity. Table 8 presents the summary data in which five treatments under two fuel to water ratio conditions were evaluated in triplicate. For most conditions (i.e., treatment x fuel to water) the variation among replicate separatory funnels was $<1 \%$ - indicating excellent repeatability.

3.3.2 Two-way ANOVA of the aqueous-phase conductivity data indicated that the fuel to water ratio did not affect aqueous-phase conductivity at the 0.05 confidence level (Tables 9 and 10).

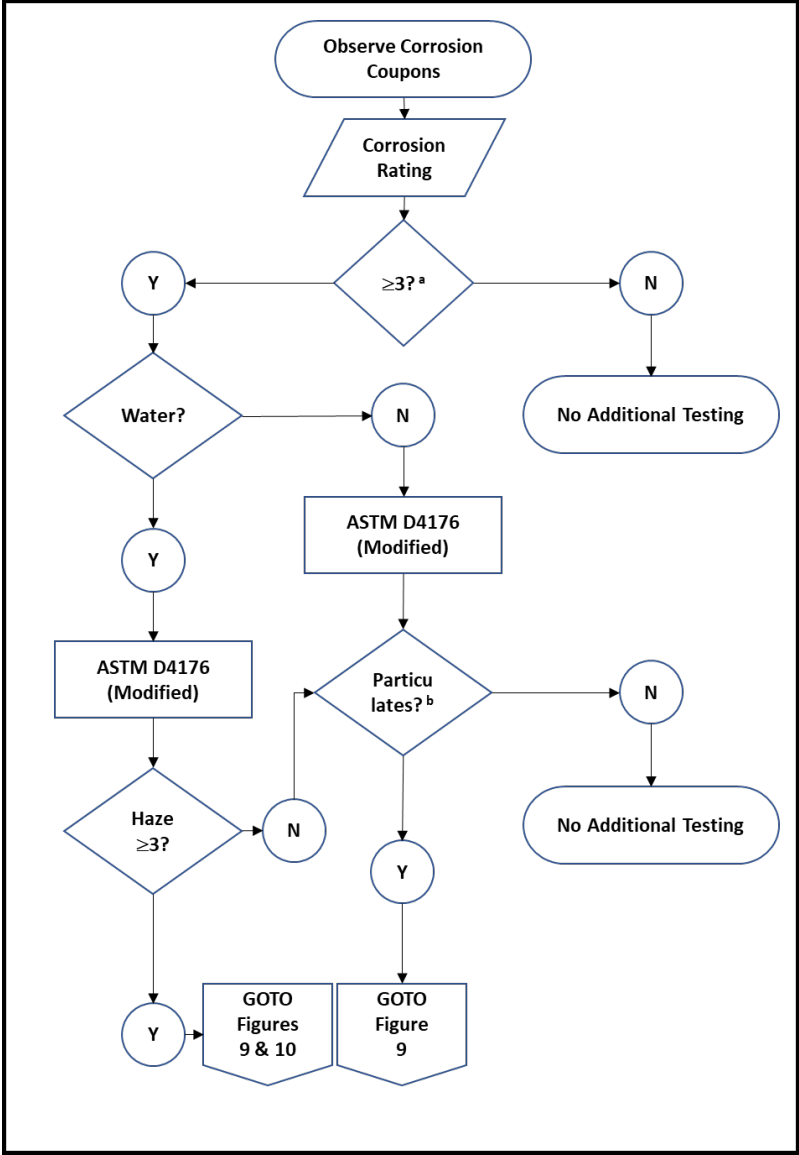


Figure 8. Flow diagram part 1 – observation-based testing – gross observations.

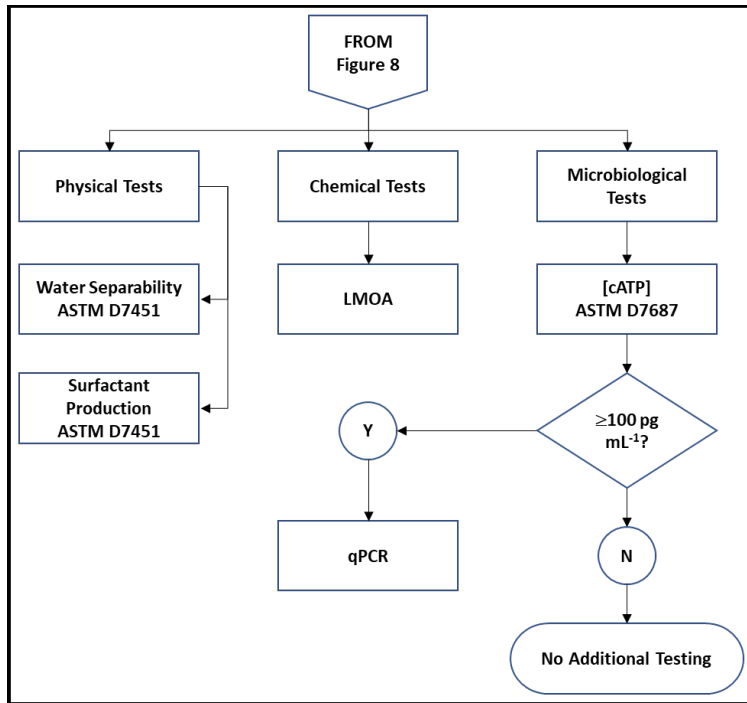


Figure 9. Flow diagram part 2 – observation-based testing – physical, chemical, and microbiological tests.

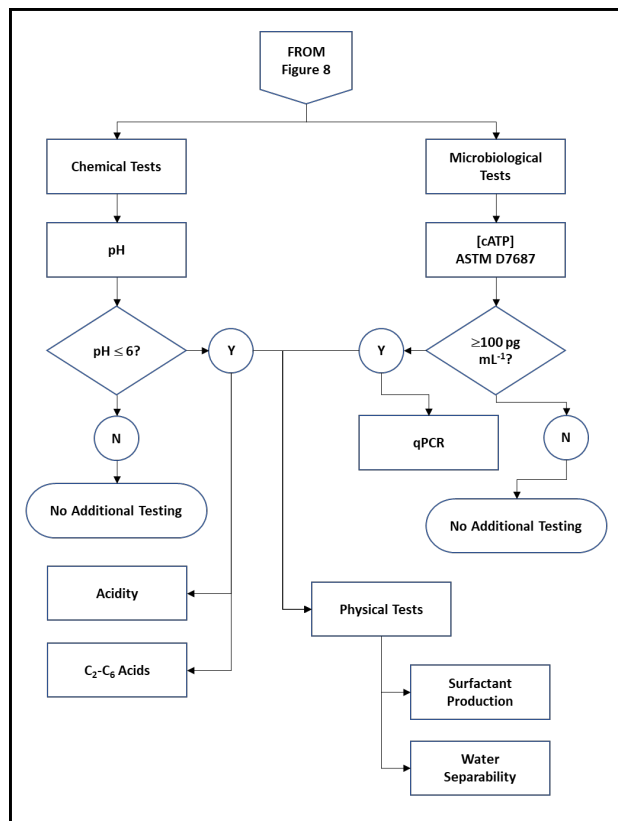


Figure 10. Flow diagram part 3 – observation-based testing – additional physical, chemical, and microbiological tests.

3.3.3 The results of the partitioning study supported the decision to use 2 L microcosms containing 1,300 mL fuel over 700 mL aqueous solution – ~65 % vol fuel over 35 % vol aqueous solution.

Table 8. Fuel and Fuel Additive Partition Test Results – Impact of LSD to Water Ratios on Aqueous-Phase Conductivity ($\mu\text{S cm}^{-1}$) All values are averages \pm standard deviations.

Treatment	30:70	1:99	$ \Delta ^a$
All ^b	85.1 \pm 0.10	85.3 \pm 0.51	0.2
CA	86.2 \pm 0.21	86 \pm 2.4	0.2
CFI	85.5 \pm 0.42	86.1 \pm 0.26	0.6
CI	85.7 \pm 0.41	85.1 \pm 0.70	0.6
MAL	85.0 \pm 0.40	86.1 \pm 0.35	1.1

Notes:

- $|\Delta|$ - absolute value of the difference of average conductivities in microcosms with 3:70 versus 1:99 water to fuel ratio microcosms.
- All – conductivity additive (CA), cold flow improver (CFI), corrosion inhibitor (CI), and mono-acid lubricity additive (MAL).

Table 9. Two-way ANOVA – Five additive treatments x two fuel to water ratios – summary statistics (sums, averages and variances are conductivities in $\mu\text{S cm}^{-1}$).

SUMMARY	Full	CI	CA	CFI	MAL	Total
<i>Fuel to water</i>						
<i>=70:30</i>						
Count	3	3	3	3	3	15
Sum	255	257	259	257	255	1283
Average	85	86	86	86	85	86
Variance	0.01	0.16	0.04	0.17	0.16	0.30
<i>99:1</i>						
Count	3	3	3	3	3	15
Sum	256	255	258	258	258	1286
Average	85	85	86	86	86	86
Variance	0.26	0.49	6.0	0.07	0.12	1.2
<i>Total</i>						
Count	6	6	6	6	6	
Sum	511	512	517	515	513	
Average	85	85	86	86	86	
Variance	0.13	0.37	2.4	0.19	0.52	

Table 10. Two-way ANOVA – Five additive treatments x two fuel to water ratios – ANOVA.

<i>Source of Variation</i>	<i>SS</i>	<i>df</i>	<i>MS</i>	<i>F</i>	<i>P-value</i>	<i>F crit</i>
Fuel to water	0.34	1	0.341	0.455	0.508	4.351
Additive	2.91	4	0.726	0.968	0.447	2.866
Interaction	2.94	4	0.735	0.979	0.441	2.866
Within	15.01	20	0.751			
Total	21.20	29				

3.4 STATISTICAL ANALYSIS

3.4.1 Background

3.4.1.1 Before providing details of the results from each type of test performed on microcosm specimens, the statistical analysis will be presented. This top-down approach is meant to provide readers with insight to the study’s overall results before delving into the details of individual parameters.

3.4.1.2 The statistical analyses presented here test the *null hypothesis* (H_0) for each of the independent variables main and two-way interaction effects. In this study, H_0 postulates that variable X, or its interaction effect did not covary with corrosion on test coupons. Corrosion was assessed as corrosion rating (CR_x , where X was the aqueous, fuel, vapor phase or aqueous-fuel interface) or general corrosion rate (GCR).

3.4.1.3 Two types of potential errors affect the interpretation of statistical computations. A *Type 1* error occurs when the null hypothesis is incorrectly rejected – i.e., the calculations are interpreted as indicating that a statistically significant relationship exists when it does not. Conversely, a *Type 2* error occurs when the null hypothesis is incorrectly accepted – i.e., a statistically significant relationship is incorrectly classified as no relationship. The *P-value* (or *P*) statistic indicates the probability of a Type 1 error being made. Thus, when $P \leq 0.05$, there is $\leq 5\%$ probability of a Type 1 error.

3.4.1.4 $P \leq 0.05$ is commonly used as the threshold for deciding whether to reject H_0 , and was the criterion used to assess significance in this study.

3.4.1.5 The statistical analyses presented below include computations suggesting the direction and magnitude of the observed relationships. *Direction* refers to whether corrosion was greater or diminished when a variable was present. Negative values indicated that there was less coupon corrosion when the variable was present than when it was not. Positive values indicate that there was more severe corrosion. This is not proof of cause and effect. *Correlation* does not imply *causation* [36]. *The test plan was designed to determine correlations only.* Readers are reminded not to assume that either positive or negative correlations reported below imply any cause and effect relationships.

3.4.2 Tier 1 - Stepwise Ordinal Logistic Regression for Aqueous-Fuel Interface

3.4.2.1 The full analysis is provided in Appendix C. This section highlights the inferences drawn from the computations.

3.4.2.2 Table 11 highlights the statistically significant correlations between independent variables and corrosion ratings (CR) on corrosion coupon face and edge surfaces in contact with the aqueous, fuel-aqueous-interface (*interface*), and fuel phases, and edge only in contact with the vapor phase. Note that correlation can be either *positive* (the values of both parameters move in the same direction – both either increase or decrease) or *negative* (the value of each parameter moves in the opposite direction of the other – as one increases the other decreases, and vice versa).

- Green and red shaded cells indicated that H_0 was rejected. Green shaded cells containing the “↓” symbol indicated that CR was significantly less when the variable was present than when it was absent. Per 3.4.1.4, as used throughout this discussion, *significant* implies $P \leq 0.05$.
- Red shaded cells containing the “↑” indicated that the CR was significantly greater when the variable was present than when it was absent. Substantial ATP-bioburdens developed in both challenged (intentionally inoculated with microbes recovered from contaminated USTs) and unchallenged (microbes present as contaminants in the fuels used for this study) microcosms. Consequently, “Microbes” as used in the following tables indicates that an intentional challenge population had been added to the microcosm.
- Gray shaded cells indicate that there was no significant relationship between the controlled variable (*treatment*) and CR.
 - f) Sulfur – LSD = present; ULSD = absent.
 - g) ↑ More deterioration when variable was present than when it was absent.
 - h) ↓ Less deterioration when variable was present than when it was absent.
- Microbes – microcosm challenged intentionally (see 3.5).
- The CR at T_{wk6} and later was ≥ 4 in all four-phase microcosms but ≤ 2 in all two-phase microcosms. This demonstrated that increased corrosivity was unequivocally correlated with the presence of an aqueous-phase. Consequently, water was not among the controlled variables included in Tables 11 and 12.
- There were no significant correlations between the individual treatments and CR on coupon surfaces exposed to the aqueous-phase. However, several significant two-way interaction effects were observed on coupon faces and edges. The interaction effect between sulfur and CFI on aqueous-phase, coupon edge surfaces indicates that CR in microcosms containing LSD + CFI was greater than in those containing ULSD + CFI.
- Only treatments with one or more significant correlations with CR were included in Table 11.

3.4.2.3 Summary statistics for treatments and CR were presented in Table 12. Only main effects and two-way interaction effects were shown. The cell shading scheme was the same as for Table 10.

- The T_{wk1} to T_{wk12} category includes data from all 12 weeks (week 1, 2, 3, 4, 6, 9 and 12).
- The T_{wk12} statistics told a different story than the T_{wk1} to T_{wk12} computations.
- In the T_{wk12} analysis, ethanol was the only main factor that correlated with high CR ratings. Four two-way interactions (ethanol + CI, MAL + FRP, sulfur + CA, and sulfur + CFI) correlated with more aggressive CR scores.
- The main factors, FAME and CI were each correlated with less aggressive CR scores, as was the interaction between ethanol and microbial challenge.
- The T_{12wk} relationships between treatments and CR scores observed for ethanol, FAME, CI, ethanol + microbes, and MAL + FRP were also significant for the T_{wk1} to T_{wk12} computations.
- Additionally, the main effects of sulfur and microbial challenge – not significant per the T_{wk12} analytics – were significant when data from all 12 weeks were included in the computations.
- When all 12-weeks’ data were considered, there was also a significant correlation between CR and the ethanol + CA interaction.

Table 11. Relationships between independent variables and CR – 12-week microcosm study.

Variable	CR ^a x Phase							
	Aqueous		Aqueous-Fuel Int _b		Fuel		Vapor	
	Face	Edge	Face	Edge	Face	Edge	Face ^c	Edge
Sulfur ^d								↑
Microbes ^e				↓				
FAME				↓	↓			
Glycerin					↓			
Ethanol			↓					
MAL				↓				
CFI				↓	↓			↓
CI			↓	↓	↓			
CA					↓			
CFI + Microbes				↓				↓
CI + Microbes				↓				
CI + MAL					↑	↑		
Ethanol + CA	↓							
Ethanol + Microbes				↑				
FAME + CA	↓	↓						
FAME + CFI		↓						
FAME + Microbes				↓				
Glycerin + CFI		↓						
MAL + CA		↓						
MAL + Microbes								↑
Sulfur + CA	↑	↑						
Sulfur + FAME					↓			
Sulfur + CFI		↑						

Notes:

- a) CR – corrosion rating.
- b) Aqueous-fuel int – interface.
- c) Vapor phase face – no significant correlations.
- d) ↑ (red fill) More deterioration when variable was present than when it was absent.
 ↓ (green fill) Less deterioration when variable was present than when it was absent.
 No arrow (grey fill) no statistically significant relationship.
- e) Microbes – microcosm challenged intentionally (see 3.5).

3.4.2.4 Relationships between average weight loss (ΔM %), total corrosion ratings (CR), and gross observation-based overall risk ratings (RS_{GO}) were determined. As discussed in Section 3.6.1, only CR observations at the coupon-fuel-aqueous-phase, three-way-interface (CR_I) were used in the statistical analysis of these three parameters. Table 13 showed which main and two-way variables correlated with significant differences in the observed parameters. Table 14 provided a summary of the ANOVA calculations found in Appendix C. Both Tables showed that water was the only variable that had the same impact on all three parameters. The relationship between ATP-bioburdens and corrosion were not included in the ordinal logistic regression analysis.

Table 12. Summary ANOVA statistics, stepwise regression – aqueous-fuel interface 12-week microcosm study at T_{12wk} and throughout 12-week exposure period.

Variable	Coupon Surface Corrosion Rating at Aqueous-Fuel Interface							
	T_{12wk}				T_{1wk} to T_{12wk}			
	Estimate	Std Error	Chi ²	P	Estimate	Std Error	Chi ²	P
Sulfur ^a	0.18	0.25	0.55	0.46	0.36	0.091	15.26	<0.0001
Microbes ^b	-0.44	0.25	3.11	0.078	0.22	0.091	6.06	0.014
FAME	-0.54	0.256	4.51	0.034	-0.22	0.09	5.67	0.017
Glycerin	-0.35	0.25	2.01	0.16	-0.43	0.093	21.49	<0.0001
Ethanol	0.71	0.26	7.27	0.007	0.37	0.091	16.1	<0.0001
MAL	-0.22	0.24	0.81	0.37	0.98	0.090	1.18	0.28
CFI	0.17	0.24	0.47	0.49	0.16	0.090	3.16	0.076
CI	-0.61	0.26	5.66	0.017	-0.31	0.091	11.85	0.0006
CA	0.14	0.25	0.33	0.57	0.082	0.09	0.82	0.36
FRP	0.23	0.24	0.90	0.34	0.090	0.091	0.99	0.32
Ethanol + Microbes	-0.50	0.25	3.92	0.048	-0.3	0.091	11.17	0.0008
Ethanol + CA					0.41	0.092	19.36	<0.0001
Ethanol + CI	0.63	0.26	5.87	0.015				
MAL + FRP	0.62	0.26	5.87	0.015	0.39	0.91	18.03	<0.0001
Sulfur + CA	0.38	0.92	16.59	<0.0001				
Sulfur + CFI	0.32	0.091	12.36	0.0004				

Notes:

- a) Sulfur – LSD = present; ULSD = absent.
- b) Microbes – microcosm challenged intentionally (see 3.5).

3.4.2.5 Concerns about the 12-week exposure period being insufficient proved to be unfounded. As shown in Figure 11, by T_{wk6} the probability of $CR_I = 5$ ($P_{CR_I=5}$) was 67 % and by T_{wk12} $P_{CR=5}$ was 85 %.

3.4.2.6 Microcosms treated with corrosion inhibitor (CI) had lower CR and RS_{GO} scores than those that were not. Figure 12, excerpted from Appendix C, illustrates the differences between CI-treated and untreated microcosms. Microcosms that had not been treated with corrosion inhibitor had an 90% probability of $CR \geq 3$ at T_{wk2} . It was T_{wk6} before CI-treated microcosms had an 80 % probability of $CR \geq 3$. Moreover, the rate ($\Delta P_{CR \geq 3} dt^{-1}$ – where ΔP is the probability change dt is time lapsed in weeks) at which the probability of $CR \geq 3$ ($P_{CR \geq 3}$) increased was substantially greater in untreated than in CI-treated microcosms ($\Delta P_{CR \geq 3} dt^{-1} = 0.4 \text{ week}^{-1}$ versus 0.1 – Figure 12a). Throughout the study, the weekly $P_{CR \geq 3}$ for CI-treated microcosms was less than the $P_{CR \geq 3}$ for untreated ones (Figure 12b). Figure 12 also illustrates a phenomenon that was common among the four-phase microcosms. In most microcosms, $\Delta P_{CR \geq 3} dt^{-1}$ approached zero after week 4. This was partially an artifact of CR. Once $CR = 5$, $\Delta P_{CR \geq 3} dt^{-1} = 0$. It was impossible to exceed 100 % coverage.

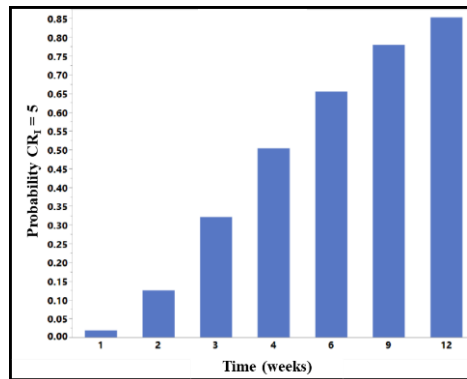


Figure 11. $P_{CR=5}$ (vertical axis) versus exposure period (weeks) – from Appendix C, page C-59.

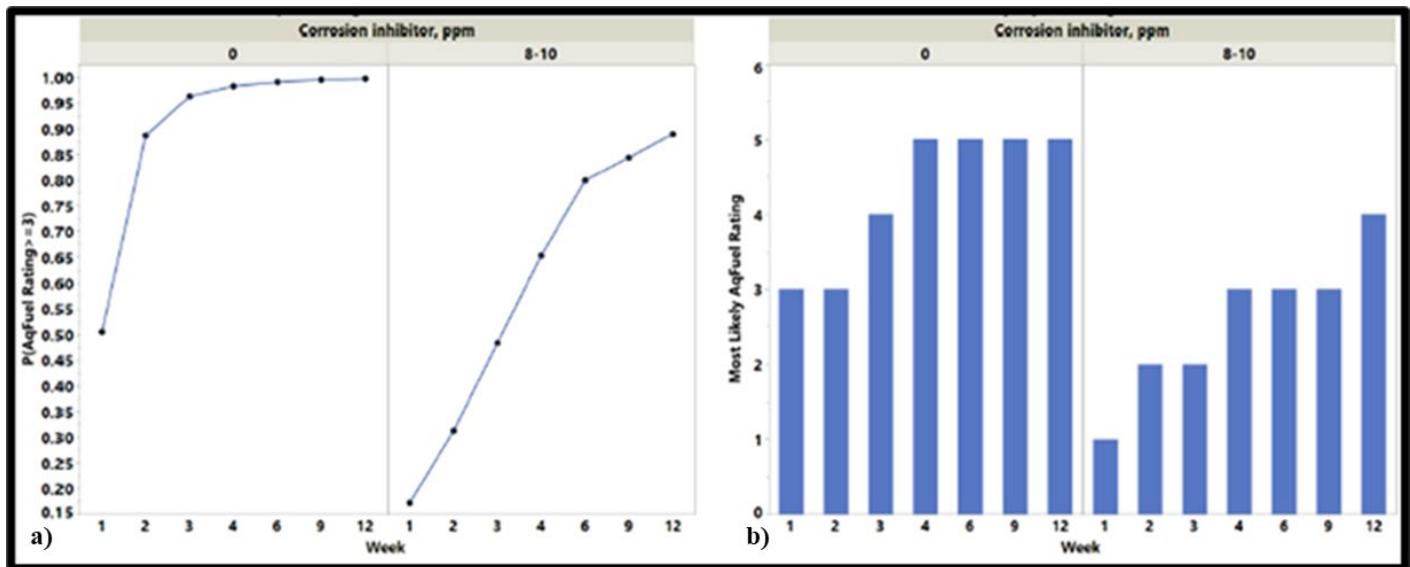


Figure 12. Relationship between CI and $P_{CR \geq 3}$ with and without CI-treatment

a) $P_{CR \geq 3}$ versus T_x , where X is weeks; b) most likely corrosion severity rating by week – from Appendix C, page C-60.

Table 13. Relationships between independent and dependent variables – 12-week microcosm study.

Variable	Relationship x Parameter		
	ΔM (%) ^a	CR ^b	RS _{GO} ^c
Sulfur		↑ ^d	↑
Water	↑	↑	↑
Microbes ^e		↓	↑
FAME			
Glycerin	↓		
Ethanol			↓
MAL			
CFI			
CI		↓	↓
CA			
FRP	↓		
CFI + CA	↑		
Ethanol + CFI			↓
Ethanol + CI			↓
Ethanol + Microbes		↑	↓
FAME + CI			↓
FAME + Water		↓	
FAME + FRP			↓
Microbes + Glycerin	↑		
Sulfur + Water			↔ ^f
Sulfur + Glycerin			↓
Sulfur + Microbes			↓

Notes:

- a) ΔM % – average corrosion coupon weight lost $T_{wk12} - T_{wk0}$.
- b) CR – total corrosion rating in the invert emulsion (fuel-water interface) zone.
- c) RS_{GO} – microcosm gross observation risk rating.
- d) ↑ More deterioration when variable was present than when it was absent.
↓ Less deterioration when variable was present than when it was absent.
- e) Microbes – microcosm challenged intentionally (see 3.5).
- f) ↔ Interaction effect between ULSD and water present for RS_{GO}.

Table 14. Summary ANOVA statistics, stepwise regression between independent and dependent variables – 12-week microcosm study.

Variable	Parameter											
	$\Delta M \% ^a$				CR ^b				RS _{GO} ^c			
	Estimate	Std Error	t-Ratio	P	Estimate	Std Error	t-Ratio	P	Estimate	Std Error	t-Ratio	P
Sulfur	-0.000094	0.018	-0.05	0.96	-0.032	0.016	-1.98	0.051	0.15	0.044	3.38	0.001
Water	-0.14	0.032	-4.43	<0.001	-0.59	0.028	-21.4	<0.0001	-0.85	0.052	-16.2	<0.0001
Microbes ^d	-0.017	0.020	-0.83	0.41	0.013	0.018	0.75	0.46	-0.19	0.032	-5.99	<0.0001
FAME	0.023	0.018	1.25	0.21	0.039	0.023	1.70	0.093	0.044	0.029	1.5	0.14
Glycerin	0.031	0.020	1.54	0.13	0.0073	0.017	0.42	0.67	-0.016	0.032	-0.49	0.63
Ethanol	0.023	0.020	0.11	0.91	-0.019	0.018	-1.10	0.27	0.20	0.032	6.19	<0.0001
MAL	-0.012	0.019	-0.65	0.52	-0.013	0.023	-0.57	0.57	0.033	0.030	1.22	0.23
CFI	0.0038	0.018	0.21	0.84	0.0083	0.016	0.51	0.61	0.045	0.030	1.52	0.13
CI	0.019	0.019	1.00	0.32	0.075	0.016	4.7	<0001	0.073	0.029	2.49	0.014
CA	-0.027	0.019	-1.45	0.15	-0.00022	0.016	-0.01	0.99	0.0099	0.029	0.34	0.73
FRP	0.022	0.019	1.15	0.25	0.00094	0.016	0.06	0.96	0.028	0.03	0.93	0.35
CFI + CA	0.044	0.019	2.34	0.021					-0.11	0.029	-3.67	0.0004
CFI + CI	0.040	0.019	2.17	0.032								
CFI + FRP					0.045	0.016	2.83	0.0056				
CI + FRP	0.033	0.019	1.78	0.078								
Ethanol + FAME					0.033	0.018	1.88	0.063				
Ethanol + Microbes					0.071	0.018	4.03	0.0001	-0.032	0.032	-1.02	0.31
Ethanol + CFI									-0.094	0.030	-3.18	0.0019
Ethanol + CI	0.040	0.019	2.11	0.038					-0.10	0.030	-3.49	0.0007
Ethanol + MAL	0.051	0.019	2.67	0.0088					0.031	0.030	1.05	0.30
Ethanol + FRP					0.025	0.016	1.54	0.13				
FAME + CI									-0.54	0.029	-1.84	0.069
FAME + Water					-0.047	0.023	-2.04	0.044				
FAME + FRP									-0.97	0.029	-3.33	0.0012
Glycerin + CFI					-0.013	0.016	-0.79	0.43				
Glycerin + FRP	0.058	0.019	3.07	0.0027					-0.046	0.030	-1.57	0.12

Table 14. Continued

Variable	Parameter											
	$\Delta M \%$				Corrosion Rating				RS _{GO}			
	Estimate	Std Error	t-Ratio	P	Estimate	Std Error	t-Ratio	P	Estimate	Std Error	t-Ratio	P
Glycerin + MAL									-0.054	0.030	-1.82	0.072
Microbes + Glycerin	0.067	0.020	3.26	0.0015					-0.089	0.032	-2.81	0.0059
Microbes + MAL	0.036	0.018	1.92	0.058	0.031	0.018	1.79	0.076				
MAL + CI					0.034	0.016	2.16	0.033	0.05	0.030	1.75	0.083
MAL + CFI	0.047	0.019	2.52	0.013								
MAL + FRP	0.036	0.018	1.96	0.053					0.056	0.030	1.94	0.055
Sulfur + Water									0.33	0.044	7.39	<0.0001
Sulfur + Ethanol					0.025	0.016	1.52	0.13				
Sulfur + Glycerin									-0.053	0.02	-1.66	0.10
Sulfur + Microbes					0.028	0.016	1.72	0.088	-0.07	0.03	-2.28	0.025
Sulfur + CA					-0.045	0.016	-2.80	0.0061				

Notes:

- a) $\Delta M \%$ – average corrosion coupon weight lost $T_{wk12} - T_{wk0}$.
- b) CR – corrosion rating in the invert emulsion (fuel-water interface) zone.
- c) RS_{GO} – microcosm gross observation risk rating.
- d) Microbes – microcosm challenged intentionally (see 3.5).

3.4.3 Tier 2 - Stepwise Regression of Corrosion Rating Changes between T_0 and T_{6wk} .

3.4.3.1 As illustrated in Figure 12, the rate at which CR changed from week to week ($\Delta P_{CR \geq 3} dt^{-1}$) was greatest during the first four weeks of exposure. Figure 13 illustrates this phenomenon, common among the four-phase but absent in the three-phase microcosms.

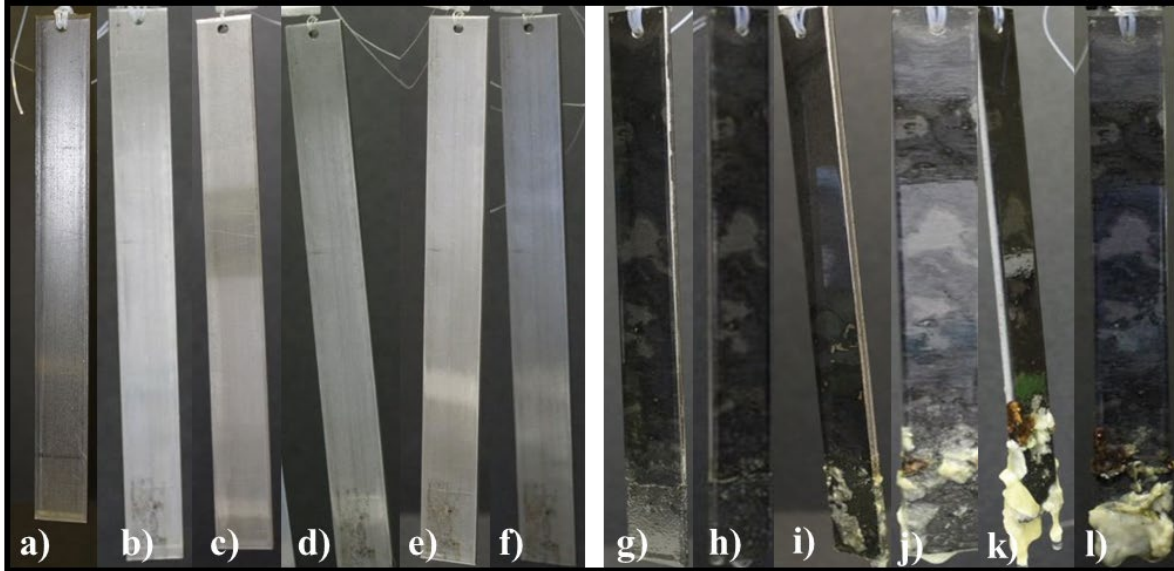


Figure 13. Corrosion coupons – a) through f): Microcosm 1, coupon 1-2, at weeks 1, 2, 3, 4, 6, and 12; g) through l) Microcosm 4, coupon 4-2, at weeks 1, 2, 3, 4, 6, and 12.

3.4.3.2 The Tier 2 analysis determined significant main and two-factor interaction relationships between each of the 11 factors on the weekly $\Delta CR dt^{-1}$ during the period T_{wk1} and T_{wk6} . Only CR at the fuel-aqueous interface (CR_I) was analyzed. The full analysis was provided in Appendix D.

3.4.3.3 Table 15 (adopted from Appendix D) was a summary of the ANOVA statistics.

3.4.3.4 The week to week $\Delta CR dt^{-1}$ changes in CI-treated microcosms were significantly less than those in untreated ones. This was illustrated graphically in Figure 14.

3.4.3.5 Table 15 shows that there were significant interaction effects between:

- CA + CFI
- CFI + CI
- Ethanol + CA
- Microbial challenge + CI

3.4.3.6 Figure 14 illustrated the respective week to week $\Delta CR dt^{-1}$ changes in CI-treated and CI-untreated microcosms. The plot represented averages among all CI-treated and untreated microcosms, respectively. The convergence of the two curves between T_{wk4} and T_{wk5} reflected the upper limit of CR scoring. As CR scores approached 5, $\Delta CR dt^{-1}$ approached zero.

Table 15. ANOVA, F-test summary statistics for week to week $\Delta CR dt^{-1}$ between T_{wk1} and T_{wk6} .

Variable	SS	F_{calc}	P
Sulfur ^a	0.0017	0.0498	0.824
Microbes ^b	0.011	0.328	0.568
FAME	0.020	0.569	0.453
Glycerin	0.0029	0.0836	0.773
Ethanol	0.014	0.389	0.534
MAL	0.0073	0.211	0.647
CFI	0.031	0.896	0.346
CI	0.854	24.4	<0.0001 ^c
CA	0.012	0.354	0.554
FRP	0.032	0.920	0.340
CFI + CA	0.162	4.65	0.034
CFI + CI	0.25	7.32	0.0082
Ethanol + CA	0.259	7.41	0.0078
Ethanol + CI	0.114	3.25	0.075
Glycerin + Microbes	0.091	2.60	0.110
Glycerin + CFI	0.13	3.60	0.061
Glycerin + CI	0.11	3.25	0.075
Microbes + CI	0.16	4.47	0.037

Notes:

- a) Sulfur – LSD = present; ULSD = absent.
- b) Microbes – microcosm challenged intentionally (see 3.5).
- c) Yellow highlighting indicated F_{calc} (the computed value of F) was significant.

3.4.3.7 Figure 15 compared weekly average CR scores in CI-treated and CI-untreated microcosms. At T_{wk1} there was no apparent difference in average CR scores between treated and untreated microcosms. However, from T_{wk2} through T_{wk6} the average CR scores for CI-treated microcosms were consistently lower than those for CI-untreated microcosms.

3.4.3.8 The interaction effect between CI-treatment and microbial challenge was one of the significant interaction effects. The main effect of microbial challenge was not significant. There were 11 microcosms (six unchallenged and five challenged) for which weekly CR scores and T_{wk12} ATP test data were available. Table 16 summarized the average CR scores in the aqueous-phase and at the aqueous-fuel interface at T_{wk1} , T_{wk4} , and $\Delta CR (CR_{wk4} - CR_{wk1})$. Week 4 observations were used because $CR_{wk6} = CR_{wk4}$ in these 11 microcosms. Table 17 summarized one-way ANOVA computations for the 11 microcosms. Tables 16 and 17 corroborated the microbial challenge results presented in Table 15.

Table 16. Effect of microbial challenge on CR between weeks 1 and 4 – summary statistics. Values are $CR_{AVG \pm s}$.

Treatment	Phase					
	Aqueous			Aqueous-Fuel Interface		
	Week		ΔCR	Week		ΔCR
	1	4		1	4	
Challenged	1.6±0.55	1.8±0.55	0.2±0.45	1.4±0.55	3±1.5	1±1.3
Unchallenged	1.5±.55	2.2±0.41	0.7±0.82	1.2±0.41	2.2±0.98	1±0.89

Table 17. Effect of microbial challenge on CR between weeks 1 and 4 – ANOVA summary.

Parameter	F_{calc}^a	P
CR_{WK4-AQ}	2.02	0.19
CR_{WK4-I}	0.58	0.46
ΔCR_{AQ}	1.29	0.28
ΔCR_I	0.09	0.77

Note: a) F_{calc} – computed value of the F-statistic. F_{crit} – the critical value of F at the 95 % confidence level was 5.12 ($F_{crit [1,10; \alpha=0.05]} = 5.12$).

Figure 16 illustrated the CI-microbial challenge interaction effect. In unchallenged microcosms at T_{wk6} , $CR_{CI-Treated}$ was less than $CR_{CI-Untreated}$. A similar relationship between CR and CI-treatment was also seen in the challenged microcosms, but the magnitude of the difference was significantly greater – reflecting the CI-microbial challenge interaction effect.

3.4.3.9 Appendix D provided analogous plots illustrating several of the interaction effects reported in Table 15 and explained in the case of the CI-microbial challenge interaction.

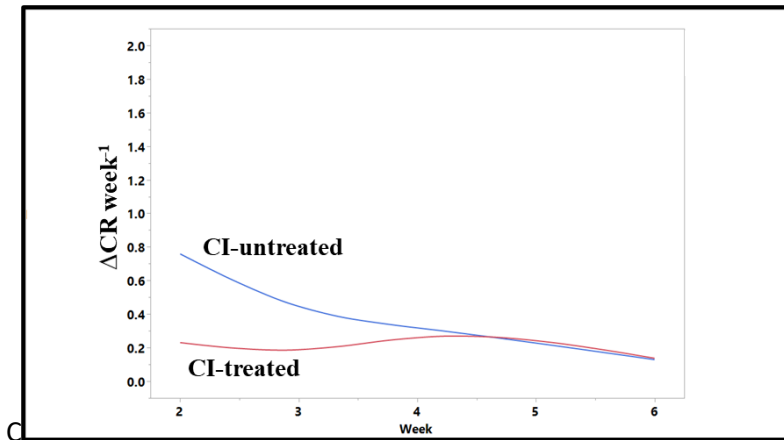


Figure 14. Impact of CI on $\Delta CR \text{ week}^{-1}$ – from Appendix D, page D-6.

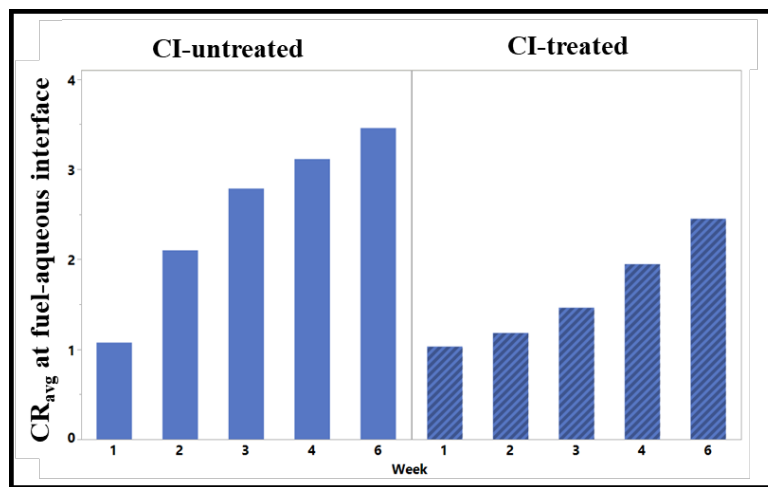


Figure 15. Comparison of weekly CR_{avg} between CI-treated and CI-untreated microcosms – from Appendix D, page D-6.

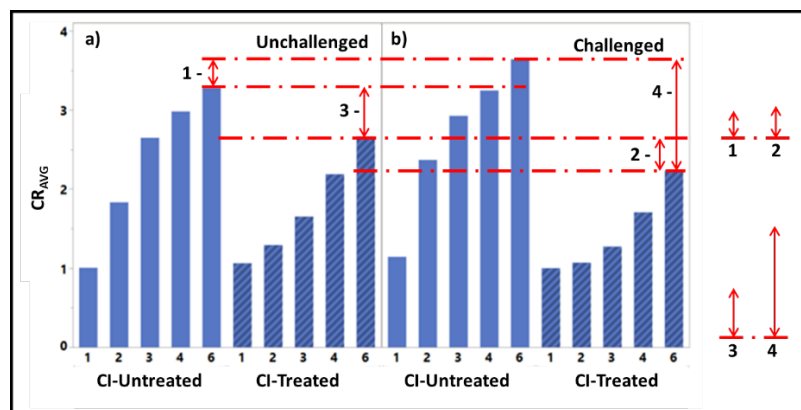


Figure 16. CI-microbial challenge interaction effect – a) microbially challenged microcosms; b) unchallenged microcosms (from Appendix D, page D-7).

Double arrows show magnitude of ΔCR at $T_{wk6} - 1 - \Delta CR_{Untreated - Unchallenged \text{ v. Challenged}}$; $2 - \Delta CR_{Treated - Unchallenged \text{ v. Challenged}}$; $3 - \Delta CR_{Unchallenged - Treated \text{ v. Untreated}}$; $4 - \Delta CR_{Challenged - Treated \text{ v. Untreated}}$.

3.4.3.10 When interpreting these statistics, it was important to recognize that they indicated apparently significant relationships but did not suggest cause and effect. Regarding the CI-microbial challenge interaction effect on CR, the greater difference between CI-treated and untreated microcosms that had been intentionally inoculated (i.e., *challenged*) than in those that had not, was counter-intuitive. It might have reflected the differences in the microbial populations in challenged versus unchallenged microcosms. These differences were addressed in Section 3.7.2.2.7 and 3.7.4.2.4, below.

3.4.4 Tier 3 -Semi-quantitative Analysis of Microcosms Containing Steel Coupons that Exhibited High Corrosion Severity

3.4.4.1 The Tier 1 and 2 results provided statistical outcomes that indicated significant correlations between microcosm content and CR_I and CR_{AQ}. The Tier 3 analysis focused on microcosms in which CR = 5 at T_{wk9} or earlier.

3.4.4.2 To accomplish this analysis, the corrosion ratings assigned at the end of various weeks were grouped and used to create several CR scenarios. For each corrosion rating scenario (for example CR = 5 at T_{wk6}):

- The number of microcosms for a given CR-scenario were tallied.
- The subset that contained each of the 11 controlled variables was tallied.
- The percentage of microcosms positive for treatment X was computed (i.e., 4 of the 7 microcosms for which CR = 5 at T_{wk6} contained ULSD. $(4 \div 7) \times 100 = 57\%$).
- Percentage categories were assigned (0%, <33%, 50%, >66%, 100%) such that if the percentage of microcosms in which the variable was present was >0 but <33 % it would be scored as “<33 %”; if present in $\geq 33\%$ to $\leq 66\%$ of the jars it was scored “50 %”; and present in >66 % but <100 %, it was scored “>66 %.” Consequently, in the CR = 5 at T_{wk6} scenario, ULSD was recorded as 50 %.
- Microcosms were grouped by *scenario*, based on the number of microcosms that contained each factor. For example, for the first scenario in Table 18, the corrosion rating had reached 5 at 6 weeks, thus indicating aggressive corrosion. There were only 7 microcosms that fit this scenario and of those microcosms, 100% contained water, about half of the microcosms contained ULSD, glycerin, ethanol, CFI additive, and/or FRP, none of them contained biodiesel, more than 66% of them had been challenged with microbes, more than 66% contained MAL, and less than 33% of them contained corrosion inhibitor and/or conductivity additive. The additional scenarios shown in Table 18 followed the same pattern of development. This semi-quantitative approach considered that any factor for which a non-50% result is shown may have been trending toward association of that factor with either decreased or increased likelihood of corrosion.

3.4.4.3 Table 18 lists six CR-scenarios and showed the relationship between the 11 independent variables and each scenario.

3.4.4.4 Again, using the CR = 5 at T_{wk6} scenario:

- All of the microcosms contained an aqueous-phase – indicating a strong positive correlation between this factor and CR-scenario.
- Most (>66 %) been microbially challenged – indicating a strong positive correlation between this factor and CR-scenario.
- None contained FAME – indicating a strong negative correlation between this factor and CR-scenario.
- ULSD, glycerin, ethanol, CFI, and FRP were present in approximately half of the microcosms – indicating the absence of any relationship between these factors and the CR-scenario.

- MAL was present in >66 % of the microcosms – indicating a positive relationship between its presence and the CR-scenario.
- CI and CA together were present in <33 % of the microcosms – indicating a negative relationship between their presence and the CR-scenario.

3.4.4.5 All corrosion coupons had CR = 1 at T₀. Over time, CR_{AQ} and CR_I increased in a subset of microcosms. The trends are plotted in Figure 17. At T_{wk12} six microcosms (19, 105, 114, 115, 122, and 123) had CR = 3 and one (19) had CR = 4 on aqueous-phase coupon surfaces (Figure 17a). As noted previously, corrosion was more aggressive at the aqueous-fuel interface (Figure 17b). By T_{wk12} 10 microcosms had CR = 4 at the aqueous-fuel interface (13, 47, 68, 73, 101, 111, 116, 123, 126, and 127), and eight microcosms had CR = 5 (19, 21, 57, 70, 84, 101, 102, and 105). As indicated in Table 18, free-water and microbial contamination were the only controlled variables consistently present in microcosms in which aggressive corrosion was observed.

3.4.4.6 Tier 3 analysis, observations summary:

- Two-phase microcosm CR scores at T₁₂ were all 1.
- At T_{wk12} the four-phase microcosm, aqueous-phase CR scores ranged from 2 (44 microcosms) to 4 (1 microcosm). Accelerated corrosion occurred only in microcosms that had an aqueous-phase.
- Corrosion was more aggressive at the aqueous-fuel interface than on any other coupon surface.
- Four-phase microcosm, CR_I scores at T₁₂ were all ≥2 and 17 were ≥4.

Table 18. Tier 3 statistical analysis - corrosion rating scenarios.

CR-scenario ^a	Number ^b of Microcosms	[S] (ULSD)	FAME	Water	Glycerin	Ethanol	Challenge Population	MAL	CFI	CI	CA	FRP
CR = 5 @ T _{wk6}	7	50%	0%	100%	50%	50%	>66%	>66%	50%	<33%	<33%	50%
CR = 4 @ T _{wk6}	38	50%	<33%	100%	50%	50%	>66%	50%	50%	<33%	50%	50%
CR = 3 or 4 @ T _{wk2} and CR = 4 or 5 @ T _{wk6}	19	50%	<33%	100%	50%	50%	>66%	50%	<33%	<33%	50%	50%
CR = 3 or 4 @ T _{wk2}	24	50%	<33%	100%	50%	50%	>66%	50%	50%	<33%	50%	50%
CR = 2 or 3 @ T _{wk1} and CR = 4 or 5 @ T _{wk6}	23	>66%	<33%	100%	50%	<33%	>66%	50%	50%	<33%	50%	50%
CR = 2 or 3 @ T _{wk1}	36	50%	<33%	100%	50%	50%	50%	50%	50%	50%	50%	50%
CR = 1 or 2 @ T _{wk12}	34	50%	>66%	0%	50%	50%	50%	>66%	50%	>66%	50%	50%

Notes:

a) CR Scenarios are for overall CR.

b) The column total = 181 microcosms. 53 microcosms were classified as belonging to two categories – for example, some of the microcosms included in the CR = 5 @ T_{wk6} scenario were also included in the CR = 3 or 4 @ T_{wk2} and CR = 4 or 5 @ T_{wk6} scenario count.

- At T_{wk12} four-phase microcosm, aqueous-fuel CR scores ranged from 2 (41 microcosms) to 5 (8 microcosms).
- Controlled variables that were not associated with either more or less aggressive corrosion included fuel grade ([S]), glycerin, ethanol, MAL, CFI, CI, CA, or FRP.
- Corrosion aggressivity was slightly more common in microbially challenged than in unchallenged microcosms. Ten of 17 microcosms with $CR \geq 4$ at the aqueous-fuel interface (59 %) had been challenged. This includes 4 of 8 with $CR = 5$ and 6 of 10 with $CR = 4$.
- Controlled variables associated with less aggressive corrosion included FAME and CI.
- Among the microcosms with $CR \leq 2$ at T_{wk12} , > 66 % contained one or more of FAME, MAL, or CI.

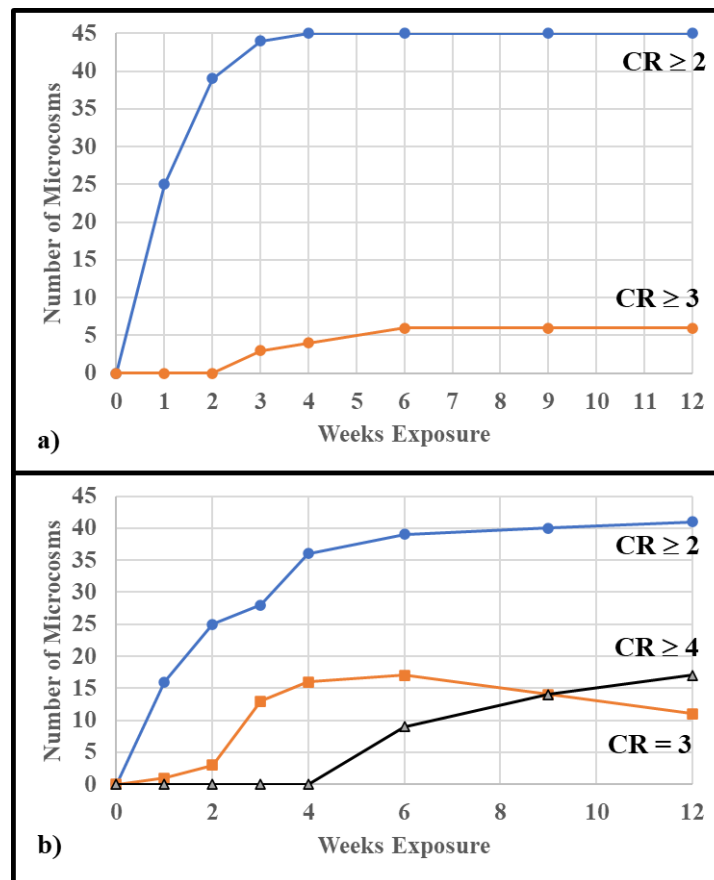


Figure 17. CR rating frequencies by week – a) aqueous-phase exposure; b) aqueous-fuel interface exposure.

3.5 MICROCOSM GROSS OBSERVATIONS

3.5.1 Conceptual Overview

- 3.5.1.1 Gross observations – recording the appearance of each phase of a sample – provided useful information about the sample’s condition. Although, ASTM D4176 [21] focused on reporting fuel haze and particulates, all of the parameters listed in Table 4 were integral to an assessment of the condition of the system from which a sample was collected.
- 3.5.1.2 The test microcosms simulated UST fuel-water, fuel-vapor-phase, and fuel-surface conditions. The gross observation parameters listed in Table 4 addressed the appearances of fuel, fuel-water interface (invert emulsion, or *rag*, layer, and fuel-associated bottoms-water – the aqueous-phase).
- 3.5.1.3 Scoring was based on biodeterioration risk as recommended by Hartman *et al.* [38] and modified for fuel retail and fleet fuel facilities by Passman (unpublished). For each parameter, results were divided into two or three risk categories. Depending on the parameter, results in the *negligible-risk* range were assigned a score of either 0 or 1, these in the *moderate-risk* range were assigned a score of either 2 or 3, and those in the *high-risk* range were scored as either 4 or 5.
- 3.5.1.4 Hartman and his colleagues developed the system to assess biodeterioration risks in NATO’s strategic reserves of finished fuels [38]. When used for system biodeterioration risk assessments, gross observations are one of seven parameter categories. The others include climate, engineering, maintenance, chemistry (fuel and fuel-associated water), physical testing, and microbiology.
- 3.5.1.5 Normally, gross observations include inspection of system components for corrosion. Given that corrosion was the primary dependent variable assessed in this study and has been addressed in 3.3.2, 3.2.3, and 3.3.4, corrosion results were omitted from gross observations.

3.5.2 Observations

- 3.5.2.1 Microcosms were photographed and observed at T_{wk3} , T_{wk4} , T_{wk6} , T_{wk9} and T_{wk12} . A summary of the overall T_x gross observation risk scores (RS_{GO}) were provided in Table 19.
- 3.5.2.2 Figure 18 illustrated T_{wk3} , T_{wk6} , and T_{wk12} microcosms with $RS_{GO} = 0$ and $RS_{GO} = 5$, respectively.
- 3.5.2.3 Fifty of the 128 microcosms had $RS_{GO} \leq 1$ at T_{wk12} . More than half (58 %) of these low RS_{GO} microcosms had an aqueous-phase.
- 3.5.2.4 Eight (28 %) of the 29 $RS_{GO} \leq 1$ microcosms that contained an aqueous-phase had been intentionally challenged with a microbial inoculum. Among these eight, seven contained ethanol, six were B5 blends, and five were LSD. Ethanol seemed to be the only common factor among low RS_{GO} microcosms that had been challenged.
- 3.5.2.5 Moderate to high RS_{GO} are typically associated with uncontrolled microbial contamination – i.e., ATP-bioburdens $\geq 3\text{Log}_{10}$ pg mL⁻¹ in the aqueous-phase, $\geq 1\text{Log}_{10}$ pg mL⁻¹ in the fuel-phase, or both.
- 3.5.2.6 To assess the relationship between ATP-bioburden and RS_{GO} , correlation coefficients (r) and percent agreement (after ATP-data were transformed to attribute scores, they were compared with RS_{GO} scores) were computed between these two variables.

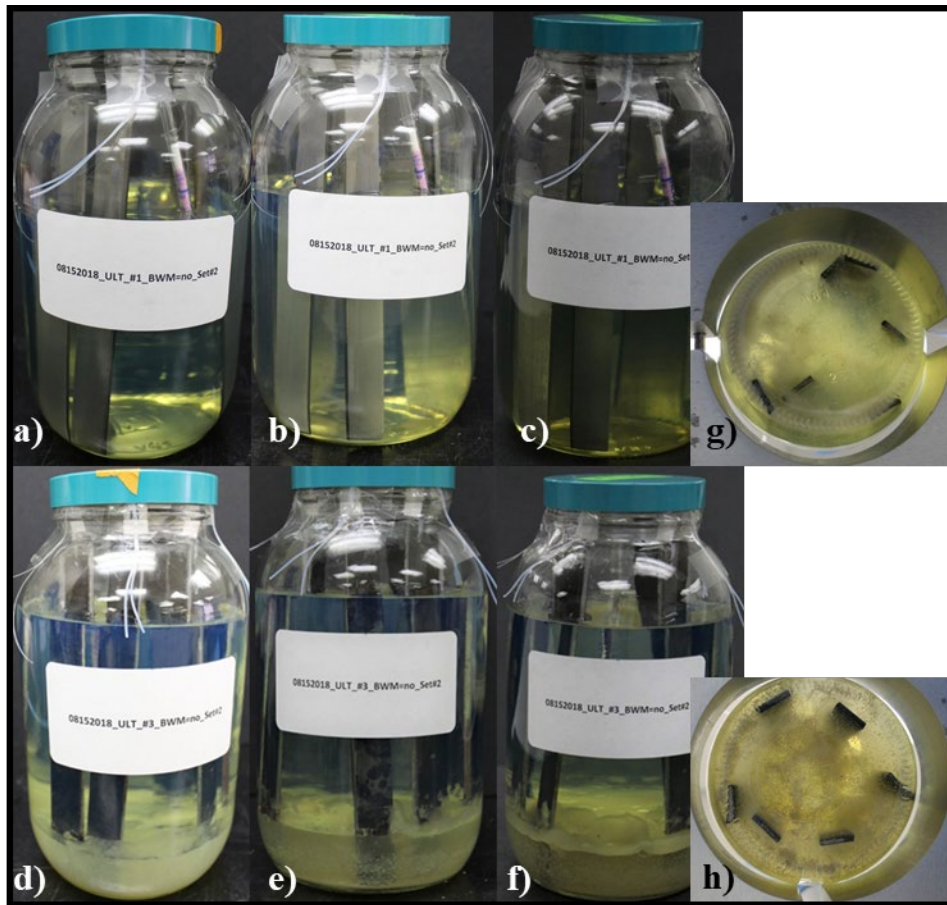


Figure 18. Microcosm gross observations – a) through c) microcosm 1 at T_{wk3} , T_{wk6} , and W_{wk12} (all $RS_{GO} = 0$); d) through f) microcosm 3 at T_{wk3} , T_{wk6} , and W_{wk12} (all $RS_{GO} = 5$); g) microcosm 1, bottom view at T_{wk12} ; h) microcosm 3, bottom view at T_{wk12} .

Table 19. Gross observation, overall risk scores (RS_{GO}) for microcosms at weeks 3, 4, 6, 9, and 12.

Microcosm	Overall Risk Score/Week					Microcosm	Overall Risk Score/Week					Microcosm	Overall Risk Score/Week				
	3	4	6	9	12		3	4	6	9	12		3	4	6	9	12
1	0	0	0	0	0	26	0	0	0	0	0	51	0	0	0	0	0
2	0	0	0	0	0	27	0	0	0	0	0	52	0	0	0	0	0
3	3	5	5	5	5	28	3	3	5	5	5	53	3	5	5	5	5
4	3	3	3	5	5	29	3	3	3	3	3	54	1	1	1	1	3
5	3	5	5	5	5	30	1	1	3	5	5	55	0	0	0	0	0
6	0	0	0	0	0	31	3	3	3	3	5	56	0	0	0	3	3
7	0	0	0	0	0	32	3	3	3	3	3	57	3	3	3	3	3
8	0	0	0	0	0	33	0	0	0	0	0	58	3	3	3	3	5
9	0	0	0	0	0	34	0	0	0	1	1	59	0	0	0	0	0
10	3	3	3	5	5	35	3	3	5	5	5	60	3	3	3	3	3
11	3	3	3	3	3	36	0	0	0	0	0	61	0	0	0	0	0
12	0	1	1	1	1	37	3	3	3	5	5	62	3	3	3	3	5
13	3	3	3	3	3	38	3	3	5	5	5	63	0	0	0	0	0
14	0	0	0	0	0	39	1	3	3	5	5	64	0	0	0	0	0
15	0	1	1	1	1	40	3	3	3	3	5	65	0	0	0	0	0
16	0	0	0	0	0	41	0	0	0	3	3	66	3	3	5	5	5
17	0	0	0	0	0	42	0	0	0	0	0	67	3	3	3	5	5
18	0	0	0	0	0	43	0	0	0	0	0	68	1	1	3	3	3
19	1	1	1	1	1	44	1	1	1	3	3	69	0	3	3	5	5
20	0	1	1	1	1	45	3	5	5	5	5	70	3	3	3	3	5
21	3	3	5	5	5	46	3	3	5	5	5	71	0	0	0	3	3
22	3	1	1	3	3	47	0	0	0	5	5	72	3	3	3	3	3
23	1	1	1	5	5	48	5	5	5	5	5	73	1	1	1	1	1
24	1	1	3	3	3	49	3	5	5	5	5	74	0	1	3	5	5
25	3	3	3	3	3	50	0	0	0	0	0	75	3	3	3	5	5

Table 19. Continued

Microcosm	Overall Risk Score/Week				
	3	4	6	9	12
76	0	0	0	1	3
77	1	1	1	1	3
78	0	0	3	5	5
79	1	3	5	5	5
80	3	3	3	5	5
81	0	1	1	3	5
82	0	0	0	0	0
83	3	3	3	3	3
84	1	1	3	5	5
85	0	0	0	3	3
86	1	3	3	3	3
87	0	0	0	0	0
88	0	0	0	0	0
89	0	0	3	3	3
90	0	0	0	0	0
91	0	0	0	0	0
92	1	1	1	1	1
93	1	1	1	1	1
94	3	3	3	3	3

Microcosm	Overall Risk Score/Week				
	3	4	6	9	12
95	0	0	0	0	0
96	1	1	1	1	3
97	0	0	0	0	0
98	0	0	3	3	5
99	0	0	0	0	0
100	3	3	3	3	3
101	3	3	3	3	5
102	3	3	3	5	5
103	3	3	5	5	5
104	0	0	0	0	0
105	3	3	3	3	3
106	3	3	3	5	5
107	3	3	5	5	5
108	0	0	0	0	5
109	1	1	1	3	3
110	0	0	1	3	3
111	1	1	1	1	1
112	1	3	3	3	3
113	1	1	1	1	1

Microcosm	Overall Risk Score/Week				
	3	4	6	9	12
114	0	0	0	1	1
115	1	1	1	1	1
116	3	3	3	3	5
117	1	1	3	3	3
118	0	0	0	0	0
119	3	3	3	3	3
120	0	0	0	0	0
121	0	0	0	0	0
122	0	0	0	3	3
123	0	0	0	0	0
124	0	0	0	0	0
125	1	1	3	3	3
126	0	0	0	0	0
127	1	1	3	5	5
128	3	3	3	3	3

3.5.2.6.1 Table 20 summarized the relationships between RS_{GO} and corrosion ratings (CR).

Table 20. Relationship between microcosm gross observation risk scores (RS_{GO}) and corrosion ratings (CR).

Parameter	Week	r ^a	P ^b	$RS_{GO} = CR$	$RS_{GO} < CR$	$RS_{GO} > CR$
RS_{GO} v. CR_{AQ} ^c	6	-0.17	0.22	4%	44%	52%
	9	-0.090	0.52	6%	37%	57%
	12	-0.12	0.39	6%	35%	59%
RS_{GO} v. CR_I ^d	6	0.35	0.0095	17%	52%	31%
	9	0.072	<0.0001	13%	46%	41%
	12	0.14	0.31	19%	41%	41%

Notes:

- a) r – correlation coefficient.
- b) P – P-value for $\alpha = 0.05$.
- c) CR_{AQ} – Corrosion rating, aqueous-phase coupon face.
- d) CR_I – Corrosion rating, aqueous-fuel interface coupon face.

Although the correlation coefficients between RS_{GO} and CR_I were significant at T_{wk6} and T_{wk9} , none were strong. Bottom-sample gross-observations have been used for decades to assess system and product deterioration [11], [39].

At T_{wk12} , RS_{GO} underestimated aqueous-phase corrosion in 35 % of the microcosms. Given that coupon edge CR were typically 2 or 3 points greater than face CR, RS_{GO} seemed to be underestimating corrosion risk. The apparent disconnect between CR and RS_{GO} observed in this study’s microcosms, suggested a need to conduct comprehensive field studies to objectively assess the correlation between these two variables.

3.5.2.6.2 Table 21 summarized the relationships between RS_{GO} and ATP-bioburdens. Aqueous and fuel-phase planktonic ([cATP]), and aqueous and aqueous-fuel-interface surface ([tATP]) bioburden-based risk scores (RS_{ATP}) generally resulted in biodeterioration risk scores that were equal to or greater than those from gross observations. The exception was fuel-phase [cATP] (1.9 ± 0.83) which yielded a lower attribute score than the RS_{GO} in 7 of the 9 microcosms from which fuel [cATP] was tested.

3.5.2.6.3 Correlations between RS_{GO} and $RS_{[cATP]}$ were significant for all pairs except RS_{GO} v. [cATP]_{Fuels-phase}.

3.5.2.6.4 The ATP and other microbiological test results will be treated in more detail in Section 3.6.

Table 21. Relationship between microcosm gross observation and [ATP]-based risk scores (RS_{GO} and RS_{ATP} , respectively).

Parameters	r^a	$r_{crit.}^b$	P^c	$RS_{GO} = RS_{ATP}$	$RS_{GO} < RS_{ATP}$	$RS_{GO} > RS_{ATP}$
RS_{GO} v. [cATP] _{Aqueous-phase}	0.55	0.30	0.0001	59%	25%	16%
RS_{GO} v. [cATP] _{Fuel-phase}	0.66	0.67	0.053	11%	11%	78%
RS_{GO} v. [tATP] _{Aqueous-phase}	0.66	0.30	<0.0001	50%	25%	25%
RS_{GO} v. [tATP] _{Interface}	0.64	0.47	0.0043	61%	17%	22%

Notes:

- a) r – correlation coefficient.
- b) $R_{crit.}$ – the minimum value of r considered to be significant at $\alpha = 0.05$, based on the number of data points, n , and computed from $n - 2$.
- c) P – P-value for $\alpha = 0.05$.

3.6 CORROSION

3.6.1 Coupon Corrosion Ratings

- 3.6.1.1 Coupon corrosion rating (CR) was the primary parameter considered in the statistical analysis reported in Section 3.4. Only observations not previously addressed were considered in this section.
- 3.6.1.2 Weekly CR scores for aqueous, fuel-aqueous-interface, fuel, and vapor-phase contact zones were reported at T_{wk1} , T_{wk2} , T_{wk3} , T_{wk4} , T_{wk6} , T_{wk9} , and T_{wk12} and provided in Appendix F, Table F.1. Coupon face and edge observations were reported.
- 3.6.1.3 As noted in 3.5.2.6.1, in many microcosms, $CR_{edge} > CR_{face}$ in each contact zone.
- 3.6.1.4 It was possible that biomass accumulation interfered with CR reporting. Figures 13i through 13l illustrated the challenge. In each of these Figures (microcosm 4 at T_{wk4} , T_{wk6} , and T_{wk12}) the face of the coupon that had been in contact with the aqueous-phase, was coated by an off-white mass.
- 3.6.1.5 Corrosion on microcosm 19 coupons was more easily visualized than in other microcosms (Figure 19).

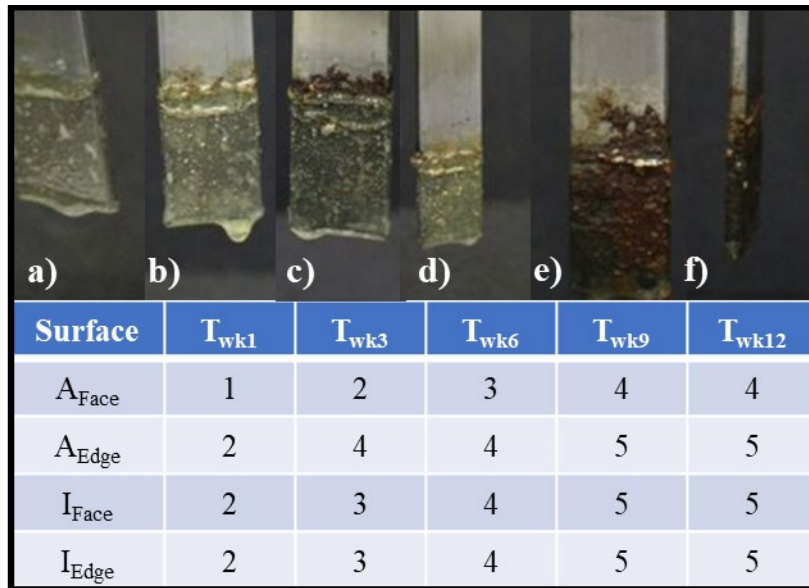


Figure 19. Microcosm 19 corrosion coupons with CR provided

a) T_{wk1}; b) T_{wk3}; c) T_{wk6}; d) T_{wk9}; e) T_{wk12}; f) coupon edge @ T_{wk12}. Values for CR per surface are from Appendix F, Table F.1.

Figure 19 also illustrated the subjectivity of corrosion ratings. By T_{wk1} (Figure 19a), the face of the coupon that was exposed to the microcosm's aqueous-phase had a uniform grey patina. The CR = 2. A biofilm coating was already visible. At T_{wk6} face CR at the aqueous-fuel interface was scored 4 and at T_{wk9} CR = 5. However, corrosion at the interface at T_{wk6} (Figure 19c) appears to have been heavier than at T_{wk9} (Figure 19d). As with microcosm 4, it was possible that biofilm coating affected CR reporting. A single analyst performed all CR observations. Although all photographs were to have been taken under nominally identical conditions, a comparison of image size and color, suggest that week-to-week photography setup differences could have been sufficient to impact scoring. Some of the subjectivity might have been addressed by having had at least three analysts independently record CR.

3.6.2 General Corrosion Rate – Coupon Weight Loss

3.6.2.1 After 12-weeks of exposure (T_{wk12}) triplicate coupons were removed from each microcosm and stored in resealable plastic bags for general corrosion rate (GCR) testing.

3.6.2.2 Actual preparation for GCR testing per 2.6.5.1 was initiated at T_{wk18}. Individual coupon GCR were computed from equations (1) and (2). Then average GCR and standard deviations ($\overline{GCR} \pm s$) were computed.

3.6.2.2.1 The % weight loss (DM %) and ($\overline{GCR} \pm s$) data were provided in Appendix G, Table G.1.

3.6.2.2.2 There was considerable variability among replicate coupons. The average coefficient of variation (CV % = (s / \overline{GCR}) x 100) was 89 % and CV % ranged from 0 % (microcosm 35) to 4,300 % (microcosm 104).

3.6.2.2.3 Microcosms with the greatest and least ($\overline{GCR} \pm s$) were compared for commonalities (Table 22).

- All four microcosms with the greatest ($\overline{GCR} \pm s$) had four phases, had been CA-treated, and had no FRP coupon. Microcosm 87 – with the fifth greatest ($\overline{GCR} \pm s$) had three phases.
- There were no other common, controlled variables among these microcosms.
- Among the microcosms with the least ($\overline{GCR} \pm s$), only microcosm 63 contained ethanol.

- Note that GCRs were negative (net weigh gains) in 26 microcosms (24 % of the 123 microcosms from which coupon GCR were determined). When observed, weight gain was an artifact of weight measurement variability.

Table 22. Test condition profiles in microcosms with greatest and least ($\overline{GCR} \pm s$).

Microcosm	GCR (mpy) (AVG \pm s)	Grade	FAME	Water	Glycerin	Ethanol	Challenge	MAL	CFI	CI	CA	FRP Coupon
44	1 \pm 1.0	ULSD	+	+	-	-	-	+	+	-	+	-
3	1.4 \pm 0.26	ULSD	-	+	-	-	-	-	-	+	+	-
56	1 \pm 1.1	LSD	+	+	+	-	-	-	-	-	+	-
36	1.2 \pm 0.17	ULSD	-	+	-	+	-	+	+	+	+	-
87	1.0 \pm 0.52	LSD	+	-	-	-	-	-	-	-	-	-
8	-0.4 \pm 0.17	ULSD	+	-	-	-	-	-	+	-	-	+
9	-0.4 \pm 0.17	ULSD	+	-	-	-	-	+	+	+	+	+
57	-0.5 \pm 0.52	LSD	-	+	+	-	-	+	+	+	+	-
53	-0.5 \pm 0.14	LSD	-	+	-	-	+	-	+	-	-	+
120	-0.5 \pm 0.62	LSD	+	-	-	-	-	+	-	-	-	+
63	-0.6 \pm 0.40	LSD	+	+	+	+	+	-	-	+	-	+

3.6.2.2.4 To assess worst case effects, Table F.2 ranked microcosms based on the greatest GCR (GCR_{max}) among triplicate coupons.

3.6.2.2.5 Microcosms with individual coupons that had the greatest GCR_{max} were also compared for commonalities (Table 23).

- All of the microcosms with the greatest GCR_{max} had four phases and treated with CA. None were microbially challenged intentionally nor had FRP coupons.
- None of the other controlled factors were uniformly present or absent from these four microcosms.
- Among the microcosms in which maximum coupon weight increases were reported, there were no common, controlled variables.

Table 23. Test condition profiles in microcosms with greatest and least GCR_{max}.

Microcosm	GCR (mpy _{max})	Grade	FAME	Water	Glycerin	Ethanol	Challenge	MAL	CFI	CI	CA	FRP Coupon
3	3.14	ULSD	-	+	-	-	-	-	-	+	+	-
44	2.96	ULSD	+	+	-	-	-	+	+	-	+	-
56	2.90	LSD	+	+	+	-	-	-	-	-	+	-
104	2.28	ULSD	-	+	+	+	-	+	+	-	+	-
63	-0.18	LSD	+	+	+	+	+	-	-	+	-	+
128	-0.18	LSD	+	+	+	+	+	-	+	-	-	-
8	-0.21	ULSD	+	-	-	-	-	-	+	-	-	+
9	-0.21	ULSD	+	-	-	-	-	+	+	+	+	+
53	-0.35	LSD	-	+	-	-	+	-	+	-	-	+

3.6.2.2.6 Among the 123 microcosms for which GCR observations were reported, 68 % had GCR_{max} < 1.0 mpy (Table 24). Only four microcosms have GCR_{max} ≥ 2mpy.

3.6.2.2.7 The maximum GCR values were significant (at $\alpha = 0.05$ – i.e., GCR_{max} > 1.5 %) for only 20 coupons (5.4 % of 369 coupons examined).

3.6.2.3 In most industrial systems, corrosion coupons are nominally exposed to homogeneous physicochemical conditions – they are fully immersed in a single type of fluid. Although it was recognized during the test design effort that corrosion coupons would be exposed to either three (in microcosms without an aqueous phase) or four (in microcosms with an aqueous-phase) phases, it was anticipated that localized, severe corrosion would be reflected in overall coupon weight-loss. The interface zone was such a small portion of each coupon’s total mass. No attempt was made to either determine the interface zone’s contribution to coupon weight-loss or extrapolate interface weight-loss data to estimate what total coupon GCR would have been had entire coupons been exposed to interface conditions.

Table 24. GCR_{max} (mpy) distribution among 123 microcosms for which GCR was reported.

Statistic	GCR (mpy, max)			
	≥ 3	≥ 2 to < 3	≥ 1 to < 2	< 1
n of 123	4	0	35	84
%	3%	0%	28%	68%

3.6.2.4 The GCR data demonstrated that localized corrosion varied in its severity and dimensions (coverage area) on replicate coupons. This variability translated into substantial GCR variability among replicates. The impact of this variability was illustrated in Table 25.

- There were no significant correlations between corrosion risk scores (CR_{AQ} and CR_I) and GCR.
- The absence of significant correlations between other uncontrolled variables were discussed in Sections 3.5.2 and 3.6.3.
- Consequently, although GCR was intended to have been a primary uncontrolled variable for assessing the impact of test conditions on corrosivity, ultimately CR scores were used instead.

Table 24. Correlation coefficients among dependent variables – [ATP], CGR_{Std} and CR.

Relationship	Statistic			
	r	r _{crit}	P	n
[cATP] _A v. GCR	0.14	0.019	0.22	79
[cATP] _I v. GCR	0.05	0.28	0.85	17
[tATP] _A v. GCR	0.17	0.43	0.32	36
[tATP] _I v. GCR	0.04	0.19	0.89	16
[cATP] _A v. CR _{AQ}	0.31	0.27	0.85	38
[cATP] _A v. CR _I	-0.11	0.27	0.51	38
CR _{AQ} v. GCR	0.27	0.27	0.10	39
CR _I v. GCR	0.10	0.27	0.56	39

3.6.3 Corrosion Morphology and Elemental Composition

3.6.3.1 Post-exposure, a subset of seven microcosms were selected based on their end-of study gross appearance (microcosm and coupons) and independent variables. Table 26 showed the independent variable profile of the selected microcosms. Table 27 summarized their T_{wk12} RS_{GO}, CR, and ATP-bioburden profiles.

Table 25. Corrosion product analysis microcosm subset – independent variable profiles. ^a

Microcosm #	Fuel Grade	Biodiesel (%)	Glycerin (mg/L)	Ethanol (mg/L)	Microbial Challenge	MAL (mg/L)	CFI (mg/L)	CI (mg/L)	CA	FRP Coupon
35	ULSD	0	0	0	Yes	0	0	0	0	Yes
40	ULSD	0	5000	10000	0	0	0	0	0	Yes
77	ULSD	5	0	10000	Yes	0	200	0	0	0
85	LSD	0	5000	0	0	0	200	0	2.5±0.5	Yes
100	ULSD	0	0	10000	Yes	0	200	0	2.5±0.5	Yes
105	ULSD	0	5000	10000	Yes	200	200	9±1	0	Yes
109	ULSD	5	0	10000	Yes	200	0	0	2.5±0.5	Yes

Note: a) All selected microcosms had four phases: vapor, fuel, aqueous-fuel interface, and aqueous.

Table 26. Corrosion product analysis microcosm subset –dependent variable profiles.

Microcosm	RS _{GO}	CR T _{wk12}		STD GCR _{AVG}	ATP-bioburden T _{wk12}			
					[cATP] Log ₁₀ pg/mL		[tATP] (Log ₁₀ pg/cm ²)	
		Aq. Phase	Interface		Aq. Phase	Interface	Aq. Phase	Interface
35	5	3	5	0.082	4.17	N.D. ^a	N.D.	N.D.
40	5	4	5	0.258	N.D.	N.D.	3.31	N.D.
77	3	3	5	0.373	2.76	2.22	3.90	3.49
85	3	4	5	0.151	1.34	N.D.	3.40	N.D.
100	3	3	5	0.081	3.11	N.D.	4.09	3.84
105	3	3	5	0.492	3.74	N.D.	N.D.	N.D.
109	3	3	4	1.2	4.75	N.D.	3.84	N.D.

Note: a) N.D. – not determined.

3.6.3.2 One steel specimen from each microcosm was extracted from its environment after 18 weeks of exposure and examined per Section 2.6.5.2.

3.6.3.3 Microscopy and EDS focused on the 4 cm to 5 cm length of coupon face that had been exposed to the microcosm’s aqueous, interface, and fuel phases. No corrosion deposits were observed on coupon surfaces exposed to either the fuel-vapor-phase interface or vapor-phase. The size of the coupon subsections was limited by SEM chamber space restraints.

3.6.3.4 Corrosion deposit images are provided in the following subsections, but no attempt was made to speculate on deposit-formation mechanisms.

3.6.3.5 Full image and spot (0.05 mm² to 0.7 mm²) areas within the images’ elemental analysis were analyzed by EDS.

3.6.3.6 The whole image corrosion deposit elemental profiles were provided in Table 28. There were no discernable relationships for:

- Concentration of any element or elements and liquid phase with which coupon had been in contact,
- Concentration of any element or elements and independent variables,
- Concentration of any element and dependent variables.

3.6.3.7 Among these seven microcosms, correlation coefficients among, carbon (C), oxygen (O), iron (Fe), potassium (K), phosphorous (P), sulfur (S), and manganese (Mn) were computed for corrosion deposits in each coupon zone. These were the elements detected in the majority of analyses. The correlation matrixes were provided in Table 29.

- In aqueous phase deposits:
 - [Fe] had a strong negative correlation with [C] and [O], respectively ($P_{[\alpha=0.05]} < 0.02$).
 - [C] and [O] had a strong positive correlation ($P_{[\alpha=0.05]} = 0.038$).
 - [Mn] had a strong negative correlation with [O].
- In aqueous-fuel interface deposits:
 - [Fe] had a strong negative correlation with [C] and [O], respectively ($P_{[\alpha=0.05]} < 0.02$).
 - [C] and [O] had a strong positive correlation ($P_{[\alpha=0.05]} = 0.038$).

- In fuel-phase deposits:
 - [Fe] had a strong negative correlation with [C] ($P_{[\alpha=0.05]} = 0.0058$) but not with [O] ($P_{[\alpha=0.05]} = 0.24$).
 - [S] had a strong negative correlation with [C] ($P_{[\alpha=0.05]} = 0.024$).
- In aqueous-phase and interface deposits there was a strong correlation ($r = 0.78 - df = 47, \alpha = 0.05, P = <0.00001$) between [C] and [O]. However, in fuel-phase deposits, $r = 0.24$. The correlation between the concentrations of these two elements was not significant ($P_{[\alpha=0.05]} = 0.60$). This observation coupled with the strong negative correlation between [Fe] and [C] and [O], respectively, in all three phases, suggested that the detected [C]s and [O]s were from residual biofilm. The correlation coefficients between $[C]_{\text{Aqueous}}$ and $[O]_{\text{Aqueous}}$ and $[tATP]_{\text{Aqueous}}$ were not significant ($P \geq 0.22 - \text{Tables 30 and 31}$). Interface [tATP] was tested on coupons from only two of the seven microcosms listed in Tables 27 and 30. Consequently, correlations between element concentrations and $[tATP]_{\text{interface}}$ could not be computed.
- A strong positive correlation between [Fe] and [O] would be expected in deposits rich in iron oxides. The negative relationship was surprising, but this study was not designed to investigate factors contributing to this relationship.
- Measurable [C] is not typically detected in EDS analysis of petroleum system corrosion deposits (Passman, unpublished). As with the [Fe] and [O] relationship, detection of 7 wt. % to 23 wt. % (14 ± 6.2 wt. %), 6 wt. % to 40 wt. % (20 ± 11 wt. %), and 7 wt. % to 18 wt. % (14 ± 4.1 wt. %) carbon in the aqueous-phase, interface, and fuel-phase coupon corrosion deposits was surprising. However, this study was not designed to investigate factors contributing to this relationship.

Table 27. Corrosion deposit elemental analysis by EDS. All values are in wt. %.

1. Aqueous-phase deposits

Element	Microcosm							AVG	s	Min	Max	CV ^a
	35	40	77	85	100	105	109					
C	20.6	6.7	15	23.2	9.9	10.7	9.8	13.7	6.2	6.7	23.2	0.45
O	24.5	21.2	14.9	18.6	9.2	14.8	22.4	17.9	5.3	9.2	24.5	0.30
Zn	0.6	0.4	0.2	BDL ^b	BDL	BDL	BDL	0.4	0.2	BDL	0.6	0.50
Na	0.1	BDL	BDL	0.1	BDL	0.3	BDL	0.2	0.1	BDL	0.3	0.69
Mg	0.6	0.1	0.2	0.1	BDL	0.2	BDL	0.2	0.2	BDL	0.6	0.86
Al	0.4	0.3	0.3	0.1	0.3	0.6	0.2	0.3	0.2	0.1	0.6	0.50
Si	0.3	0.3	0.3	0.1	0.2	0.4	0.2	0.3	0.1	0.1	0.4	0.38
P	7.7	0.2	0.2	4.1	0.9	4.2	1.1	2.6	2.8	0.2	7.7	1.1
S	0.3	0.3	0.3	0.1	0.3	0.4	0.2	0.3	0.1	0.1	0.4	0.35
Cl	0.4	BDL	0.1	BDL	0.1	BDL	BDL	0.2	0.2	BDL	0.4	0.87
K	1.1	0.2	0.1	1.3	0.1	BDL	0.2	0.5	0.5	BDL	1.3	1.1
Ca	0.5	BDL	BDL	0.2	0.1	0.2	BDL	0.3	0.2	BDL	0.5	0.69
Mn	0.7	1.5	1.1	0.7	0.9	0.9	0.5	0.9	0.3	0.5	1.5	0.36
Fe	42.2	69.0	66.7	51.3	77.7	66.1	65.2	62.6	11.9	42.2	77.7	0.19
N	BDL	BDL	BDL	BDL	0.4	1.1	1.2	0.9	0.4	0.4	1.2	0.48
Ni	BDL	BDL	BDL	BDL	BDL	BDL	BDL	BDL	BDL	BDL	BDL	

2. Aqueous-fuel interface deposits

Element	Microcosm							AVG ^a	s ^b	Min	Max	CV ^c
	35	40	77	85	100	105	109					
C	14.2	6.4	18.8	40.2	11.4	10.3	21.6	17.6	11.2	6.4	40.2	0.64
O	20.3	22.9	20.1	31.0	22.7	18.2	21.3	22.4	4.1	18.2	31	0.19
Zn	BDL ^d	0.6	BDL	0.3	0.6	BDL	0.3	0.5	0.2	0.3	0.6	0.38
Na	0.2	BDL	BDL	BDL	BDL	0.2	BDL	0.2	0.0	BDL	0.2	0.00
Mg	0.3	BDL	0.3	0.1	0.1	0.1	BDL	0.2	0.1	BDL	0.3	0.61
Al	0.9	0.5	0.1	0.1	0.1	0.5	0.4	0.4	0.3	0.1	0.9	0.80
Si	0.5	0.6	0.1	0.1	0.1	0.2	0.2	0.3	0.2	0.1	0.6	0.81
P	2.2	0.2	0.4	0.4	2	2.5	0.6	1.2	1.0	0.2	2.5	0.84
S	0.6	0.4	0.2	0.3	0.2	0.3	0.2	0.3	0.1	0.2	0.6	0.47
Cl	0.1	BDL	BDL	BDL	BDL	BDL	BDL	0.1	BDL	BDL	0.1	
K	1.3	BDL	0.4	BDL	0.2	0.2	0.7	0.6	0.5	BDL	1.3	0.82
Ca	0.2	BDL	0.3	0.2	0.1	BDL	BDL	0.2	0.1	BDL	0.3	0.41
Mn	0.9	0.5	0.8	0.2	0.4	1.3	0.6	0.7	0.4	0.2	1.3	0.54
Fe	56.4	67.3	58.6	27.1	62.3	64.9	52.6	55.6	13.5	27.1	67.3	0.24
N	1.3	BDL	BDL	BDL	BDL	1.3	1.5	1.4	0.1	BDL	1.5	0.08
Ni	BDL	BDL	BDL	BDL	BDL	BDL	BDL	BDL	BDL	BDL	BDL	

3. Fuel-phase deposits

Element	Microcosm							AVG	s	Min	Max	CV
	35	40	77	85	100	105	109					
C	16.2	6.6	12.2	12.4	17.2	18.2	16.4	14.2	4.1	6.6	18.2	0.29
O	19.2	21.5	17.1	21.7	21.7	24	13	19.7	3.7	13	24	0.19
Zn	0.2	0.5	0.2	0.4	0.3	0.2	BDL	0.3	0.1	BDL	0.5	0.42
Na	0.2	0.2	0.2	0.2	BDL	BDL	0.1	0.2	0.0	BDL	0.2	0.25
Mg	0.2	1.3	0.1	0.9	BDL	0.1	BDL	0.5	0.5	BDL	1.3	1.1
Al	1.7	1.5	0.5	0.5	0.4	0.2	0.4	0.7	0.6	0.2	1.7	0.80
Si	0.5	1.6	0.4	0.3	0.2	0.1	0.2	0.5	0.5	0.1	1.6	1.1
P	0.4	0.1	0.2	0.6	0.1	BDL	0.1	0.3	0.2	BDL	0.6	0.83
S	0.6	1.0	0.3	0.3	0.3	0.1	BDL	0.4	0.3	0.1	1	0.74
Cl	BDL	BDL	BDL	BDL	BDL	BDL	BDL	BDL	BDL	BDL	BDL	
K	1.8	0.1	1.5	1.5	1.1	0.4	0.5	1.0	0.7	0.1	1.8	0.66
Ca	0.3	BDL	0.2	1.1	0.1	BDL	0.3	0.4	0.4	BDL	1.1	1.0
Mn	1.1	0.6	1.1	0.8	0.8	0.9	0.6	0.8	0.2	0.6	1.1	0.25
Fe	56.3	65.8	66	59.1	57.8	54.6	67.1	61.0	5.2	54.6	67.1	0.09
N	1.3	BDL	BDL	BDL	BDL	1.2	1.1	1.2	0.1	1.1	1.3	0.08
Ni	BDL	BDL	BDL	BDL	BDL	BDL	BDL	BDL	BDL	BDL	BDL	

Notes:

- a) AVG – average.
- b) s – standard deviation
- c) CV – coefficient of variation ($s \div \text{AVG}$).
- d) BDL – below detection limit – not detected.

Table 28. Corrosion deposit elemental profile correlation coefficients ($|r|_{\text{crit [5 df; } \alpha = 0.05]} = 0.75$). Significant correlation coefficients are highlighted in bold font.

1. Aqueous-phase deposits.

<i>Element</i>	<i>C</i>	<i>O</i>	<i>Fe</i>	<i>K</i>	<i>P</i>	<i>S</i>	<i>Mn</i>
C	1.00						
O	0.78	1.00					
Fe	-0.98	-0.84	1.00				
K	-0.12	-0.44	0.09	1.00			
P	-0.42	-0.49	0.35	0.37	1.00		
S	-0.21	-0.07	0.06	0.54	0.30	1.00	
Mn	-0.51	-0.84	0.55	0.36	0.60	0.23	1.00

2. Aqueous-fuel interface deposits.

<i>Element</i>	<i>C</i>	<i>O</i>	<i>Fe</i>	<i>K</i>	<i>P</i>	<i>S</i>	<i>Mn</i>
C	1.00						
O	0.78	1.00					
Fe	-0.98	-0.84	1.00				
K	-0.12	-0.44	0.09	1.00			
P	-0.42	-0.49	0.35	0.37	1.00		
S	-0.21	-0.07	0.06	0.54	0.30	1.00	
Mn	-0.51	-0.84	0.55	0.36	0.60	0.23	1.00

3. Fuel-phase deposits.

<i>Element</i>	<i>C</i>	<i>O</i>	<i>Fe</i>	<i>K</i>	<i>P</i>	<i>S</i>	<i>Mn</i>
C	1.00						
O	0.24	1.00					
Fe	-0.90	-0.51	1.00				
K	0.11	-0.64	-0.01	1.00			
P	-0.24	-0.30	0.07	0.73	1.00		
S	-0.82	-0.19	0.65	-0.15	0.12	1.00	
Mn	0.04	-0.57	0.12	0.72	0.29	-0.08	1.00

3.6.3.8 The results of these analyses of each of the microcosms listed in Tables 26 and 27 were reported in the following sets of Figures.

Table 30. Aqueous-phase and interface corrosion deposit ATP, carbon (C), oxygen(O), and iron (Fe) concentrations. All values are in wt. %.

Microcosm	Log ₁₀ [tATP] ^a		[C]		[O]		[Fe]	
	A ^b	I ^c	A	I	A	I	A	I
35	N.D. ^d	N.D.	20.6	14.2	24.5	20.3	42.2	56.4
40	3.31	N.D.	6.7	6.4	21.2	22.9	69.0	67.3
77	3.90	3.49	15	18.8	14.9	20.1	66.7	58.6
85	3.40	N.D.	23.2	40.2	18.6	31.0	51.3	27.1
100	4.09	3.84	9.9	11.4	9.2	22.7	77.7	62.3
105	N.D.	N.D.	10.7	10.3	14.8	18.2	66.1	64.9
109	3.84	N.D.	9.8	21.6	22.4	21.3	65.2	52.6

Notes:

- a) Log₁₀ [tATP] values are in Log₁₀ pg cm⁻².
- b) A – aqueous-phase.
- c) I – aqueous-phase-fuel interface.
- d) N.D. – not determined (not tested).

Table 31. Correlation coefficients – corrosion deposit ATP, carbon (C), oxygen(O), and iron (Fe) concentrations.

	[tATP]	[C]	[O]	[Fe]
[tATP]	1.00			
[C]	-0.21	1.00		
[O]	-0.67	-0.05	1.00	
[Fe]	0.61	-0.82	-0.53	1.00

3.6.3.8.1 The Figures with SEM images include EDS elemental analysis. Most of the elements were listed with their chemical symbol and the letter K (for example, in Figure 22, carbon was listed as “CK”). A few elements were listed with the letter L (for example, in Figure 22, zinc was listed as “ZnL”).

- The K and L notations referred to x-ray emission lines. They were based on the energy released when electrons transitioned from one principal quantum number (i.e., an electrons quantum state) to another [40].
- The energy released was measured in electron volts (eV)
- Figure 20a illustrated the Siegbahn notations for K, L, and M emissions. The alphanumeric (1s, 2s, 2p, etc.) values referred to the origin and destination atomic orbitals.
- Figure 20b illustrated the results of an EDS scan. The counts were photon emissions detected. Elements were identified based on the energy at which their emissions are detected. Thus, the peak at 3.7 KeV (1 KeV = 1,000 eV) was characteristic of antimony (Sb).

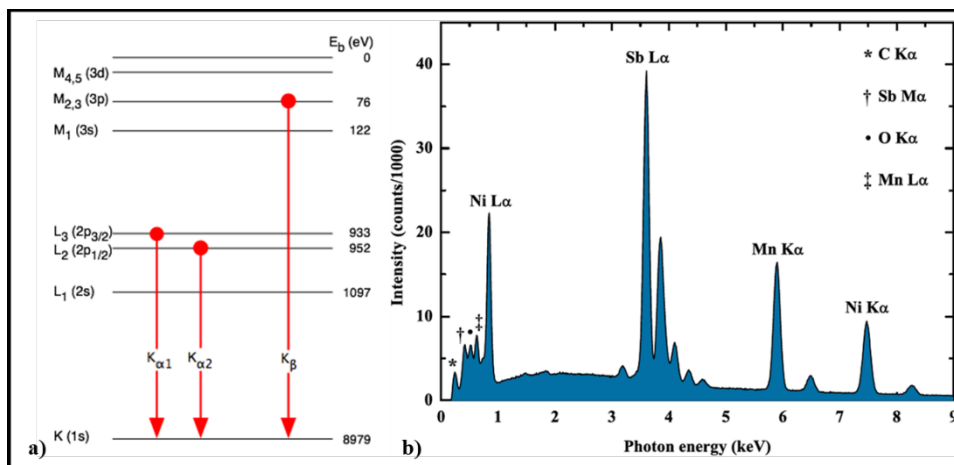


Figure 20. EDS basics – a) x-ray emission lines; b) example of EDS spectrograph.

- The bottom row of each analysis included the phrase *Matrix Correction ZAF*. This indicated that the values on the chart had been corrected for atomic number (Z), self-absorption (A), and fluorescence (F) effects.
- The two data columns reported relative concentrations of the detected elements. The *Wt%* column listed the weight percentage of the total emissions represented by each element. The *At%* column listed the relative molar (i.e., number of atoms) abundance of each element. For example, in Figure 22, the data for C and Fe were:

Element	Atomic Number (Z)	Atomic Mass (A)	Wt%	At%
C	6	12	20.6	39.1
Fe	26	56	42.2	17.2

- The atomic mass of Fe (A_{Fe}) is $4.7 \times A_C$. On a Wt. % basis, Fe represented a greater percentage of the corrosion deposit. To illustrate this point, consider rust (iron oxide – Fe_2O_3). The Fe % as weight fraction = 78 %, but as molar (atomic) fraction = 40 %.

3.6.3.8.2 Full corrosion analysis would have included micrographs of the coupon surface underneath corrosion deposits. The focus of this study was on the relationship between the controlled variables and corrosion development. A detailed assessment of either corrosion deposits or metal surfaces – including determination of the specific processes by which corrosion developed in the different zones within each microcosm or among different microcosms was not part of the study. Consequently, in the following subsections, minimal interpretation of the Figures was provided.

3.6.3.8.3 Microcosm 35 (Figures 21 through 24)

- The general corrosion product was enriched for carbon and oxygen. This is typical for corrosion product that forms in hydrocarbon environments.
- The aqueous-phase corrosion product phosphorous (P) concentration ([P]) was elevated (9.9 wt. % overall, 7.7 wt. % in spot scan. Given that [P] of the steel from which the coupons were produced was < 0.05 wt. %, adsorption from the overlying biofilm was the most likely mechanism.

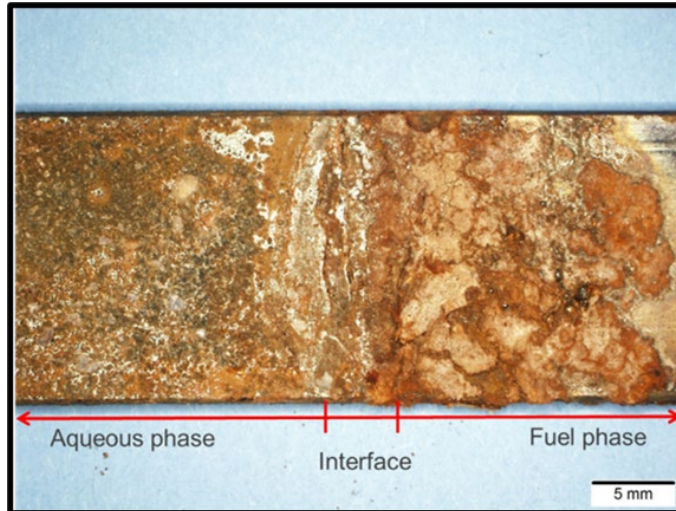


Figure 21. Optical micrograph of microcosm #35 specimen with annotated regions of interest.

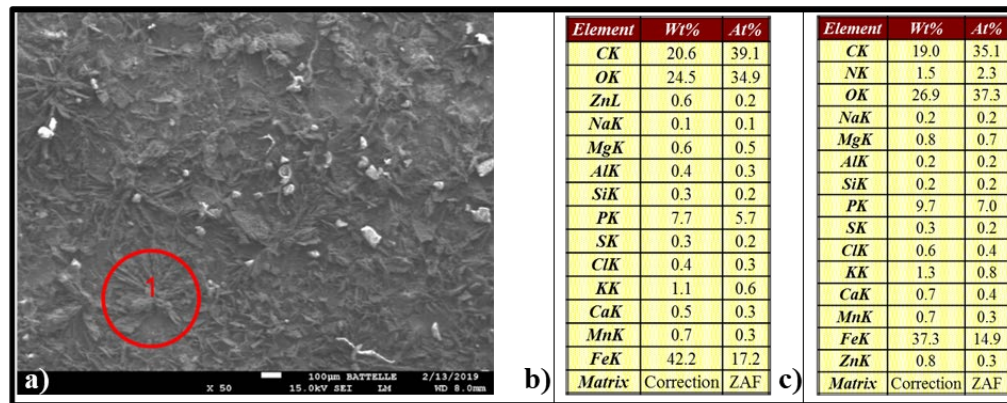


Figure 22. Microcosm #35 – a) SEM micrograph of aqueous-phase corrosion product; b) overall EDS data; c) spot scan (1) EDS data (area $\approx 0.14 \text{ mm}^2$).

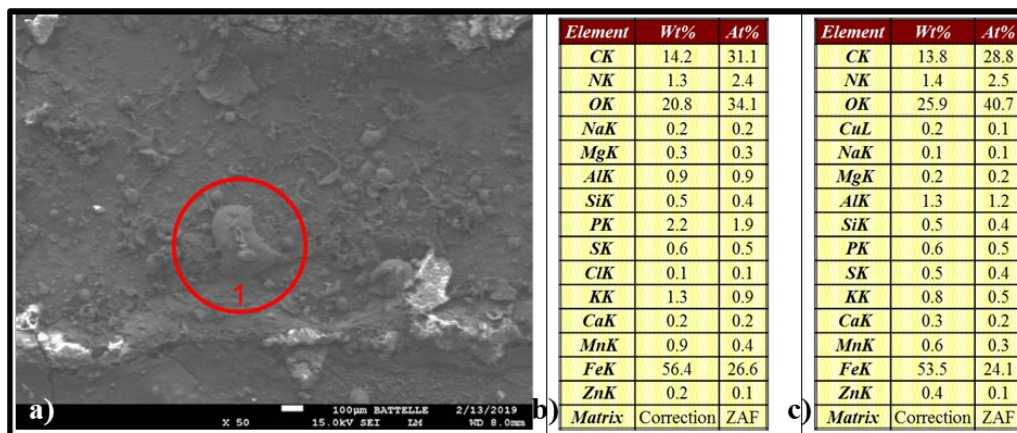


Figure 23. Microcosm #35 – a) SEM micrograph of aqueous-fuel interface corrosion product; b) overall EDS data, c) spot scan (1) EDS data (area $\approx 0.26 \text{ mm}^2$).

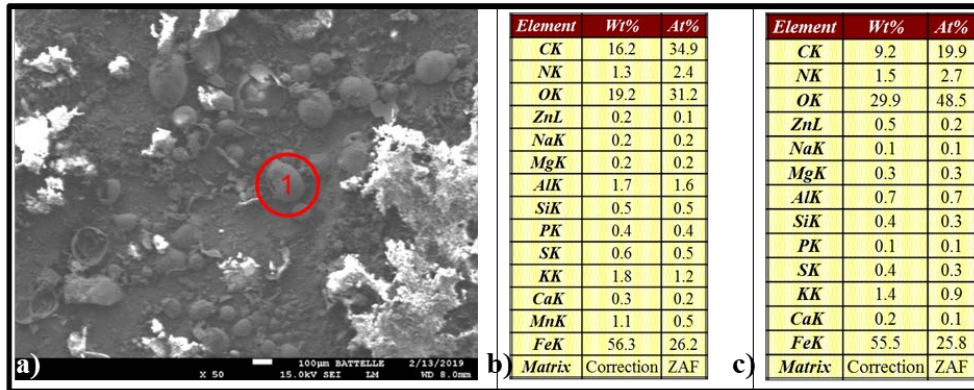


Figure 24. Microcosm #35 – a) SEM micrograph of fuel-phase corrosion product; b), overall EDS data; c) spot scan (1) EDS data (area $\approx 0.07 \text{ mm}^2$).

3.6.3.8.4 Microcosm 40 (Figures 25 through 28).

- The elemental profile of the microcosm 40 corrosion product was unexceptional. Elevated oxygen concentration ([O]) reflected metal (iron – Fe) oxide formation.
- The elevated carbon content was likely attributable to the hydrocarbon environment out of which the steel coupon was pulled.
- In the fuel phase there is an increased content of magnesium (Mg), aluminum (Al), and silicon (Si). These can be trace elemental additions in some low alloy steels as evidenced by their background appearance in most of the spectra generated during this analysis. In the corrosion product formed in microcosm #40, they have complexed in higher quantities than nominal.

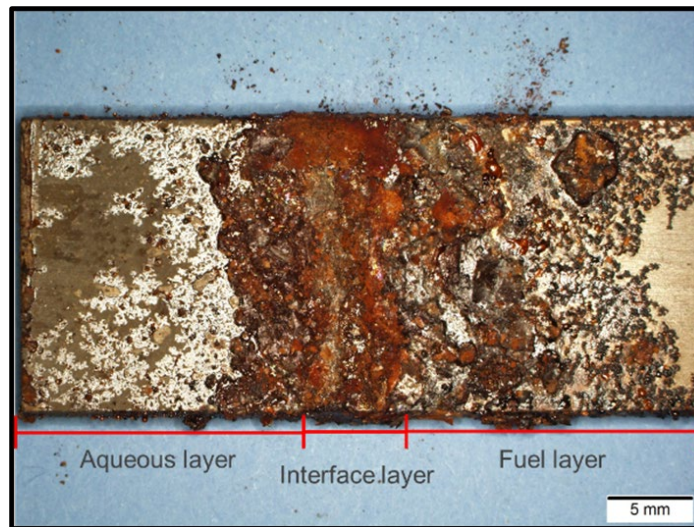


Figure 25. Optical micrograph of microcosm #40 specimen.

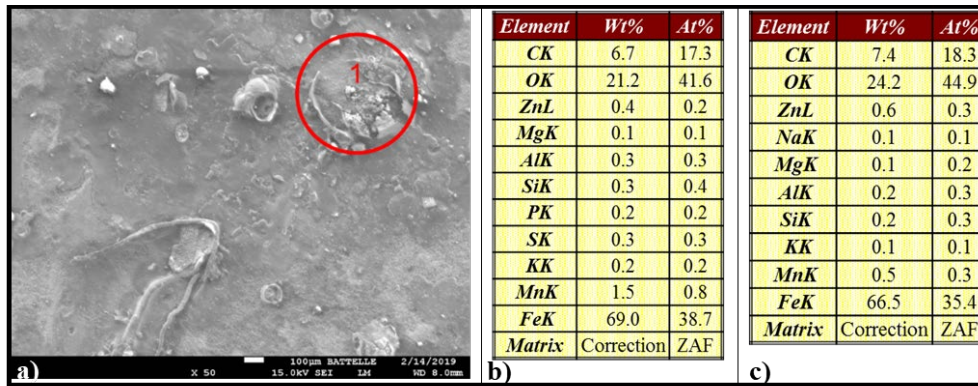


Figure 26. Microcosm #40 – a) SEM micrograph of aqueous-phase corrosion product; b) overall EDS data; c) spot scan (1) EDS data.

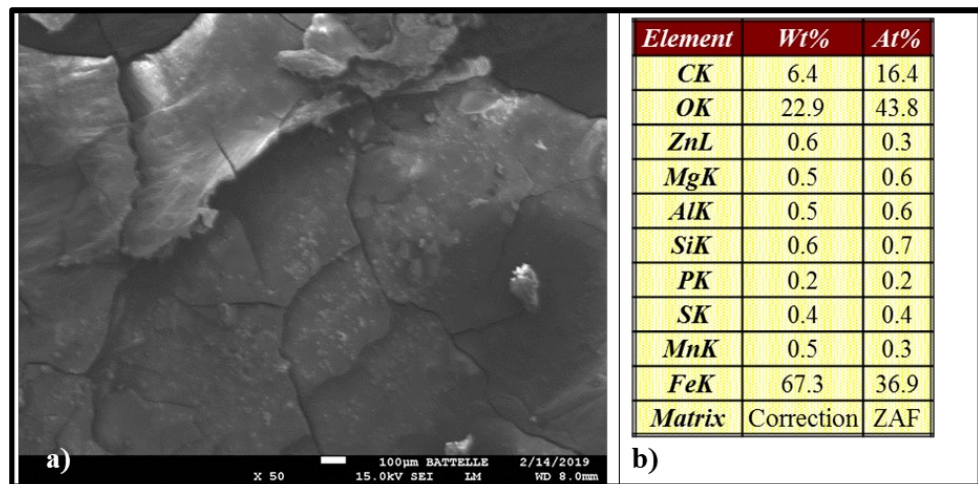


Figure 27. Microcosm #40 – a): SEM micrograph of aqueous-fuel interface corrosion product; b) overall EDS data – no heterogeneity observed.

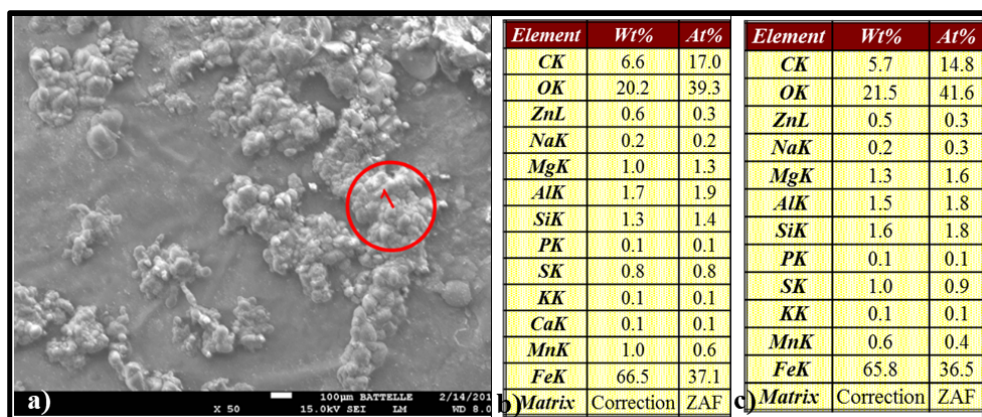


Figure 28. Microcosm #40 – a) SEM micrograph of fuel-phase corrosion product; b) overall EDS data; c) spot scan (1) EDS data.

3.6.3.8.5 Microcosm 77 (Figures 29 through 32)

- The [K] in the fuel-phase deposit was 15x that found in the aqueous phase deposit. Potassium is not an element found in low-carbon steel. Consequently, it had to have come from the microcosm fluids. Bushnell-Hass medium [18] includes monopotassium phosphate (KPO_4), dipotassium phosphate (K_2PO_4) and potassium nitrate (KNO_3). However, if the potassium from the aqueous phase was incorporated into corrosion deposits, detectable (≥ 0.1 wt. %) [K]_s should have been present in all aqueous-phase and interface deposits.
 - [K] was BDL in the microcosm 105 aqueous-phase corrosion deposit.
 - [K] was BDL in the microcosm 40 and 85 interface corrosion deposits.
 - [K] was ≥ 0.1 in all fuel-phase corrosion deposits.
 - Based on these data, [K] in corrosion deposits did not seem to be associated with Bushnell-Haas medium being present.
- Microcosm 77 included CFI – the composition of which was undisclosed. However, CFI was not present in microcosm 109 in which the [K] enrichment in the interface deposit relative to the aqueous-phase deposit was comparable to that in microcosm 77 (i.e., $[\text{K}]_I = 3.5 [\text{K}]_A$, where I and A were the interface and aqueous-phase corrosion deposits, respectively).
- The third likely factor was microbial load.
 - If total ATP-bioburden contributed to [K] enrichment, then the bioburdens in microcosms 77 and 109 would be expected to be comparable. Aqueous-phase and interface planktonic bioburden data were available for both microcosms. Corrosion-coupon surface bioburden data were only available for microcosm 77. Microcosm 77 aqueous-phase bioburden ($[\text{cATP}]_A = 2.76 \text{ Log}_{10} \text{ pg mL}^{-1}$) ranked 37th among the 44 microcosms. Microcosm 109 aqueous-phase bioburden ($[\text{cATP}]_A = 4.75 \text{ Log}_{10} \text{ pg mL}^{-1}$) ranked 13th among the 44 microcosms. However, their respective interface bioburdens were nearly the same, at $[\text{cATP}]_I = 3.90 \text{ Log}_{10} \text{ pg mL}^{-1}$ in microcosm 77 and $[\text{cATP}]_I = 3.84 \text{ Log}_{10} \text{ pg mL}^{-1}$ in microcosm 109. This suggests a relationship between $[\text{cATP}]_I$ and [K] enrichment in the interface corrosion deposits. However, $[\text{cATP}]_I \geq 3.3 \text{ Log}_{10} \text{ pg mL}^{-1}$ in the other EDS examined microsomes. Given that $[\text{K}]_I$ ranged from < 0.1 wt. % to 1.3 wt. % but $[\text{cATP}]_I$ was $3.7 \pm 0.34 \text{ Log}_{10} \text{ pg mL}^{-1}$, there did not appear a direct relationship between potassium enrichment in interface corrosion deposits and interface ATP-bioburdens.
- In fuel-phase deposits, [K] ranged from 0.1 wt. % to 1.8 wt. %. There was no other evidence that minerals from the Bushnell-Haas medium had migrated into the fuel-phase. The data collected were insufficient to identify the mechanism by which potassium was enriched in the interface corrosion deposits of some but not all four-phase microcosms.

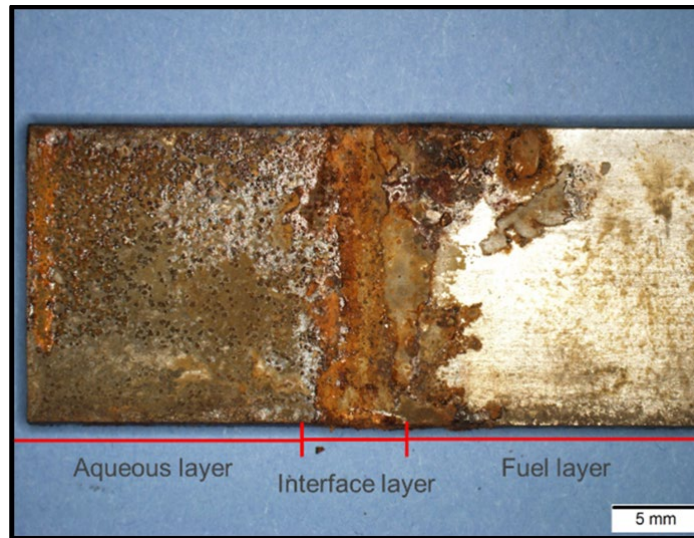


Figure 29. Optical micrograph of microcosm #77 specimen.

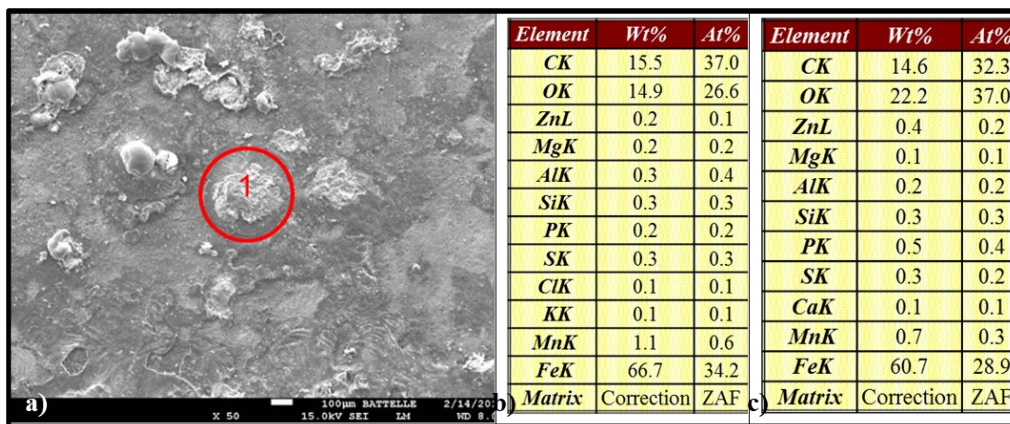


Figure 30. Microcosm #77 – a) SEM Micrograph of aqueous-phase corrosion product; b) overall EDS data; c) spot scan (1) EDS data.

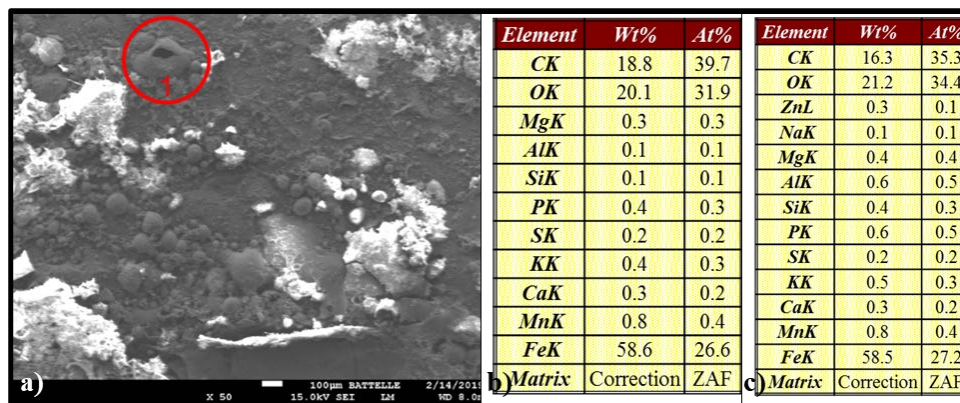


Figure 31. Microcosm #77 – a) SEM micrograph of aqueous-fuel interface corrosion product; b) overall EDS data; c) spot scan (1) EDS data.

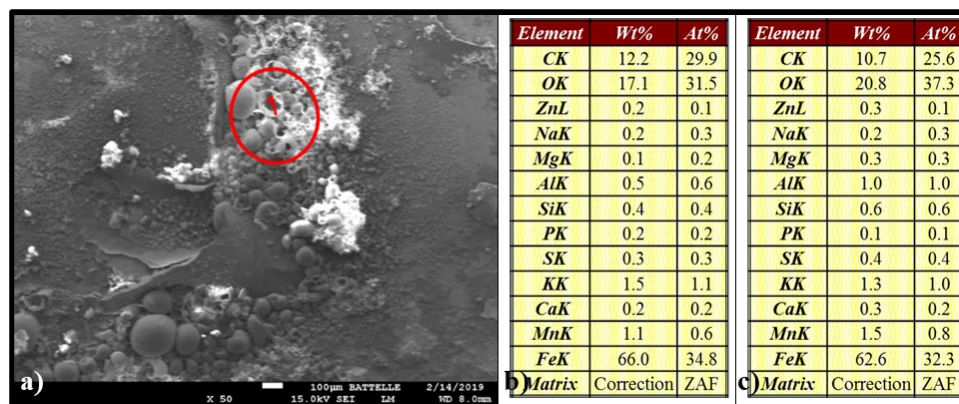


Figure 32. Microcosm #77 – a) SEM micrograph of fuel-phase corrosion product; b) overall EDS data; c) spot scan (1) EDS data.

3.6.3.8.6 Microcosm 85 (Figures 33 through 36)

- The corrosion deposit formed on the microcosm #85 corrosion coupon was more morphologically homogenous than that observed on the other coupons in this subset.
- There was significant charging of the oxide even after gold coating, so micrographs were difficult to render with a high degree of fidelity.
- Phosphorous ($[P]_A$) in the aqueous phase corrosion product was enriched relative to $[P]_I$ and $[P]_F$ (wt. % $[P]_A$, $[P]_I$ and $[P]_F = 4.1, 0.4, \text{ and } 0.6$, respectively). Other microcosms in the subset in which the relative $[P]_A$ enrichment was observed were microcosm #35 and #105. The common properties of the microcosms 35 and 85 included the presence of an aqueous-phase, and absence of MAL and CI. All other controlled variables – including fuel grade – differed. There were no readily apparent reasons for $[P]_A$ to have been enriched relative to the other phases of their respective microcosms or relative to the $[P]_I$ s observed in the other five microcosms, regardless of phase.

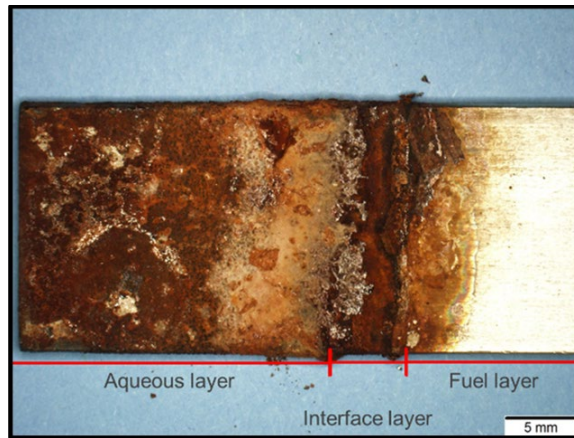


Figure 33. Optical micrograph of microcosm #85 specimen.

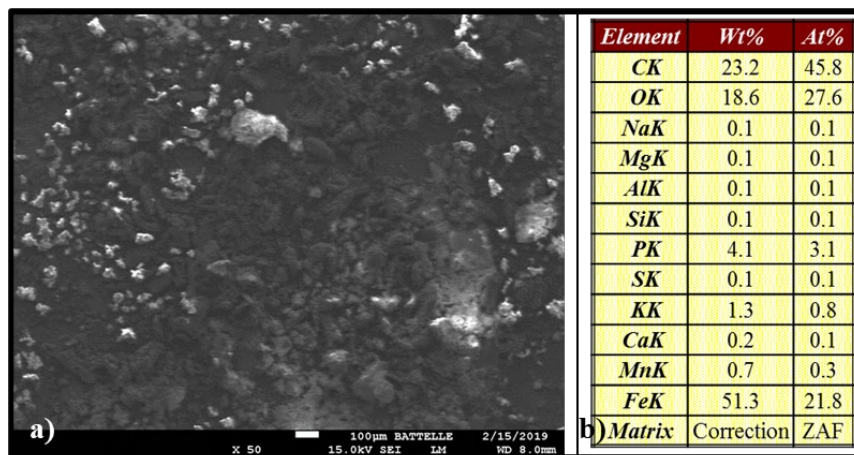


Figure 34. Microcosm #85 – a) SEM micrograph of aqueous-phase corrosion product; b) overall EDS data – no heterogeneity observed.

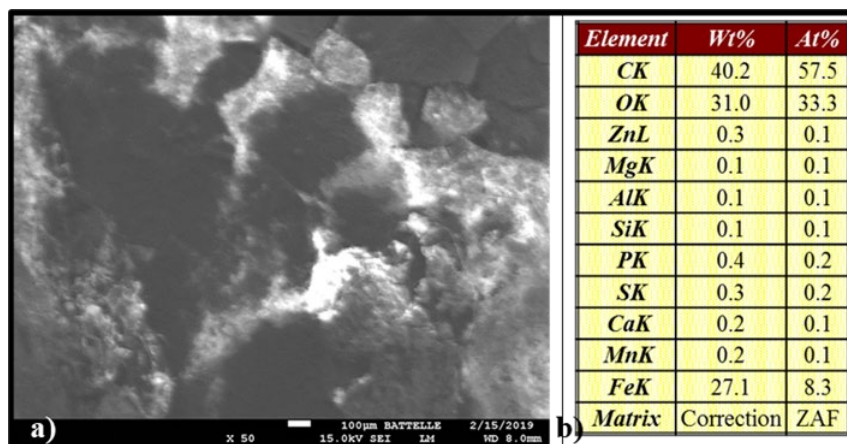


Figure 35. Microcosm #85 – a) SEM micrograph of aqueous-fuel interface corrosion product; b) overall EDS data – no heterogeneity observed.

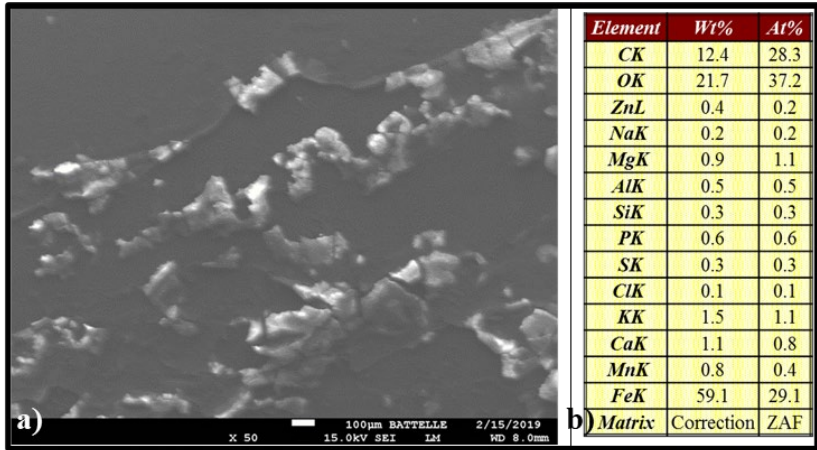


Figure 36. Microcosm #85 – a) SEM micrograph of fuel-phase corrosion product; b) overall EDS data – no heterogeneity observed.

3.6.3.8.7 Microcosm 100 (Figures 37 through 40)

- The density of corrosion deposit coverage over the three exposure phases of the coupon shown in Figure 37 was less than that on any of the other six coupons included in the subset.
- The aqueous-phase and interface corrosion products had slightly elevated [P]s (wt. % = 0.9 and 2.0, respectively) relative to the fuel-phase deposit ([P] = 0.1 wt. %). However, overall (i.e., SEM field-wade) [P]s were substantially less than those reported for microcosms 35 and 85 for aqueous-phase deposits.
- However, as seen in Figure 38, there was a local area (~0.8 mm²) in which [P] = 11 wt. %.

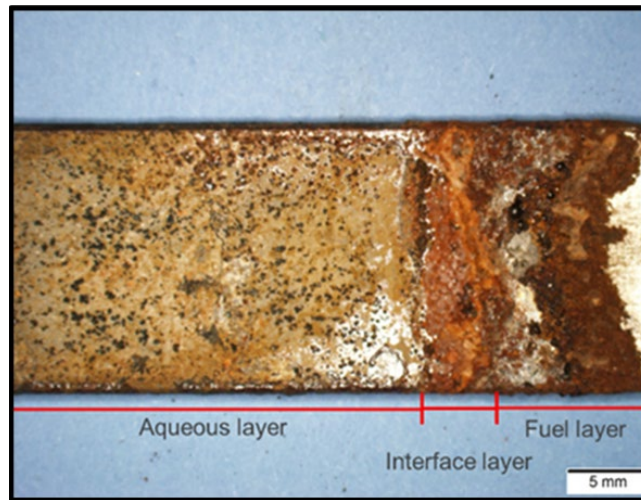


Figure 37. Optical micrograph of microcosm #100 specimen.

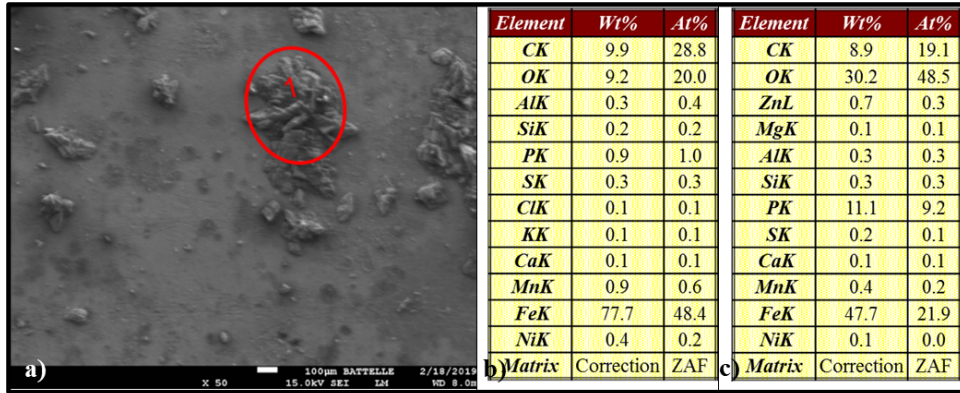


Figure 38. Microcosm #100 – a) SEM micrograph of aqueous-phase corrosion product; b) overall EDS data; c) spot scan (1) EDS data.

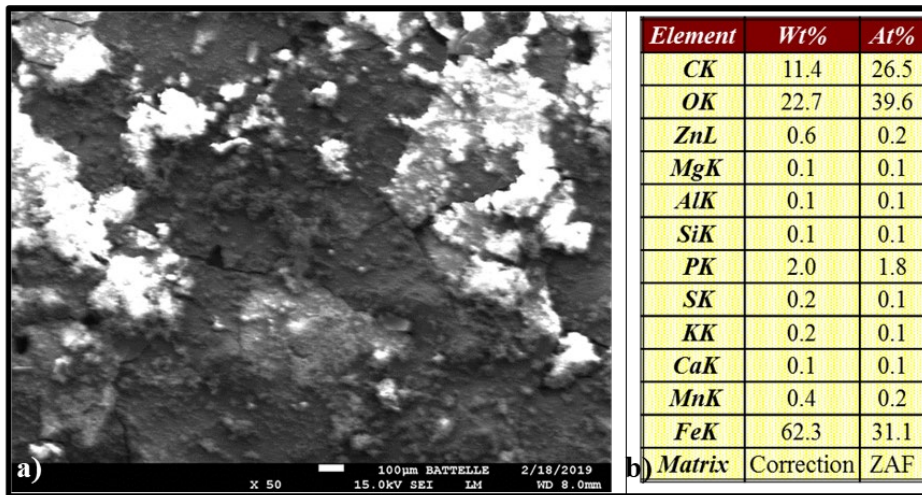


Figure 39. Microcosm #100 – a) SEM micrograph of aqueous-fuel interface corrosion product; b) overall EDS data – no heterogeneity observed.

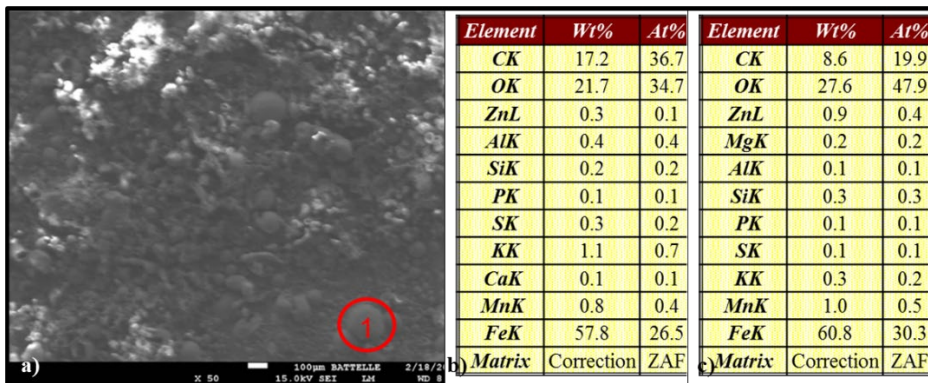


Figure 40. Microcosm #100 – a) SEM micrograph of fuel-phase corrosion product; b) overall EDS data; c) spot scan (1) EDS elemental data.

3.6.3.8.8 Microcosm 105 (Figures 41 through 45)

- Corrosion deposition was comparable to that seen on the microcosm 100 coupon.
 - Both microcosms contained ULSD, ethanol, CFI, and an FRP coupon, and were challenged with the microbial inoculum.
 - Microcosm 100 was not treated with glycerin or CI, but microcosm 105 was.
 - Neither microcosm was treated with FAME.
- The [P] was enriched in the aqueous and interface corrosion deposits relative to [P]_A or [P]_F (wt. % [P]_I, [P]_A, and [P]_F = 2.5, 4.2, and <0.1, respectively).

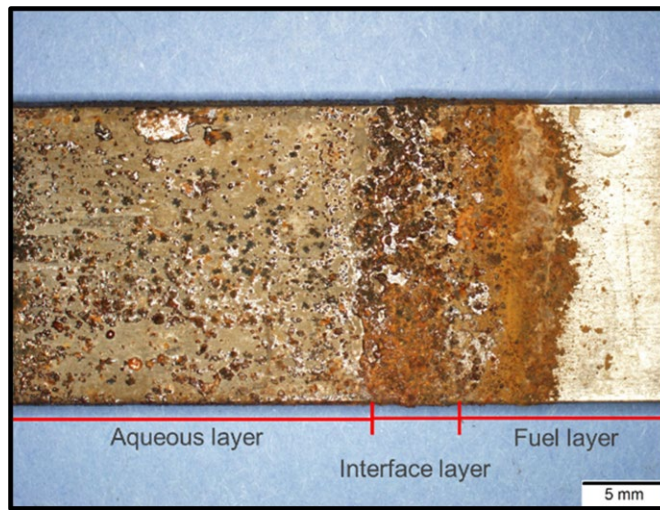


Figure 41. Optical micrograph of microcosm #105 specimen.

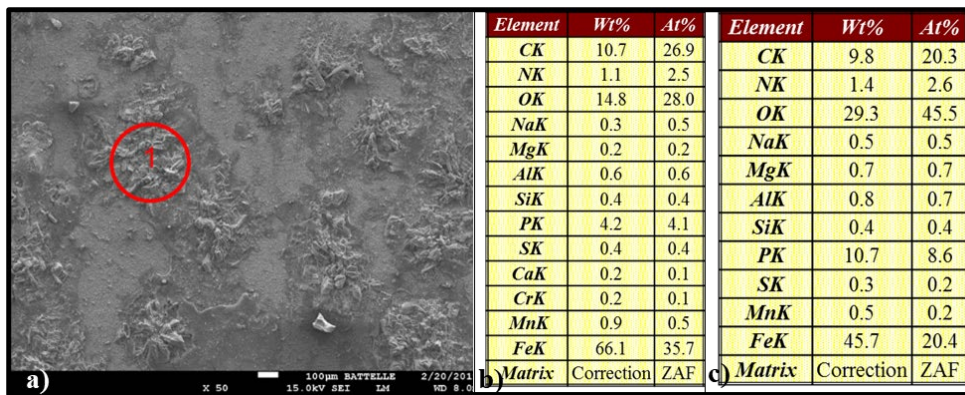


Figure 42. Microcosm #105 – a) SEM micrograph of aqueous-phase corrosion product; b) overall EDS data; c) spot scan (1) EDS data.

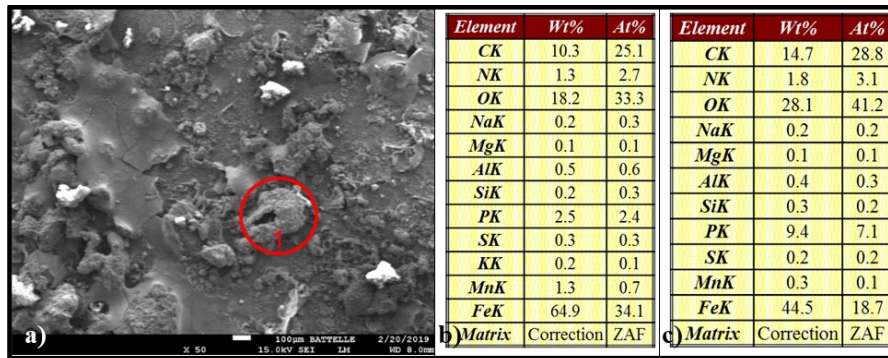


Figure 43. Microcosm #105 – a) SEM micrograph of aqueous-fuel interface corrosion product; b) overall EDS data; c) spot scan (1) EDS data.

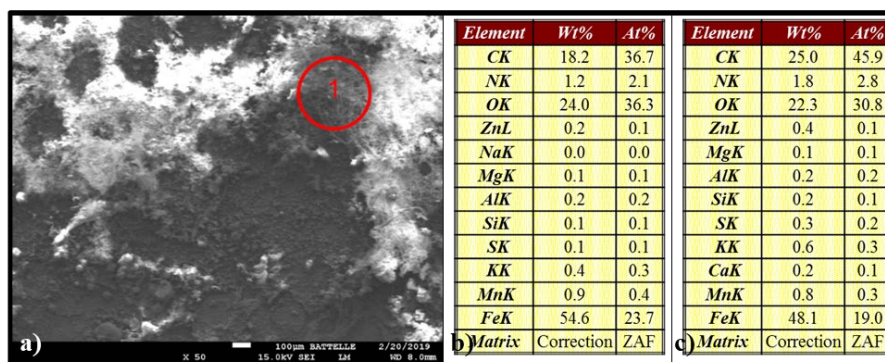


Figure 44. Microcosm #105 – a) SEM micrograph of fuel-phase corrosion product; b) overall EDS data; c) spot scan (1) EDS data.

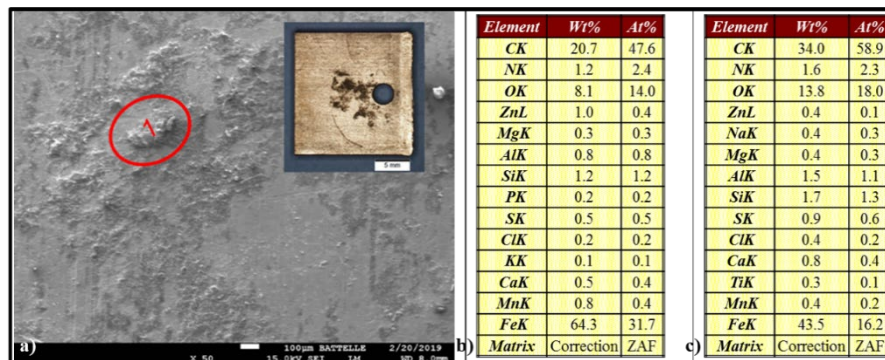


Figure 45. Microcosm #105 – a) SEM micrograph of vapor-phase corrosion product (inset - ~310 mm² area around hole through which monofilament from which coupon hung was threaded); b) overall EDS data; c) spot scan (1) EDS data.

3.6.3.8.9 Microcosm 109 (Figures 46 through 50)

- Although the fuel was treated with FAME but not with CFI or CI, corrosion deposition on the microcosm 109 coupon was similar to that on coupons from microcosms 100 and 105.

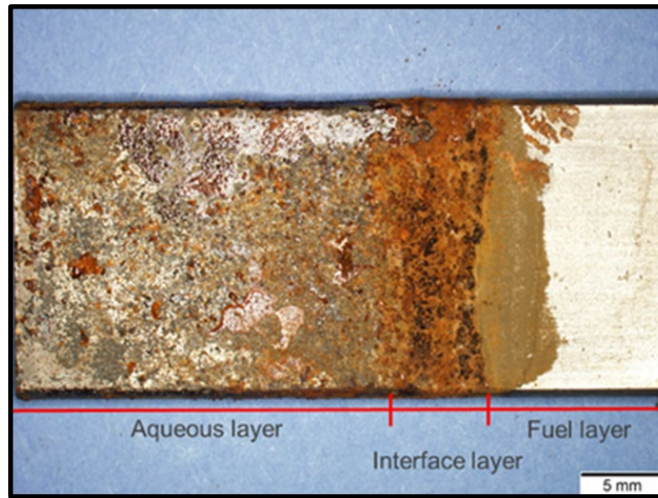


Figure 46. Optical micrograph of microcosm #109 specimen.

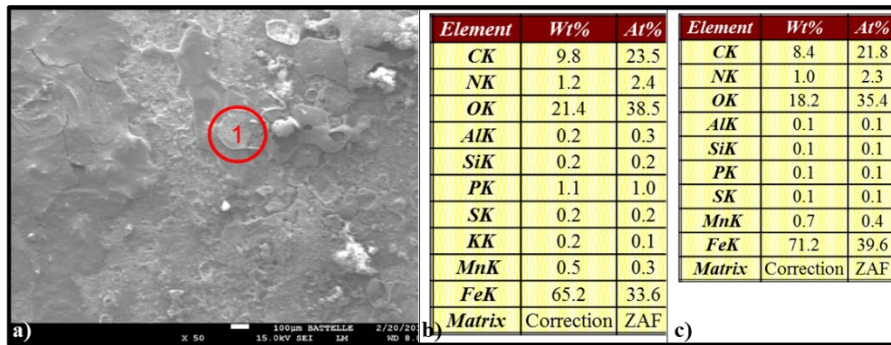


Figure 47. Microcosm #109 – a) SEM micrograph of aqueous-phase corrosion product; b) overall EDS data; c) spot scan (1) EDS data.

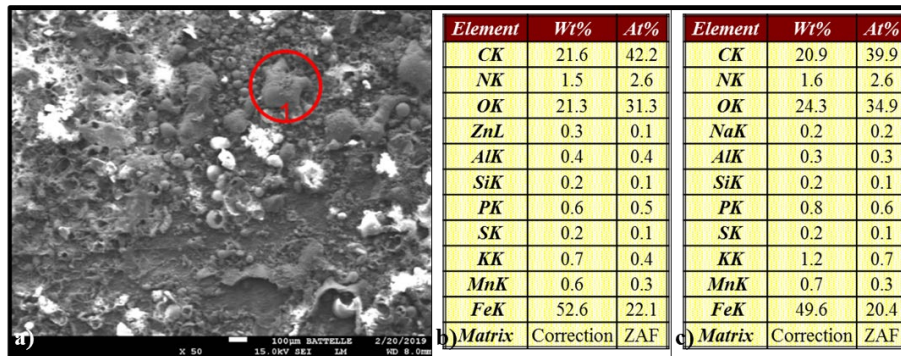


Figure 48. Microcosm #109 – a) SEM micrograph of aqueous-fuel interface corrosion product; b) overall EDS data; c) spot scan (1) EDS data.

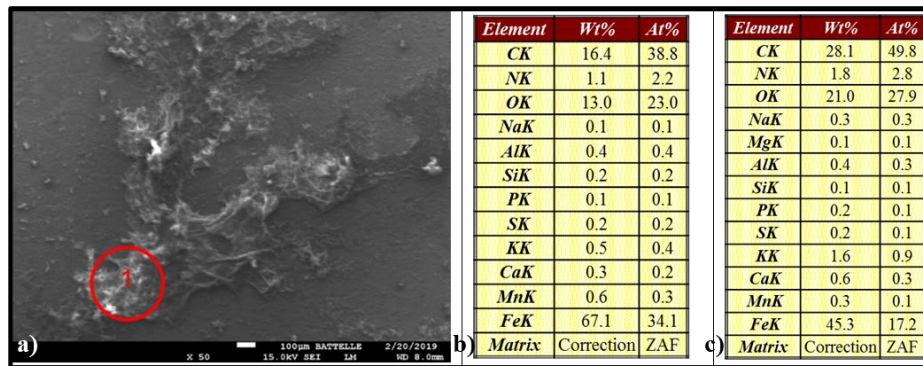


Figure 49. Microcosm #109 – a) SEM micrograph of fuel-phase corrosion product; b) overall EDS data; c) spot scan (1) EDS data.

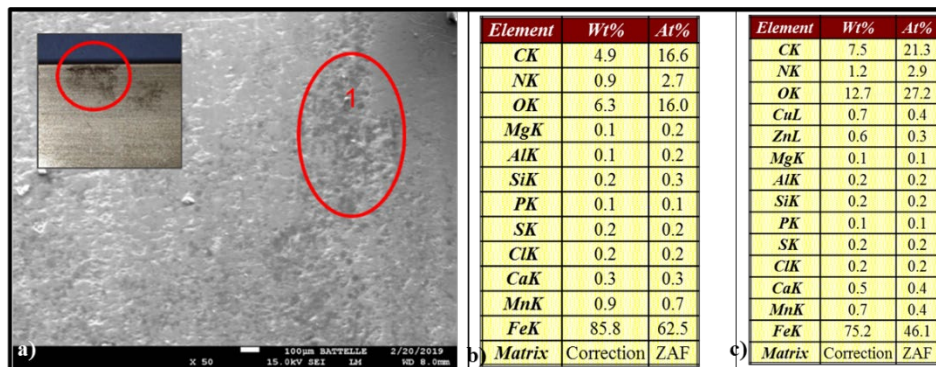


Figure 50. Microcosm #109 – a) SEM micrograph of fuel-phase (~2 cm to 3 cm above fuel-water interface) corrosion product (inset – unmeasured area near coupon edge); b) overall EDS data; c) spot scan (1) EDS data.

- 3.6.3.9 As explained in the introduction (Section 1.2), the purpose of this study was to identify significant relationships between a selected set of controlled variables and corrosion in a microcosm array. Consequently, the primary dependent variable was corrosion rating (CR) of coupons exposed to each of the microcosm phases (3.6.1). The additional dependent variables recorded were used to provide additional insights as to how corrosion varied as a function of the main and two-way interaction effects of the controlled variables.
- 3.6.3.10 The CR data showed an unequivocal relationship with water contact. Corrosion was observed on coupons in all microcosms that contained an aqueous-phase.
- 3.6.3.11 In contrast, the GCR data did not appear to correlate with any of the main or interaction effects.
- 3.6.3.12 There were no unequivocal relationships between corrosion morphology as visualized under low powered light microscopy and SEM.

- 3.6.3.13 Similarly, there were no unequivocal relationships between corrosion deposit, elemental profiles and either independent or other dependent variables (i.e., CR, RS_{GO} , or [ATP]). However, one exception was found. There was a correlation between $[K]_{interface}$ and microbes as mentioned in section 3.5.3.8.5., K might have originated from Bushnell-Haas medium.
- 3.6.3.14 Corrosion coupons were fabricated from grade 1018 low-carbon steel. The elemental composition of Grade 1018 steel is provided in Table 32.

Table 32. Grade 1018 low-carbon steel elemental composition.

Element	wt %	
	min	max
C	0.13	0.2
Mn	0.3	0.9
P	0.0	0.04
Si	0.15	0.3
S	0.0	0.5
Fe	99.42	98.06

3.6.3.15 The [P] in several deposits was several orders of magnitude greater than that expected due to leaching from the alloy. For example, all of the microcosms (35, 100, 105) with $[P] \geq 2$ in the interface deposit were microbially challenged. However, microcosm 77 ($[P] = 0.4$ wt. %) was also challenged. Still elevated [P] seems to be associated with the intentional challenge, particularly at the aqueous-fuel interface. Unfortunately, biofilm ATP-bioburden data were available for only two coupons.

- Microcosm 77: $\text{Log}_{10} [tATP]_I = 3.49 \text{ pg cm}^{-2}$.
- Microcosm 100 ($[P] = 2.0$ wt. %): $\text{Log}_{10} [tATP]_I = 3.84 \text{ pg cm}^{-2}$.
- Although the [P] in microcosm 100 was 5x that in microcosm 77, the ATP-bioburdens on coupon surfaces at the aqueous-fuel interface were not substantially different. However – as will be discussed in Section 3.6 – the types of microbes within the biofilm community are likely to determine the community's biodeteriogenic activity.

3.6.3.16 Similarly, N and K enrichment in coupon deposits most likely reflect microbial activity.

3.6.3.17 An alternative explanation for K enrichment is the dissolution of potassium-based catalyst from FRP. Potassium-based catalysts are sometimes utilized in production of fiber-reinforced plastics. It is unknown whether a potassium-based catalyst was used in the production of the FRP from which coupons were fabricated for this study.

- Although FRP coupons were in microcosms 35 and 85 – both of which had deposits with the greatest [K]s – FRP coupons were also present in microcosms 40 and 105 – the two with the lowest [K] in their corrosion deposits.

3.6.3.18 In summary, corrosion deposit analysis indicates that typical galvanic chemical corrosion occurred on all coupons exposed to a microcosm aqueous-phase. More severe corrosion in the aqueous-fuel interface zone might reflect an MIC role, but there is no unequivocal evidence of MIC damage.

3.7 MICROBIOLOGY

3.7.1 Overview

- 3.7.1.1 Adenosine triphosphate (ATP) was the primary parameter used to monitor microbial loads (bioburdens) in microcosms. Because bioburden quantification is test-method dependent, *bioburden* as used in this report referred to *ATP-bioburden*. ATP-bioburden was reported as $\text{Log}_{10}[\text{ATP}]$ in pg mL^{-1} for fluid samples and pg cm^{-2} for surface samples. Additionally, fluid sample [ATP] included only ATP from within intact cells – *cellular ATP* (cATP). Surface sample [ATP] included cATP, plus free ATP (ATP that was dissolved in the fluid) and cell-fragment ATP (any ATP that was bound to cell fragments that remained intact after cells lysed upon death). Consequently, surface sample [ATP] is reported as *total ATP* (tATP). Although the [cATP] cell^{-1} can vary from 0.5 fg cell^{-1} to 6.5 fg cell^{-1} ($1 \text{ fg} = 10^{-15} \text{ g}$) [41, 42], nearly sixty years of reports have shown that an estimate of 1 fg cell^{-2} correlates well with other bioburden estimates [43, 44, and 45]. ASTM Method D7687 [15] relies on filtration and wash steps to separate whole cells from cell debris. Once these interferences are removed, the whole cells are intentionally lysed to release cATP. The protocol used to detect biofilm ATP does not include these preliminary steps. Consequently, tATP is reported. One limitation of ATP testing is that the [cATP] in dormant cells is orders of magnitude less than [cATP] in metabolically active cells. This means that dormant cells are not typically detected. Although a protocol for detecting dormant cells has been developed [44], it was not used in this project.
- 3.7.1.2 Genomic test methods have evolved rapidly over the course of the past 20 years [46, 47]. Currently the three major categories are quantitative polymerase chain reaction (qPCR), next generation sequencing (NGS), and whole genome sequencing (WGS). qPCR methods use a short section of ribonucleic acid (RNA) or deoxyribonucleic acid (DNA) as a primer to quantitatively detect microbes. It is generally believed that if the primer targets a section of the genome that is ancient, then the results are representative of most or all of the microbes present. Conversely, if the primer is for a gene that is unique to a single type of microbe (operational taxonomic unit – OTU), qPCR can be used to detect and quantify the presence of that OTU. 16S rRNA and 18S rRNA analyses are types of next generation sequencing (NGS) methodology that provide a relatively rapid assessments of the types of microbes (operational taxonomic units – OTUs) present in mixed populations. 16S rRNA is used to detect prokaryotes (bacteria and archaea) and 18S RNA is used to detect eukaryotes (fungi). WGS examines the entire genomes of microbes in test specimens. In this study, 16S and 18S NGS testing was used to profile microbial populations (*metagenomes*) in selected underground storage tank (UST) and microcosms.

3.7.2 Adenosine Triphosphate

3.7.2.1 Challenge population development

- 3.7.2.1.1 The FCP consensus was to use microbes indigenous to UST as the challenge population source material.
- 3.7.2.1.2 Bottom-samples were collected from six ULSD UST and shipped to Battelle, Columbus OH, for testing and further processing. Upon receipt, bottoms-water specimens were tested by ASTM D7687. The results were summarized in Table 33. Aqueous-phase ATP-bioburdens were classified as *heavy* if $[\text{cATP}] \geq 3\text{Log}_{10} \text{ pg mL}^{-1}$ (i.e., $\geq 10^3 \text{ pg mL}^{-1}$) [48].

Table 29. ATP-bioburdens in ULSD UST bottoms-water samples.

Sample ID	[cATP]	
	(pg mL ⁻¹)	(Log ₁₀ pg mL ⁻¹)
1	100	2.02
2	1	0.00
3	3	0.48
4	40,000	4.60
5	12,000	4.08
6	28,000	4.45

3.7.2.1.3 Bottoms-water samples 1, 2, and 3 were pooled to create primary inoculum #1, and 4, 5, and 6 were pooled to create primary inoculum #2.

3.7.2.1.4 Per 2.4.2, 20 mL of primary inoculum was added to LSD microcosms (500 mL fuel over 100 mL Bushnell-Haas medium) and left to stand at room temperature for a week. These were designated a primary (1°) microcosms.

3.7.2.1.5 After a week, aqueous-phase specimens were collected for ATP testing.

3.7.2.1.6 The ATP-bioburden of robust microbial populations will increase from <2 Log₁₀ pg mL⁻¹ to ≥4 Log₁₀ pg mL⁻¹ within a week. If 1° [cATP] ≥4 Log₁₀ pg mL⁻¹ when tested after one week, 10 mL of aqueous-phase fluid was transferred to secondary ULSD or LSD (2°) microcosms and left to incubate at room temperature for two-weeks. The 4 Log₁₀ pg mL⁻¹ lower control limit was selected to ensure microbial population robustness.

3.7.2.1.7 If 2° aqueous-phase [cATP] ≥4 Log₁₀ pg mL⁻¹ when tested after two weeks, the high bioburden aqueous-phase portions of replicate microcosms were pooled to use as challenge inocula for the 120-day study. Only the aqueous-phases of inoculum #2 2° microcosms were pooled and used to challenge the test microcosms.

3.7.2.1.8 The 1° and 2° microcosm ATP-bioburden data were reported in Table 34.

Table 30. ATP-bioburdens in aqueous-phases of 1° and 2° microcosms.

Sample	[cATP]	
	(pg mL ⁻¹)	(Log ₁₀ pg mL ⁻¹)
1° Microcosm 1	22,000	4.34
1° Microcosm 2	10,000	4.00
2° Microcosm 1	12,000	4.08
2° Microcosm 2	12,000	4.08

3.7.2.2 ATP-bioburdens in test microcosms.

- 3.7.2.2.1 The project QAPP called for weekly aqueous-phase [cATP] testing. During the final test plan design effort, this schedule was modified to be conditional (Figure 8). The Figure 8 flow diagram was based on the expectation that $CR \geq 3$ and fuel haze rating ≥ 3 would generally be concomitant. In actuality, there was no direct relationship between CR and haze rating. Consequently, limited ATP testing was performed between T_{wk0} and T_{wk9} .
- 3.7.2.2.2 ATP testing was performed on six T_0 and nine T_{wk4} microcosms, but only microcosm 77 was common to the two sample sets (Table 35). Three of the six microcosms tested at T_0 had been challenged, as had five of the eight tested at T_{wk4} .
- 3.7.2.2.3 Figure 51 showed the $\text{Log}_{10}[\text{cATP}] (\overline{[\text{cATP}]} \pm s)$ for challenged and unchallenged microcosms. Although ATP bioburdens in the two uninoculated microcosms tested at T_0 were in the negligible range ($[\text{cATP}] = 0.4 \pm 0.12 \text{ Log}_{10} \text{ pg mL}^{-1}$ – T_0 fuel-phase [cATP] in these two microcosms were $\leq 1 \text{ pg mL}^{-1}$), by T_{wk4} $[\text{cATP}] = 3.6 \pm 0.9 \text{ Log}_{10} \text{ pg mL}^{-1}$.
- 3.7.2.2.4 A limited number of microcosms were tested for ATP-bioburden before T_{wk9} . Among those that were tested before T_{wk9} , the ATP-bioburdens in challenged versus unchallenged microcosms were significantly different at T_{wk0} and T_{wk4} , but not at T_{wk6} ($F_{[1,4 \text{ df}]} = 0.0003$, $P = 0.99$). Through T_{wk4} the average ATP-bioburden in the aqueous-phase of challenged microcosms was 10-times greater than that in unchallenged microcosms.
- 3.7.2.2.5 Assuming that the T_0 and T_{wk4} microcosms tested were representative of all of the unchallenged microcosms, the ATP-bioburden in the unchallenged microcosms tested at T_{wk4} indicated that dormant microbes that had been present in the fuel provided for this study had settled into the aqueous-phases, become metabolically active, and subsequently proliferated. As discussed in Section 3.6.2.2.11 and shown in Table 36, this phenomenon of dormant microbes slowly becoming metabolically active is consistent with the positive correlation between aqueous-phase corrosion ratings (CR_{AQ}) and [cATP].
- 3.7.2.2.6 The complete ATP dataset was provided in Appendix H and was analyzed thoroughly by Passman *et al.* in a paper presented at the 16th International Symposium on the Stability and Handling of Liquid Fuels [48]. The paper was provided as Attachment 1.
- 3.7.2.2.7 When the T_{wk12} aqueous-phase ATP-bioburdens in all four-phase microcosms were compared, $\text{Log}_{10} [\text{cATP}] = 3 \pm 3.0 \text{ Log}_{10} \text{ pg mL}^{-1}$ and $4.0 \pm 0.13 \text{ Log}_{10} \text{ pg mL}^{-1}$ in unchallenged and challenged microcosms, respectively. The difference was significant ($F_{[1,44 \text{ df}]} = 10.3$, $P=0.0024$). As reflected in the large standard deviation, in unchallenged microcosms ranged from $0.32 \text{ Log}_{10} \text{ pg mL}^{-1}$ to $5.74 \text{ Log}_{10} \text{ pg mL}^{-1}$ ($[\text{cATP}]_{\text{max}} - [\text{cATP}]_{\text{min}} = 5.42 \text{ Log}_{10} \text{ pg mL}^{-1}$). The range was much smaller in challenged microcosms ($2.75 \text{ Log}_{10} \text{ pg mL}^{-1}$ to $5.3 \text{ Log}_{10} \text{ pg mL}^{-1}$ ($[\text{cATP}]_{\text{max}} - [\text{cATP}]_{\text{min}} = 2.55 \text{ Log}_{10} \text{ pg mL}^{-1}$). Table 36 summarized the controlled variables of the challenged and unchallenged microcosms with aqueous-phase $[\text{cATP}]_{\text{min}}$ and $[\text{cATP}]_{\text{max}}$ at T_{wk12} . These observations suggested that microbial contamination distribution in the fuels used to prepare the microcosms was quite heterogeneous. It is possible that cell masses (*flocs*) were present in some volumes of fuel used to fill microcosms jars, but not others. Also, the concept of *critical inoculum* – the minimum number of microbial cells needed to enable a population to reproduce successfully – is common knowledge in microbiology. It is possible that the chemical environment in some microcosms was sufficiently hostile to prevent indigenous microbes from reproducing. It was likely that the challenge inoculum bioburden was consistently greater than the critical inoculum. Consequently, there was substantially less aqueous-phase ATP-bioburden variability among challenged microcosms.

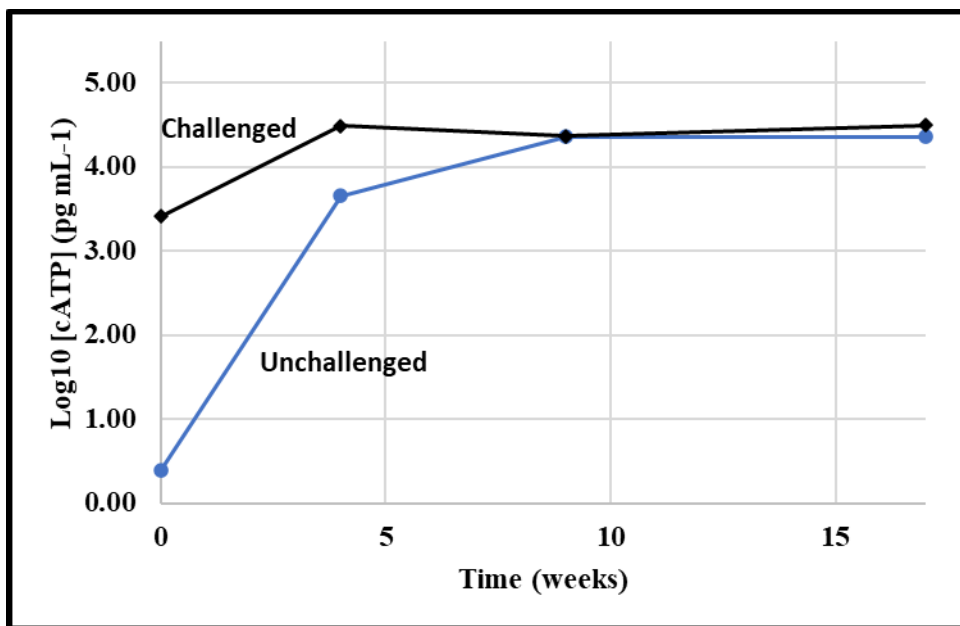


Figure 51. Log₁₀ [cATP] ($\overline{[cATP]} \pm s$) versus time (weeks) between T₀ and T_{wk9} (black line – intentionally challenged; blue line – unchallenged).

Table 5. Microcosms tested for [cATP] at T₀, T_{wk4}, and T_{wk9}, with indication of whether they were intentionally challenged with 2° microcosm inoculum.

Microcosm	Tested			Challenged
	T _{wk0}	T _{wk4}	T _{wk9} ^a	+ or -
3	N	Y	Y	-
4	N	Y	Y	+
9	N	Y	Y	-
29	Y	N	N	+
30	N	Y	Y	-
35	N	Y	Y	+
39	N	Y	Y	+
40	Y	N	N	-
57	Y	N	N	-
66	Y	N	N	-
74	N	Y	Y	-
77	Y	Y	Y	+
86	N	Y	Y	+
119	Y	N	N	+

Note: a) Most, but not all of the microcosms with an aqueous-phase were tested at T_{wk9}.

3.7.2.2.8 Correlations between [cATP] in aqueous, fuel, and interface zones were compared as were correlations between [cATP] and [tATP]. The correlation coefficients were compiled into Table 37.

- [cATP] in the aqueous-phase correlated significantly with [cATP] in the sediment and interface zones, but not with [cATP] in the fuel-phase. It appeared that the invert-emulsion layer functions as a barrier to ATP-bioburden incursion into the fuel-phase.

Table 31. Controlled variable profiles of challenged and unchallenged microcosms with aqueous-phase [cATP]_{min} and [cATP]_{max} at T_{wk12}.

Property	Unchallenged		Challenged	
Log₁₀ [cATP]	0.32	5.74	2.76	5.3
Fuel	LSD	ULSD	ULSD	LSD
FAME	B5	B5	B0	B5
Glycerin	+	+	+	-
Ethanol	+	+	-	-
MAL	-	-	-	-
CFI	+	+	-	+
CI	-	-	+	-
CA	-	-	+	-
FRP	-	+	-	+

- Sessile ATP-bioburdens showed a similar pattern. Aqueous-phase [tATP] on steel coupons correlated strongly with interface [tATP] but not with fuel-phase [tATP].
- The correlation between aqueous-phase [tATP] and interface [tATP] on FRP coupons was statistically significant but marginally so ($r^2 = 0.34$, $P = 0.04$).
- Interestingly, aqueous-phase [cATP] and [tATP] correlated with one another, but interface [cATP] and [tATP] did not.

3.7.2.2.9 Additionally, [cATP] and [tATP] were profiled as functions of microcosm phase. Figure 52 profiled [cATP] and Figure 53 profiled [tATP].

- Typical bioburden profiles show maxima within the invert emulsion layer [49]. However, in this study, at T_{wk12}, [cATP] was slightly greater in the aqueous-phase ($\text{Log}_{10} [\text{cATP}] = 4.0 \pm 2.6 \text{ pg mL}^{-1}$) than in the interface zone ($\text{Log}_{10} [\text{cATP}] = 3.0 \pm 2.4$). This could have been due to either a greater percentage of dormant microbes within the invert emulsion, a high ratio of extracellular polymeric substance (EPS) to cells, or a combination of the two. The apparent difference could also have been a statistical artifact of the [cATP] variability in both phases, among microcosms (three-phase data were collected at T_{wk12} for only 20 microcosms).
- Negligible ($\text{Log}_{10} [\text{tATP}] = 0.9 \pm 0.2 \text{ pg cm}^{-2}$) ATP-bioburdens were detected on coupons surfaces that had been exposed to the vapor-phase.
- As with planktonic ATP-bioburdens, the greatest [tATP] were recovered from coupons surfaces that had been exposed to the aqueous-phase ($\text{Log}_{10} [\text{tATP}] = 3.0 \pm 1.2 \text{ pg cm}^{-2}$), followed by the interface ($\text{Log}_{10} [\text{tATP}] = 1.5 \pm 1.4 \text{ pg cm}^{-2}$), and fuel-phase ($\text{Log}_{10} [\text{tATP}] = 1.0 \pm 1.5 \text{ pg cm}^{-2}$), surfaces.

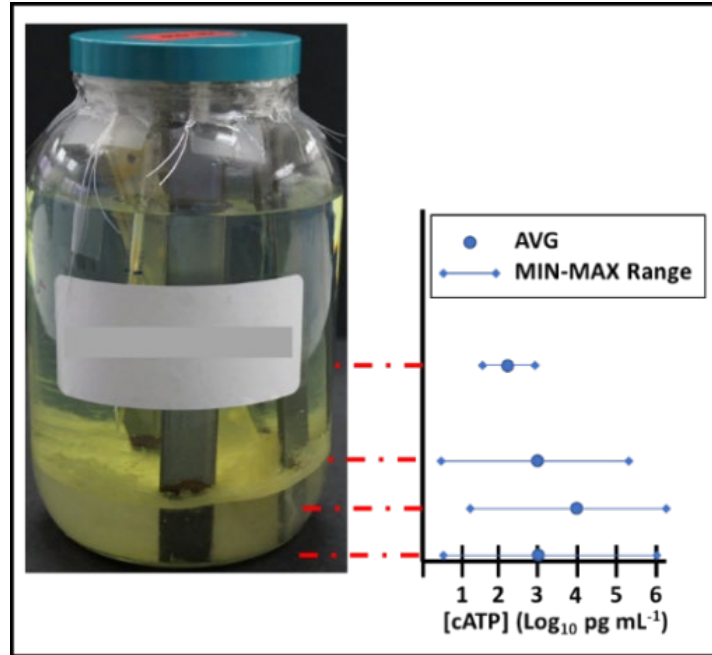


Figure 52. Planktonic ATP-bioburden profile in fuel over aqueous-phase microcosm. Averages and ranges are for 20 microcosms.

Table 32. ATP-bioburden correlation coefficients between planktonic and sessile populations in different microcosm phases.

Interface	r^2	r^2_{crit}	n	P
Planktonic ([cATP])				
Aqueous-phase & sediment	0.95	0.9	4	0.03
Aqueous-phase & interface	0.45	0.18	21	0.0009
Aqueous-phase & Fuel	0.38	0.45	9	0.08
Interface & Fuel	0.75	0.56	7	0.01
Sessile ([tATP])				
<i>Carbon steel coupons</i>				
Aqueous-phase & interface	0.61	0.21	18	0.0001
Aqueous-phase & Fuel	0.37	0.36	11	0.05
<i>Epoxy resin coupons</i>				
Aqueous-phase & interface	0.34	0.3	13	0.04
<i>Carbon steel & epoxy resin coupons</i>				
Aqueous-phase	0.34	0.65	6	0.23
Sessile - Planktonic				
Aqueous-phase	0.69	0.1	39	<0.0000
Interface	0.52	0.56	7	0.06

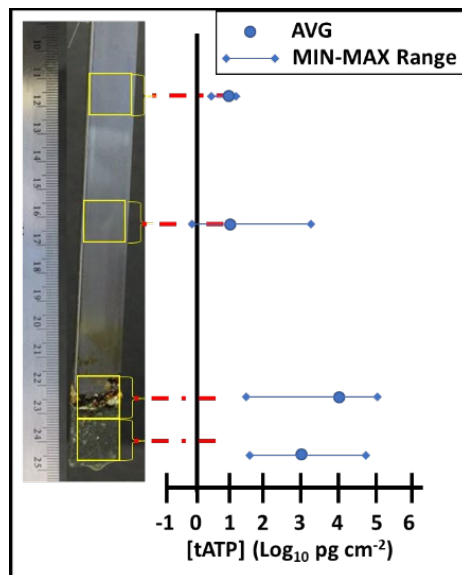


Figure 53. Sessile ATP-bioburden profile on low-carbon steel corrosion coupons in fuel over aqueous-phase microcosms. Averages and ranges are for 18 microcosms.

3.7.2.2.10 There were no significant relationships between the controlled variables and T_{wk12} aqueous-phase ATP-bioburdens (Table 38).

3.7.2.2.11 There is a considerable body of literature on the subject of microbiologically influenced corrosion (MIC) [50 to 54]. Results from two previous UST surveys [6, 7] suggested there was a direct relationship between microbial contamination and corrosion in ULSD fuel systems.

- There were no apparent correlations between either planktonic or sessile bioburdens and CGR in the microcosms for which ATP and corrosion rate data were available (Table 35).
- As reported in Table 20, at T_{wk12} RS_{GO} did not correlate with either CR_{AQ} or CR_I .
- As reported in Table 21, at T_{wk12} $[cATP]_{AQ}$ correlated strongly with RS_{GO} .
- The correlation coefficient calculations were based on 6 to 79 data pairs, depending on the pairs (“n” in Table 39). At apparent absence of significant correlations could have been partially due to the limited number of data sets for some of the parameter pairs.
- The most aggressive corrosion was seen in a 1 cm to 2 cm band at the aqueous-fuel interface. In this zone, the coupon surface was exposed to invert emulsions and metabolically active microbial communities. Biofilm accumulation was also greatest in this zone – providing conditions conducive to localized corrosion cells.
- The localized appearance of substantial corrosion is likely to have biased the general corrosion rate (GCR) results (see 3.6.2). GCR is typically calculated on coupons that are exposed entirely to a single fluid (water, crude oil, petroleum product, etc.).
- Most importantly, the original expectation was that $[ATP]$ in the unchallenged microcosms would have remained at $< 2 \text{ Log}_{10} \text{ pg mL}^{-1}$ – providing a clear distinction between bioburdens in challenged and unchallenged microcosms. Although the aqueous-phase $\overline{[cATP]}_{\text{Challenged}} > \overline{[cATP]}_{\text{Unchallenged}}$, by T_{wk12} , 56 % of the unchallenged microcosms supported ATP-bioburdens $\geq 3 \text{ Log}_{10} \text{ pg mL}^{-1}$. This ATP-bioburden similarity between challenged and unchallenged microcosms is likely to have obscured any controlled variable effects.

Table 33. ANOVA Summary effect of controlled variables on T_{wk12} aqueous-phase [cATP].

Statistic	Sulfur		Biodiesel (%)		Glycerin (ppm)		Ethanol (ppm)		Microbes	
	LSD	ULSD	B0	B5	+ ^a	-	+ ^b	-	+ ^c	-
AVG	4.2	4.4	3.9	3.5	4.2	4.5	4.5	4.2	4.5	4.1
s	0.77	0.69	0.98	1.48	0.86	0.54	0.54	0.95	0.66	0.75
F	0.69		0.02		0.42		0.84		1.58	
P	0.42		0.90		0.52		0.37		0.22	
F-crit	4.38		4.35		4.38		4.38		4.38	

Statistic	MAL ^d		CI ^f		Conductivity Additive		FRP Material		
	+ ^e	-	-	+ ^g	-	+ ^h	-	+	-
AVG	4.5	4.3	0.7	4.3	4.4	4.3	4.5	4.4	4.3
s	0.79	0.70	0.18	0.69	0.83	0.66	0.81	0.84	0.59
F		0.65		0.001		0.36		0.01	
P		0.43		0.97		0.56		0.93	
F-crit		4.38		4.38		4.38		4.41	

Notes:

- a) Glycerin +: 5,000 ppm
- b) Ethanol +: 10,000 ppm
- c) Microbes +: Challenged
- d) MAL – mon-acid lubricity additive
- e) MAL +: 200 ppm
- f) CI – corrosion inhibitor
- g) CI +: 8ppm to 10 ppm
- h) Conductivity additive +: 2 ppm to 3 ppm

Table 39. Correlations between general corrosion rates and gross observations, respectively and [ATP].

Relationship	Statistic			
	r	r _{crit}	P	n
GCR v. [cATP]_{AQ}	0.14	0.019	0.22	79
GCR v. [tATP]_{AQ}	0.17	0.43	0.32	36
GCR v. [cATP]_I	0.05	0.28	0.85	17
GCR v. [tATP]_I	0.04	0.19	0.89	16
GCR v. CR_{AQ}	0.27	0.27	0.10	39
GCR v. CR_I	0.10	0.27	0.56	39
CR_{AQ} v. [cATP]_{AQ}	0.031	0.27	0.85	38
CR_{AQ} v. [cATP]_I	-	0.72	-	6
CR_{AQ} v. [tATP]_{AQ}	0.090	0.33	0.66	26
CR_{AQ} v. [tATP]_I	-0.20	0.58	0.60	9
CR_I v. [cATP]_{AQ}	-0.11	0.27	0.51	38
CR_I v. [tATP]_{AQ}	0.35	0.72	0.50	6
CR_I v. [cATP]_I	-0.026	0.33	0.90	26
CR_I v. [tATP]_I	-0.49	0.58	0.18	9

3.7.3 Microscopy

3.7.3.1 Microscopic observations were performed on aqueous-phase and interface jar wall specimens, and coupon scrapings from microcosms for which gross observations and [cATP]s indicated that fungal biomass was present. Appendix I, Table I.1 listed 36 specimens examined from 30 microcosms and provided descriptions of the images included in Appendix I.

3.7.3.2 Appendix I, Figure I.1 included 30 micrographs from 28 microcosms.

3.7.3.3 Of the 30 microcosms from which specimens were examined microscopically, 25 (80 %) had unequivocal fungal growth as evidenced by the presence of fungal hyphae (*hyphae* are tubular filaments that make up the vegetative mass of molds), yeast cells, or both.

3.7.3.3.1 The tentative classification of fungal taxa provided in Table H.1 is based on morphology [55] (Figure 54 illustrated the primary morphological properties used to identify fungi):

- Width and length of cells in hyphae.
- Septation between cells in hyphae.
- Location and distribution of spores.
- Dimorphism – dimorphic fungi can appear as molds or yeasts (single cells that reproduce by budding). For dimorphic fungi, the predominant form is typically dictated by temperature – with higher temperatures favoring the yeast form.

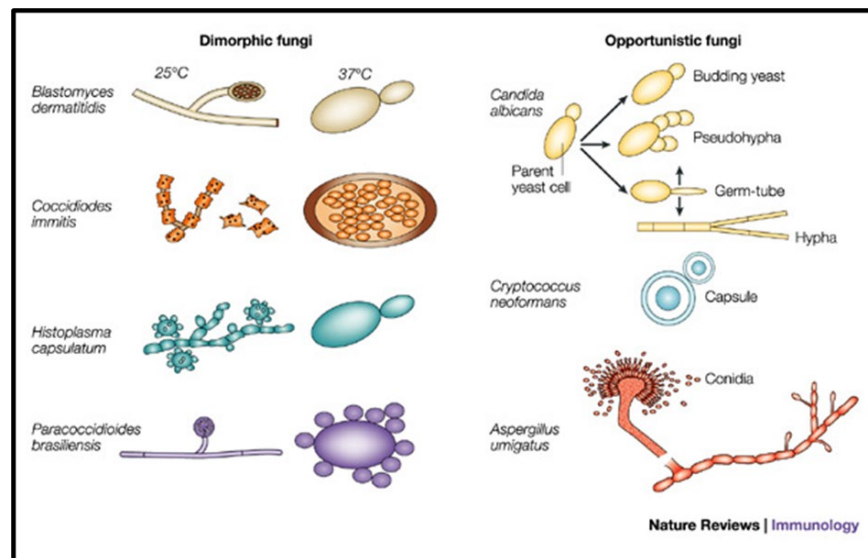


Figure 54. Primary morphological features used to classify molds

(Source: <https://www.bioidea.net/static/media/uploads/nature-rev-LRomani-InfectFungi.jpg>).

3.7.3.3.2 Definitive identification relies on genomic testing. Fungal genomic data was discussed in section 3.7.4.3.4.

3.7.3.4 Table 40 lists the fungal genera and species tentatively identified in the test matrix microcosms and Figure 55 illustrates their taxonomical relationships.

- Figure 55 was a simplified taxonomic map. Unlike lines in phylogenetic trees (*dendograms*), the lines in Figure 54 did not reflect genetic histories from domains through species. The dashed lines at each level indicated that there are taxa within that taxonomic level that were not included in the Figure. For example, there are 100's of *Aspergillus* species of which only

five were listed. Although it was not detected, *Hormoconis resiniae* (now classified as *Amorphotheca resiniae* [56]) was included because it is routinely cited as the predominant fuel-infecting fungal species [57].

Table 40. Tentative classification of fungal taxa identified in test microcosms and listing of the microcosms in which they were observed.

Genus	Species	Microcosms
<i>Aspergillus</i>	<i>fumigates</i>	110, 122, 126, 128
	<i>nidulans</i>	28, 32, 46, 76, 85
	<i>niger</i>	28, 32, 46, 76, 85, 126, 127
	<i>oryzae</i>	3, 41, 45, 61, 67, 70, 78, 79, 86, 93, 99
	<i>terreus</i>	102, 110, 122, 126, 127
<i>Candia</i>	spp.	41, 47, 48, 49, 61, 67, 70, 78, 79, 86, 93, 99
<i>Paracoccidioides</i>	spp.	28, 45, 46, 76, 85, 102, 109, 110, 122, 126, 127

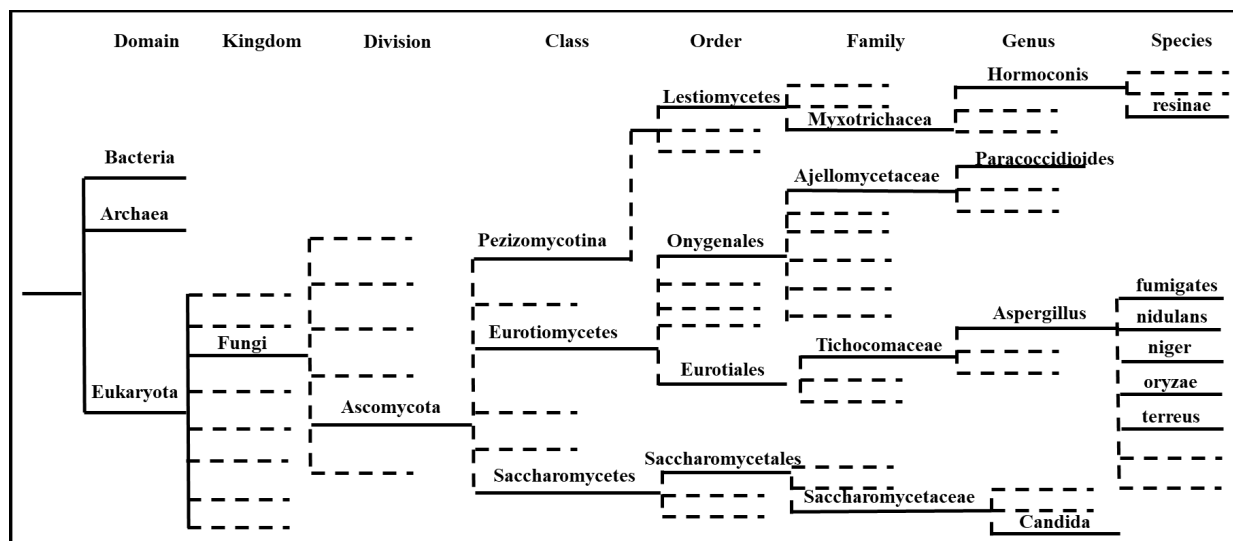


Figure 55. Taxonomic tree of fungal taxa detected in test microcosms.

- 3.7.3.4.1 Except for microcosms 126 and 127 in which *Aspergillus niger* was identified, Table J.1 indicated “*A. nidulans* or *A. niger*.” This uncertainty was reflected in the dual listings in Table 40.
- 3.7.3.4.2 No attempt was made to provide species identifications for fungi tentatively identified as belonging to either *Candida* or *Paracoccidioides* genera.
- 3.7.3.4.3 Figure 56 provided examples of two of the photomicrographs included in Appendix I.

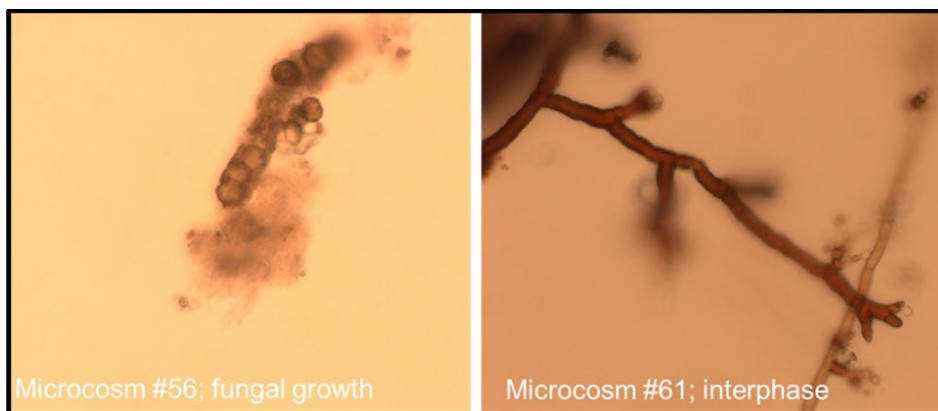


Figure 56. Illustrative microscopic images of fungal growth from microcosms #56 and #61.

3.7.3.4.4 The taxa tentatively identified in Table I.1 were all ubiquitous members of soil microbiomes. Consequently, it was reasonable to speculate that airborne fungal spores (*aerospora*) were introduced into fuel tanks either through vents or with surface runoff introduced through fill-line, spill containment well, overflow return valves.

3.7.4 Genomics

3.7.4.1 Concept

3.7.4.1.1 Although the use of genetic material to identify microbes was pioneered more than a half-century ago [58], 21st century developments in genomic test methodology have made it practical to reliably test fuel and fuel-associated waters [59 and 60].

3.7.4.1.2 At present, there are two relevant categories of genomic tests – quantitative polymerase chain reaction (qPCR) and next generation sequencing (NGS – also referred to as high-throughput sequencing, massively parallel sequencing, or deep sequencing).

- For qPCR testing a short sequence of nucleotides is used as a primer. Depending on the primer selected, qPCR can be used to quantify the population density (gene copies mL⁻¹) of the general microbial population, that of specific taxa (for example the bacterium *Pseudomonas aeruginosa*), or functional groups (for example, sulfate reducing bacteria). ASTM subcommittee D02.14 on Stability, Cleanliness and Compatibility of Liquid Fuels is currently drafting a proposed new *standard practice for quantification of microbial contamination in liquid fuels and fuel-associated water by quantitative Polymerase Chain Reaction (qPCR)*.
- NGS uses the 16S RNA gene for bacteria and 18S RNA gene for fungi. In both cases, the gene contains *conserved* zones (nucleotide sequences that are identical in all bacteria or fungi, respectively) and *hypervariable* zones (nucleotide sequences that are unique to a single type of microbe – operational taxonomic unit – OTU). The 18S RNA region – also known as the *internal transcribed spacer* (ITS) region – in fungi is more hypervariable and therefore preferred for fungal NGS testing.
- Thus, qPCR is a quantitative tool and NGS is a qualitative tool, best used to determine what OTUs are present in specimens or as a semi-quantitative tool to compare the abundance of each OTU relative to the others detected.
- The precision and accuracy of the sequencing data depend on several critical variables.
 - Specimen concentration – typically specimens are either filtered or centrifuged to obtain a mass of cells from which to extract DNA. Given the heterogeneous distribution of microbes in fuels [61], the specimen concentration step can be a substantial source of variation.

- DNA extraction – to be detected, DNA must be separated from the cells from which it originates. Microbial cells differ in the ease with which they are lysed (broken open). Cells that are not lysed will not be detected by genomic test methods.
- Classification – DNA detected by genomic test methods is compared with known OTU DNA profiles stored in databases. The statistics used to match DNA in specimens with DNA profiles in databases is quite complex. Matches are based on percent similarities and can be biased by the types of microbial DNA profiles archived in the metagenome database used. The details are not reported in this document, but specimens from the pooled UST bottoms-waters were sent to two independent labs for 16S and 18S sequencing. The results provided by one lab were clearly erroneous. The list of OTU detected had no similarities to published fuel microbiome profiles. Moreover, it was substantially different from profiling performed in-house at Battelle. This illustrates the importance of using only properly vetted metagenomic software and databases.

3.7.4.1.3 In this project, 16S and ITS sequencing was used to characterize the microbiomes in specimens collected from two UST bottoms-water specimens (Appendix J, Tables J.1 and J.2) and the 21 microcosms listed in Table 41. The ATP-bioburdens in all cases were $[cATP] > 4 \text{Log}_{10} \text{ pg mL}^{-1}$ or $[tATP] > 4 \text{Log}_{10} \text{ pg cm}^{-2}$.

3.7.4.1.4 Specimens were analyzed as described in Section 2.6.6.2.2. The complete data set was provided in Appendix J Tables J.3 through J.24 and Figures J.1 through J.12.

3.7.4.2 Diversity within microcosms

3.7.4.2.1 A total of 139 OTU were detected among 21 microcosms.

3.7.4.2.2 The number of OTU recovered ranged from one (microcosm 76) to 47 (microcosm 40). However, many of these OTU were detected at abundance $< 0.06\%$ repeatability limit as discussed in section 3.7.4.3.6.

- The number of OTU recovered was not related to the ATP-bioburden. Microcosms 3, 36, and 40 had the greatest number of OTU ($S \geq 40$). Microcosms 76, 102, 47, and 47 had the least number of OTU ($S \leq 5$).
- Table 42 compared the aqueous-phase bioburdens from these microcosms. A one-way ANOVA computation determined that $F_{\text{Obs}} = 0.17$, where $F_{\text{crit}[1,4; \alpha = 0.05]} = 7.71$ and $P = 0.72$. This means that there is no significant relationship between the number of OTU detected and the $[cATP]$.
- Shannon-Wiener diversity indices (H) ranged from 0.0 to 2.09 in challenged microcosms and from 0.52 to 1.79 in unchallenged microcosms (Table 43). The value of H increases with the number of OTU detected. $H = 0$ (microcosm 76) indicated that only one OTU was detected.
- The maximum possible Shannon-Wiener diversity index (H_{max}) is simply $\text{Ln } S$ – the natural logarithm of S . It is used to compute *evenness* (E).
- Evenness is an expression of the relative abundances of OTU in a specimen. When all OTU are present in the same proportion, $H = H_{\text{max}}$ and $E (H \div H_{\text{max}} = 1)$.
- Other than microcosms 76, $E_{\text{microcosm}}$ ranged from 0.01 (microcosm 45) to 0.57 (microcosm 102).
- As will be discussed further, below, duplicate specimens from microcosm 45 were tested. The S -values were 5 and 7 for 45A and B, respectively. *Massilia* sp. WG5 (a soil bacterium) accounted for $>98\%$ of the recovered gene copies mL^{-1} in both microcosms. There were four other OTU recovered from microcosm 45A and six others from microcosm 45B.

Table 41. Microcosms specimens tested by 16S and ITS sequencing.

Microcosm #	Sample Source	NGS Analysis
3	aqueous-phase and coupon	16S and ITS
4	aqueous-phase	16S
21	aqueous-phase	16S
28	aqueous-phase	16S and ITS
32	aqueous-phase and coupon	16S
36	aqueous-phase and coupon	16S
40	swab of FRP (in DI water)	16S
40	aqueous-phase	16S
45	fuel-phase	16S, 2 biological replicates
46	sediment	16S
47	aqueous-phase	16S and ITS
48	aqueous-phase and coupon	16S
56	aqueous-phase and coupon	16S
57	steel coupon	16S
76	aqueous-phase and coupon	16S and ITS
78	aqueous-phase and coupon	16S
81	aqueous-fuel interface	16S, 2 biological replicates
102	aqueous-phase and coupon	16S
110	aqueous-phase	16S and ITS
126	aqueous-phase and coupon	16S and ITS
127	aqueous-phase and coupon	16S and ITS

Table 42. ATP-bioburden comparison between microcosms from which greatest and least number of OTU were recovered from aqueous-phase specimens.

Microcosm	S	[cATP] _{AQ}
3	41	4.80
36	45	0.48
40	47	5.17
76	1	N.D. ^a
102	4	3.72
47	5	4.70
57	5	3.82

Note: a) N.D. Not determined.

Table 43. Microbial diversity in samples selected for sequencing – Shannon-Weiner Diversity Index (H), number of OTU (S), maximum possible diversity index (H_{max}), and evenness (E).

Microcosm	H	S	H _{max} (Ln S)	E	Microcosm	H	S	H _{max} (Ln S)	E
<u>3</u> ^a	1.77	41	3.71	0.48	48	1.17	17	2.83	0.41
4	0.68	9	2.20	0.31	56	0.60	6	1.79	0.34
21	0.53	11	2.40	0.22	57	0.03	5	1.61	0.02
28	0.78	12	2.48	0.32	76	0	1	0	1
32	0.17	7	1.95	0.09	78	1.16	12	2.48	0.47
36	2.10	45	3.81	0.55	81A	0.79	10	2.30	0.35
40	1.95	47	3.85	0.51	81B	0.73	14	2.64	0.28
45A ^b	0.01	5	1.61	0.01	102	0.43	4	1.39	0.31
45B	0.02	7	1.95	0.01	110	0.88	8	2.08	0.42
46	0.76	8	2.08	0.37	126	2.07	38	3.64	0.57
47	0.49	5	1.61	0.31	127	0.64	32	3.47	0.19

Notes:

- a) Uninoculated (unchallenged) microcosms – microcosm number is underlined.
- b) Duplicate specimens were collected from microcosms 45 and 81. Diversity statistics are reported as 45A and 45B, and 81A and 81B for the respective replicate A & B specimens.

3.7.4.2.3 One-way ANOVA was used to determine the impact of the population source (challenge population or indigenous growth) on S, H, H_{max}, and E, where S was the number of OTU in the specimen, and E was evenness as computed from $H \div H_{max}$ (Table 44).

Table 34. Population diversity differences between challenged and unchallenged microcosms (F_{crit}[1,19; α = 0.05] = 4.38).

Parameter	F _{obs}	P-value
S	1.40	0.25
H	0.69	0.42
H_{max}	0.43	0.52
E	0.54	0.47

- There were no significant differences in the diversity parameters between challenged and unchallenged microcosms. This means that by T_{wk12} microbial diversity in unchallenged microcosms was comparable to that in challenged microcosms. This similarity might explain that corrosion ratings in challenged and unchallenged microcosms, at the fuel-aqueous-phase interface and in the aqueous-phase were statistically indistinguishable at T_{wk12}.

3.7.4.3 Microbiome taxonomy

3.7.4.3.1 The previous section focused on the statistics of diversity in the microcosms. This section will report the types of microbes detected.

3.7.4.3.2 Tables J.3 through J.24 listed the taxa reported from each specimen. The Krona plots in Figures J.1 through J.11 show in graphic form the same information listed in Tables J.3 through J.24.

- Krona plots provide a visual image of the OTU detected, their relative abundances and taxonomic relationships [62].
- As illustrated in Figure 57, each ring represents a different taxonomic level – ranging from domain (ring closest to *root*) to strain or biovariant (a subdivision of strain). The percentage of the circle shaded by a taxon’s ring (for example, in Figure 57, at the phylum level, Proteobacteria account for ~64 % of the ring, Firmicutes account for ~34 %, and “2-more” account for the remaining ~2 %) indicates its relative abundance.

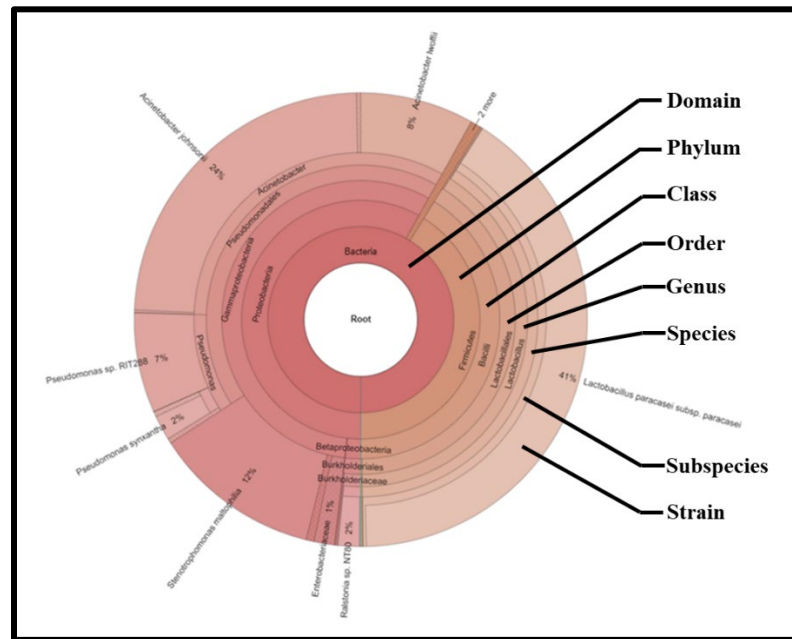


Figure 57. Krona plot for microcosm 40, illustrating significance of each ring.

3.7.4.3.3 Overall, *Acinetobacter johnson*, *Lactobacillus acidipiscis*, and *L. paracasei* were recovered most commonly, although their relative abundances, when present, ranged from <0.1 % to > 88 % (Table 45). In six of the microcosms tested by 16S and ITS (5, 56, 57, 76, 102, and 110), a single OTU represented >99% of the total microbiome. Moreover, in four of these six microcosms (57, 76, 102, and 110), the dominant taxon was *Pseudomonas sp.*

3.7.4.3.4 There were apparent qualitative differences between challenged and unchallenged microcosms.

- Table 46 listed the taxa most commonly detected in specimens from challenged microcosms.
 - One or more *Lactobacillus* spp. were detected in each of the challenged microcosms.
 - The fungus *Aspergillus fischeri* was detected in five of the seven challenged microcosms tested by 16S and ITS.

Table 45. Relative abundances of the three most commonly detected taxa in microcosms tested by 16S and ITS. Values are percentages.

Microcosm	<i>Acinetobacter johnsonii</i>	<i>Lactobacillus acidipiscis</i>	<i>Lactobacillus paracasei</i>
4	0.01	0.29	0.31
21	-	10.91	86.00
28	-	57.42	40.79
36	41.22	-	-
40	23.90	-	40.80
45 ^a	0.04	-	0.05
46	-	55.21	43.65
47	0.02	81.25	-
48	0.05	52.46	30.09
56	0.04	-	-
78	-	61.01	-
81 ^a	0.02	8.85	74.28
102	-	0.01	76.54
126	23.50	-	-
127	4.55	0.02	88.17
# microcosms	10	10	10
% microcosms	50	50	50

Note: a) values are averages between duplicate specimens.

- Additional microbial diversity observations at the species level:
 - *Lactobacillus* spp. were the most prevalent in all of the challenged microcosms with highest percentage of relative abundance ranging from 52 % to 76 %.
 - *Bacillus* was the second most abundant genus in challenged microcosms. Its relative abundance was greatest (31 %) in microcosm 4 – B0 ULSD treated with CFI and CA.
 - Species of the petroleum diesel fuel degrading genus *Oerskovia* were present only in microcosm 48 – B5 ULSD with glycerin added.
 - Species of *Porphyromonas* were found in 3 of 7 microcosms.

Table 46. List of microbial taxa detected in specimens from challenged microcosms. Numbers indicate percentage of relative abundance. Colors indicate the OTU's relative abundance - high (≥ 5 % shades of blue, darkening with increased %) to low (red).

Genus and species/ Microcosm #	4	21	28	32	46	48	81
<i>Acinetobacter johnsonii</i>	0.01					0.05	0.03
<i>Acinetobacter lwoffii</i>						0.02	
<i>Aspergillus fischeri</i>	0.09	0.01	0.06			0.02	0.02
<i>Bacillus circulans</i>	31.1	1.97	0.18		0.08	10.55	5.06
<i>Haemophilus parainfluenzae</i>		0.01	0.06				
<i>Lactobacillus acidipiscis</i>	0.29	10.91	0.06	0.12	0.08	52.46	17.69
<i>Lactobacillus casei</i>	0.07	0.04	0.04		0.04	0.05	0.06
<i>Lactobacillus paracasei</i>	0.31	0.27	0.19	0.02	0.16	30.09	76.54
<i>Lactobacillus rhammosus</i>	0.1	0.8	0.11	0.1	0.15	0.56	0.55
<i>Lactococcus lactis subsp. lactis</i>							0.01
<i>Oerskovia sp.</i>						6.13	
<i>Porphyromonas sp.</i>		0.01	0.08				0.01
<i>Pseudomonas sp.</i>			0.01	0.01		0.03	
<i>Stenotrophomonas maltophilia</i>				0.01			
<i>Streptococcus cristatus</i>							0.01

- Table 47 listed the taxa most commonly detected in specimens from unchallenged microcosms.
 - No OTU was present in all tested microcosm.
 - The dominant or most prevalent organisms by microcosm were common hydrocarbon degrading species of *Acinetobacter*, *Lactobacillus*, and *Pseudomonas*.
 - *Pseudomonas* spp. were recovered in specimens from eight of the 13 microcosms on which NGS testing was performed. Various *Pseudomonas* spp. are known to be hydrocarbon degraders (i.e., they are *hydrocarbonoclastic* – using hydrocarbons as their sole carbon food source) [63].
 - *Acinetobacter* spp. were recovered from seven and *Lactobacillus* spp. from five.
 - *Methylobacterium* sp. was recovered from microcosm 56. Members of this genus are known to corrode copper. In microcosm 56 – which contained B0 LSD, glycerin, and CA – the *Methylobacterium* OTU accounted for 99 % of the microbiome.
 - None of the fungal taxa identified tentatively in 3 were detected by ITS.
- Although there were no significant differences in population diversity and a marginal difference in average [cATP]_{AQ}, the taxa in T_{wk12} unchallenged differed substantially from those in challenged microcosms.
- The two most likely sources of the unchallenged microcosm bioburdens were the fuel samples and laboratory air.

Table 47. List of microbial taxa detected in specimens from unchallenged microcosms. Numbers indicate percentage of relative abundance. Colors indicate the OTU's relative abundance - high (≥ 5 % shades of blue, darkening with increased %) to low (red).

Species/ Microcosm #	3	36	40	45	47	56	57	76	78	102	110	126	127
<i>Acinetobacter sp.</i>		38	33	0.02	0.002	0.004						30	6
<i>Bacillus coagulans</i>		0.02											
<i>Blastomonas sp.</i>	0.1												
<i>Caballeronia zhejiangensis</i>		0.08	0.03				0.02					0.02	
<i>Cronobacter turicensis</i>		0.27	0.4									0.37	0.12
<i>Cutibacterium acnes</i>												0.02	0.02
<i>Edaphobacter aggregans</i>	0.06												
<i>Enterobacter sp.</i>		0.8	0.67										0.15
<i>Ensifer sp.</i>									0.24				
<i>Flavobacterium sp.</i>		0.02										0.1	
<i>Gemella sanguinis</i>			0.14										
<i>Hammondia hammondi</i>	0.42											0.11	
<i>Klebsiella aerogenes</i>		0.67	0.38									0.8	0.04
<i>Lactobacillus acidipiscis</i>			40.94		0.09				0.06	0.01			88.45
<i>Lysinibacillus xylanilyticus</i>		0.04											
<i>Leifsonia aquatica</i>	0.03												
<i>Leptothrix cholodnii</i>	0.02												
<i>Massilia sp.</i>				99									
<i>Mesorhizobium sp.</i>	3.83				0.02				0.16				
<i>Methylobacterium sp.</i>	0.33				19	99			0.33	0.2			
<i>Methyloversatilis discipulorum</i>	0.35												
<i>Mycolicibacterium mucogenicum</i>	0.83												
<i>Novosphingobium nitrogenifigens</i>	1.64												
<i>Paraprevotella clara</i>			0.06										
<i>Pantholops hodgsonii</i>	0.08												
<i>Paraburkholderia fungorum</i>	13.19												
<i>Paraburkholderia phytofirmans</i>	1.12												
<i>Pelomonas sp.</i>		0.5	0.12									0.34	0.02
<i>Penicillium solitum</i>													0.06
<i>Porphyromonas sp.</i>		0.88	0.48	0.02								0.12	
<i>Pseudomonas sp.</i>		17.38	9.66				1	100		99.79	99.79	54.1	1.96
<i>Prevotella nanceiensis</i>		0.08											
<i>Ralstonia sp.</i>	53.2	2.3	1.63									1.4	0.19
<i>Reyranella massiliensis</i>	0.12												
<i>Sphingomonas sp.</i>	5.62	0.09										0.03	0.04
<i>Sphingopyxis sp.</i>	0.08												
<i>Stenotrophomonas maltophilia</i>						0.06						12.04	2.72
<i>Variovorax paradoxus</i>	1.52												

- Had laboratory air – introduced during microcosm sampling and other manipulations during which microcosms were uncovered – been the source of microbes infecting the unchallenged microcosms, population profiles in the two types of microcosms would likely have been substantially more similar.
- As discussed at considerable length in Passman, 2013 [11], microbes that contaminate fuel early in the distribution process (i.e., in refinery tanks) can remain dormant and be transported throughout the fuel channel.

- In challenged microcosms, the microbes in the inoculum were likely to have been sufficient to prevent those introduced as fuel contaminants from proliferating.
 - In unchallenged microcosms, absent the competition from the inoculum population, microbes settling from the fuel into the aqueous-phase had an opportunity to proliferate.
 - In future studies in which the role of microbes will be considered, all fluids should be filter-sterilized (i.e., pressure filtered through a 0.1 μm filter) before use.
- 3.7.4.3.5 Comparison of the OTU detected in specimens from challenged T_{wk12} microcosms and the challenge microbiome indicated that they were quite dissimilar. As illustrated in Figure 58, T_{wk12} microbiomes in challenged microcosms were no more similar to the initial challenge microbiome than they were to T_{wk12} unchallenged microbiomes. Each was <2 % similar to the other.
- Population succession in closed systems is well documented [64]. Invariably, one or more taxa become more predominant and others less.
 - In extreme cases, taxa that represent negligible fraction of the original microbiome become dominant over time.
 - It is rare for taxa undetected initially to become so dominant as to eclipse the initially predominant taxa.
 - The rationale for including genomic testing in this study was to determine if there was any clear relationship between the types of microbes present and corrosion aggressiveness. In-depth monitoring of population dynamics was beyond the project's scope. Consequently, there were insufficient data collected to further examine how populations in challenged and unchallenged microcosms evolved during the 12-week incubation period.
- 3.7.4.3.6 As noted above, duplicate specimens from microcosms 45 and 81 were collected and tested by 16S and ITS. The objective was to get some idea of the variability between replicate analyses.
- Although their diversity statistics (Table 44) were similar, the duplicate microcosm 45 specimens were quite different from one another at both the genus and species levels (Figure 59a). Of a total of nine OTU detected in microcosm 45 specimens, only 3 were detected in both. However, *Massilia* sp. (a Gram-negative, rod-shaped, bacterial species belonging to the beta-proteobacteria class) accounted for > 99 % of the total microbiome in both specimens. Figure J.5 (Appendix J) shows Krona diagrams that illustrate the weighted relative abundances of OTU recovered from the two replicate samples.
 - In contrast to the microcosm 45 duplicate specimens, those from microcosm 81 were quite similar. Specimens 81A and 81B had 2 and 4 unique OTU, respectively, but nine of 15 OTU were detected in both specimens. In particular, *L. paracasei* plus *L. acidipiscis* accounted for 93 % and 94 %, of the total microbiome in microcosms 81A and 81B respectively, and *B. circulans* represented an additional 6 % and 5 %, respectively, so that the three OTU represented $\geq 99\%$ of microbiomes in the two replicate specimens. Figure J.9 (Appendix J) shows Krona diagrams that illustrate the weighted relative abundances of OTU recovered from the two replicate samples.
 -
 - These observations highlighted two challenges with 16S and ITS testing:
 - The sources of variability are still being evaluated [59] and can include:
 - Heterogeneous distribution of bioburden in sample source,
 - Heterogeneous distribution in sample,
 - Differences in cell lysis efficacies among replicate specimens,

- Differences in software analysis of DNA – assigning identical DNA to different OTU.
- Per the last bullet above, the reliability of OTU assignment remains to be fully validated. As ecological databases grow, classifications will become more reliable.

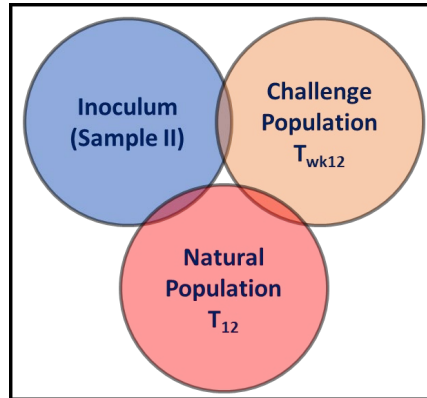


Figure 58. Venn diagram illustrating differences among the three microbial populations recovered from microcosms.

The overlap among the original challenge population (Inoculum), the population in challenged microcosms at T_{wk12}, and the population that developed in unchallenged microcosms at T_{wk12} was <2 %.

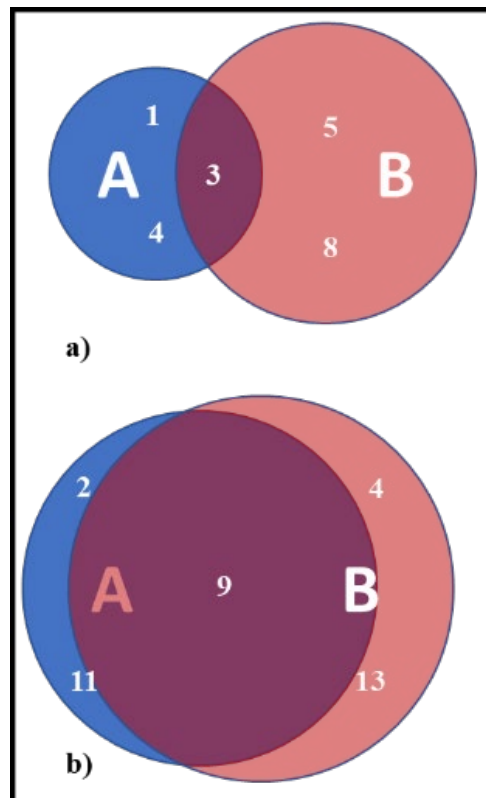


Figure 59. Venn diagrams of taxonomic profile similarities between replicate specimens – a) microcosm 45; b) microcosm 81.

3.8 CHEMISTRY

3.8.1 Sulfur Concentration

3.8.1.1 The fuel samples received at Battelle were mislabeled. The LSD was identified as ULSD and vice versa. In June 2018, specimens were sent to a third part laboratory (ALS, Houston, TX) for testing. The sulfur concentration of fuel originally labelled as LSD was $4 \mu\text{g g}^{-1}$ and that of the fuel labelled as ULSD was $274 \mu\text{g g}^{-1}$. The respective fuel containers were relabeled, and all subsequent testing including all microcosms testing was performed with correctly identified fuels. The original intention was to perform the partition coefficient studies (3.2) in LSD. Performing them in ULSD had no impact on subsequent testing.

3.8.2 Vapor-phase Low Molecular Weight Organic Acids

3.8.2.1 The decision to use this particular style of acetic acid Dräger tubes was unfortunate. These tubes were designed to detect gas or vapor-phase acetic acid in air that was actively drawn through the tube.

3.8.2.1.1 For use, both ends of the tube are broken off, one end is inserted into a hand-held vacuum device, and air is drawn into the tube at a known flow-rate for a known time interval.

3.8.2.1.2 The graduations on the tube indicate the acetic acid concentration in a known volume of air.

3.8.2.1.3 Figure 60a illustrated acetic acid Dräger tube design (image from Gastec No. 81 Instructions for acetic acid detector tube, Gastec Corporation, Kanagawa, Japan). Figure 60b illustrated the color change that occurs when acetic acid contacts the indicator medium. The tube in this Figure, indicates that the acetic acid concentration in the sampled air was $\sim 7 \text{ mg m}^{-3}$ (ppmv).

3.8.2.1.4 As shown in Figure 7, there was no active air-flow through the Dräger tubes suspended into the test microcosms. It was erroneously assumed that acetic acid would diffuse through the fuel phase and into the tube, despite the absence of any air flow. At T_{wk12} , all of the Dräger tubes remained pink. If low molecular weight organic acids (LMOA) such as acetic acid were produced, they remained undetected. We conclude that the Dräger tubes were used incorrectly, and results are therefore meaningless.

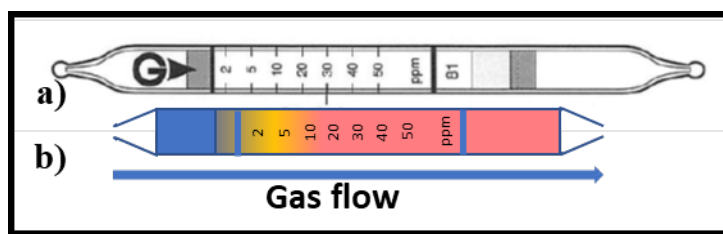


Figure 60. Acetic acid Dräger tube -a) schematic from manufacturer's instruction sheet; b) simulation of color change when acetic acid concentration is $\sim 7 \text{ ppmv}$ (mg m^{-3}) in sampled air.

3.8.3 Aqueous-phase Low Molecular Weight Organic Acids

3.8.3.1 In fuel systems that include a free-water phase, low molecular weight organic acids (LMOA) can be produced either through abiotic chemical reactions or as microbial metabolites.

3.8.3.1.1 When LMOA are *biogenic* – produced as microbial metabolites – the various C₂ through C₆ carboxylic acids are produced in the course of glucose metabolism via the citric acid cycle (AKA the *Krebs Cycle*, or *Tricarboxylic Acid Cycle*). These include: acetic (C₂H₄O₂), pyruvic (C₃H₄O₂), malic, (C₄H₉O₅), fumaric (C₄H₄O₄), succinic (C₄H₆O₄), α-ketoglutaric (C₅H₆O₅), isocitric (C₆H₈O₇), cis-aconitic (C₆H₆O₆), and citric (C₆H₈O₇) [65]. The LMOA are classified as *weak acids*. A weak acid is one that partially dissociates into ions in aqueous solutions. For example, acetic acid dissociates to acetate (C₂H₃O₂⁻) and a proton (H⁺):



- Weak organic acids underlying biofilms can be directly corrosive [53] so acid corrosion can be caused by the accumulation of LMOA formed from the reactions described above, or a combination of both [65, 66].
- If the only or primary LMOA present is acetic, its creation can be either abiogenic, biogenic, or both. Members of the genera *Acetobacter* and *Gluconobacter* ferment ethanol to acetic acid through a three-step metabolic pathway [66]. Additionally, ethanol can be oxidized to acetic acid abiotically.

3.8.3.1.2 Abiotic oxidation of fuel additives or fuel molecules can also generate LMOA. For example, methane can be oxidized to form formic acid.

3.8.3.2 To determine whether LMOA were accumulating in the test microcosms' aqueous-phases, and whether such accumulation was primarily biogenic, a subset of microcosms was tested for LMOA.

3.8.3.2.1 The LMOA data are presented in Table 48.

3.8.3.2.2 All of the tested microcosms had acetic acid concentrations $\geq 33 \text{ mg mL}^{-1}$.

3.8.3.2.3 The three microcosms (77, 86, and 96) in which the acetic acid concentrations were $\geq 3,000 \text{ mg mL}^{-1}$ had been treated with ethanol and microbially challenged. They varied with regard to fuel grade and presence of FAME.

Table 8. LMOA detected in aqueous-phase specimens from selected microcosms sampled at T_{wk12}.

Acid (mg mL ⁻¹) ^a	Microcosm									
	15	21	32	35	39	53	77	79	86	96
Acetic (C ₂)	96	40	152	33	111	45	3126	214	3756	3818
Propionic (C ₃)	63	52	64	<0.1	0	64	62	51	209	107
Isobutyric (C ₄)	0.01 ^b	0.01	0.01	<0.01 ^c	0	0.01	0.01	<0.01	99	16
Butanoic (butyric - C ₄)	0.01	0.01	0.84	0.01	0.01	7.1	3.0	0.01	164	47
3-Methyl butanoic (isovaleric - C ₅)	1.5	<0.01	0.71	<0.01	0.01	9.71	<0.1	<0.01	139	35
Pentanoic (valeric - C ₅)	0.01	0.01	3.08	0.01	0.01	9.4	0.55	0.01	196	54
4-Methyl pentanoic acid (C ₅)	24.65	14.07	28.77	<0.01	13.76	34	22	14	202	71
Hexanoic (C ₆)	8.3	-8.8 ^d	11.45	<0.01	0.01	14	2.2	0.01	265	77
Heptanoic (C ₇)	48.25	23.58	59.88	19.87	27.6	44	32	<0.1	303	119

Notes:

- Only LMOA detected in one or more microcosms are listed. Those likely to be biogenic are highlighted in **bold font**.
- The method's limits of detection and quantification were 0.001 mg mL⁻¹ and 0.01 mg mL⁻¹, respectively. Detection of the analyte in this range was reported as *trace* and listed as 0.01 mg mL⁻¹.
- If an analyte was not detected, it was reported as below the detection limit – <0.01 mg mL⁻¹.
- Analytical artifact.

3.8.3.2.4 Microcosm 15 was also treated with ethanol, but it had not been challenged. The acetic acid concentration in his microcosm was 96 mg mL⁻¹.

3.8.3.2.5 Acetic acid represented from 20 % to 96 % of the LMOA total.

- It was 20 % of the total 230 mg LMOA mL⁻¹ detected in microcosm 53 and 96 % of the total 3,200 mg LMOA mL⁻¹ detected in microcosm 77.
- Microcosm 53 was B0 LSD and microcosm 77 was B5 ULSD + 10,000 ppm ethanol. Both microcosms had been microbially challenged. There were insufficient microcosms tested for LMOA to determine whether either the fuel grade or presence of FAME affected the results.

3.8.3.2.6 Microcosms 21, 35, and 53 all had <100 mg acetic acid mL⁻¹. Although all three had been intentionally challenged, none were dosed with ethanol. All three were B0 LSD. However, per 3.6.3.2.3, neither fuel grade nor FAME appeared to be relevant factors.

3.8.3.2.7 The only controlled factor difference between the microcosms with >3,000 mg acetic acid mL⁻¹ and those with <160 mg acetic acid mL⁻¹ was the presence of ethanol and microbes. This observation supports the hypothesis that acetic acid creation is linked to microbial action on ethanol contamination in diesel fuel UST.

3.8.3.2.8 All of the microcosms except 35 and 39 (both microbially challenged, B0 ULSD with no ethanol added) had ≥3 LMOA that were Krebs cycle byproducts (3.8.3.1.1).

3.8.3.2.9 In most of the microcosms the concentration of abiogenic acids (i.e., 4-Methyl pentanoic acid + hexanoic + heptanoic acid) was >40 mg mL⁻¹.

- The three microcosms with <40 mg abiogenic acids were 21, 32 and 79.

- Microcosm 21 contained B0 LSD + glycerin and microbial challenge.
 - Microcosm 32 contained B5 LSD + glycerin, microbes, CFI and FRP.
 - Microcosm 79 contained B5 ULSD, but neither glycerin nor microbial challenge.
- There were no universally common controlled variables among the six microcosms with ≥ 50 mg abiotic acid mL^{-1} other than none contained either CA or CI.
- 3.8.3.2.10 The data suggest that LMOA were both produced in and partitioned into the aqueous-phase. The former was likely through microbial activity. The latter was abiotic. However, there were insufficient data to support an unequivocal statement beyond noting the near universality of LMOA in aqueous-phase specimens.
- 3.8.3.2.11 There were no T_0 , $T_{\text{wk}4}$ or $T_{\text{wk}9}$ data against which to compare the $T_{12\text{wk}}$ acid concentrations. Results from early in the study would have helped to differentiate between partitioning and acid creation.
- 3.8.3.2.12 Comparison of total LMOA concentrations ([LMOA]) and $T_{\text{wk}12}$ coupon corrosion ratings (CR) on aqueous-phase and interface surfaces indicated that there were no significant correlations between either CR_{AQ} or CR_{I} and [LMOA] (Figure 61). The critical value of r was 0.55 and the P -values for CR_{AQ} and CR_{I} versus [LMOA] were 0.88 and 0.68 respectively.
- 3.8.3.2.13 A limited number of microcosms were tested for LMOA at T_0 , $T_{4\text{w}}$, $T_{9\text{w}}$, and $T_{12\text{w}}$. Additionally, 28 microcosms were tested at $T_{9\text{w}}$ and $T_{12\text{w}}$. The data from Appendix H, Tables H.2 and H.3 are plotted in Figure 62 and show that 25 of 28 samples tested (89%) had measurable concentrations of acetic acid at $T_{12\text{w}}$. Also, 13 of 28 samples (46%) had C_3 to C_7 organic acids at $T_{12\text{w}}$. In many, but not all of these microcosms, LMOA concentration generally increased with time. Acetic acid concentration increased from $T_{9\text{w}}$ to $T_{12\text{w}}$ in 20 of 27 samples tested (74%), whereas acetic acid decreased in only 5 of 27 samples (19%) over the same time period. Acetic acid (a C_2 acid) formed earlier than C_3 to C_7 LMOA in 13 of 29 samples (45%) containing acetic acid at $T_{9\text{w}}$. However, among 29 microcosms in which LMOA with $C_{>2}$ were detected concurrently with acetic acid at $T_{12\text{w}}$, only two (7%) had LMOA with $C_{>2}$ at $T_{9\text{w}}$. Acetic acid formation nearly always preceded or accompanied heavier LMOA formation.

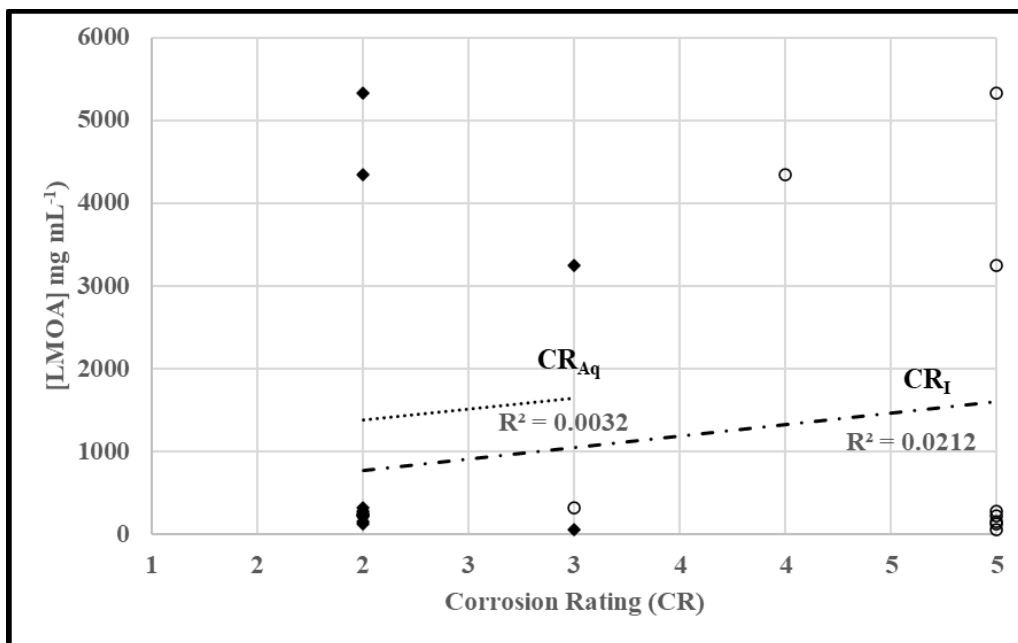


Figure 61. Relationship between aqueous-phase and interface corrosion coupon corrosion ratings and [LMOA] – ♦ - CR_{AQ}; ° - CR_I.

3.8.4 Aqueous-phase alcohols

3.8.4.1 The same ten samples analyzed for LMOA were also analyzed for alcohol (methanol, ethanol, and glycerol). Table 49 presented the alcohol data.

3.8.4.2 Ethanol was detected in all ethanol-treated microcosms.

3.8.4.3 Glycerol ($\geq 150 \text{ mg mL}^{-1}$) was detected in all glycerol-treated microcosms. Trace concentrations of glycerol (0.19 mg mL^{-1} to 1.4 mg mL^{-1}) were detected in microcosms to which glycerol had not been added intentionally.

3.8.4.3.1 Among the microcosms with traces of glycerol only microcosm 77 had been treated with FAME.

3.8.4.3.2 It was most likely that glycerol detected in aqueous-phase specimens had partitioned from the fuel-phase. Again, there were insufficient samples tested to support any unequivocal statement.

Table 49. Methanol, ethanol, and glycerol in selected microcosm aqueous-phase specimens at T_{wk12}.

Analyte (mg mL ⁻¹)	Microcosm									
	15	21	32	35	39	53	77	79	86	96
Methanol	0	0	2.1	0	0	0	0	0	0	0
Ethanol	30	0	0	0	0	0	25	0	16	23
Glycerol	190	0.36	170	1.4	150	0.19	1.2	330	160	210

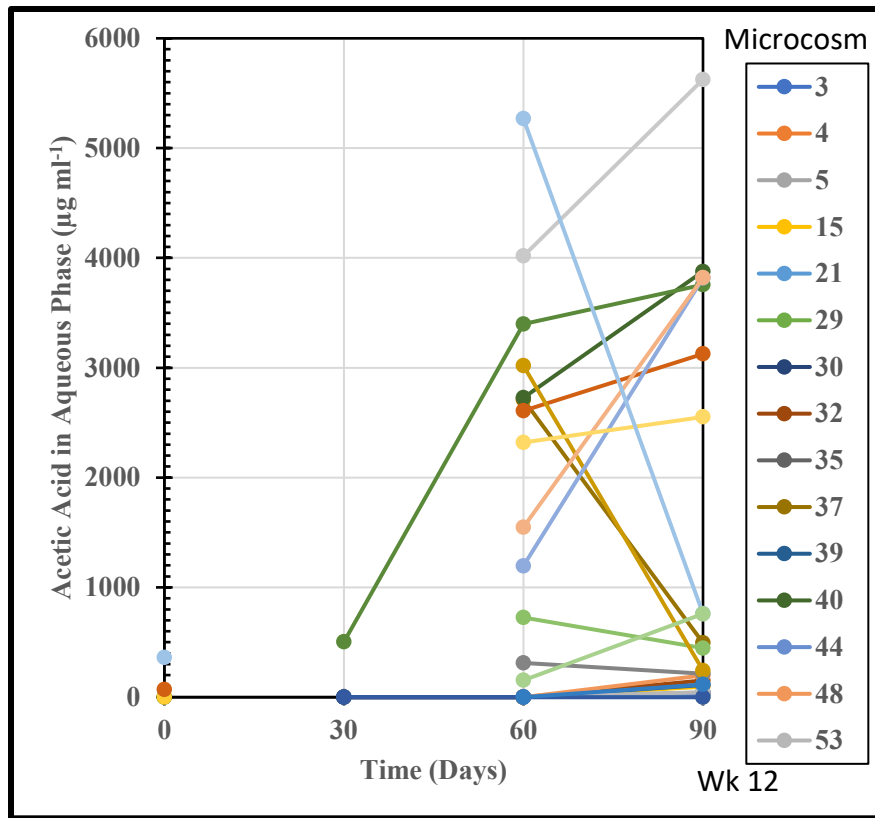


Fig 62. Acetic acid concentration as a function of microcosm incubation time.

3.8.5 Surfactant

3.8.5.1 As defined in ASTM D7261 [16] Surfactants are surface active materials (or agent) “that could disarm (deactivate) filter separator (coalescing) elements so that free water is not removed from the fuel in actual service.” Surface active materials are commonly organic molecules that have a polar (*hydrophilic* – “water loving”) head and a non-polar (*hydrophobic* – “water hating”) tail (Figure 62a). When fuel, water, and surfactant molecules are present in a vessel, the surfactant molecules encapsulate water into droplets (*micelles*) (Figure 62b) and create invert emulsions (water micelles in fuel – Figures 62c and 62d). *Biosurfactants* are surfactants produced by organisms.

3.8.5.1.1 There are 1,000s of biosurfactants [67].

3.8.5.1.2 Common biosurfactants include lipopeptides and glycolipids [68].

3.8.5.2 The presence of surfactants in fuel is most commonly determined by testing the ease with which fuel and water separate after having been mixed. ASTM D7261 [16] uses a separometer to homogenize fuel and water, and then determine separability on a scale of 0 to 100. ASTM D7451 [17] is a visual rating method in which 80 mL of test fuel and 20 mL water (or other aqueous solution) are placed into a graduated tube, mixed by shaking, and permitted to settle. Fuel haze, the degree of phase separation, and the interface appearance are assigned scores.

3.8.5.3 Twenty-eight microcosms were tested by both ASTM D7261 and ASTM D7451 for the presence of surfactants in fuel-phase specimens using equipment donated by Emcee Electronics (Venice, FL). The results were presented in Table 50. Table 50a included the data from ULSD microcosms and Table 50b included the data from LSD microcosms. All tested microcosms had an aqueous-phase.

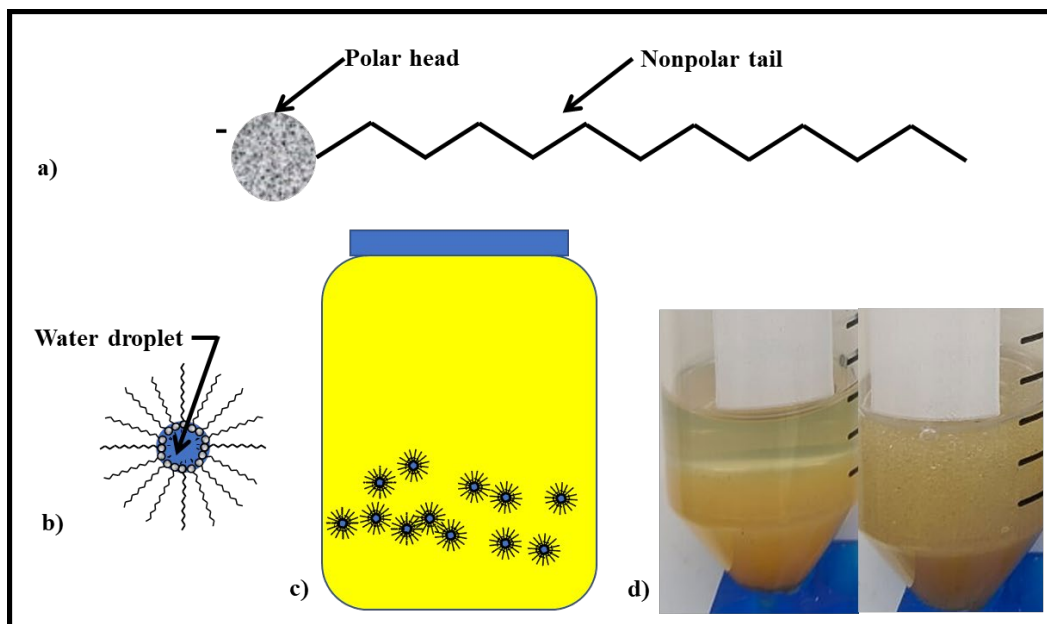


Figure 62. Surfactants – a) schematic of surfactant molecule showing polar head and nonpolar tail; b) schematic of invert-emulsion micelle showing polar heads encapsulating water droplet and nonpolar tails extending into the medium (i.e., fuel); c) schematic of invert emulsion micelles dispersed in fuel; d) photo of 10 mL each fuel and water – left: before shaking; right: 24h after shaking (note stability of invert emulsion).

3.8.5.4 Surfactant data from ULSD specimens were compared against those from LSD specimens. A summary of the ANOVA statistics was provided in Table 51.

3.8.5.4.1 The D7261 DSEP ratings were significantly greater in ULSD than in LSD – indicating that, in general, water separated more readily from ULSD than LSD.

3.8.5.4.2 Corroborating the D7261 data, D7451 fuel haze ratings were an average of 2 points greater in LSD (5 ± 1) than in ULSD (3 ± 1).

3.8.5.4.3 Notwithstanding substantial variability among microcosms, the presence of FAME (i.e., B5) degraded water separability significantly ($F_{\text{calc}} = 9.7$; $F_{\text{crit}}[\text{df } 1,26; \alpha = 0.05] = 4.24$; $P = 9.7E-5$).

- DSEP in B0 ULSD = 70 ± 29 and in B5 ULSD = 20 ± 35 .
- DSEP in B0 LSD = 16 ± 24 and in B5 LSD = 0.0 ± 0.00 .

3.8.5.4.4 Among D7451 properties, the fuel-water separation (SR_{F-W}) and interface condition ratings (CoR_i) were significantly better in ULSD than in LSD. This is not surprising as LSD has more polar organic molecules than does ULSD.

Table 50a. Fuel-water separability properties in microcosm ULSD.

Microcosm	Fuel Grade	D7261		D7451		
		DSEP	Water (mL)	Haze	SR _{F-W} ^a	CoR _I ^b
1	B0 ULSD	94	19	3	3	1b
3	B0 ULSD	96	9.5	2	2	1b
4	B0 ULSD	92	9.5	2	2	1b
5	B0 ULSD	81	10	2	2	2
6	B5 ULSD	0	<5	6	3	4
10	B5 ULSD	0	8.5	2	3	3
11	B0 ULSD	0	8	6	3	3
35	B0 ULSD	97	9.5	2	2	1b
37	B0 ULSD	93	10	3	3	2
99	B0 ULSD	69	9.5	3	2	1b
100	B0 ULSD	52	8.5	3	2	4
103	B0 ULSD	75	9	2	2	3
106	B0 ULSD	54	9	3	2	2
111	B5 ULSD	61	8	4	3	4
AVG ± s		62 ± 37	9 ± 4	3 ± 1.4	2.4 ± 0.51	2 ± 1

Notes:

- a) SR_{F-W} – Fuel-water separation rating.
- b) CoR_I – Interface condition rating.

Table 50b. Fuel-water separability properties in microcosm LSD.

Microcosm	Fuel Grade	D7261		D7451		
		DSEP	Water (mL)	Haze	SR _{F-W} ^a	CoR _I ^b
17	B0 LSD	0	7.5	6	3	4
29	B0 LSD	0	7.5	6	3	4
52	B0 LSD	0	9	5	3	2
53	B0 LSD	45	10	5	3	3
54	B0 LSD	43	9.5	5	3	3
58	B0 LSD	0	9	5	3	3
64	B5 LSD	0	9	5	2	3
82	B0 LSD	0	26	2	3	2
83	B0 LSD	0	8.5	6	3	3
91	B5 LSD	0	8	6	3	4
96	B5 LSD	0	7	6	3	4
116	B0 LSD	54	10.5	5	3	3
123	B5 LSD	0	5	6	2	4
128	B5 LSD	0	8.5	6	2	3
AVG ± s		10 ± 20	10 ± 4.9	5 ± 1.1	2.8 ± 0.43	3.2 ± 0.70

Notes:

- c) SR_{F-W} – Fuel-water separation rating.
- d) CoR_I – Interface condition rating.

Table 51. ANOVA summary – impact of fuel grade on fuel-water separability properties

(F_{Crit}[df 1,26; α = 0.05] = 4.22).

Parameter	F _{calc}	P
D7261 DESP	21.00	9.70E-05
D7451 -Water (mL)	0.069	0.79
D7451 - Fuel Haze	22	6.80E-05
D7451 - SR_{F-W}^a	4.0	0.056
D7451 - CoR_I^b	5.23	0.03

Notes:

- a) SR_{F-W} – Fuel-water separation rating.
- b) CoR_I – Interface condition rating.

3.8.5.5 If degraded fuel-water separability was caused by biosurfactant production, ATP-bioburdens those microcosms in which DSEP >50 might have been significantly less than those with DSEP <50. To test this, a one-way ANOVA was computed to determine if DSEP and [cATP] were related.

3.8.5.5.1 There were 23 microcosms for which [cATP]_{AQ} and DSEP data were available. DSEP > 50 in 11 and <50 in 12.

3.8.5.5.2 No significant difference in [cATP]_{AQ} was observed. F_{Calc} = 0.0026 (F_{Crit}[df 1,21; α = 0.05] = 4.32 and P = 0.96).

3.8.5.5.3 However, as discussed above and in Passman, 2012 [11], bioburden and specific types of biodeteriogenic activities are not necessarily correlated with total bioburdens. Specific types of metabolic activities are functions of the microbial taxa present, the physiological state of each OTU, and chemical signaling among members of the microbiome community. Without further analysis [67, 68] it is impossible to determine whether and what surfactants were in the microcosms with low DSEP values. Additional analysis was beyond the scope of this project.

3.8.5.5.4 Ten microcosms were analyzed for both fuel phase properties and aqueous phase composition at T_{12w} as shown in Tables 52a and 52b. Fuel property analysis included ASTM D4176 [24] Method D7261 [17], and D7451 [16]. The ASTM D4176 test method for haze is designed to detect the presence of free water and particulate matter in fuel. Test results were reported as a rating from 1 to 5 with 1 being clear with no haze. ASTM D7261 was designed to determine the presence of surfactants in fuel which hinder the ability of filter separators to separate free water from fuel. Test results were reported as a rating from 100 to 50 with 100 being the best separability. ASTM D7451 was designed to detect the presence of water-soluble or partially water-soluble components in fuel which could affect the interface and interfere with the fuel's water separation properties. Test results included three parameters: 1) fuel clarity rating from 1 to 6 with 1 being clear and 6 being opaque, 2) fuel-water separability rating from 1 to 3 with 1 being complete absence of emulsions or precipitates at the fuel-water interface, and 3) interface condition rating from 1 to 4 with 1 being clear and clean.

- As shown in Table 52a, the D4176 haze ratings showed no sensitivity to total oxygenate concentration. Although total oxygenate concentration in the water phase varied by more than two orders of magnitude from 35 to nearly 4600 $\mu\text{g ml}^{-1}$, the fuel phase remained clear with a haze rating of 1.
- Water separability methods, D7261 and D7451, showed much greater sensitivity to total oxygenates. D7261 water separability showed a trend from good separability (ratings > 90) for fuel in contact with water containing < 150 $\mu\text{g ml}^{-1}$ total oxygenates to poor separability for most microcosms with total oxygenates > 150 $\mu\text{g ml}^{-1}$ in the aqueous-phase as shown in Figure 63. Similarly, D7451 fuel clarity ratings tended to increase as total oxygenate concentration increased (Figure 64). Additionally, the Interface Condition Rating worsened as the total oxygenate concentration increased (Figure 65). while Water Separability Rating (Figure 66) did not correlate significantly with oxygenate concentration. However, despite the weak overall correlation, separability worsened when total oxygenate concentration was $\geq 150 \mu\text{g mL}^{-1}$.
- Results for ASTM D7451 Water separability also correlated negatively with LMOA and alcohol concentrations in the aqueous-phase (Figures 67 and 68, respectively). Water Separability ratings generally decreased with increasing LMOA and alcohol concentrations.
- Aqueous composition included Low Molecular weight Organic Acids (LMOA) and alcohols. Individual component concentrations and total oxygenate concentrations (sum of LMOA and alcohols) in the aqueous phase are shown in Table 52b.
- These results suggested that LMOA and alcohols impaired fuels' separability characteristics. They also demonstrate the value of D7261 and D7451 Water Separability tests to detect the effects of LMOA and alcohols on fuel separability. The Water Separability tests detected the presence of LMOA and alcohols whereas D4176 Haze did not.

Table 52a. Fuel properties for ten selected microcosms.

Microcosm	ASTM D4176 Haze by Visual	D7261 Water Separability	D7451 Water Separability - Aq. Vol. (mL)	D7451 Fuel Clarity Rating	D7451 Fuel-Water Separability Rating	D7451 Interface Condition Rating	D7451 Interface Condition Rating
3	1	96	9.5	2	2	1	B
4	1	92	9.5	2	2	1	B
5	1	81	10	2	2	2	
35	1	97	9.5	2	2	1	B
37	1	93	10	3	3	2	
53	1	45	10	5	3	3	
83	1	0	8.5	6	3	3	
96	1	0	7	6	3	4	
99	1	69	9.5	3	2	1	B
100	1	52	8.5	3	2	4	

Table 52b. Aqueous-phase properties for ten selected microcosms.

Microcosm	Acetic Acid (µg/mL)	Total Organic Acids (µg/mL)	Ethanol (µg/mL)	Glycerin (µg/mL)	Total Alcohols (µg/mL)	Total Oxygenates (µg/mL)
3	34	34	4.3	15	20	54
4	33	33	0.0	2.4	2.4	35
5	42	54	0.0	131	131	184
35	33	53	0.0	1.4	1.4	54
37	495	495	13	0.1	13	508
53	45	228	0.0	0.2	0.2	228
83	243	243	10	0.1	10	253
96	3818	4344	23	213	235	4580
99	117	117	33	1.6	35	152
100	3820	3820	26	2.0	28	3848

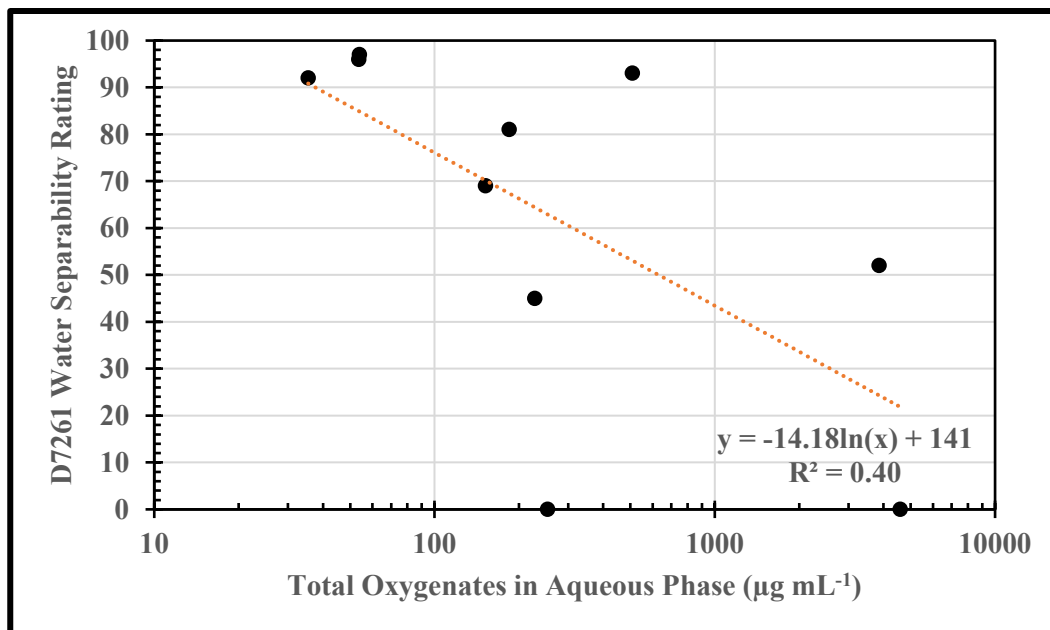


Fig 63. Effect of Total Oxygenates on D7261 Water Separability.

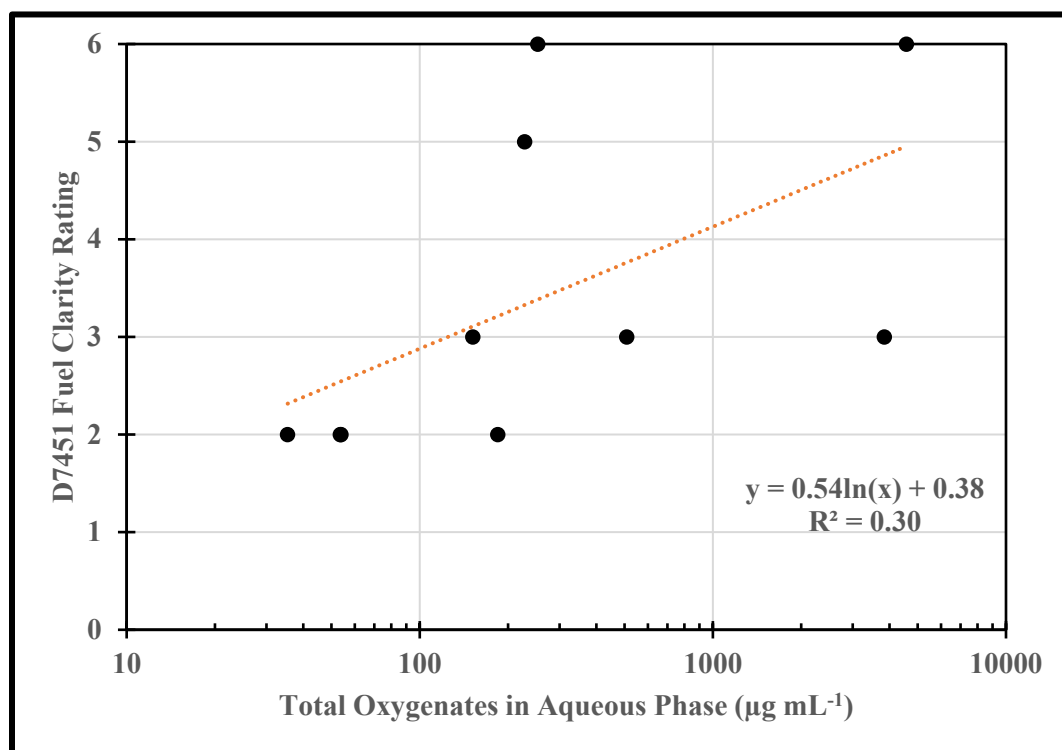


Fig 64. Effect of Total Oxygenates on ASTM D7451 Fuel Clarity Ratings.

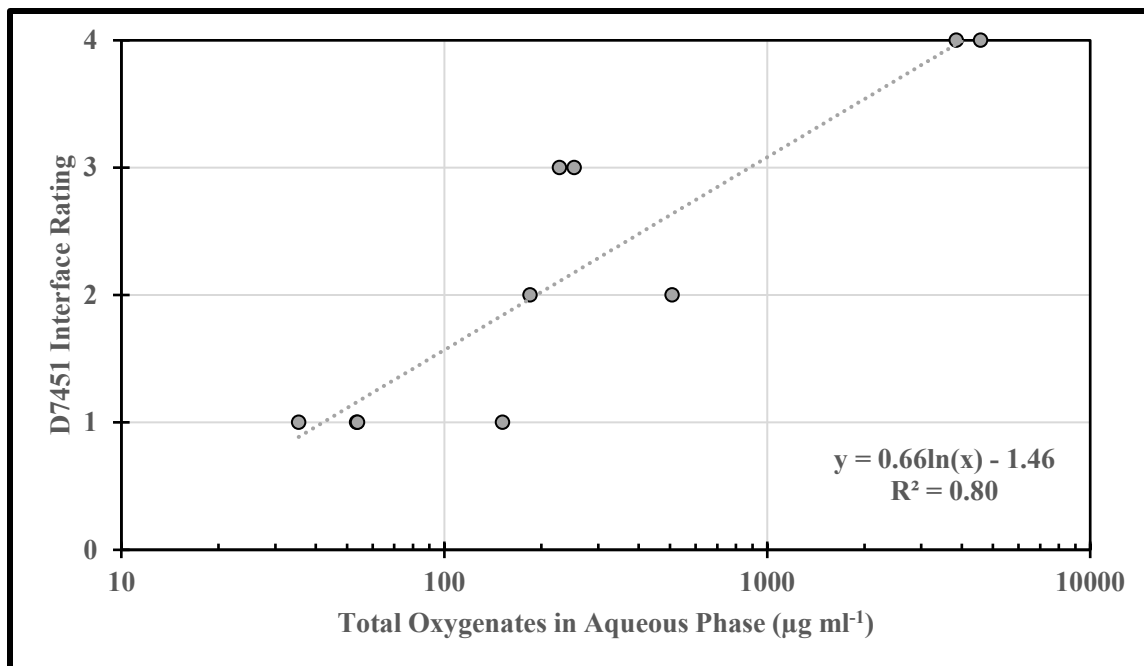


Fig 65. Effect of Total Oxygenates on ASTM D7451 Interface Rating.

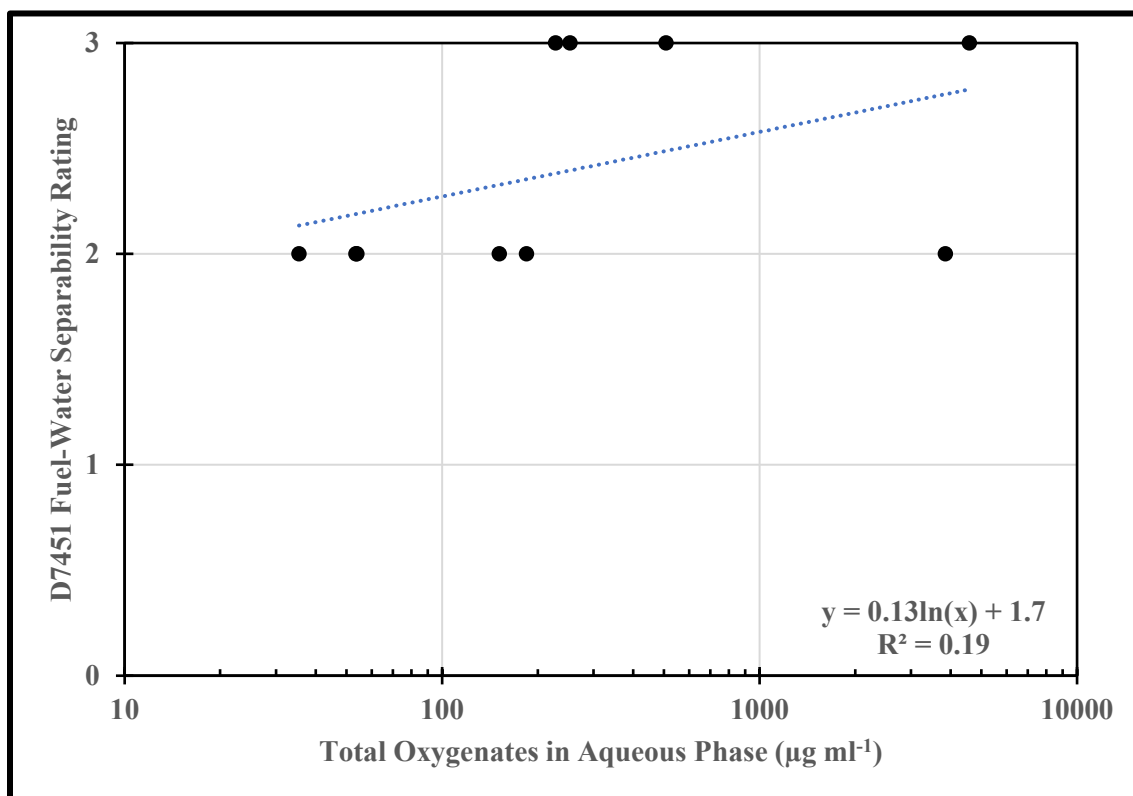


Fig 66. Effect of Total Oxygenates on ASTM D7451 Water Separability.

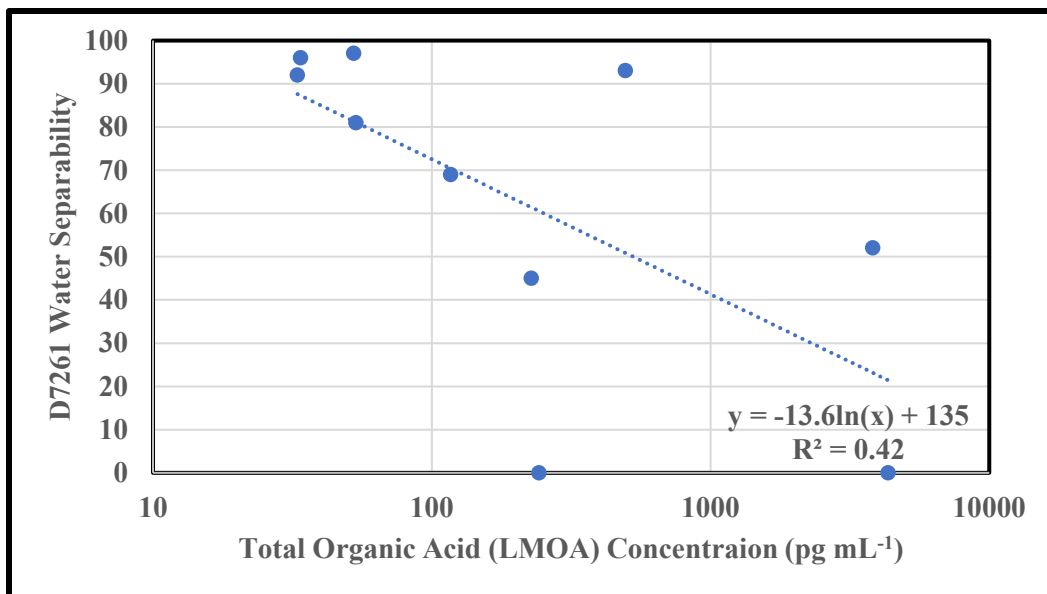


Fig 67. Effect of Total Organic Acid Concentration on Water Separability.

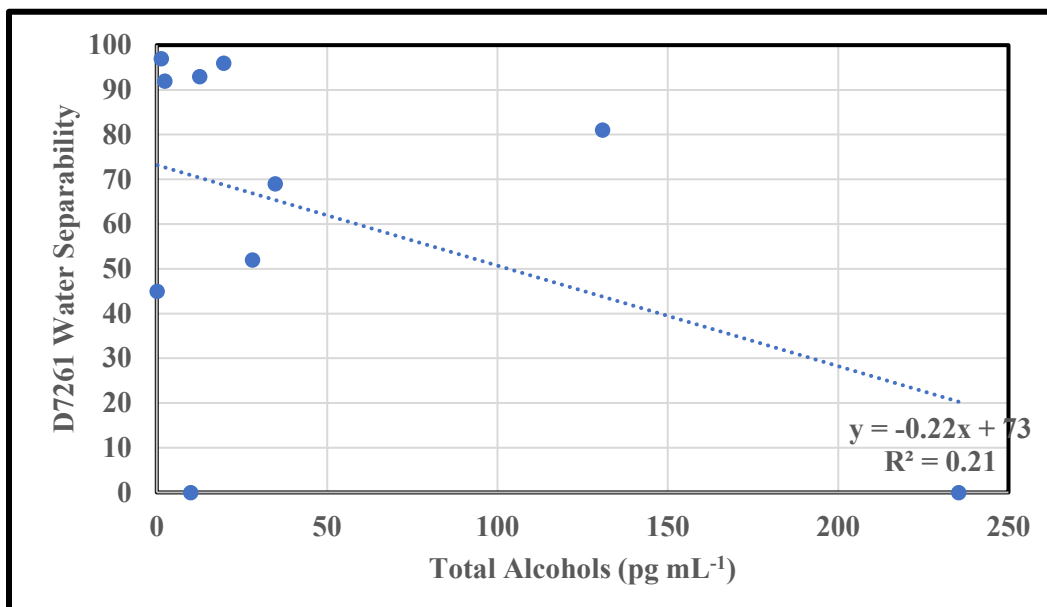


Fig 68. Effect of Alcohol Concentration on Water Separability.

3.9 RESULTS SUMMARY

3.9.1 Microcosm Design

3.9.1.1 Preliminary testing established that contrary to conventional wisdom, partitioning of polar fuel additives is not affected by the fuel to water ratio. This finding has important ramifications regarding microcosm design. It validates the used of lower fuel to water ratios – such as 70 to 30 – instead of the commonly used 100 parts fuel to one-part water.

3.9.1.2 The microcosm design did not adequately accommodate for vapor-phase analysis since the Dräger tubes were used incorrectly.

3.9.2 Fractional-factorial Test Plan

3.9.2.1 The test plan was adequate to meet the study's objective of identifying the primary or interaction-effect relationships between eleven controlled variables and corrosion on steel coupons.

3.9.2.2 The 12-week exposure period was sufficient for severe ($CR > 3$) corrosion to occur on coupons.

3.9.3 Relationships between Controlled Variables and Corrosion

3.8.3.1 The only controlled variable (factor) that had an unequivocal impact on corrosion was water.

3.9.3.1.1 Corrosion was more severe in microcosms that had an aqueous-phase than in those that did not.

3.9.3.1.2 Corrosion ratings (CR) at the fuel-aqueous-phase interface (CR_I) were generally greater than those elsewhere on coupons. Also, for each exposure phase (i.e., aqueous, interface, fuel, and vapor), CR on the coupons' edges were greater than on their faces.

3.9.3.2 The impact of microbial activity on corrosion was largely obscured by high ATP-bioburdens (i.e., $[cATP] \geq 3\text{Log}_{10} \text{ pg mL}^{-1}$) in unchallenged (uninoculated) microcosms. Some of the statistical calculations indicated that corrosion was more severe in challenged than in unchallenged microcosms but no unequivocal statement could be made based on the data set.

3.9.3.3 Statistical analysis of the relationships between the controlled variables and CR indicated a number of statistically significant (i.e., P-values < 0.05) but subtle relationships.

3.9.3.3.1 The following factors correlated positively with CR:

- Water
- Ethanol + microbial challenge (interaction effect)
- The following factors correlated negatively with CR:
- Microbial challenge
- CI
- FAME + water (interaction effect)

3.9.3.3.2 CRV-edge in LSD microcosms was $>$ CRV-edge in ULSD microcosms.

3.9.3.3.3 There was a positive correlation between $CR_{I\text{-edge}}$ and the interaction of ethanol + microbial challenge.

3.9.3.3.4 Overall, the following factors have a negative correlation with $CR_{I\text{-edge}}$:

- Microbial challenge

- FAME
- CFI
- CI
- CI + microbial challenge
- FAME + microbial challenge

3.9.3.4 The following factors correlated positively with GCR:

- Water
- CFI + CA (interaction effect)
- Microbial challenge + glycerin (interaction effect)

3.9.3.5 The following factors correlated negatively with GCR:

- Glycerin
- FRP

3.9.4 Relationships between Controlled Variables and Gross Observations

3.9.4.1 3.8.4.1 The following factors correlated positively with gross-observation risk scores (RS_{GO}):

- Sulfur concentration (fuel grade) (i.e. CR_{LSD} > CR_{ULSD})
- Water
- Microbial challenge

3.9.4.2 The following factors correlated negatively with RS_{GO}:

- Primary factors:
 - CI
 - Ethanol
- Interactions:
 - Ethanol + CI
 - Ethanol + CFI
 - Ethanol + microbial challenge
 - FAME + CI
 - FAME + FRP
 - Sulfur concentration + glycerin
 - Sulfur concentration + microbial challenge

3.9.5 Relationships among Uncontrolled Variables

3.9.5.1 There was no significant correlation between CR and GCR.

3.9.5.1.1 In 68 % (84) of the microcosms $\overline{GCR} < 1.0$ mpy.

3.9.5.1.2 In 2 % (3) of the microcosms $\overline{GCR} \geq 2.3$ mpy.

3.9.5.2 There was no significant correlation between GCR and [ATP] (including cATP and tATP in all microcosm phases).

3.9.5.3 ATP-bioburdens

3.9.5.3.1 There were no significant correlations between controlled variables and ATP-bioburdens.

3.9.5.3.2 By T_{wk4}, aqueous-phase cATP concentrations ([cATP]_{AQ}) were $\geq 3 \text{ Log}_{10} \text{ pg mL}^{-1}$ in >50 % of all microbially challenged and unchallenged microcosms.

3.9.5.3.3 At T_{wk4} , $\overline{[cATP]}$ in microbially challenged microcosms was greater than that in unchallenged microcosms, but at T_{wk9} $\overline{[cATP]}$ in microbially challenged and unchallenged microcosms were no longer significantly different. However, $[cATP]$ in some unchallenged remained low throughout the study.

- Given that in the 1° and 2° microcosms used to cultivate and condition the challenge population, $[cATP] \geq 4 \text{ Log}_{10} \text{ pg mL}^{-1}$ within two-weeks, the substantial ATP-bioburdens in test microcosms, by T_{wk12} was expected.
- The high ATP-bioburdens in unchallenged microcosms were surprising given that $[cATP]$ was $< 0.5 \text{ pg mL}^{-1}$ (below detection limits) in the fuels (ULSD and LSD) at T_0 . These results suggest that commercial fuels transport dormant microbes that can become reactivated when water is present.

3.9.5.3.4 ATP-bioburdens were greatest in aqueous-phase specimens and least in fuel-phase specimens.

- The somewhat greater ATP-bioburdens in the aqueous-phase relative to the aqueous-fuel interface seemed to contradict historical (culture test based) reports of the greatest bioburdens being within the interface zone.
- The observation of $[cATP]_{AQ} > [cATP]_I$ might have reflected the relative abundance of dormant cells within biofilms.

3.9.5.4 Genomics

3.9.5.4.1 Population diversity was assessed based on number of OTU detected (S), diversity index (H), and evenness (E).

- S ranged from 1 (microcosm 76) to 47 (microcosm 40). There were no apparent relationships between controlled variables or ATP-bioburdens and S, or between S and corrosivity.
- H ranged from 0.0 (microcosm 76) and 2.1 (microcosm 36). There were no apparent relationships between controlled variables or ATP-bioburdens and H, or between H and corrosivity.
- E ranged from 0.01 (microcosm 45) to 0.57 (microcosm 102). There were no apparent relationships between controlled variables or ATP-bioburdens and E, or between E and corrosivity.

3.9.5.4.2 Taxonomic profiles indicated that there was little similarity between the T_{wk12} and challenge inoculum populations. Most taxa detected in challenged microcosms at T_{wk12} had not been detected in the challenge cell suspension. Conversely, nearly all taxa detected in the challenge cell suspension were apparently absent from T_{wk12} specimens.

3.9.5.4.3 At T_{wk12} , taxonomic profiles of specimens from challenged microcosms were distinct from those of specimens from unchallenged microcosms. Thus, although there were a few OTU recovered from both the challenge suspension and either challenged or unchallenged microcosms, none were detected in all three.

3.9.5.4.4 When all OTU were considered, replicate specimens from microcosm 45 showed substantial taxonomic difference. In contrast, replicate specimens from microcosm 81 were substantially similar to one another. However, when only the OTU that represented $>99\%$ of the total microbiomes in the respective pairs of duplicate samples, the same OTU were recovered as the dominant taxa. This reflected excellent agreement for dominant OTU.

3.9.5.5 Chemistry

3.9.5.5.1 Acetic acid – presumably, the metabolic by-product of ethanol bio-oxidation – was the predominant LMOA detected in microcosm specimens.

- 3.9.5.5.2 There were no significant correlations between [LMOA] and either CR_{AQ} or CR_I.
- 3.9.5.5.3 The only controlled factor difference between microcosms with >3,000 mg mL⁻¹ acetic acid and those with <160 mg mL⁻¹ acetic acid was the presence of ethanol and microbes. This observation supports the hypothesis that acetic acid creation is linked to microbial action on ethanol contamination in diesel fuel UST.
- 3.9.5.5.4 At T_{12w}, 89% of aqueous samples tested contained acetic acid and nearly half (46%) contained C₃ to C₇ LMOA. Additionally, LMOA concentration generally – but not invariably – increased with time. Between T_{wk9} to T_{wk12}, acetic acid concentration increased in 74% and decreased in 19 % of the microcosms tested. Acetic acid formation nearly always preceded or accompanied C₃ to C₇ LMOA formation.
- 3.9.5.5.5 The fuel separability properties of ULSD were significantly better than those of LSD.
- 3.9.5.5.6 Presence of LMOA and alcohols correlated negatively with fuels’ water separability characteristics but had little effect on fuels’ visual appearance as measured by D4176 Haze. Similarly, aqueous phase total oxygenates concentrations ≥150 µg mL⁻¹ was associated with decreased water separability. These results suggested that D7261 and D7451 were sensitive to elevated LMOA, alcohol, and oxygenates concentrations, but D4176 haze ratings were not.

4 LESSONS LEARNED

4.1 TEST PLAN AND MICROCOSM DESIGN

- 4.1.1 The test plan focused on the relationship between a set of eleven controlled variables and two uncontrolled variables – corrosion ratings and general corrosion risk.
- 4.1.1.1 To provide supplemental information intended to help explain the observed relationships between the controlled variables and the two corrosion parameters, additional tests were included in the design.
- 4.1.1.2 To balance the FCP’s desire to obtain useful data and the need to control project costs, certain tests were made conditional (see 3.1.10).
- 4.1.1.2.1 As depicted in Figure 8 the sole criterion for additional testing was CR_I ≥ 3.
- In retrospect, the CR corrosion rating at the aqueous-fuel interface should have been the designated parameter, rather than simply CR.
 - By T_{wk1} CR_I ≥ 3 on coupons in a substantial number of microcosms. However, the additional testing specified in Figure 8 was not performed. Presumably, this was because the project team used CR_{AQ} to determine whether additional testing was needed. Consequently, in future studies, samples should be collected and tested during the first four weeks.
 - RS_{GO} should have been used instead of *Particulates* as a criterion for additional testing. Few microcosms had >25 % particulate coverage of jar bottoms at T_{wk12}, but some had RS_{GO} ≥ 3 by T_{wk1}.
 - Also, in retrospect CR_I and RS_{GO} – the gross observation-based risk score should have been identified as co-criteria for additional testing. Additional testing would then have been conditional on either CR_I or RS_{GO} ≥ 3.

4.1.1.2.2 The test plan did not specify a requirement for at least a subset of microcosms to be tested at T_0 to establish a baseline for all dependent variables. Consequently, the rates of change during the first month of testing could not be determined. In future projects, a representative number of microcosms should be tested for all dependent variables at T_0 .

4.1.2 The microcosm design was not suitable for inclusion of vapor-phase LMOA detection.

4.1.2.1 As discussed in 3.7.2, the Dräger tubes used to detect LMOA produced in the liquid phases or vapor-phase did neither.

4.1.2.1.1 If vapor-phase LMOA are to be detected using a permanently installed device, that device should not contact the microcosm's liquids.

4.1.2.1.2 Any LMOA that accumulate in a microcosm's vapor-phase are likely to disperse rapidly, each time the lid is removed.

- Weekly observations of permanently installed detectors would permit determination of LMOA evolution rates (week to week increases in total [LMOA] detected by sensor or weekly sensor replacement).
- Although it is a more expensive option, an alternative approach would have been to fit microcosm lids with a septum. Each week before the lid was removed for coupon inspection, a headspace specimen could have been collected using a syringe designed for GC-MS sampling. The specimen would have then been analyzed by GS-MS or other suitable GC protocol to profile and quantify vapor-phase [LMOA].

4.1.2.1.3 At most retail facilities, ullage (the difference between the fuel volume present and a tank's capacity) is dynamic. Fuel draw-downs and deliveries mix the fuel and caused 30 % to 60 % ullage volume changes with each product turnover cycle.

- The importance of simulating UST fluid flow dynamics is unclear in an evaluation of factors influencing corrosion.
- It might be beneficial to conduct a small study to compare LMOA accumulation and coupon corrosion ratings in static and dynamic microcosms.

4.1.3 Fuel preparation

4.1.1.1 In future studies, fuels provided to testing labs should include chain-of-custody forms and a certificate of analysis.

4.1.3.1.1 The fuels received at Battelle had been mislabeled. A simple certificate of analysis that included an indication of the fuel's color would have enabled the identification of the labelling error before they began project work. Additionally, the fuel samples should have been tested per ASTM D975 to confirm the critical fuel properties of each fuel sample received.

4.1.3.1.2 ATP-bioburden testing does not detect dormant microbes. Although microbes could have been introduced into microcosms as the jars were being set up, it is more likely that they were present in a dormant state in the fuels provided for the study.

4.1.3.1.3 In future studies:

- Received fuels should be tested by both ASTM D6974 [69] and D7687.
- Before being dispensed into microcosms, fuels should be pressure filtered through a 0.1 μm filter into sterile or, minimally, chemically clean containers.

4.2 ANALYSIS

4.2.1 Subset Selection

- 4.2.1.1 Subsets of microcosms were selected for genomic and chemical testing. Although these subsets included a similar number of microcosms, relatively few microcosms were subjected to a full set of tests (i.e., [cATP]_{AQ}, [cATP]_I, [cATP]_F, [tATP]_{AQ}, [tATP]_I, [tATP]_F, NGS, LMOA, alcohols, surfactants).
- 4.2.1.2 Microcosms selected for multi-parameter testing should be from the same sub-group so that relationships among uncontrolled and controlled variables can be assessed.
- 4.2.1.3 Some testing (for example [tATP], ASTM D7164, and D7451) was performed as extracurricular add-on efforts by FCP members. Future studies should incorporate increased up-front planning and coordination during project to ensure that full data sets for a given microcosm are created.

4.2.2 Corrosion Ratings

- 4.2.2.1 Although corrosion coupons were pulled weekly for observation, CR data were not recorded until later in the study. Delays in recording CR data were likely to have contributed to the failure to perform the additional conditional tests specified in Figures 8, 9, and 10 during T_{wk1} through T_{wk3}.
- 4.2.2.2 In future studies, observations must be completed in accordance with the QAPP. Photos are essential for illustration purposes but are inadequate for testing per the RFP.
- 4.2.2.3 By T_{wk2} CR_{AQ} ≠ CR_I ≠ CR_F. As indicated under 4.1.1.2, additional tests should have been triggered by the highest CR_X. Considerable data were lost because only CR_{AQ} data were used as the criterion for additional testing.
- 4.2.2.4 Substantial differences in CR_X translated into the questionable relevance of GCR data.
- 4.2.2.4.1 Typically, coupons used to determine GCR are fully immersed in a single vapor or fluid phase. It is assumed that for any area of a coupon, weight loss will be uniform within the test method's reproducibility coefficient. For this reason, in future studies it may be more appropriate to evaluate corrosion rates separately within the various zones (vapor, fuel, fuel-water interface, and aqueous). This may be accomplished either by evaluating each corrosion zone separately on a single coupon, or using separate coupons in each zone.
- 4.2.2.4.2 At T_{wk12} CR_I ≥ 4 on many coupons. However, the area in contact with the invert-emulsion or emulsion-free aqueous-fuel interface was typically <10 % of the coupon's total surface area.
- 4.2.2.4.3 Alternative parameters should be considered in lieu of GCR.
- Corrosion deposit mass
 - Corrosion deposit minerology
 - Profilometry
 - Sub-deposit coupon morphology (i.e., pitting topology, erosion wear, etc.)

4.2.3 Microbiology

- 4.2.3.1 Biofilm testing was not included in the initial test plan. Added as an extracurricular parameter (2.6.6.1.2), [tATP] data provided important, relevant information about the relationship between sessile population bioburdens and corrosion ratings. Biofilm bioburden testing should be included in future fuel corrosivity studies.

- 4.2.3.2 Microscopy of suspected fungal masses in T_{wk12} microcosms provided little useful information. The taxa that were tentatively identified based on their morphologies were not detected by ITS sequencing testing. Without substantial labor spent isolating individual fungal taxa and running physiological tests, there is no basis for assessing the accuracy of either the genomic or morphological results. Low-magnification microscopy of fungal masses should be omitted from future projects except for those in which detection and taxonomic classification of fungi is a primary objective. The apparent disagreement between taxa identified by microscopy and genomic testing raises questions about why the results are different and which method is more accurate. Although this question is likely beyond the scope, it would be an interesting topic of future study.
- 4.2.3.3 The absence of any OTU profile commonalities among microcosms raised many questions about the utility of this technology in microcosm studies. To better understand populations during the test period, genomic testing should be performed periodically – minimally at monthly intervals, and samples for genomic testing should be drawn from the same microcosm sub-set.
- 4.2.3.3.1 Quantitative polymerase chain reaction (qPCR) and NGS testing is being performed on specimens collected from all microcosms that had an aqueous-phase.
- In January 2020, microcosms with an aqueous-phase were transported from Battelle to Marathon Petroleum’s Refining, Analytical, and Development (RAD) lab in Catlettsburg, KY.
 - In February 2020, microcosms were tested by D7687, and specimens were collected for genomic testing.
 - Once the data are available, ATP, qPCR, and NGS data from 18-month microcosms will be compared, and 18-month NGS data will be compared against the T_{wk12} data provided in this report.
 - A stand-alone report will be shared with members of the FCP.
 - An assessment of lessons learned from the genomic testing performed as part of the project is pending the completion of the stand-alone report.

4.2.4 Data Interpretation

- 4.2.4.1 The test plan was designed to assess first and second order *relationships* between controlled and uncontrolled variables under laboratory conditions.
- 4.2.4.2 Readers of this report are cautioned not to conflate *correlation* (i.e., two or more parameters show similar trends – it seems to always rain when I wear my brown shoes) with *causation* (intentional changes to one or more controlled variables is reflected in changes to one or more dependent variables – the water in the pot over the fire grew warmer until it boiled).
- 4.2.4.3 Similarly, the statistical relationships provided in this report indicate the probability that there is a relationship between controlled (independent) and uncontrolled (dependent) variables. In a fractional-factorial test plan, there are insufficient data on which to perform principle component analysis (a set of statistical tools used to assess the magnitude of relationships among variables).

5 CONCLUSIONS

5.1 PRIMARY FACTORS AFFECTING CORROSIVITY IN FUEL MICROCOSMS

- 5.1.1 Mild steel corrosion was unequivocally associated with the presence of an aqueous-fuel interface and, by extension, the presence of free-water. By the end of the test period, $CR_I \geq 4$ were observed in all microcosms that included an aqueous-phase. Water was the only independent variable that correlated positively with all of the independent variables.
- 5.1.2 Despite the interference effect of indigenous microbial growth in unchallenged microcosms, it can be tentatively concluded that the presence of the intentional challenge population- originating from retail UST systems in which moderate to severe corrosion was observed – correlated with increased corrosion severity. The conclusion is not unequivocal because the relationship between microbial challenge and corrosion varied, depending on the statistical treatment of the data. Some of the analyses indicated no correlation. Others indicated a positive correlation.
- 5.1.3 Neither [S] (fuel grade) nor FAME – the two primary factors that differentiate contemporary fuels from those used historically – correlated significantly with either GCR or CR. However, some of the analyses indicated that there was a significant positive correlation between CR and [S]. Similarly, although FAME did not correlate to CR or GCR by some analyses, it correlated negatively by other analyses.
- 5.1.4 None of the other independent variables had consistently significant correlation coefficients with the dependent variables. For example, depending on the analysis, ethanol was positively, negatively, or not significantly correlated with CR. However, presence of ethanol combined with microbial challenge correlated well with high concentrations of acetic acid in the aqueous phase. This observation supports the hypothesis that acetic acid formation is linked to microbial action on ethanol contamination in the diesel fuel UST.

5.2 INDEPENDENT VARIABLE INTERACTIONS

- 5.2.1 None of the independent variable two-way interactions were correlated consistently with either CR or GCR. For example, at T_{wk12} , ethanol + microbial challenged correlated positively with CR_{I-E} (CR on coupon edge at interface). However, the correlation was negative with $\Delta CR dt^{-1}$ – the rate at which CR increased during the period week 1 to week 6.
- 5.2.2 There was minimal indication that FRP was a relevant variable. The correlation between MAL + FRP and $\Delta CR dt^{-1}$ was statistically significant, but not supported by any other indication that FRP either as a primary factor or interacting factor correlated with any of the dependent variables.

6 RECOMMENDATIONS

6.1 MICROCOSM DESIGN

- 6.1.1 2 L microcosms are adequate and appropriate for bench-scale fuel corrosivity studies.
- 6.1.2 The use of 800 mL to 1000 mL over 200 mL to 500 mL of an aqueous-phase is also appropriate. It provides adequate volumes of both phases for specimen collection during the course of a study.
- 6.1.3 To simulate UST fluid dynamic condition while minimizing VOC loss, provisions should be made for periodic removal and replacement of approximately 60 % of the fuel volume. This can be accomplished by simply siphoning fuel from the microcosm.

- 6.1.3.1 Preferably, the microcosm lid would be fitted with inlet and outlet tubing.
- 6.1.3.1.1 Inlet tubing would open either at or below the aqueous-fuel interface.
- 6.1.3.1.2 Outlet tubing would open at a level approximately 30 % above the aqueous-fuel interface.
- 6.1.3.2 Fuel removal should be accomplished either by siphoning or peristaltic pump.
- 6.1.3.3 Fuel replacement should be by gravity delivery.
- 6.1.3.4 All components should be equipped with vent filters to reduce the risk of introducing external (i.e., laboratory air) contamination during fluid movement.
- 6.1.4 Microcosm lids should be fitted with a septum to facilitate vapor-phase specimen collection.
- 6.1.5 If an installed volatile acid detector is to be used, it should be a device that does not contact the fuel-phase.
- 6.1.6 All materials used in microcosms should minimally be chemically cleaned, and optimally sterilized before use. Fuels should be filter sterilized per 4.1.3.1.3 before being dispensed into microcosms.

6.2 SPECIMEN COLLECTION

- 6.2.1 The use of both scheduled and conditional specimen collection is appropriate.
- 6.2.2 The conditional criteria for conditional sampling should be modified so that either $CR_I \geq 3$ or $RS_{GO} \geq 3$ triggers collection.
- 6.2.3 Regardless of whether specimens are collected per a schedule or because of conditional criteria, they should be tested for all dependent variables included in the test plan design.
- 6.2.4 Observational data used to determine the need for conditional sample collection should be recorded as scheduled. Delayed observations of photos prevented potentially critical T_{wk1} to T_{wk4} conditional sampling and testing from being completed.

6.3 INDEPENDENT FACTOR SELECTION

- 6.3.1 Future testing should focus on:
 - 6.3.1.1 Ethanol
 - 6.3.1.2 Microbial contamination
 - 6.3.1.3 Sulfur concentration
 - 6.3.1.4 FAME
- 6.3.2 In addition to the presence of water, these four factors seemed to correlate with either significantly increased or decreased corrosivity.

6.4 TEST PLAN DESIGN

- 6.4.1 Future microcosm studies should include replicate microcosms and – if there is a desire to determine magnitude of effects – multiple tiers of each controlled variable.

- 6.4.1.1 Replicate microcosms will make it possible to differentiate between apparent correlations due to random variations and those due to actual relationships. The inconsistencies among correlations observed in this study could have reflected either actual differences in relationships (for example, when a controlled variable or variable-pair correlated with CR at a given observation time, but not with $\Delta CR dt^{-1}$).
- 6.4.1.2 Multiple tiers will facilitate differentiation between coincidental covariation and causal relationships. Suggested multiple tiered factors include:
- 6.4.1.2.1 Multiple FAME concentrations (for example: 0 wt. %, 1 wt. %, 5 wt. %, and 10 wt. %).
- 6.4.1.2.2 Multiple FAME sources (i.e., soy, rapeseed or canola, animal or poultry fat, palm, and coconut).
- 6.4.2 Extend exposure period to two-years. During extracurricular testing performed at T_{18mo} , substantial vapor-phase corrosion was observed on coupons for which CR_V at T_{wk12} was ≤ 2 .
- 6.4.2.1 Focus on early (T_0 to T_{wk6}) and longer term (T_{3mo} to T_{24mo}) relationships.
- 6.4.2.1.1 During early period, complete observations, specimen collection, and analysis weekly.
- 6.4.2.1.2 During longer term period, complete observations, specimen collection, and analysis quarterly (i.e., at T_{mo3} , T_{mo6} , T_{mo9} , T_{12mo} , T_{mo15} , T_{mo18} , T_{mo21} , and T_{mo24}). If the values of dependent variables at T_{6mo} are not significantly different from the values at T_{3mo} , the intervals should be extended to six-months (T_{mo6} , T_{mo12} , T_{mo18} , and T_{mo24}).
- 6.4.3 To accommodate logistical constraints, a series of single factor or two-factor test plans should be executed.
- 6.4.3.1 For example, a test plan to investigate the relationships between FAME, [S], and microbial contamination would require 146 microcosms:
- Two types of FAME (for example, soy and animal/poultry fat) x four FAME concentrations (see 6.4.1.2.1).
 - Three [S]s: ULSD, LSD, and HSD.
 - Microbial challenge – present or absent.
 - Aqueous-phase-free controls:
 - Fuel only – ULSD
 - Fuel (ULSD) + FAME (soy @ 5 wt. %)
- 6.4.3.1.1 Triplicate microcosms: 8 FAME x 3 [S] x 2 microbial challenge x 3 replicates = 48 combinations of test conditions x 3 replicates = 144 microcosms. Plus 2 controls = 146 microcosms.
- 6.4.3.1.2 Using duplicates instead of triplicates would reduce the total number of microcosms to 98. However, if there are substantial differences between duplicate microcosms, it would be difficult to distinguish between outliers and random variation.

6.5 DEPENDENT VARIABLES

- 6.5.1 Except for GCR, the dependent variables that were included in this study were appropriate. GCR measurements obfuscated the substantial differences in corrosion that occurred on coupon surfaces exposed to the aqueous, interface, fuel, and vapor-phases respectively.
- 6.5.2 Additional variables that should be considered for inclusion in future studies include:

- 6.5.3 Profilometry to quantify corrosion on different areas of coupons surfaces – particularly at the fuel-water interface.
 - 6.5.3.1 qPCR for total microbial bioburden and for acid producing bacteria.
 - 6.5.3.2 Profilometry (for example atomic force microscopy and optical interferometry) and mineralogy of corrosion deposits to determine whether corrosion mechanisms vary with test conditions.
 - 6.5.3.3 Examination of unexposed and under-deposit corrosion coupon surfaces.
 - 6.5.3.4 Volatile organic acid accumulation in the vapor-phase.

7 REFERENCES

1. NACE, 2013. NACE Glossary of Corrosion Terms, CORROSION. 1964;20(8):267t-268t. <https://doi.org/10.5006/0010-9312-20.8.267t> or <https://www.nace.org/glossary/corrosion-terminology-c>.
2. Koch, G., Varney, J., Thompson, N., Moghissi, O., Gould, M., and Payer, J. 2016. International measures of prevention, application, and economics of corrosion technologies study. NACE International, Houston. 216 pp. <http://impact.nace.org/documents/Nace-International-Report.pdf>.
3. The World Bank. 2018. Gross domestic product data. The World Bank, IRBD-IDA. <http://data.worldbank.org/indicator/NY.GNP.MKTP.PP.CD>.
4. Pearson, G. and Oudijk, G., 1993. Investigation and remediation of petroleum product releases from residential storage tanks. Groundwater Monitoring & Remediation, 13(3):124-128. <https://doi.org/10.1111/j.1745-6592.1993.tb00081.x>.
5. Sowards, J.W. and Mansfield, E., 2014. Corrosion of copper and steel alloys in a simulated underground storage-tank sump environment containing acid-producing bacteria. Corrosion Science, 2014. 87: p. 460-471. <http://dx.doi.org/10.1016/j.corsci.2014.07.009>.
6. Battelle, 2012. Corrosion in systems storing and dispensing ultra low sulfur diesel (ULSD), hypotheses investigation, study no. 10001550 Final Report, 146 pp, Battelle Memorial Institute, Columbus, OH. <https://fuelmanagementservices.com/pdfs/ULSDStoringSystemCorrosion.pdf>.
7. U.S. EPA, 2016. Investigation of corrosion-influencing factors in underground storage tanks with diesel service, EPA 510-R-16-001, 68 pp, United States Environmental Protection Agency, Washington, DC. https://www.epa.gov/sites/production/files/2016-07/documents/diesel-corrosion-report_0.pdf.
8. Sissine, F., 2007. Energy independence and security act of 2007: a summary of major provisions. Congressional Research Service, Washington DC. 27 pp. https://www1.eere.energy.gov/manufacturing/tech_assistance/pdfs/crs_report_energy_act_2007.pdf.
9. ASTM, 2019. ASTM D8011-19, Standard specification for ethanol fuel blends for flexible-fuel automotive spark-ignition engines. ASTM International, West Conshohocken, PA, www.astm.org.
10. NPN, 1998. Market Facts 1998. National Petroleum News, Chicago, 146 pp. Available from <https://searchworks.stanford.edu/view/10048374>.

11. Passman, F.J., 2012. Microbial contamination control in fuels and fuel systems since 1980 – a review. *International Biodeterioration & Biodegradation* 81(1): 87-104, <http://dx.doi.org/10.1016/j.ibiod.2012.08.002>.
12. ASTM, 2017. G1-03(2017)e1, Standard practice for preparing, cleaning, and evaluating corrosion test specimens, ASTM International, West Conshohocken, PA, 2015, www.astm.org.
13. ASTM, 2015. C581-15, Standard practice for determining chemical resistance of thermosetting resins used in glass-fiber-reinforced structures intended for liquid service, ASTM International, West Conshohocken, PA, www.astm.org.
14. ASTM, 2014. D7464-14, Standard practice for manual sampling of liquid fuels, associated materials and fuel system components for microbiological testing. ASTM International, West Conshohocken, PA, www.astm.org.
15. ASTM, 2017. D7687-17, Standard test method for measurement of cellular adenosine triphosphate in fuel and fuel-associated water with sample concentration by filtration. ASTM International, West Conshohocken, PA, www.astm.org.
16. ASTM, 2017. D7261-17, Standard test method for determining water separation characteristics of diesel fuels by portable separator. ASTM International, West Conshohocken, PA, www.astm.org.
17. ASTM, 2016. D7451-16, Standard test method for water separation properties of light and middle distillate, and compression and spark ignition fuels. ASTM International, West Conshohocken, PA, www.astm.org.
18. Bushnell, L. and H. Haas, The utilization of certain hydrocarbons by microorganisms. *Journal of Bacteriology*, 1941. 41(5): p. 653. <https://www.ncbi.nlm.nih.gov/pmc/articles/PMC374727/pdf/jbacter00729-0101.pdf>.
19. ASTM, 2016. D4294-16e1, Standard test method for sulfur in petroleum and petroleum products by energy dispersive x-ray fluorescence spectrometry. ASTM International, West Conshohocken, PA, www.astm.org.
20. ASTM, 2016, D5453-16e1, Standard test method for determination of total sulfur in light hydrocarbons, spark ignition engine fuel, diesel engine fuel, and engine oil by ultraviolet fluorescence. ASTM International, West Conshohocken, PA, www.astm.org.
21. ASTM, 2015. D7039-15a, Standard test method for sulfur in gasoline, diesel fuel, jet fuel, kerosene, biodiesel, biodiesel blends, and gasoline-ethanol blends by monochromatic wavelength dispersive X-ray Fluorescence Spectrometry. ASTM International, West Conshohocken, PA, www.astm.org.
22. ASTM, 2016. D6304-16e1, Standard test method for determination of water in petroleum products, lubricating oils, and additives by coulometric Karl Fischer titration. ASTM International, West Conshohocken, PA, www.astm.org.
23. ASTM, 2014. D4176-04(2014), Standard test method for free water and particulate contamination in distillate fuels (visual inspection procedures). ASTM International, West Conshohocken, PA, www.astm.org.

24. ASTM, 2017. D1500-12(2017), Standard test method for ASTM color of petroleum products (ASTM Color Scale). ASTM International, West Conshohocken, PA, 2015, www.astm.org.
25. NACE, 2001. TM0172-2001-SG, Determining corrosive properties of cargoes in petroleum product pipelines. NACE International, Houston, TX, www.nace.org.
26. Adorno, M.A.T., Hirasawa, J. S., & Varesche, M. B. A., 2014. Development and validation of two methods to quantify volatile acids (C2-C6) by GC/FID: headspace (automatic and manual) and liquid-liquid extraction (LLE). *American Journal of Analytical Chemistry*, 5(07): 406-414. DOI: 10.4236/ajac.2014.57049.
27. Andrade, C., & Alonso, C., 1996. Corrosion rate monitoring in the laboratory and on-site. *Construction and Building Materials*, 10(5):315-328. [https://doi.org/10.1016/0950-0618\(95\)00044-5](https://doi.org/10.1016/0950-0618(95)00044-5).
28. Klindworth, A., Pruesse, E., Schweer, T., Peplies, J., Quast, C., Horn, M., & Glöckner, F. O., 2013. Evaluation of general 16S ribosomal RNA gene PCR primers for classical and next-generation sequencing-based diversity studies. *Nucleic acids research*, 2013. 41(1):e1, 11pp. <https://doi.org/10.1093/nar/gks808>.
29. Spellerberg, I.F., & Fedor, P. J., 2003. A tribute to Claude Shannon (1916–2001) and a plea for more rigorous use of species richness, species diversity and the ‘Shannon–Wiener’ Index. *Global ecology and Biogeography*, 12(3):177-179. <https://doi.org/10.1046/j.1466-822X.2003.00015.x>.
30. NACE, 2014. Corrosion Costs and Preventive Strategies in the United States. Publication No. FHWA-RD-01-156, U.S. Department of Transportation, Federal Highway Administration, McLean, VA, 12 pp.
31. James, G., Witten, D., Hastie, T., Tibshirani, R., 2017. *An introduction to statistical learning: with applications in R* (Springer Texts in Statistics) 1st ed. 2013, Corr. 7th printing 2017 Edition, Springer, New York, 426 pp. ISBN-13: 978-1461471370.
32. CRC, 2014. Diesel Fuel Storage and Handling Guide, CRC Report No. 667. Coordinating Research Council, Inc. Alpharetta, GA, 32 pp. <http://crcsite.wpengine.com/wp-content/uploads/2019/05/CRC-667.pdf>.
33. Motor Vehicle Diesel Fuel Standards and Requirements, 40 CFR § 80.520, <https://www.law.cornell.edu/cfr/text/40/80.520>.
34. Energy Policy Act of 2005, Public Law 109–58—AUG. 8, 2005, 551 pp. <https://www.congress.gov/109/plaws/publ58/PLAW-109publ58.pdf>.
35. Gonzalez-Pajuelo M, Meynial-Salles I, Mendes F, Andrade J C, Vasconcelos I, Soucaille P., 2005. Metabolic engineering of clostridium acetobutylicum for the industrial production of 1,3-propanediol from glycerol. *Metabolic Engineering* 7: 329-336. doi:10.1016/j.ymben.2005.06.001.
36. Aldrich, J. 1995. Correlations genuine and spurious in Pearson and Yule. *Statistical Sci.* 10(4): 363-376. https://projecteuclid.org/download/pdf_1/euclid.ss/1177009870.

37. Passman, F. J., McFarland, B. L., and Hillyer, M. J., 2001. Oxygenated Gasoline Biodeterioration and its Control in Laboratory Microcosms. *Intl. Biodeter. Biodeg.* 47(2): 95-106. PII: S0964-8305(00)00080-9.
38. Hartman, J., Geva, J., Fass, R., 1992. A computerized expert system for diagnosis and control of microbial contamination in jet fuel and diesel fuel storage systems. In: Giles, H.N. (Ed.), *Proceedings of the Fourth International Conference on Stability and Handling of Liquid Fuels*, Orlando, Florida, 19e22 November 1991. U.S. Department of Energy, Washington, pp: 153-166.
39. Conlette, O.C., Emmanuel, N. E., & Chijoke, O. G., 2016 Methanogen population of an oil production skimmer pit and the effects of environmental factors and substrate availability on methanogenesis and corrosion rates. *Microbial ecology*, 2016. 72(1), 175-184.
<http://doi.org/10.1007/s00248-016-0764-2>.
40. Siegbahn, M. 1916. Relations between the K and L series of the high-frequency spectra. *Nature* 96: 676. <https://doi.org/10.1038/096676b0>.
41. Holm-Hansen, O. and Booth, C. R., 1966. The measurement of adenosine triphosphate in the ocean and its ecological significance. *Limnology and oceanography* 11(4): 510-519.
<https://doi.org/10.4319/lo.1966.11.4.0510>.
42. Hamilton, R.D., and Holm-Hansen, O., 1967. Adenosine triphosphate content of marine bacteria. *Limnology and Oceanography* 12(2):319-324. <https://doi.org/10.4319/lo.1967.12.2.0319>.
43. Christian, R. R., Hanson, R. B. and Newell, S. Y., 1982. Comparison of methods for measurement of bacterial growth rates in mixed batch cultures. *Appl. Env. Microbiol.*, 43(5):1160-1165.
[http://dx.doi.org/0099-2240/82/051160-06\\$02.00/0](http://dx.doi.org/0099-2240/82/051160-06$02.00/0).
44. Passman, F. J., Egger, G. L. II, Hallahan S., Skinner, B. W., and Deschepper, M., 2009. Real-time testing of bioburdens in metalworking fluids using adenosine triphosphate as a biomass indicator. *Tribology Transactions* 52(6):788-792. <http://dx.doi.org/10.1080/10402000903097486>.
45. Passman, F.J. and Küenzi, P., 2015. A Differential Adenosine Triphosphate Test Method for Differentiating between Bacterial and Fungal Contamination in Water-Miscible Metalworking Fluids” *International Biodeterioration & Biodegradation* 99:125-137. <https://doi.org/10.1016/j.ibiod.2015.01.006>.
46. Whitaker, R. J. and Banfield, J. F., 2006. Population genomics in natural microbial communities. *Trends in Ecology & Evolution*, 21(9): 508-516. <https://doi.org/10.1016/j.tree.2006.07.001>.
47. Sansonetti, P. J., 2018. Dealing with variability and complexity: challenges in disentangling microbial communities. *FEMS Microbiology Reviews*, 42:113-115.
<https://doi.org/10.1093/femsre/fux058>.
48. Passman, F.J., Schmidt, J, Lewis, R.P. and Christian, P., 2019. The relationship between planktonic and sessile microbial population adenosine triphosphate in diesel fuel microcosms. In: R. E. Morris. Ed. *Proceedings of the 16th International Symposium on the Stability and Handling of Liquid Fuels*, 08 to 12 September 2019, Long Beach, USA (2019). <http://iash.conferencespot.org/69070-iash-1.4569809/t001-1.4569870/f0010-1.4570090/a036-1.4570109/ap103-1.4570112> .

49. Hill, E.C., Hill, G.C., 1994. Microbial proliferation in bilges and its relation to pitting corrosion of hull plate of in-shore vessels. Transactions of the Institute of Marine Engineers 105 (4), 174-182. <https://s3-eu-west-1.amazonaws.com/media.echamicrobiology.co.uk/2016/05/Microbial-Proliferation-in-Bilges-and-its-Relation-to-Pitting-Corrosion-of-Hull-Plate-of-Inshore-Vessels.pdf>.
50. Videla, H.A., 2000. An overview of mechanisms by which sulphate-reducing bacteria influence corrosion of steel in marine environments. Biofouling, 15(1-3):37-47. <https://doi.org/10.1080/08927010009386296>.
51. Videla, H.A. and Herrera, L.K., 2005. Microbiologically influenced corrosion: looking to the future. Int Microbiol, 8(3):169-180. <http://scielo.isciii.es/pdf/im/v8n3/04%20Videla.pdf>.
52. Viera, M.R. and Videla, H.A., 1993. Biodeterioration of materials: microbiological corrosion and biofouling. Rev Argent Microbiol, 25(3):157-170. PMID: 8140248.
53. Uprety, B.K., Venkatesagowda, B., and Rakshit, S.K., 2017. Current prospects on production of microbial lipid and other value-added products using crude glycerol obtained from biodiesel industries. BioEnergy Research, 10(4):1117-1137. <https://doi.org/10.1007/s12155-017-9857-0>.
54. Little, B. and Lee, J, Eds. 2007. Microbiologically influenced corrosion. John Wiley & Sons, Inc. 279 pp., ISBN 978-0-471-77276-7.
55. Webster, J., & Weber, R., 2007. Introduction to fungi. Cambridge University Press.867 pp. ISBN 9780521014830.
56. Parbery, D.G., 1969. *Amorphotheca resinae* gen. nov., sp. nov.: The perfect state of *Cladosporium resinae*. Australian Journal of Botany, 17(2):331-357. <https://doi.org/10.1071/BT9690331>.
57. Rafin, C. and Veignie, E., 2019. *Hormoconis resinae*, the kerosene fungus, In: McGenity T. Ed. Taxonomy, Genomics and Ecophysiology of Hydrocarbon-Degrading Microbes. Handbook of Hydrocarbon and Lipid Microbiology. Springer, Cham pp 1-20. https://doi.org/10.1007/978-3-319-60053-6_3-1.
58. Marmur, J. and Doty, P., 1962. Determination of the base composition of deoxyribonucleic acid from its denaturation temperature. J. Molec. Biol. 5:109-118. [https://doi.org/10.1016/S0022-2836\(62\)80066-7](https://doi.org/10.1016/S0022-2836(62)80066-7).
59. Rauch, M.E., Graef, H.W., Rozenzhak, S.M. Jones, S. E., Bleckmann, C. A., Kruger, R. L., Naik, R.R., and Stone, M. O., 2006. Characterization of microbial contamination in United States Air Force aviation fuel tanks. J Ind Microbiol Biotechnol, 33(1): p. 29-36. <https://doi.org/10.1007/s10295-005-0023-x>.
60. Radwan, O., Gunasekera, T.S., Ruiz, O.N., 2018. Robust Multiplex Quantitative Polymerase Chain Reaction Assay for Universal Detection of Microorganisms in Fuel. Energy & Fuels, 32, 10530-10539. DOI:10.1021/acs.energy&fuels.8b02292.
61. Passman, F. J., 2018. Chapter 8 – Sampling. In: S. J. Rand and A. W. Verstuyft, Eds. ASTM Manual 1 – Significance of Tests for Petroleum Products–9th Edition, ASTM International, West Conshohocken, PA, pp: 119-142 (2018). ISBN 978-0-8031-7108-4.

62. Ondov, B. D., Bergman, N. H., and Phillippy, A. M., 2011. Interactive metagenomic visualization in a web browser. *BMC Bioinformatics* 12:385-994. <http://www.biomedcentral.com/1471-2105/12/385>.
63. Firmino, F. C., Porcellato, D., Cox, M., Suen, G., Broadbent, J. R., and Steele, L. J., 2020. Characterization of microbial communities in ethanol biorefineries. *J. of Industrial Microbiol. Biotech.* 47:183–195. <https://doi.org/10.1007/s10295-019-02254-7>.
64. Pacwa-Płociniczak, M., Płaza, G. A., Poliwoda, A., and Piotrowska-Seget, Z., 2014. Characterization of hydrocarbon-degrading and biosurfactant-producing *Pseudomonas* sp. P-1 strain as a potential tool for bioremediation of petroleum-contaminated soil. *Environ Sci Pollut Res Int.* 21(15): 9385–9395. <https://doi.org/10.1007/s11356-014-2872-1>.
65. Passman, F. J., 2019. Chapter 35 - Biodeterioration. In Totten, G.E, Shah, R. J., and Forester, D. R., Eds. *ASTM Manual 37, 2nd Ed.*, ASTM International, West Conshohocken, PA, pp: 1237-1268. <https://doi.org/10.1520/MNL3720150021>.
66. Chinnawirotpisan, P., Theeragool, G., Limtong, S., Toyama, H., Adachi, O. O., Matsushita, K., 2003. Quinoprotein alcohol dehydrogenase is involved in catabolic acetate production, while NAD-dependent alcohol dehydrogenase in ethanol assimilation in *Acetobacter pasteurianus* SKU1108. *J. Biosci. Bioeng.*, 96(6):564-571. [https://doi.org/10.1016/S1389-1723\(04\)70150-4](https://doi.org/10.1016/S1389-1723(04)70150-4).
67. Youssef, N., Mostafa S. Elshahed, M. S., and McInerney, M. J., 2009. Chapter 6 - Microbial Processes in Oil Fields: Culprits, Problems, and Opportunities. *Adv. Appl. Microbiol* 66: 141-251. ISSN 0065-2164, [https://doi.org/10.1016/S0065-2164\(08\)00806-X](https://doi.org/10.1016/S0065-2164(08)00806-X).
68. Vijayakumar, S., and Saravanan, V., 2015. Biosurfactants-Types, Sources and Applications. *Research Journal of Microbiology* 10(5): 181-192. ISSN 1816-4935 / DOI: 10.3923/jm.2015.181.192.
69. ASTM, 2016. D6974-16, Standard Practice for Enumeration of Viable Bacteria and Fungi in Liquid Fuels—Filtration and Culture Procedures. ASTM International, West Conshohocken, PA, 2016, www.astm.org.

8 GLOSSARY

bacterium (*pl. bacteria*), *n*—a single cell microorganism characterized by the absence of defined intracellular membranes that define all higher life forms. All bacteria are members of the biological diverse kingdoms *Prokaryota* and *Archaeobacteriota*. Individual taxa within these kingdoms are able to thrive in environments ranging from sub-zero temperatures, such as in frozen foods and polar ice, to superheated waters in deep-sea thermal vents, and over the pH range <2.0 to >13.0. Potential food sources range from single carbon molecules (carbon dioxide and methane) to complex polymers, including plastics. Oxygen requirements range from obligate anaerobes, which die on contact with oxygen, to obligate aerobes, which die if oxygen pressure falls below a species-specific threshold.

bioburden, *n*—the level of microbial contamination (*biomass*) in a system. Typically, bioburden is defined in terms of either biomass or numbers of cells per unit volume or mass or surface area material tested (g biomass/mL; g biomass/g; cells/mL sample, and so forth). The specific parameter used to define bioburden depends on critical properties of the system evaluated and the investigator's preferences.

biodeterioration, *n*—the loss of commercial value or performance characteristics, or both, of a product (fuel) or material (fuel system) through biological processes.

biofilm, *n*—a film or layer of microorganisms, biopolymers, water, and entrained organic and inorganic debris that forms as a result of microbial growth and proliferation at phase interfaces (liquid-liquid, liquid-solid, liquid-gas, and so forth) (synonym: *skinnogen layer*).

bioinformatics, *n* – an interdisciplinary branch of statistics and molecular biology that uses information technology and analytics to understand biological data.

biomass, *n*—biological material including any material other than fossil fuels which is or was a living organism or component or product of a living organism. In biology and environmental science, biomass is typically expressed as density of biological material per unit sample volume, area, or mass (g biomass/g (or /mL or /cm²) sample); when used for products derived from organisms biomass is typically expressed in terms of mass (kg, MT, etc.) or volume (L, m³, bbl, etc.). Products of living organisms include those materials produced directly by living organisms as metabolites (for example, ethanol, various carbohydrates and fatty acids), materials manufactured by processing living organisms (for example, pellets manufactured by shredding and pelletizing plant material) and materials produced by processing living organisms, their components or metabolites (for example, transesterified oil; also called biodiesel).

biosurfactant, *n*—a biologically produced molecule that acts as a soap or detergent.

consortium (*pl. consortia*), *n*—microbial community comprised of more than one species that exhibits properties not shown by individual community members. Consortia often mediate biodeterioration processes that individual taxa cannot.

controlled variable (factor), *n* – in statistics, a predetermined element of a test plan. For example, in this study, the presence or absence of additives such as cold flow improver are controlled variables – also referred to as *independent variables*.

Dräger tube, *n* – glass or polymeric, tubular vessel, packed with a porous substance that has been impregnated with an indicator dye that will change colors proportionally to the concentration of an analyte present in air or gas that is drawn through the tube by a vacuum device.

factor, *n* – in statistics, a variable in an experiment. Factors can be controlled (independent) or uncontrolled (dependent). See *controlled variable* and *uncontrolled variable* definitions.

fatty acid, n. – a class of organic molecules that include a carboxyl group (-COOH) and a hydrocarbon chain. *Saturated* fatty acids have no carbon to carbon double bonds and have the general formula $\text{CH}_3(\text{CH}_2)_n\text{COOH}$, where n is the number of CH_2 groups in the hydrocarbon chain. *Unsaturated* fatty acids have one or more carbon to carbon double bonds.

fatty acid methyl ester (FAME), n – the esterification reaction product of a fatty acid with methanol. FAME molecules have the general formula $\text{R}-\overset{\text{O}}{\parallel}{\text{C}}-\text{OH}$ where R is the hydrocarbon chain. FAME is commonly called biodiesel.

fungus (pl. fungi), n—single cell (typically yeasts) or filamentous (molds) microorganisms that share the property of having the true intracellular membranes (organelles) that characterize all higher life forms (*Eukaryotes*).

Internal Transcribed Spacer (ITS), n—segment of DNA situated between ribosomal RNA genes, that can be sequenced in order to classify fungi.

discussion – ITS sequencing is the genetic test method used to classify fungi.

low molecular weight acid (LMWA), n – see low molecular weight organic acid. LMWA is term used by the manufacturer of the Dräger tubes used in this study.

low molecular weight organic acid (LMOA), n – a molecule with one to 6 carbon atoms, terminating with a carboxyl group (see *fatty acid*).

metabolite, n—a chemical substance produced by any of the many complex chemical and physical processes involved in the maintenance of life.

metagenome, n – the genetic content of any group of microorganisms.

microbiologically influenced corrosion (MIC), n—corrosion that is enhanced by the action of microorganisms in the local environment.

microcosm, n – a miniature system used to model larger systems.

next generation sequencing (NGS), n – in genetic testing, is a class of high throughput DNA analysis technologies used to classify organisms based on their genetic properties. Synonyms include *high-throughput sequencing* and *massive parallel sequencing*.

polymerase chain reaction (PCR), n – a family of biochemical methods in which repeated cycles of heating and cooling are used to create millions of copies of DNA from a single copy.

quantitative polymerase chain reaction (qPCR), n – a variant of PCR in which the number of DNA copies produced is monitored as a function of time and the signal generated by the DNA concentration in test specimens is compared to that from a standard curve.

ribosomal ribonucleic acid (rRNA), n – the component of living cells in which proteins are synthesized.

discussion – ribosomes contain messenger RNA (mRNA) that transfers genetic information from DNA to rRNA. The rRNA assembles amino acids to produce polypeptides and proteins. 16S rRNA is the component of the 30S subunit of prokaryotic ribosomes that is code for by the 16S rRNA gene. This gene is the region of DNA used to identify OTUs in a specimen.

uncontrolled variable (factor), n – in statistics a parameter whose value is dependent on test conditions. For example, in this study, corrosion ratings and ATP-bioburdens were uncontrolled variables – also referred to as *dependent variables*.

APPENDIX A
Microcosm Test Condition Matrix

Table A.1 Fractional factorial fuel corrosivity test plan – microcosm details.

#	Group	Sulfur	Biodiesel (%)	Water	Glycerin (ppm)	Ethanol (ppm)	Microorganisms	Mono-acid lubricity (MAL) additive (ppm)	Cold flow improver (CFI) additive (ppm)	Corrosion inhibitor (ppm)	Conductivity Additive (ppm)	FRP Material
1	1	ULSD	0	0	0	0	0	200	0	0	0	0
2	1	ULSD	0	0	0	0	0	200	200	0	2-3	Present
3	1	ULSD	0	Present	0	0	0	0	0	8-10	2-3	0
4	1	ULSD	0	Present	0	0	Present	0	200	0	2-3	0
5	1	ULSD	0	Present	5000	0	Present	0	200	0	2-3	Present
6	1	ULSD	5	0	0	0	0	0	0	0	2-3	Present
7	1	ULSD	5	0	0	0	0	0	0	8-10	2-3	0
8	1	ULSD	5	0	0	0	0	0	200	0	0	Present
9	1	ULSD	5	0	0	0	0	200	200	8-10	2-3	Present
10	1	ULSD	5	Present	0	0	Present	200	0	8-10	0	Present
11	1	ULSD	5	Present	0	10000	0	0	0	0	2-3	Present
12	1	ULSD	5	Present	0	10000	0	0	200	8-10	0	0
13	1	ULSD	5	Present	0	10000	Present	200	200	8-10	2-3	0
14	1	ULSD	5	Present	5000	0	0	200	0	8-10	0	Present
15	1	ULSD	5	Present	5000	10000	0	200	200	0	0	Present
16	1	LSD	0	0	0	0	0	0	0	8-10	0	0
17	1	LSD	0	0	0	0	0	200	0	0	2-3	0
18	1	LSD	0	0	0	0	0	200	200	8-10	2-3	0
19	1	LSD	0	Present	0	0	0	0	200	8-10	2-3	Present
20	1	LSD	0	Present	0	0	0	200	200	0	0	Present
21	1	LSD	0	Present	0	0	Present	200	200	8-10	2-3	Present
22	1	LSD	0	Present	0	10000	0	0	200	0	0	0
23	1	LSD	0	Present	0	10000	0	200	0	0	2-3	Present
24	1	LSD	0	Present	5000	10000	0	0	200	8-10	0	0
25	1	LSD	0	Present	5000	10000	Present	200	0	8-10	2-3	Present

26	1	LSD	5	0	0	0	0	0	200	0	2-3	0
27	1	LSD	5	0	0	0	0	0	200	8-10	0	Present
28	1	LSD	5	Present	0	0	Present	0	200	8-10	0	0
29	1	LSD	5	Present	0	0	Present	200	0	0	0	0
30	1	LSD	5	Present	5000	0	0	200	200	0	0	0
31	1	LSD	5	Present	5000	0	Present	0	0	0	2-3	Present
32	1	LSD	5	Present	5000	0	Present	0	200	0	0	Present
33	2	ULSD	0	0	0	0	0	0	200	8-10	2-3	0
34	2	ULSD	0	Present	0	0	0	200	0	0	0	0
35	2	ULSD	0	Present	0	0	Present	0	0	0	0	Present
36	2	ULSD	0	Present	0	10000	0	200	200	8-10	2-3	0
37	2	ULSD	0	Present	0	10000	Present	200	0	0	2-3	0
38	2	ULSD	0	Present	5000	0	Present	0	0	8-10	2-3	Present
39	2	ULSD	0	Present	5000	0	Present	200	0	0	0	Present
40	2	ULSD	0	Present	5000	10000	0	0	0	0	0	Present
41	2	ULSD	0	Present	5000	10000	0	200	0	8-10	0	0
42	2	ULSD	5	0	0	0	0	200	0	0	2-3	0
43	2	ULSD	5	0	0	0	0	200	200	8-10	0	0
44	2	ULSD	5	Present	0	0	0	200	200	0	2-3	0
45	2	ULSD	5	Present	0	0	0	200	200	8-10	0	Present
46	2	ULSD	5	Present	0	0	Present	200	200	0	2-3	Present
47	2	ULSD	5	Present	5000	0	0	0	0	8-10	0	0
48	2	ULSD	5	Present	5000	0	Present	0	0	0	0	0
49	2	ULSD	5	Present	5000	0	Present	200	200	0	0	0
50	2	LSD	0	0	0	0	0	0	0	0	2-3	Present
51	2	LSD	0	0	0	0	0	200	200	0	0	Present
52	2	LSD	0	Present	0	0	0	200	0	8-10	0	0
53	2	LSD	0	Present	0	0	Present	0	200	0	0	Present
54	2	LSD	0	Present	0	0	Present	200	200	0	2-3	0

#	Group	Sulfur	Biodiesel (%)	Water	Glycerin (ppm)	Ethanol (ppm)	Microorganisms	Mono-acid lubricity (MAL) additive (ppm)	Cold flow improver (CFI) additive (ppm)	Corrosion inhibitor (ppm)	Conductivity Additive (ppm)	FRP Material
---	-------	--------	---------------	-------	----------------	---------------	----------------	--	---	---------------------------	-----------------------------	--------------

55	2	LSD	0	Present	0	10000	0	200	0	8-10	0	Present
56	2	LSD	0	Present	5000	0	0	0	0	0	2-3	0
57	2	LSD	0	Present	5000	0	0	200	200	8-10	2-3	0
58	2	LSD	0	Present	5000	0	Present	200	200	8-10	0	Present
59	2	LSD	5	Present	0	0	0	0	0	8-10	2-3	Present
60	2	LSD	5	Present	0	10000	Present	0	0	8-10	2-3	0
61	2	LSD	5	Present	5000	0	0	200	0	0	2-3	Present
62	2	LSD	5	Present	5000	0	Present	0	200	8-10	2-3	0
63	2	LSD	5	Present	5000	10000	0	0	200	0	0	Present
64	2	LSD	5	Present	5000	10000	Present	200	0	8-10	0	0
65	3	ULSD	0	0	0	0	0	200	0	8-10	0	Present
66	3	ULSD	0	Present	0	0	Present	200	200	8-10	0	0
67	3	ULSD	0	Present	0	10000	0	200	200	0	0	Present
68	3	ULSD	0	Present	0	10000	Present	0	0	8-10	0	0
69	3	ULSD	0	Present	5000	0	0	0	200	0	0	0
70	3	ULSD	0	Present	5000	0	Present	0	200	8-10	0	Present
71	3	ULSD	0	Present	5000	10000	0	0	0	8-10	2-3	Present
72	3	ULSD	0	Present	5000	10000	Present	0	0	0	2-3	0
73	3	ULSD	0	Present	5000	10000	Present	0	200	8-10	2-3	0
74	3	ULSD	5	Present	0	0	0	0	200	0	0	Present
75	3	ULSD	5	Present	0	0	Present	200	0	8-10	2-3	0
76	3	ULSD	5	Present	0	10000	0	200	0	8-10	2-3	Present
77	3	ULSD	5	Present	0	10000	Present	0	200	0	0	0
78	3	ULSD	5	Present	5000	0	0	0	200	8-10	2-3	0
79	3	ULSD	5	Present	5000	0	0	200	0	0	2-3	0
80	3	LSD	0	Present	0	0	Present	0	0	8-10	2-3	Present
81	3	LSD	0	Present	0	0	Present	200	0	0	2-3	Present
82	3	LSD	0	Present	0	10000	0	0	0	0	2-3	0
83	3	LSD	0	Present	0	10000	Present	200	200	0	0	0

#	Group	Sulfur	Biodiesel (%)	Water	Glycerin (ppm)	Ethanol (ppm)	Microorganisms	Mono-acid lubricity (MAL) additive (ppm)	Cold flow improver (CFI) additive (ppm)	Corrosion inhibitor (ppm)	Conductivity Additive (ppm)	FRP Material
---	-------	--------	---------------	-------	----------------	---------------	----------------	--	---	---------------------------	-----------------------------	--------------

84	3	LSD	0	Present	5000	0	0	0	0	8-10	0	Present
85	3	LSD	0	Present	5000	0	0	0	200	0	2-3	Present
86	3	LSD	0	Present	5000	10000	Present	0	0	0	0	Present
87	3	LSD	5	0	0	0	0	0	0	0	0	0
88	3	LSD	5	0	0	0	0	200	0	8-10	2-3	Present
89	3	LSD	5	Present	0	0	0	0	0	0	0	0
90	3	LSD	5	Present	0	0	0	0	200	0	2-3	0
91	3	LSD	5	Present	0	10000	0	200	200	0	2-3	Present
92	3	LSD	5	Present	0	10000	Present	200	200	8-10	0	Present
93	3	LSD	5	Present	5000	0	Present	200	0	8-10	0	Present
94	3	LSD	5	Present	5000	0	Present	200	200	8-10	2-3	Present
95	3	LSD	5	Present	5000	10000	0	0	200	8-10	2-3	Present
96	3	LSD	5	Present	5000	10000	Present	200	200	0	2-3	0
97	4	ULSD	0	0	0	0	0	0	200	0	0	0
98	4	ULSD	0	Present	0	0	0	200	0	0	2-3	Present
99	4	ULSD	0	Present	0	10000	0	0	200	8-10	0	Present
100	4	ULSD	0	Present	0	10000	Present	0	200	0	2-3	Present
101	4	ULSD	0	Present	0	10000	Present	200	0	8-10	2-3	Present
102	4	ULSD	0	Present	5000	0	0	200	200	8-10	2-3	Present
103	4	ULSD	0	Present	5000	0	Present	200	0	8-10	2-3	0
104	4	ULSD	0	Present	5000	10000	0	200	200	0	2-3	0
105	4	ULSD	0	Present	5000	10000	Present	200	200	8-10	0	Present
106	4	ULSD	5	Present	0	0	Present	0	0	0	2-3	0
107	4	ULSD	5	Present	0	0	Present	0	200	8-10	2-3	Present
108	4	ULSD	5	Present	0	10000	0	200	0	0	0	0
109	4	ULSD	5	Present	0	10000	Present	200	0	0	0	Present
110	4	ULSD	5	Present	5000	10000	0	0	200	0	2-3	0
111	4	ULSD	5	Present	5000	10000	Present	0	0	8-10	0	Present
112	4	ULSD	5	Present	5000	10000	Present	200	0	0	2-3	Present

#	Group	Sulfur	Biodiesel (%)	Water	Glycerin (ppm)	Ethanol (ppm)	Microorganisms	Mono-acid lubricity (MAL) additive (ppm)	Cold flow improver (CFI) additive (ppm)	Corrosion inhibitor (ppm)	Conductivity Additive (ppm)	FRP Material
---	-------	--------	---------------	-------	----------------	---------------	----------------	--	---	---------------------------	-----------------------------	--------------

113	4	ULSD	5	Present	5000	10000	Present	200	200	8-10	2-3	0
114	4	LSD	0	Present	0	10000	Present	0	200	8-10	2-3	0
115	4	LSD	0	Present	0	10000	Present	200	0	8-10	0	0
116	4	LSD	0	Present	5000	0	Present	0	0	8-10	0	0
117	4	LSD	0	Present	5000	0	Present	200	0	0	0	0
118	4	LSD	0	Present	5000	10000	0	200	0	0	0	Present
119	4	LSD	0	Present	5000	10000	Present	200	200	0	2-3	Present
120	4	LSD	5	0	0	0	0	200	0	0	0	Present
121	4	LSD	5	0	0	0	0	200	200	8-10	0	0
122	4	LSD	5	Present	0	0	0	200	0	8-10	2-3	0
123	4	LSD	5	Present	0	10000	0	0	0	8-10	0	Present
124	4	LSD	5	Present	0	10000	0	200	200	8-10	0	0
125	4	LSD	5	Present	0	10000	Present	0	0	0	2-3	Present
126	4	LSD	5	Present	5000	10000	0	0	0	8-10	2-3	0
127	4	LSD	5	Present	5000	10000	0	200	0	0	2-3	0
128	4	LSD	5	Present	5000	10000	Present	0	200	0	0	0

#	Group	Sulfur	Biodiesel (%)	Water	Glycerin (ppm)	Ethanol (ppm)	Microorganisms	Mono-acid lubricity (MAL) additive (ppm)	Cold flow improver (CFI) additive (ppm)	Corrosion inhibitor (ppm)	Conductivity Additive (ppm)	FRP Material
---	-------	--------	---------------	-------	----------------	---------------	----------------	--	---	---------------------------	-----------------------------	--------------

APPENDIX B
LC-MS TEST METHOD PARAMETERS

Single Quadrupole Acquisition Method - MS Parameters Report

Method file	D:\MassHunter\GCMS\1\methods\DB5-1hr.M
Tune file	ATUNE.U
Ion source	EI
Source temperature (°C)	230
Quad temperature (°C)	150
Fixed Electron energy (eV)	70.0
Acquisition Type	Scan
Stop time (min)	10.00
Solvent delay (min)	0.00
Trace Ion Detection	False
Gain Factor	1
EM Saver	False
EM Saver Limit	N/A

Scan Time Segments

Time	Start Mass	End Mass	Threshold	Scan Speed
0.00	17	500	200	1,562 [N=2]

Timed Events

Time	Type of Event	Parameter
------	---------------	-----------

Real-Time Plots

Type of Plot	Label	Low Mass	High Mass
Total Ion	N/A	N/A	N/A
Spectrum	N/A	N/A	N/A
Extracted Ion	Scan 1-1	17	550

Identification of Potential Parameters
Causing Corrosion of Metallic Components
in Diesel Underground Storage Tanks
(CRC Project No. DP-07-16)
Matrix Analysis

Jo Martinez

Staff Statistician, Chevron

August 19, 2019

Agenda

- Summary of Conclusions
- Matrix Design
- Rating Data
- Statistical Method
- Model Results
 - Aqueous (p. 7)
 - Aqueous Edge (p. 22)
 - Aqueous/Fuel Interface (p. 43)
 - Aqueous/Fuel Interface Edge (p. 61)
 - Fuel (p. 82)
 - Fuel Edge (p. 104)
 - Vapor (p. 116)
 - Vapor Edge (p. 122)

Summary of Conclusions

The following effects showed significant changes in corrosion rating as depicted in the logistic model predictions or most likely ratings (none for Vapor phase):

Aqueous	AqEdge	AqFuel	AqFuel Edge	Fuel	Fuel Edge	Vapor Edge
						↓ULSD
			↓Biodiesel	↓Biodiesel		
			↓Microbes			
			↓MAL Additive			
	↑CFI Additive, LSDF					
		↓Corrosion Inhibitor	↓Corrosion Inhibitor	↓Corrosion Inhibitor		
				↓Biodiesel, LSDF		
	↓ULSD, CFI Additive					↓ULSD, Water
↓ULSD, Conductivity Additive	↓ULSD, Conductivity Additive					↓ULSD, CFI Additive
				↓Biodiesel, Glycerin		
			↓Biodiesel, Ethanol			
			↓Biodiesel, Microbes			
		↓Biodiesel, CFI Additive				
	↓Glycerin, CFI Additive			↓Conductivity Additive, Water		
			↓CFI Additive, Glycerin			
		↓Ethanol, Microbes	↓Ethanol, Microbes	↓Glycerin, FRP-Material		
			↑Ethanol, Microbes			
↓Ethanol, Conductivity Additive				↓Corrosion Inhibitor, Ethanol		
						↑MAL Additive, Microbes
						↓CFI Additive, Microbes
			↓Corrosion Inhibitor, Microbes	↓Corrosion Inhibitor, Microbes		
			↓Corrosion Inhibitor, MAL Additive	↓Corrosion Inhibitor, MAL Additive		
	↓MAL Additive, Conductivity Additive			↑Corrosion Inhibitor, MAL Additive	↑Corrosion Inhibitor, MAL Additive	
		↓Corrosion Inhibitor, CFI Additive				
			↓CFI Additive, Conductivity Additive			
				↓CFI Additive, FRP-Material		↓CFI Additive, FRP-Material
				↓Corrosion Inhibitor, FRP-Material		
				↓Conductivity Additive, FRP-Material		

Note: ↓ lower corrosion rating, ↑ higher corrosion rating, Absence, Presence

Matrix Design

- **Fractional Factorial Design:** $2^{11-4} = 128$ tests
- **Factors (Levels):**
 - Sulfur (LSDF, ULSD)
 - Biodiesel, % (0, 5)
 - Water (0, Present)
 - Glycerin, ppm (0, 5000)
 - Ethanol, ppm (0, 10000)
 - Microbes (0, Present)
 - Mono Acid Lubricity (MAL) Additive, ppm (0, 200)
 - Cold Flow Improver (CFI) Additive, ppm (0, 200)
 - DSA-type Corrosion Inhibitor, ppm (0, 8-10)
 - Conductivity Additive, ppm (0, 2-3)
 - FRP Material (0, Present)
- **Response:** Average Corrosion Severity Rating for Samples 1-3
- **Objective:** Determine factors affecting Corrosion

Average Corrosion Severity Rating Data

- Repeated Measurements per matrix condition
 - Time (week): 7 (1, 2, 3, 4, 6, 9, 12)
 - Phase (location): 8 (Aqueous, Aqueous Edge, Aqueous/Fuel Interface, Aqueous/Fuel Interface Edge, Fuel, Fuel Edge, Vapor, Vapor Edge)
 - Total measurements per condition: 56
- Rating Scheme
 - 1 – little to no visible corrosion product
 - 2 – light/superficial corrosion
 - 3 – mild, but obvious corrosive attack
 - 4 – greater than 50% zonal coverage
 - 5 – heavy/full/coverage/zonal spread
- Analyses performed on Week 12 and on all weeks (Time) average corrosion severity rating for each of the following phases:
 - Aqueous
 - Aqueous Edge
 - Aqueous/Fuel Interface
 - Aqueous/Fuel Interface Edge
 - Fuel
 - Fuel Edge
 - Vapor
 - Vapor Edge

Ordinal Logistic Regression

- Modeled 106 average corrosion severity rating data in Aqueous, Aqueous Edge, Aqueous/Fuel interface and Aqueous/Fuel Edge interface
 - 22 out of 128 conditions are without Water
- Modeled 128 average corrosion severity rating data in Fuel, Fuel Edge, Vapor and Vapor Edge phases
- **Corrosion Severity Rating** is an ordinal type of data so Ordinal Logistic Regression is used to analyze this data
- Response variable is the **Probability of Corrosion Severity (0-1)**
 - E.g. $P(\text{Aq/Fuel Rating} \geq 3) = 0.8$
- Regressed **Corrosion Severity Rating** on:
 - Main effects (10 or 11)
 - Two-factor interaction effects (45 or 52)
- Stepwise Ordinal Logistic Regression was applied for variable selection

Aqueous Phase

Conclusions (Aqueous Phase)

Average Corrosion Severity Rating (average of 3 samples)

- 5% Biodiesel has **lower** probability of high corrosion severity than zero Biodiesel
- 10000 ppm of Ethanol has **higher** probability of high corrosion severity than zero Ethanol
- Presence of Microbes has **lower** probability of high corrosion severity than the absence of Microbes
- 8-10 ppm Corrosion inhibitor has **lower** probability of high corrosion severity than zero corrosion inhibitor
- LSDF has **lower** probability of high corrosion severity than ULSD in the presence of Microbes
- LSDF has **lower** probability of high corrosion severity than ULSD without CFI additive while it has **higher** probability with CFI additive
- LSDF has **lower** probability of high corrosion severity than ULSD without Conductivity additive while it has **higher** probability with Conductivity additive
- 10000 ppm Ethanol has **higher** probability of high corrosion severity than without Ethanol in the absence of Microbes
- 10000 ppm Ethanol has **lower** probability of high corrosion severity than zero Ethanol with Conductivity additive while it has **higher** probability without Conductivity additive
- 200 ppm MAL additive has **lower** probability of high corrosion severity than zero MAL additive in the presence of FRP Material while it has **higher** probability in the absence of FRP Material

Average Corrosion Severity Rating by Time (Week)

- Probability of high corrosion severity in Week 2 is significantly higher than Week 1, and Week 3 is significantly higher Week 2

Stepwise Ordinal Logistic Regression

Aqueous Phase – Week 12

Whole Model Test			
Model	-LogLikelihood	DF	ChiSquare Prob>ChiSq
Difference	25.146607	16	50.29321 <.0001*
Full	65.023302		
Reduced	90.169908		
RSquare (U)	0.2789		
AICc	176.884		
BIC	218.652		
Observations (or Sum Wgts)	106		
Fit Details			
Measure	Training	Definition	
Entropy RSquare	0.2789	1-Loglike(model)/Loglike(0)	
Generalized RSquare	0.4621	$(1-(L(0)/L(model))^{(2/n)})/(1-L(0)^{(2/n)})$	
Mean -Log p	0.6134	$\sum -\log(p_{ij})/n$	
RMSE	0.4348	$\sqrt{\sum (y_{ij}-p_{ij})^2/n}$	
Mean Abs Dev	0.3420	$\sum y_{ij}-p_{ij} /n$	
Misclassification Rate	0.2453	$\sum (p_{ij} \neq p_{Max})/n$	
N	106	n	
Lack Of Fit			
Source	DF	-LogLikelihood	ChiSquare Prob>ChiSq
Lack Of Fit	299	65.023302	130.0466
Saturated	315	0.000000	Prob>ChiSq
Fitted	16	65.023302	1.0000

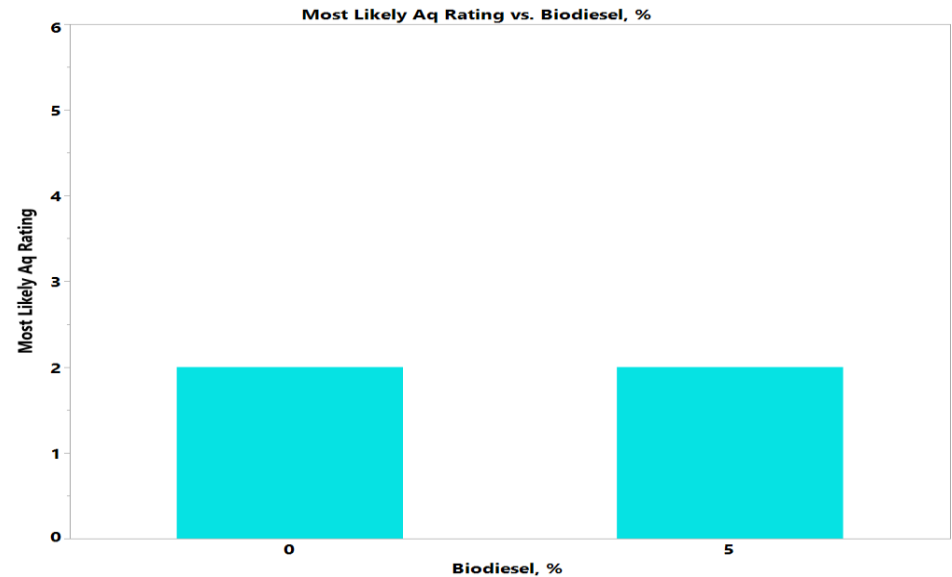
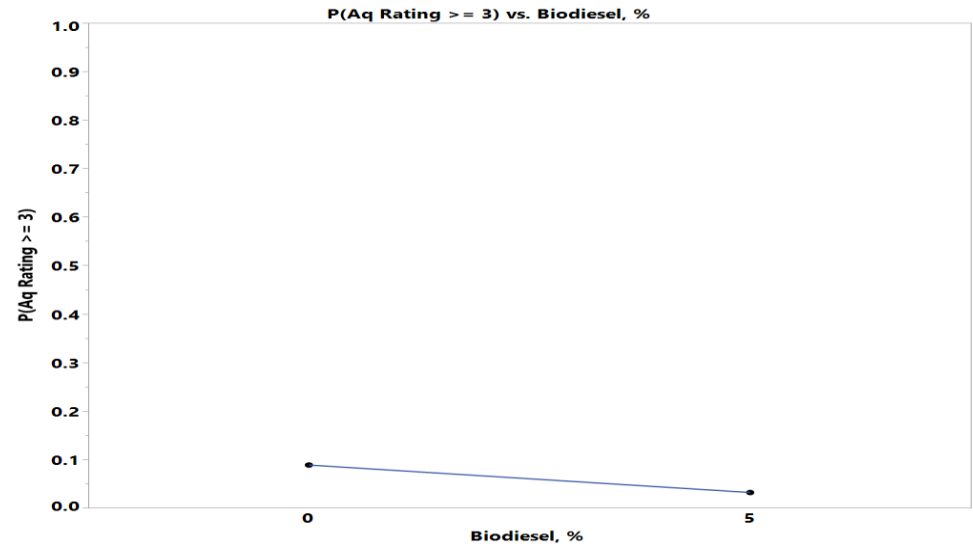
Parameter Estimates				
Term	Estimate	Std Error	ChiSquare	Prob>ChiSq
Intercept[1]	-3.7365251	0.5708586	42.84	<.0001*
Intercept[2]	2.17208207	0.365532	35.31	<.0001*
Intercept[3]	4.52957967	0.6495163	48.63	<.0001*
Sulfur[LSDf]	0.18184084	0.2448408	0.55	0.4577
Biodiesel, %[0]	-0.5433041	0.2559302	4.51	0.0338*
Glycerin, ppm[0]	-0.3518723	0.248167	2.01	0.1562
Ethanol, ppm[0]	0.71158042	0.2638271	7.27	0.0070*
Mircobes[0]	-0.444817	0.2524353	3.11	0.0781
MAL additive, ppm[0]	-0.2200302	0.2446519	0.81	0.3685
CFI additive, ppm[0]	0.16769537	0.2438245	0.47	0.4916
Corrosion inhibitor, ppm[0]	-0.6148249	0.2585284	5.66	0.0174*
Conductivity additive, ppm[0]	0.14091691	0.2469439	0.33	0.5682
FRP Material[0]	0.23137556	0.244541	0.90	0.3441
Sulfur[LSDf]*Mircobes[0]	-0.7847733	0.2710492	8.38	0.0038*
Sulfur[LSDf]*CFI additive, ppm[0]	0.42283281	0.2460738	2.95	0.0857
Sulfur[LSDf]*Conductivity additive, ppm[0]	0.51293217	0.2528561	4.12	0.0425*
Ethanol, ppm[0]*Mircobes[0]	-0.4990156	0.2519469	3.92	0.0476*
Ethanol, ppm[0]*Conductivity additive, ppm[0]	0.63226333	0.2609579	5.87	0.0154*
MAL additive, ppm[0]*FRP Material[0]	0.62048169	0.2561888	5.87	0.0154*

Biodiesel Effect – Aq Phase

- 5% Biodiesel has **lower** probability of high corrosion severity than zero Biodiesel

	Biodiesel, %	
	0	5
Aq12	N	N
1	2	7
2	41	36
3	7	9
4	4	0

	Biodiesel, %	
	0	5
Aq12	N	N
1		
2		
3		
4		

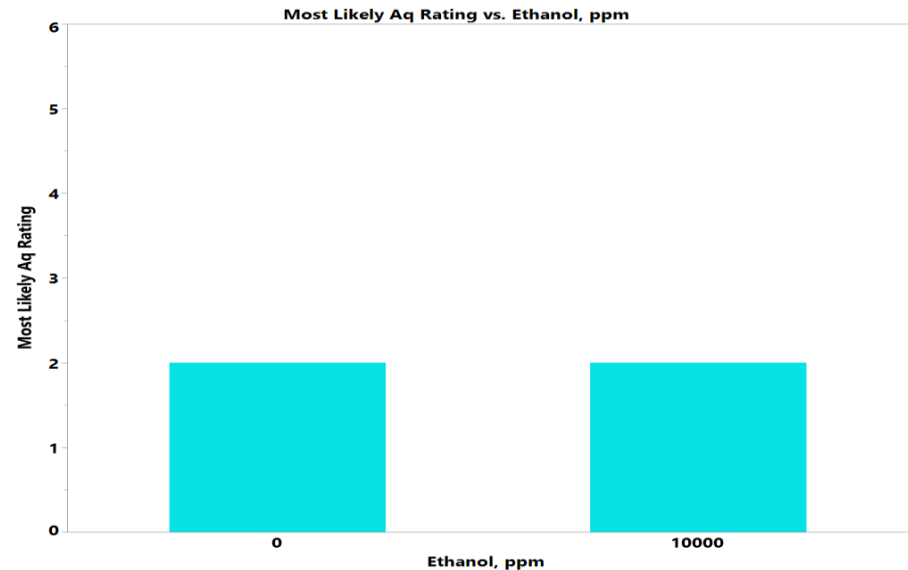
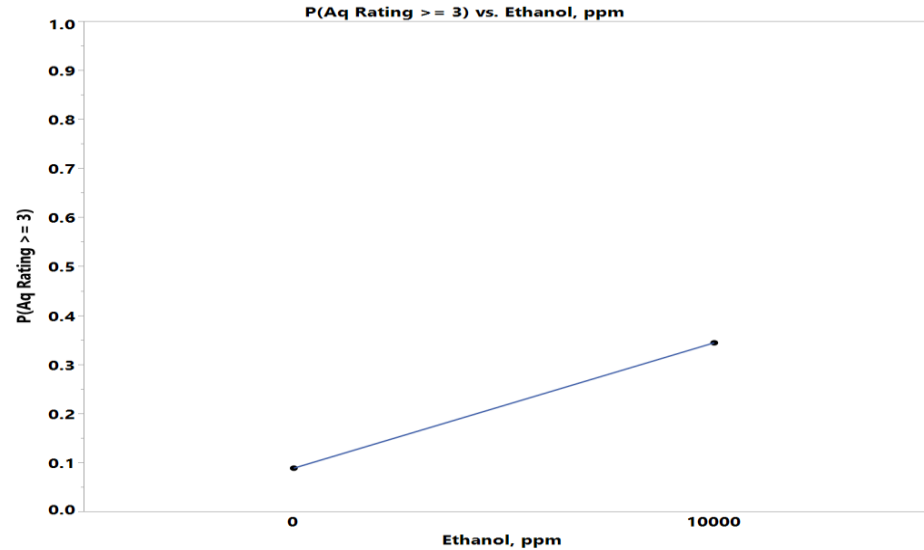
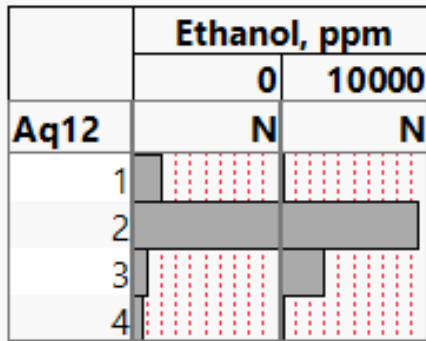


Where((Sulfur = LSDF) and (Glycerin = 0) and (Microbes = 0) and (Ethanol = 0) and (MAL additive = 0) and (CFI additive = 0) and (Corrosion inhibitor = 0) and (Conductivity Additive = 0) and (FRP Material = 0))

Ethanol Effect – Aq Phase

- 10000 ppm of Ethanol has **higher** probability of high corrosion severity than zero Ethanol

	Ethanol, ppm	
	0	10000
Aq12	N	N
1	8	1
2	40	37
3	4	12
4	3	1



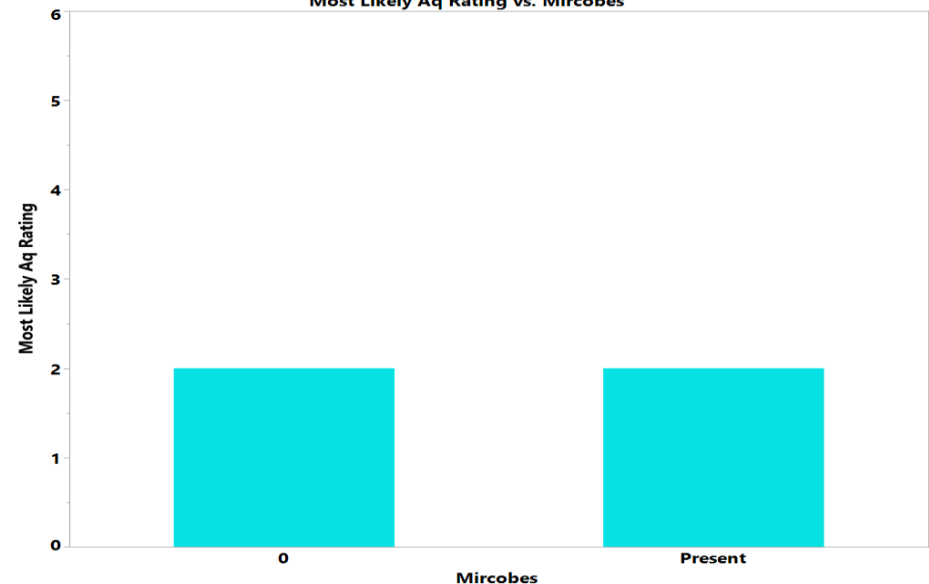
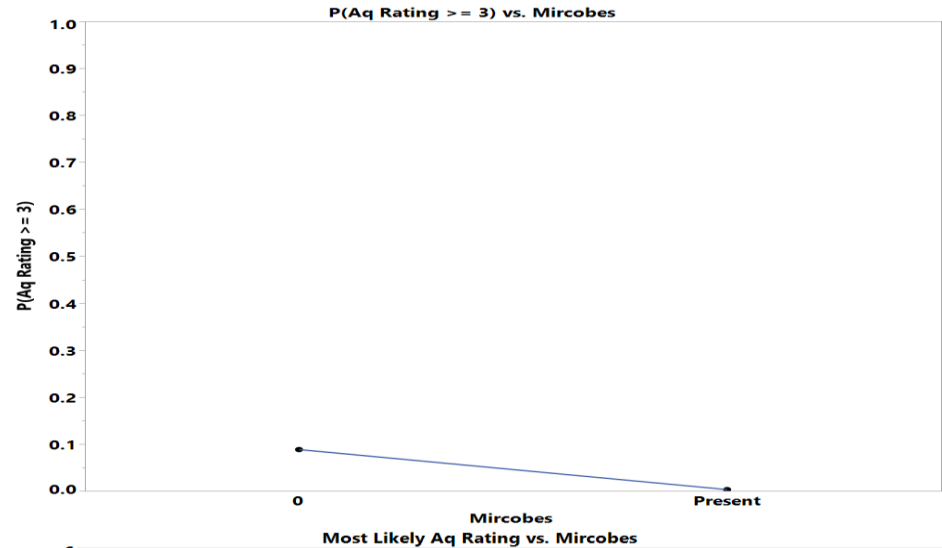
Where((Sulfur = LSDF) and (Water = 0) and (Glycerin = 0) and (Microbes = 0) and (Biodiesel = 0) and (MAL additive = 0) and (CFI additive = 0) and (Corrosion inhibitor = 0) and (Conductivity Additive = 0) and (FRP Material = 0))

Microbes Effect – Aq Phase

- Presence of Microbes has **lower** probability of high corrosion severity than the absence of Microbes

	Microbes	
	0	Present
Aq12	N	N
1	3	6
2	36	41
3	8	8
4	4	0

	Microbes	
	0	Present
Aq12	N	N
1		
2		
3		
4		

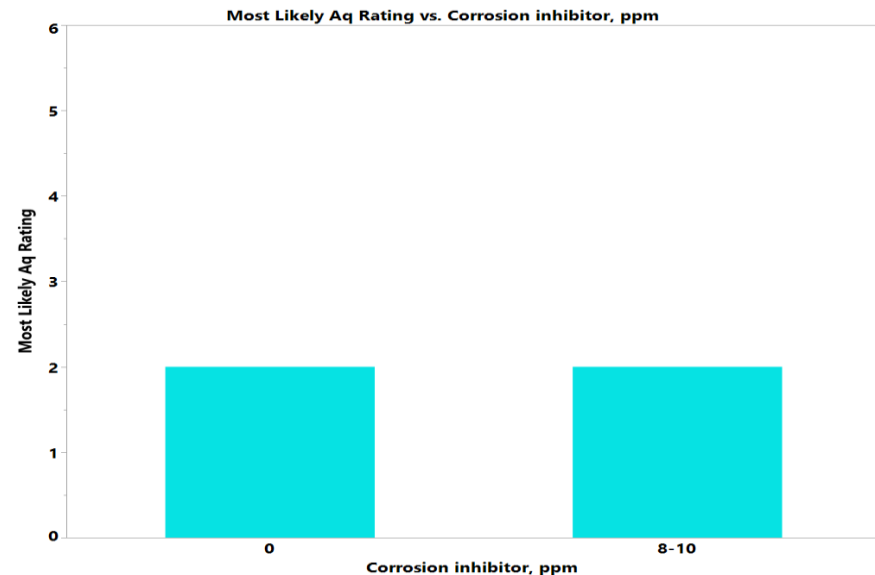
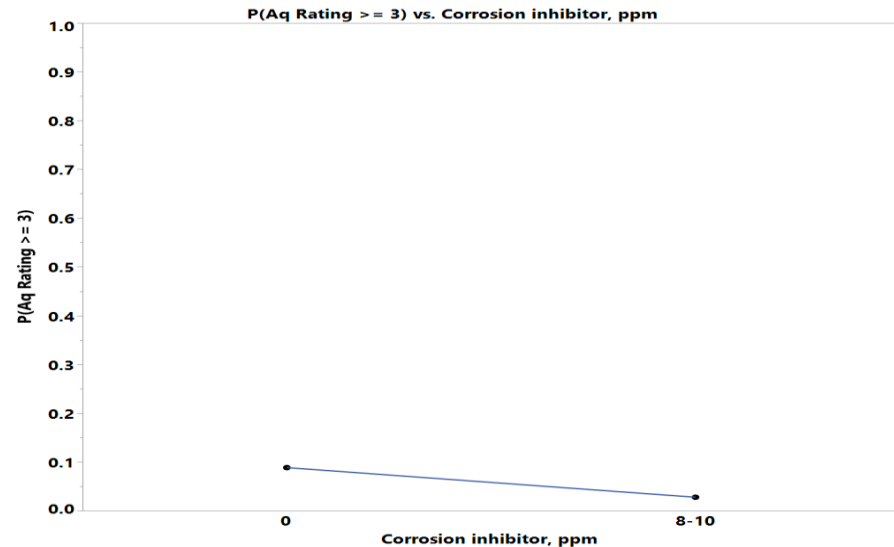


Corrosion Inhibitor Effect – Aq Phase

- 8-10 ppm Corrosion inhibitor has **lower** probability of high corrosion severity than zero corrosion inhibitor

	Corrosion inhibitor, ppm	
	0	8-10
Aq12	N	N
1	3	6
2	37	40
3	11	5
4	3	1

	Corrosion inhibitor, ppm	
	0	8-10
Aq12	N	N
1		
2		
3		
4		

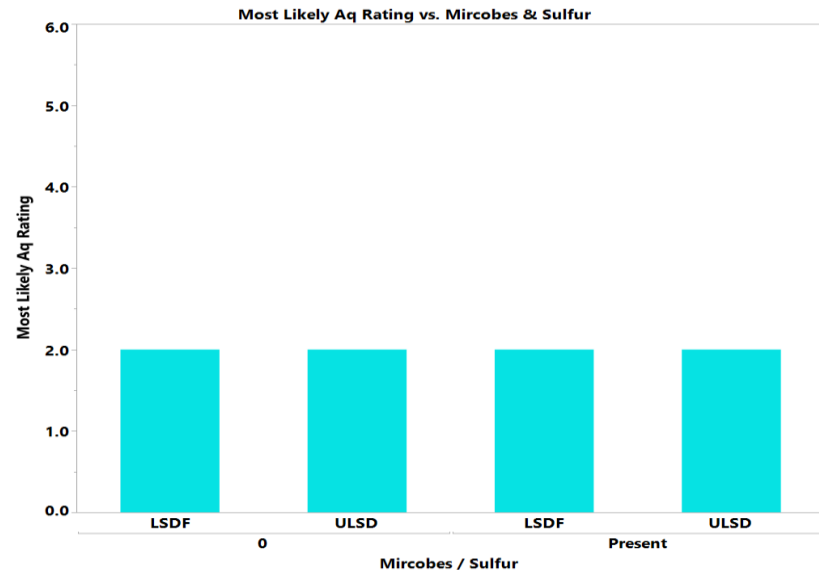
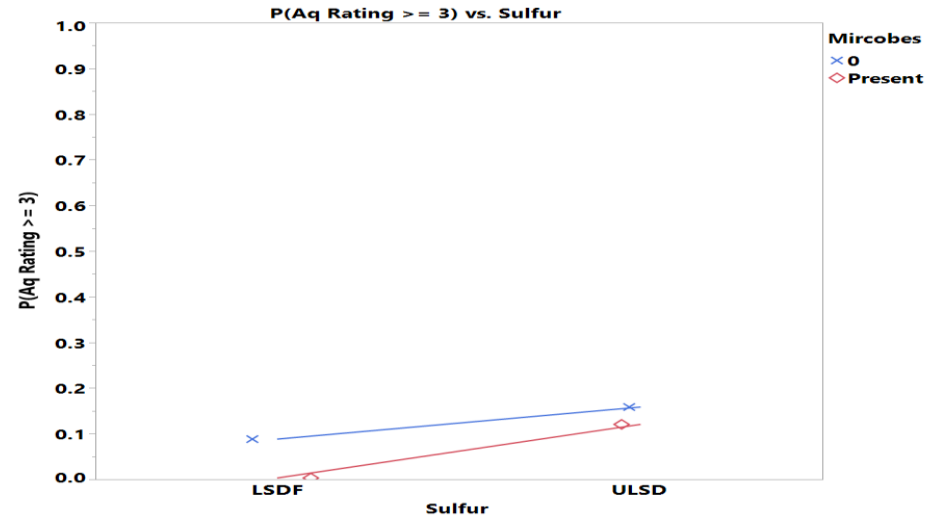
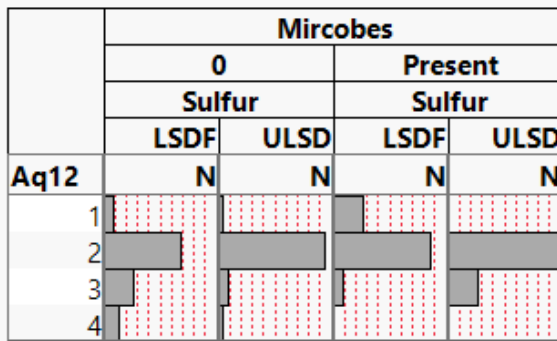


Where((Biodiesel = 0) and (Water = 0) and (Glycerin = 0) and (Microbes = 0) and (Ethanol = 0) and (MAL additive = 0) and (CFI additive = 0) and (Sulfur= LSDF) and (Conductivity Additive = 0) and (FRP Material = 0))

Sulfur-Microbes Interaction Effect

- LSDF has **lower** probability of high corrosion severity than ULSD when in the presence of Microbes

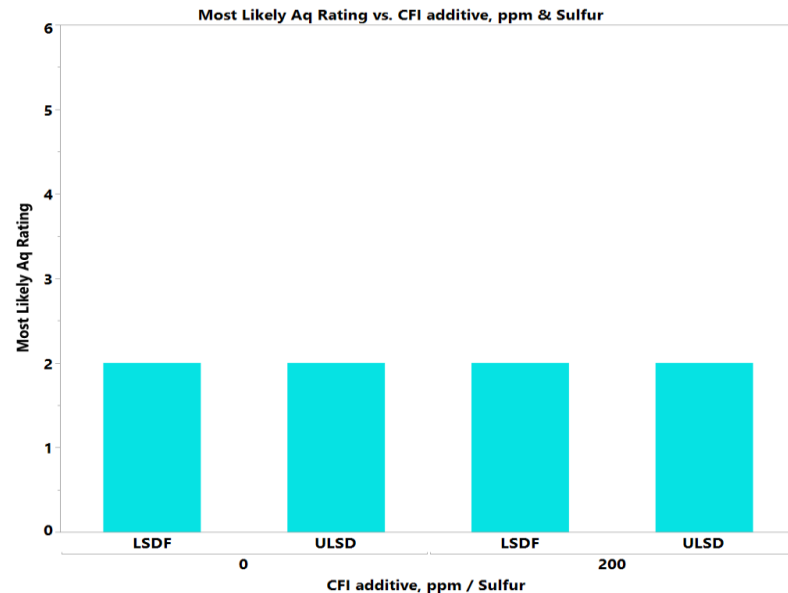
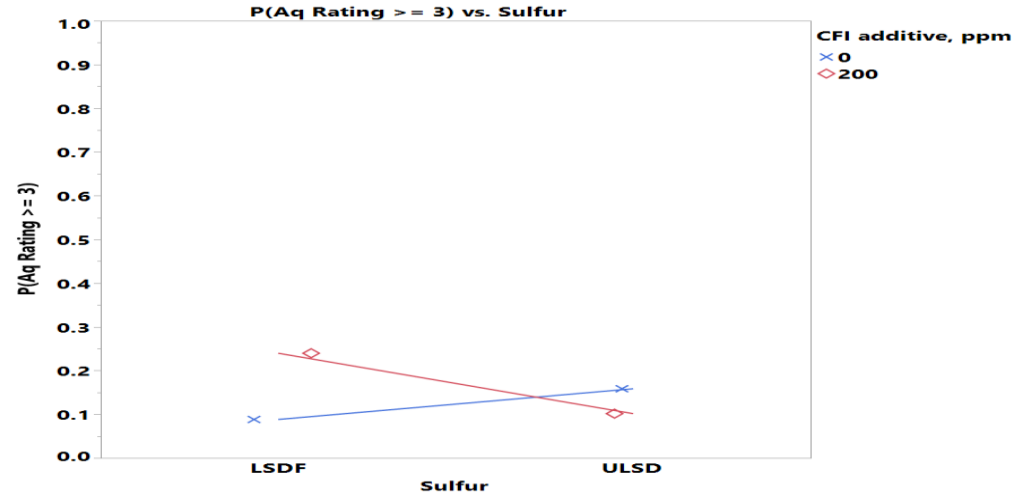
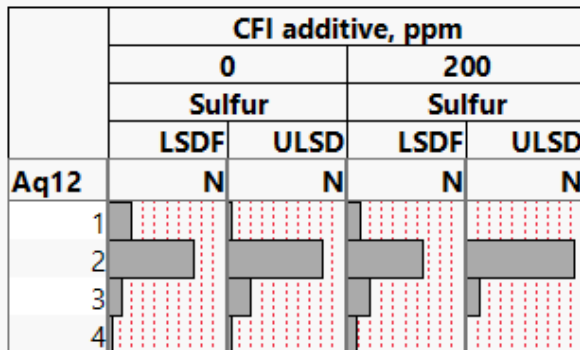
	Microbes			
	0		Present	
	Sulfur		Sulfur	
	LSDF	ULSD	LSDF	ULSD
Aq12	N	N	N	N
1	2	1	6	0
2	15	21	19	22
3	6	2	2	6
4	3	1	0	0



Sulfur-CFI Additive Interaction Effect

- LSDF has **lower** probability of high corrosion severity than ULSD **without** CFI additive while it has **higher** probability **with** CFI additive

	CFI additive, ppm			
	0		200	
	Sulfur		Sulfur	
	LSDF	ULSD	LSDF	ULSD
Aq12	N	N	N	N
1	5	1	3	0
2	18	20	16	23
3	3	5	5	3
4	1	1	2	0



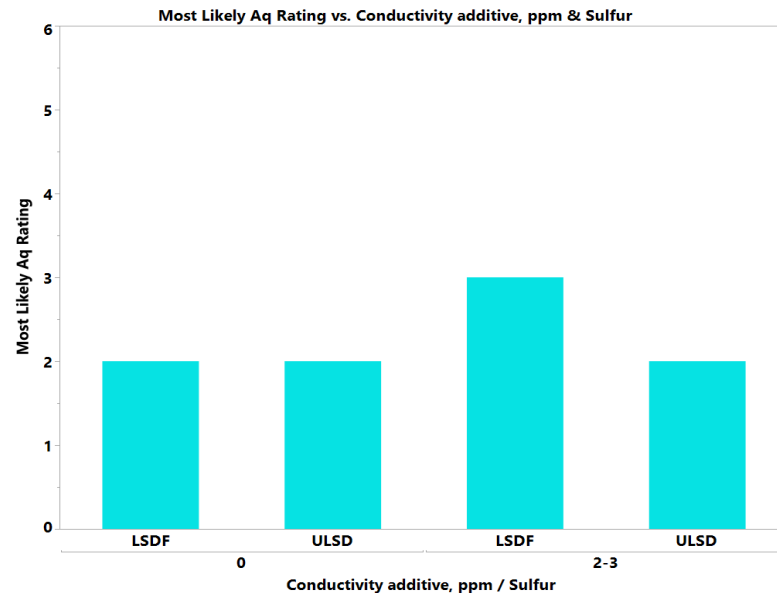
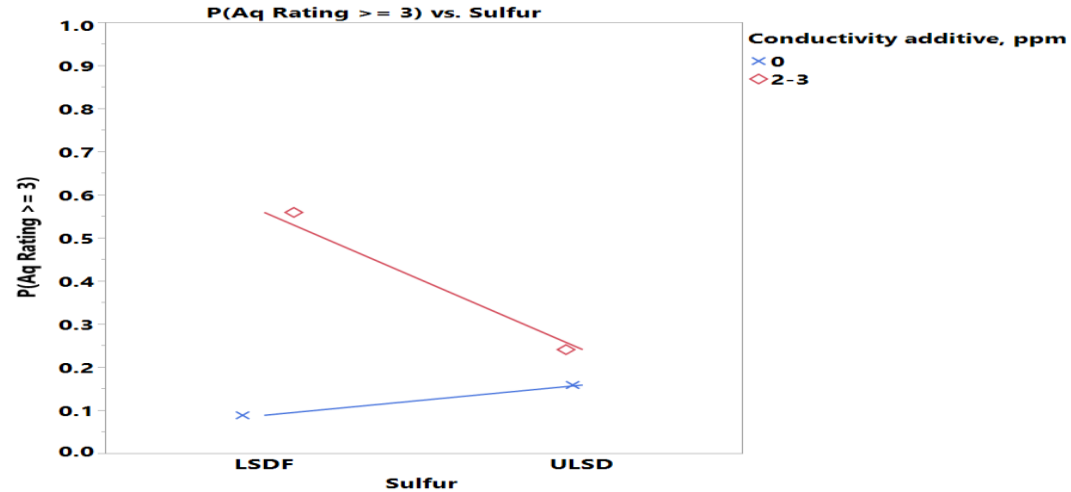
Where((Glycerin = 0) and (Microbes = 0) and (MAL additive = 0) and (Biodiesel = 0) and (Corrosion inhibitor = 0) and (Conductivity Additive = 0) and (FRP Material = 0) and (Ethanol = 0))

Sulfur-Conductivity Additive Interaction Effect

- LSDF has **lower** probability of high corrosion severity than ULSD **without** Conductivity additive while it has **higher** probability **with** Conductivity additive

	Conductivity additive, ppm			
	0		2-3	
	Sulfur		Sulfur	
	LSDF	ULSD	LSDF	ULSD
Aq12	N	N	N	N
1	5	1	3	0
2	17	18	17	25
3	4	5	4	3
4	0	1	3	0

	Conductivity additive, ppm			
	0		2-3	
	Sulfur		Sulfur	
	LSDF	ULSD	LSDF	ULSD
Aq12	N	N	N	N
1				
2				
3				
4				



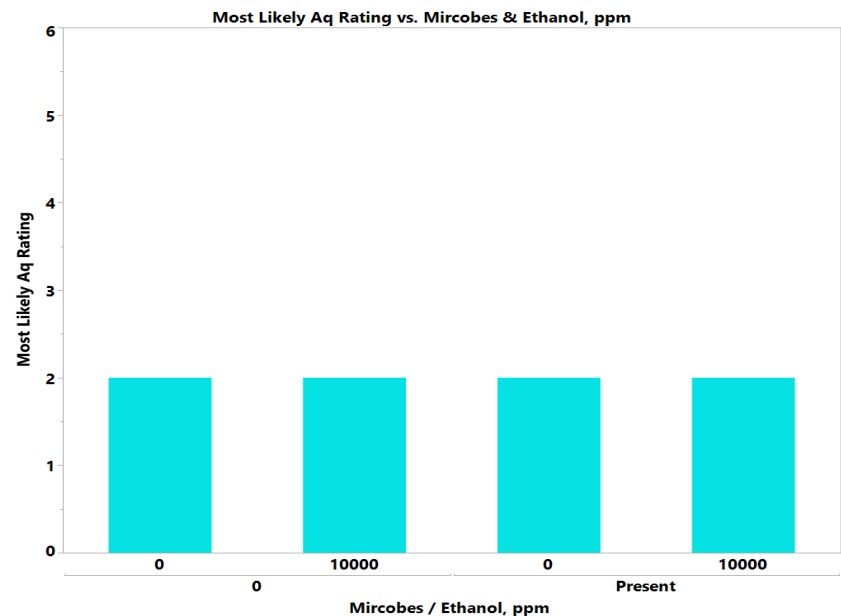
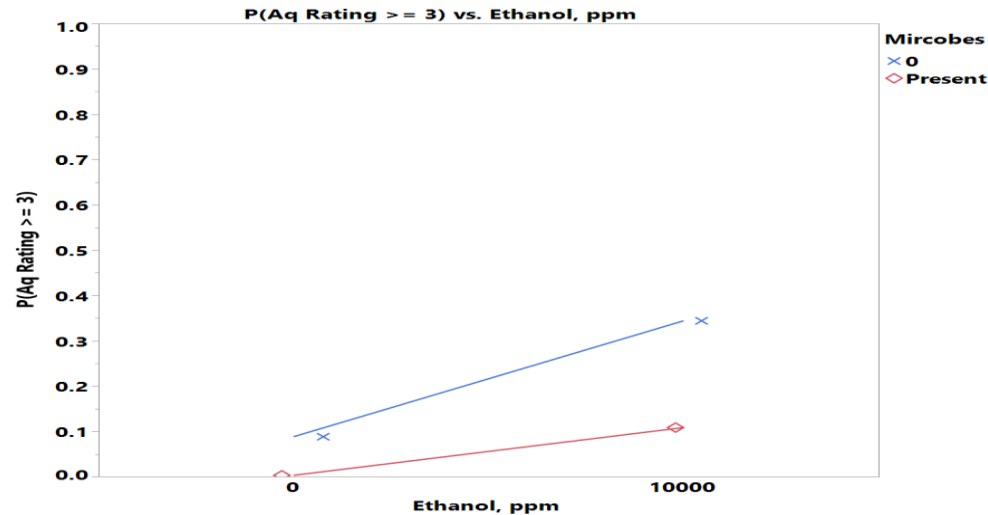
Where((Glycerin = 0) and (Microbes = 0) and (MAL additive = 0) and (CFI additive = 0) and (Corrosion inhibitor = 0) and (Biodiesel = 0) and (FRP Material = 0) and (Ethanol = 0))

Ethanol-Microbes Interaction Effect

- 10000 ppm Ethanol has **higher** probability of high corrosion severity than zero Ethanol in the absence of Microbes

	Microbes			
	0		Present	
	Ethanol, ppm		Ethanol, ppm	
	0	10000	0	10000
Aq12	N	N	N	N
1	3	0	5	1
2	16	20	24	17
3	3	5	1	7
4	3	1	0	0

	Microbes			
	0		Present	
	Ethanol, ppm		Ethanol, ppm	
	0	10000	0	10000
Aq12	N	N	N	N
1				
2				
3				
4				



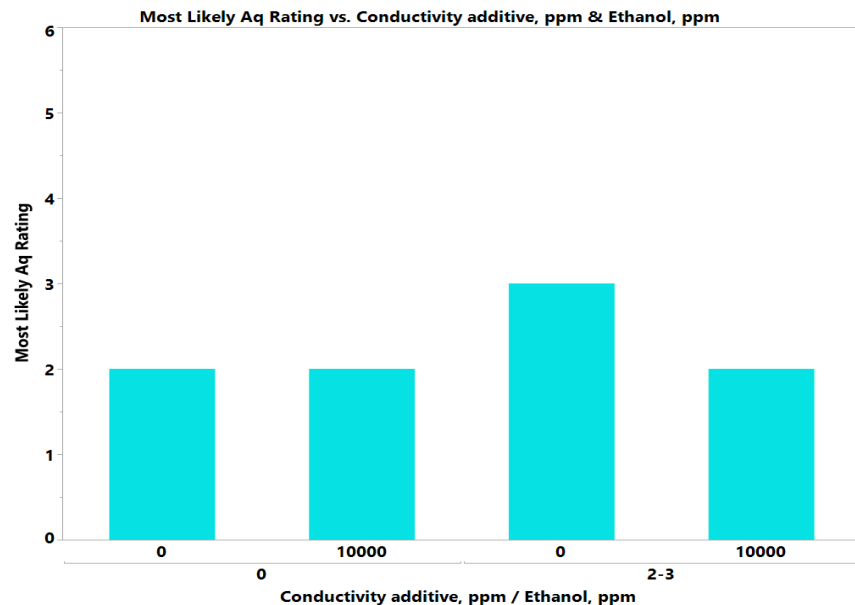
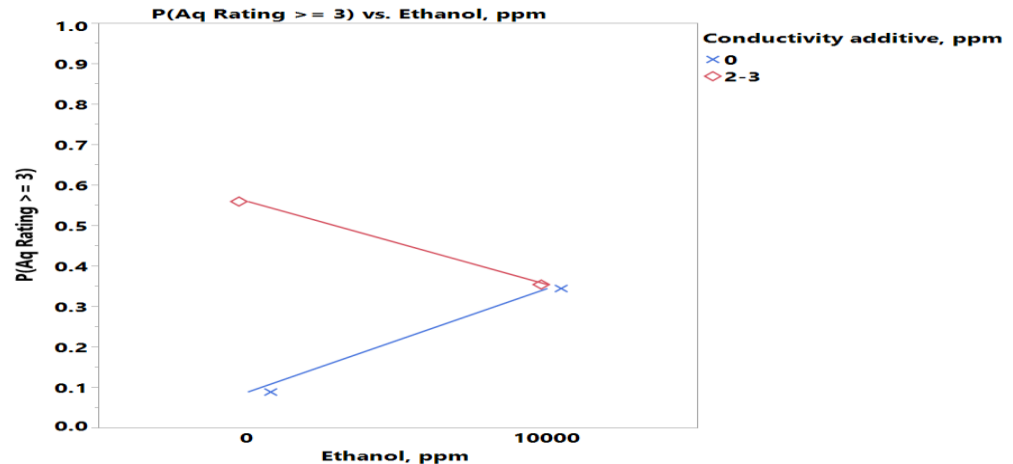
Where((MAL additive = 0) and (Corrosion inhibitor = 0) and (Conductivity Additive = 0) and (FRP Material = 0) and (Sulfur = LSDF) and (Biodiesel = 0) and (CFI additive = 0) and (Glycerin = 0))

Ethanol-Conductivity Additive Interaction Effect

- 10000 ppm Ethanol **has lower** probability of high corrosion severity than zero Ethanol **with** Conductivity additive while it **has higher** probability **without** Conductivity additive

	Conductivity additive, ppm			
	0		2-3	
	Ethanol, ppm		Ethanol, ppm	
	0	10000	0	10000
Aq12	N	N	N	N
1	5	1	3	0
2	20	15	20	22
3	1	8	3	4
4	0	1	3	0

	Conductivity additive, ppm			
	0		2-3	
	Ethanol, ppm		Ethanol, ppm	
	0	10000	0	10000
Aq12	N	N	N	N
1				
2				
3				
4				



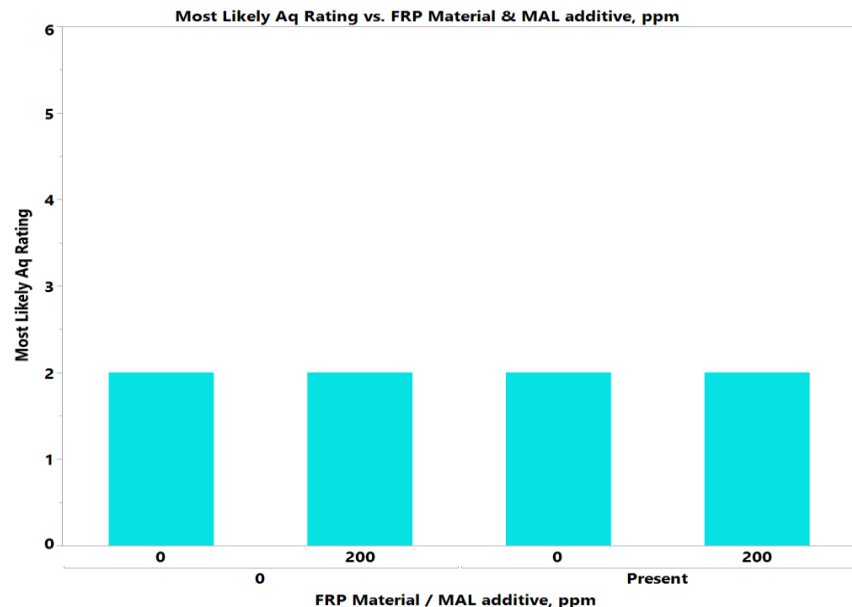
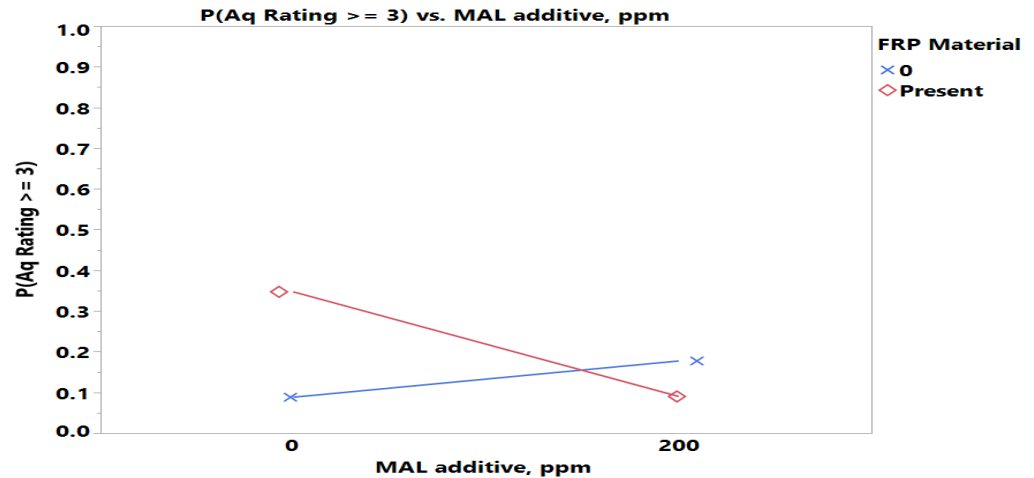
Where (MAL additive = 0) and (Corrosion inhibitor = 0) and (Microbes = 0) and (FRP Material = 0) and (Sulfur = LSDF) and (Biodiesel = 0) and (CFI additive = 0) and (Glycerin = 0)

MAL Additive-FRP Material Interaction Effect

- 200 ppm MAL additive has lower probability of high corrosion severity than zero MAL in the presence of FRP Material while it has higher probability in the absence of FRP Material

	FRP Material			
	0		Present	
	MAL additive, ppm		MAL additive, ppm	
	0	200	0	200
Aq12	N	N	N	N
1	4	0	1	4
2	17	24	17	19
3	4	3	4	5
4	1	0	3	0

	FRP Material			
	0		Present	
	MAL additive, ppm		MAL additive, ppm	
	0	200	0	200
Aq12	N	N	N	N
1	4	0	1	4
2	17	24	17	19
3	4	3	4	5
4	1	0	3	0



Where((Corrosion inhibitor = 0) and (Sulfur = LSDF) and (Biodiesel = 0) and (CFI additive = 0) and (Glycerin = 0) and (Microbes = 0) and (Ethanol = 0) and (Conductivity Additive = 0))

Ordinal Logistic Regression

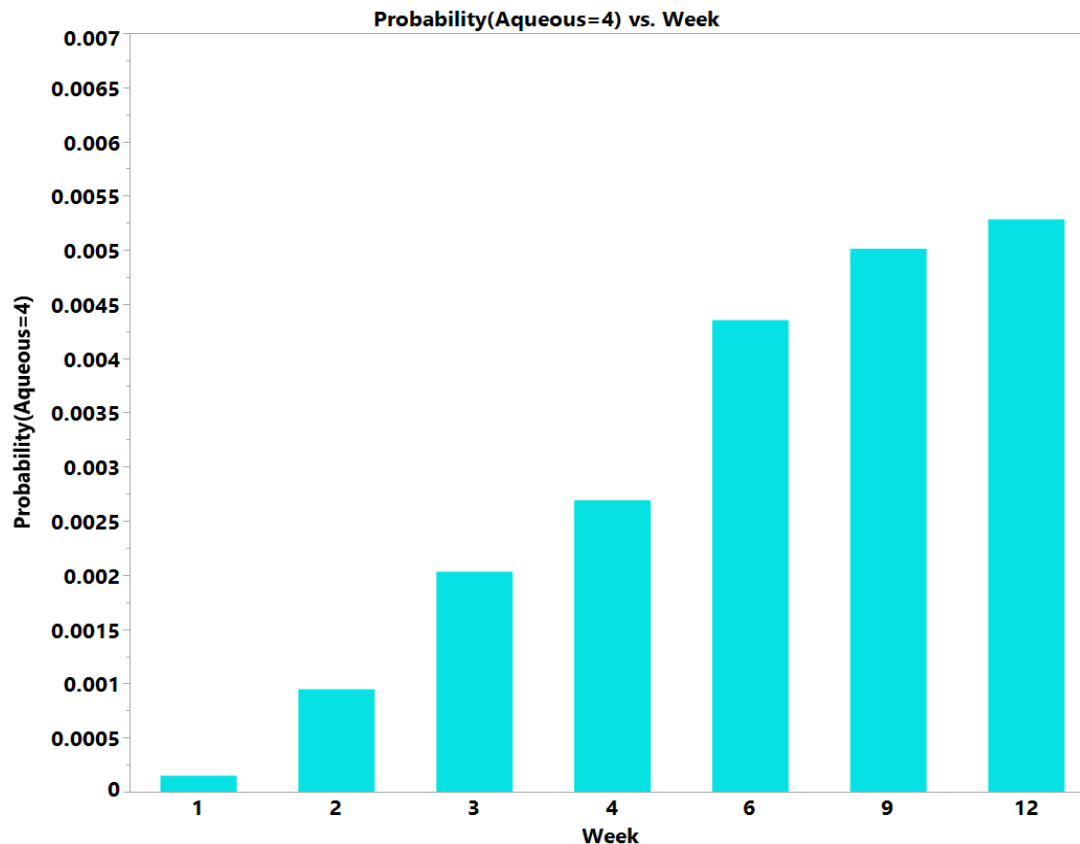
Aq Phase – All Weeks

Whole Model Test				
Model	-LogLikelihood	DF	ChiSquare	Prob>ChiSq
Difference	153.54307	22	307.0861	<.0001*
Full	458.87226			
Reduced	612.41533			
RSquare (U)	0.2507			
AICc	969.56			
BIC	1082.98			
Observations (or Sum Wgts)	742			
Fit Details				
Measure	Training Definition			
Entropy RSquare	0.2507	1-Loglike(model)/Loglike(0)		
Generalized RSquare	0.4194	$(1-(L(0)/L(model))^{(2/n)})/(1-L(0)^{(2/n)})$		
Mean -Log p	0.6184	$\sum -\log(\rho[j])/n$		
RMSE	0.4415	$\sqrt{\sum (y[j]-\rho[j])^2/n}$		
Mean Abs Dev	0.3568	$\sum y[j]-\rho[j] /n$		
Misclassification Rate	0.2547	$\sum (\rho[j] \neq \rhoMax)/n$		
N	742	n		
Lack Of Fit				
Source	DF	-LogLikelihood	ChiSquare	
Lack Of Fit	2201	458.87226	917.7445	
Saturated	2223	0.00000	Prob>ChiSq	
Fitted	22	458.87226	1.0000	

Parameter Estimates				
Term	Estimate	Std Error	ChiSquare	Prob>ChiSq
Intercept[1]	0.26136317	0.2196206	1.42	0.2340
Intercept[2]	5.46419525	0.3302785	273.71	<.0001*
Intercept[3]	8.14756113	0.4846874	282.57	<.0001*
Sulfur[LSDF]	0.35554435	0.0910064	15.26	<.0001*
Biodiesel[0]	-0.2150993	0.0903395	5.67	0.0173*
Glycerin[0]	-0.4297413	0.092704	21.49	<.0001*
Ethanol[0]	0.36605119	0.0913197	16.07	<.0001*
Mircobes[0]	-0.2234803	0.0907772	6.06	0.0138*
MAL additive[0]	0.09786026	0.0902557	1.18	0.2783
CFI additive[0]	0.15987529	0.0899721	3.16	0.0756
Corrosion inhibitor[0]	-0.3126017	0.0908115	11.85	0.0006*
Conductivity Additive[0]	0.08157754	0.0899556	0.82	0.3645
FRP Material[0]	0.09006014	0.0907396	0.99	0.3209
Sulfur[LSDF]*Mircobes[0]	-0.4998287	0.0940967	28.22	<.0001*
Sulfur[LSDF]*CFI additive[0]	0.31941601	0.0908432	12.36	0.0004*
Sulfur[LSDF]*Conductivity Additive[0]	0.37663185	0.0924695	16.59	<.0001*
Ethanol[0]*Mircobes[0]	-0.3048957	0.0912253	11.17	0.0008*
Ethanol[0]*Conductivity Additive[0]	0.40832393	0.09281	19.36	<.0001*
MAL additive[0]*FRP Material[0]	0.39040806	0.0919411	18.03	<.0001*
Week[2-1]	-1.8455397	0.3311125	31.07	<.0001*
Week[3-2]	-0.7645191	0.3447316	4.92	0.0266*
Week[4-3]	-0.2818174	0.3457953	0.66	0.4151
Week[6-4]	-0.4830882	0.3409517	2.01	0.1565
Week[9-6]	-0.1415323	0.3328443	0.18	0.6707
Week[12-9]	-0.0529518	0.3299836	0.03	0.8725

Corrosion by Time (Week)

- Probability of high corrosion severity in Week 2 is significantly higher than Week 1, and Week 3 is significantly higher Week 2



Where((Sulfur = LSDF) and (Biodiesel = 0) and (Glycerin = 0) and (Ethanol = 0) and (Microbes = 0) and (MAL additive = 0) and (CFI additive = 0) and (Corrosion Inhibitor = 0) and (Conductivity Additive = 0) and (FRP Material = 0))

Aqueous Edge Phase

Conclusions (Aqueous Edge Phase)

Average Corrosion Severity Rating (average of 3 samples)

- ULSD has **higher** probability of high corrosion severity than LSDF
- 5% Biodiesel has **lower** probability of high corrosion severity than zero Biodiesel
- Presence of Microbes has **lower** probability of high corrosion severity than the absence of Microbes
- 200 ppm MAL additive has **lower** probability of high corrosion severity than zero MAL additive
- 200 ppm CFI additive has **higher** probability of high corrosion severity than zero CFI additive
- LSDF has **lower** probability of high corrosion severity than ULSD with Biodiesel
- LSDF has **lower** probability of high corrosion severity than ULSD in the presence of Microbes
- LSDF has **lower** probability of high corrosion severity than ULSD without CFI additive while it has **higher** probability with CFI additive
- LSDF has **lower** probability of high corrosion severity than ULSD without Conductivity additive while it has **higher** probability with Conductivity additive
- LSDF has **lower** probability of high corrosion severity than ULSD in the absence of FRP Material
- 5000 ppm Glycerin has **lower** probability of high corrosion severity than zero Glycerin with CFI additive while it has **higher** probability with CFI additive
- 10000 ppm Ethanol has **lower** probability of high corrosion severity than zero Ethanol without FRP Material while it has **higher** probability with FRP Material
- 200 ppm MAL additive has **lower** probability of high corrosion severity than zero MAL additive in the presence of Microbes
- 200 ppm MAL additive has **lower** probability of high corrosion severity than zero MAL additive with Conductivity additive
- 8-10 ppm Corrosion inhibitor has **lower** probability of high corrosion severity than zero corrosion inhibitor in the presence of FRP Material while it has **higher** probability in the absence of FRP Material

Average Corrosion Severity Rating by Time (Week)

- Probability of high corrosion severity in Week 2 is significantly higher than Week 1, and Week 3 is significantly higher Week 2
- Probability of high corrosion severity in Week 2 is **higher** than Week 1 more significantly without MAL additive than with MAL additive

Stepwise Ordinal Logistic Regression

Aqueous Edge Phase – Week 12

Whole Model Test				
Model	-LogLikelihood	DF	ChiSquare	Prob>ChiSq
Difference	37.876361	20	75.75272	<.0001*
Full	49.836520			
Reduced	87.712880			
RSquare (U)	0.4318			
AICc	162.488			
BIC	211.596			
Observations (or Sum Wgts)	106			

Fit Details		
Measure	Training	Definition
Entropy RSquare	0.4318	1-Loglike(model)/Loglike(0)
Generalized RSquare	0.6313	$(1-(L(0)/L(model))^{(2/n)})/(1-L(0)^{(2/n)})$
Mean -Log p	0.4702	$\sum -\log(p_{ij})/n$
RMSE	0.3949	$\sqrt{\sum (y_{ij}-p_{ij})^2/n}$
Mean Abs Dev	0.2759	$\sum y_{ij}-p_{ij} /n$
Misclassification Rate	0.2075	$\sum (p_{ij} \neq p_{Max})/n$
N	106	n

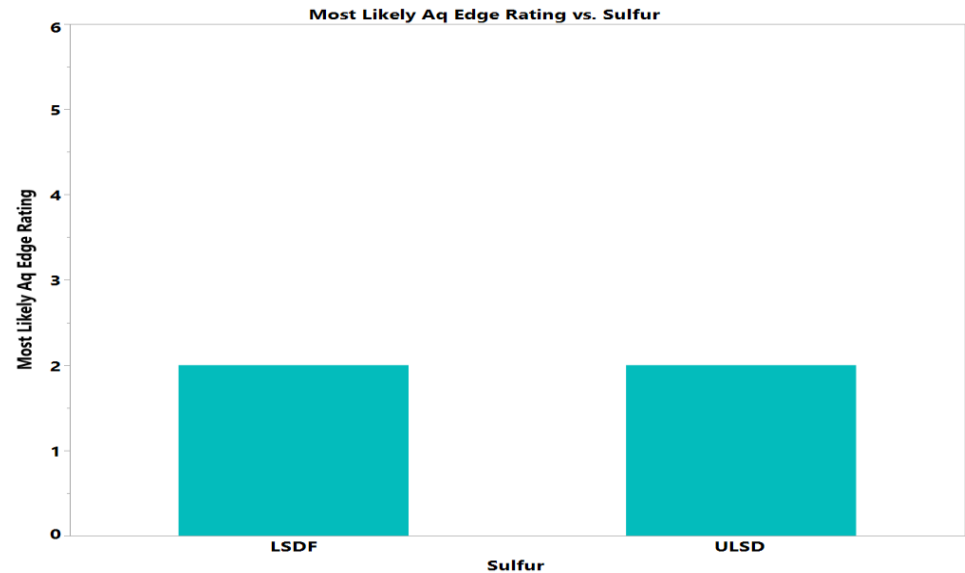
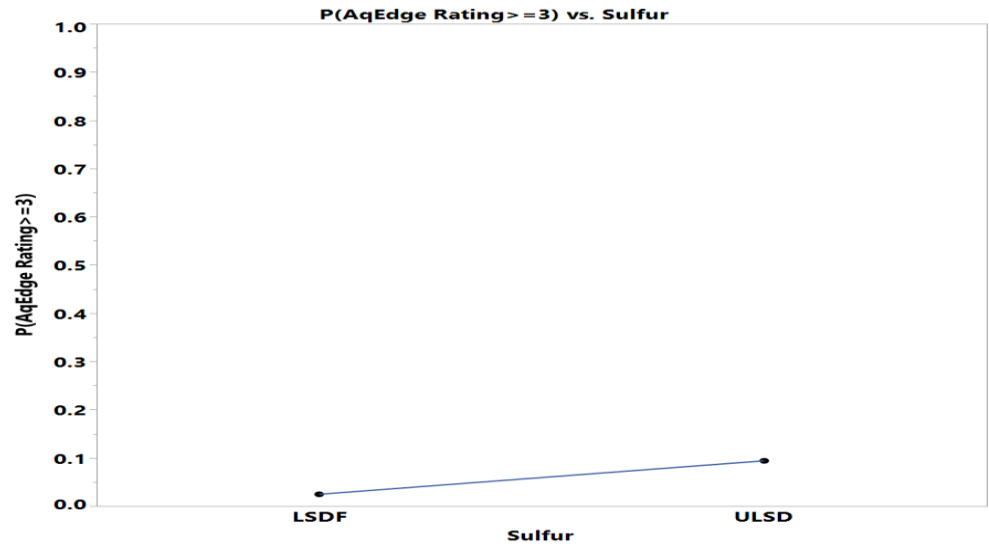
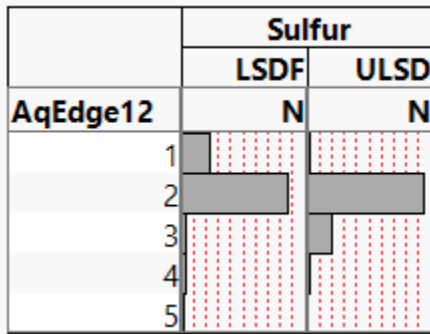
Lack Of Fit			
Source	DF	-LogLikelihood	ChiSquare
Lack Of Fit	400	49.836520	99.67304
Saturated	420	0.000000	Prob>ChiSq
Fitted	20	49.836520	1.0000

Parameter Estimates				
Term	Estimate	Std Error	ChiSquare	Prob>ChiSq
Intercept[1]	-5.4346685	1.0622037	26.18	<.0001*
Intercept[2]	4.31371423	0.8520604	25.63	<.0001*
Intercept[3]	6.74993038	1.1406156	35.02	<.0001*
Intercept[4]	8.62401115	1.5694466	30.19	<.0001*
Sulfur[LSDf]	1.65885574	0.5065922	10.72	0.0011*
Biodiesel, %[0]	-0.9131635	0.3173911	8.28	0.0040*
Glycerin, ppm[0]	0.07056478	0.288247	0.06	0.8066
Ethanol, ppm[0]	0.14301504	0.2956149	0.23	0.6285
Mircobes[0]	-0.7521436	0.318037	5.59	0.0180*
MAL additive, ppm[0]	-1.1767574	0.3843635	9.37	0.0022*
CFI additive, ppm[0]	0.66246986	0.3388644	3.82	0.0506
Corrosion inhibitor, ppm[0]	-0.3500382	0.2865734	1.49	0.2219
Conductivity additive, ppm[0]	0.04344821	0.2988026	0.02	0.8844
FRP Material[0]	-0.0233202	0.2896033	0.01	0.9358
Sulfur[LSDf]*Biodiesel, %[0]	-1.0377895	0.3368246	9.49	0.0021*
Sulfur[LSDf]*Mircobes[0]	-1.3858691	0.412043	11.31	0.0008*
Sulfur[LSDf]*CFI additive, ppm[0]	0.93502712	0.3439142	7.39	0.0066*
Sulfur[LSDf]*Conductivity additive, ppm[0]	1.12019354	0.3601293	9.68	0.0019*
Sulfur[LSDf]*FRP Material[0]	-0.5824447	0.3106422	3.52	0.0608
Glycerin, ppm[0]*CFI additive, ppm[0]	0.56444751	0.2951556	3.66	0.0558
Ethanol, ppm[0]*FRP Material[0]	-0.5409977	0.3065379	3.11	0.0776
Mircobes[0]*MAL additive, ppm[0]	-0.7530773	0.333216	5.11	0.0238*
MAL additive, ppm[0]*Conductivity additive, ppm[0]	0.91745315	0.364471	6.34	0.0118*
Corrosion inhibitor, ppm[0]*FRP Material[0]	0.76805843	0.3155629	5.92	0.0149*

Sulfur Effect – Aq Edge Phase

- ULSD has **higher** probability of high corrosion severity than LSDF

	Sulfur	
	LSDF	ULSD
AqEdge12	N	N
1	10	1
2	38	42
3	2	9
4	2	1
5	1	0

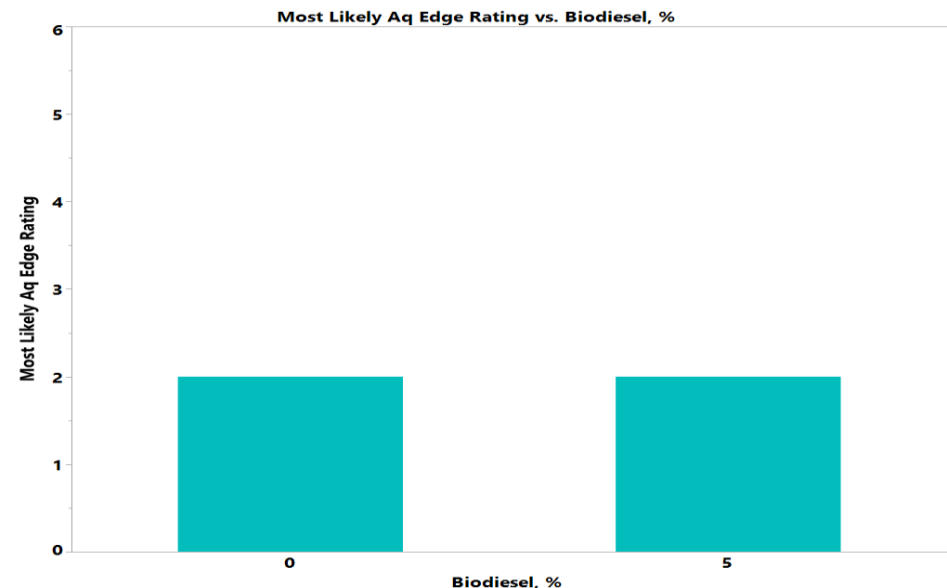
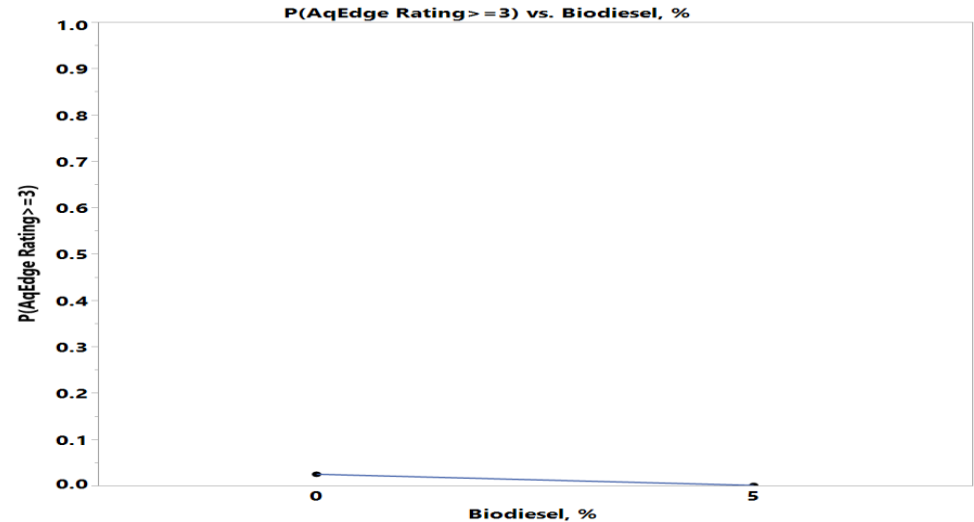
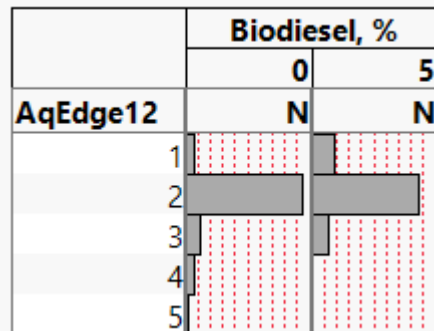


Where((Biodiesel = 0) and (Glycerin = 0) and (Microbes = 0) and (Ethanol = 0) and (MAL additive = 0) and (CFI additive = 0) and (Corrosion inhibitor = 0) and (Conductivity Additive = 0) and (FRP Material = 0))

Biodiesel Effect – Aq Edge Phase

- 5% Biodiesel has **lower** probability of high corrosion severity than zero Biodiesel

	Biodiesel, %	
	0	5
AqEdge12	N	N
1	3	8
2	42	38
3	5	6
4	3	0
5	1	0



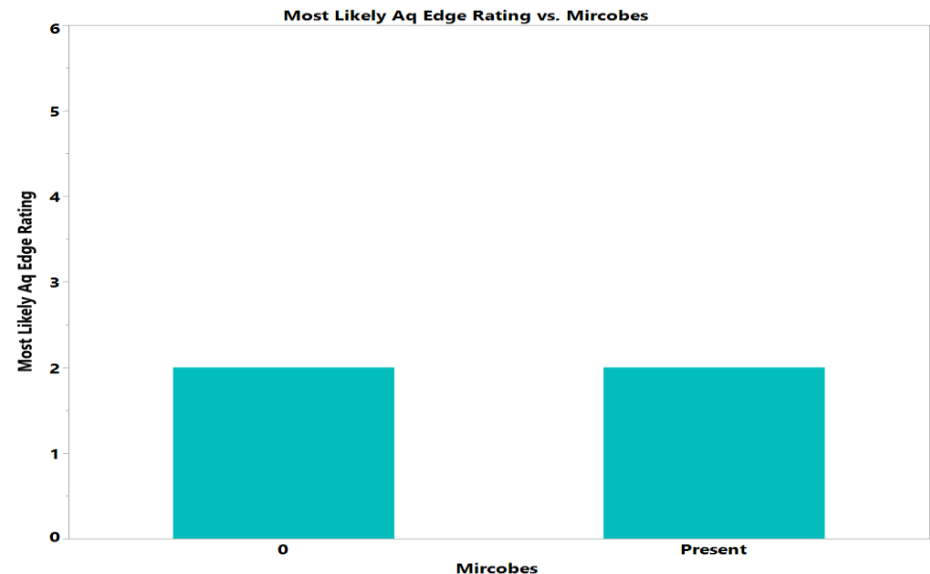
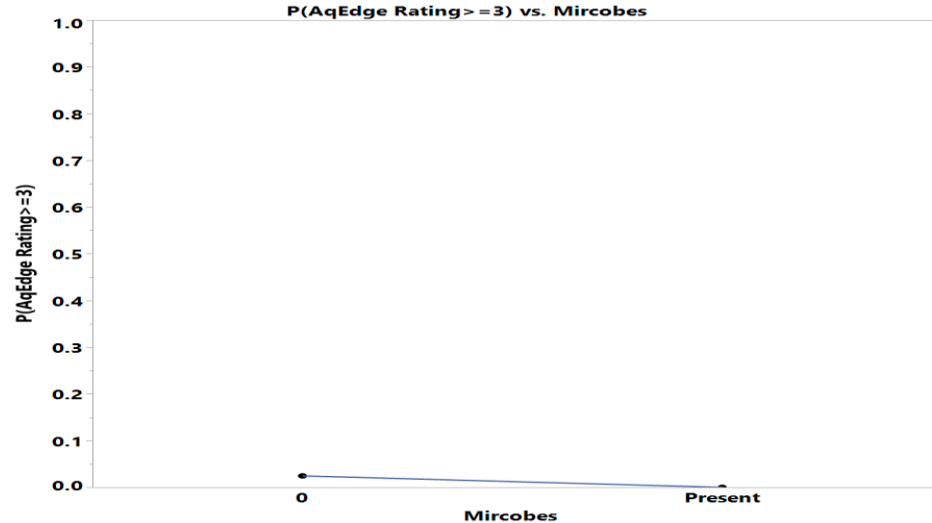
Where((Sulfur = LSDF) and (Glycerin = 0) and (Microbes = 0) and (Ethanol = 0) and (MAL additive = 0) and (CFI additive = 0) and (Corrosion inhibitor = 0) and (Conductivity Additive = 0) and (FRP Material = 0))

Microbes Effect – Aq Edge Phase

- Presence of Microbes has **lower** probability of high corrosion severity than the absence of Microbes

	Microbes	
	0	Present
AqEdge12	N	N
1	3	8
2	39	41
3	5	6
4	3	0
5	1	0

	Microbes	
	0	Present
AqEdge12	N	N
1		
2		
3		
4		
5		

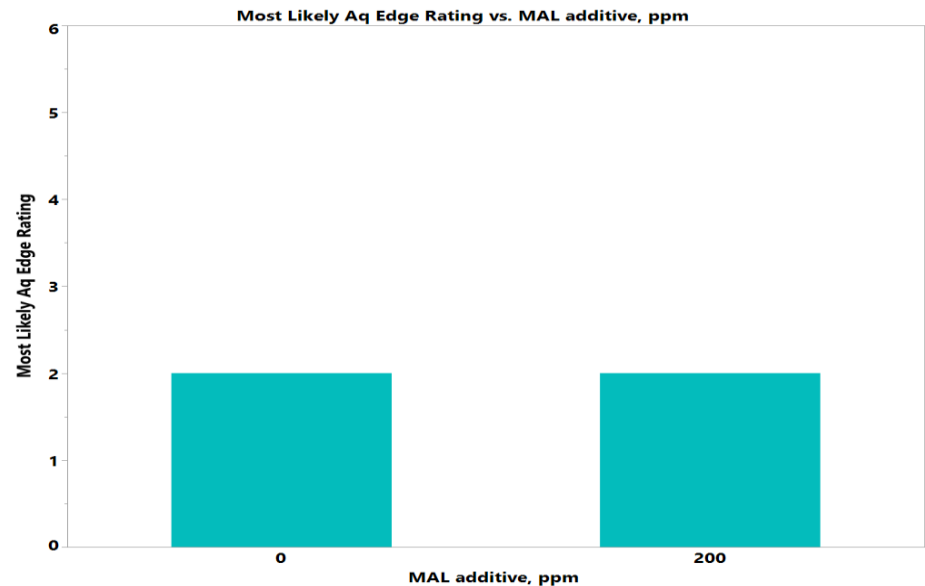
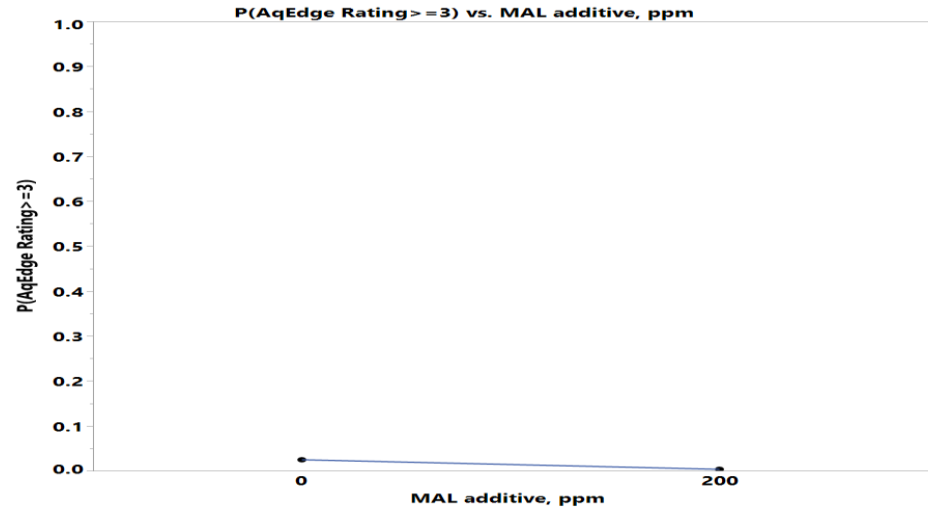
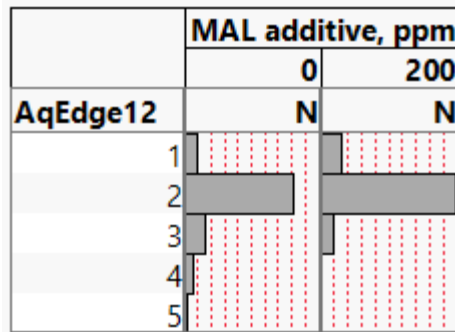


Where((Sulfur = LSDF) and (Glycerin = 0) and (Biodiesel = 0) and (Ethanol = 0) and (MAL additive = 0) and (CFI additive = 0) and (Corrosion inhibitor = 0) and (Conductivity Additive = 0) and (FRP Material = 0))

MAL Additive Effect – Aq Edge Phase

- 200 ppm MAL additive has **lower** probability of high corrosion severity than zero MAL additive

		MAL additive, ppm	
		0	200
AqEdge12		N	N
1		4	7
2		36	44
3		7	4
4		3	0
5		1	0



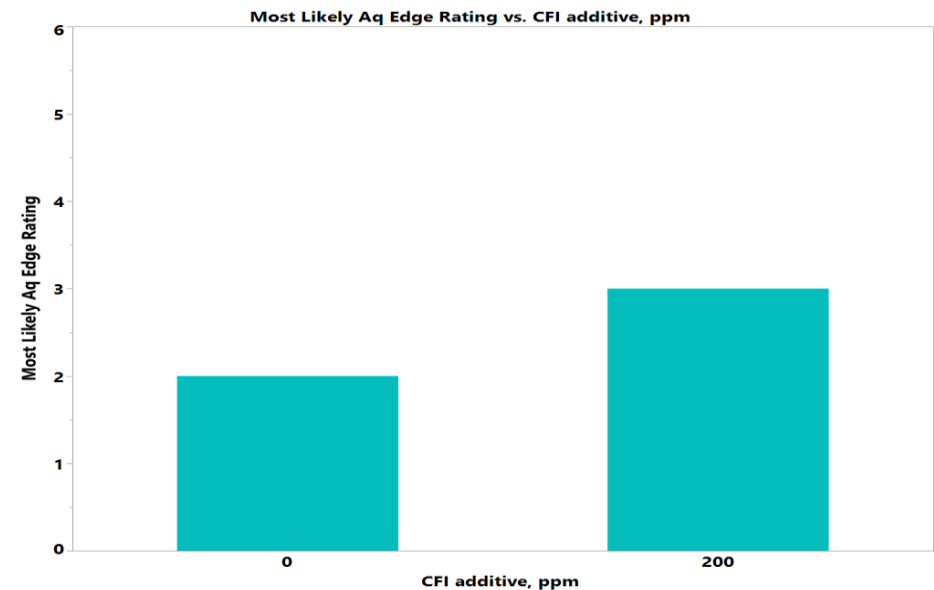
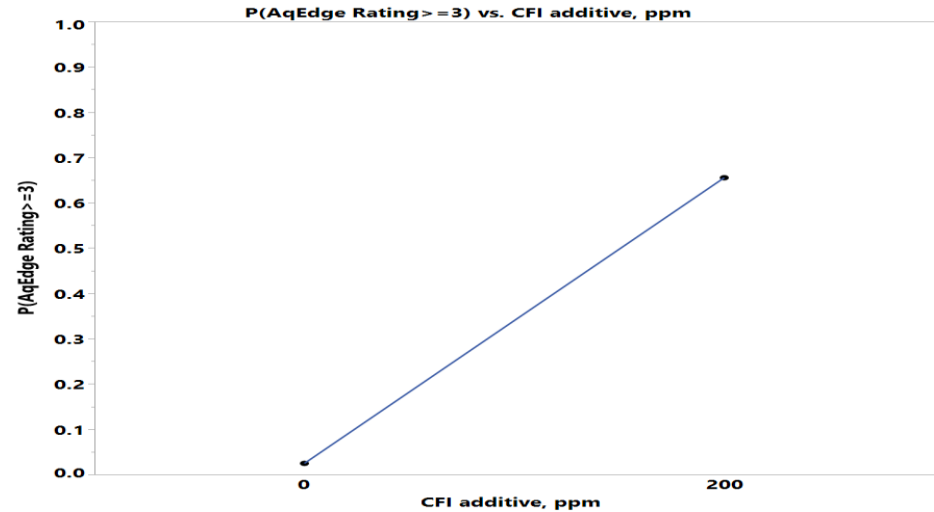
Where((Sulfur = LSDF) and (Glycerin = 0) and (Biodiesel = 0) and (Ethanol = 0) and (Microbes = 0) and (CFI additive = 0) and (Corrosion inhibitor = 0) and (Conductivity Additive = 0) and (FRP Material = 0))

CFI Additive Effect – Aq Edge Phase

- 200 ppm CFI additive has **higher** probability of high corrosion severity than zero CFI additive

	CFI additive, ppm	
	0	200
AqEdge12	N	N
1	6	5
2	41	39
3	5	6
4	2	1
5	0	1

	CFI additive, ppm	
	0	200
AqEdge12	N	N
1		
2		
3		
4		
5		



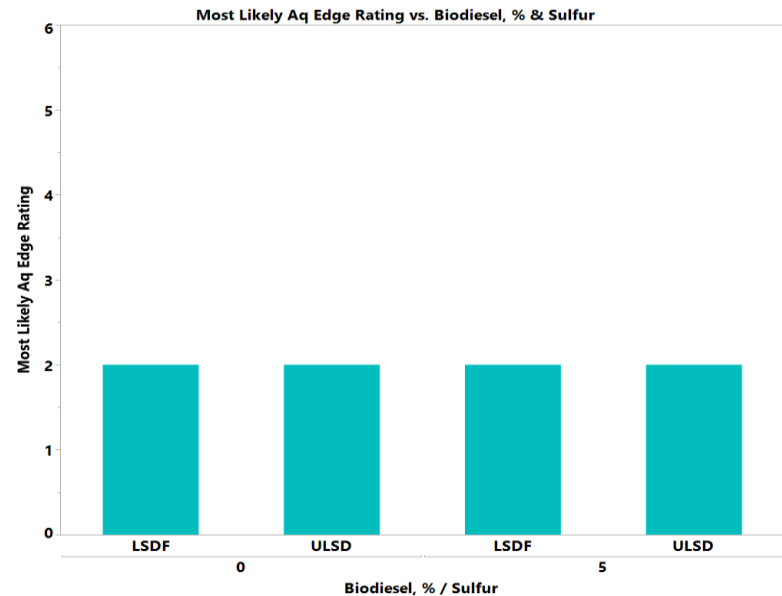
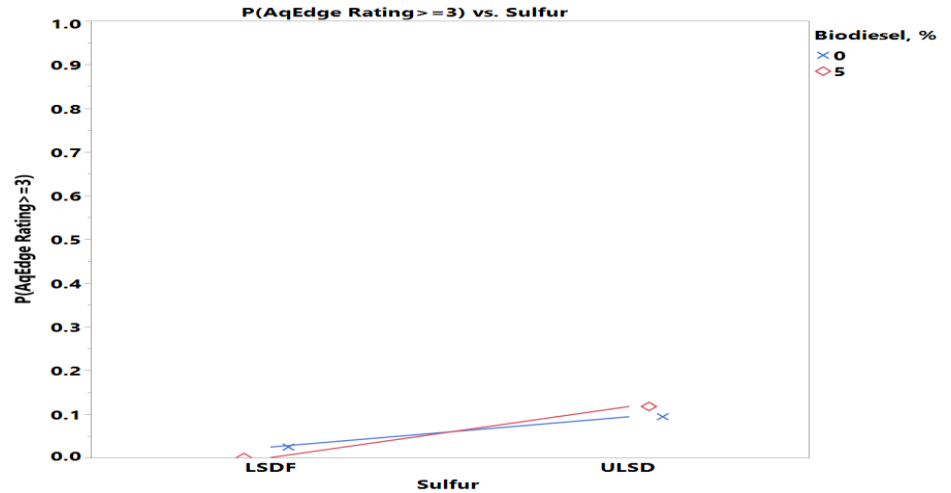
Where((Sulfur = LSDF) and (Glycerin = 0) and (Biodiesel = 0) and (Ethanol = 0) and (MAL additive = 0) and (Microbes = 0) and (Corrosion inhibitor = 0) and (Conductivity Additive = 0) and (FRP Material = 0))

Sulfur-Biodiesel Interaction Effect

- LSDF has **lower** probability of high corrosion severity than ULSD with Biodiesel

	Biodiesel, %			
	0		5	
	Sulfur		Sulfur	
	LSDF	ULSD	LSDF	ULSD
AqEdge12	N	N	N	N
1	2	1	8	0
2	21	21	17	21
3	1	4	1	5
4	2	1	0	0
5	1	0	0	0

	Biodiesel, %			
	0		5	
	Sulfur		Sulfur	
	LSDF	ULSD	LSDF	ULSD
AqEdge12	N	N	N	N
1				
2				
3				
4				
5				



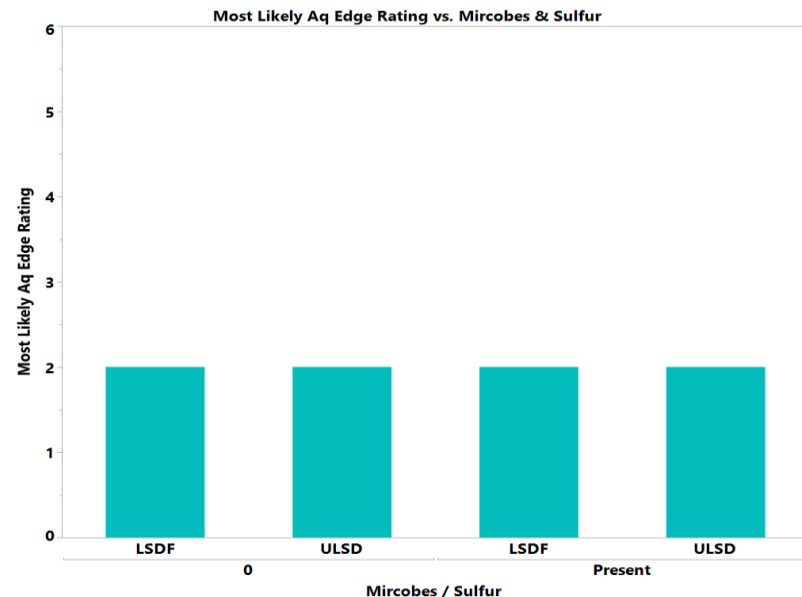
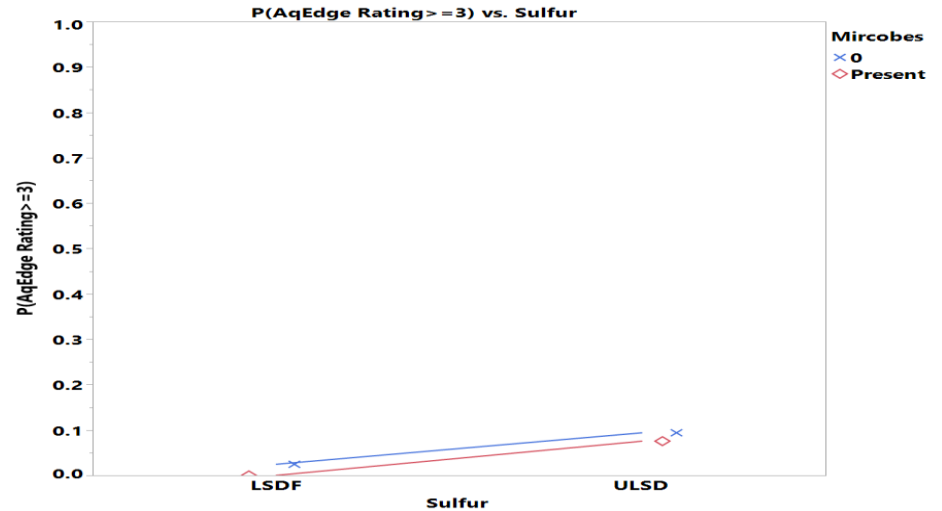
Where((Glycerin = 0) and (Ethanol = 0) and (MAL additive = 0) and (CFI additive = 0) and (Corrosion inhibitor = 0) and (Conductivity Additive = 0) and (FRP Material = 0) and (Microbes = 0))

Sulfur-Microbes Interaction Effect

- LSDF has **lower** probability of high corrosion severity than ULSD with Microbes

	Microbes			
	0		Present	
	Sulfur		Sulfur	
	LSDF	ULSD	LSDF	ULSD
AqEdge12	N	N	N	N
1	2	1	8	0
2	19	20	19	22
3	2	3	0	6
4	2	1	0	0
5	1	0	0	0

	Microbes			
	0		Present	
	Sulfur		Sulfur	
	LSDF	ULSD	LSDF	ULSD
AqEdge12	N	N	N	N
1				
2				
3				
4				
5				

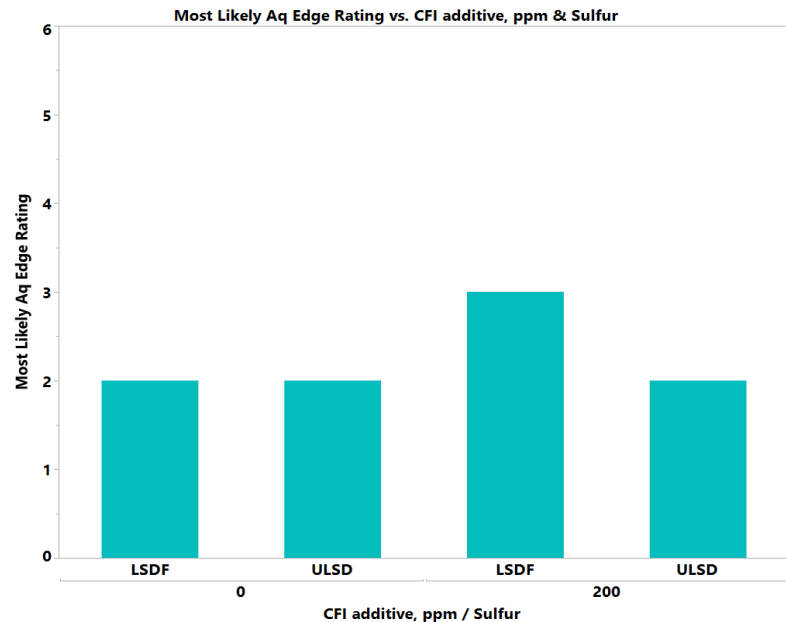
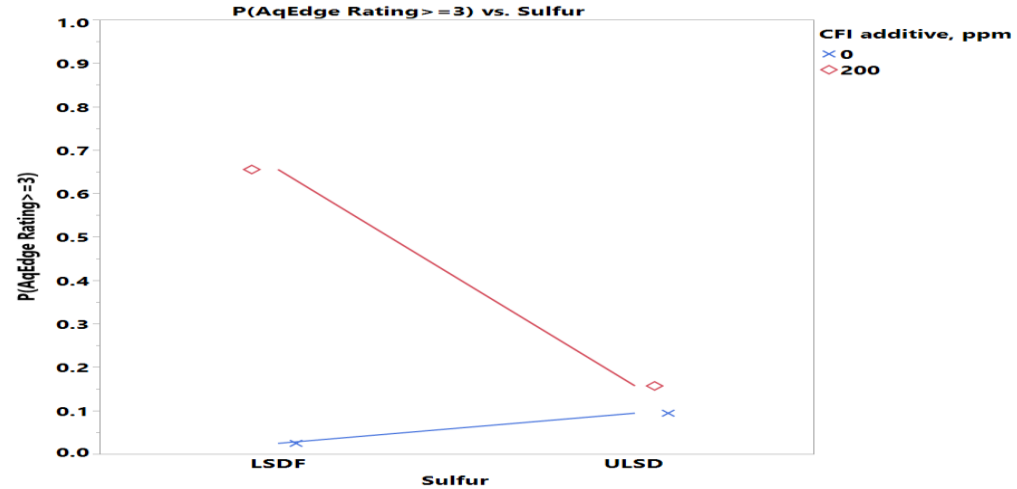
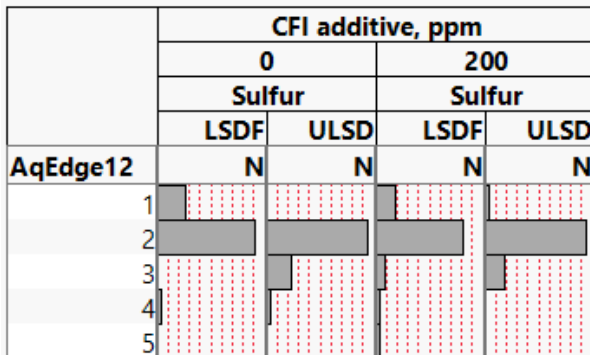


Where((Glycerin = 0) and (Ethanol = 0) and (MAL additive = 0) and (CFI additive = 0) and (Corrosion inhibitor = 0) and (Conductivity Additive = 0) and (FRP Material = 0) and (Biodiesel = 0))

Sulfur-CFI Additive Interaction Effect

- LSDF has **lower** probability of high corrosion severity than ULSD **without** CFI additive while it has **higher** probability **with** CFI additive

	CFI additive, ppm			
	0		200	
	Sulfur		Sulfur	
	LSDF	ULSD	LSDF	ULSD
AqEdge12	N	N	N	N
1	6	0	4	1
2	20	21	18	21
3	0	5	2	4
4	1	1	1	0
5	0	0	1	0



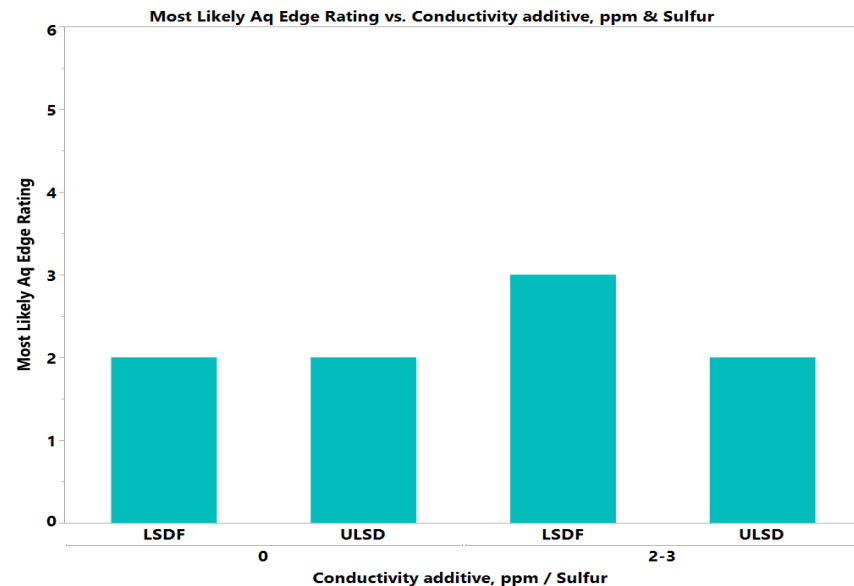
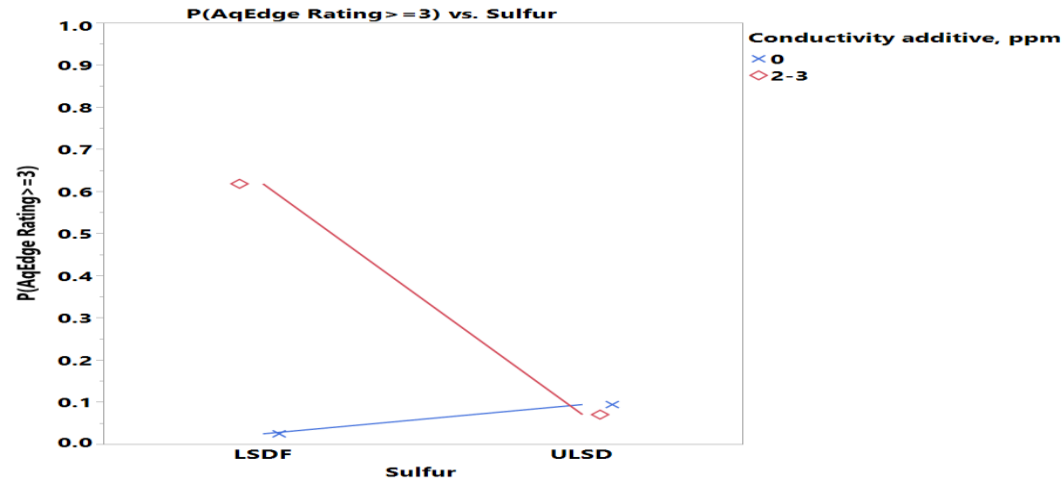
Where((Glycerin = 0) and (Microbes = 0) and (MAL additive = 0) and (Biodiesel = 0) and (Corrosion inhibitor = 0) and (Conductivity Additive = 0) and (FRP Material = 0) and (Ethanol = 0))

Sulfur-Conductivity Additive Interaction Effect

- LSDF has **lower** probability of high corrosion severity than ULSD **without** Conductivity additive while it has **higher** probability **with** Conductivity additive

	Conductivity additive, ppm			
	0		2-3	
	Sulfur		Sulfur	
	LSDF	ULSD	LSDF	ULSD
AqEdge12	N	N	N	N
1	6	0	4	1
2	19	18	19	24
3	1	6	1	3
4	0	1	2	0
5	0	0	1	0

	Conductivity additive, ppm			
	0		2-3	
	Sulfur		Sulfur	
	LSDF	ULSD	LSDF	ULSD
AqEdge12	N	N	N	N
1				
2				
3				
4				
5				

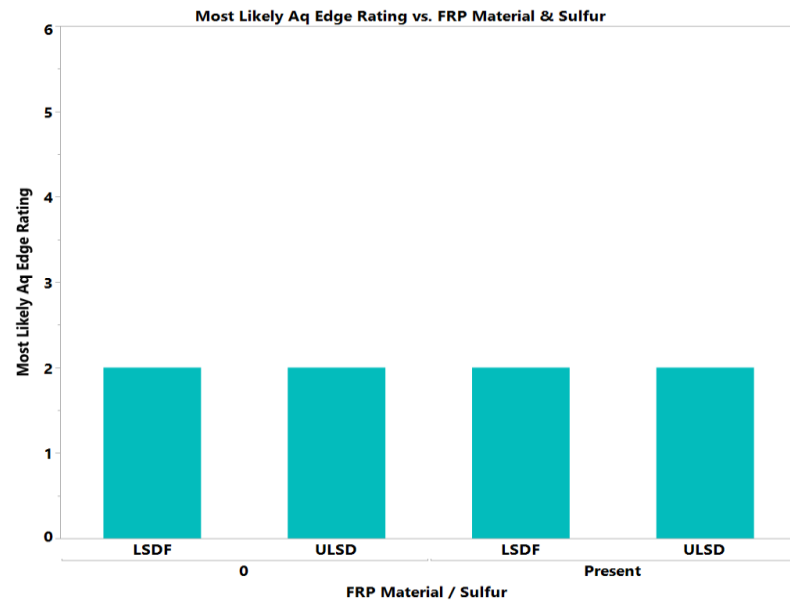
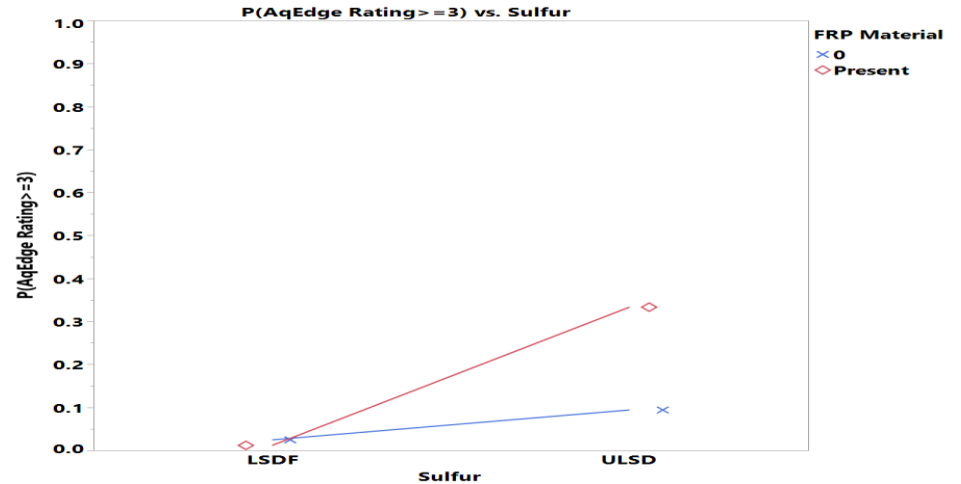
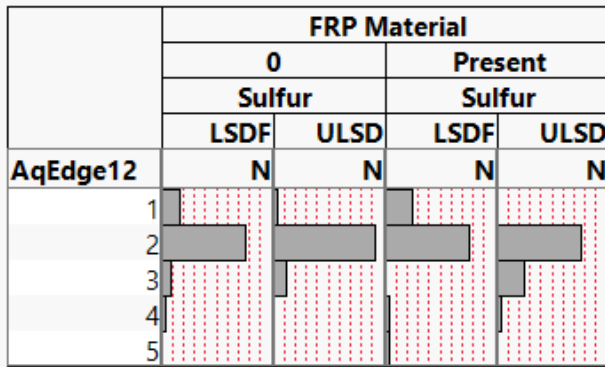


Where((Glycerin = 0) and (Microbes = 0) and (MAL additive = 0) and (CFI additive = 0) and (Corrosion inhibitor = 0) and (Biodiesel = 0) and (FRP Material = 0) and (Ethanol = 0))

Sulfur-FRP Material Interaction Effect

- LSDF has **lower** probability of high corrosion severity than ULSD without FRP Material

	FRP Material			
	0		Present	
	Sulfur		Sulfur	
	LSDF	ULSD	LSDF	ULSD
AqEdge12	N	N	N	N
1	4	1	6	0
2	19	23	19	19
3	2	3	0	6
4	1	0	1	1
5	0	0	1	0



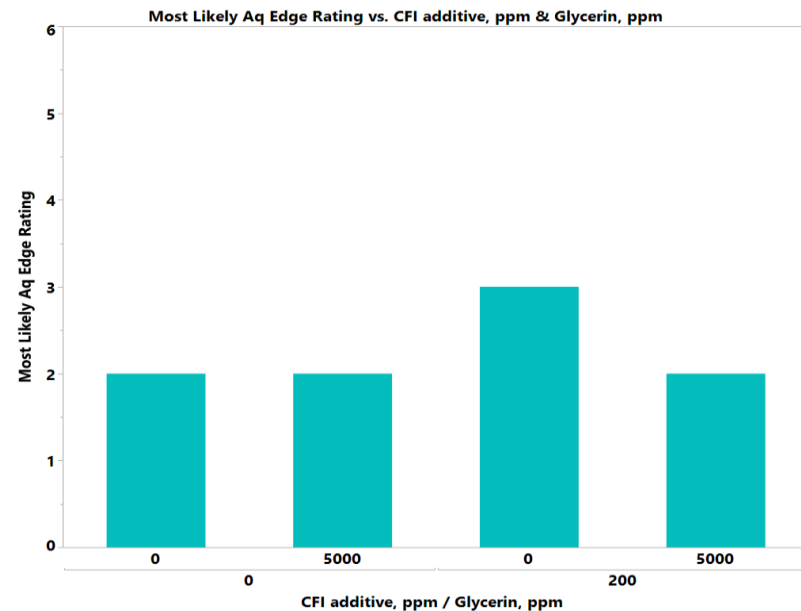
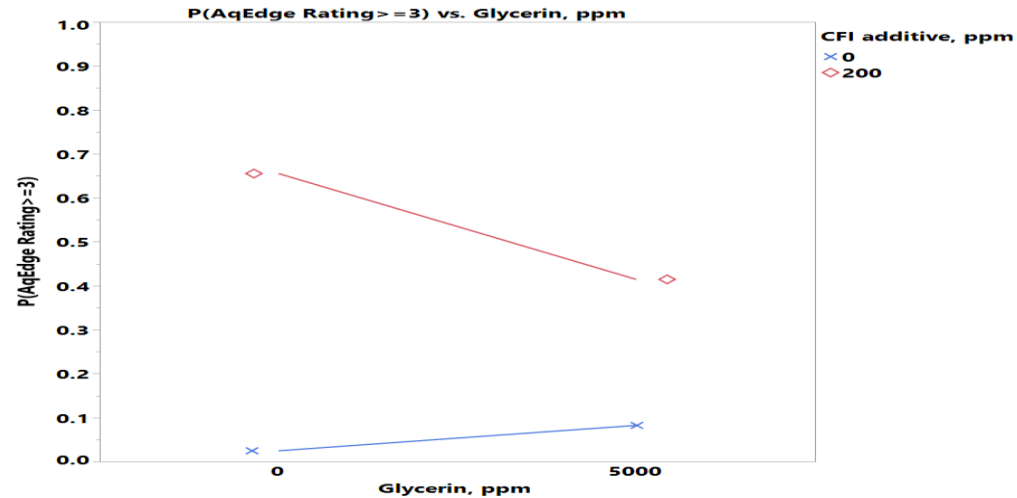
Where((Glycerin = 0) and (Microbes = 0) and (MAL additive = 0) and (CFI additive = 0) and (Corrosion inhibitor = 0) and (Biodiesel = 0) and (Conductivity additive = 0) and (Ethanol = 0))

Glycerin-CFI Additive Interaction Effect

- 5000 ppm Glycerin has **lower** probability of high corrosion severity than zero Glycerin **with** CFI additive while it has **higher** probability **with** CFI additive

	CFI additive, ppm			
	0		200	
	Glycerin, ppm		Glycerin, ppm	
	0	5000	0	5000
AqEdge12	N	N	N	N
1	3	3	2	3
2	22	19	19	20
3	3	2	5	1
4	0	2	0	1
5	0	0	1	0

	CFI additive, ppm			
	0		200	
	Glycerin, ppm		Glycerin, ppm	
	0	5000	0	5000
AqEdge12	N	N	N	N
1				
2				
3				
4				
5				



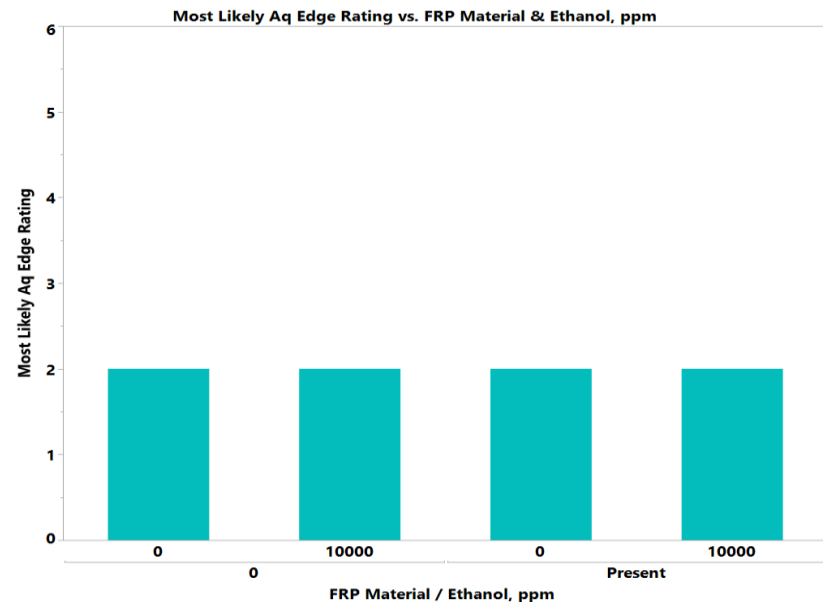
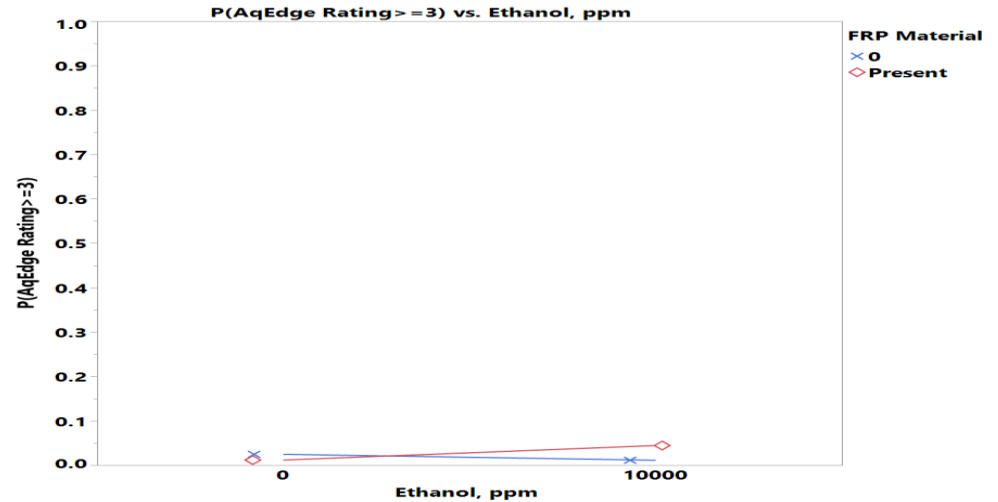
Where((Ethanol = 0) and (Microbes = 0) and (MAL additive = 0) and (Biodiesel = 0) and (Corrosion inhibitor = 0) and (Conductivity Additive = 0) and (FRP Material = 0) and (Ethanol = 0))

Ethanol-FRP Material Interaction Effect

- 10000 ppm Ethanol has **lower** probability of high corrosion severity than zero Ethanol **without** FRP Material while it has **higher** probability **with** FRP Material

	FRP Material			
	0		Present	
	Ethanol, ppm		Ethanol, ppm	
	0	10000	0	10000
AqEdge12	N	N	N	N
1	2	3	4	2
2	21	21	21	17
3	3	2	1	5
4	1	0	1	1
5	0	0	1	0

	FRP Material			
	0		Present	
	Ethanol, ppm		Ethanol, ppm	
	0	10000	0	10000
AqEdge12	N	N	N	N
1				
2				
3				
4				
5				

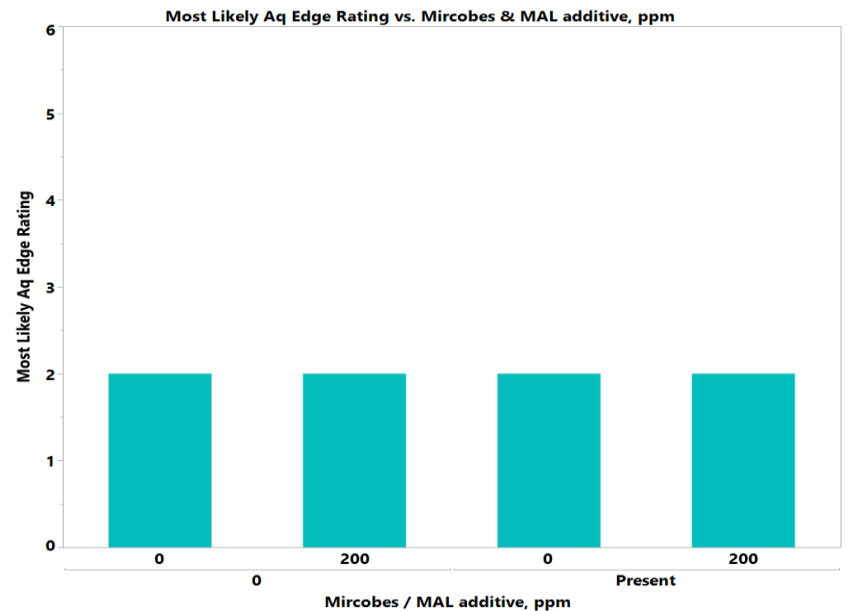
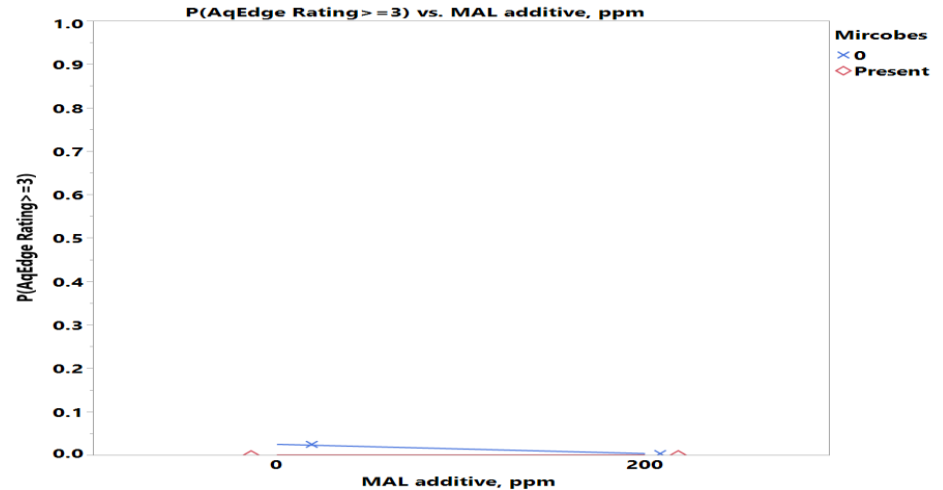
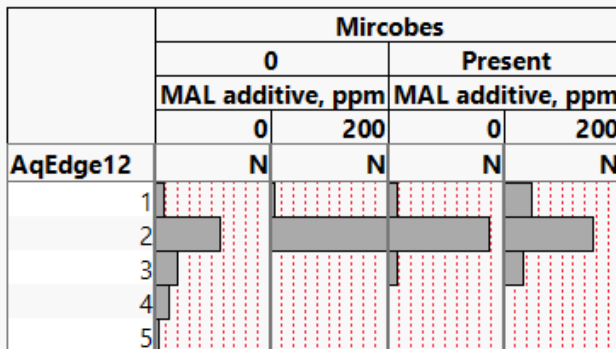


Where((MAL additive = 0) and (Corrosion inhibitor = 0) and (Microbes= 0) and (Conductivity additive= 0) and (Sulfur = LSDF) and (Biodiesel = 0) and (CFI additive = 0) and (Glycerin = 0))

MAL Additive-Microbes Interaction Effect

- 200 ppm MAL additive has **lower** probability of high corrosion severity than zero MAL additive in the presence of Microbes

	Microbes			
	0		Present	
	MAL additive, ppm		MAL additive, ppm	
	0	200	0	200
AqEdge12	N	N	N	N
1	2	1	2	6
2	14	25	22	19
3	5	0	2	4
4	3	0	0	0
5	1	0	0	0



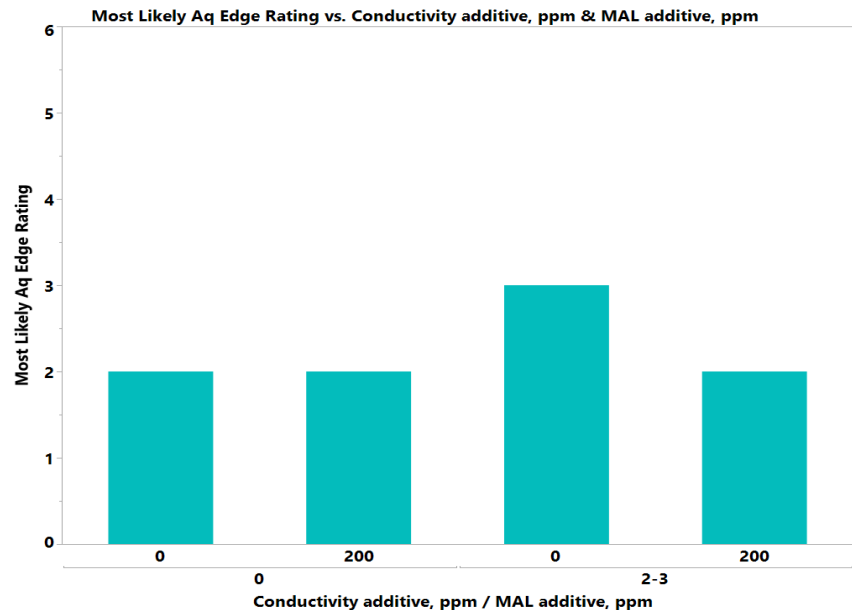
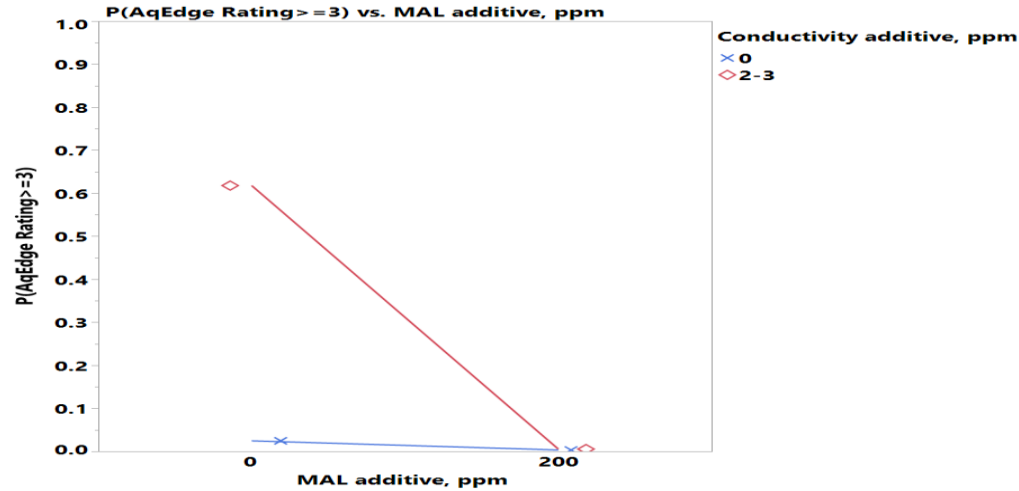
Where((Ethanol = 0) and (Corrosion inhibitor = 0) and (Conductivity Additive = 0) and (FRP Material = 0) and (Sulfur = LSDF) and (Biodiesel = 0) and (CFI additive = 0) and (Glycerin = 0))

MAL Additive-Conductivity Additive Interaction Effect

- 200 ppm MAL additive has **lower** probability of high corrosion severity than zero MAL additive with Conductivity additive

	Conductivity additive, ppm			
	0		2-3	
	MAL additive, ppm		MAL additive, ppm	
	0	200	0	200
AqEdge12	N	N	N	N
1	3	3	1	4
2	16	21	20	23
3	4	3	3	1
4	1	0	2	0
5	0	0	1	0

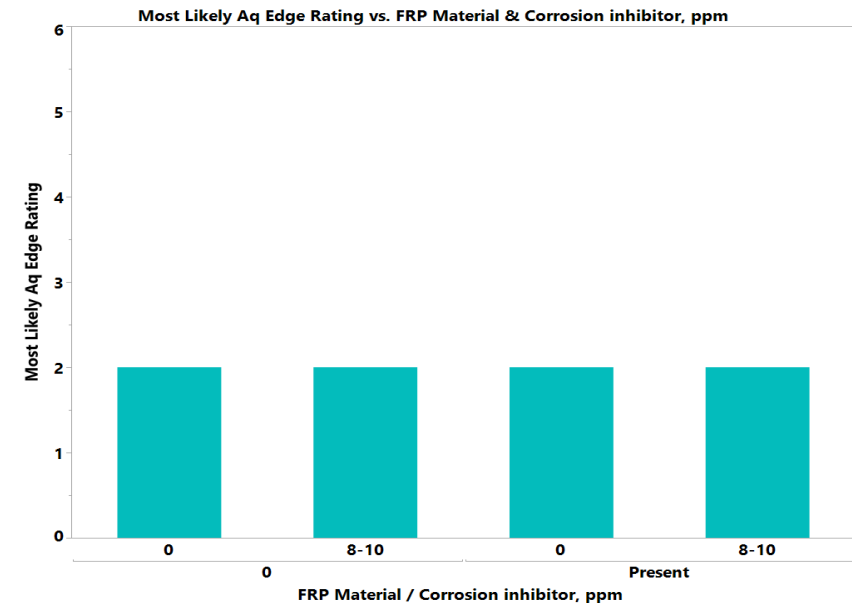
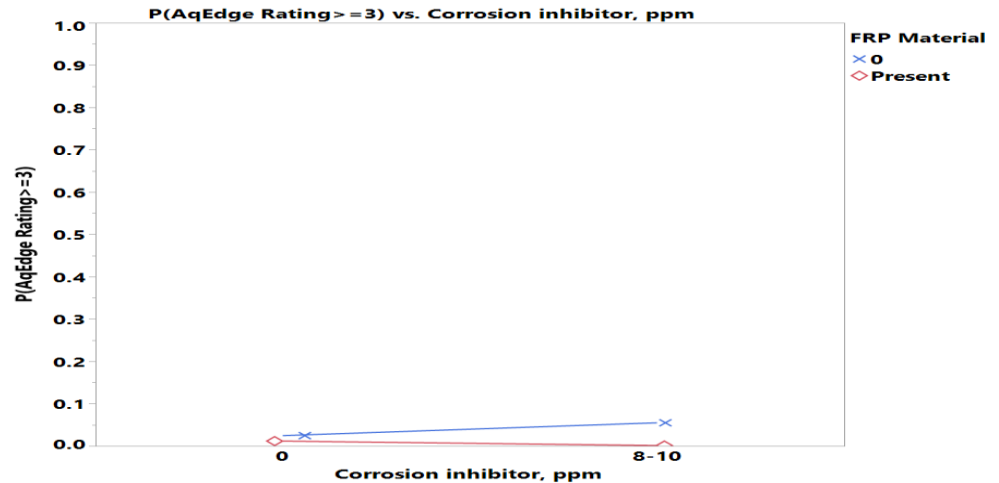
	Conductivity additive, ppm			
	0		2-3	
	MAL additive, ppm		MAL additive, ppm	
	0	200	0	200
AqEdge12	N	N	N	N
1	[Bar chart showing distribution]		[Bar chart showing distribution]	
2	[Bar chart showing distribution]		[Bar chart showing distribution]	
3	[Bar chart showing distribution]		[Bar chart showing distribution]	
4	[Bar chart showing distribution]		[Bar chart showing distribution]	
5	[Bar chart showing distribution]		[Bar chart showing distribution]	



Where((Corrosion inhibitor = 0) and (Sulfur = LSDF) and (Biodiesel = 0) and (CFI additive = 0) and (Glycerin = 0) and (Microbes = 0) and (Ethanol = 0) and (FRP Material = 0))

Corrosion Inhibitor-FRP Material Interaction Effect

- 8-10 ppm Corrosion inhibitor has **lower** probability of high corrosion severity than zero corrosion inhibitor **with** FRP Material while it has **higher** probability **without** FRP Material



	FRP Material			
	0		Present	
	Corrosion inhibitor, ppm		Corrosion inhibitor, ppm	
	0	8-10	0	8-10
AqEdge12	N	N	N	N
1	3	2	2	4
2	21	21	18	20
3	2	3	5	1
4	1	0	2	0
5	0	0	0	1

	FRP Material			
	0		Present	
	Corrosion inhibitor, ppm		Corrosion inhibitor, ppm	
	0	8-10	0	8-10
AqEdge12	N	N	N	N
1				
2				
3				
4				
5				

Where((MAL additive = 0) and (Sulfur = LSDF) and (Microbes= 0) and (Biodiesel = 0) and (Sulfur = LSDF) and (Biodiesel = 0) and (CFI additive = 0) and (Glycerin = 0))

Ordinal Logistic Regression

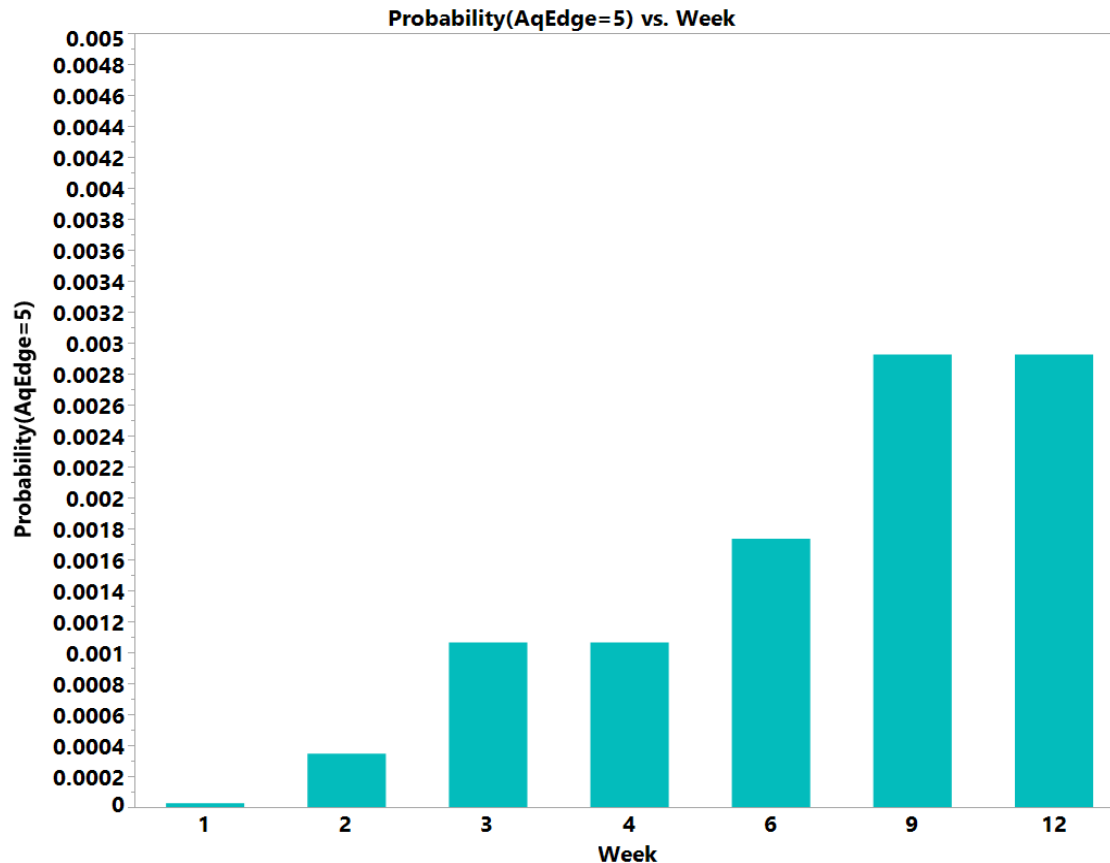
Aq Edge Phase – All Weeks

Whole Model Test				
Model	-LogLikelihood	DF	ChiSquare	Prob> ChiSq
Difference	183.89652	32	367.793	<.0001*
Full	412.88004			
Reduced	596.77656			
RSquare (U)	0.3081			
AICc	901.539			
BIC	1063.7			
Observations (or Sum Wgts)	742			
Fit Details				
Measure	Training Definition			
Entropy RSquare	0.3081	1-Loglike(model)/Loglike(0)		
Generalized RSquare	0.4887	$(1-(L(0)/L(model))^{(2/n)})/(1-L(0)^{(2/n)})$		
Mean -Log p	0.5564	$\sum -\log(p[j])/n$		
RMSE	0.4232	$\sqrt{\sum (y[j]-p[j])^2/n}$		
Mean Abs Dev	0.3253	$\sum y[j]-p[j] /n$		
Misclassification Rate	0.2399	$\sum (p[j] \neq pMax)/n$		
N	742	n		
Lack Of Fit				
Source	DF	-LogLikelihood	ChiSquare	Prob> ChiSq
Lack Of Fit	2932	412.88004	825.7601	
Saturated	2964	0.00000		
Fitted	32	412.88004	1.0000	

Parameter Estimates				
Term	Estimate	Std Error	ChiSquare	Prob> ChiSq
Intercept[1]	0.48897829	0.2363441	4.28	0.0386*
Intercept[2]	6.53381414	0.399481	267.51	<.0001*
Intercept[3]	8.5680742	0.5008843	292.61	<.0001*
Intercept[4]	10.4007562	0.8535129	148.49	<.0001*
Sulfur[LSDf]	0.67569851	0.1044884	41.82	<.0001*
Biodiesel[0]	-0.3974869	0.0973975	16.66	<.0001*
Glycerin[0]	-0.1928147	0.0958872	4.04	0.0443*
Ethanol[0]	-0.1281836	0.095915	1.79	0.1814
Mircobes[0]	-0.2000608	0.0958702	4.35	0.0369*
MAL additive[0]	0.1278048	0.2356784	0.29	0.5876
CFI additive[0]	0.22616942	0.0978653	5.34	0.0208*
Corrosion inhibitor[0]	-0.0695503	0.0954229	0.53	0.4661
Conductivity Additive[0]	0.1173634	0.0959565	1.50	0.2213
FRP Material[0]	0.06652598	0.095331	0.49	0.4853
Sulfur[LSDf]*Biodiesel[0]	-0.6507046	0.1018823	40.79	<.0001*
Sulfur[LSDf]*Mircobes[0]	-0.5915629	0.1010172	34.29	<.0001*
Sulfur[LSDf]*CFI additive[0]	0.37380385	0.0975831	14.67	0.0001*
Sulfur[LSDf]*Conductivity Additive[0]	0.60651795	0.1020254	35.34	<.0001*
Sulfur[LSDf]*FRP Material[0]	-0.2792221	0.0979986	8.12	0.0044*
Glycerin[0]*CFI additive[0]	0.31571066	0.097402	10.51	0.0012*
Ethanol[0]*FRP Material[0]	-0.315511	0.0990303	10.15	0.0014*
Mircobes[0]*MAL additive[0]	-0.1626037	0.0982282	2.74	0.0978
MAL additive[0]*Conductivity Additive[0]	0.26313135	0.097575	7.27	0.0070*
Corrosion inhibitor[0]*FRP Material[0]	0.40321854	0.097674	17.04	<.0001*
Week[2-1]	-1.9973226	0.3568078	31.33	<.0001*
Week[3-2]	-1.0262737	0.3647332	7.92	0.0049*
Week[4-3]	-0.1213767	0.3632709	0.11	0.7383
Week[6-4]	-0.3641299	0.3614478	1.01	0.3137
Week[9-6]	-0.3217986	0.3534159	0.83	0.3625
Week[12-9]	-0.0615251	0.3482954	0.03	0.8598
Week[2-1]*MAL additive[0]	-0.6215944	0.3463308	3.22	0.0727
Week[3-2]*MAL additive[0]	-0.0998202	0.3598407	0.08	0.7815
Week[4-3]*MAL additive[0]	0.12137666	0.3632709	0.11	0.7383
Week[6-4]*MAL additive[0]	-0.124496	0.360818	0.12	0.7301
Week[9-6]*MAL additive[0]	-0.2019183	0.3531327	0.33	0.5675
Week[12-9]*MAL additive[0]	0.06152506	0.3482954	0.03	0.8598

Corrosion by Time (Week)

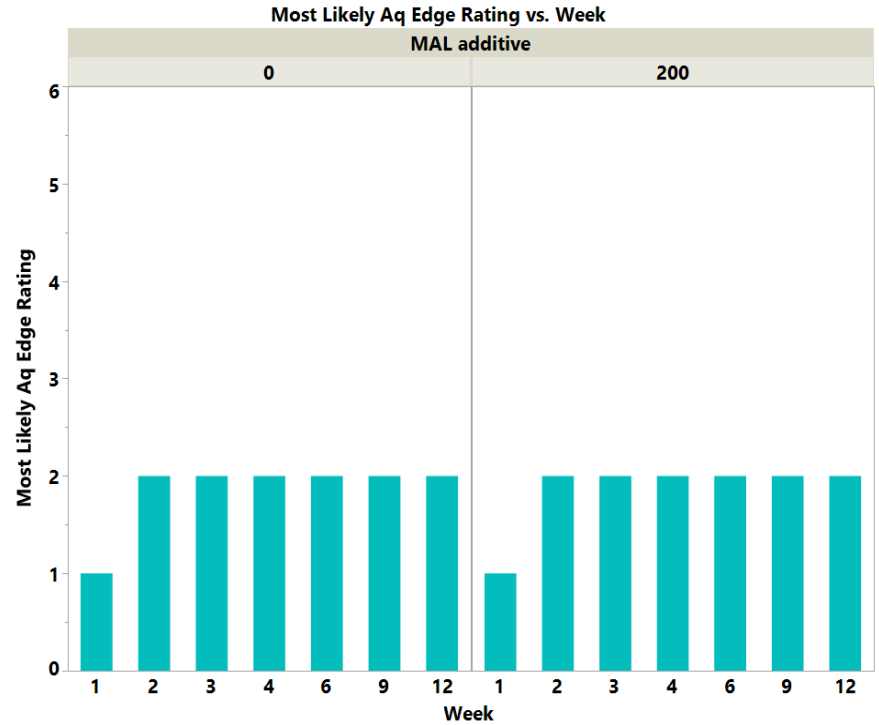
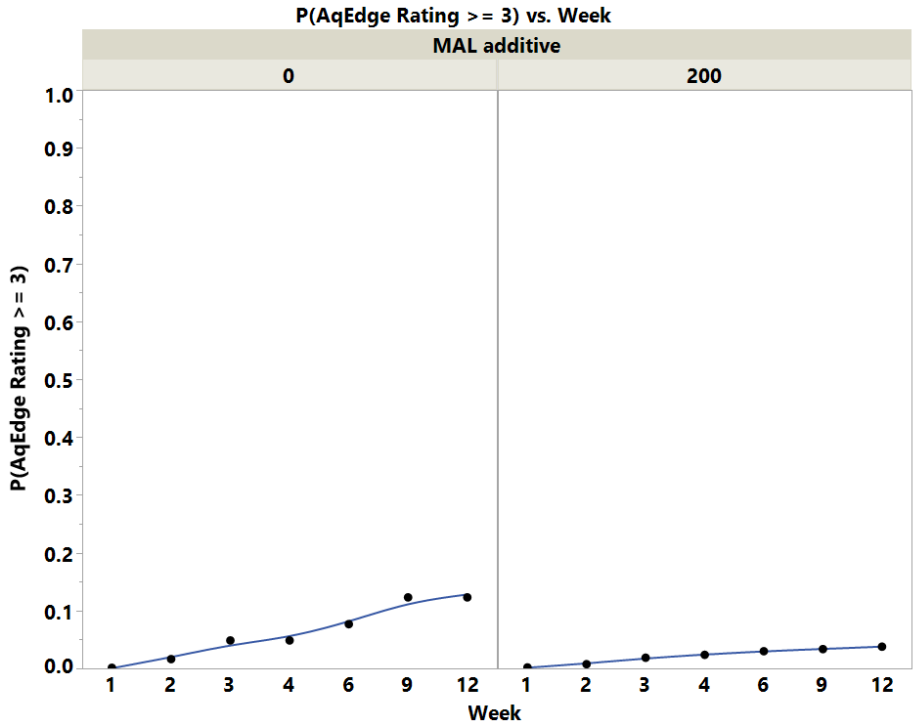
- Probability of high corrosion severity in Week 2 is significantly higher than Week 1, and Week 3 is significantly higher Week 2



Where((Sulfur = LSDF) and (Biodiesel = 0) and (Glycerin = 0) and (Ethanol = 0) and (Microbes = 0) and (MAL additive = 0) and (CFI additive = 0) and (Corrosion Inhibitor = 0) and (Conductivity Additive = 0) and (FRP Material = 0))

MAL Additive Effect by Time (Week)

- Probability of high corrosion severity in Week 2 is **higher** than Week 1 more significantly without MAL additive than with MAL additive



Where((Sulfur = LSDF) and (Biodiesel = 0) and (Glycerin = 0) and (Ethanol = 0) and (Microbes = 0) and (Corrosion Inhibitor = 0) and (CFI additive = 0) and (Conductivity Additive = 0) and (FRP Material = 0))

Aqueous/Fuel Phase

Conclusions (Aqueous/Fuel Phase)

Average Corrosion Severity Rating (average of 3 samples)

- ULSD has marginally **higher** probability of high corrosion severity than LSDF
- 5% Biodiesel has **lower** probability of high corrosion severity than zero Biodiesel
- 200ppm MAL additive has **lower** probability of high corrosion severity than zero MAL additive
- 8-10ppm Corrosion inhibitor has **lower** probability of high corrosion severity than zero Corrosion inhibitor
- 5% Biodiesel has **lower** probability of high corrosion severity than zero Biodiesel more significantly with Ethanol
- 5% Biodiesel has **lower** probability of high corrosion severity than zero Biodiesel more significantly with CFI Additive
- 5000ppm Glycerin has **lower** probability of high corrosion severity than zero Glycerin more significantly with Microbes
- 10000ppm Ethanol has **lower** probability of high corrosion severity than zero Ethanol more significantly without Microbes
- 10000ppm Ethanol has **lower** probability of high corrosion severity than zero Ethanol more significantly with FRP Material
- 200ppm MAL additive has **lower** probability of high corrosion severity than zero MAL additive more significantly without Conductivity Additive
- 8-10ppm Corrosion inhibitor has **lower** probability of high corrosion severity than zero Corrosion inhibitor more significantly without CFI Additive
- 8-10ppm Corrosion inhibitor has **lower** probability of high corrosion severity than zero Corrosion inhibitor more significantly without FRP Material

Average Corrosion Severity Rating by Time (Week)

- Significant weekly **increases** in probability of high corrosion severity between weeks 1, 2, 3, 4 and 6; marginal differences observed between weeks 6, 9 and 12
- More significant **increase** in probability of high corrosion severity between weeks 1 and 2 without Corrosion inhibitor than with Corrosion inhibitor

Stepwise Ordinal Logistic Regression

Aqueous/Fuel Phase – Week 12

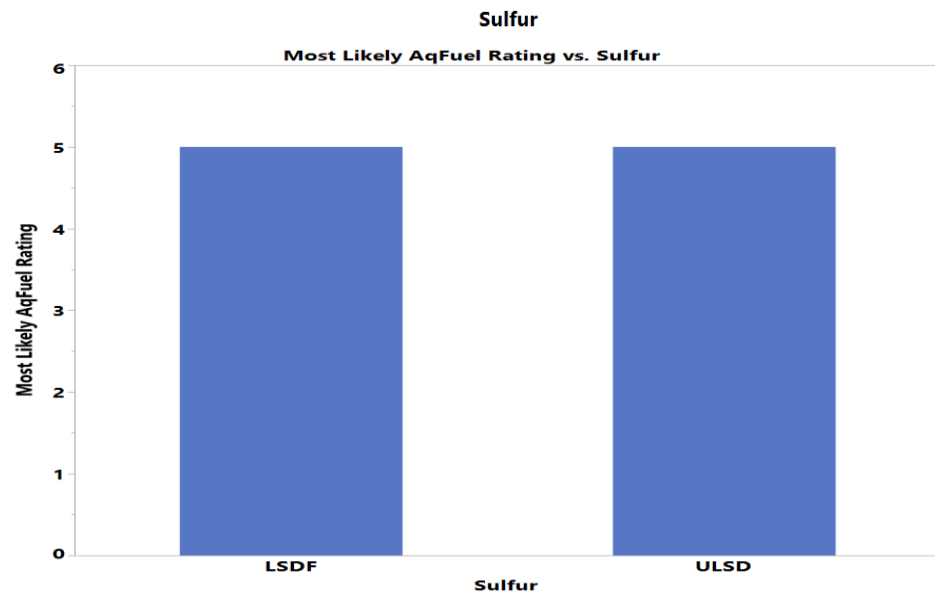
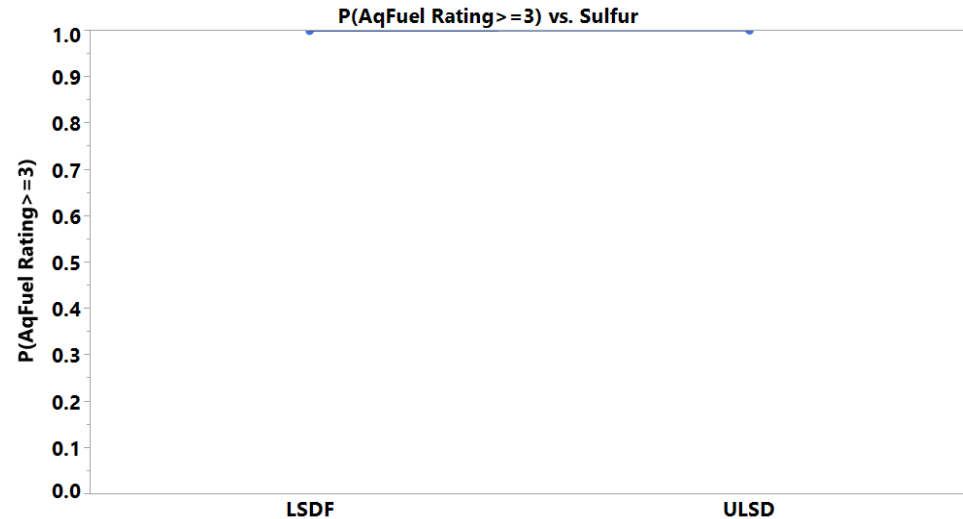
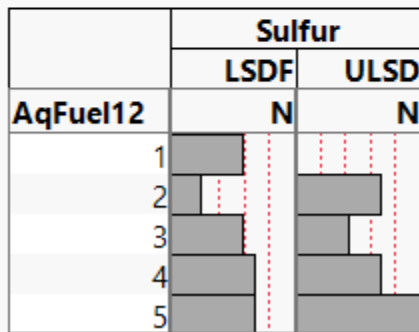
Whole Model Test				
Model	-LogLikelihood	DF	ChiSquare	Prob> ChiSq
Difference	43.33251	18	86.66503	<.0001*
Full	124.93727			
Reduced	168.26979			
RSquare (U)	0.2575			
AICc	306.067			
BIC	352.47			
Observations (or Sum Wgts)	106			
Fit Details				
Measure	Training Definition			
Entropy RSquare	0.2575	1-Loglike(model)/Loglike(0)		
Generalized RSquare	0.5829	$(1-(L(0)/L(model))^{2/n})/(1-L(0)^{2/n})$		
Mean -Log p	1.1787	$\sum -\log(p[j])/n$		
RMSE	0.6576	$\sqrt{\sum (y[j]-p[j])^2/n}$		
Mean Abs Dev	0.6203	$\sum y[j]-p[j] /n$		
Misclassification Rate	0.5660	$\sum (p[j] \neq pMax)/n$		
N	106	n		
Lack Of Fit				
Source	DF	-LogLikelihood	ChiSquare	
Lack Of Fit	402	124.93727	249.8745	
Saturated	420	0.00000	Prob> ChiSq	
Fitted	18	124.93727	1.0000	

Parameter Estimates				
Term	Estimate	Std Error	ChiSquare	Prob> ChiSq
Intercept[1]	-3.1603239	0.4087464	59.78	<.0001*
Intercept[2]	-1.4941151	0.2936386	25.89	<.0001*
Intercept[3]	-0.0357378	0.2549217	0.02	0.8885
Intercept[4]	1.73547943	0.3053234	32.31	<.0001*
Sulfur[LSDF]	0.31244169	0.1902754	2.70	0.1006
Biodiesel[0]	-1.0183733	0.2104795	23.41	<.0001*
Glycerin[0]	0.01889828	0.1887443	0.01	0.9202
Ethanol[0]	0.11108188	0.1893569	0.34	0.5575
Mircobes[0]	0.08505135	0.1920885	0.20	0.6579
MAL additive[0]	-0.4848634	0.1942636	6.23	0.0126*
CFI additive[0]	7.46739e-5	0.190296	0.00	0.9997
Corrosion inhibitor[0]	-1.0458892	0.2096881	24.88	<.0001*
Conductivity Additive[0]	-0.0646862	0.189792	0.12	0.7332
FRP Material[0]	0.01365728	0.1906959	0.01	0.9429
Biodiesel[0]*Ethanol[0]	-0.4238314	0.1941981	4.76	0.0291*
Biodiesel[0]*CFI additive[0]	0.38498093	0.1926112	3.99	0.0456*
Glycerin[0]*Mircobes[0]	0.37931689	0.192304	3.89	0.0486*
Ethanol[0]*Mircobes[0]	-1.0430881	0.2125663	24.08	<.0001*
Ethanol[0]*FRP Material[0]	-0.3918615	0.1964809	3.98	0.0461*
MAL additive[0]*Conductivity Additive[0]	-0.6864672	0.1995965	11.83	0.0006*
CFI additive[0]*Corrosion inhibitor[0]	-0.368687	0.192976	3.65	0.0561
Corrosion inhibitor[0]*FRP Material[0]	-0.580865	0.1975493	8.65	0.0033*

Sulfur Effect – Aq/Fuel Interface

- ULSD has marginally **higher** probability of high corrosion severity than LSDF

		Sulfur	
		LSDF	ULSD
AqFuel12		N	N
1	11	4	
2	7	12	
3	11	9	
4	12	12	
5	12	16	

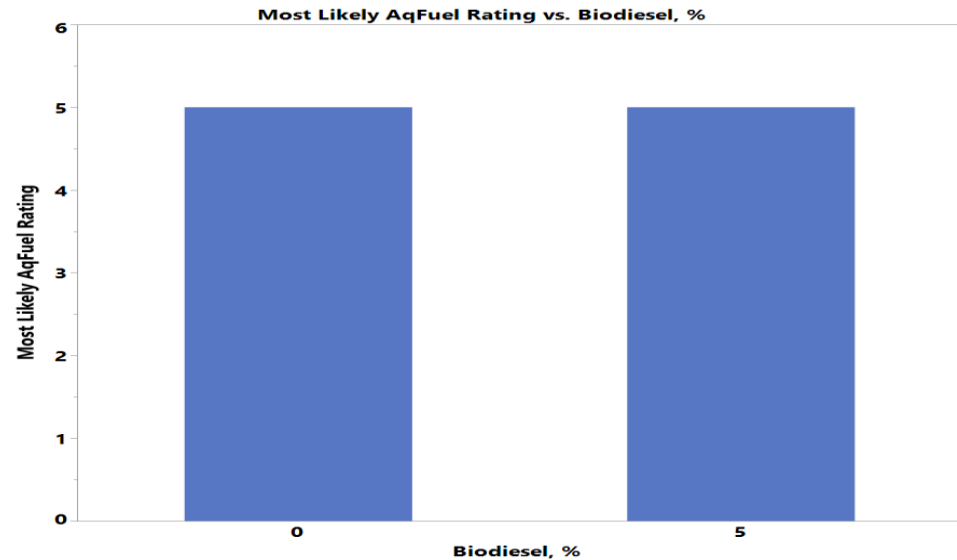
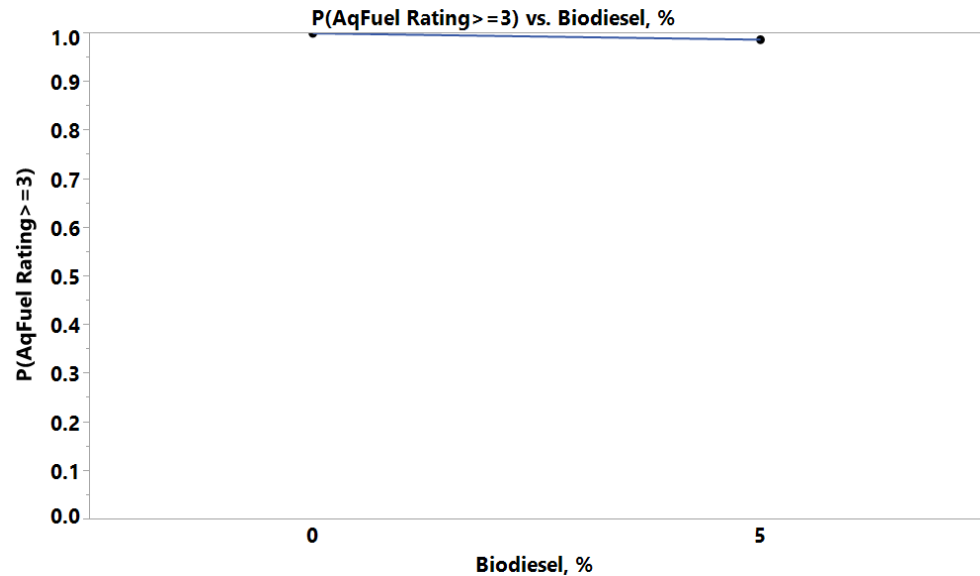
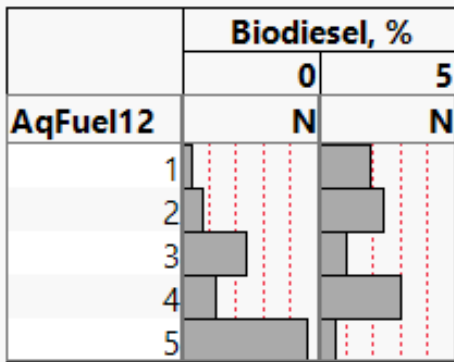


Where((Biodiesel = 0) and (Glycerin = 0) and (Microbes = 0) and (Ethanol = 0) and (MAL additive = 0) and (CFI additive = 0) and (Corrosion inhibitor = 0) and (Conductivity Additive = 0) and (FRP Material = 0))

Biodiesel Effect – Aq/Fuel Interface

- 5% Biodiesel has **lower** probability of high corrosion severity than zero Biodiesel

	Biodiesel, %	
	0	5
AqFuel12	N	N
1	4	11
2	6	13
3	13	7
4	8	16
5	23	5

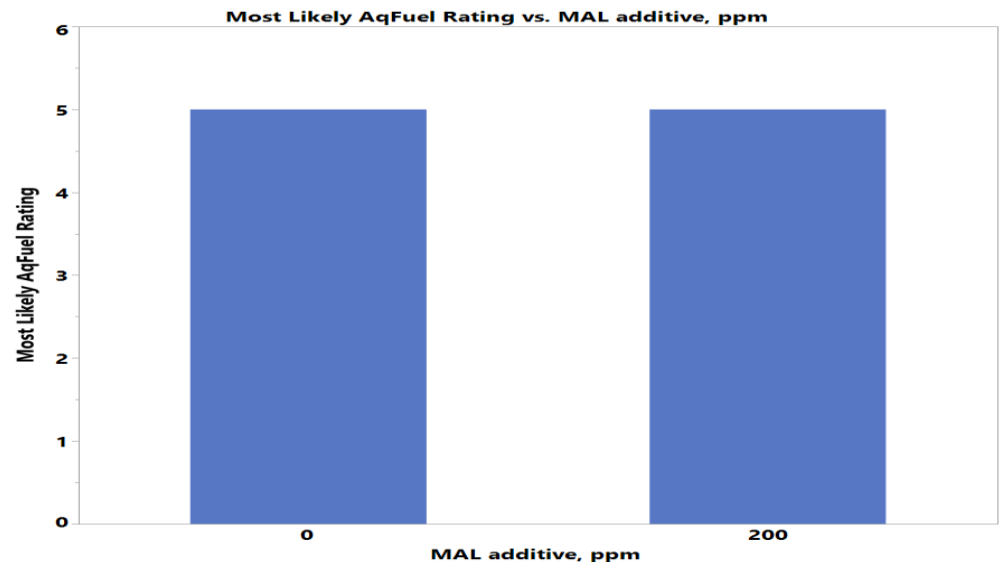
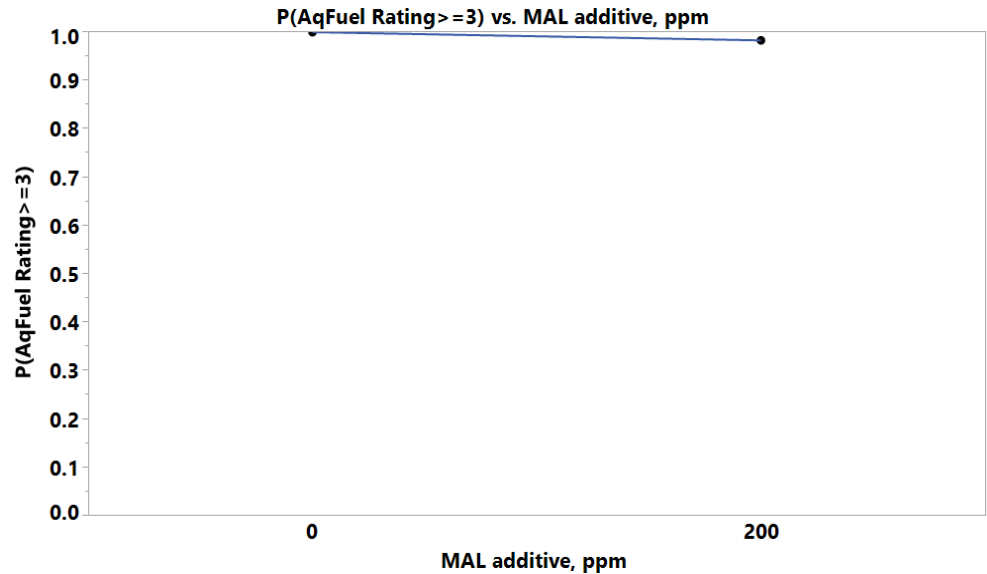
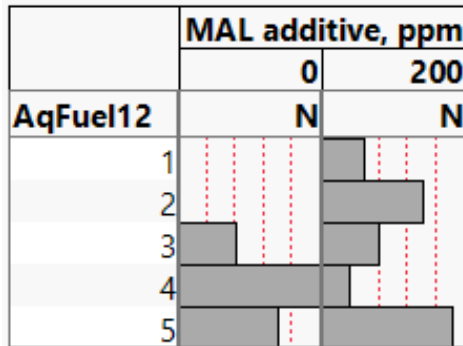


Where((Sulfur = LSDF) and (Glycerin = 0) and (Microbes = 0) and (Ethanol = 0) and (MAL additive = 0) and (CFI additive = 0) and (Corrosion inhibitor = 0) and (Conductivity Additive = 0) and (FRP Material = 0))

MAL Additive Effect – Aq/Fuel Interface

- 200ppm MAL additive has **lower** probability of high corrosion severity than zero MAL additive

	MAL additive, ppm	
	0	200
AqFuel12	N	N
1	6	9
2	6	13
3	10	10
4	16	8
5	13	15

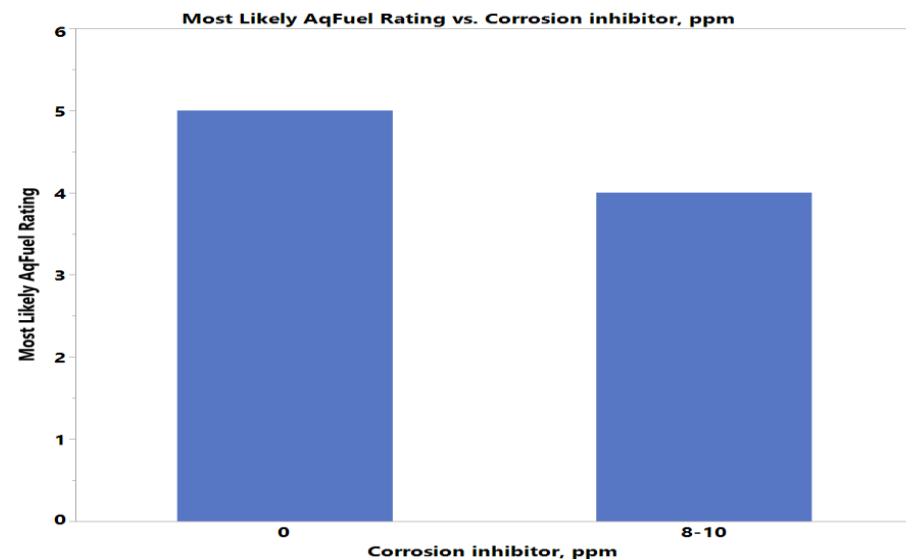
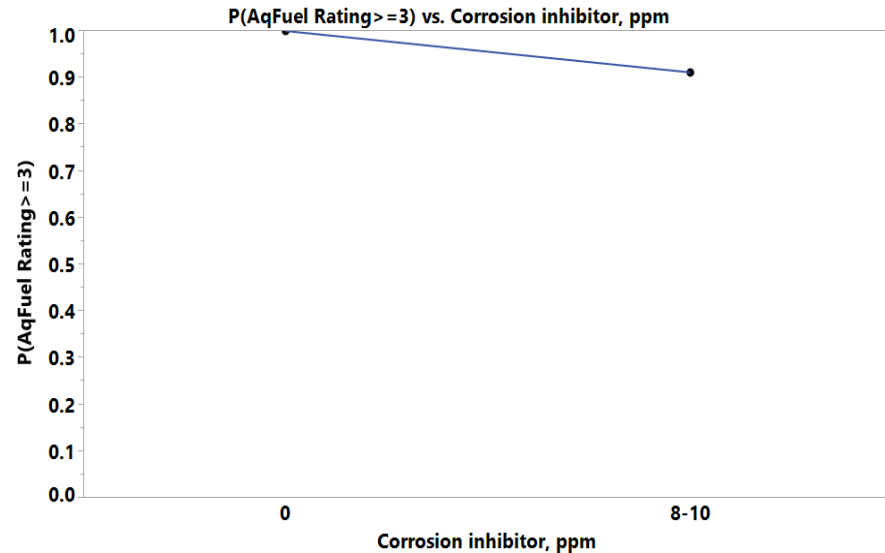
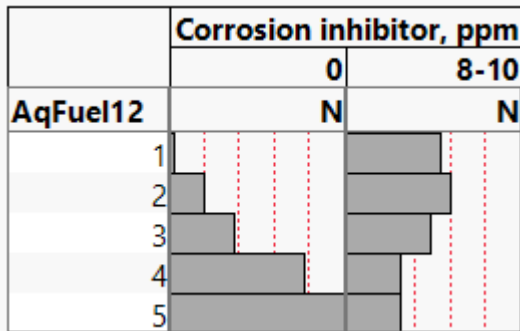


Where((Biodiesel = 0) and (Glycerin = 0) and (Microbes = 0) and (Ethanol = 0) and (Sulfur = LSDF) and (CFI additive = 0) and (Corrosion inhibitor = 0) and (Conductivity Additive = 0) and (FRP Material = 0))

Corrosion Inhibitor Effect – Aq/Fuel Interface

- 8-10ppm Corrosion inhibitor has **lower** probability of high corrosion severity than zero Corrosion inhibitor

	Corrosion inhibitor, ppm	
	0	8-10
AqFuel12	N	N
1	3	12
2	6	13
3	9	11
4	16	8
5	20	8

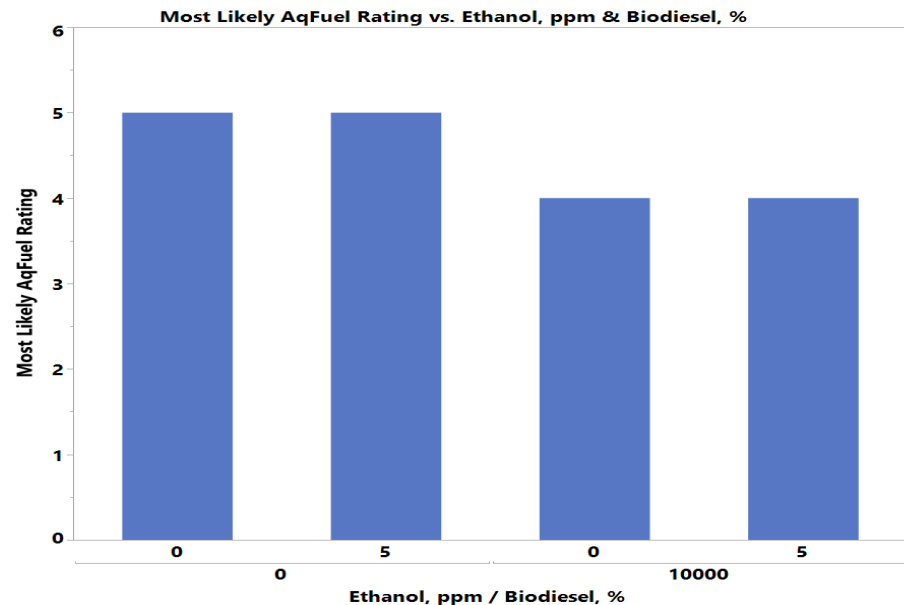
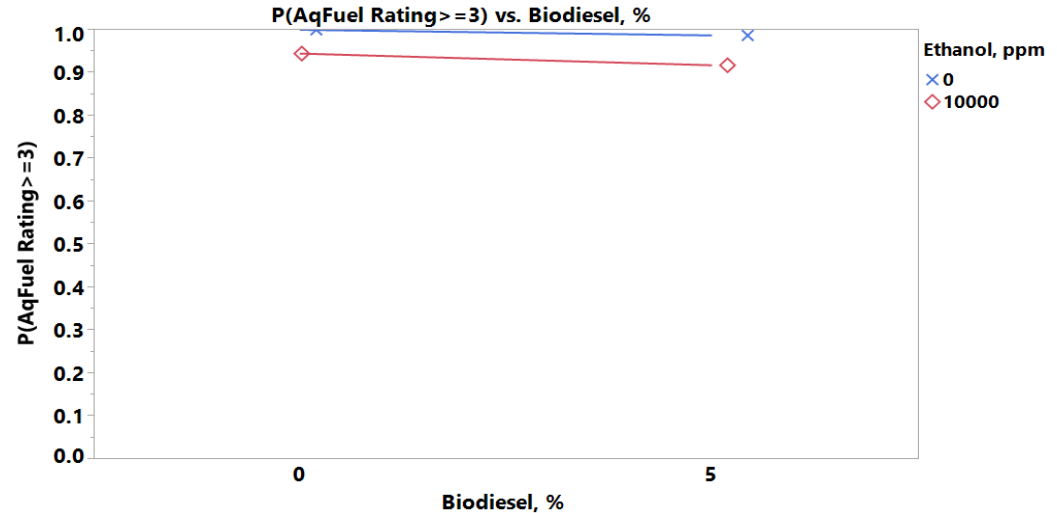
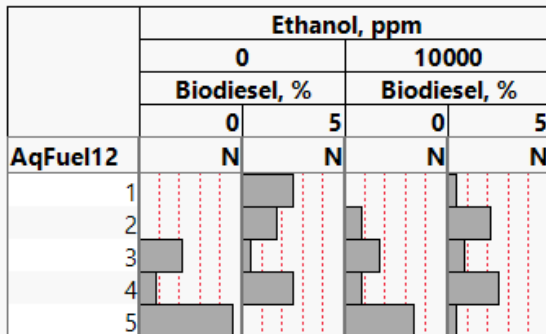


Where((Biodiesel = 0) and (Glycerin = 0) and (Microbes = 0) and (Ethanol = 0) and (MAL additive = 0) and (CFI additive = 0) and (Sulfur= LSDF) and (Conductivity Additive = 0) and (FRP Material = 0))

Biodiesel-Ethanol Interaction Effect

- 5% Biodiesel has **lower** probability of high corrosion severity than zero Biodiesel more significantly with Ethanol

	Ethanol, ppm			
	0		10000	
	Biodiesel, %		Biodiesel, %	
	0	5	0	5
AqFuel12	N	N	N	N
1	2	8	2	3
2	2	6	4	7
3	7	3	6	4
4	4	8	4	8
5	13	2	10	3

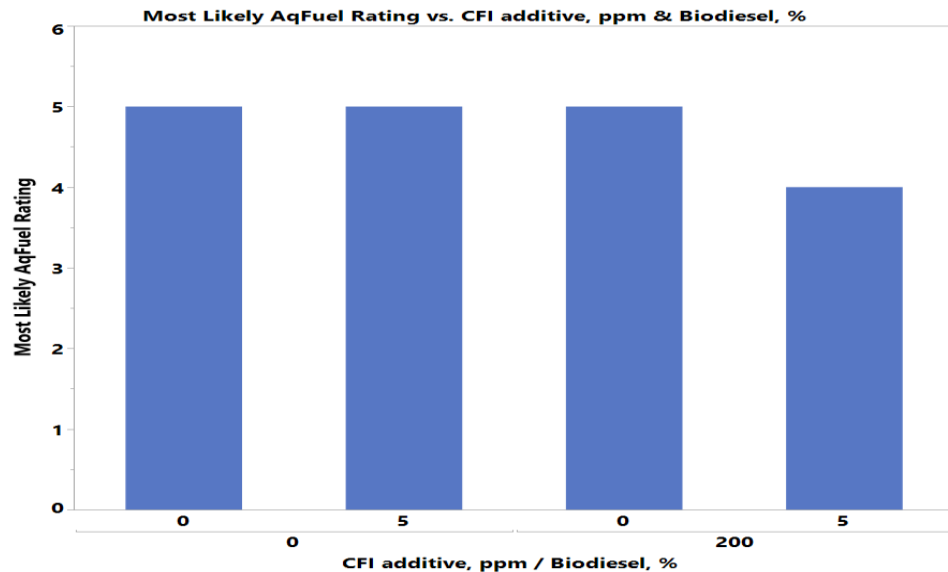
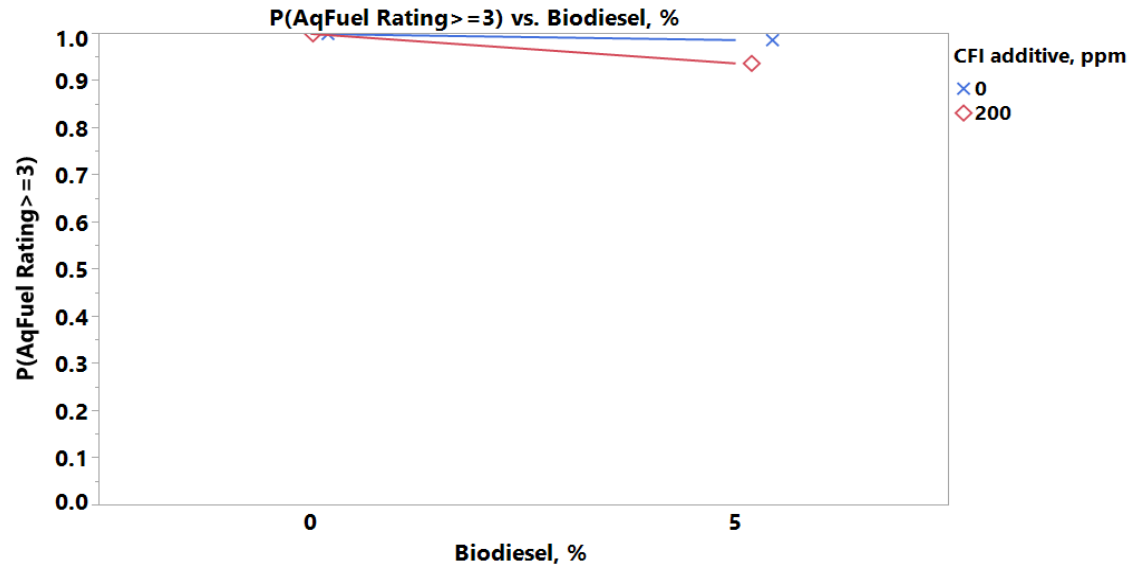
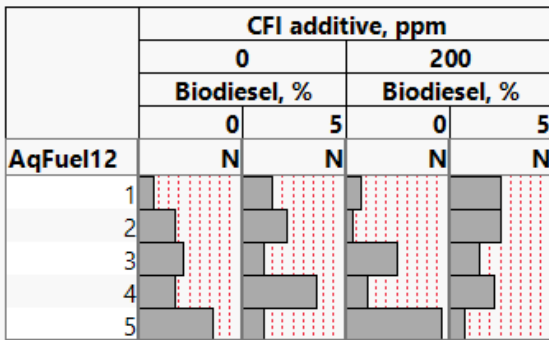


Where((Glycerin = 0) and (Microbes = 0) and (MAL additive = 0) and (CFI additive = 0) and (Corrosion inhibitor = 0) and (Conductivity Additive = 0) and (FRP Material = 0) and (Sulfur = LSDF))

Biodiesel-CFI Additive Interaction Effect

- 5% Biodiesel has **lower** probability of high corrosion severity than zero Biodiesel more significantly with CFI Additive

	CFI additive, ppm			
	0		200	
	Biodiesel, %		Biodiesel, %	
	0	5	0	5
AqFuel12	N	N	N	N
1	2	4	2	7
2	5	6	1	7
3	6	3	7	4
4	5	10	3	6
5	10	3	13	2

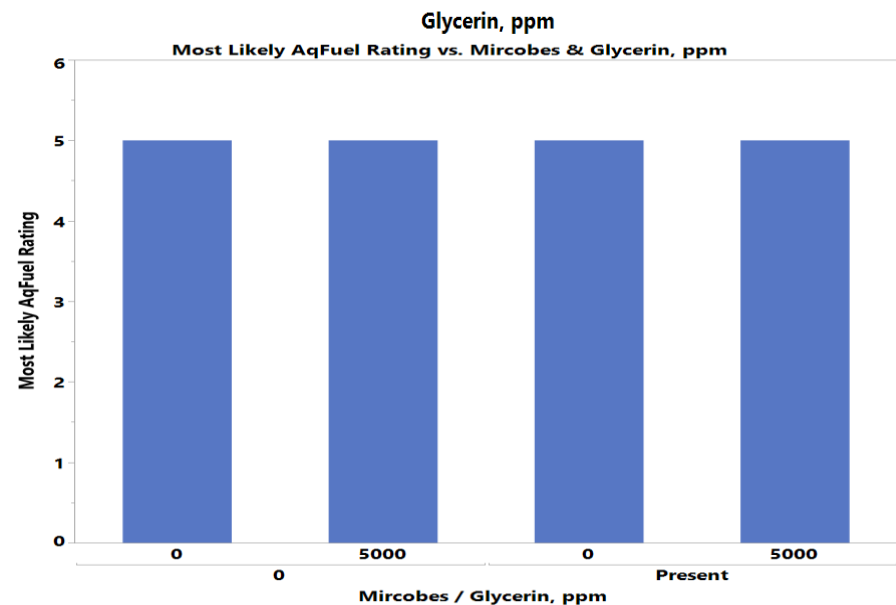
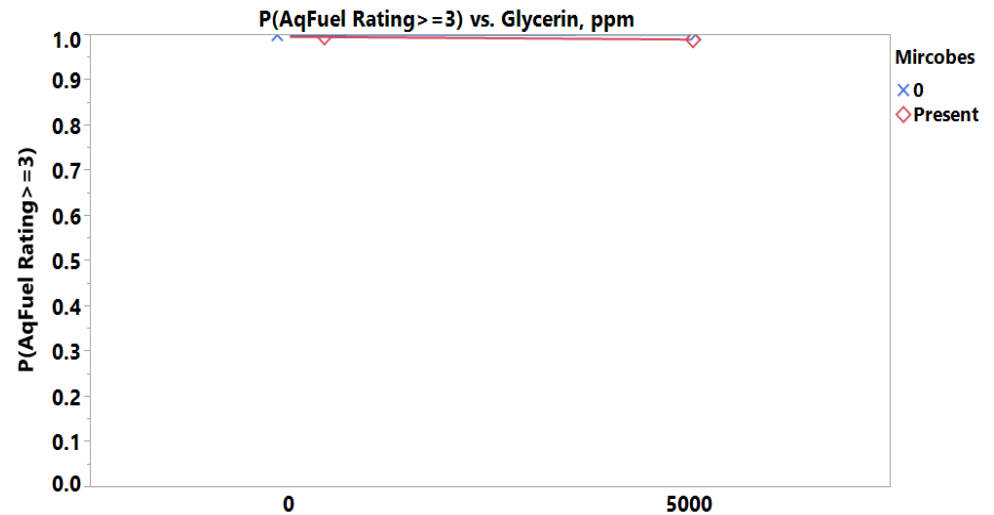
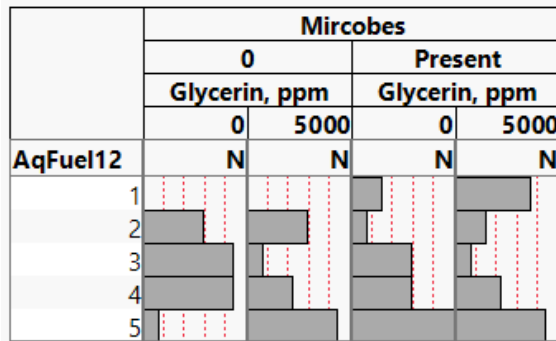


Where((Glycerin = 0) and (Microbes = 0) and (MAL additive = 0) and (Corrosion inhibitor = 0) and (Conductivity Additive = 0) and (FRP Material = 0) and (Sulfur = LSDF) and (Ethanol = 0))

Glycerin-Microbes Interaction Effect

- 5000ppm Glycerin has **lower** probability of high corrosion severity than zero Glycerin more significantly with Microbes

	Microbes			
	0		Present	
	Glycerin, ppm		Glycerin, ppm	
	0	5000	0	5000
AqFuel12	N	N	N	N
1	2	2	4	7
2	6	6	3	4
3	8	3	6	3
4	8	5	6	5
5	3	8	9	8

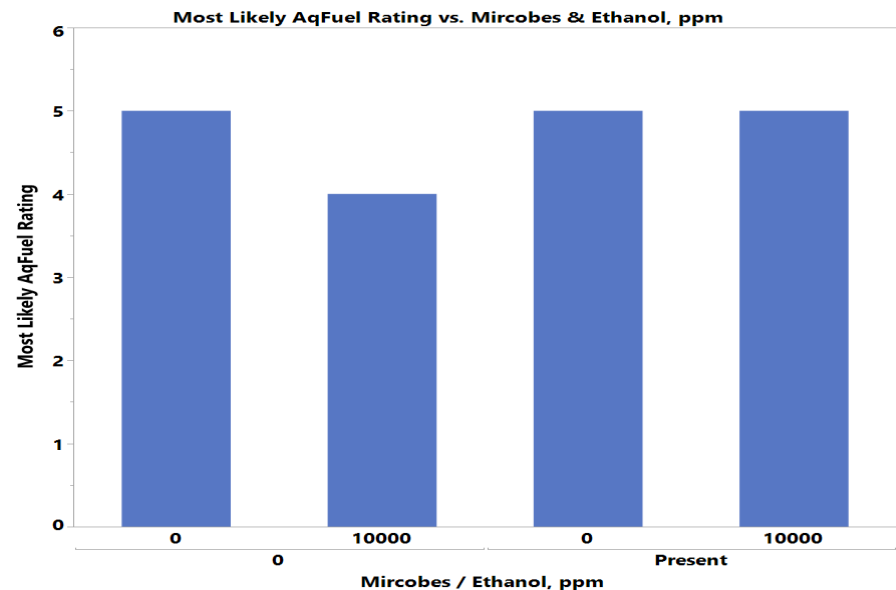
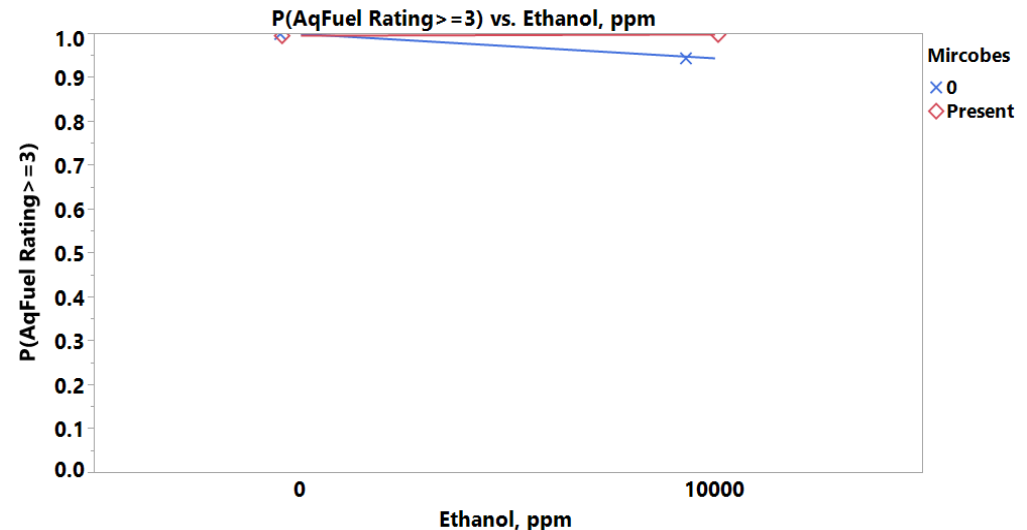
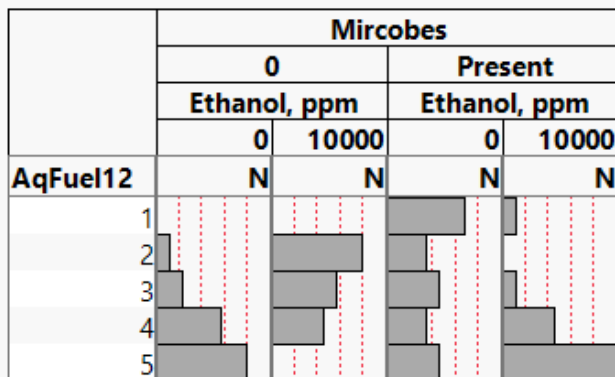


Where((MAL additive = 0) and (Corrosion inhibitor = 0) and (Conductivity Additive = 0) and (FRP Material = 0) and (Sulfur = LSDF) and (Ethanol = 0) and (Biodiesel = 0) and (CFI additive = 0))

Ethanol-Microbes Interaction Effect

- 10000ppm Ethanol has **lower** probability of high corrosion severity than zero Ethanol more significantly without Microbes

	Microbes			
	0		Present	
	Ethanol, ppm		Ethanol, ppm	
	0	10000	0	10000
AqFuel12	N	N	N	N
1	2	2	8	3
2	3	9	5	2
3	4	7	6	3
4	7	6	5	6
5	9	2	6	11



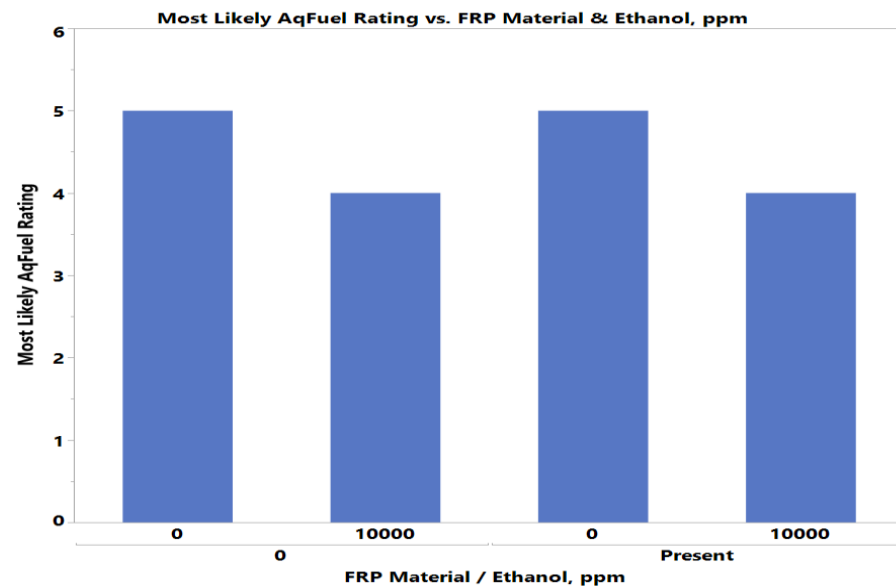
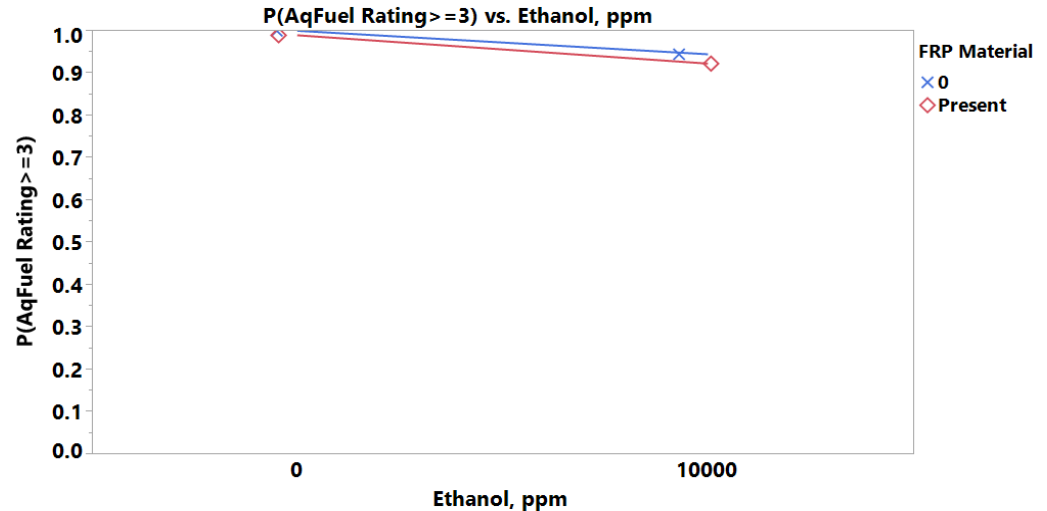
Where((MAL additive = 0) and (Corrosion inhibitor = 0) and (Conductivity Additive = 0) and (FRP Material = 0) and (Sulfur = LSDF) and (Biodiesel = 0) and (CFI additive = 0) and (Glycerin = 0))

Ethanol-FRP Material Interaction Effect

- 10000ppm Ethanol has **lower** probability of high corrosion severity than zero Ethanol more significantly with FRP Material

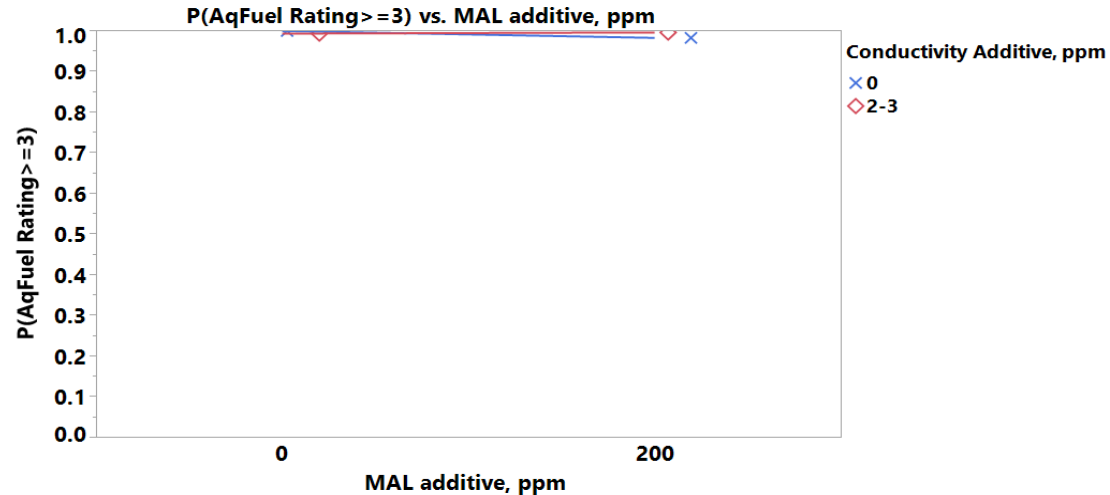
	FRP Material			
	0		Present	
	Ethanol, ppm		Ethanol, ppm	
	0	10000	0	10000
AqFuel12	N	N	N	N
1	4	5	6	0
2	3	4	5	7
3	4	4	6	6
4	9	9	3	3
5	7	4	8	9

	FRP Material			
	0		Present	
	Ethanol, ppm		Ethanol, ppm	
	0	10000	0	10000
AqFuel12	N	N	N	N
1	4	5	6	0
2	3	4	5	7
3	4	4	6	6
4	9	9	3	3
5	7	4	8	9

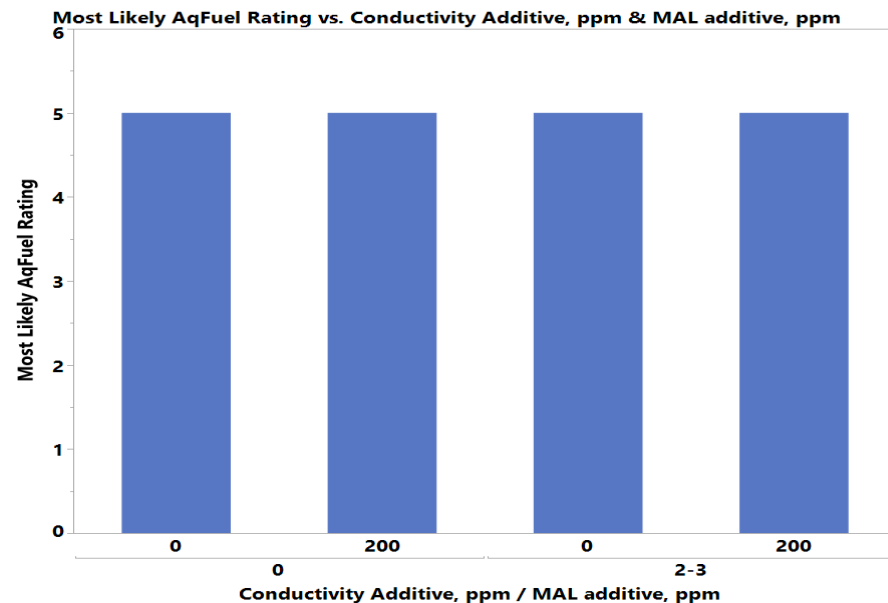
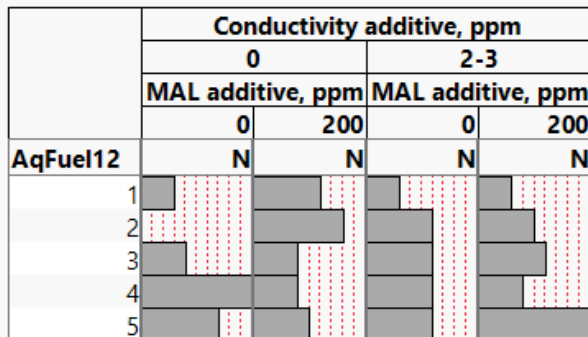


MAL Additive-Conductivity Additive Interaction Effect

- 200ppm MAL additive has **lower** probability of high corrosion severity than zero MAL additive more significantly without Conductivity Additive



	Conductivity additive, ppm			
	0		2-3	
	MAL additive, ppm		MAL additive, ppm	
	0	200	0	200
AqFuel12	N	N	N	N
1	3	6	3	3
2	0	8	6	5
3	4	4	6	6
4	10	4	6	4
5	7	5	6	10

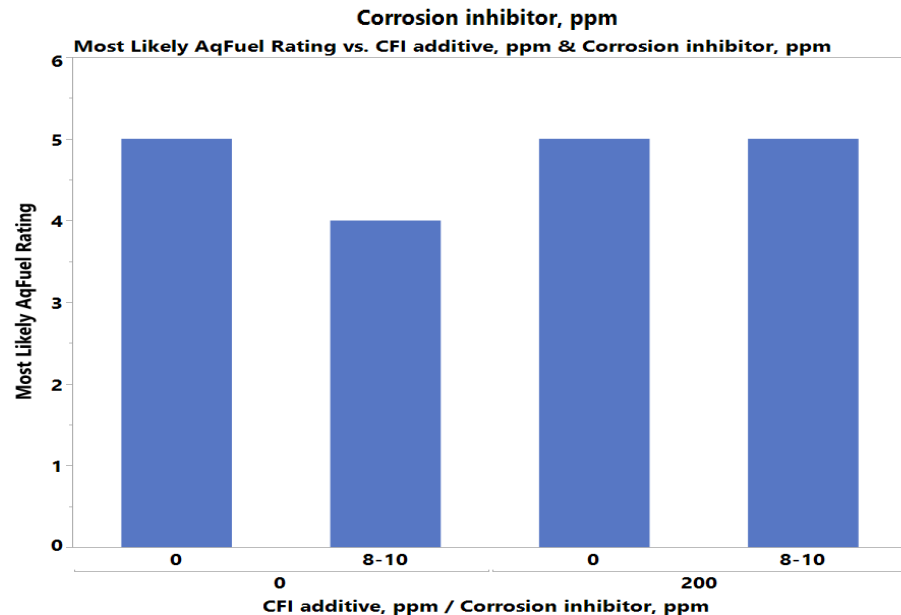
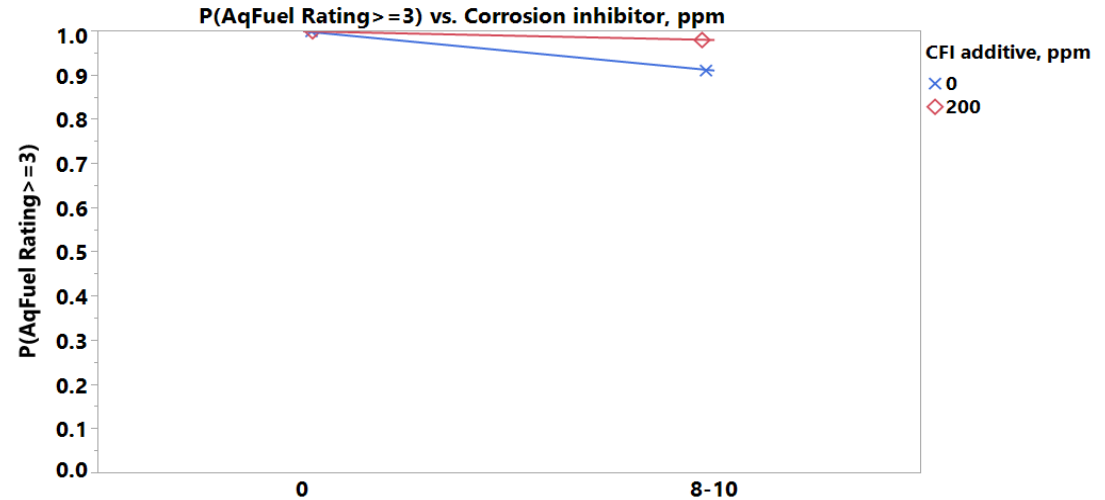
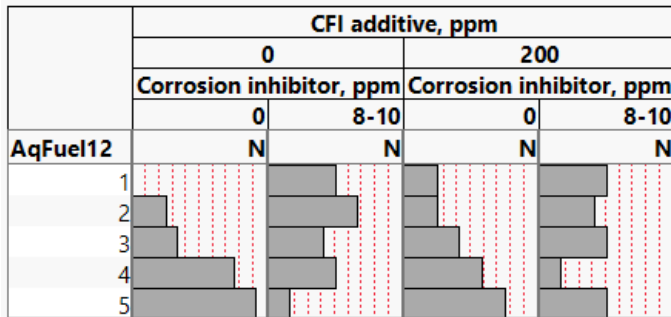


Where((Corrosion inhibitor = 0) and (Sulfur = LSDF) and (Biodiesel = 0) and (CFI additive = 0) and (Glycerin = 0) and (Microbes = 0) and (Ethanol = 0) and (FRP Material = 0))

Corrosion Inhibitor-CFI Additive Interaction Effect

- 8-10ppm Corrosion inhibitor has **lower** probability of high corrosion severity than zero Corrosion inhibitor more significantly without CFI Additive

	CFI additive, ppm			
	0		200	
	Corrosion inhibitor, ppm		Corrosion inhibitor, ppm	
	0	8-10	0	8-10
AqFuel12	N	N	N	N
1	0	6	3	6
2	3	8	3	5
3	4	5	5	6
4	9	6	7	2
5	11	2	9	6

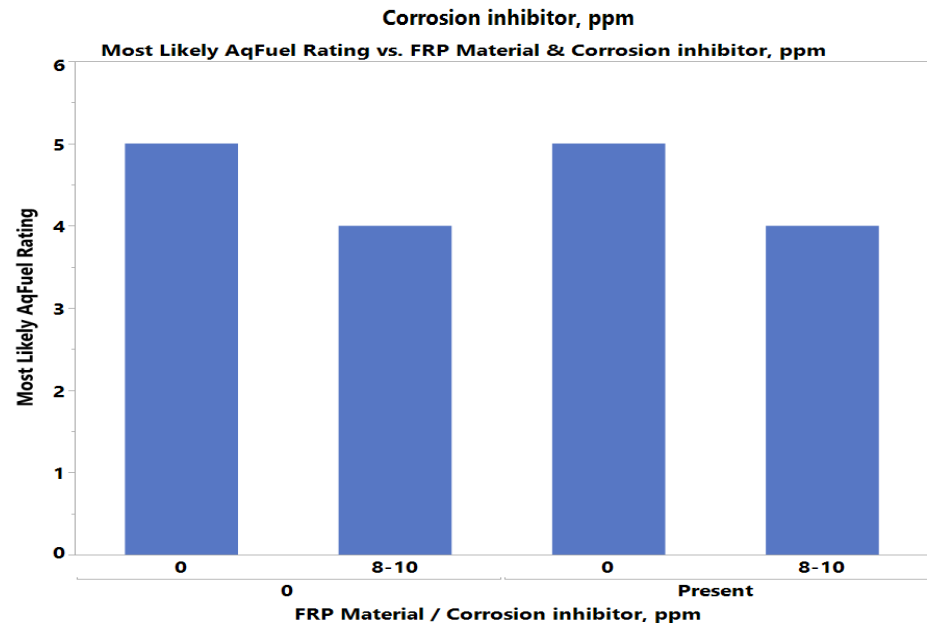
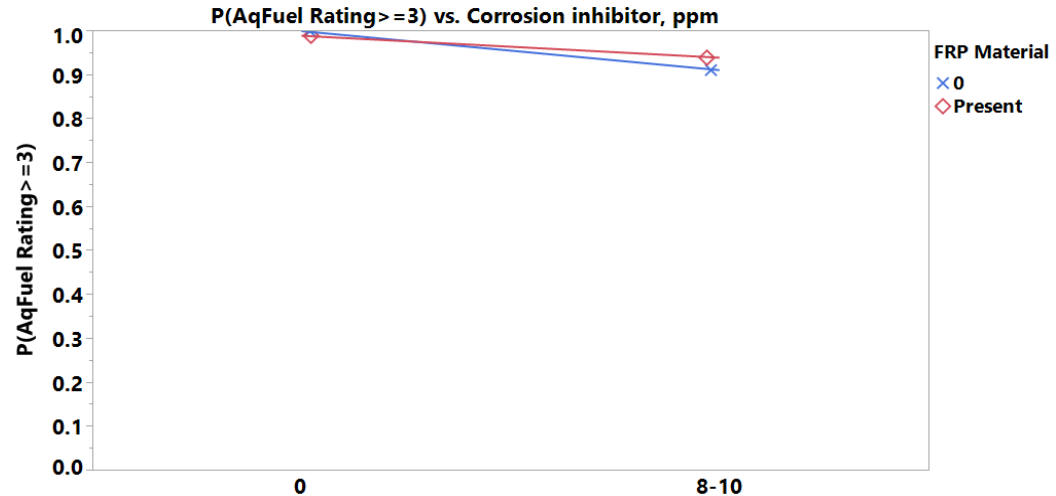
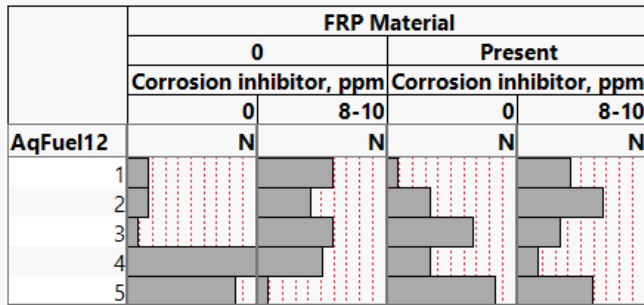


Where((Sulfur = LSDF) and (Biodiesel = 0) and (Glycerin = 0) and (Microbes = 0) and (Ethanol = 0) and (FRP Material = 0) and (MAL additive = 0) and (Conductivity Additive = 0))

Corrosion Inhibitor-FRP Material Interaction Effect

- 8-10ppm Corrosion inhibitor has **lower** probability of high corrosion severity than zero Corrosion inhibitor more significantly without FRP Material

	FRP Material			
	0		Present	
	Corrosion inhibitor, ppm		Corrosion inhibitor, ppm	
	0	8-10	0	8-10
AqFuel12	N	N	N	N
1	2	7	1	5
2	2	5	4	8
3	1	7	8	4
4	12	6	4	2
5	10	1	10	7



Where((Sulfur = LSDF) and (Biodiesel = 0) and (Glycerin = 0) and (Microbes = 0) and (Ethanol = 0) and (MAL additive = 0) and (Conductivity Additive = 0) and (CFI additive = 0))

Ordinal Logistic Regression

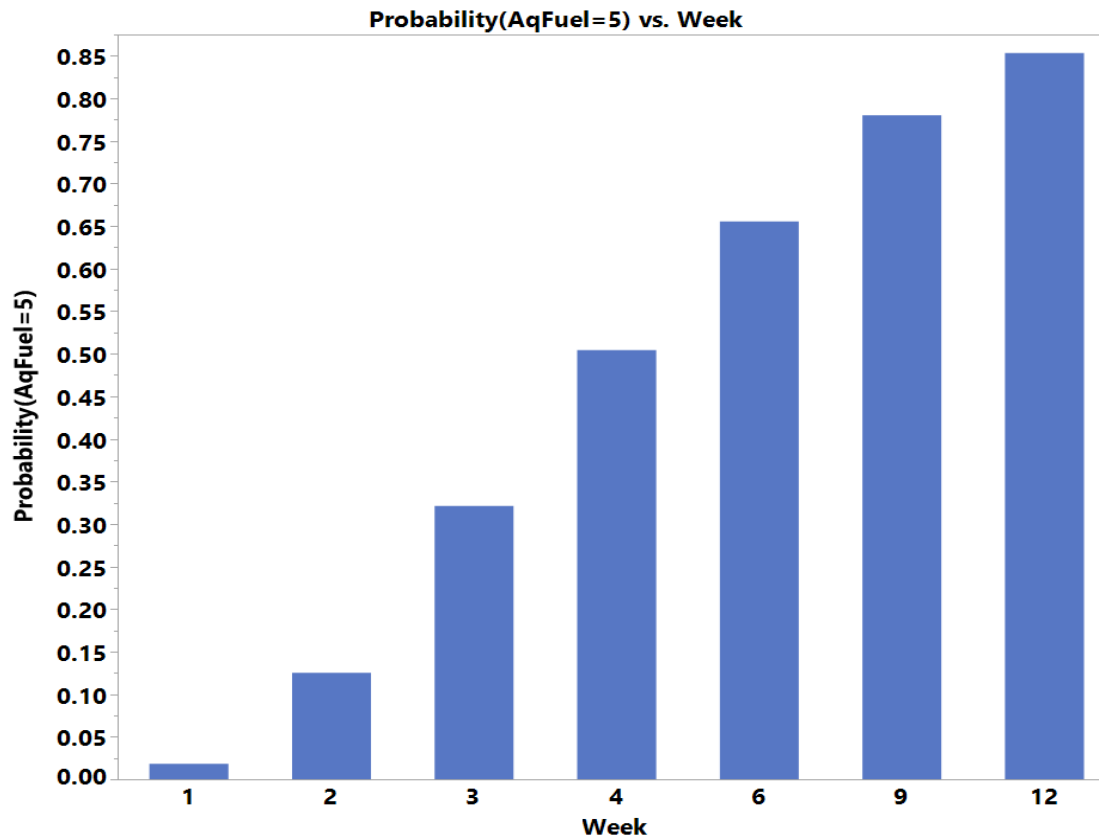
Aqueous/Fuel Phase – All Weeks

Whole Model Test				
Model	-LogLikelihood	DF	ChiSquare	Prob> ChiSq
Difference	306.1414	30	612.2827	<.0001*
Full	823.2890			
Reduced	1129.4304			
RSquare (U)	0.2711			
AICc	1717.94			
BIC	1871.3			
Observations (or Sum Wgts)	742			
Fit Details				
Measure	Training	Definition		
Entropy RSquare	0.2711	1-Loglike(model)/Loglike(0)		
Generalized RSquare	0.5899	$(1-L(0)/L(model))^{(2/n)}/(1-L(0))^{(2/n)}$		
Mean -Log p	1.1096	$\sum -\log(p[j])/n$		
RMSE	0.6410	$\sqrt{\sum (y[j]-p[j])^2/n}$		
Mean Abs Dev	0.6066	$\sum y[j]-p[j] /n$		
Misclassification Rate	0.4852	$\sum (p[j] \neq pMax)/n$		
N	742	n		
Lack Of Fit				
Source	DF	-LogLikelihood	ChiSquare	
Lack Of Fit	2934	823.28900	1646.578	
Saturated	2964	0.00000	Prob> ChiSq	
Fitted	30	823.28900	1.0000	

Parameter Estimates				
Term	Estimate	Std Error	ChiSquare	Prob> ChiSq
Intercept[1]	1.04395042	0.2317254	20.30	<.0001*
Intercept[2]	2.94877046	0.2584398	130.19	<.0001*
Intercept[3]	4.98787731	0.294321	287.20	<.0001*
Intercept[4]	6.94792772	0.3417109	413.42	<.0001*
Sulfur[LSDf]	0.15271828	0.0719382	4.51	0.0338*
Biodiesel[0]	-0.6758379	0.075833	79.43	<.0001*
Glycerin[0]	-0.1702349	0.0721731	5.56	0.0183*
Ethanol[0]	0.02473269	0.0719992	0.12	0.7312
Mircobes[0]	0.08737041	0.0723058	1.46	0.2269
MAL additive[0]	-0.3621251	0.073041	24.58	<.0001*
CFI additive[0]	-0.0294862	0.0729269	0.16	0.6860
Corrosion inhibitor[0]	-0.1243241	0.2289791	0.29	0.5872
Conductivity Additive[0]	-0.0701395	0.0723442	0.94	0.3323
FRP Material[0]	0.07307642	0.0728105	1.01	0.3155
Week[2-1]	-1.4075937	0.3050342	21.29	<.0001*
Week[3-2]	-0.9592591	0.2731586	12.33	0.0004*
Week[4-3]	-0.7330824	0.2622406	7.81	0.0052*
Week[6-4]	-0.6878877	0.25781	7.12	0.0076*
Week[9-6]	-0.4624572	0.2559279	3.27	0.0708
Week[12-9]	-0.4472684	0.2565717	3.04	0.0813
Biodiesel[0]*Ethanol[0]	-0.2227965	0.0726826	9.40	0.0022*
Biodiesel[0]*CFI additive[0]	0.26990612	0.0726395	13.81	0.0002*
Glycerin[0]*Mircobes[0]	0.14780954	0.0723661	4.17	0.0411*
Ethanol[0]*Mircobes[0]	-0.6139638	0.0755209	66.09	<.0001*
Ethanol[0]*FRP Material[0]	-0.3170003	0.0743667	18.17	<.0001*
MAL additive[0]*Conductivity Additive[0]	-0.4672656	0.073798	40.09	<.0001*
CFI additive[0]*Corrosion inhibitor[0]	-0.4133278	0.0736796	31.47	<.0001*
Corrosion inhibitor[0]*FRP Material[0]	-0.2562718	0.072755	12.41	0.0004*
Week[2-1]*Corrosion inhibitor[0]	-0.6279813	0.3025389	4.31	0.0379*
Week[3-2]*Corrosion inhibitor[0]	-0.237106	0.271536	0.76	0.3826
Week[4-3]*Corrosion inhibitor[0]	-0.0335354	0.2611696	0.02	0.8978
Week[6-4]*Corrosion inhibitor[0]	0.06188914	0.2568005	0.06	0.8096
Week[9-6]*Corrosion inhibitor[0]	-0.1601463	0.2555228	0.39	0.5308
Week[12-9]*Corrosion inhibitor[0]	-0.0471208	0.2561522	0.03	0.8540

Corrosion by Time (Week)

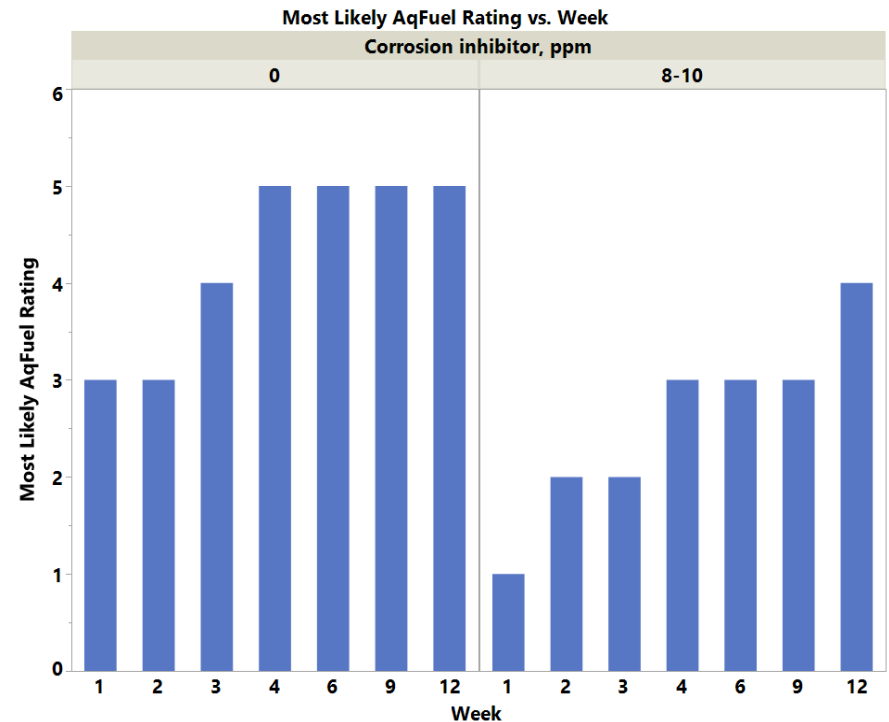
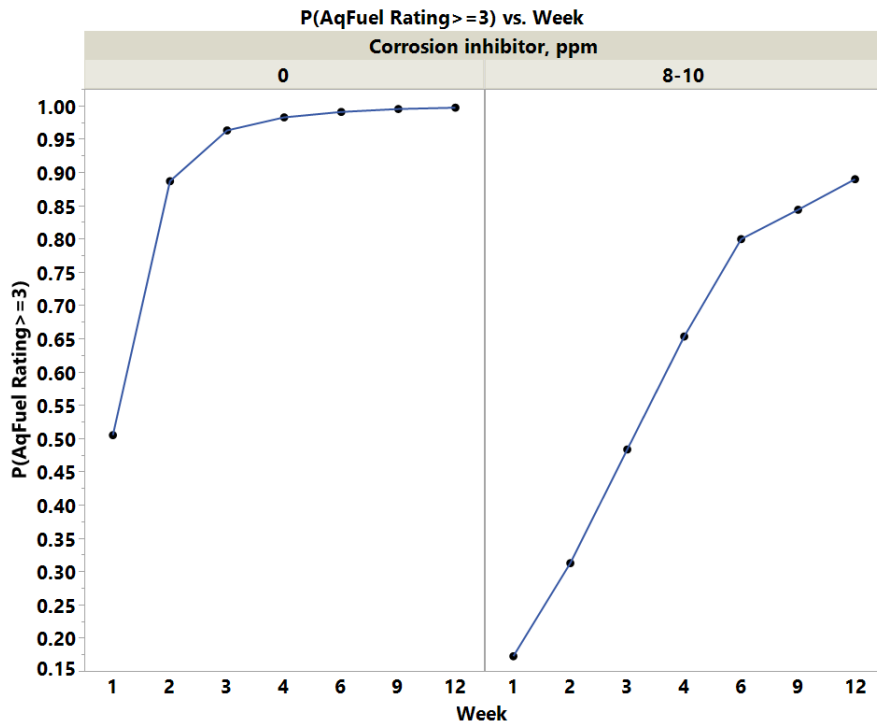
- Significant weekly **increases** in probability of high corrosion severity between weeks 1, 2, 3, 4 and 6 while marginal differences observed between weeks 6, 9 and 12



Where((Sulfur = LSDF) and (Biodiesel = 0) and (Glycerin = 0) and (Ethanol = 0) and (Microbes = 0) and (MAL additive = 0) and (CFI additive = 0) and (Corrosion Inhibitor = 0) and (Conductivity Additive = 0) and (FRP Material = 0))

Corrosion Inhibitor Effect by Time (Week)

- More significant **increase** in probability of high corrosion severity between weeks 1 and 2 without Corrosion Inhibitor than with Corrosion Inhibitor



Where((Sulfur = LSDF) and (Biodiesel = 0) and (Glycerin = 0) and (Ethanol = 0) and (Microbes = 0) and (MAL additive = 0) and (CFI additive = 0) and (Conductivity Additive = 0) and (FRP Material = 0))

Aqueous/Fuel Edge Phase

Conclusions (Aqueous/Fuel Edge Phase)

Average Corrosion Severity Rating (average of 3 samples)

- ULSD has marginally **higher** probability of high corrosion severity than LSDF
- 5% Biodiesel has **lower** probability of high corrosion severity than zero Biodiesel
- Presence of Microbes has **lower** probability of high corrosion severity than absence of Microbes
- 200ppm MAL additive has **lower** probability of high corrosion severity than zero MAL additive
- 8-10ppm Corrosion inhibitor has **lower** probability of high corrosion severity than zero Corrosion Inhibitor
- LSDF has **lower** probability of high corrosion severity than ULSD more significantly without Conductivity additive
- 5% Biodiesel has **lower** probability of high corrosion severity than zero Biodiesel without Ethanol while it has **higher** probability with Ethanol
- 5% Biodiesel has **lower** probability of high corrosion severity than zero Biodiesel more significantly with Microbes
- 5% Biodiesel has **lower** probability of high corrosion severity than zero Biodiesel more significantly with FRP Material
- 5000ppm Glycerin has **higher** probability of high corrosion severity than zero Glycerin more significantly with Ethanol
- 10000ppm Ethanol has **lower** probability of high corrosion severity than zero Ethanol more significantly without Microbes while it has **higher** probability with Microbes
- 8-10ppm Corrosion inhibitor has **lower** probability of high corrosion severity than zero Corrosion inhibitor more significantly with Microbes
- 8-10ppm Corrosion inhibitor has **lower** probability of high corrosion severity than zero Corrosion inhibitor more significantly without MAL Additive
- 200ppm CFI additive has **lower** probability of high corrosion severity than zero CFI additive more significantly without Glycerin
- 200ppm CFI additive has **lower** probability of high corrosion severity than zero CFI additive without Conductivity Additive while it has **higher** probability with Conductivity additive

Average Corrosion Severity Rating by Time (Week)

- Significant weekly **increases** in probability of high corrosion severity between weeks 1, 2, 3, 4, 6 and 9
- More significant **increase** in probability of high corrosion severity between weeks 1 and 2 without Corrosion Inhibitor than with Corrosion Inhibitor

Stepwise Ordinal Logistic Regression

Aqueous/Fuel Edge Phase – Week 12

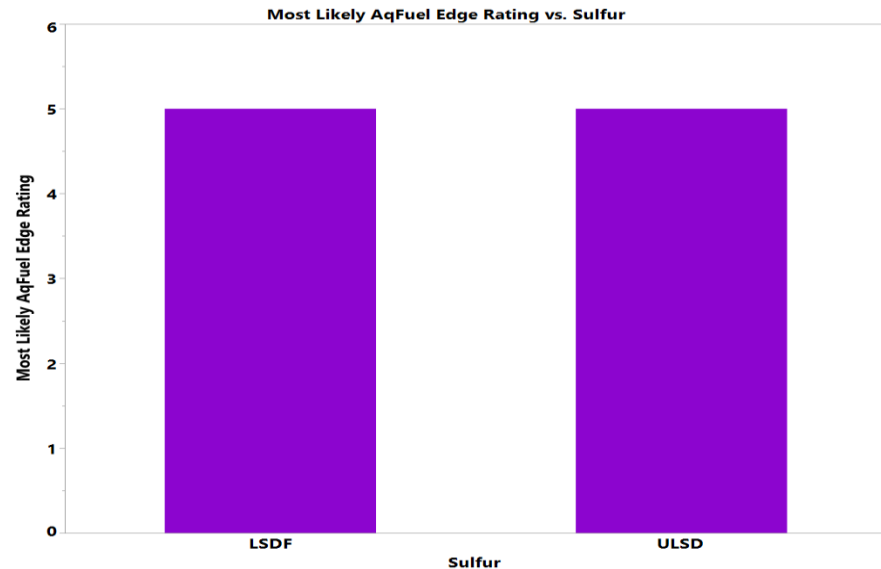
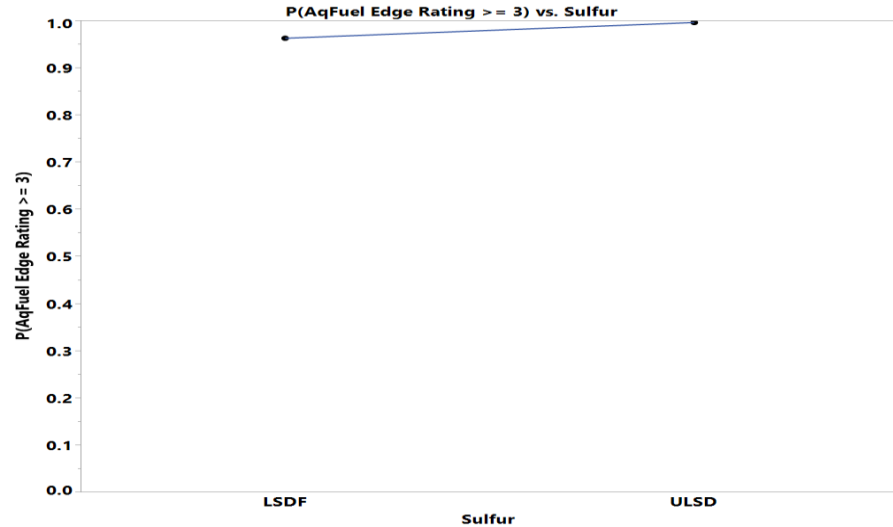
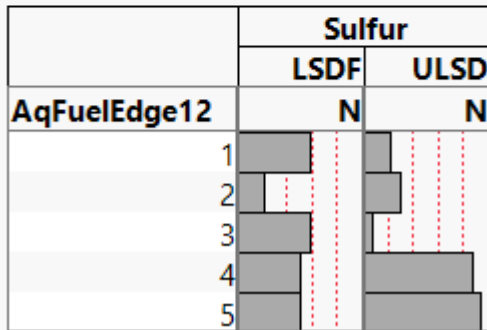
Whole Model Test			
Model	-LogLikelihood	DF	ChiSquare Prob> ChiSq
Difference	49.20814	20	98.41627 <.0001*
Full	118.09736		
Reduced	167.30550		
RSquare (U)	0.2941		
AICc	299.01		
BIC	348.117		
Observations (or Sum Wgts)	106		
Fit Details			
Measure	Training	Definition	
Entropy RSquare	0.2941	1-Loglike(model)/Loglike(0)	
Generalized RSquare	0.6317	$(1-(L(0)/L(model))^{(2/n)})/(1-L(0)^{(2/n)})$	
Mean -Log p	1.1141	$\sum -\text{Log}(\rho[j])/n$	
RMSE	0.6373	$\sqrt{\sum (y[j]-\rho[j])^2/n}$	
Mean Abs Dev	0.5736	$\sum y[j]-\rho[j] /n$	
Misclassification Rate	0.4717	$\sum (\rho[j] \neq \rho\text{Max})/n$	
N	106	n	
Lack Of Fit			
Source	DF	-LogLikelihood	ChiSquare Prob> ChiSq
Lack Of Fit	400	118.09736	236.1947
Saturated	420	0.00000	
Fitted	20	118.09736	1.0000

Parameter Estimates				
Term	Estimate	Std Error	ChiSquare	Prob> ChiSq
Intercept[1]	-2.6855935	0.3900589	47.40	<.0001*
Intercept[2]	-1.2507918	0.2887507	18.76	<.0001*
Intercept[3]	-0.0893179	0.2597402	0.12	0.7309
Intercept[4]	1.91534494	0.3241586	34.91	<.0001*
Sulfur[LSDF]	0.63237988	0.205887	9.43	0.0021*
Biodiesel, %[0]	-1.2568403	0.2350394	28.59	<.0001*
Glycerin, ppm[0]	0.23309762	0.2025433	1.32	0.2498
Ethanol, ppm[0]	0.0460159	0.2021587	0.05	0.8199
Mircobes[0]	-0.5675822	0.206934	7.52	0.0061*
MAL additive, ppm[0]	-0.474089	0.2053683	5.33	0.0210*
CFI additive, ppm[0]	-0.1112572	0.1995643	0.31	0.5772
Corrosion inhibitor, ppm[0]	-1.1842986	0.2332533	25.78	<.0001*
Conductivity additive, ppm[0]	0.25294164	0.2017477	1.57	0.2099
FRP Material[0]	-0.0508887	0.2049138	0.06	0.8039
Sulfur[LSDF]*Conductivity additive, ppm[0]	0.44354972	0.2054946	4.66	0.0309*
Biodiesel, %[0]*Ethanol, ppm[0]	-0.5899877	0.2082503	8.03	0.0046*
Biodiesel, %[0]*Mircobes[0]	0.69155806	0.2153038	10.32	0.0013*
Biodiesel, %[0]*FRP Material[0]	0.50449141	0.2048288	6.07	0.0138*
Glycerin, ppm[0]*Ethanol, ppm[0]	0.40812967	0.2063118	3.91	0.0479*
Glycerin, ppm[0]*CFI additive, ppm[0]	0.41278877	0.2022375	4.17	0.0412*
Ethanol, ppm[0]*Mircobes[0]	-0.7921748	0.2158613	13.47	0.0002*
Mircobes[0]*Corrosion inhibitor, ppm[0]	0.46737283	0.2077531	5.06	0.0245*
MAL additive, ppm[0]*Corrosion inhibitor, ppm[0]	-0.4767358	0.2090524	5.20	0.0226*
CFI additive, ppm[0]*Conductivity additive, ppm[0]	-0.5725932	0.2145551	7.12	0.0076*

Sulfur Effect – Aq/Fuel Edge Phase

- ULSD has marginally **higher** probability of high corrosion severity than LSDF

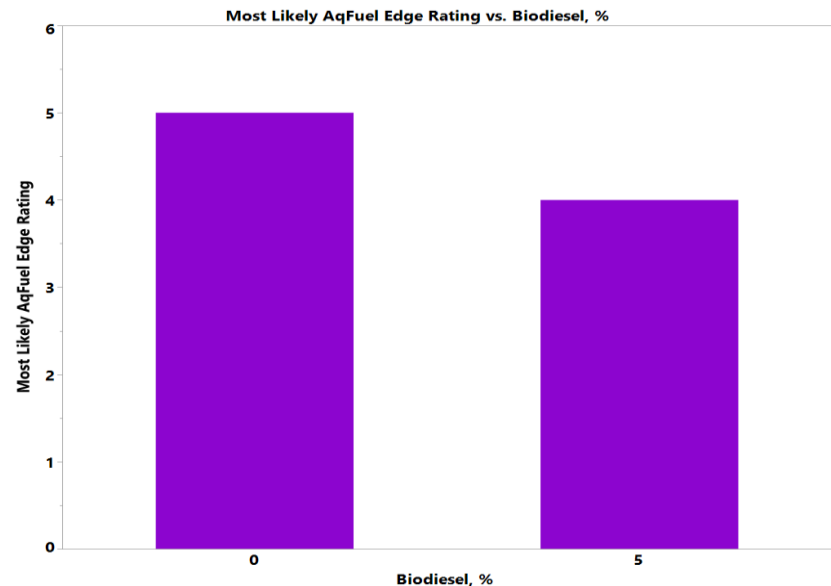
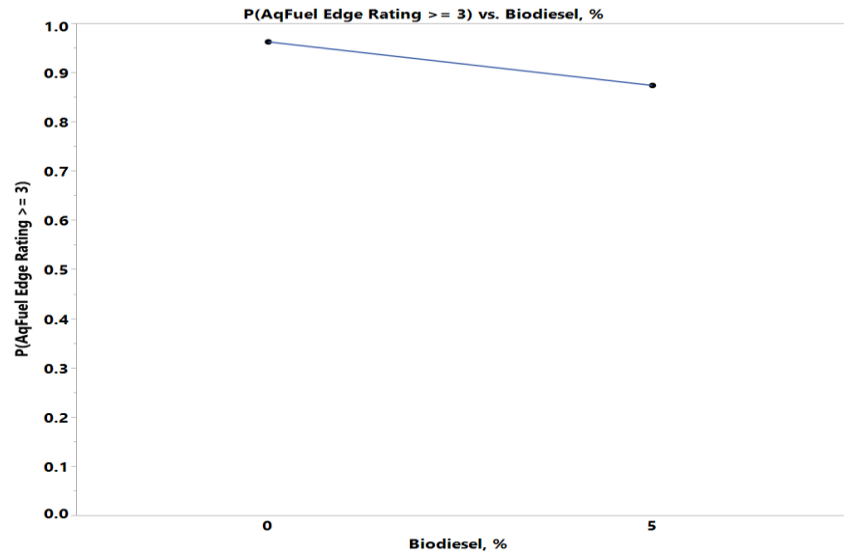
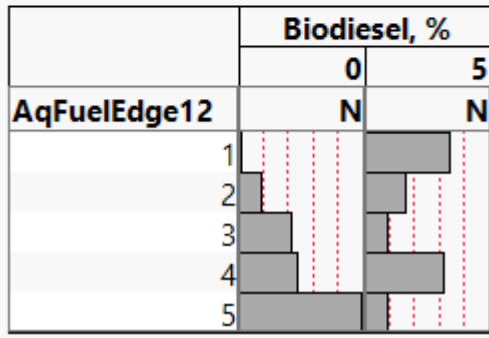
	Sulfur	
	LSDF	ULSD
AqFuelEdge12	N	N
1	12	7
2	7	8
3	12	5
4	11	16
5	11	17



Biodiesel Effect - Aq/Fuel Edge Phase

- 5% Biodiesel has **lower** probability of high corrosion severity than zero Biodiesel

	Biodiesel, %	
	0	5
AqFuelEdge12	N	N
1	3	16
2	6	9
3	11	6
4	12	15
5	22	6

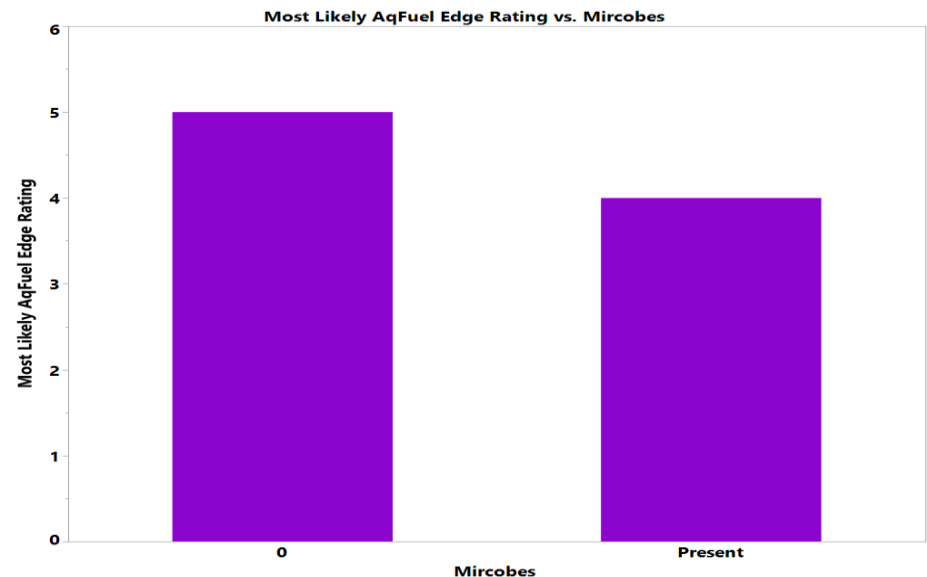
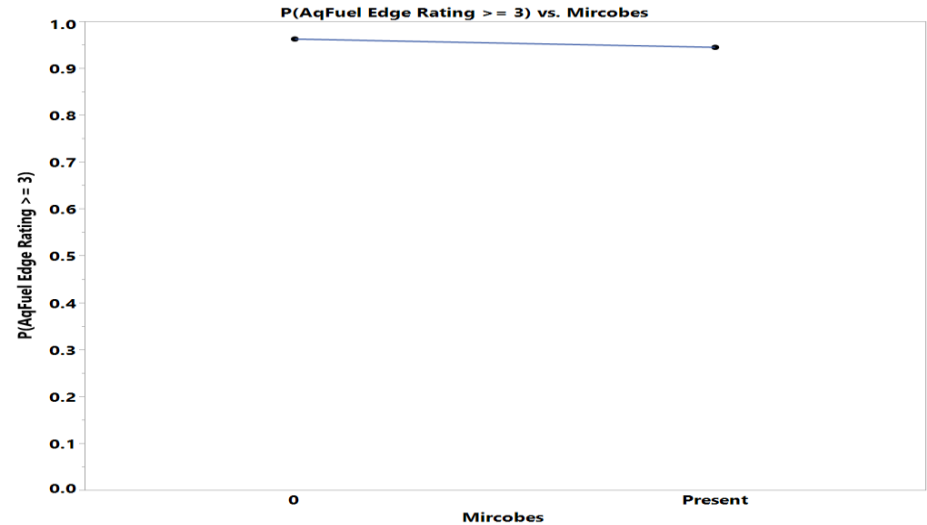
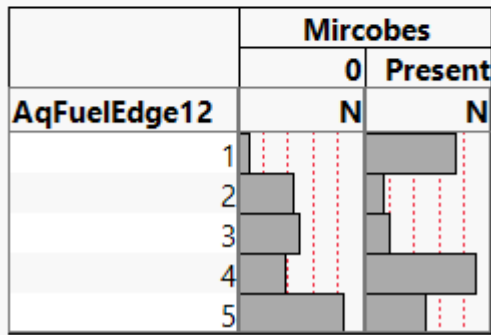


Where((Sulfur = LSDF) and (Glycerin = 0) and (Microbes = 0) and (Ethanol = 0) and (MAL additive = 0) and (CFI additive = 0) and (Corrosion inhibitor = 0) and (Conductivity Additive = 0) and (FRP Material = 0))

Microbes Effect – Aq/Fuel Edge Phase

- Presence of Microbes has **lower** probability of high corrosion severity than absence of Microbes

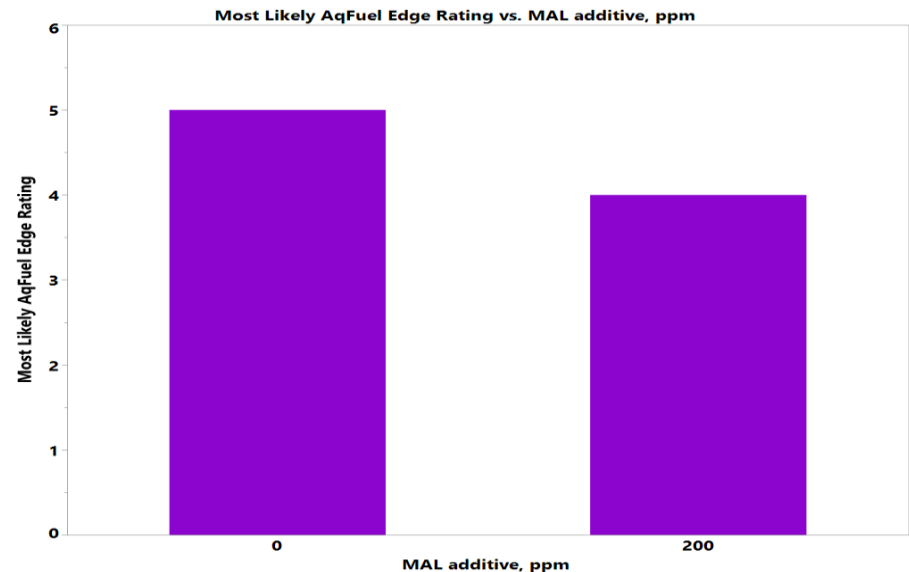
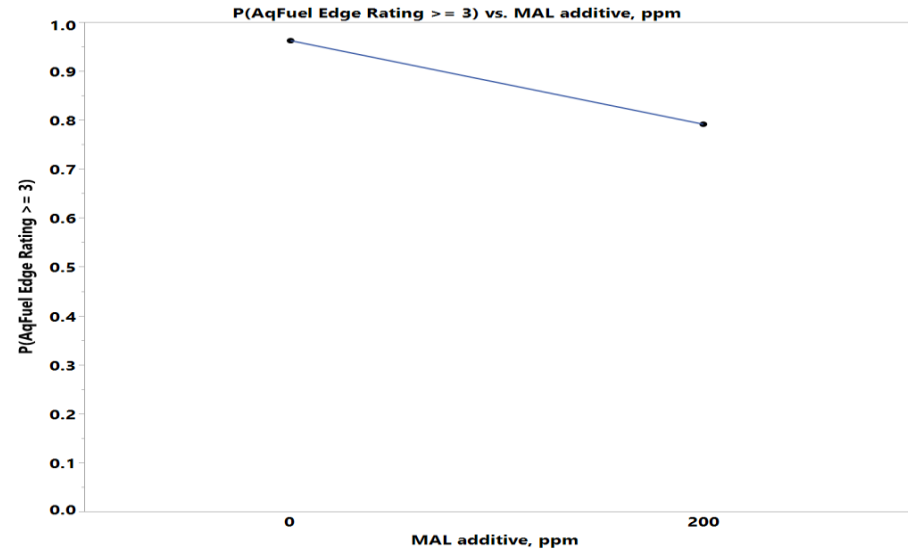
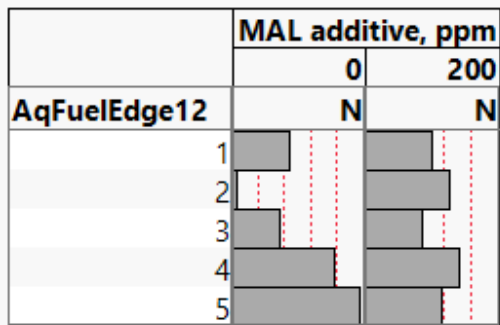
	Microbes	
	0	Present
AqFuelEdge12	N	N
1	4	15
2	10	5
3	11	6
4	9	18
5	17	11



MAL Additive Effect - Aq/Fuel Edge Phase

- 200ppm MAL additive has **lower** probability of high corrosion severity than zero MAL additive

	MAL additive, ppm	
	0	200
AqFuelEdge12	N	N
1	9	10
2	3	12
3	8	9
4	14	13
5	17	11

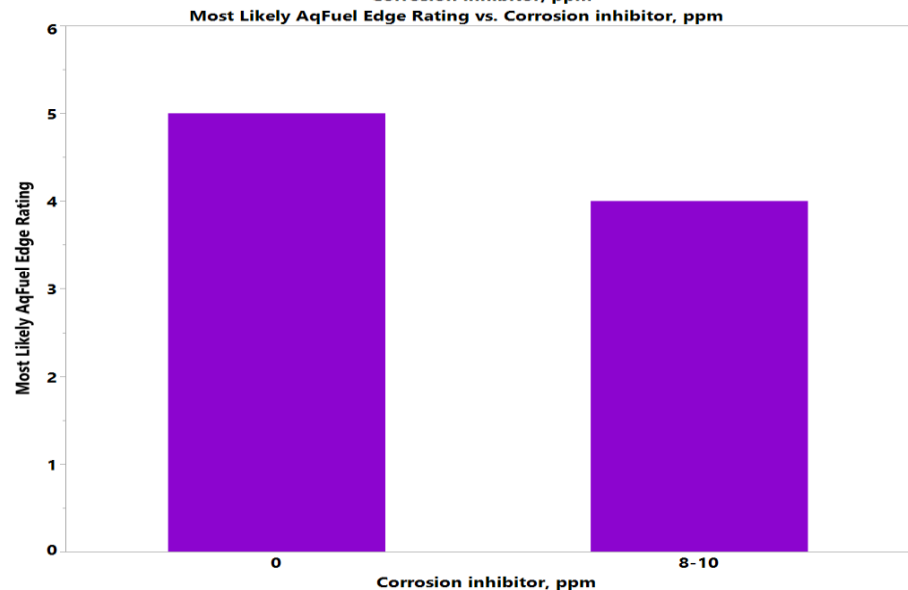
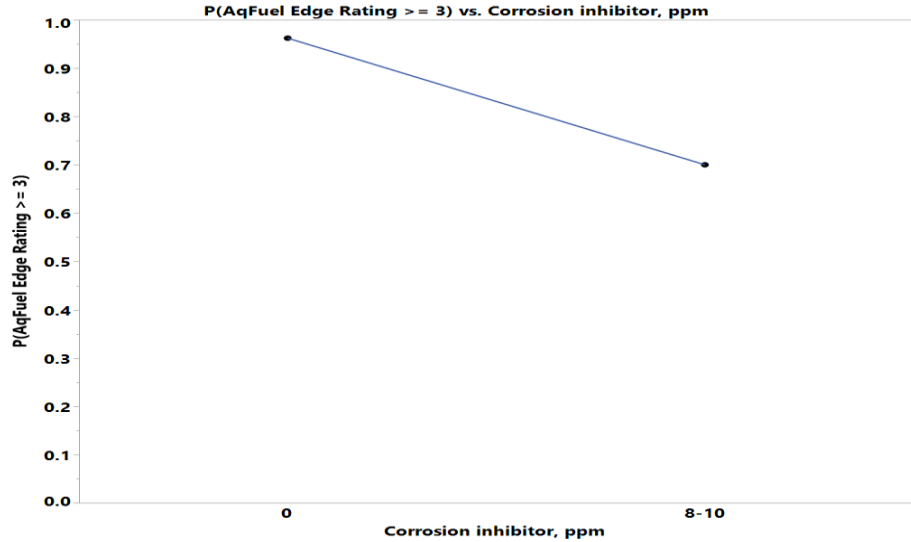
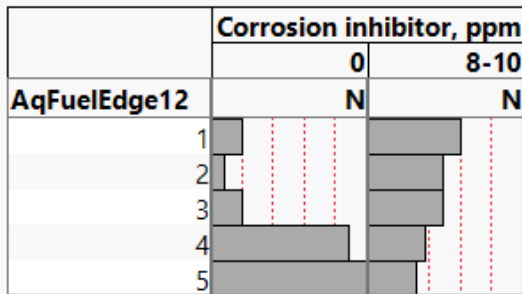


Where((Biodiesel = 0) and (Glycerin = 0) and (Microbes = 0) and (Ethanol = 0) and (Sulfur = LSDF) and (CFI additive = 0) and (Corrosion inhibitor = 0) and (Conductivity Additive = 0) and (FRP Material = 0))

Corrosion Inhibitor Effect - Aq/Fuel Edge Phase

- 8-10ppm Corrosion inhibitor has **lower** probability of high corrosion severity than zero Corrosion Inhibitor

	Corrosion inhibitor, ppm	
	0	8-10
AqFuelEdge12	N	N
1	6	13
2	4	11
3	6	11
4	18	9
5	20	8

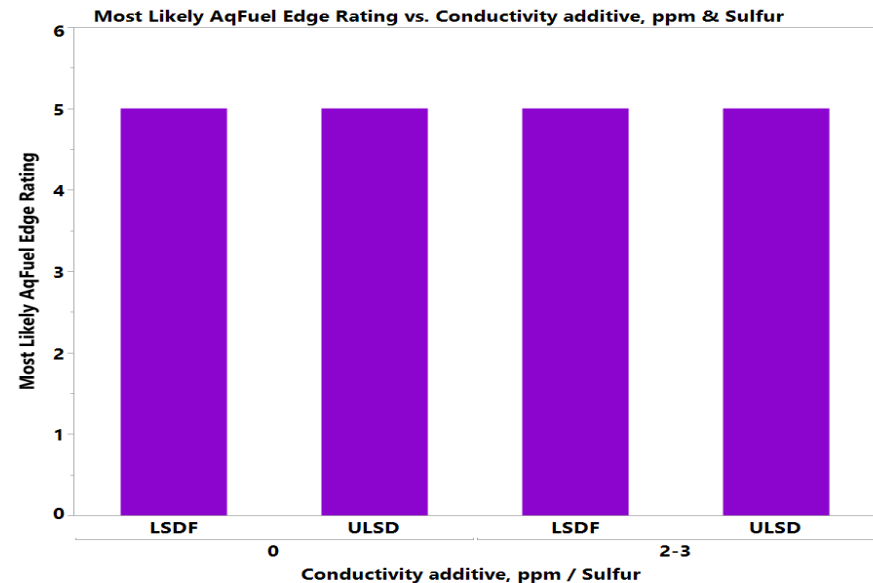
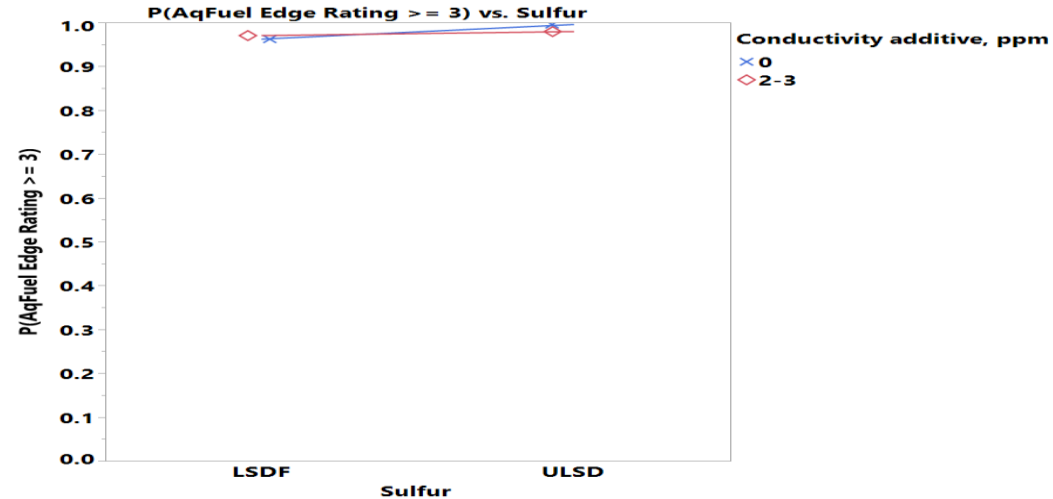
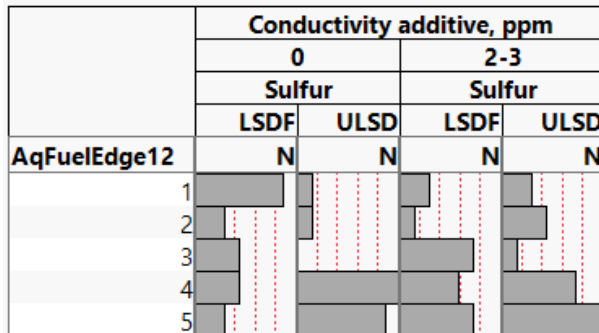


Where((Biodiesel = 0) and (Glycerin = 0) and (Microbes = 0) and (Ethanol = 0) and (MAL additive = 0) and (CFI additive = 0) and (Sulfur= LSDF) and (Conductivity Additive = 0) and (FRP Material = 0))

Sulfur-Conductivity Additive Interaction Effect

- LSDF has **lower** probability of high corrosion severity than ULSD more significantly **without** Conductivity additive

	Conductivity additive, ppm			
	0		2-3	
	Sulfur		Sulfur	
	LSDF	ULSD	LSDF	ULSD
AqFuelEdge12	N	N	N	N
1	8	3	4	4
2	4	3	3	5
3	5	2	7	3
4	5	9	6	7
5	4	8	7	9

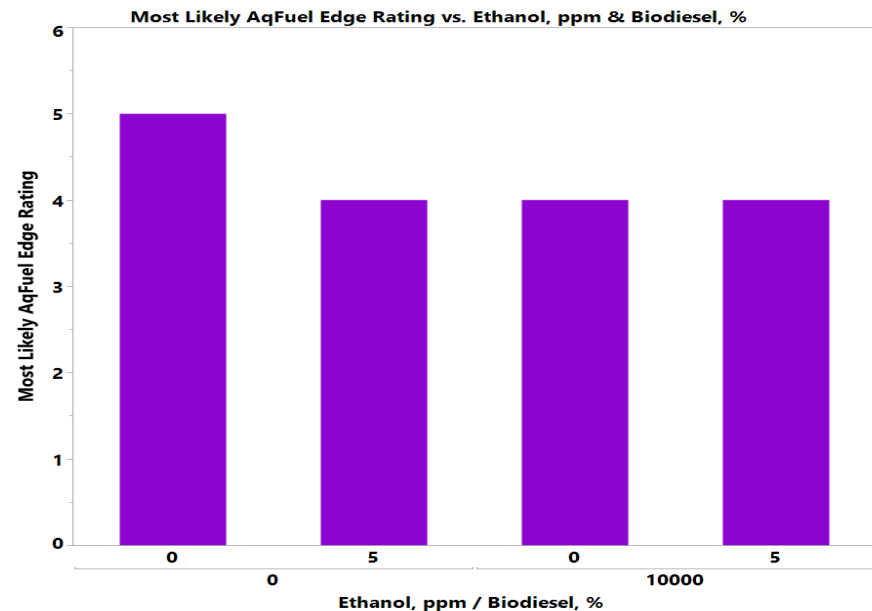
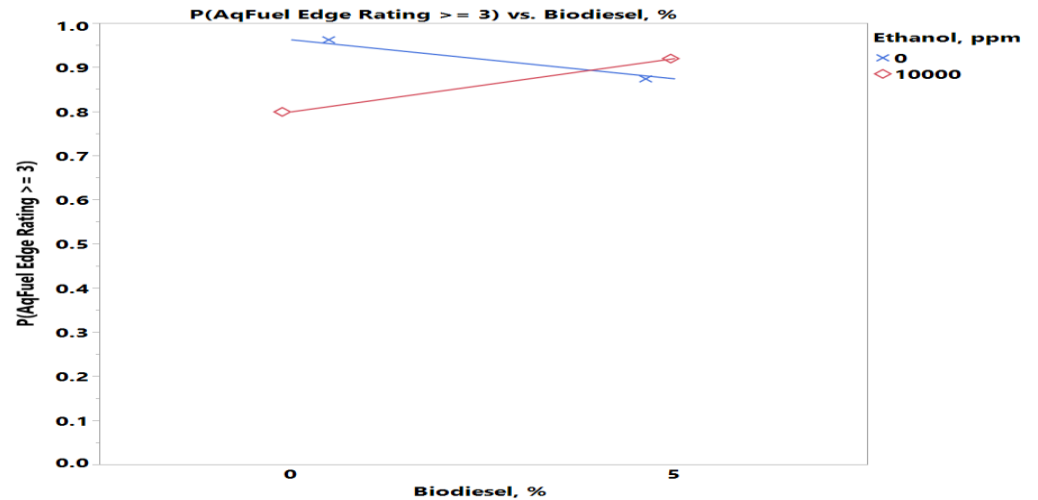
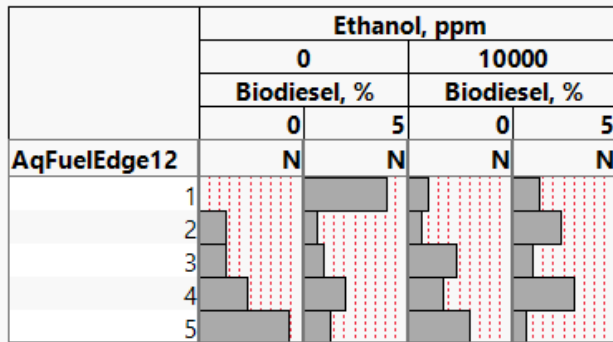


Where((Glycerin = 0) and (Microbes = 0) and (MAL additive = 0) and (CFI additive = 0) and (Corrosion inhibitor = 0) and (Biodiesel = 0) and (FRP Material = 0) and (Ethanol = 0))

Biodiesel-Ethanol Interaction Effect

- 5% Biodiesel has **lower** probability of high corrosion severity than zero Biodiesel **without** Ethanol while it has **higher** probability **with** Ethanol

	Ethanol, ppm			
	0		10000	
	Biodiesel, %	Biodiesel, %	Biodiesel, %	Biodiesel, %
AqFuelEdge12	0	5	0	5
	N	N	N	N
1	0	12	3	4
2	4	2	2	7
3	4	3	7	3
4	7	6	5	9
5	13	4	9	2

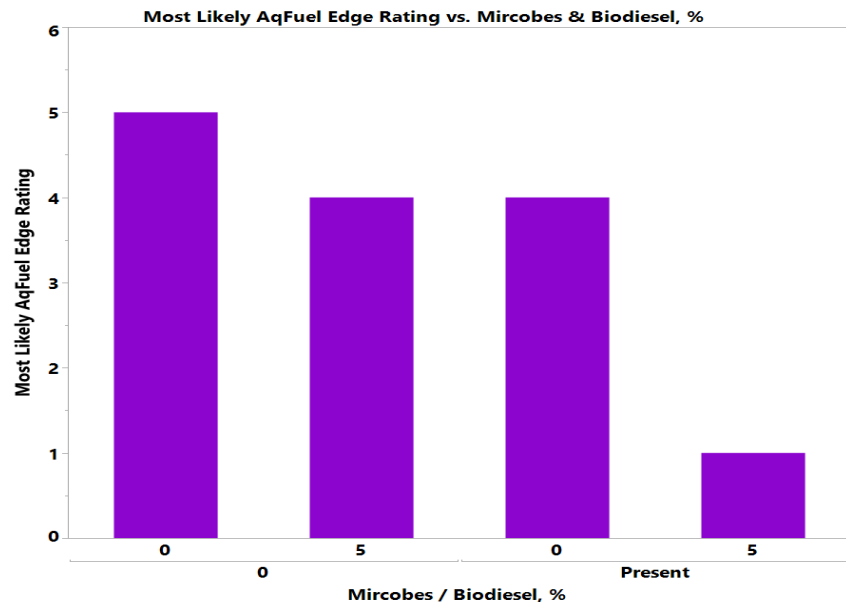
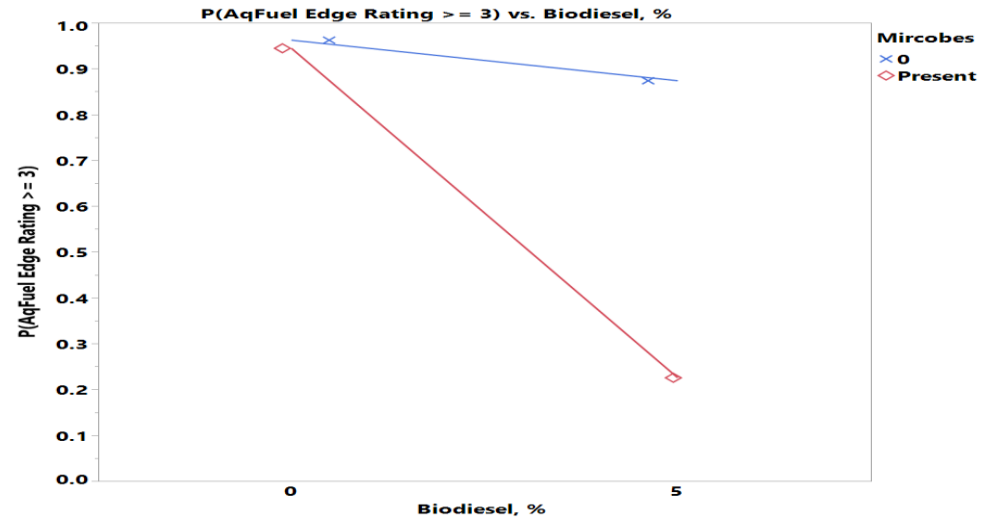
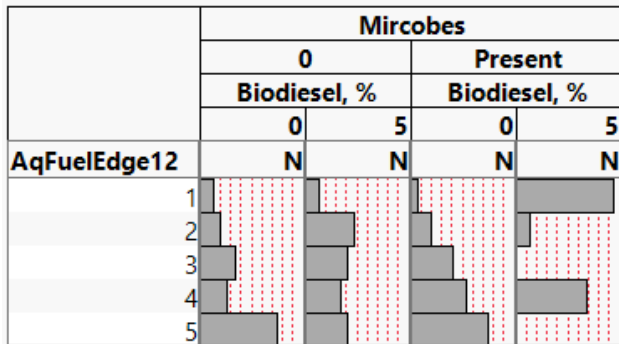


Where((Glycerin = 0) and (Microbes = 0) and (MAL additive = 0) and (CFI additive = 0) and (Corrosion inhibitor = 0) and (Conductivity Additive = 0) and (FRP Material = 0) and (Sulfur = LSDF))

Biodiesel-Microbes Interaction Effect

- 5% Biodiesel has **lower** probability of high corrosion severity than zero Biodiesel more significantly with Microbes

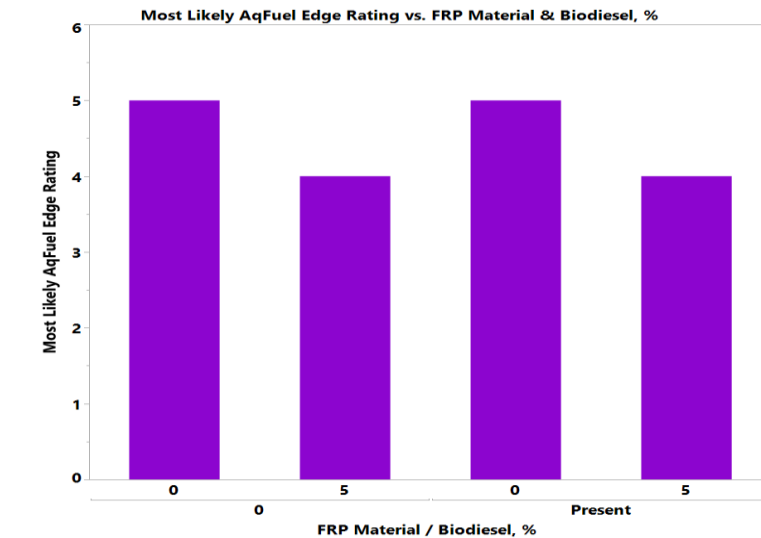
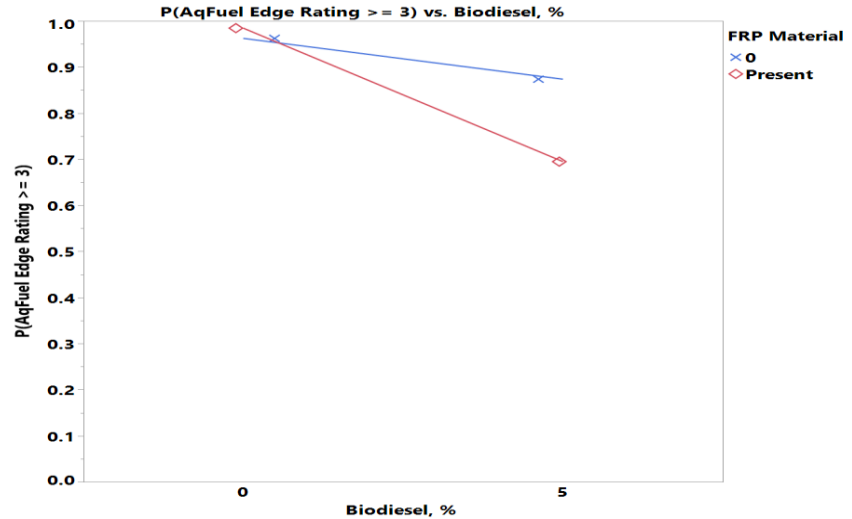
	Microbes			
	0		Present	
	Biodiesel, %		Biodiesel, %	
	0	5	0	5
AqFuelEdge12	N	N	N	N
1	2	2	1	14
2	3	7	3	2
3	5	6	6	0
4	4	5	8	10
5	11	6	11	0



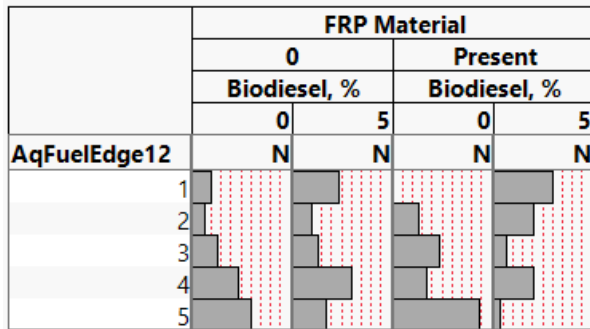
Where((Glycerin = 0) and (Ethanol = 0) and (MAL additive = 0) and (CFI additive = 0) and (Corrosion inhibitor = 0) and (Conductivity Additive = 0) and (FRP Material = 0) and (Sulfur = LSDF))

Biodiesel-FRP Material Interaction Effect

- 5% Biodiesel has **lower** probability of high corrosion severity than zero Biodiesel more significantly with FRP Material



	FRP Material			
	0		Present	
	Biodiesel, %		Biodiesel, %	
	0	5	0	5
AqFuelEdge12	N	N	N	N
1	3	7	0	9
2	2	3	4	6
3	4	4	7	2
4	7	9	5	6
5	9	5	13	1



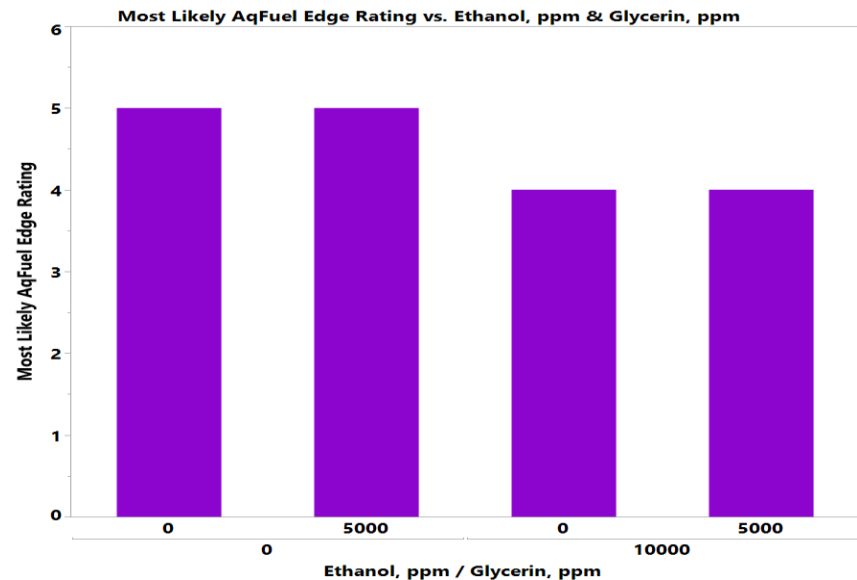
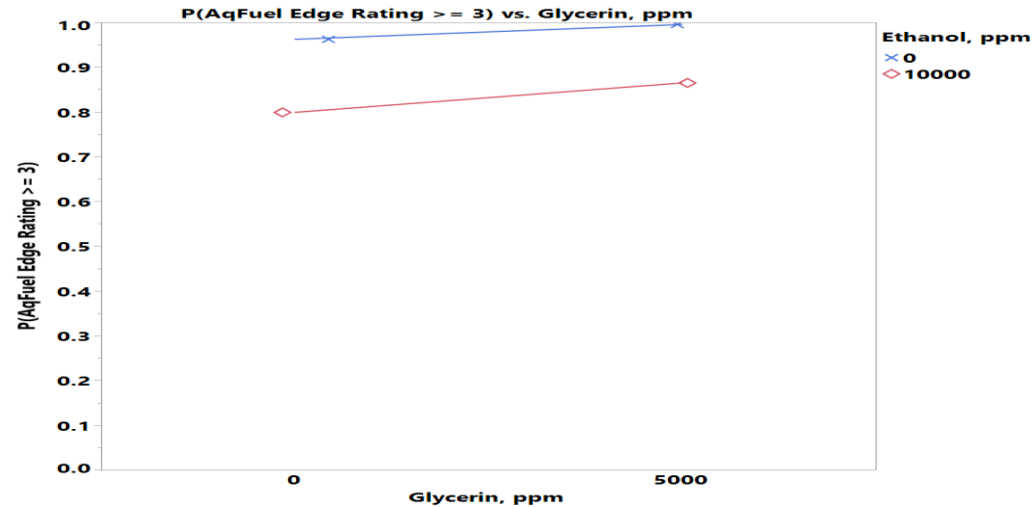
Where((Glycerin = 0) and (Microbes = 0) and (MAL additive = 0) and (Corrosion inhibitor = 0) and (Conductivity Additive = 0) and (CFI Additive = 0) and (Sulfur = LSDF) and (Ethanol = 0))

Glycerin-Ethanol Interaction Effect

- 5000ppm Glycerin has **higher** probability of high corrosion severity than zero Glycerin more significantly with Ethanol

	Ethanol, ppm			
	0		10000	
	Glycerin, ppm		Glycerin, ppm	
	0	5000	0	5000
AqFuelEdge12	N	N	N	N
1	6	6	3	4
2	2	4	4	5
3	6	1	6	4
4	8	5	10	4
5	6	11	4	7

	Ethanol, ppm			
	0		10000	
	Glycerin, ppm		Glycerin, ppm	
	0	5000	0	5000
AqFuelEdge12	N	N	N	N
1	█	█	█	█
2	█	█	█	█
3	█	█	█	█
4	█	█	█	█
5	█	█	█	█



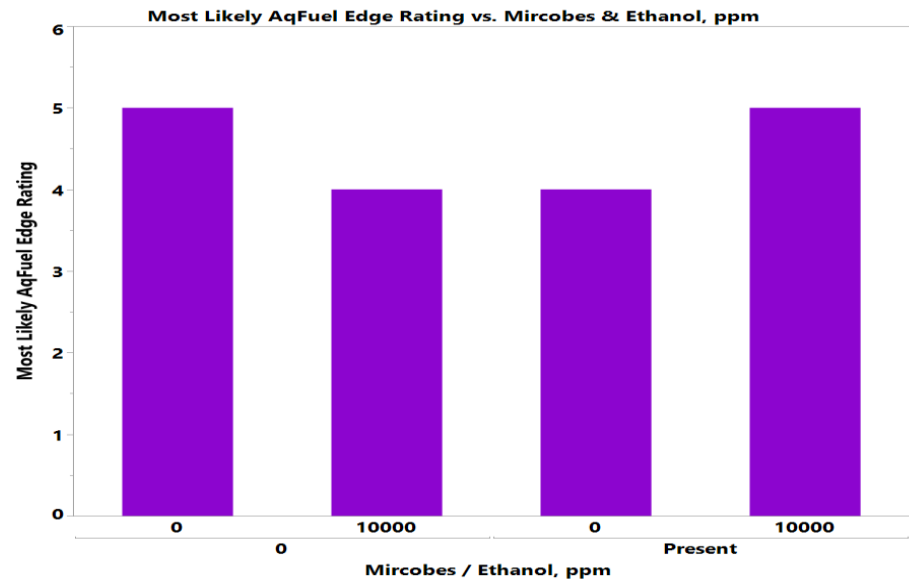
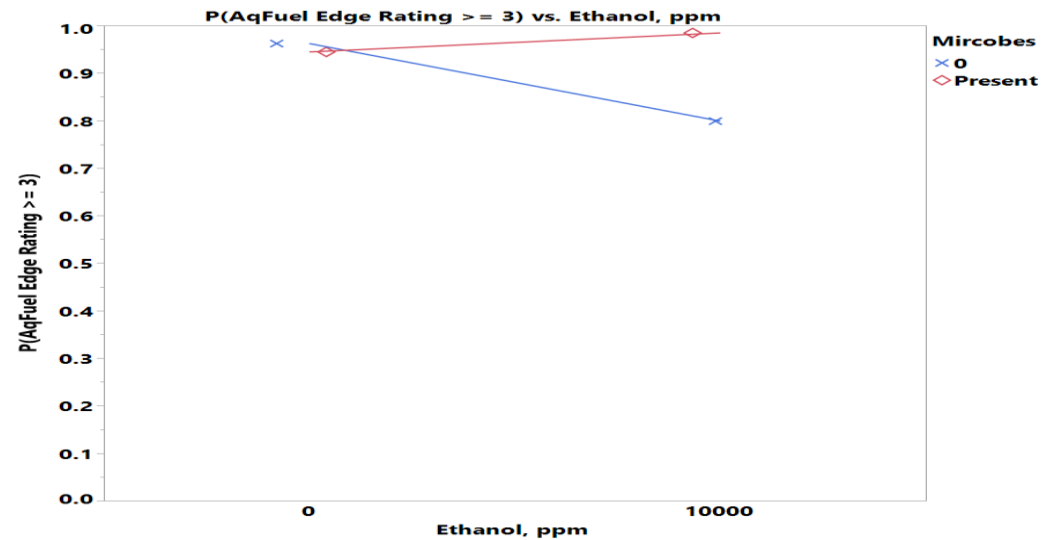
Where((MAL additive = 0) and (Corrosion inhibitor = 0) and (Conductivity Additive = 0) and (FRP Material = 0) and (Sulfur = LSDF) and (Microbes = 0) and (Biodiesel = 0) and (CFI additive = 0))

Ethanol-Microbes Interaction Effect

- 10000ppm Ethanol has **lower** probability of high corrosion severity than zero Ethanol more significantly **without** Microbes while it has **higher** probability with Microbes

	Mirco b es			
	0		Present	
	Ethanol, ppm		Ethanol, ppm	
	0	10000	0	10000
AqFuelEdge12	N	N	N	N
1	2	2	10	5
2	2	8	4	1
3	4	7	3	3
4	6	3	7	11
5	11	6	6	5

	Mirco b es			
	0		Present	
	Ethanol, ppm		Ethanol, ppm	
	0	10000	0	10000
AqFuelEdge12	N	N	N	N
1				
2				
3				
4				
5				

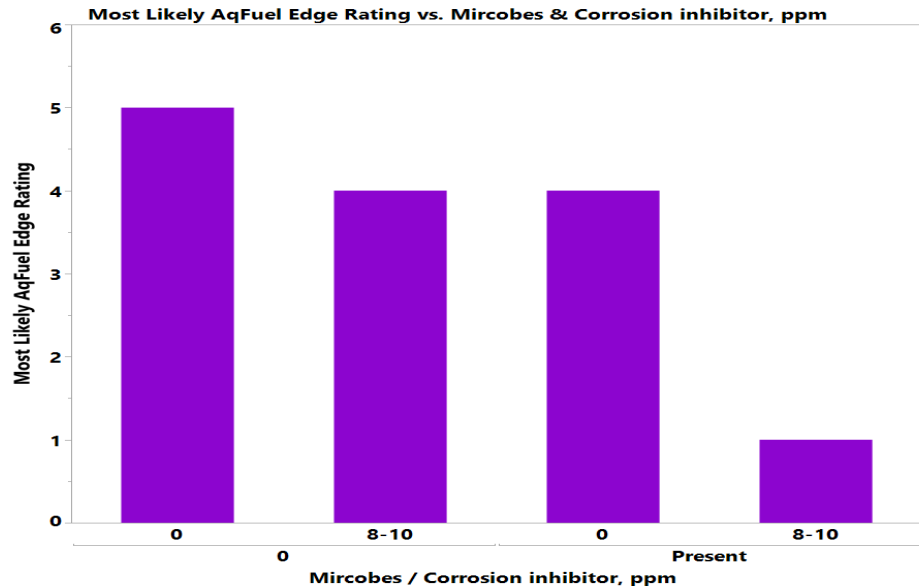
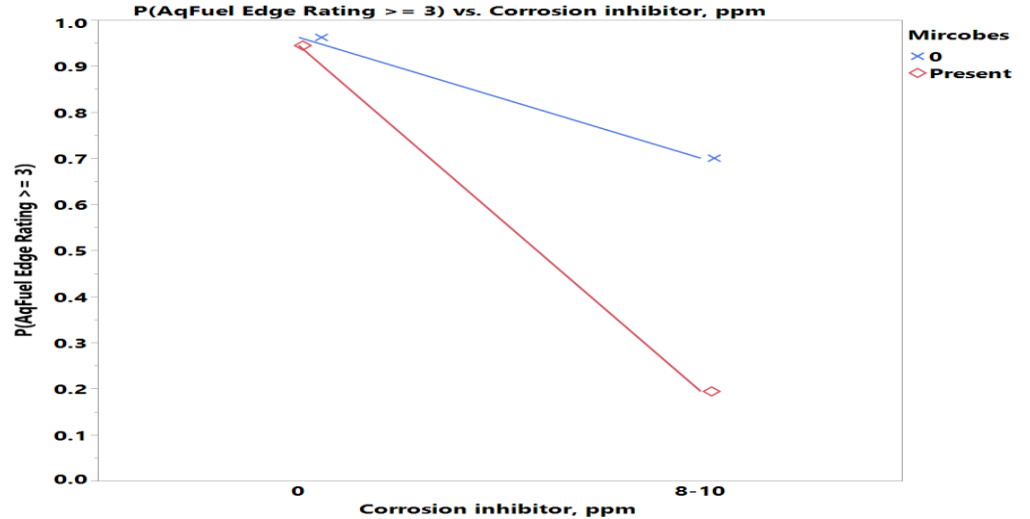
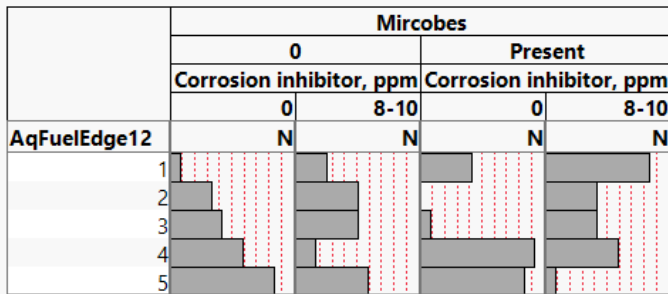


Where((MAL additive = 0) and (Corrosion inhibitor = 0) and (Conductivity Additive = 0) and (FRP Material = 0) and (Sulfur = LSDF) and (Biodiesel = 0) and (CFI additive = 0) and (Glycerin = 0))

Corrosion Inhibitor-Microbes Interaction Effect

- 8-10ppm Corrosion inhibitor has **lower** probability of high corrosion severity than zero Corrosion inhibitor more significantly with Microbes

	Microbes			
	0		Present	
	Corrosion inhibitor, ppm		Corrosion inhibitor, ppm	
	0	8-10	0	8-10
AqFuelEdge12	N	N	N	N
1	1	3	5	10
2	4	6	0	5
3	5	6	1	5
4	7	2	11	7
5	10	7	10	1

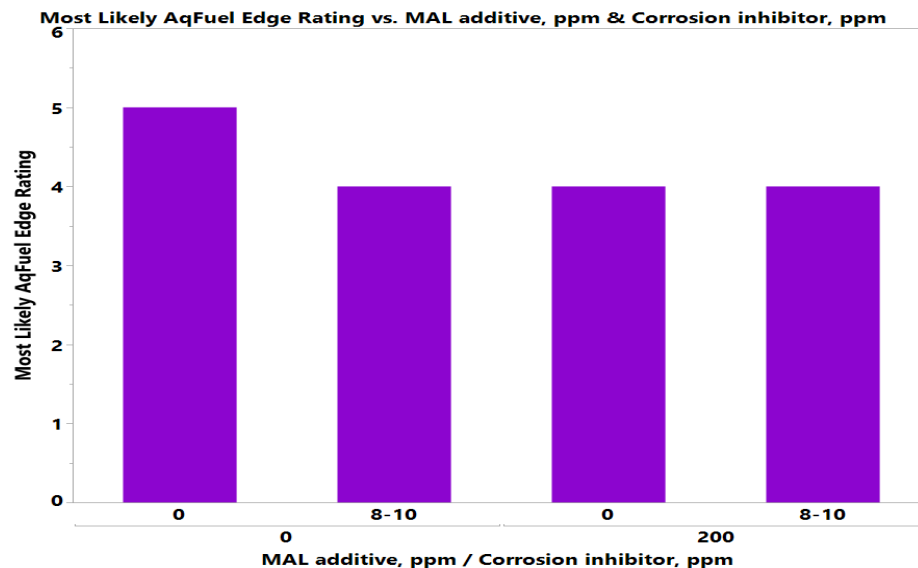
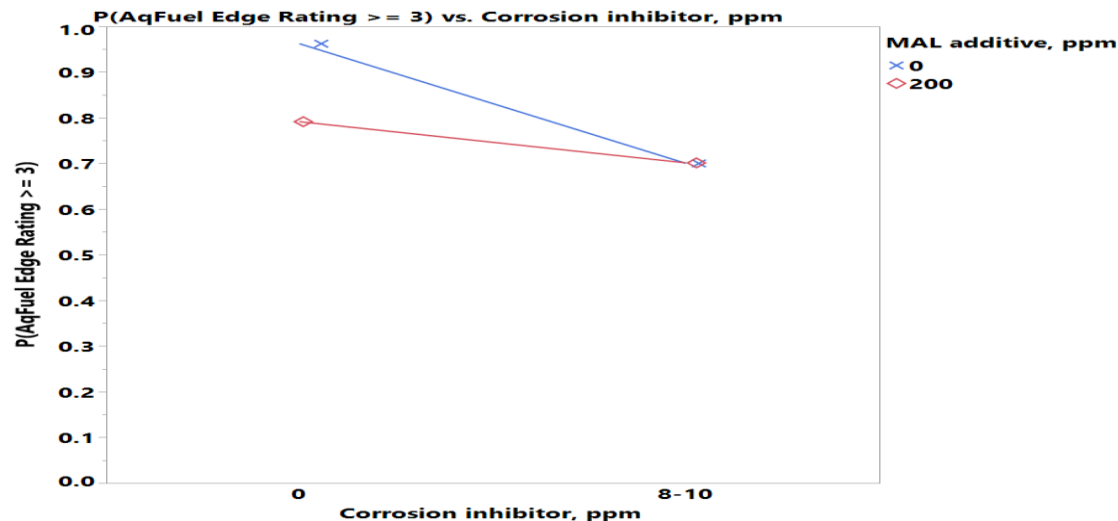
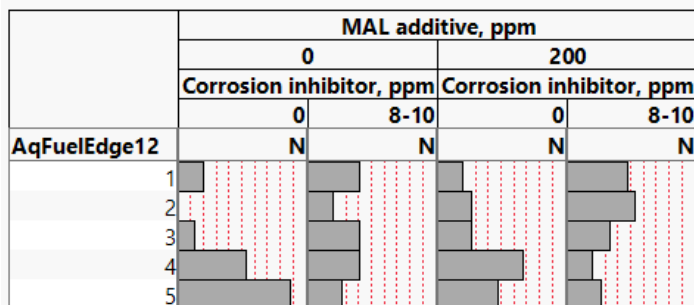


Where((Sulfur = LSDF) and (Biodiesel = 0) and (Glycerin = 0) and (CFI Additive = 0) and (Ethanol = 0) and (FRP Material = 0) and (MAL additive = 0) and (Conductivity Additive = 0))

Corrosion Inhibitor-MAL Additive Interaction Effect

- 8-10ppm Corrosion inhibitor has **lower** probability of high corrosion severity than zero Corrosion inhibitor more significantly without MAL Additive

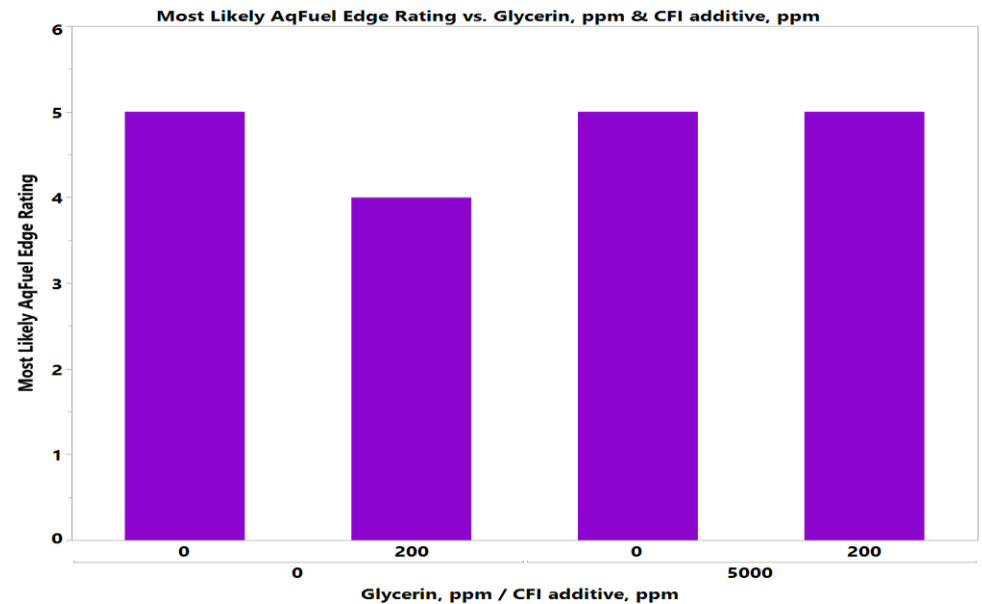
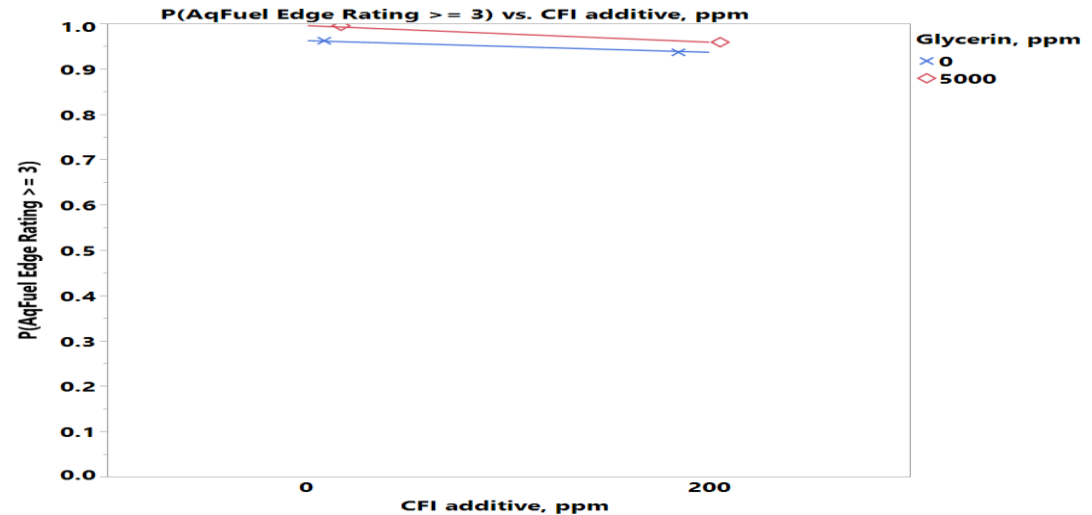
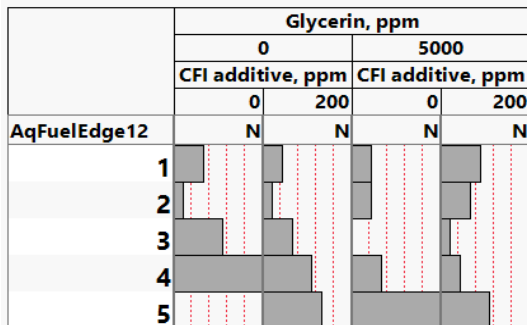
	MAL additive, ppm			
	0		200	
	Corrosion inhibitor, ppm		Corrosion inhibitor, ppm	
	0	8-10	0	8-10
AqFuelEdge12	N	N	N	N
1	3	6	3	7
2	0	3	4	8
3	2	6	4	5
4	8	6	10	3
5	13	4	7	4



CFI Additive-Glycerin Interaction Effect

- 200ppm CFI additive has **lower** probability of high corrosion severity than zero CFI additive more significantly without Glycerin

	Glycerin, ppm			
	0		5000	
	CFI additive, ppm		CFI additive, ppm	
	0	200	0	200
AqFuelEdge12	N	N	N	N
1	5	4	4	6
2	3	3	4	5
3	7	5	2	3
4	11	7	5	4
5	2	8	11	7

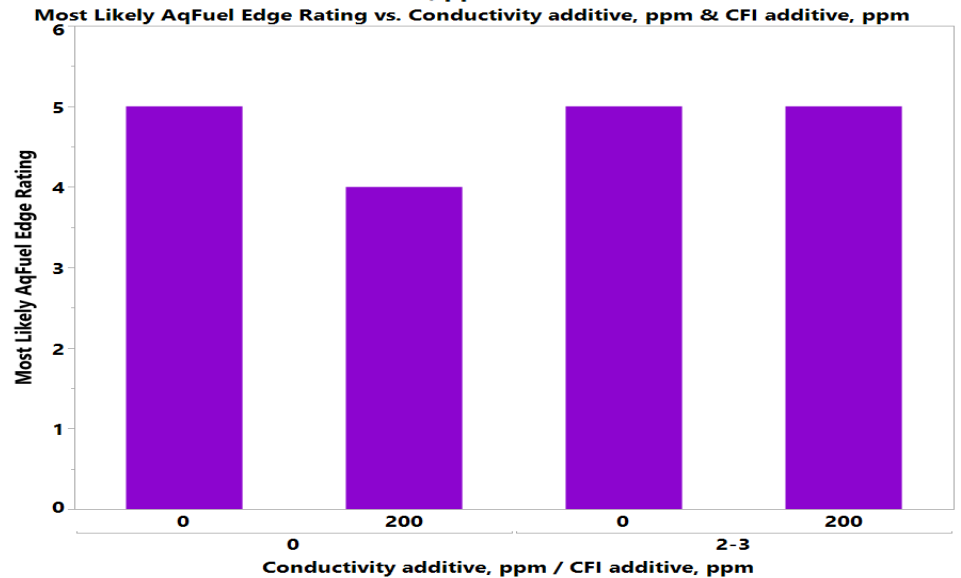
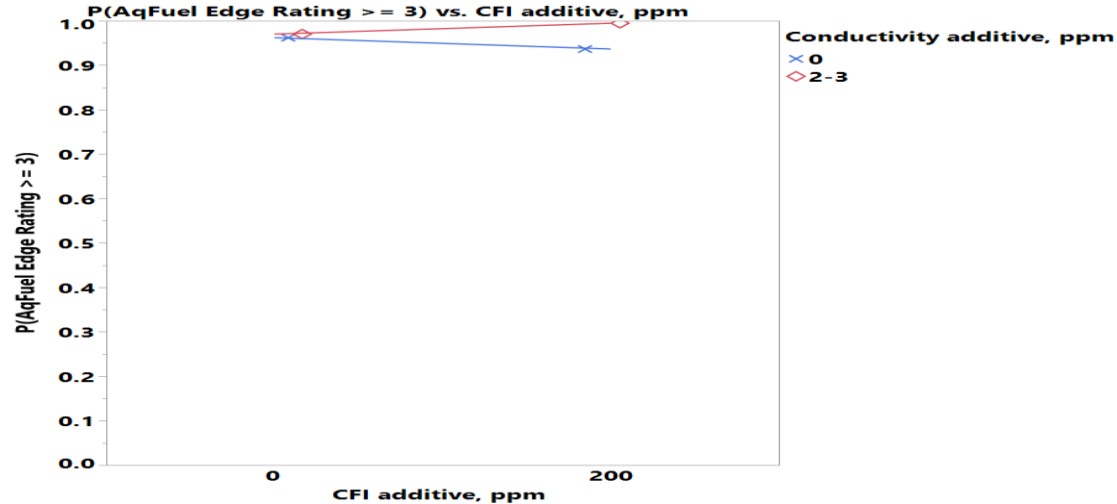
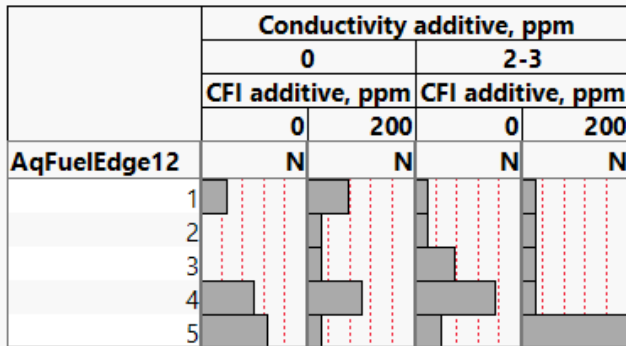


Where((MAL additive = 0) and (Corrosion inhibitor = 0) and (Conductivity Additive = 0) and (FRP Material = 0) and (Sulfur = LSDF) and (Microbes = 0) and (Biodiesel = 0) and (Ethanol = 0))

CFI Additive-Conductivity Additive Interaction Effect

- 200ppm CFI additive has **lower** probability of high corrosion severity than zero CFI additive **without** Conductivity Additive while it has **higher** probability **with** Conductivity additive

	Conductivity additive, ppm			
	0		2-3	
	CFI additive, ppm		CFI additive, ppm	
	0	200	0	200
AqFuelEdge12	N	N	N	N
1	5	6	4	4
2	3	4	4	4
3	3	4	6	4
4	7	7	9	4
5	8	4	5	11



Where((Corrosion inhibitor = 0) and (Sulfur = LSDF) and (Biodiesel = 0) and (MAL additive = 0) and (Glycerin = 0) and (Microbes = 0) and (Ethanol = 0) and (FRP Material = 0))

Ordinal Logistic Regression

Aqueous/Fuel Edge Phase – All Weeks

Whole Model Test				
Model	-LogLikelihood	DF	ChiSquare	Prob>ChiSq
Difference	336.2987	32	672.5974	<.0001*
Full	799.8034			
Reduced	1136.1021			

RSquare (U)	0.2960
AICc	1675.39
BIC	1837.54
Observations (or Sum Wgts)	742

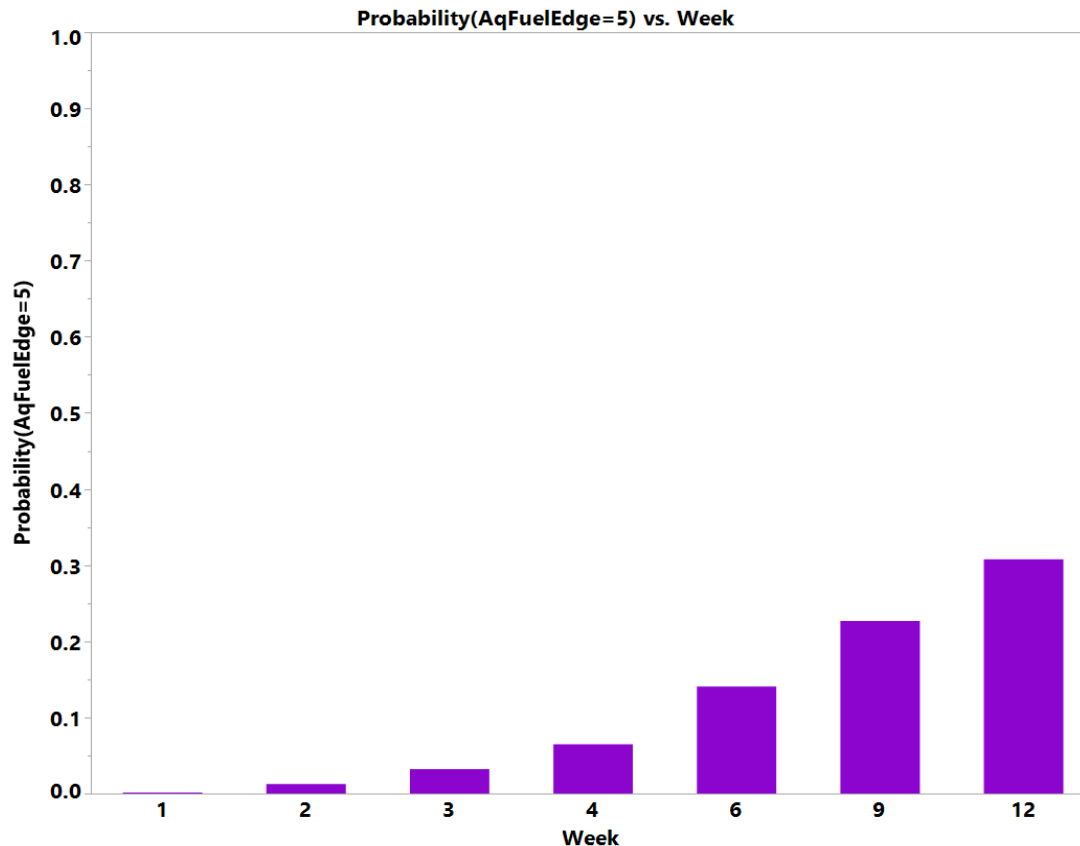
Fit Details	
Measure	Training Definition
Entropy RSquare	0.2960 1-Loglike(model)/Loglike(0)
Generalized RSquare	0.6253 $(1-(L(0)/L(model))^{(2/n)})/(1-L(0)^{(2/n)})$
Mean -Log p	1.0779 $\sum -\log(p[j])/n$
RMSE	0.6323 $\sqrt{\sum (y[j]-p[j])^2/n}$
Mean Abs Dev	0.5818 $\sum y[j]-p[j] /n$
Misclassification Rate	0.4879 $\sum (p[j] \neq \rho \text{Max})/n$
N	742 n

Lack Of Fit			
Source	DF	-LogLikelihood	ChiSquare
Lack Of Fit	2932	799.80342	1599.607
Saturated	2964	0.00000	Prob> ChiSq
Fitted	32	799.80342	1.0000

Parameter Estimates				
Term	Estimate	Std Error	ChiSquare	Prob> ChiSq
Intercept[1]	1.38356488	0.2422096	32.63	<.0001*
Intercept[2]	3.18045716	0.2686948	140.11	<.0001*
Intercept[3]	5.00127459	0.3014204	275.31	<.0001*
Intercept[4]	6.95073232	0.3503363	393.63	<.0001*
Sulfur[LSDF]	0.40145377	0.0747716	28.83	<.0001*
Biodiesel[0]	-0.8951326	0.0815563	120.46	<.0001*
Glycerin[0]	-0.0839069	0.0740732	1.28	0.2573
Ethanol[0]	0.02237183	0.0744199	0.09	0.7637
Mircobes[0]	-0.1631669	0.0752886	4.70	0.0302*
MAL additive[0]	-0.2513168	0.0743948	11.41	0.0007*
CFI additive[0]	-0.0717341	0.0738509	0.94	0.3314
Corrosion inhibitor[0]	-0.2442025	0.2365083	1.07	0.3018
Conductivity Additive[0]	0.11147108	0.0743326	2.25	0.1337
FRP Material[0]	-0.1175734	0.0756384	2.42	0.1201
Sulfur[LSDF]*Conductivity Additive[0]	0.2752387	0.0753587	13.34	0.0003*
Biodiesel[0]*Ethanol[0]	-0.4507141	0.0766308	34.59	<.0001*
Biodiesel[0]*Mircobes[0]	0.65983903	0.0784754	70.70	<.0001*
Biodiesel[0]*FRP Material[0]	0.40700504	0.0760129	28.67	<.0001*
Glycerin[0]*Ethanol[0]	0.12878035	0.0741504	3.02	0.0824
Glycerin[0]*CFI additive[0]	0.20360888	0.074436	7.48	0.0062*
Ethanol[0]*Mircobes[0]	-0.590873	0.0777622	57.74	<.0001*
Mircobes[0]*Corrosion inhibitor[0]	0.53094249	0.0767612	47.84	<.0001*
MAL additive[0]*Corrosion inhibitor[0]	-0.1951144	0.074864	6.79	0.0092*
CFI additive[0]*Conductivity Additive[0]	-0.1563179	0.0751863	4.32	0.0376*
Week[2-1]	-1.452687	0.3129942	21.54	<.0001*
Week[3-2]	-0.8696375	0.2779682	9.79	0.0018*
Week[4-3]	-0.6762442	0.267235	6.40	0.0114*
Week[6-4]	-0.776902	0.2637173	8.68	0.0032*
Week[9-6]	-0.5267078	0.261923	4.04	0.0443*
Week[12-9]	-0.4089513	0.2623371	2.43	0.1190
Week[2-1]*Corrosion inhibitor[0]	-0.6695749	0.3108064	4.64	0.0312*
Week[3-2]*Corrosion inhibitor[0]	-0.0751838	0.2765656	0.07	0.7857
Week[4-3]*Corrosion inhibitor[0]	-0.0596668	0.2662529	0.05	0.8227
Week[6-4]*Corrosion inhibitor[0]	-0.0809402	0.262319	0.10	0.7577
Week[9-6]*Corrosion inhibitor[0]	-0.0566324	0.2612397	0.05	0.8284
Week[12-9]*Corrosion inhibitor[0]	-0.0072238	0.2618998	0.00	0.9780

Corrosion by Time (Week)

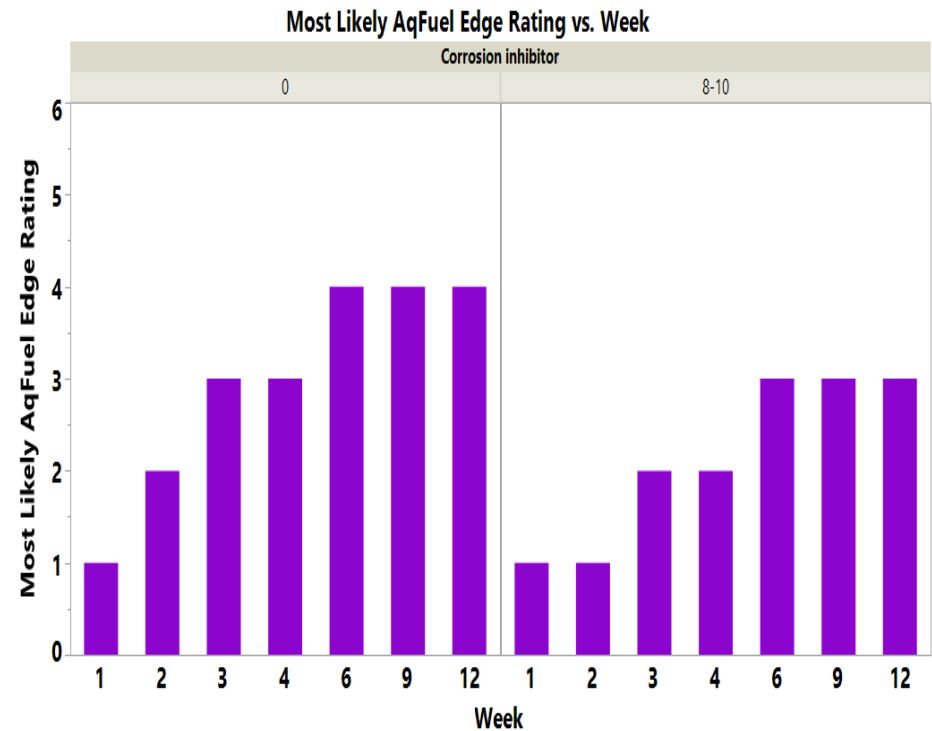
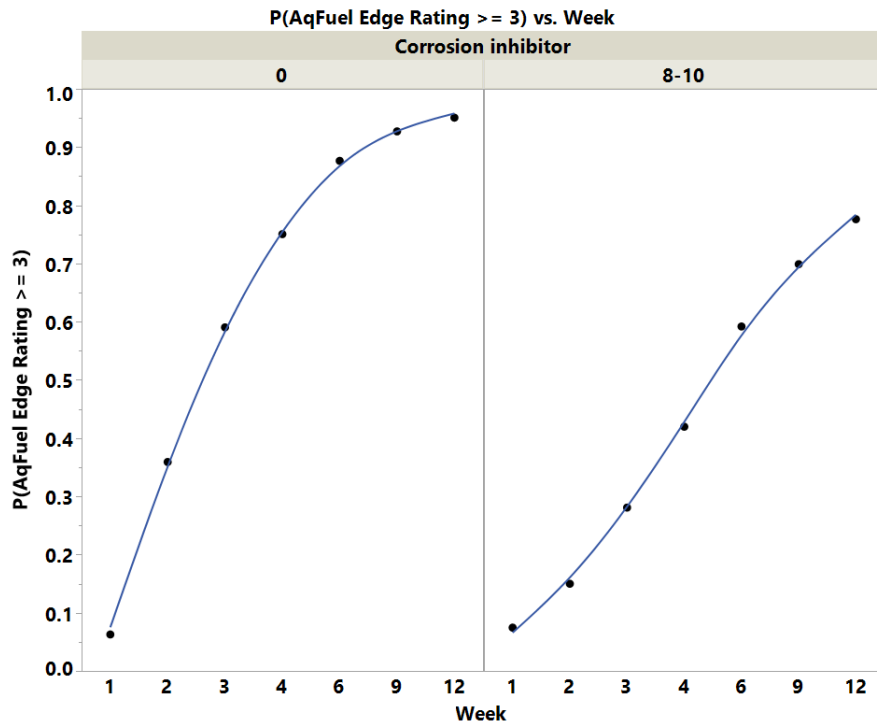
- Significant weekly **increases** in probability of high corrosion severity between weeks 1, 2, 3, 4, 6 and 9.



Where((Sulfur = LSDF) and (Biodiesel = 0) and (Glycerin = 0) and (Ethanol = 0) and (Microbes = 0) and (MAL additive = 0) and (CFI additive = 0) and (Corrosion Inhibitor = 0) and (Conductivity Additive = 0) and (FRP Material = 0))

Corrosion Inhibitor Effect by Time (Week)

- More significant **increase** in probability of high corrosion severity between weeks 1 and 2 without Corrosion Inhibitor than with Corrosion Inhibitor



Where((Sulfur = LSDF) and (Biodiesel = 0) and (Glycerin = 0) and (Ethanol = 0) and (Mircobes = 0) and (MAL additive = 0) and (CFI additive = 0) and (Conductivity Additive = 0) and (FRP Material = 0))

Fuel Phase

Conclusions (Fuel Phase)

Average Corrosion Severity Rating (average of 3 samples)

- ULSD has marginally **higher** probability of high corrosion severity than LSDF
- 5% Biodiesel has **lower** probability of high corrosion severity than zero Biodiesel
- Presence of Water has **higher** probability of high corrosion severity than absence of Water
- 8-10ppm Corrosion inhibitor has **lower** probability of high corrosion severity than zero Corrosion inhibitor
- LSDF has **lower** probability of high corrosion severity than ULSD without Ethanol
- 5% Biodiesel has **lower** probability of high corrosion severity than zero Biodiesel more significantly with LSDF
- 5% Biodiesel has **lower** probability of high corrosion severity than zero Biodiesel more significantly without Glycerin
- 5% Biodiesel has **lower** probability of high corrosion severity than zero Biodiesel more significantly with Ethanol
- 5000ppm Glycerin has **lower** probability of high corrosion severity than zero Glycerin more significantly without FRP Material
- 8-10ppm Corrosion inhibitor has **lower** probability of high corrosion severity than zero Corrosion inhibitor more significantly without Ethanol
- 8-10ppm Corrosion inhibitor has **lower** probability of high corrosion severity than zero Corrosion inhibitor without Microbes while it has **higher** probability with Microbes
- 8-10ppm Corrosion inhibitor has **lower** probability of high corrosion severity than zero Corrosion inhibitor without MAL Additive while it has **higher** probability with MAL Additive
- 8-10ppm Corrosion inhibitor has **lower** probability of high corrosion severity than zero Corrosion inhibitor more significantly without FRP Material
- 200ppm CFI Additive has **lower** probability of high corrosion severity than zero CFI additive without FRP Material while it has **higher** probability with FRP Material
- 2-3ppm Conductivity additive has **lower** probability of high corrosion severity than zero Conductivity additive without Water while it has **higher** probability with Water
- 2-3ppm Conductivity Additive has **lower** probability of high corrosion severity than zero Conductivity additive more significantly without FRP Material
- 2-3ppm Conductivity additive has **lower** probability of high corrosion severity than zero Conductivity additive more significantly with Microbes

Average Corrosion Severity Rating by Time (Week)

- Marginal weekly **increases** in probability of high corrosion severity between weeks 2 & 3 and weeks 4 & 6

Stepwise Ordinal Logistic Regression

Fuel Phase – Week 12

Whole Model Test				
Model	-LogLikelihood	DF	ChiSquare	Prob>ChiSq
Difference	37.087003	24	74.17401	<.0001*
Full	52.453802			
Reduced	89.540806			
RSquare (U)	0.4142			
AICc	170.809			
BIC	231.06			
Observations (or Sum Wgts)	128			
Fit Details				
Measure	Training	Definition		
Entropy RSquare	0.4142	1-Loglike(model)/Loglike(0)		
Generalized RSquare	0.5839	$(1-(L(0)/L(model))^{(2/n)})/(1-L(0)^{(2/n)})$		
Mean -Log p	0.4098	$\sum -\log(\rho[j])/n$		
RMSE	0.3517	$\sqrt{\sum (y[j]-\rho[j])^2/n}$		
Mean Abs Dev	0.2537	$\sum y[j]-\rho[j] /n$		
Misclassification Rate	0.1719	$\sum (\rho[j] \neq \rhoMax)/n$		
N	128	n		
Lack Of Fit				
Source	DF	-LogLikelihood	ChiSquare	
Lack Of Fit	230	52.453802	104.9076	
Saturated	254	0.000000	Prob> ChiSq	
Fitted	24	52.453802	1.0000	

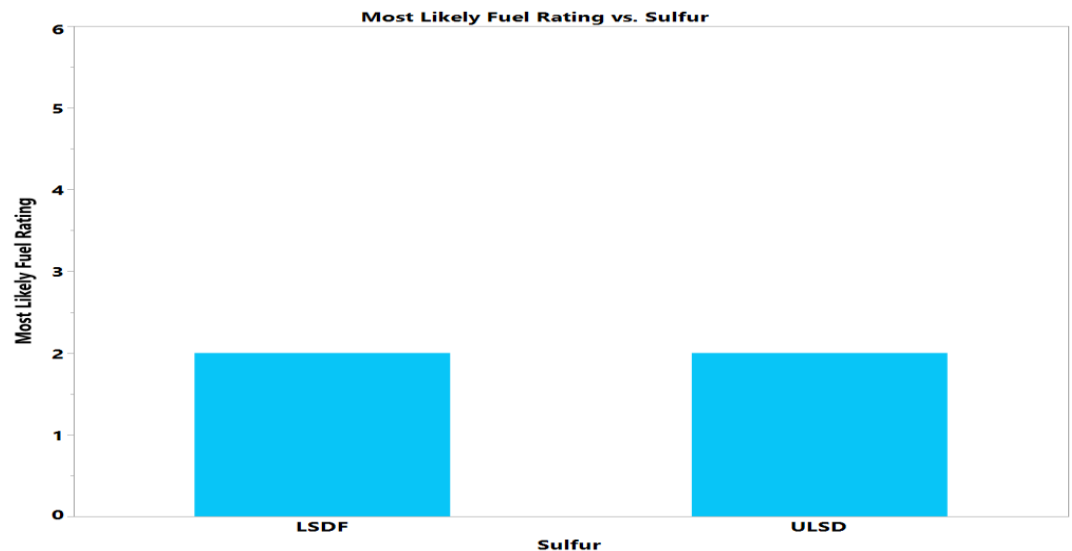
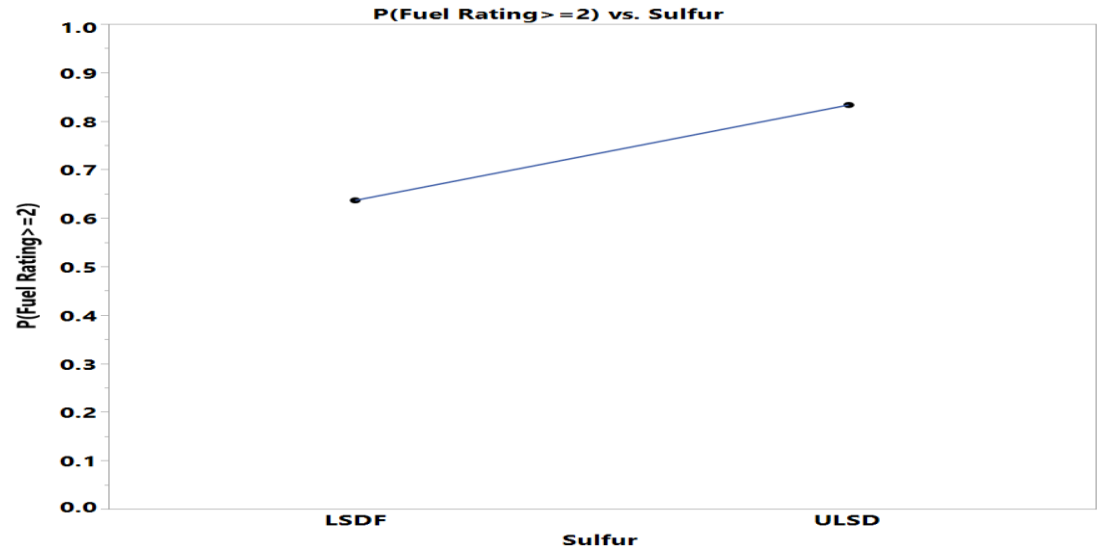
Parameter Estimates				
Term	Estimate	Std Error	ChiSquare	Prob> ChiSq
Intercept[1]	2.00633855	0.5161738	15.11	0.0001*
Intercept[2]	8.90215181	1.6711062	28.38	<.0001*
Sulfur[LSDF]	0.57428509	0.296707	3.75	0.0529
Biodiesel[0]	-0.8926615	0.2949003	9.16	0.0025*
Water[0]	1.30261073	0.473206	7.58	0.0059*
Glycerin[0]	0.4531067	0.2888359	2.46	0.1167
Ethanol[0]	-0.1352039	0.2871051	0.22	0.6377
Mircobes[0]	-0.3716031	0.2821647	1.73	0.1878
MAL additive[0]	0.13779522	0.255282	0.29	0.5894
CFI additive[0]	-0.098931	0.2593408	0.15	0.7029
Corrosion inhibitor[0]	-0.5386693	0.2776284	3.76	0.0523
Conductivity Additive[0]	-0.3358735	0.4139776	0.66	0.4172
FRP Material[0]	-0.0004951	0.26567	0.00	0.9985
Sulfur[LSDF]*Biodiesel[0]	-0.73262	0.2996302	5.98	0.0145*
Sulfur[LSDF]*Ethanol[0]	0.68218726	0.2778771	6.03	0.0141*
Biodiesel[0]*Glycerin[0]	-0.7729028	0.284317	7.39	0.0066*
Biodiesel[0]*Ethanol[0]	0.59766642	0.2926887	4.17	0.0412*
Water[0]*Conductivity Additive[0]	-0.9248099	0.4335661	4.55	0.0329*
Glycerin[0]*FRP Material[0]	-0.6004754	0.2757659	4.74	0.0294*
Ethanol[0]*Corrosion inhibitor[0]	0.55995808	0.2725104	4.22	0.0399*
Mircobes[0]*Corrosion inhibitor[0]	-0.5642727	0.2718017	4.31	0.0379*
Mircobes[0]*Conductivity Additive[0]	0.91756834	0.3181152	8.32	0.0039*
MAL additive[0]*Corrosion inhibitor[0]	-0.7392817	0.2868797	6.64	0.0100*
CFI additive[0]*FRP Material[0]	-1.06672	0.2985304	12.77	0.0004*
Corrosion inhibitor[0]*FRP Material[0]	0.50552593	0.2648497	3.64	0.0563
Conductivity Additive[0]*FRP Material[0]	-0.5220985	0.2778743	3.53	0.0603

Sulfur Effect – Fuel Phase

- ULSD has marginally **higher** probability of high corrosion severity than LSDF

	Sulfur	
	LSDF	ULSD
Fuel12	N	N
1	43	37
2	20	27
3	1	0

	Sulfur	
	LSDF	ULSD
Fuel12	N	N
1		
2		
3		

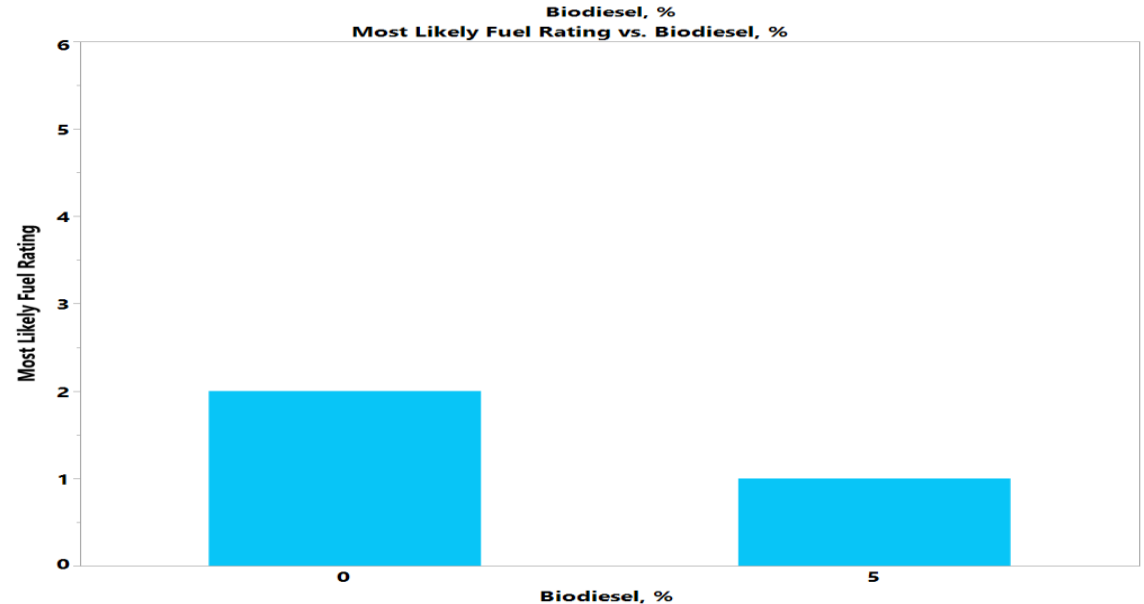
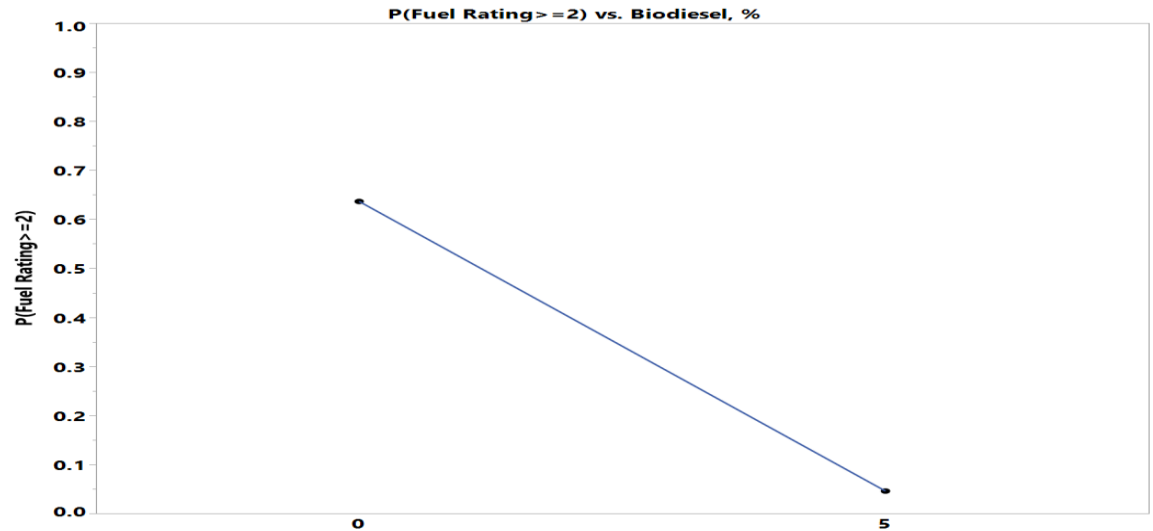
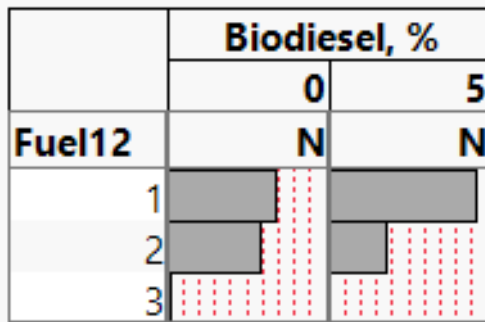


Where((Biodiesel = 0) and (Water = 0) and (Glycerin = 0) and (Microbes = 0) and (Ethanol = 0) and (MAL additive = 0) and (CFI additive = 0) and (Corrosion inhibitor = 0) and (Conductivity Additive = 0) and (FRP Material = 0))

Biodiesel Effect – Fuel Phase

- 5% Biodiesel has **lower** probability of high corrosion severity than zero Biodiesel

	Biodiesel, %	
	0	5
Fuel12	N	N
1	34	46
2	29	18
3	1	0

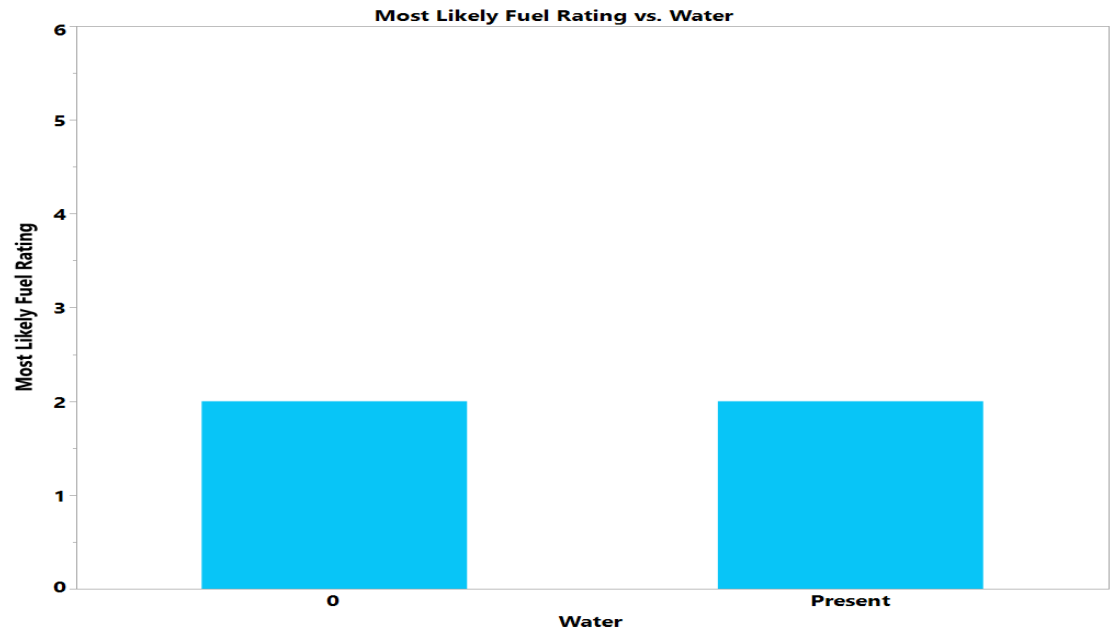
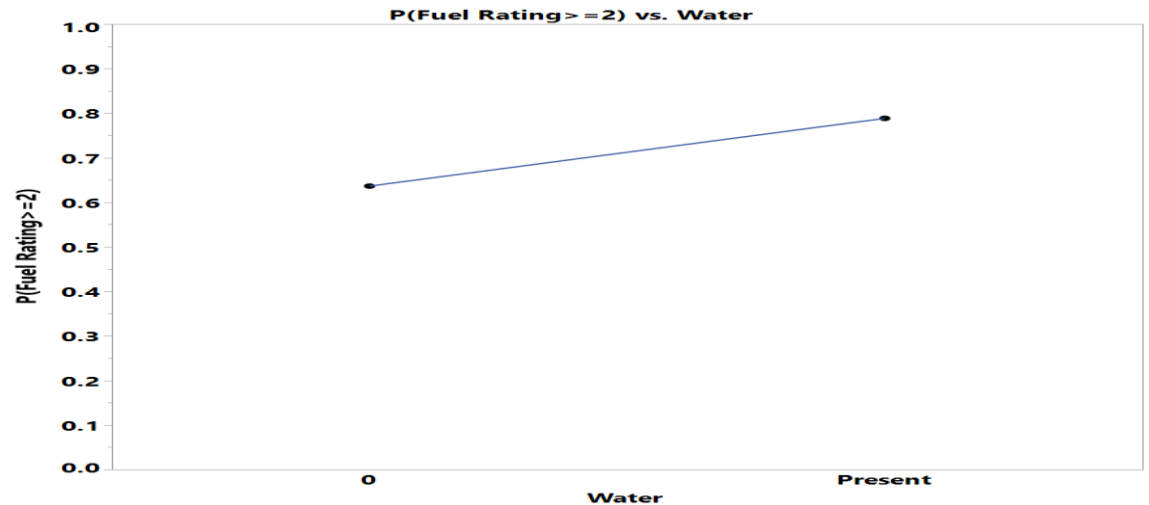


Water Effect – Fuel Phase

- Presence of Water has **higher** probability of high corrosion severity than absence of Water

		Water	
		0	Present
Fuel12	N		
	1	19	61
	2	3	44
	3	0	1

		Water	
		0	Present
Fuel12	N		
	1		
	2		
	3		

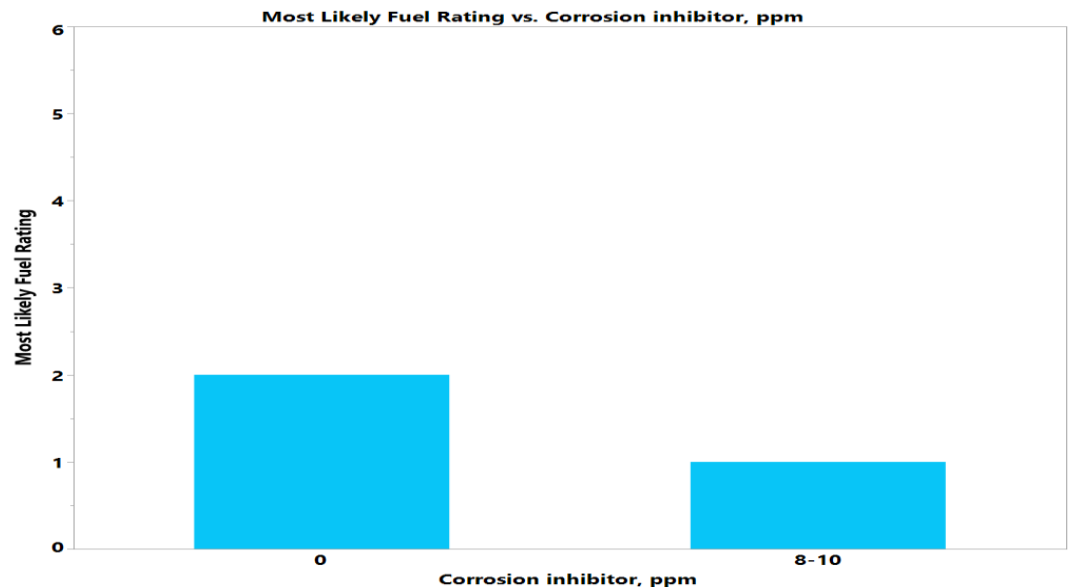
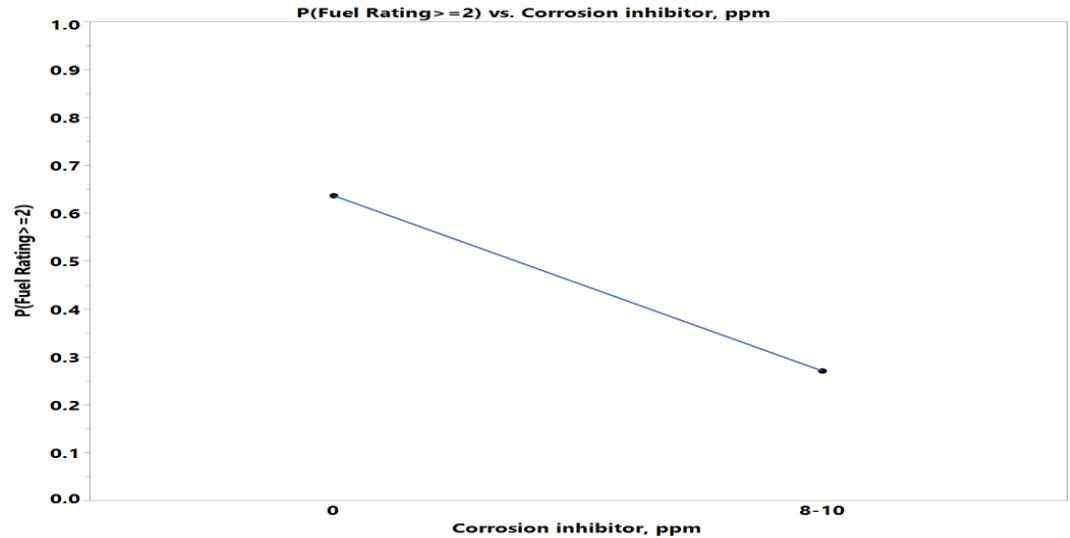
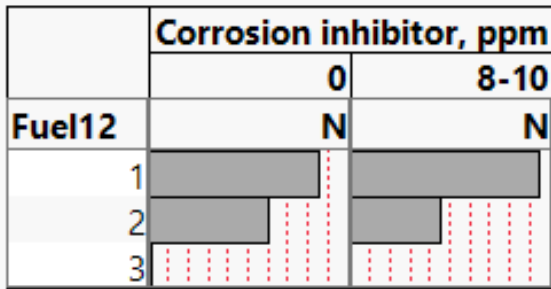


Where((Sulfur = LSDF) and (Biodiesel = 0) and (Glycerin = 0) and (Microbes = 0) and (Ethanol = 0) and (MAL additive = 0) and (CFI additive = 0) and (Corrosion inhibitor = 0) and (Conductivity Additive = 0) and (FRP Material = 0))

Corrosion Inhibitor Effect – Fuel Phase

- 8-10ppm Corrosion inhibitor has **lower** probability of high corrosion severity than zero Corrosion inhibitor

	Corrosion inhibitor, ppm	
	0	8-10
Fuel12	N	N
1	38	42
2	27	20
3	1	0

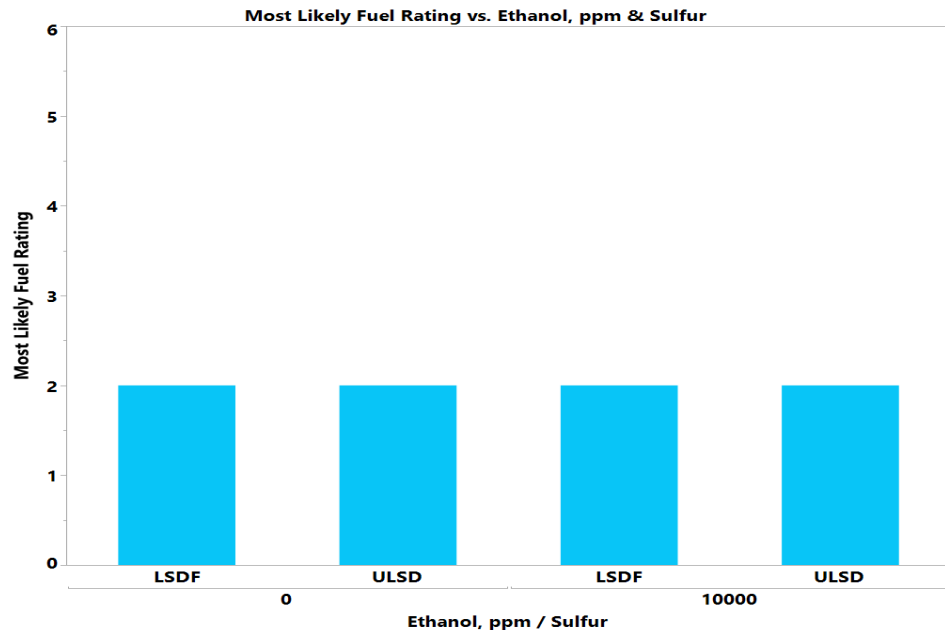
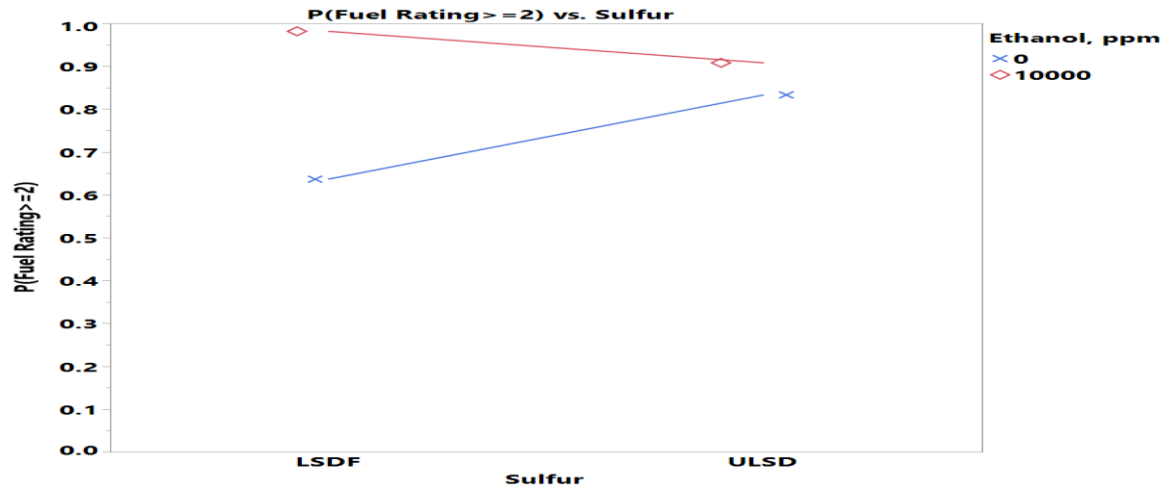
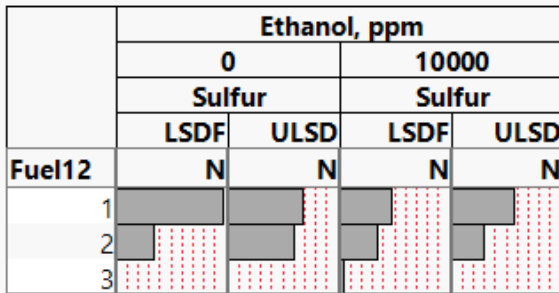


Where((Biodiesel = 0) and (Water = 0) and (Glycerin = 0) and (Microbes = 0) and (Ethanol = 0) and (MAL additive = 0) and (CFI additive = 0) and (Sulfur= LSDF) and (Conductivity Additive = 0) and (FRP Material = 0))

Sulfur-Ethanol Interaction Effect

- LSDF has **lower** probability of high corrosion severity than ULSD without Ethanol

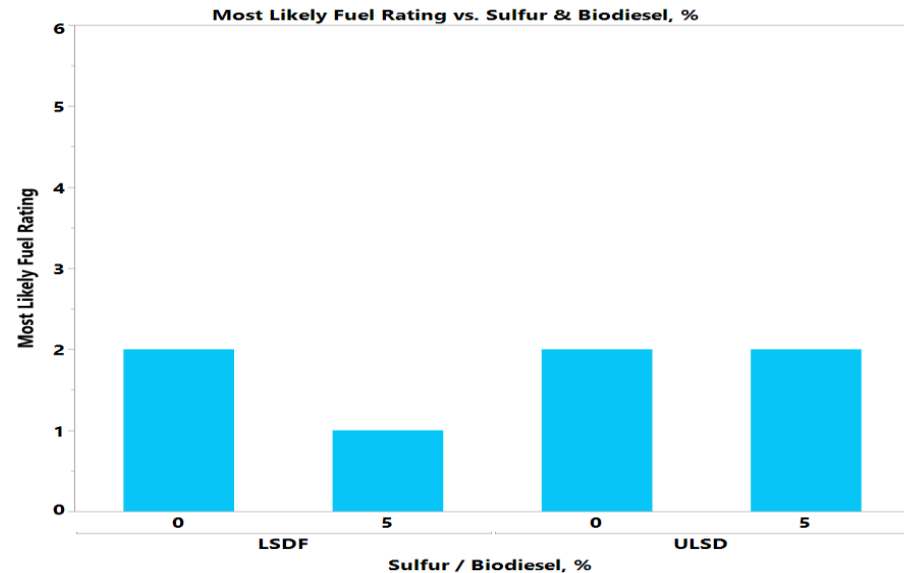
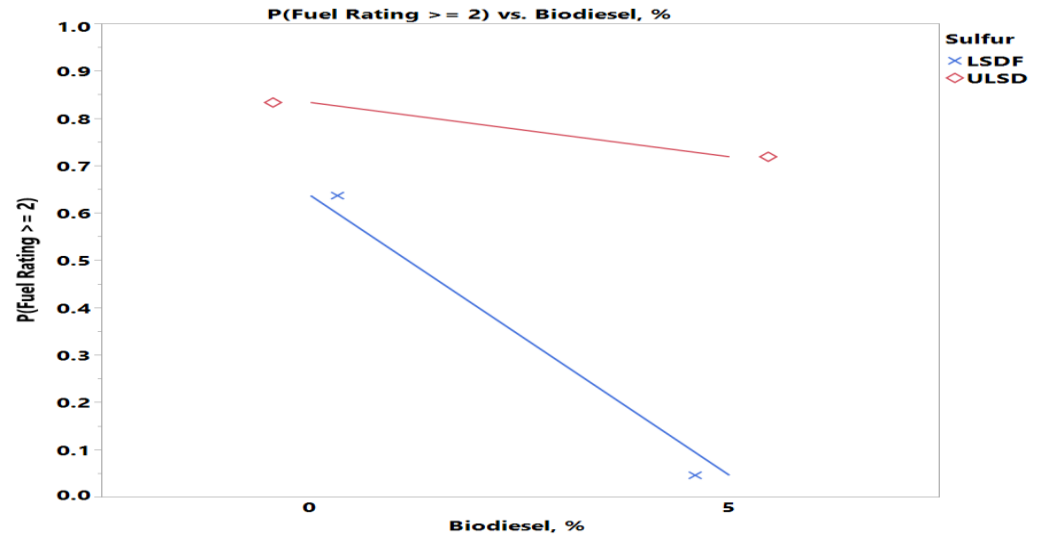
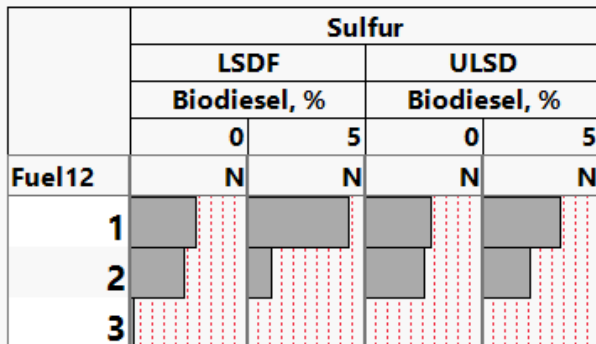
	Ethanol, ppm			
	0		10000	
	Sulfur		Sulfur	
	LSDF	ULSD	LSDF	ULSD
Fuel12	N	N	N	N
1	29	20	14	17
2	10	18	10	9
3	0	0	1	0



Biodiesel-Sulfur Interaction Effect

- 5% Biodiesel has **lower** probability of high corrosion severity than zero Biodiesel more significantly with LSDF

	Sulfur			
	LSDF		ULSD	
	Biodiesel, %		Biodiesel, %	
	0	5	0	5
Fuel12	N	N	N	N
1	17	26	17	20
2	14	6	15	12
3	1	0	0	0

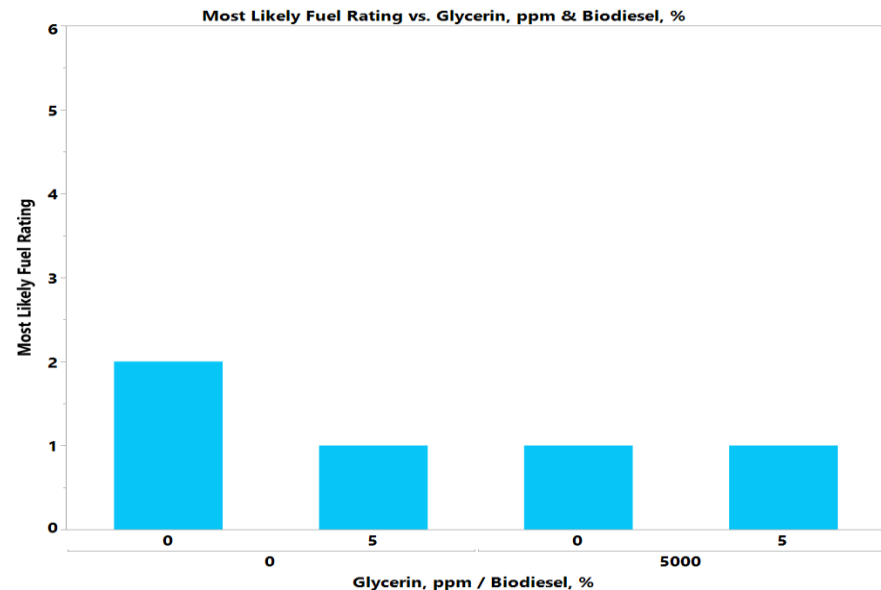
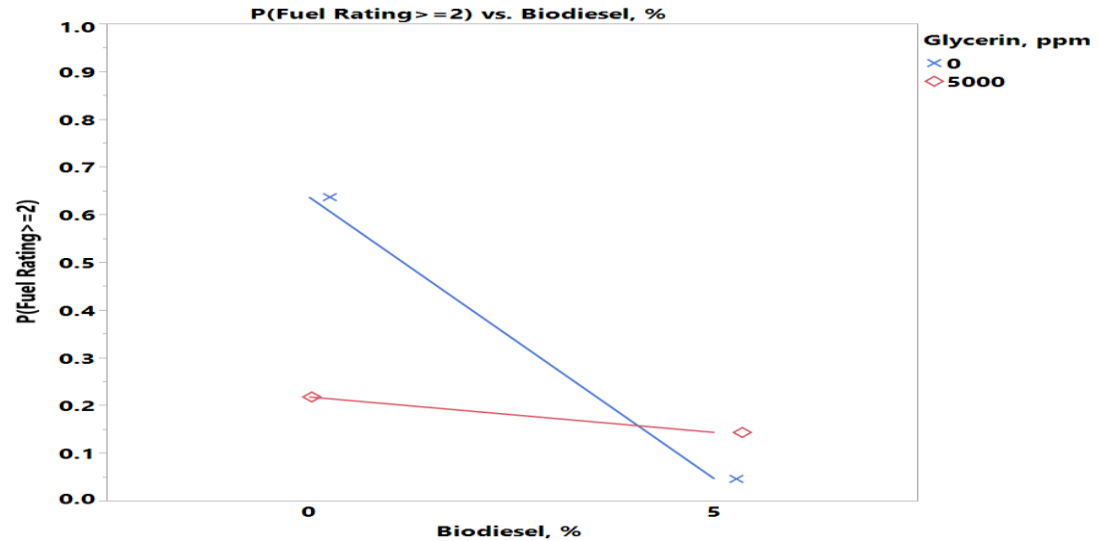
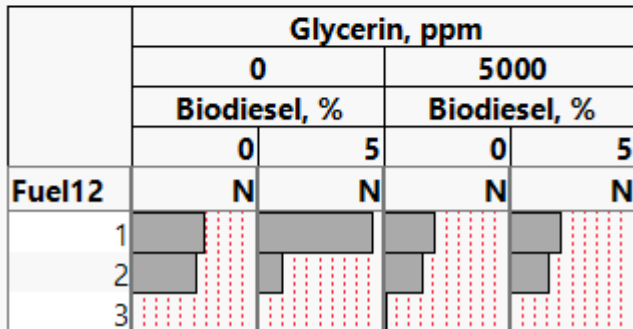


Where((Glycerin = 0) and (Water = 0) and (Microbes = 0) and (MAL additive = 0) and (CFI additive = 0) and (Corrosion inhibitor = 0) and (Conductivity Additive = 0) and (FRP Material = 0) and (Ethanol = 0))

Biodiesel-Glycerin Interaction Effect

- 5% Biodiesel has **lower** probability of high corrosion severity than zero Biodiesel more significantly without Glycerin

	Glycerin, ppm			
	0		5000	
	Biodiesel, %		Biodiesel, %	
	0	5	0	5
Fuel12	N	N	N	N
1	20	32	14	14
2	18	7	11	11
3	0	0	1	0

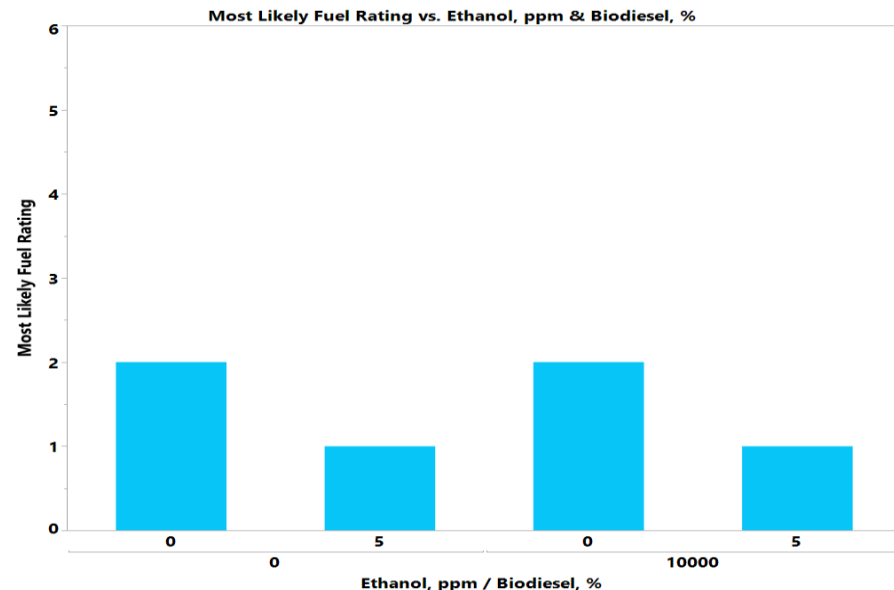
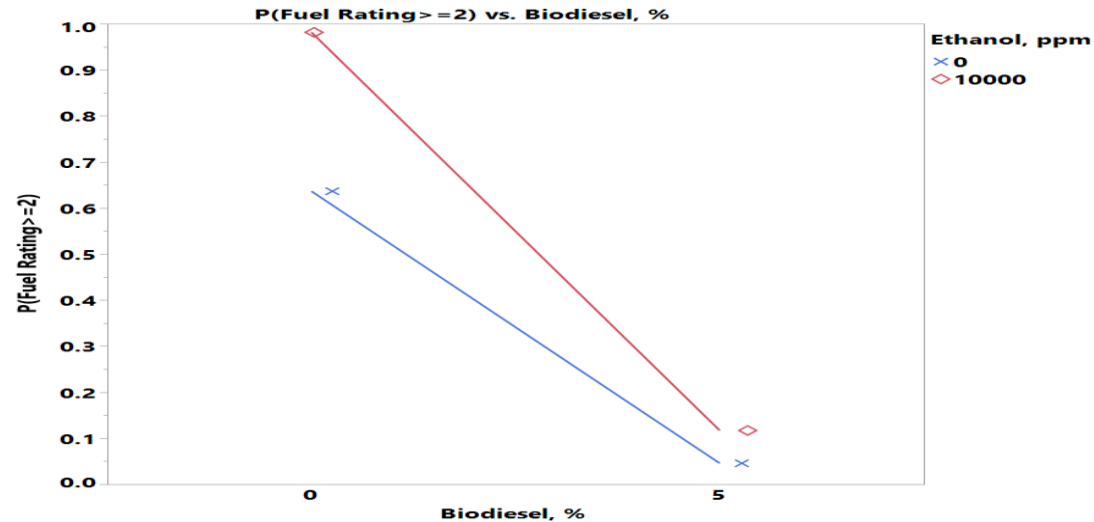
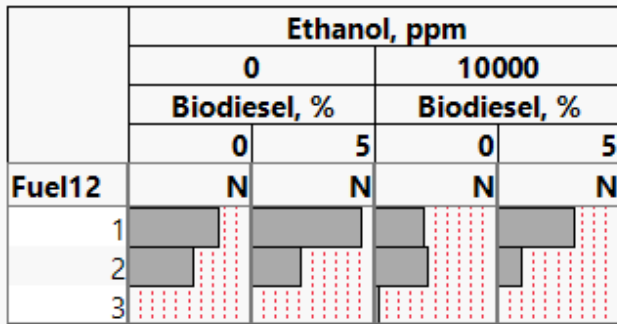


Where((Ethanol = 0) and (Water = 0) and (Microbes = 0) and (MAL additive = 0) and (CFI additive = 0) and (Corrosion inhibitor = 0) and (Conductivity Additive = 0) and (FRP Material = 0) and (Sulfur = LSDF))

Biodiesel-Ethanol Interaction Effect

- 5% Biodiesel has **lower** probability of high corrosion severity than zero Biodiesel more significantly with Ethanol

	Ethanol, ppm			
	0		10000	
	Biodiesel, %		Biodiesel, %	
	0	5	0	5
Fuel12	N	N	N	N
1	22	27	12	19
2	16	12	13	6
3	0	0	1	0



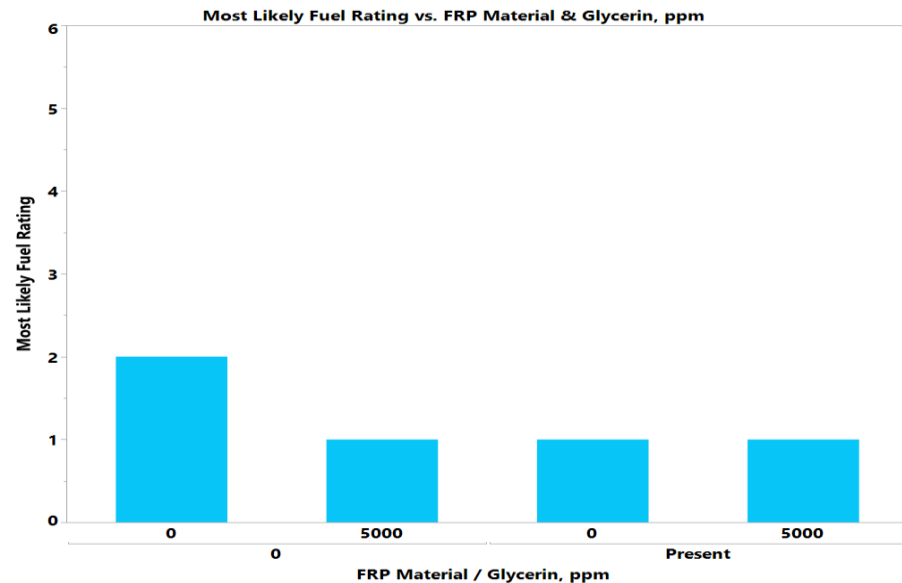
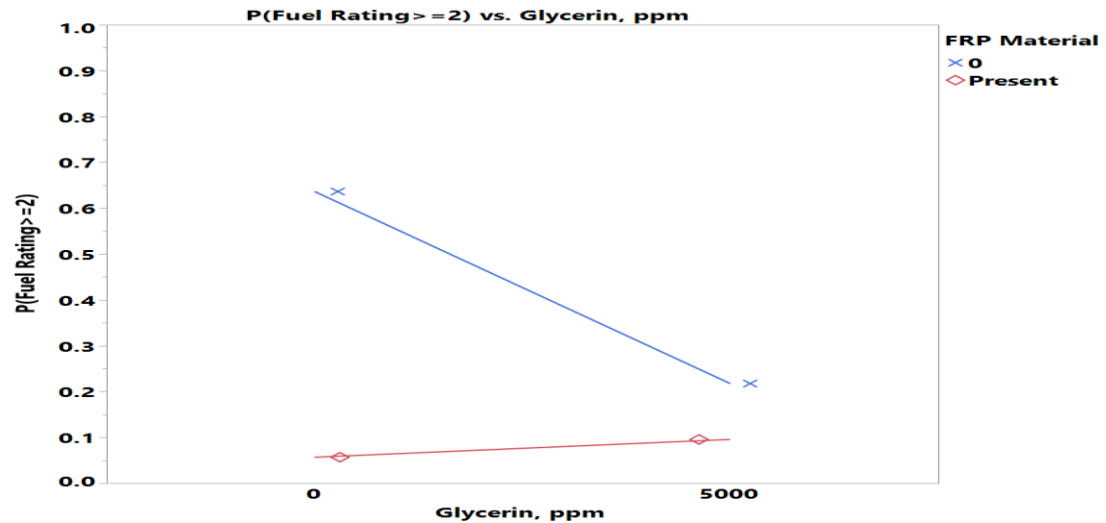
Where((Glycerin = 0) and (Water = 0) and (Microbes = 0) and (MAL additive = 0) and (CFI additive = 0) and (Corrosion inhibitor = 0) and (Conductivity Additive = 0) and (FRP Material = 0) and (Sulfur = LSDF))

Glycerin-FRP Material Interaction Effect

- 5000ppm Glycerin has **lower** probability of high corrosion severity than zero Glycerin more significantly without FRP Material

	FRP Material			
	0		Present	
	Glycerin, ppm		Glycerin, ppm	
	0	5000	0	5000
Fuel12	N	N	N	N
1	25	15	27	13
2	15	10	10	12
3	0	0	0	1

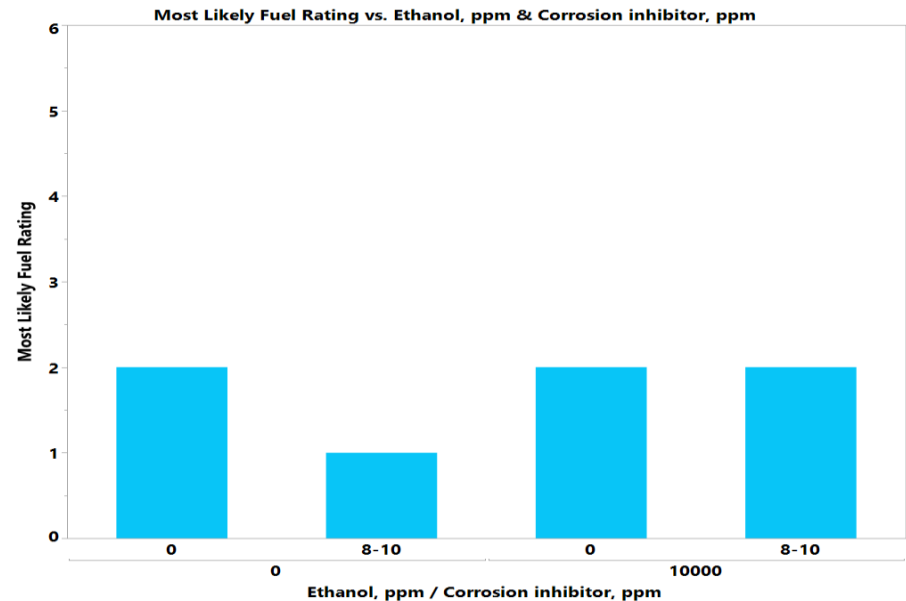
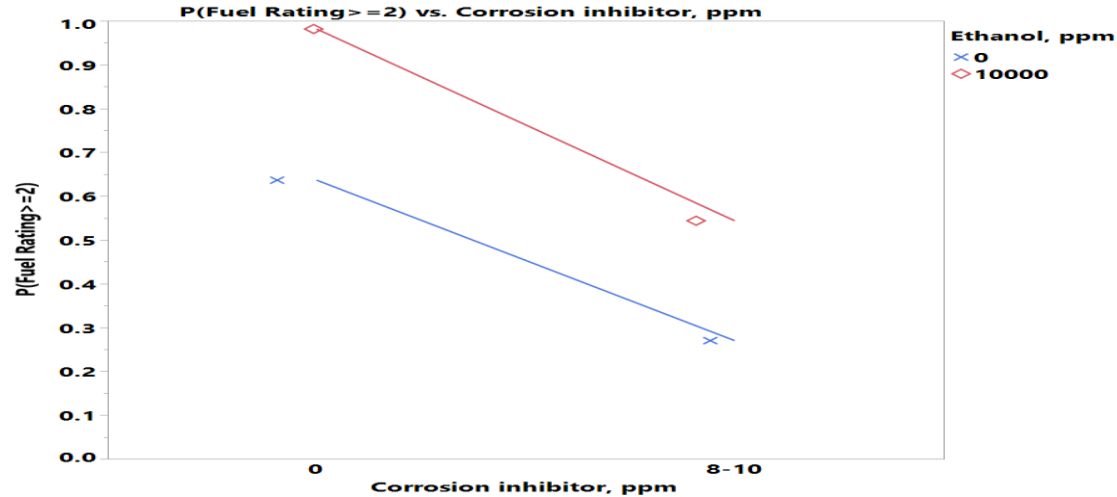
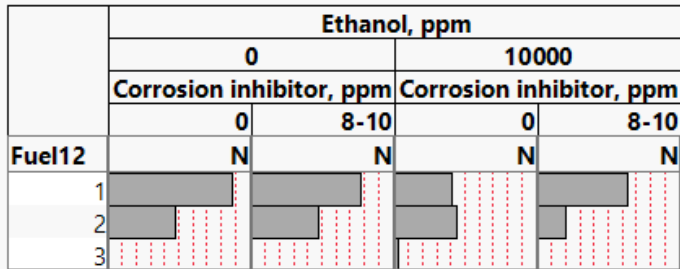
	FRP Material			
	0		Present	
	Glycerin, ppm		Glycerin, ppm	
	0	5000	0	5000
Fuel12	N	N	N	N
1				
2				
3				



Corrosion Inhibitor-Ethanol Interaction Effect

- 8-10ppm Corrosion inhibitor has **lower** probability of high corrosion severity than zero Corrosion inhibitor more significantly without Ethanol

	Ethanol, ppm			
	0		10000	
	Corrosion inhibitor, ppm		Corrosion inhibitor, ppm	
	0	8-10	0	8-10
Fuel12	N	N	N	N
1	26	23	12	19
2	14	14	13	6
3	0	0	1	0



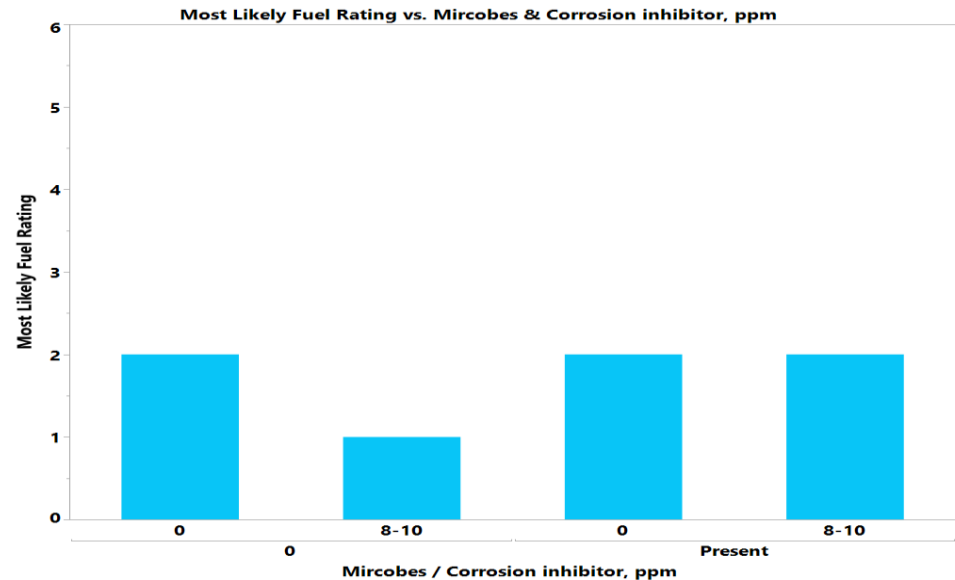
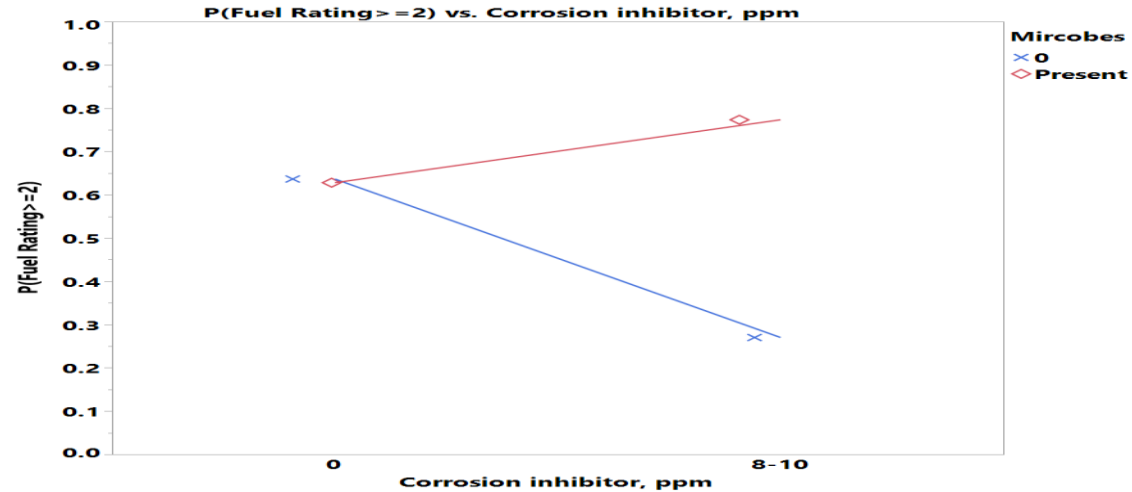
Where((Sulfur = LSDF) and (Water = 0) and (Biodiesel = 0) and (Glycerin = 0) and (Microbes = 0) and (CFI Additive= 0) and (FRP Material = 0) and (MAL additive = 0) and (Conductivity Additive = 0))

Corrosion Inhibitor-Microbes Interaction Effect

- 8-10ppm Corrosion inhibitor has **lower** probability of high corrosion severity than zero Corrosion inhibitor **without** Microbes while it has **higher** probability **with** Microbes

	Microbes			
	0		Present	
	Corrosion inhibitor, ppm		Corrosion inhibitor, ppm	
	0	8-10	0	8-10
Fuel12	N	N	N	N
1	20	25	18	17
2	19	9	8	11
3	0	0	1	0

	Microbes			
	0		Present	
	Corrosion inhibitor, ppm		Corrosion inhibitor, ppm	
	0	8-10	0	8-10
Fuel12	N	N	N	N
1	[Bar chart showing fuel rating distribution for 0 ppm inhibitor, 0 microbes]		[Bar chart showing fuel rating distribution for 0 ppm inhibitor, microbes present]	
2	[Bar chart showing fuel rating distribution for 8-10 ppm inhibitor, 0 microbes]		[Bar chart showing fuel rating distribution for 8-10 ppm inhibitor, microbes present]	
3	[Bar chart showing fuel rating distribution for 0 ppm inhibitor, 0 microbes]		[Bar chart showing fuel rating distribution for 0 ppm inhibitor, microbes present]	



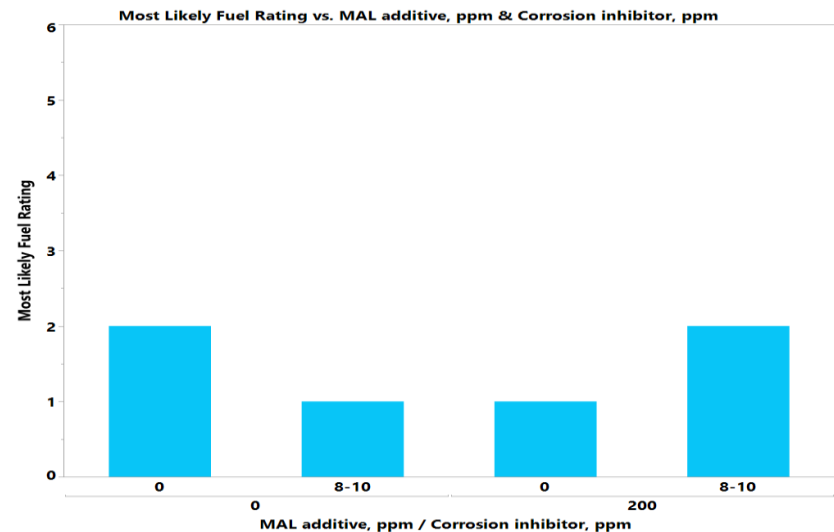
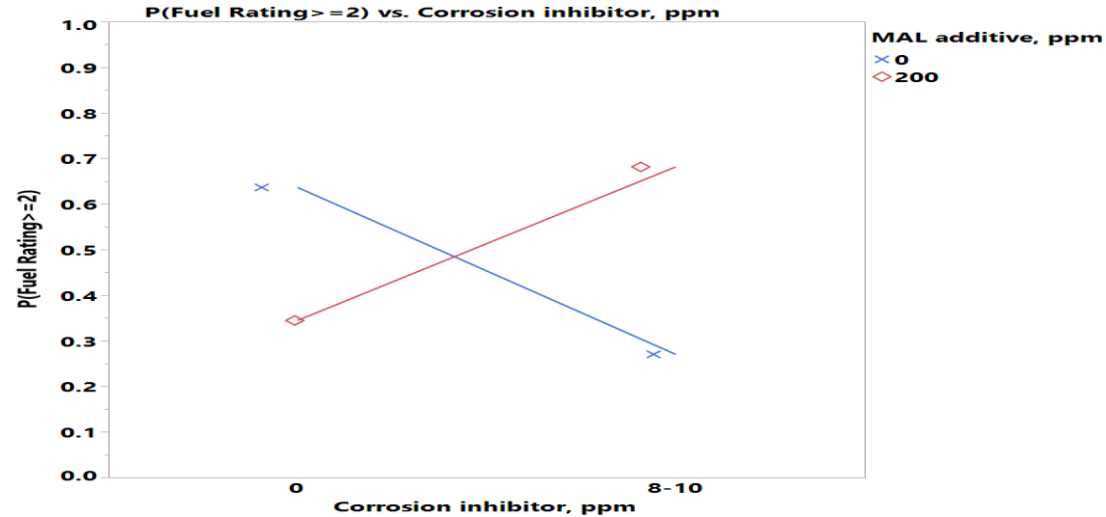
Where((Sulfur = LSDF) and (Water = 0) and (Biodiesel = 0) and (Glycerin = 0) and (Ethanol = 0) and (CFI Additive= 0) and (FRP Material = 0) and (MAL additive = 0) and (Conductivity Additive = 0))

Corrosion Inhibitor-MAL Additive Interaction Effect

- 8-10ppm Corrosion inhibitor has **lower** probability of high corrosion severity than zero Corrosion inhibitor **without** MAL Additive while it has **higher** probability **with** MAL Additive

	MAL additive, ppm			
	0		200	
	Corrosion inhibitor, ppm		Corrosion inhibitor, ppm	
	0	8-10	0	8-10
Fuel12	N	N	N	N
1	18	22	20	20
2	13	7	14	13
3	1	0	0	0

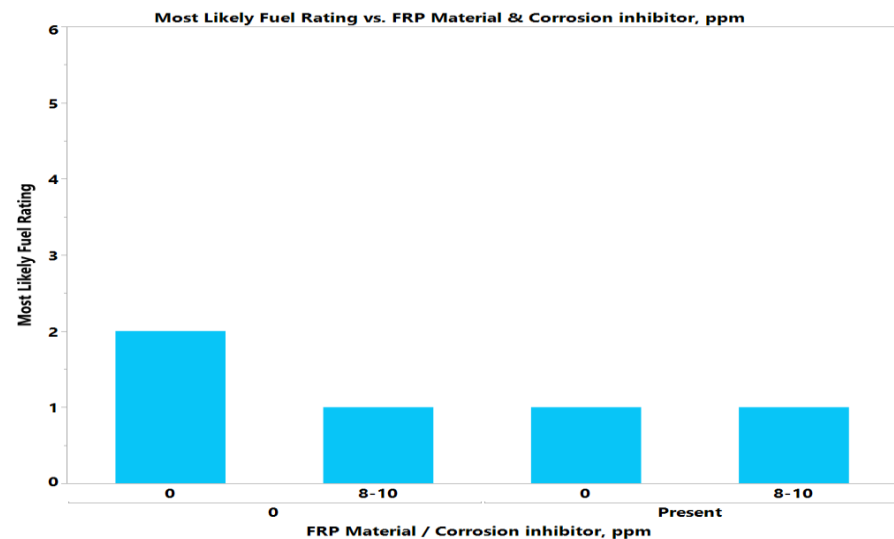
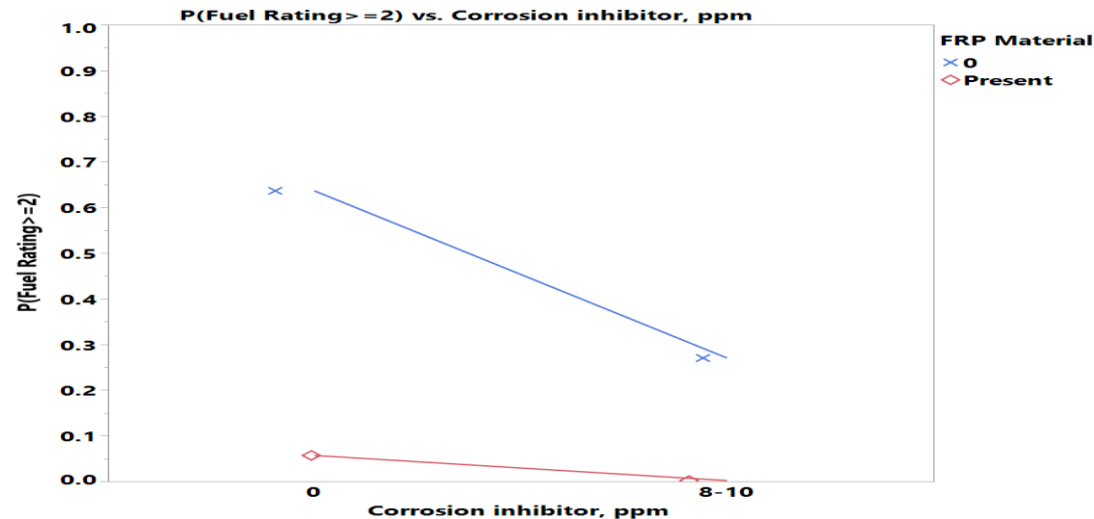
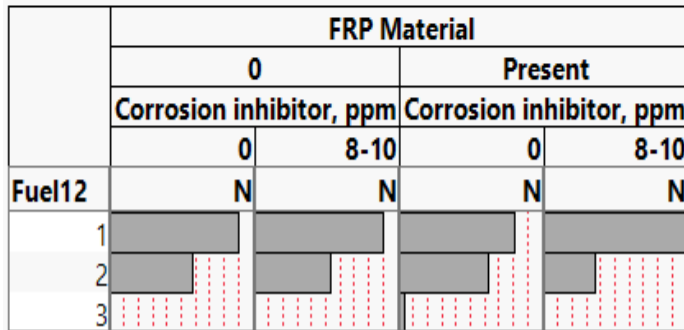
	MAL additive, ppm			
	0		200	
	Corrosion inhibitor, ppm		Corrosion inhibitor, ppm	
	0	8-10	0	8-10
Fuel12	N	N	N	N
1	[Bar chart showing fuel rating distribution for 0 ppm MAL, 0 ppm CI]		[Bar chart showing fuel rating distribution for 200 ppm MAL, 0 ppm CI]	
2	[Bar chart showing fuel rating distribution for 0 ppm MAL, 8-10 ppm CI]		[Bar chart showing fuel rating distribution for 200 ppm MAL, 8-10 ppm CI]	
3	[Bar chart showing fuel rating distribution for 0 ppm MAL, 0 ppm CI]		[Bar chart showing fuel rating distribution for 200 ppm MAL, 0 ppm CI]	



Corrosion Inhibitor-FRP Material Interaction Effect

- 8-10ppm Corrosion inhibitor has **lower** probability of high corrosion severity than zero Corrosion inhibitor more significantly without FRP Material

	FRP Material			
	0		Present	
	Corrosion inhibitor, ppm		Corrosion inhibitor, ppm	
	0	8-10	0	8-10
Fuel12	N	N	N	N
1	20	20	18	22
2	13	12	14	8
3	0	0	1	0



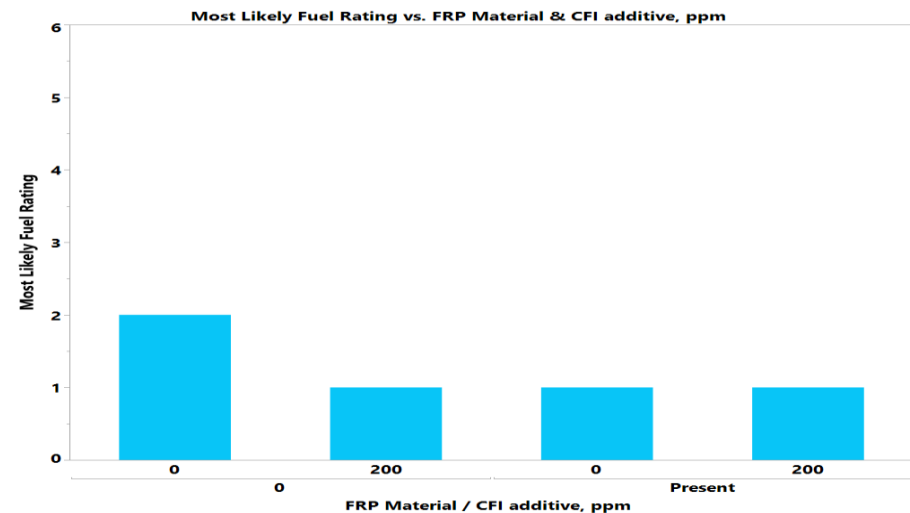
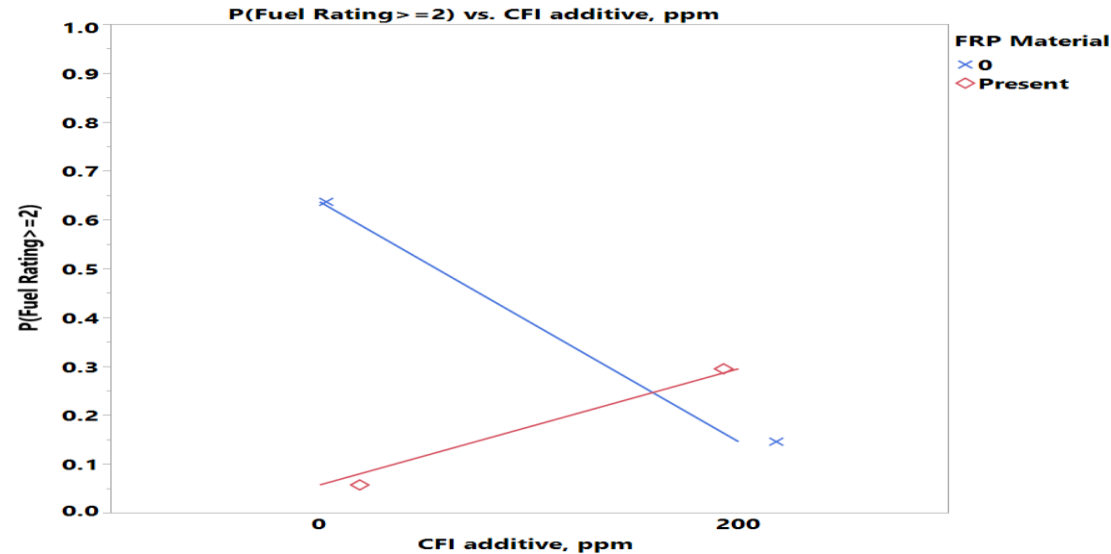
Where((Sulfur = LSDF) and (Water = 0) and (Biodiesel = 0) and (Glycerin = 0) and (Ethanol = 0) and (CFI Additive= 0) and (MAL Additive = 0) and (Microbes= 0) and (Conductivity Additive = 0))

CFI Additive-FRP Material Interaction Effect

- 200ppm CFI Additive has **lower** probability of high corrosion severity than zero CFI additive **without** FRP Material while it has **higher** probability **with** FRP Material

	FRP Material			
	0		Present	
	CFI additive, ppm		CFI additive, ppm	
	0	200	0	200
Fuel12	N	N	N	N
1	15	25	25	15
2	17	8	7	15
3	0	0	1	0

	FRP Material			
	0		Present	
	CFI additive, ppm		CFI additive, ppm	
	0	200	0	200
Fuel12	N	N	N	N
1				
2				
3				

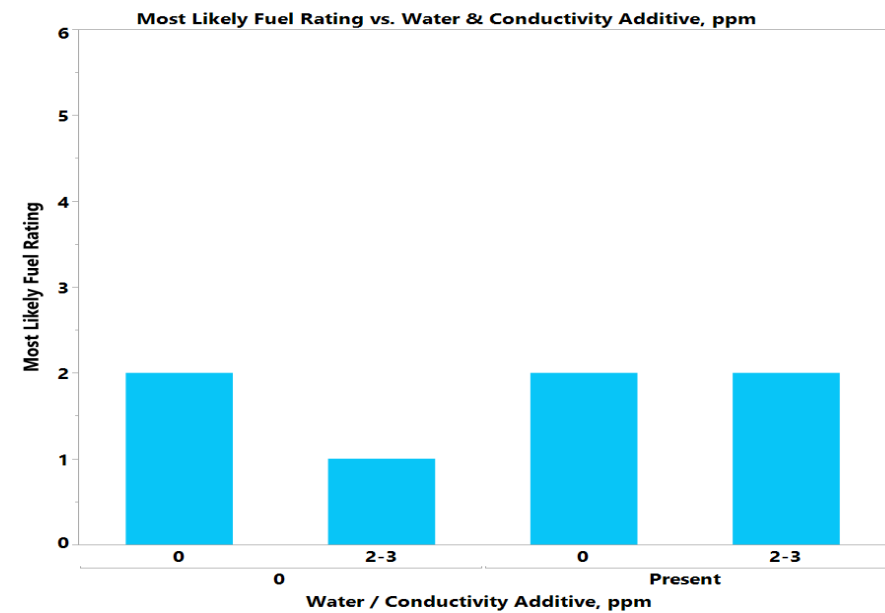
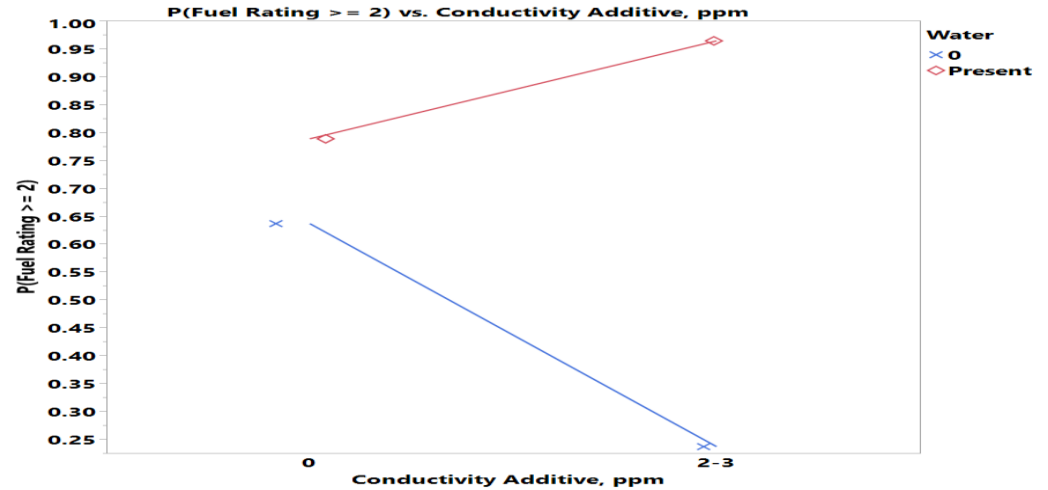
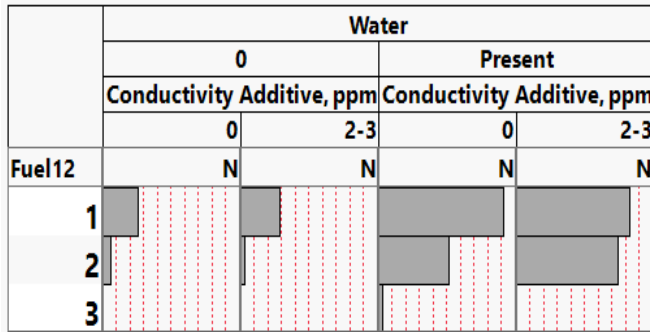


Where((Sulfur = LSDF) and (Water = 0) and (Biodiesel = 0) and (Glycerin = 0) and (Ethanol = 0) and (Corrosion Inhibitor= 0) and (MAL Additive = 0) and (Microbes= 0) and (Conductivity Additive = 0))

Conductivity Additive-Water Interaction Effect

- 2-3ppm Conductivity additive has **lower** probability of high corrosion severity than zero Conductivity additive **without** Water while it has **higher** probability **with** Water

	Water			
	0		Present	
	Conductivity Additive, ppm		Conductivity Additive, ppm	
	0	2-3	0	2-3
Fuel12	N	N	N	N
1	9	10	32	29
2	2	1	18	26
3	0	0	1	0

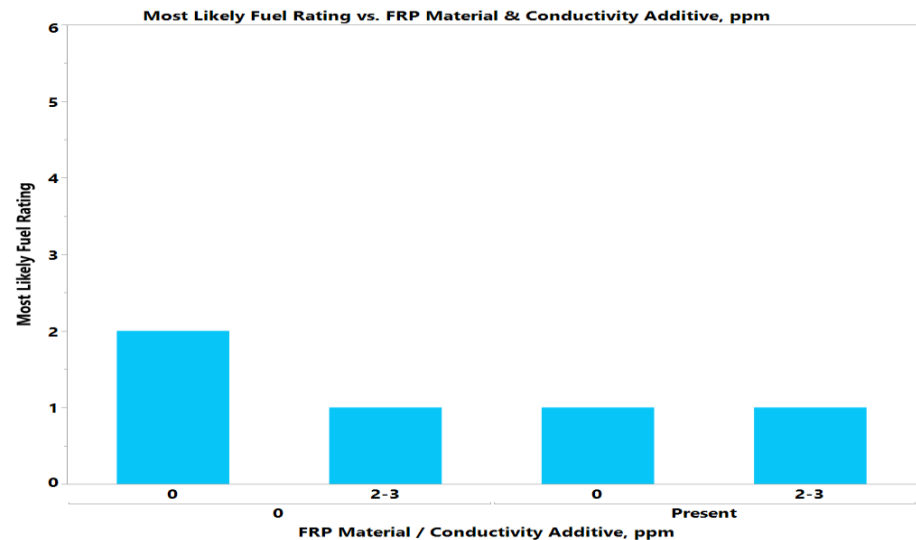
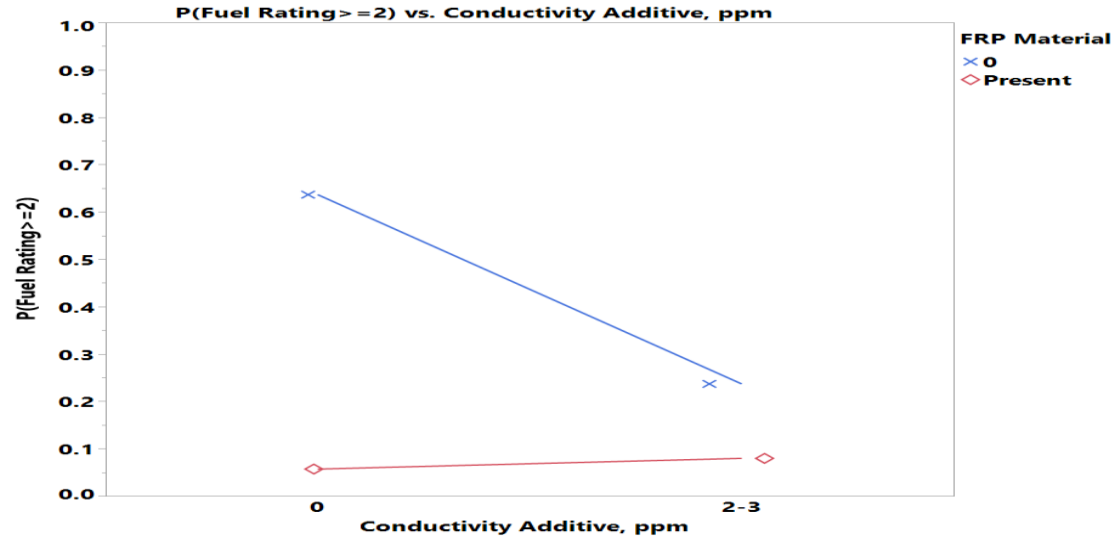
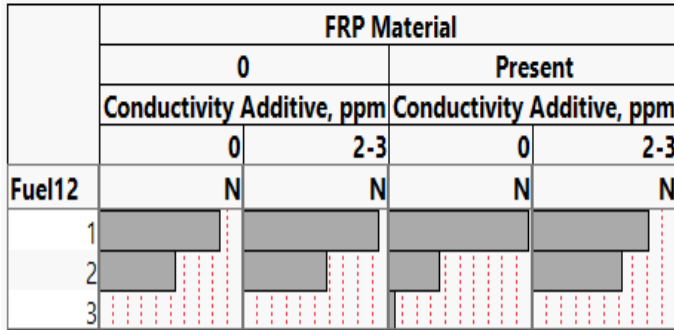


Where((Glycerin = 0) and (Biodiesel = 0) and (Microbes = 0) and (MAL additive = 0) and (CFI additive = 0) and (Corrosion inhibitor = 0) and (Ethanol = 0) and (FRP Material = 0) and (Sulfur = LSDF))

Conductivity Additive-FRP Material Interaction Effect

- 2-3ppm Conductivity Additive has **lower** probability of high corrosion severity than zero Conductivity additive more significantly without FRP Material

	FRP Material			
	0		Present	
	Conductivity Additive, ppm		Conductivity Additive, ppm	
	0	2-3	0	2-3
Fuel12	N	N	N	N
1	19	21	22	18
2	12	13	8	14
3	0	0	1	0

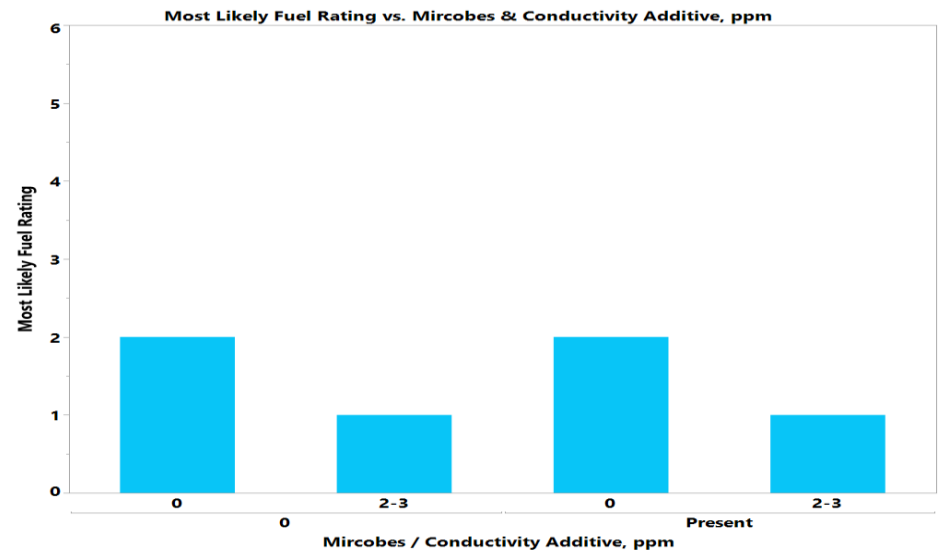
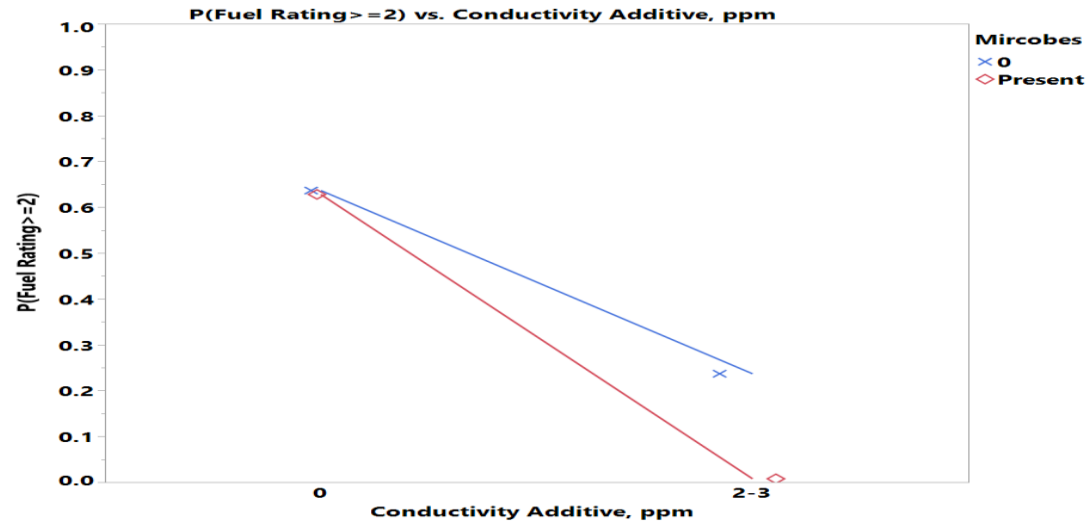
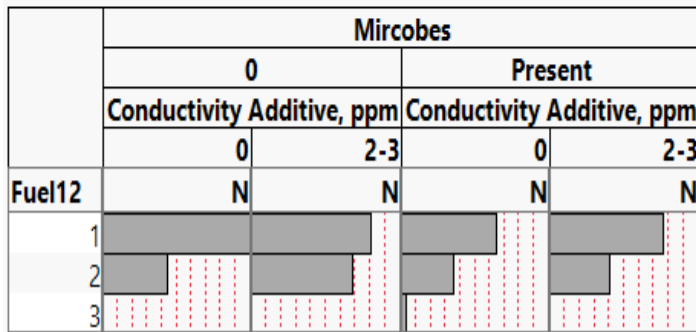


Where((Sulfur = LSDF) and (Water = 0) and (Biodiesel = 0) and (Glycerin = 0) and (Ethanol = 0) and (CFI Additive= 0) and (Corrosion Inhibitor = 0) and (Microbes= 0) and (MAL Additive = 0))

Conductivity Additive–Microbes Interaction Effect

- 2-3ppm Conductivity additive has **lower** probability of high corrosion severity than zero Conductivity additive more significantly with Microbes

	Microbes			
	0		Present	
	Conductivity Additive, ppm		Conductivity Additive, ppm	
	0	2-3	0	2-3
Fuel12	N	N	N	N
1	25	20	16	19
2	11	17	9	10
3	0	0	1	0



Where((Sulfur = LSDF) and (Water = 0) and (Biodiesel = 0) and (Glycerin = 0) and (Ethanol = 0) and (CFI Additive= 0) and (FRP Material = 0) and (Corrosion Inhibitor = 0) and (MAL Additive= 0))

Ordinal Logistic Regression

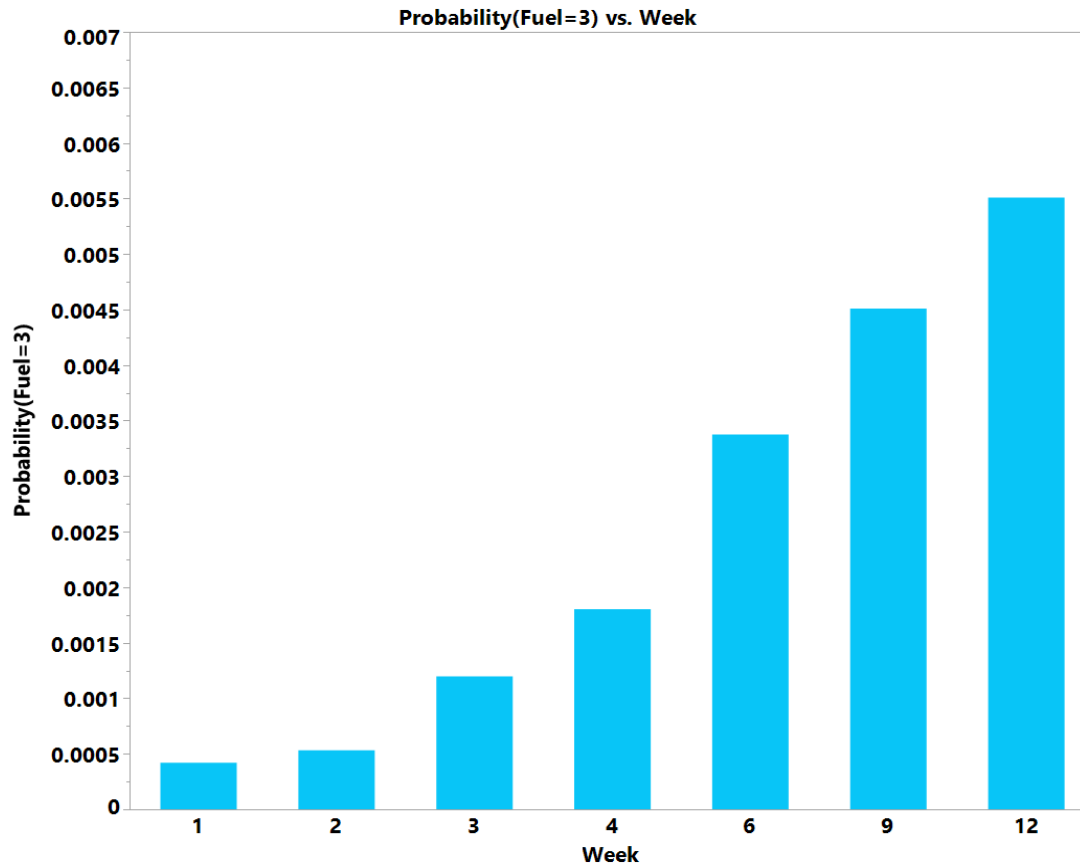
Fuel Phase – All Weeks

Whole Model Test				
Model	-LogLikelihood	DF	ChiSquare	Prob> ChiSq
Difference	160.48587	30	320.9717	<.0001*
Full	332.64701			
Reduced	493.13288			
RSquare (U)		0.3254		
AICc		731.741		
BIC		882.828		
Observations (or Sum Wgts)		896		
Fit Details				
Measure	Training	Definition		
Entropy RSquare	0.3254	1-Loglike(model)/Loglike(0)		
Generalized RSquare	0.4511	$(1-(L(0)/L(model))^{(2/n)})/(1-L(0)^{(2/n)})$		
Mean -Log p	0.3713	$\sum -\log(p[j])/n$		
RMSE	0.3426	$\sqrt{\sum (y[j]-p[j])^2/n}$		
Mean Abs Dev	0.2333	$\sum y[j]-p[j] /n$		
Misclassification Rate	0.1741	$\sum (p[j] \neq pMax)/n$		
N	896	n		
Lack Of Fit				
Source	DF	-LogLikelihood	ChiSquare	
Lack Of Fit	1760	332.64701	665.294	
Saturated	1790	0.00000	Prob> ChiSq	
Fitted	30	332.64701	1.0000	

Parameter Estimates				
Term	Estimate	Std Error	ChiSquare	Prob> ChiSq
Intercept[1]	4.26036932	0.4808395	78.50	<.0001*
Intercept[2]	10.2613665	0.9175502	125.07	<.0001*
Sulfur[LSDF]	0.29380333	0.1077874	7.43	0.0064*
Biodiesel[0]	-0.4681586	0.1059061	19.54	<.0001*
Water[0]	1.20034686	0.2943895	16.63	<.0001*
Glycerin[0]	0.34041836	0.1088009	9.79	0.0018*
Ethanol[0]	0.11893143	0.1109172	1.15	0.2836
Mircobes[0]	-0.3250782	0.107483	9.15	0.0025*
MAL additive[0]	0.184431	0.1010851	3.33	0.0681
CFI additive[0]	-0.32173	0.1038365	9.60	0.0019*
Corrosion inhibitor[0]	-0.1588444	0.1037978	2.34	0.1259
Conductivity Additive[0]	-0.8082899	0.2856117	8.01	0.0047*
FRP Material[0]	0.00640833	0.1056239	0.00	0.9516
Sulfur[LSDF]*Biodiesel[0]	-0.6510518	0.112305	33.61	<.0001*
Sulfur[LSDF]*Ethanol[0]	0.20549474	0.1016134	4.09	0.0431*
Biodiesel[0]*Glycerin[0]	-0.31457	0.1056993	8.86	0.0029*
Biodiesel[0]*Ethanol[0]	0.54106583	0.1114773	23.56	<.0001*
Water[0]*Conductivity Additive[0]	-1.2226476	0.2875715	18.08	<.0001*
Glycerin[0]*FRP Material[0]	-0.3746463	0.1045325	12.85	0.0003*
Ethanol[0]*Corrosion inhibitor[0]	0.26938763	0.1038976	6.72	0.0095*
Mircobes[0]*Corrosion inhibitor[0]	-0.3867549	0.1051876	13.52	0.0002*
Mircobes[0]*Conductivity Additive[0]	0.452917	0.1124559	16.22	<.0001*
MAL additive[0]*Corrosion inhibitor[0]	-0.1742336	0.1045903	2.78	0.0957
CFI additive[0]*FRP Material[0]	-0.8787151	0.1147779	58.61	<.0001*
Corrosion inhibitor[0]*FRP Material[0]	0.22096674	0.1009571	4.79	0.0286*
Conductivity Additive[0]*FRP Material[0]	-0.2340347	0.1039755	5.07	0.0244*
Week[2-1]	-0.2401865	0.4913259	0.24	0.6249
Week[3-2]	-0.8098366	0.4332672	3.49	0.0616
Week[4-3]	-0.410392	0.3717556	1.22	0.2696
Week[6-4]	-0.6284928	0.342334	3.37	0.0664
Week[9-6]	-0.2907763	0.3225484	0.81	0.3673
Week[12-9]	-0.2011369	0.31648	0.40	0.5251

Corrosion by Time (Week)

- Marginal weekly **increases** in probability of high corrosion severity between weeks 2 & 3 and weeks 4 & 6.



Where((Sulfur = LSDF) and (Water = 0) and (Biodiesel = 0) and (Glycerin = 0) and (Ethanol = 0) and (Microbes = 0) and (MAL additive = 0) and (CFI additive = 0) and (Corrosion Inhibitor = 0) and (Conductivity Additive = 0) and (FRP Material = 0))

Fuel Edge Phase

Conclusions (Fuel Edge Phase)

Average Corrosion Severity Rating (average of 3 samples)

- Presence of FRP Material has **lower** probability of high corrosion severity than the absence of FRP Material
- LSDF has **lower** probability of high corrosion severity than ULSD with Ethanol while it has **higher** probability without Ethanol
- Presence of FRP Material has **lower** probability of high corrosion severity than the absence of FRP Material without CFI additive while it has **higher** probability with CFI additive
- 8-10ppm Corrosion inhibitor has **lower** probability of high corrosion severity than zero Corrosion inhibitor more significantly without CFI additive
- 8-10ppm Corrosion inhibitor has **higher** probability of high corrosion severity than zero Corrosion inhibitor more significantly with MAL additive
- 8-10ppm Corrosion inhibitor has **higher** probability of high corrosion severity than zero Corrosion inhibitor more significantly without Conductivity additive
- 8-10ppm Corrosion inhibitor has **higher** probability of high corrosion severity than zero Corrosion inhibitor more significantly without FRP Material

Average Corrosion Severity Rating by Time (Week)

- Marginal weekly **increases** in probability of high corrosion severity between weeks 1 & 2 and weeks 2 & 3

Stepwise Ordinal Logistic Regression

Fuel Edge Phase – Week 12

Whole Model Test

Model	-LogLikelihood	DF	ChiSquare	Prob>ChiSq
Difference	19.81536	17	39.63072	0.0015*
Full	102.73115			
Reduced	122.54652			

RSquare (U)	0.1617
AICc	253.313
BIC	302.503
Observations (or Sum Wgts)	128

Fit Details

Measure	Training	Definition
Entropy RSquare	0.1617	1-Loglike(model)/Loglike(0)
Generalized RSquare	0.3123	$(1-(L(0)/L(model))^{(2/n)})/(1-L(0)^{(2/n)})$
Mean -Log p	0.8026	$\sum -\log(p_{ij})/n$
RMSE	0.5247	$\sqrt{\sum (y_{ij}-p_{ij})^2/n}$
Mean Abs Dev	0.4864	$\sum y_{ij}-p_{ij} /n$
Misclassification Rate	0.3359	$\sum (p_{ij} \neq p_{Max})/n$
N	128	n

Lack Of Fit

Source	DF	-LogLikelihood	ChiSquare
Lack Of Fit	364	102.73115	205.4623
Saturated	381	0.00000	Prob>ChiSq
Fitted	17	102.73115	1.0000

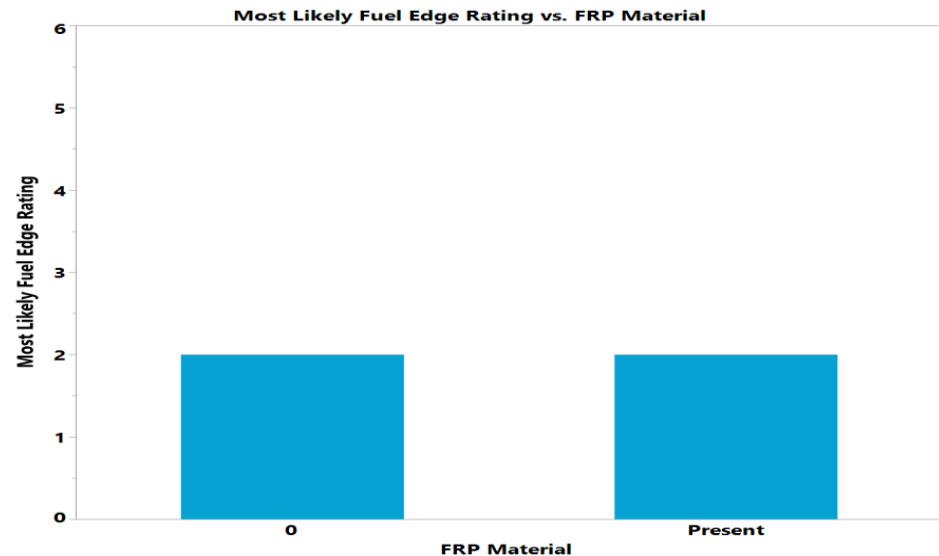
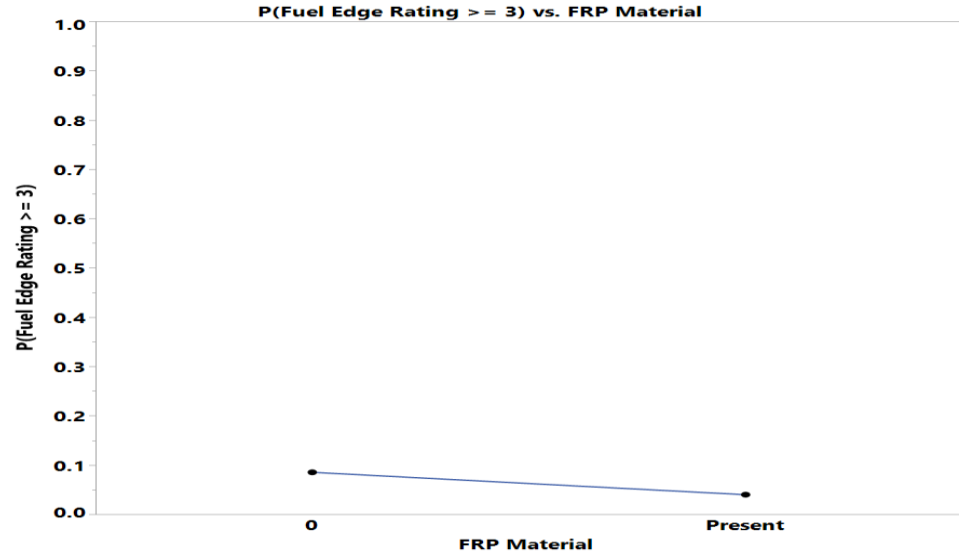
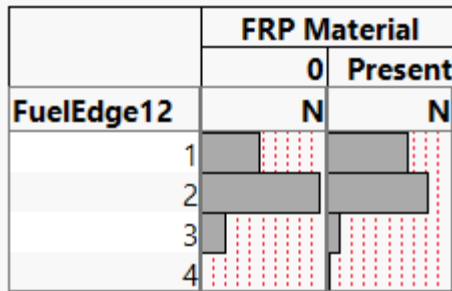
Parameter Estimates

Term	Estimate	Std Error	ChiSquare	Prob>ChiSq
Intercept[1]	-0.8695467	0.3246824	7.17	0.0074*
Intercept[2]	2.73357894	0.4369952	39.13	<.0001*
Intercept[3]	5.6659384	1.066124	28.24	<.0001*
Sulfur[LSDf]	-0.0006874	0.1882037	0.00	0.9971
Biodiesel, %[0]	-0.0265826	0.1853165	0.02	0.8859
Water[0]	0.02755414	0.3034716	0.01	0.9277
Glycerin, ppm[0]	0.04815449	0.2029895	0.06	0.8125
Ethanol, ppm[0]	0.14450407	0.2058948	0.49	0.4828
Mircobes[0]	-0.0168347	0.2038182	0.01	0.9342
MAL additive, ppm[0]	-0.0707856	0.1856924	0.15	0.7031
CFI additive, ppm[0]	-0.0052965	0.1855035	0.00	0.9772
Corrosion inhibitor, ppm[0]	0.28499869	0.1864424	2.34	0.1264
Conductivity Additive, ppm[0]	-0.1969941	0.1867748	1.11	0.2916
FRP Material[0]	-0.3613312	0.187949	3.70	0.0545
Sulfur[LSDf]*Ethanol, ppm[0]	-0.5838031	0.1953579	8.93	0.0028*
MAL additive, ppm[0]*Corrosion inhibitor, ppm[0]	-0.4245416	0.1895207	5.02	0.0251*
CFI additive, ppm[0]*Corrosion inhibitor, ppm[0]	0.53620357	0.1929855	7.72	0.0055*
CFI additive, ppm[0]*FRP Material[0]	-0.484677	0.1934839	6.28	0.0122*
Corrosion inhibitor, ppm[0]*Conductivity Additive, ppm[0]	0.32947609	0.1876411	3.08	0.0791
Corrosion inhibitor, ppm[0]*FRP Material[0]	0.44103763	0.1924867	5.25	0.0219*

FRP Material Effect – Fuel Edge Phase

- Presence of FRP Material has **lower** probability of high corrosion severity than the absence of FRP Material

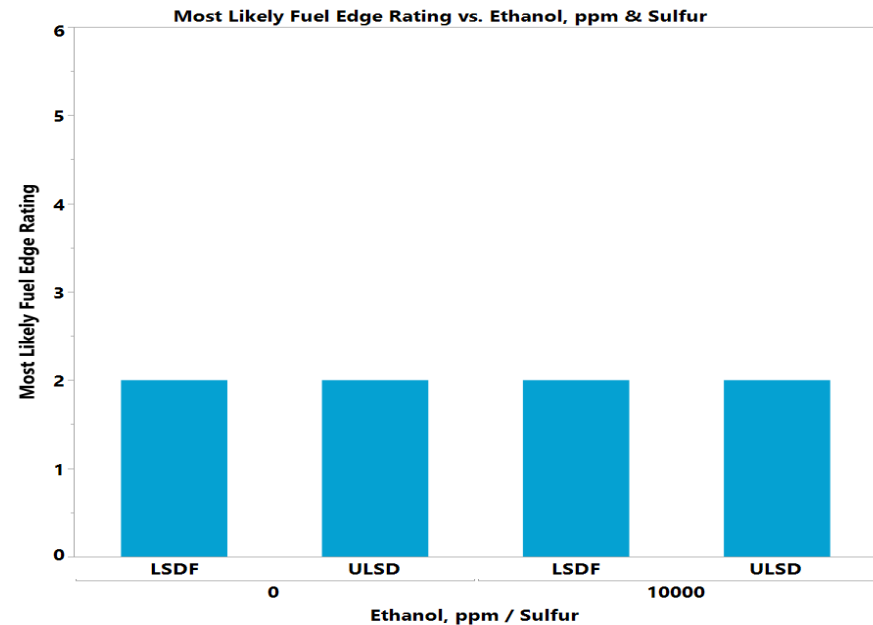
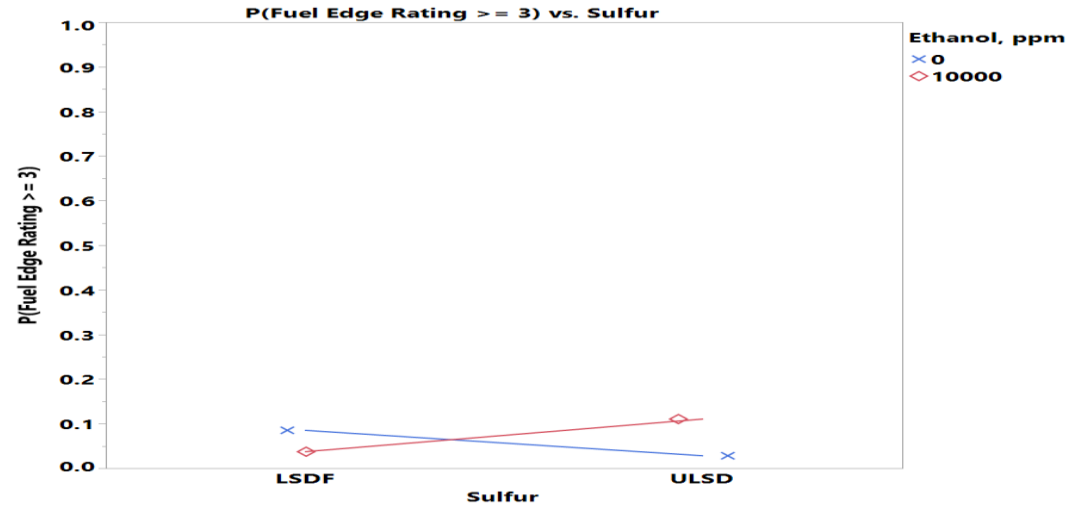
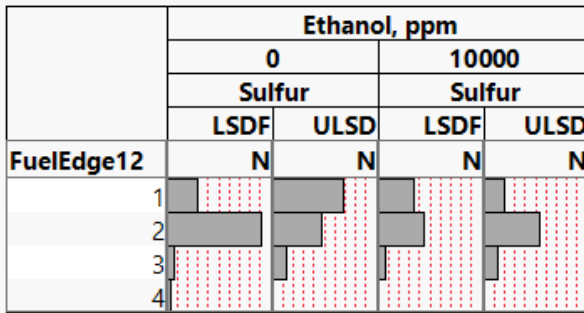
	FRP Material	
	0	Present
FuelEdge12	N	N
1	19	26
2	38	32
3	8	4
4	0	1



Sulfur-Ethanol Interaction Effect

- LSDF has **lower** probability of high corrosion severity than ULSD **with** Ethanol while it has **higher** probability **without** Ethanol

	Ethanol, ppm			
	0		10000	
	Sulfur		Sulfur	
	LSDF	ULSD	LSDF	ULSD
FuelEdge12	N	N	N	N
1	9	20	10	6
2	27	14	13	16
3	2	4	2	4
4	1	0	0	0

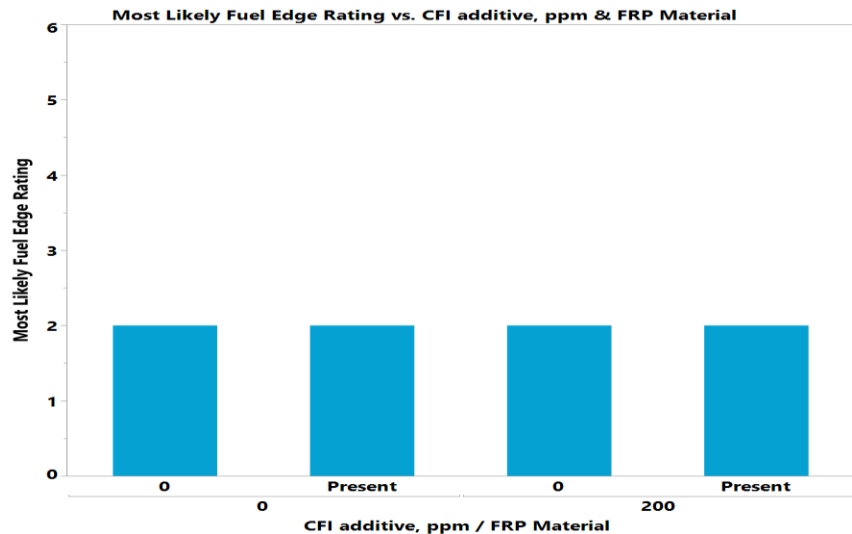
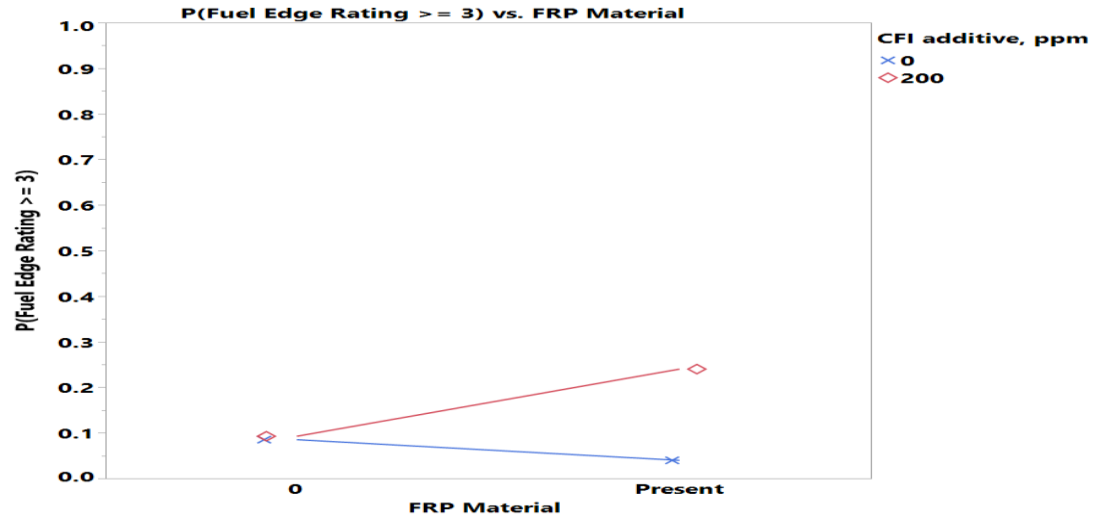


FRP Material-CFI Additive Interaction Effect

- Presence of FRP Material has **lower** probability of high corrosion severity than the absence of FRP Material **without** CFI additive while it has **higher** probability **with** CFI additive

	CFI additive, ppm			
	0		200	
	FRP Material		FRP Material	
	0	Present	0	Present
FuelEdge12	N	N	N	N
1	8	15	11	11
2	18	18	20	14
3	6	0	2	4
4	0	0	0	1

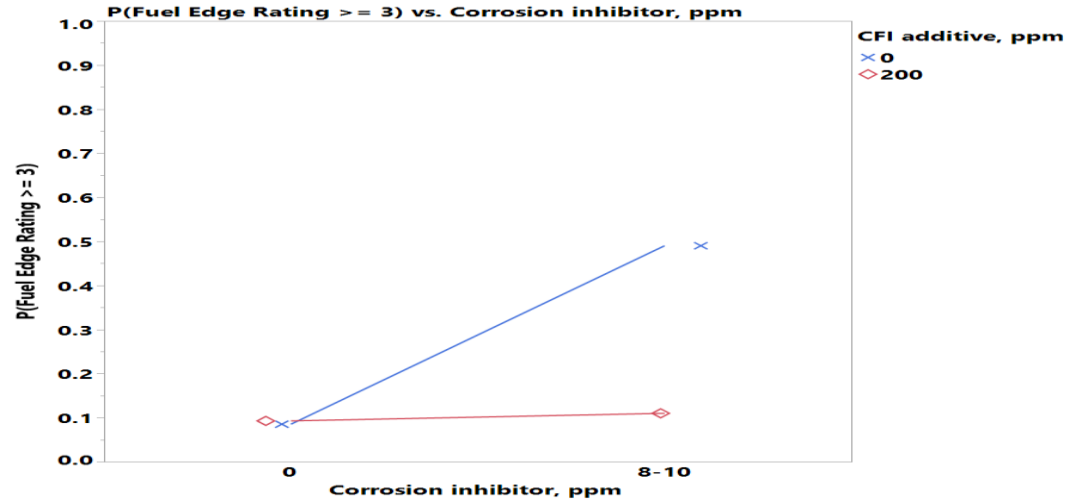
	CFI additive, ppm			
	0		200	
	FRP Material		FRP Material	
	0	Present	0	Present
FuelEdge12	N	N	N	N
1	8	15	11	11
2	18	18	20	14
3	6	0	2	4
4	0	0	0	1



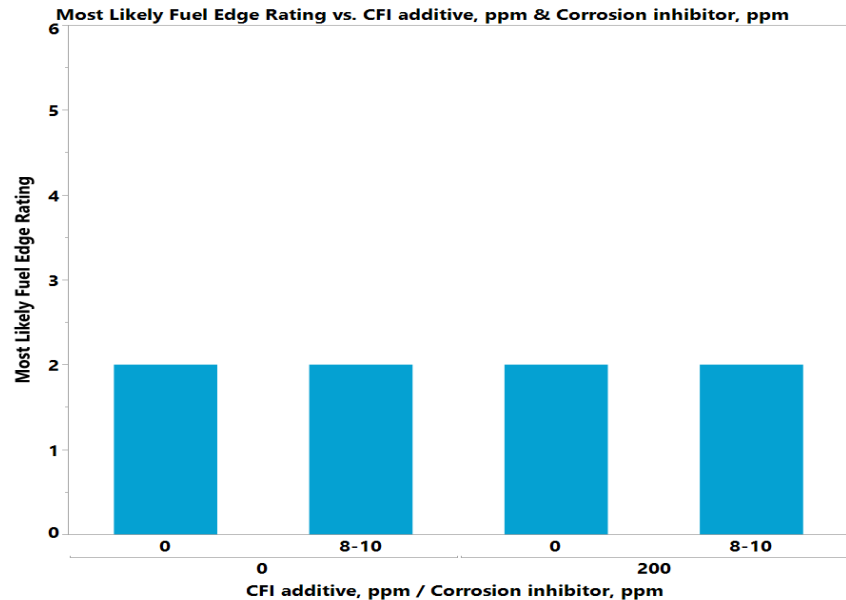
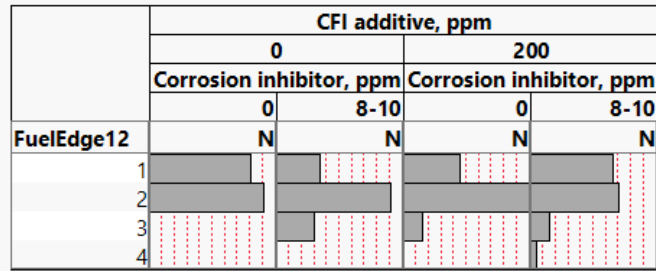
Where((Sulfur = LSDF) and (Water = 0) and (Biodiesel = 0) and (Glycerin = 0) and (Ethanol = 0) and (Corrosion Inhibitor= 0) and (MAL Additive = 0) and (Microbes= 0) and (Conductivity Additive = 0))

Corrosion Inhibitor-CFI Additive Interaction Effect

- 8-10ppm Corrosion inhibitor has **lower** probability of high corrosion severity than zero Corrosion inhibitor more significantly without CFI additive



	CFI additive, ppm			
	0		200	
	Corrosion inhibitor, ppm		Corrosion inhibitor, ppm	
FuelEdge12	0	8-10	0	8-10
	N	N	N	N
1	16	7	9	13
2	18	18	20	14
3	0	6	3	3
4	0	0	0	1

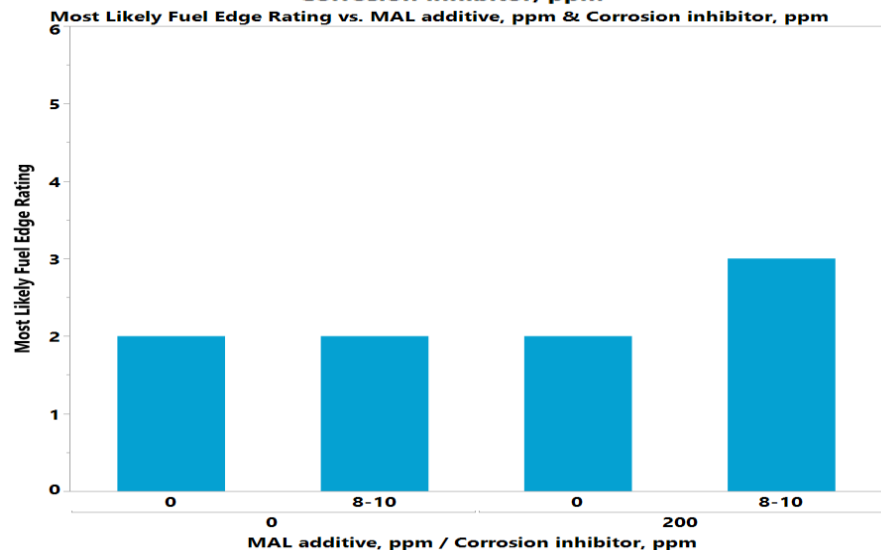
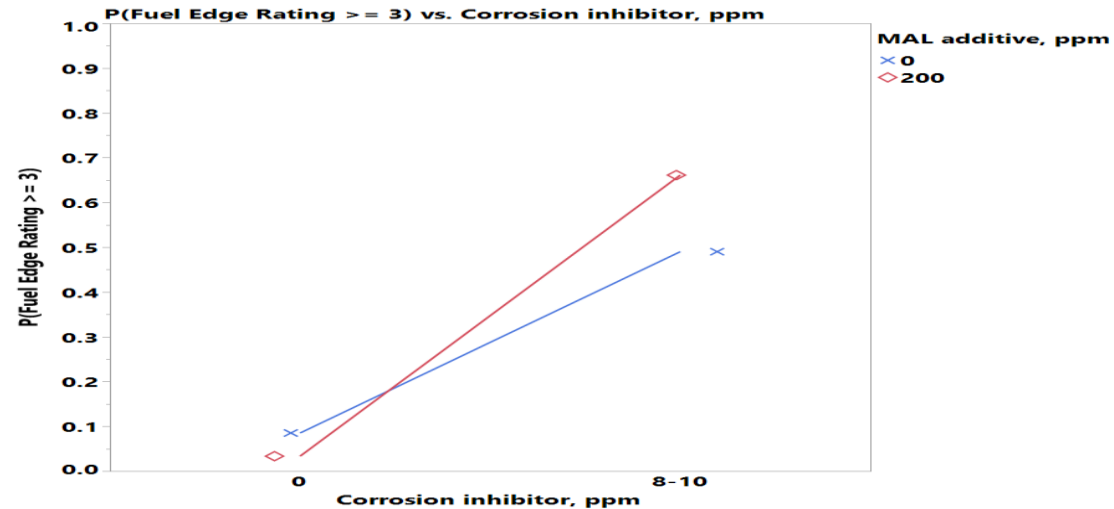
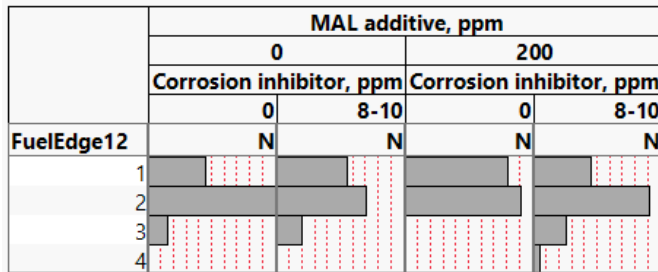


Where((Sulfur = LSDF) and (Water = 0) and (Biodiesel = 0) and (Glycerin = 0) and (Microbes = 0) and (Ethanol= 0) and (FRP Material = 0) and (MAL additive = 0) and (Conductivity Additive = 0))

Corrosion Inhibitor-MAL Additive Interaction Effect

- 8-10ppm Corrosion inhibitor has **higher** probability of high corrosion severity than zero Corrosion inhibitor more significantly with MAL additive

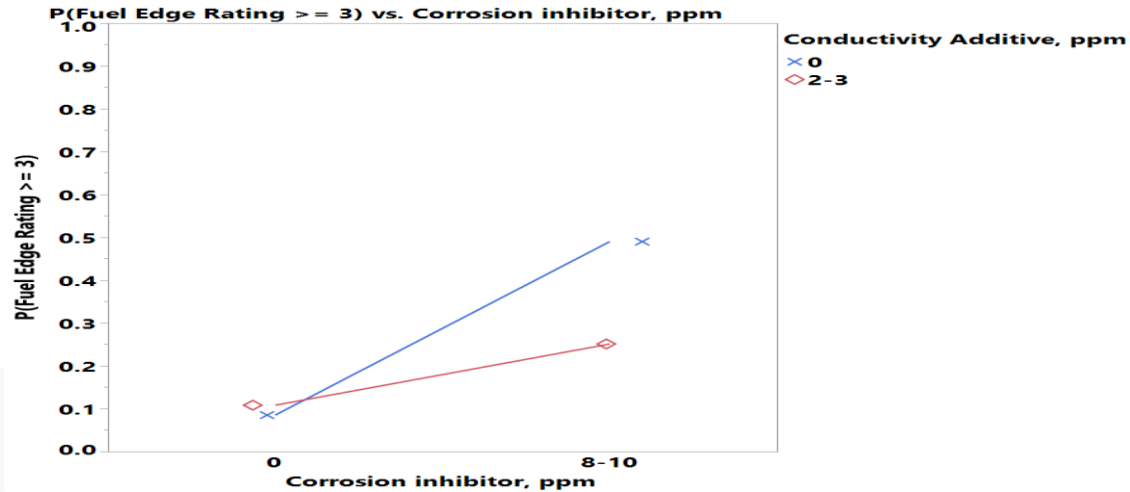
	MAL additive, ppm			
	0		200	
	Corrosion inhibitor, ppm		Corrosion inhibitor, ppm	
	0	8-10	0	8-10
FuelEdge12	N	N	N	N
1	9	11	16	9
2	20	14	18	18
3	3	4	0	5
4	0	0	0	1



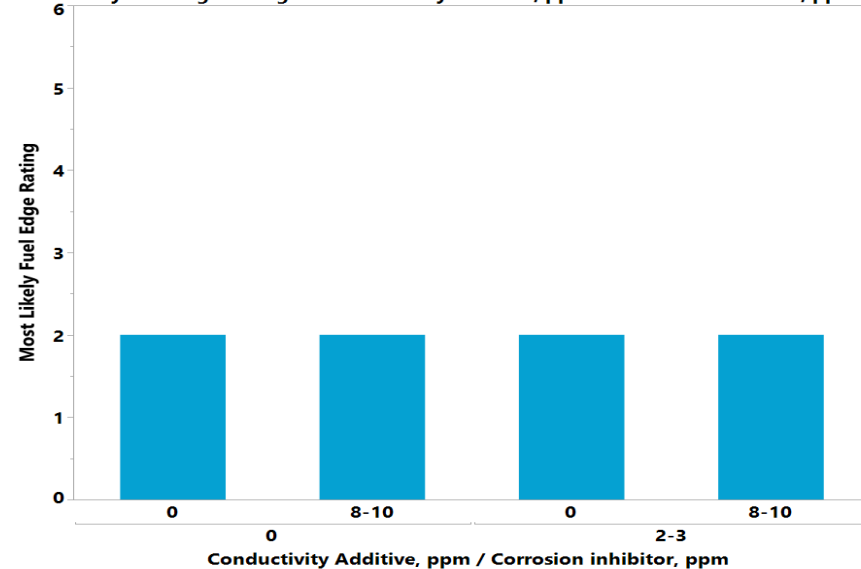
Where((Sulfur = LSDF) and (Water = 0) and (Biodiesel = 0) and (Glycerin = 0) and (Ethanol = 0) and (CFI Additive= 0) and (FRP Material = 0) and (Microbes= 0) and (Conductivity Additive = 0))

Corrosion Inhibitor-Conductivity Additive Interaction Effect

- 8-10ppm Corrosion inhibitor has **higher** probability of high corrosion severity than zero Corrosion inhibitor more significantly without Conductivity additive



Most Likely Fuel Edge Rating vs. Conductivity Additive, ppm & Corrosion inhibitor, ppm



	Conductivity Additive, ppm			
	0		2-3	
	Corrosion inhibitor, ppm		Corrosion inhibitor, ppm	
	0	8-10	0	8-10
FuelEdge12	N	N	N	N
1	13	7	12	13
2	17	16	21	16
3	2	6	1	3
4	0	1	0	0

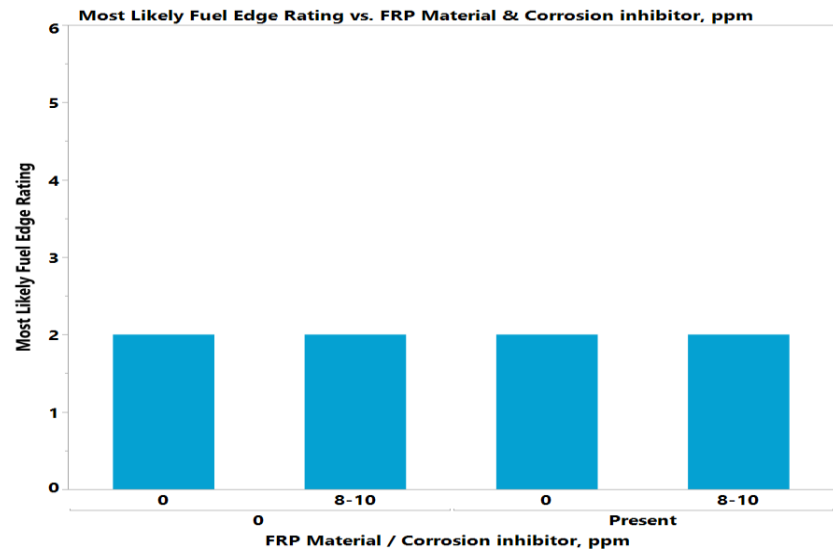
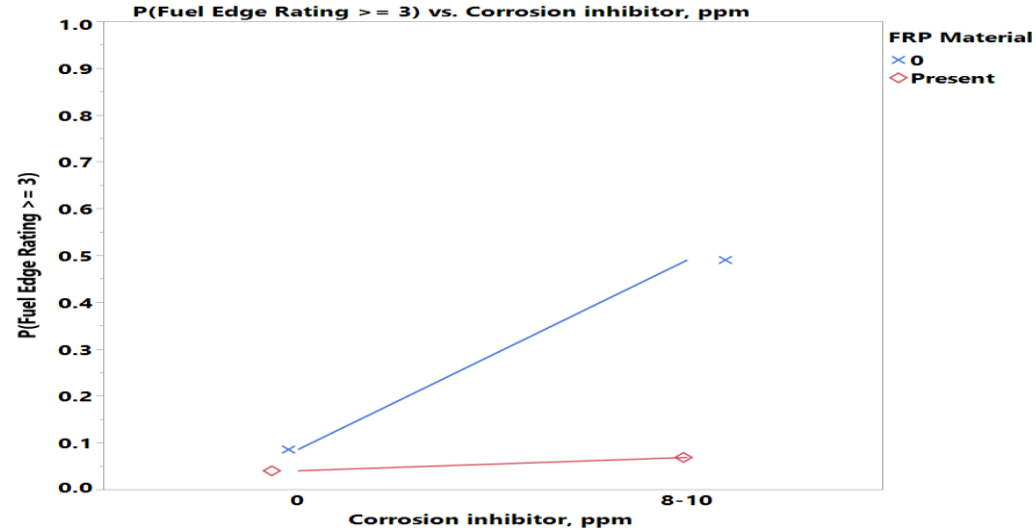
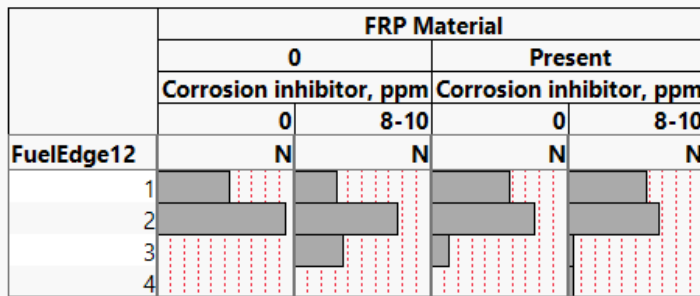
	Conductivity Additive, ppm			
	0		2-3	
	Corrosion inhibitor, ppm		Corrosion inhibitor, ppm	
	0	8-10	0	8-10
FuelEdge12	N	N	N	N
1	13	7	12	13
2	17	16	21	16
3	2	6	1	3
4	0	1	0	0

Where((Sulfur = LSDF) and (Water = 0) and (Biodiesel = 0) and (Glycerin = 0) and (Ethanol = 0) and (CFI Additive= 0) and (FRP Material = 0) and (MAL additive = 0) and (Microbes= 0))

Corrosion Inhibitor-FRP Material Interaction Effect

- 8-10ppm Corrosion inhibitor has **higher** probability of high corrosion severity than zero Corrosion inhibitor more significantly without FRP Material

	FRP Material			
	0		Present	
	Corrosion inhibitor, ppm		Corrosion inhibitor, ppm	
	0	8-10	0	8-10
FuelEdge12	N	N	N	N
1	12	7	13	13
2	21	17	17	15
3	0	8	3	1
4	0	0	0	1



Where((Sulfur = LSDF) and (Water = 0) and (Biodiesel = 0) and (Glycerin = 0) and (Ethanol = 0) and (CFI Additive= 0) and (MAL Additive = 0) and (Microbes= 0) and (Conductivity Additive = 0))

Stepwise Ordinal Logistic Regression

Fuel Edge Phase – All Weeks

Whole Model Test

Model	-LogLikelihood	DF	ChiSquare	Prob>ChiSq
Difference	124.11217	23	248.2243	<.0001*
Full	688.67957			
Reduced	812.79174			

RSquare (U)	0.1527
AICc	1430.97
BIC	1554.11
Observations (or Sum Wgts)	896

Fit Details

Measure	Training	Definition
Entropy RSquare	0.1527	$1 - \text{Loglike}(\text{model}) / \text{Loglike}(0)$
Generalized RSquare	0.2891	$(1 - (L(0)/L(\text{model}))^{2/n}) / (1 - L(0)^{2/n})$
Mean -Log p	0.7686	$\sum -\text{Log}(p[j]) / n$
RMSE	0.5181	$\sqrt{\sum (y[j] - p[j])^2 / n}$
Mean Abs Dev	0.4758	$\sum y[j] - p[j] / n$
Misclassification Rate	0.3717	$\sum (p[j] \neq \text{pMax}) / n$
N	896	n

Lack Of Fit

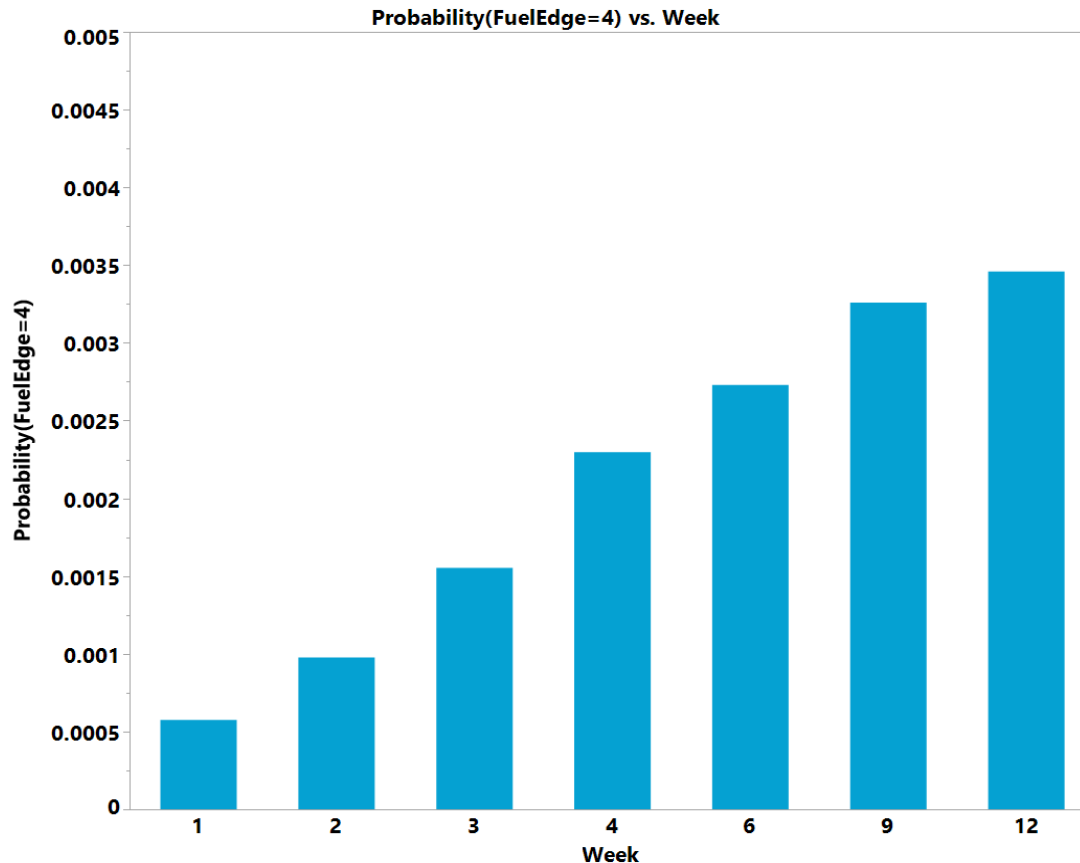
Source	DF	-LogLikelihood	ChiSquare
Lack Of Fit	2662	688.67957	1377.359
Saturated	2685	0.00000	Prob>ChiSq
Fitted	23	688.67957	1.0000

Parameter Estimates

Term	Estimate	Std Error	ChiSquare	Prob>ChiSq
Intercept[1]	1.19159904	0.2321494	26.35	<.0001*
Intercept[2]	4.48560673	0.2857018	246.50	<.0001*
Intercept[3]	7.7746791	0.6418287	146.73	<.0001*
Sulfur[LSDF]	-0.1025527	0.0720123	2.03	0.1544
Biodiesel[0]	-0.0284259	0.0710187	0.16	0.6890
Water[0]	0.2357536	0.1170398	4.06	0.0440*
Glycerin[0]	-0.002455	0.0772807	0.00	0.9747
Ethanol[0]	0.00951662	0.078373	0.01	0.9034
Mircobes[0]	-0.0317495	0.0776302	0.17	0.6826
MAL additive[0]	0.09677358	0.0710808	1.85	0.1734
CFI additive[0]	0.03943924	0.0709165	0.31	0.5781
Corrosion inhibitor[0]	0.22219011	0.0713831	9.69	0.0019*
Conductivity Additive[0]	-0.216684	0.0715423	9.17	0.0025*
FRP Material[0]	-0.3353889	0.0717699	21.84	<.0001*
Sulfur[LSDF]*Ethanol[0]	-0.5457027	0.0743142	53.92	<.0001*
MAL additive[0]*Corrosion inhibitor[0]	-0.2507227	0.0717608	12.21	0.0005*
CFI additive[0]*Corrosion inhibitor[0]	0.25639804	0.071929	12.71	0.0004*
CFI additive[0]*FRP Material[0]	-0.371069	0.0727192	26.04	<.0001*
Corrosion inhibitor[0]*Conductivity Additive[0]	0.36287703	0.0718653	25.50	<.0001*
Corrosion inhibitor[0]*FRP Material[0]	0.34825207	0.0722395	23.24	<.0001*
Week[2-1]	-0.5319419	0.2849273	3.49	0.0619
Week[3-2]	-0.4634271	0.267421	3.00	0.0831
Week[4-3]	-0.3919054	0.2589518	2.29	0.1302
Week[6-4]	-0.1732748	0.2555932	0.46	0.4978
Week[9-6]	-0.1774339	0.2546552	0.49	0.4860
Week[12-9]	-0.0601959	0.2541676	0.06	0.8128

Corrosion by Time (Week)

- Marginal weekly **increases** in probability of high corrosion severity between weeks 1 & 2 and weeks 2 & 3.



Where((Sulfur = LSDF) and (Water = 0) and (Biodiesel = 0) and (Glycerin = 0) and (Ethanol = 0) and (Microbes = 0) and (MAL additive = 0) and (CFI additive = 0) and (Corrosion Inhibitor = 0) and (Conductivity Additive = 0) and (FRP Material = 0))

Vapor Phase

Conclusions (Vapor Phase)

Average Corrosion Severity Rating (average of 3 samples)

- 8-10ppm Corrosion inhibitor has **lower** probability of high corrosion severity than zero Corrosion inhibitor

Average Corrosion Severity Rating by Time (Week)

- No significant weekly increases in probability of high corrosion severity

Stepwise Ordinal Logistic Regression

Vapor Phase – Week 12

Whole Model Test				
Model	-LogLikelihood	DF	ChiSquare	Prob>ChiSq
Difference	5.770556	11	11.54111	0.3991
Full	50.071850			
Reduced	55.842407			
RSquare (U)	0.1033			
AICc	129.337			
BIC	163.22			
Observations (or Sum Wgts)	128			
Fit Details				
Measure	Training	Definition		
Entropy RSquare	0.1033	1-Loglike(model)/Loglike(0)		
Generalized RSquare	0.1481	$(1-(L(0)/L(model))^{2/n})/(1-L(0)^{2/n})$		
Mean -Log p	0.3912	$\sum -\log(p[j])/n$		
RMSE	0.3408	$\sqrt{\sum (y[j]-p[j])^2/n}$		
Mean Abs Dev	0.2237	$\sum y[j]-p[j] /n$		
Misclassification Rate	0.1406	$\sum (p[j] \neq pMax)/n$		
N	128	n		
Lack Of Fit				
Source	DF	-LogLikelihood	ChiSquare	
Lack Of Fit	243	50.071850	100.1437	
Saturated	254	0.000000	Prob>ChiSq	
Fitted	11	50.071850	1.0000	

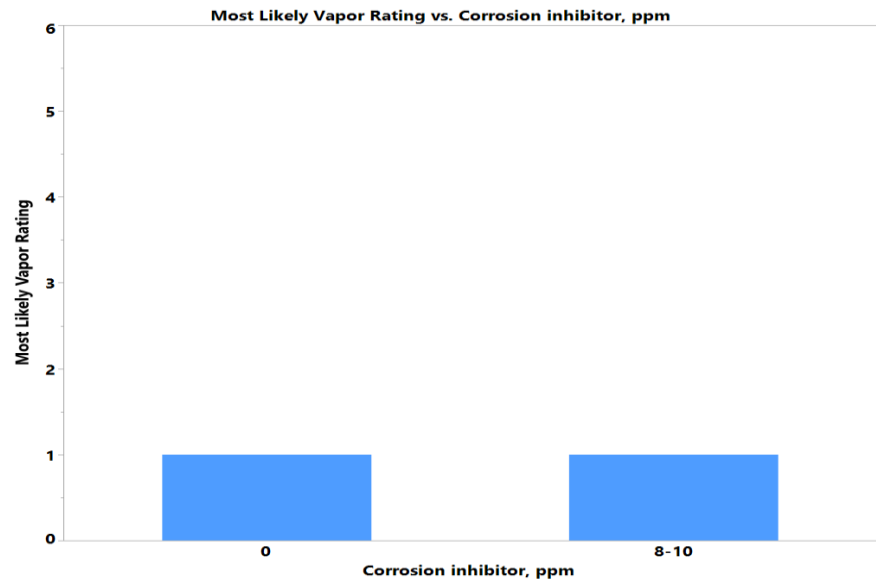
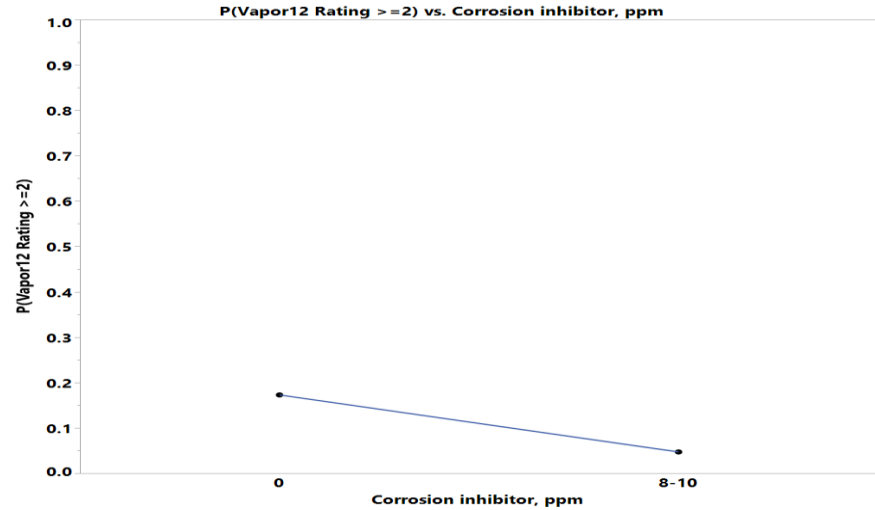
Parameter Estimates				
Term	Estimate	Std Error	ChiSquare	Prob>ChiSq
Intercept[1]	2.09914321	0.4684941	20.08	<.0001*
Intercept[2]	5.23609511	1.0808277	23.47	<.0001*
Sulfur[LSDf]	-0.0356523	0.2677398	0.02	0.8941
Biodiesel, %[0]	0.19062982	0.2712432	0.49	0.4822
Water[0]	-0.2135916	0.3967507	0.29	0.5903
Glycerin, ppm[0]	-0.2103409	0.3141134	0.45	0.5031
Ethanol, ppm[0]	-0.2309558	0.3139263	0.54	0.4619
Mircobes[0]	0.09501979	0.3101981	0.09	0.7594
MAL additive, ppm[0]	0.39704795	0.2809151	2.00	0.1575
CFI additive, ppm[0]	-0.059196	0.2683056	0.05	0.8254
Corrosion inhibitor, ppm[0]	-0.7219821	0.3080245	5.49	0.0191*
Conductivity Additive, ppm[0]	0.10948965	0.2684073	0.17	0.6833
FRP Material[0]	0.14762355	0.2684103	0.30	0.5823

Corrosion Inhibitor Effect – Vapor Phase

- 8-10ppm Corrosion inhibitor has **lower** probability of high corrosion severity than zero Corrosion inhibitor

	Corrosion inhibitor, ppm	
	0	8-10
Vapor12	N	N
1	52	58
2	13	4
3	1	0

	Corrosion inhibitor, ppm	
	0	8-10
Vapor12	N	N
1		
2		
3		



Ordinal Logistic Regression

Vapor Phase – All Weeks

Whole Model Test

Model	-LogLikelihood	DF	ChiSquare	Prob>ChiSq
Difference	41.15762	17	82.31524	<.0001*
Full	267.17365			
Reduced	308.33127			

RSquare (U)	0.1335
AICc	573.215
BIC	663.508
Observations (or Sum Wgts)	896

Fit Details

Measure	Training	Definition
Entropy RSquare	0.1335	1-Loglike(model)/Loglike(0)
Generalized RSquare	0.1764	$(1-(L(0)/L(model))^{(2/n)})/(1-L(0)^{(2/n)})$
Mean -Log p	0.2982	$\sum -\log(\rho[j])/n$
RMSE	0.2963	$\sqrt{\sum (y[j]-\rho[j])^2/n}$
Mean Abs Dev	0.1709	$\sum y[j]-\rho[j] /n$
Misclassification Rate	0.1060	$\sum (\rho[j] \neq \rho_{Max})/n$
N	896	n

Lack Of Fit

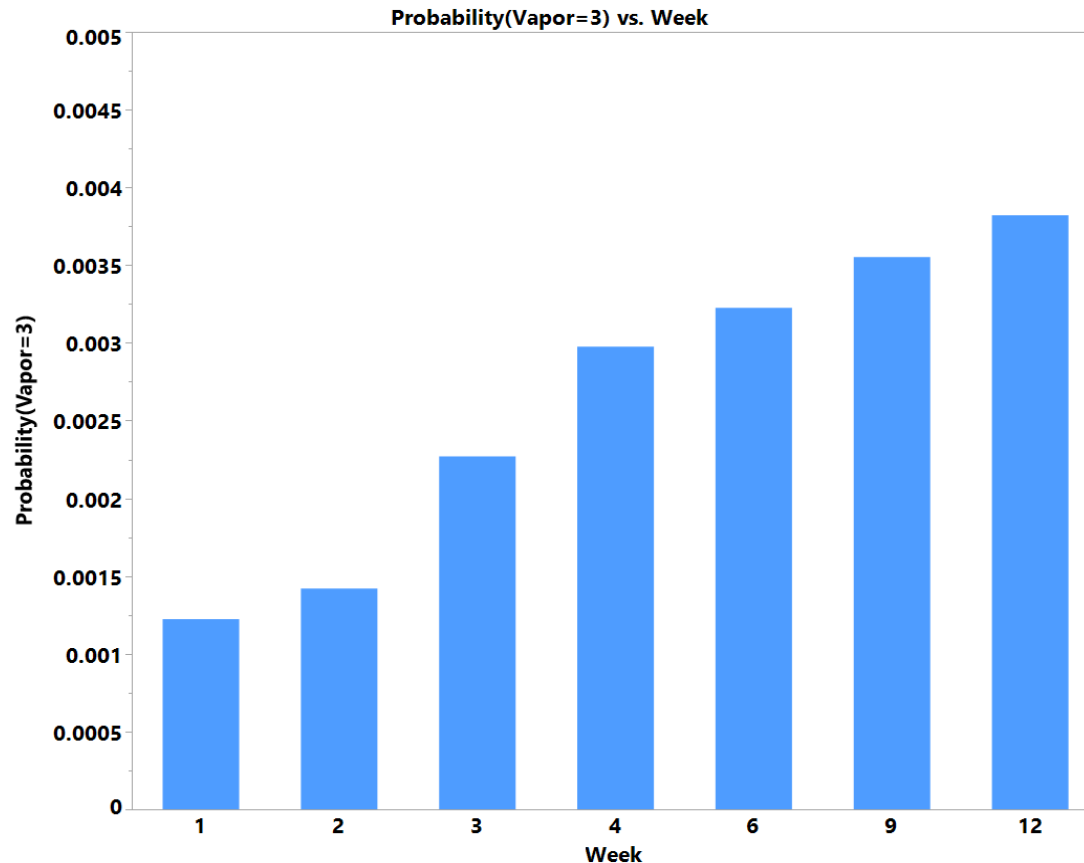
Source	DF	-LogLikelihood	ChiSquare
Lack Of Fit	1773	267.17365	534.3473
Saturated	1790	0.00000	Prob>ChiSq
Fitted	17	267.17365	1.0000

Parameter Estimates

Term	Estimate	Std Error	ChiSquare	Prob>ChiSq
Intercept[1]	3.3090726	0.439762	56.62	<.0001*
Intercept[2]	7.35728236	0.8224963	80.01	<.0001*
Sulfur[LSDf]	-0.1779263	0.116721	2.32	0.1274
Biodiesel[0]	0.23500516	0.1183936	3.94	0.0472*
Water[0]	-0.1754453	0.1728995	1.03	0.3102
Glycerin[0]	-0.219162	0.1356746	2.61	0.1062
Ethanol[0]	-0.0825177	0.133268	0.38	0.5358
Mircobes[0]	0.0360613	0.1329778	0.07	0.7863
MAL additive[0]	0.50762976	0.1255483	16.35	<.0001*
CFI additive[0]	-0.0396595	0.1161781	0.12	0.7328
Corrosion inhibitor[0]	-0.844393	0.1428676	34.93	<.0001*
Conductivity Additive[0]	0.00237859	0.1157402	0.00	0.9836
FRP Material[0]	0.10545649	0.1160902	0.83	0.3637
Week[2-1]	-0.1495365	0.5484359	0.07	0.7851
Week[3-2]	-0.4693246	0.4914888	0.91	0.3396
Week[4-3]	-0.2716056	0.4284771	0.40	0.5262
Week[6-4]	-0.0809839	0.403688	0.04	0.8410
Week[9-6]	-0.0965716	0.3928967	0.06	0.8058
Week[12-9]	-0.0734932	0.3830715	0.04	0.8479

Corrosion by Time (Week)

- No significant weekly increases in probability of high corrosion severity.



Where((Sulfur = LSDF) and (Biodiesel = 0) and (Water = 0) and (Glycerin = 0) and (Ethanol = 0) and (Microbes = 0) and (MAL additive = 0) and (CFI additive = 0) and (Corrosion Inhibitor = 0) and (Conductivity Additive = 0) and (FRP Material = 0))

Vapor Edge Phase

Conclusions (Vapor Edge Phase)

Average Corrosion Severity Rating (average of 3 samples)

- LSDF has significantly **higher** probability of high corrosion severity than ULSD
- 10000ppm Ethanol has **lower** probability of high corrosion severity than zero Ethanol
- Presence of Microbes has **lower** probability of high corrosion severity than absence of Microbes
- 200ppm MAL additive has **higher** probability of high corrosion severity than zero MAL additive
- ULSD has **lower** probability of high corrosion severity than LSDF more significantly without Water
- ULSD has **lower** probability of high corrosion severity than LSDF more significantly with Microbes
- ULSD has **lower** probability of high corrosion severity more significantly without CFI additive
- 5% Biodiesel has **lower** probability of high corrosion severity without Conductivity additive while it has **higher** probability with Conductivity additive
- 5000ppm Glycerin has **higher** probability of high corrosion severity than zero Glycerin more significantly with Ethanol
- 5000ppm Glycerin has **higher** probability of high corrosion severity than zero Glycerin without MAL additive while it has **lower** probability with MAL additive
- 10000ppm Ethanol has **lower** probability of high corrosion severity than zero Ethanol without Microbes while it has **higher** probability with Microbes
- 200ppm MAL additive has **higher** probability of high corrosion severity more significantly with Microbes
- 200ppm MAL additive has **higher** probability of high corrosion severity than zero MAL additive more significantly without FRP Material
- 200ppm CFI additive has **lower** probability of high corrosion severity than zero CFI additive without Microbes
- 200ppm CFI additive has **lower** probability of high corrosion severity than zero CFI additive more significantly without FRP Material

Average Corrosion Severity Rating by Time (Week)

- Significant weekly **increase** in probability of high corrosion severity between weeks 2 and 3

Stepwise Ordinal Logistic Regression

Vapor Edge Phase – Week 12




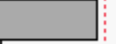


Whole Model Test				
Model	-LogLikelihood	DF	ChiSquare	Prob>ChiSq
Difference	37.07867	22	74.15734	<.0001*
Full	72.10841			
Reduced	109.18708			
RSquare (U)	0.3396			
AICc	203.867			
BIC	260.666			
Observations (or Sum Wgts)	128			
Fit Details				
Measure	Training	Definition		
Entropy RSquare	0.3396	1-Loglike(model)/Loglike(0)		
Generalized RSquare	0.5373	$(1-(L(0)/L(model))^{(2/n)})/(1-L(0)^{(2/n)})$		
Mean -Log p	0.5633	$\sum -\log(p[j])/n$		
RMSE	0.4387	$\sqrt{\sum (y[j]-p[j])^2/n}$		
Mean Abs Dev	0.3661	$\sum y[j]-p[j] /n$		
Misclassification Rate	0.3125	$\sum (p[j] \neq pMax)/n$		
N	128	n		
Lack Of Fit				
Source	DF	-LogLikelihood	ChiSquare	
Lack Of Fit	232	72.108409	144.2168	
Saturated	254	0.000000	Prob>ChiSq	
Fitted	22	72.108409	1.0000	

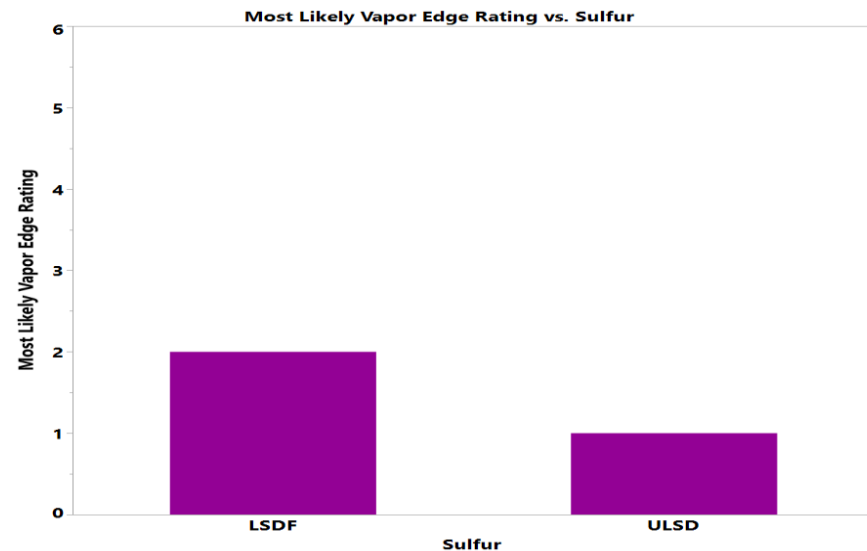
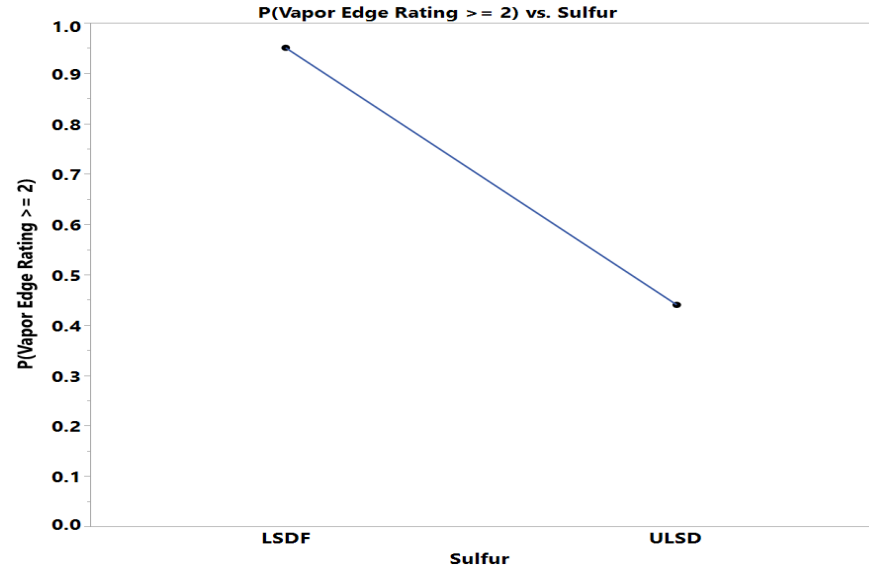
Parameter Estimates				
Term	Estimate	Std Error	ChiSquare	Prob>ChiSq
Intercept[1]	-0.9502933	0.4150776	5.24	0.0221*
Intercept[2]	4.65462269	0.7588687	37.62	<.0001*
Sulfur[LSDF]	-0.9448946	0.3268755	8.36	0.0038*
Biodiesel, %[0]	-0.0913234	0.2167017	0.18	0.6734
Water[0]	0.06545512	0.3901074	0.03	0.8668
Glycerin, ppm[0]	0.31871628	0.2360489	1.82	0.1769
Ethanol, ppm[0]	0.49793969	0.2403154	4.29	0.0383*
Mircobes[0]	1.00073103	0.2684625	13.90	0.0002*
MAL additive, ppm[0]	0.57013865	0.2370865	5.78	0.0162*
CFI additive, ppm[0]	0.06408712	0.2185573	0.09	0.7693
Corrosion inhibitor, ppm[0]	-0.0711371	0.2141625	0.11	0.7398
Conductivity Additive, ppm[0]	-0.2780122	0.2174731	1.63	0.2011
FRP Material[0]	0.17698932	0.2173389	0.66	0.4154
Sulfur[LSDF]*Water[0]	-0.6850694	0.3224266	4.51	0.0336*
Sulfur[LSDF]*Mircobes[0]	0.55655106	0.2431582	5.24	0.0221*
Sulfur[LSDF]*CFI additive, ppm[0]	-0.5240349	0.2219753	5.57	0.0182*
Biodiesel, %[0]*Conductivity Additive, ppm[0]	-0.5721203	0.2249411	6.47	0.0110*
Glycerin, ppm[0]*Ethanol, ppm[0]	-0.4116634	0.2411353	2.91	0.0878
Glycerin, ppm[0]*MAL additive, ppm[0]	0.54227438	0.2295042	5.58	0.0181*
Ethanol, ppm[0]*Mircobes[0]	-0.7030588	0.2487142	7.99	0.0047*
Mircobes[0]*MAL additive, ppm[0]	-0.5586439	0.2356354	5.62	0.0177*
Mircobes[0]*CFI additive, ppm[0]	-0.8923464	0.2401072	13.81	0.0002*
MAL additive, ppm[0]*FRP Material[0]	0.36065092	0.2205178	2.67	0.1019
CFI additive, ppm[0]*FRP Material[0]	-0.4247211	0.2192966	3.75	0.0528

Sulfur Effect – Vapor Edge Phase

- LSDF has significantly **higher** probability of high corrosion severity than ULSD

	Sulfur	
	LSDF	ULSD
VaporEdge12	N	N
1	21	29
2	38	33
3	5	2

	Sulfur	
	LSDF	ULSD
VaporEdge12	N	N
1		
2		
3		

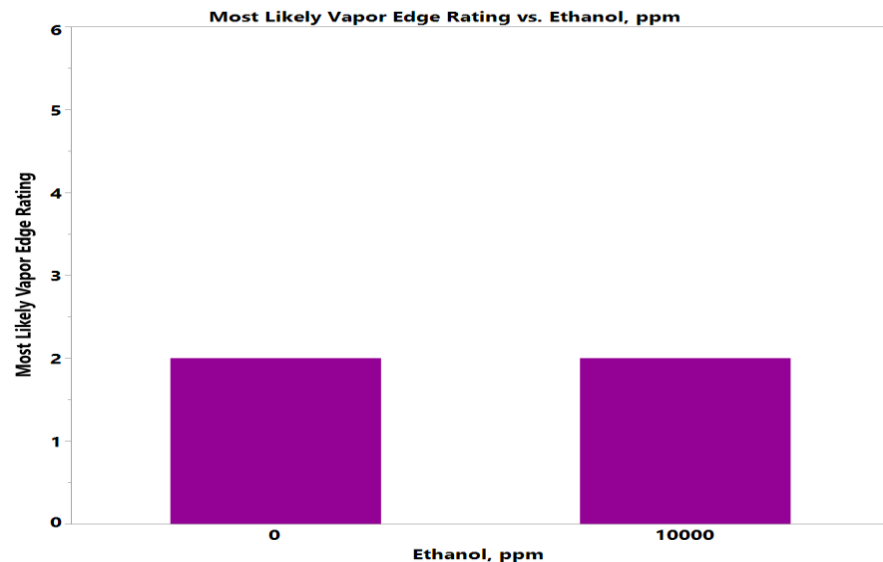
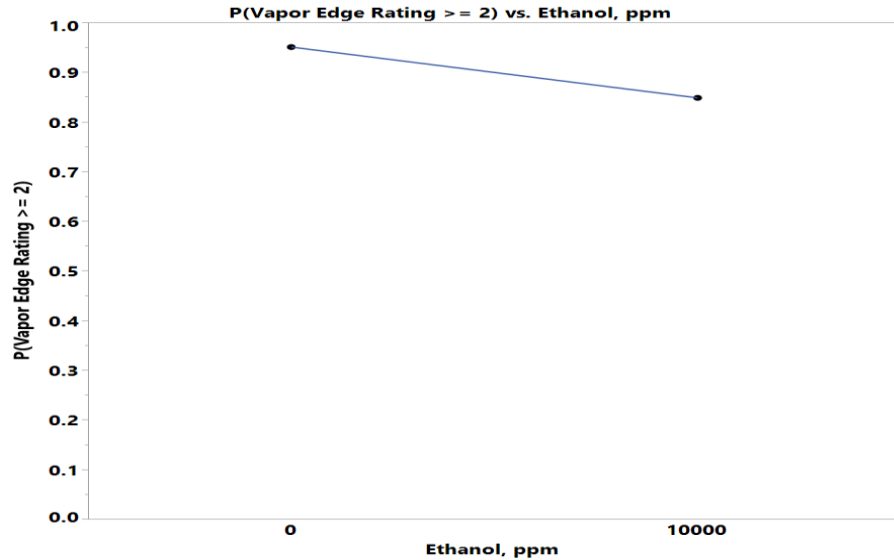


Ethanol Effect – Vapor Edge Phase

- 10000ppm Ethanol has **lower** probability of high corrosion severity than zero Ethanol

	Ethanol, ppm	
	0	10000
VaporEdge12	N	N
1	33	17
2	42	29
3	2	5

	Ethanol, ppm	
	0	10000
VaporEdge12	N	N
1		
2		
3		

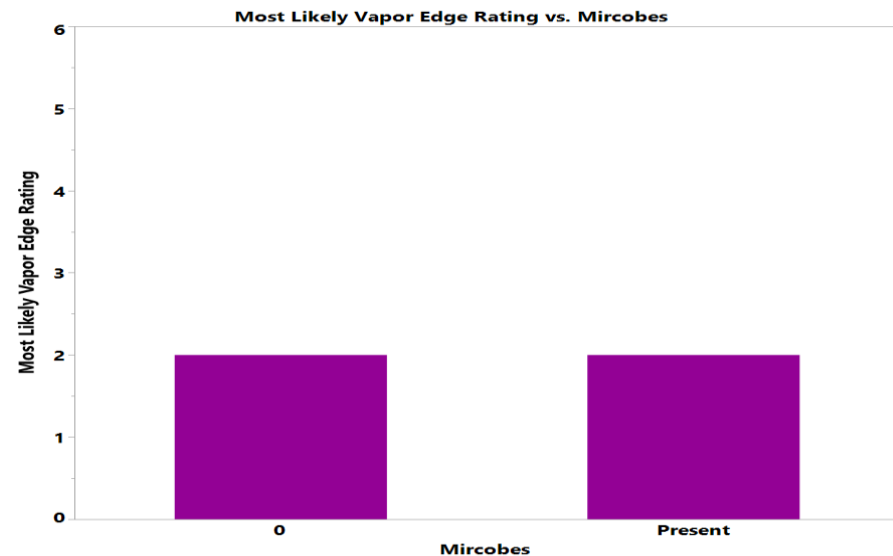
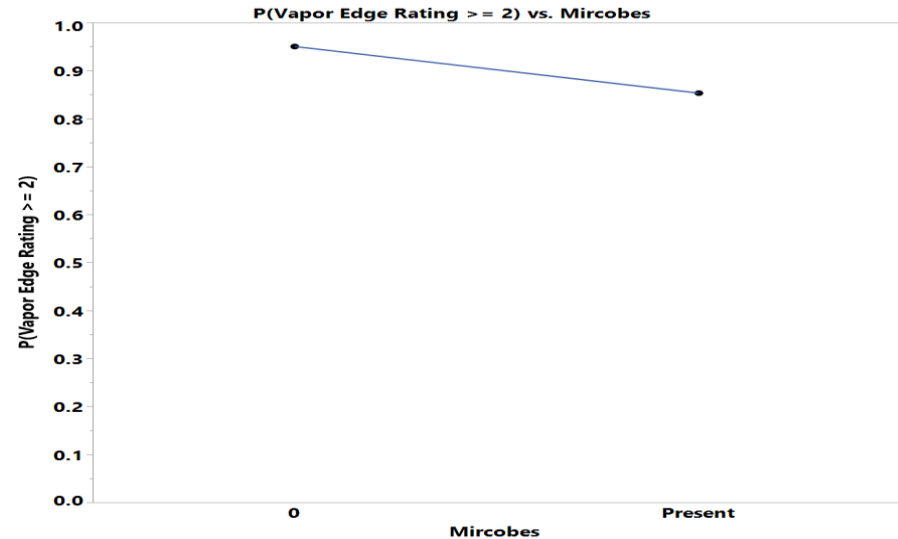


Microbes Effect – Vapor Edge Phase

- Presence of Microbes has **lower** probability of high corrosion severity than absence of Microbes

	Microbes	
	0	Present
VaporEdge12	N	N
1	35	15
2	37	34
3	1	6

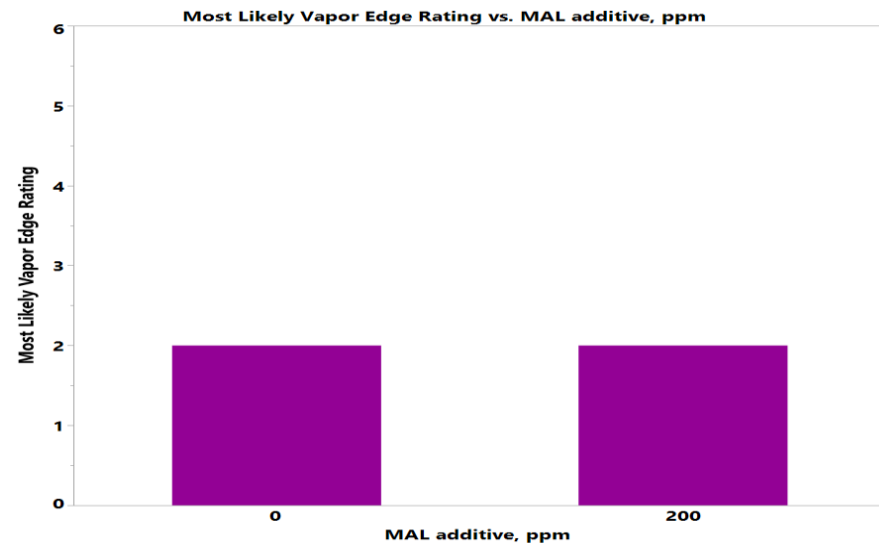
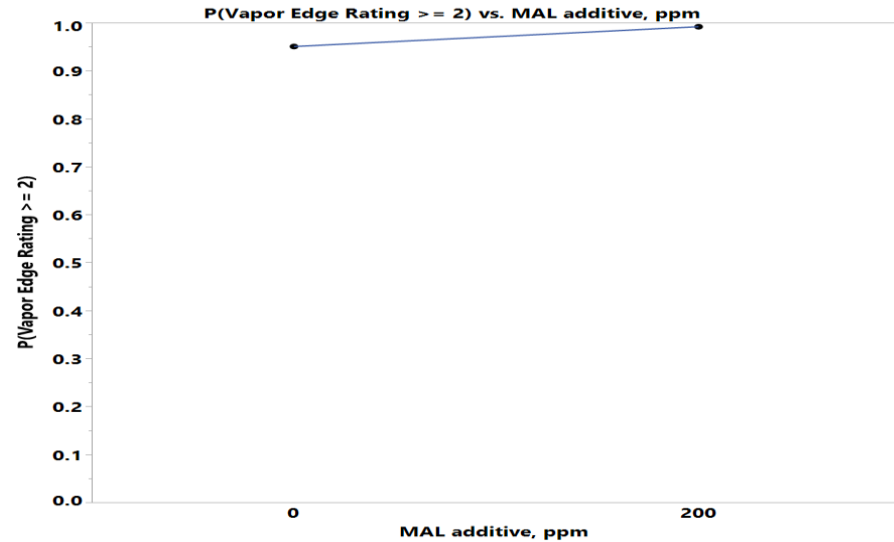
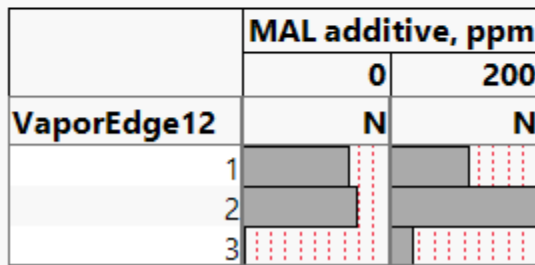
	Microbes	
	0	Present
VaporEdge12	N	N
1		
2		
3		



MAL Additive Effect – Vapor Edge Phase

- 200ppm MAL additive has **higher** probability of high corrosion severity than zero MAL additive

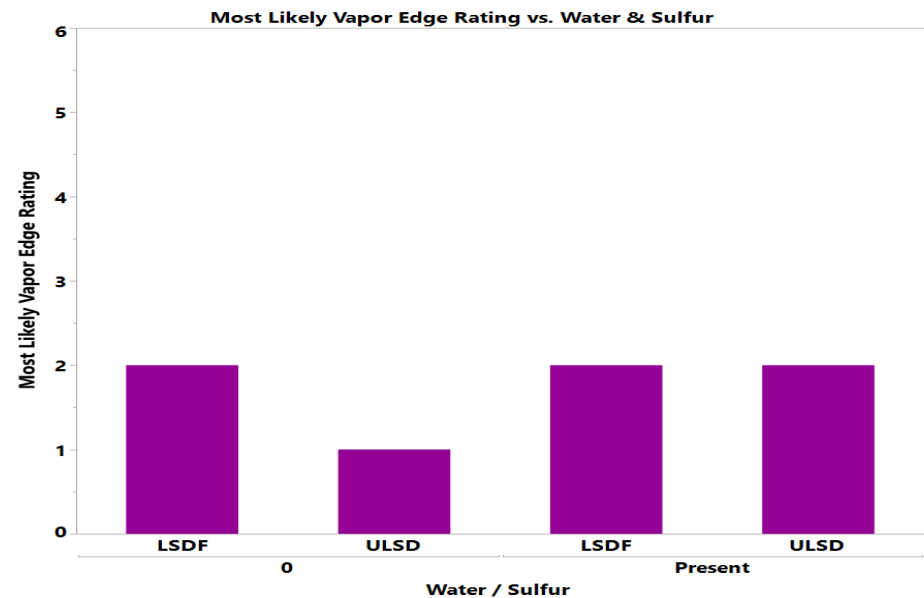
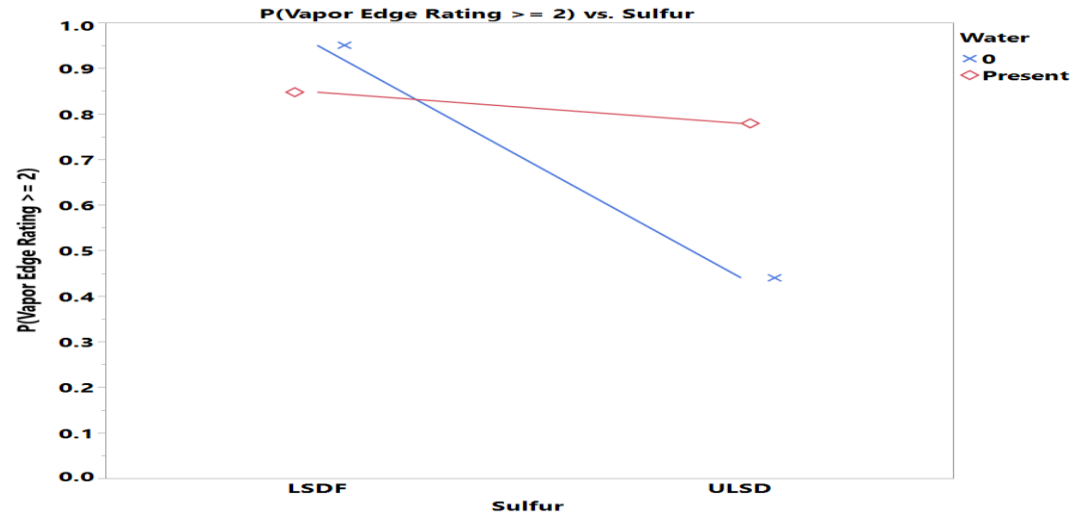
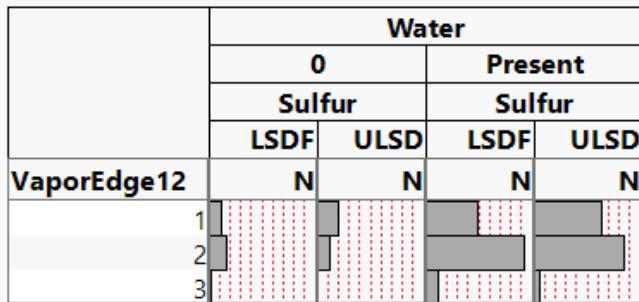
		MAL additive, ppm	
		0	200
VaporEdge12		N	N
1		29	21
2		31	40
3		1	6



Sulfur-Water Interaction Effect

- ULSD has **lower** probability of high corrosion severity than LSDF more significantly without Water

	Water			
	0		Present	
	Sulfur		Sulfur	
	LSDF	ULSD	LSDF	ULSD
VaporEdge12	N	N	N	N
1	4	7	17	22
2	6	4	32	29
3	1	0	4	2

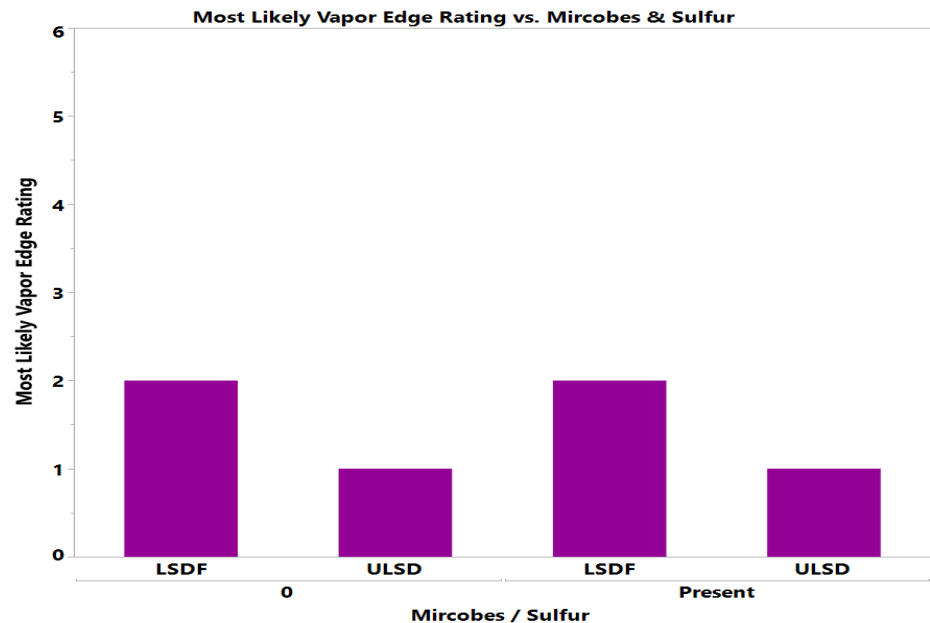
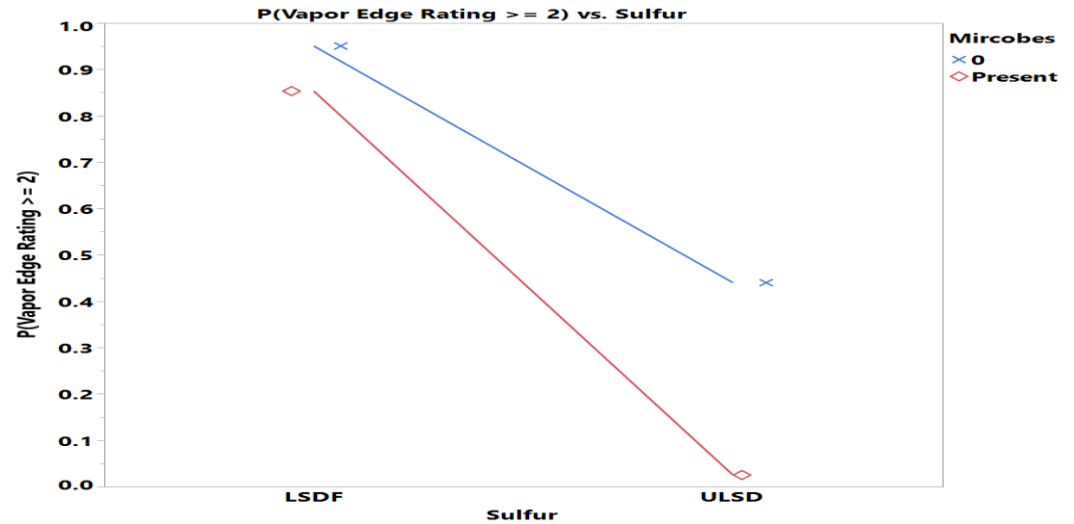


Sulfur-Microbes Interaction Effect

- ULSD has **lower** probability of high corrosion severity than LSDF more significantly with Microbes

	Microbes			
	0		Present	
	Sulfur		Sulfur	
	LSDF	ULSD	LSDF	ULSD
VaporEdge12	N	N	N	N
1	17	18	4	11
2	19	18	19	15
3	1	0	4	2

	Microbes			
	0		Present	
	Sulfur		Sulfur	
	LSDF	ULSD	LSDF	ULSD
VaporEdge12	N	N	N	N
1	[Bar chart showing counts for Microbes=0, Sulfur=LSDF]		[Bar chart showing counts for Microbes=Present, Sulfur=LSDF]	
2	[Bar chart showing counts for Microbes=0, Sulfur=ULSD]		[Bar chart showing counts for Microbes=Present, Sulfur=ULSD]	
3	[Bar chart showing counts for Microbes=0, Sulfur=LSDF]		[Bar chart showing counts for Microbes=Present, Sulfur=ULSD]	



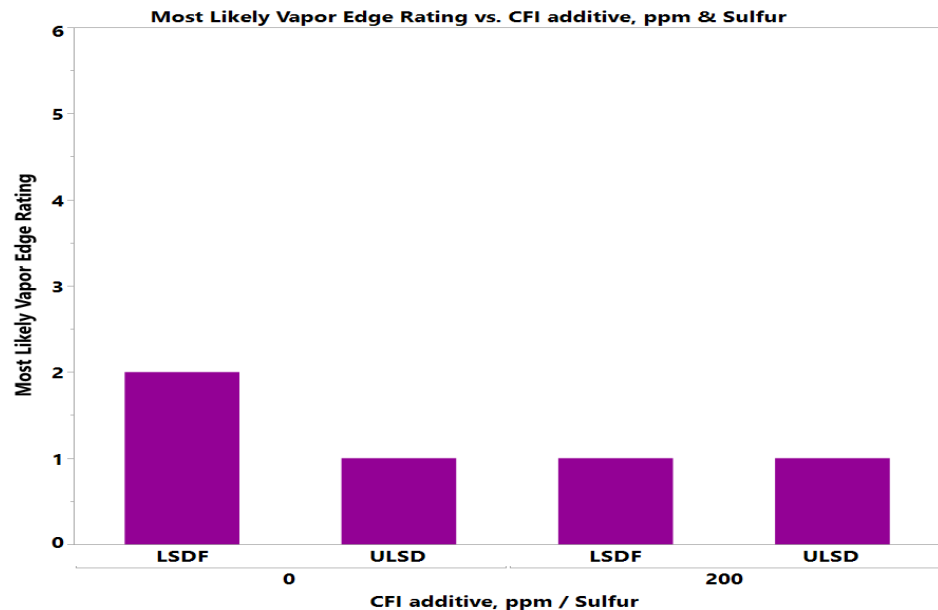
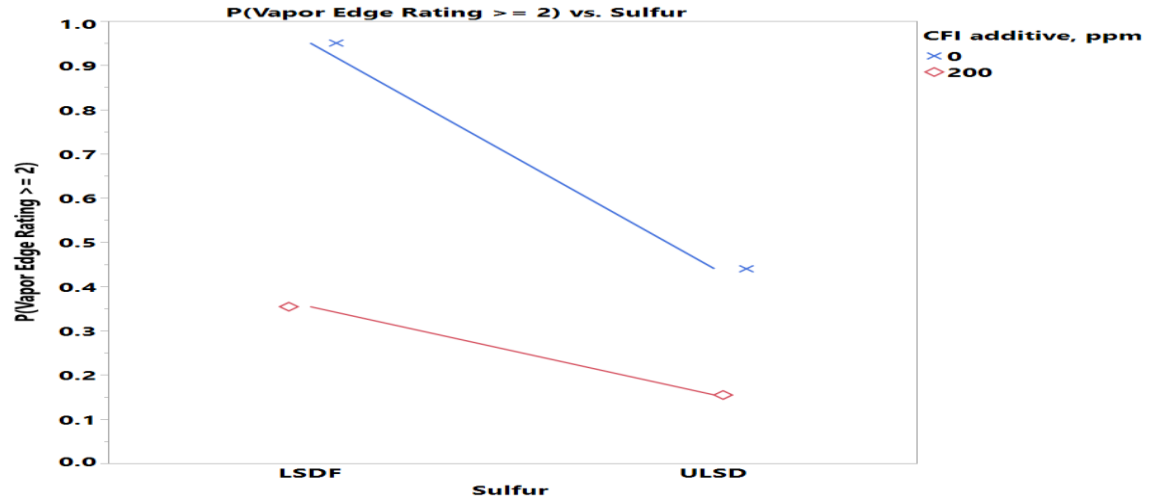
Where((Glycerin = 0) and (Water = 0) and (Biodiesel = 0) and (MAL additive = 0) and (CFI additive = 0) and (Corrosion inhibitor = 0) and (Conductivity Additive = 0) and (FRP Material = 0) and (Corrosion inhibitor = 0))

Sulfur-CFI Additive Interaction Effect

- ULSD has **lower** probability of high corrosion severity more significantly without CFI additive

	CFI additive, ppm			
	0		200	
	Sulfur		Sulfur	
	LSDF	ULSD	LSDF	ULSD
VaporEdge12	N	N	N	N
1	7	15	14	14
2	24	17	14	16
3	2	0	3	2

	CFI additive, ppm			
	0		200	
	Sulfur		Sulfur	
	LSDF	ULSD	LSDF	ULSD
VaporEdge12	N	N	N	N
1				
2				
3				

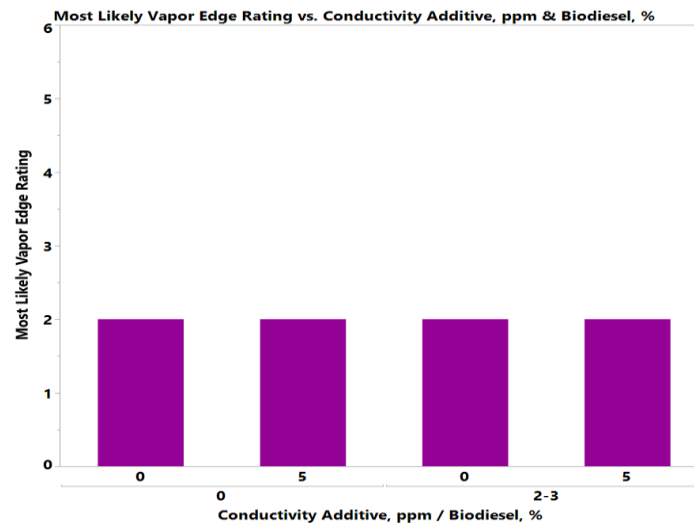
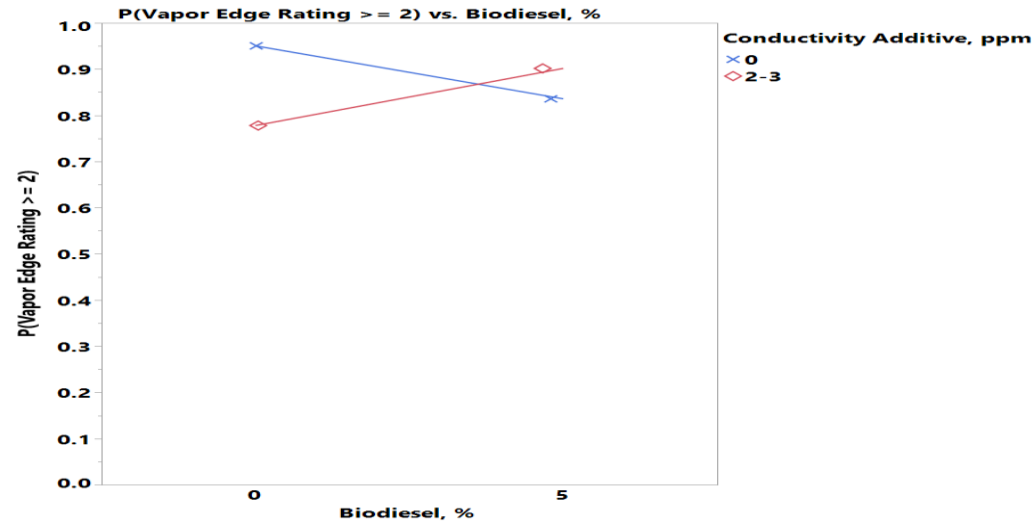


Biodiesel-Conductivity Additive Interaction Effect

- 5% Biodiesel has **lower** probability of high corrosion severity **without** Conductivity additive while it has **higher** probability **with** Conductivity additive

	Conductivity Additive, ppm			
	0		2-3	
	Biodiesel, %		Biodiesel, %	
	0	5	0	5
VaporEdge12	N	N	N	N
1	8	14	16	12
2	20	16	16	19
3	3	1	1	2

	Conductivity Additive, ppm			
	0		2-3	
	Biodiesel, %		Biodiesel, %	
	0	5	0	5
VaporEdge12	N	N	N	N
1				
2				
3				

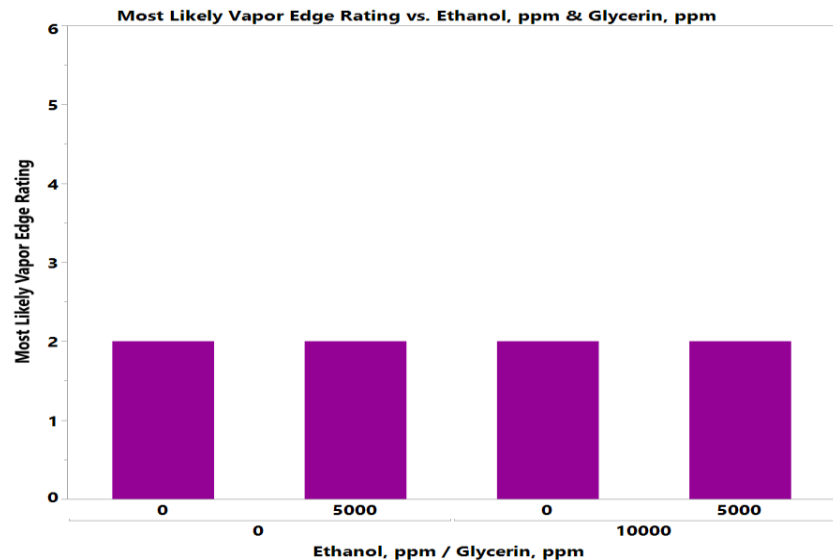
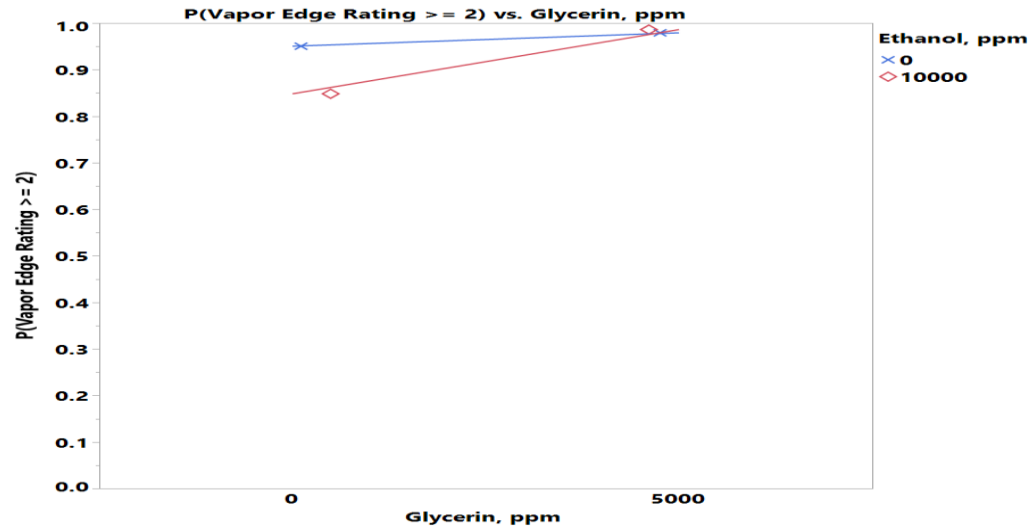


Glycerin-Ethanol Interaction Effect

- 5000ppm Glycerin has **higher** probability of high corrosion severity than zero Glycerin more significantly with Ethanol

	Ethanol, ppm			
	0		10000	
	Glycerin, ppm		Glycerin, ppm	
	0	5000	0	5000
VaporEdge12	N	N	N	N
1	22	11	12	5
2	26	16	13	16
3	2	0	2	3

	Ethanol, ppm			
	0		10000	
	Glycerin, ppm		Glycerin, ppm	
	0	5000	0	5000
VaporEdge12	N	N	N	N
1				
2				
3				

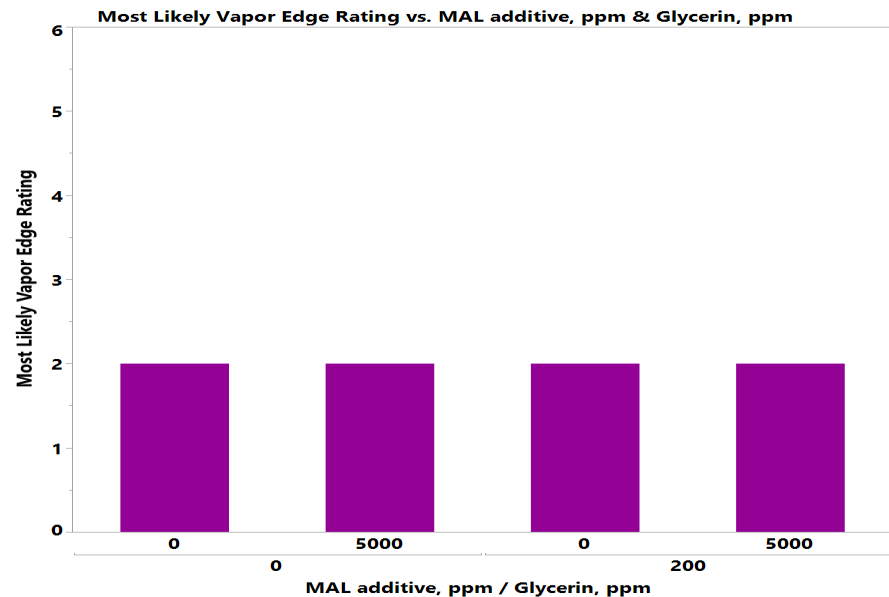
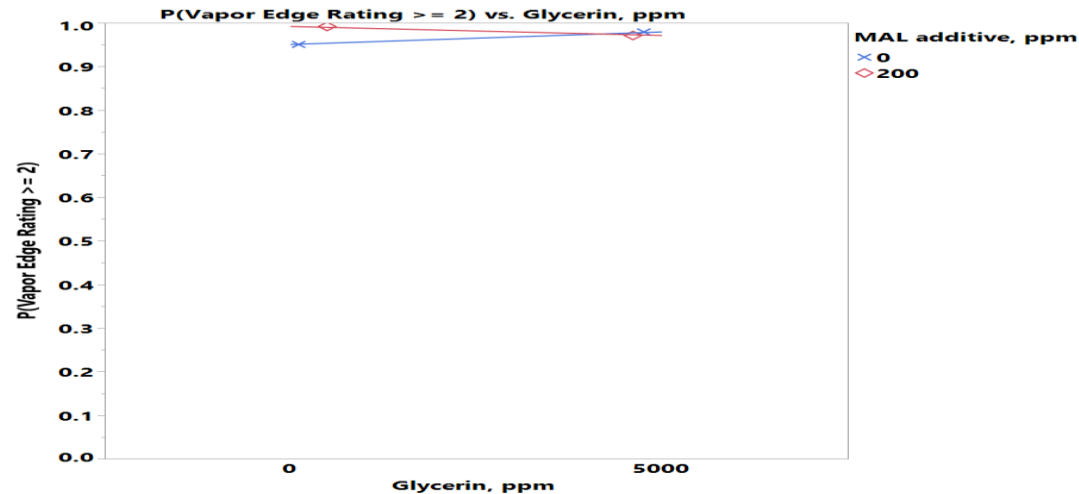


Glycerin-MAL Additive Interaction Effect

- 5000ppm Glycerin has **higher** probability of high corrosion severity than zero Glycerin **without** MAL additive while it has **lower** probability **with** MAL additive

	MAL additive, ppm			
	0		200	
	Glycerin, ppm		Glycerin, ppm	
	0	5000	0	5000
VaporEdge12	N	N	N	N
1	20	9	14	7
2	15	16	24	16
3	0	1	4	2

	MAL additive, ppm			
	0		200	
	Glycerin, ppm		Glycerin, ppm	
	0	5000	0	5000
VaporEdge12	N	N	N	N
1	20	9	14	7
2	15	16	24	16
3	0	1	4	2

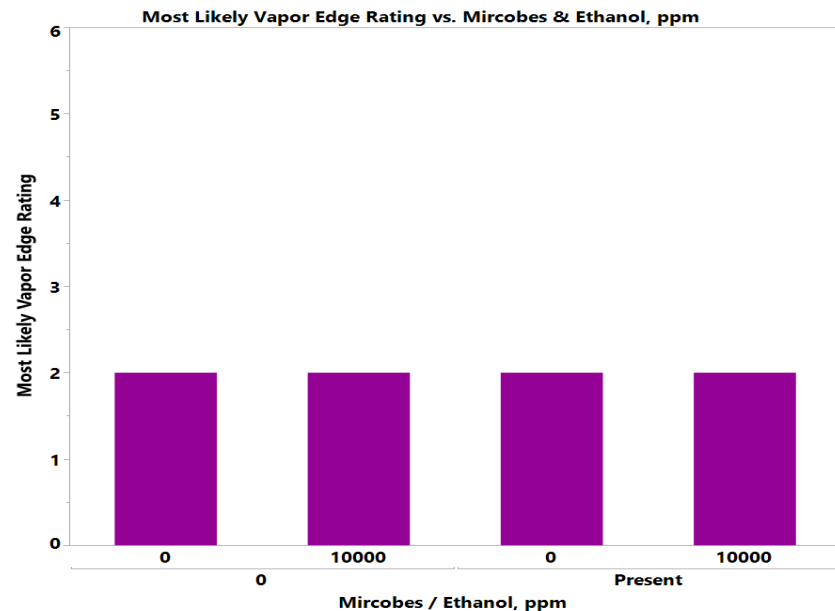
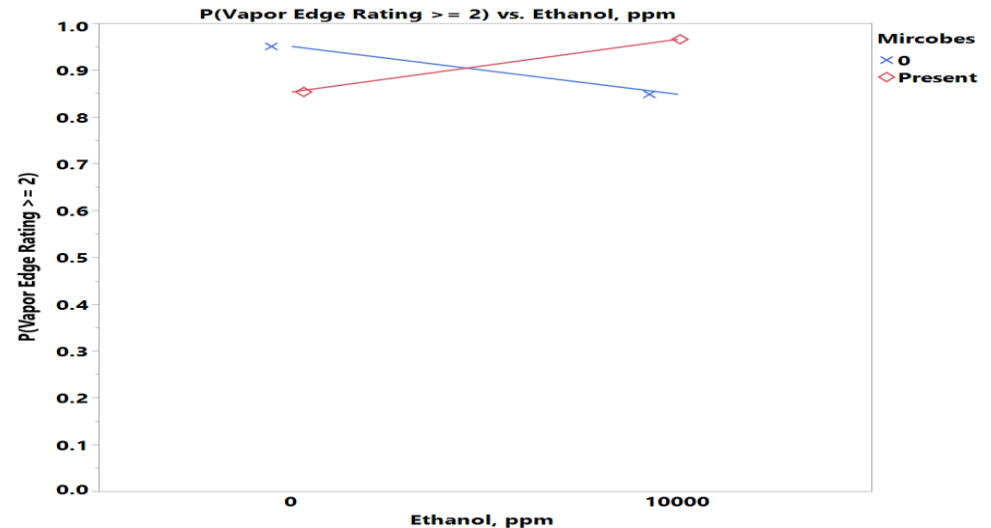


Ethanol-Microbes Interaction Effect

- 10000ppm Ethanol has **lower** probability of high corrosion severity than zero Ethanol **without** Microbes while it has **higher** probability **with** Microbes

	Microbes			
	0		Present	
	Ethanol, ppm		Ethanol, ppm	
	0	10000	0	10000
VaporEdge12	N	N	N	N
1	22	13	11	4
2	24	13	18	16
3	1	0	1	5

	Microbes			
	0		Present	
	Ethanol, ppm		Ethanol, ppm	
	0	10000	0	10000
VaporEdge12	N	N	N	N
1				
2				
3				

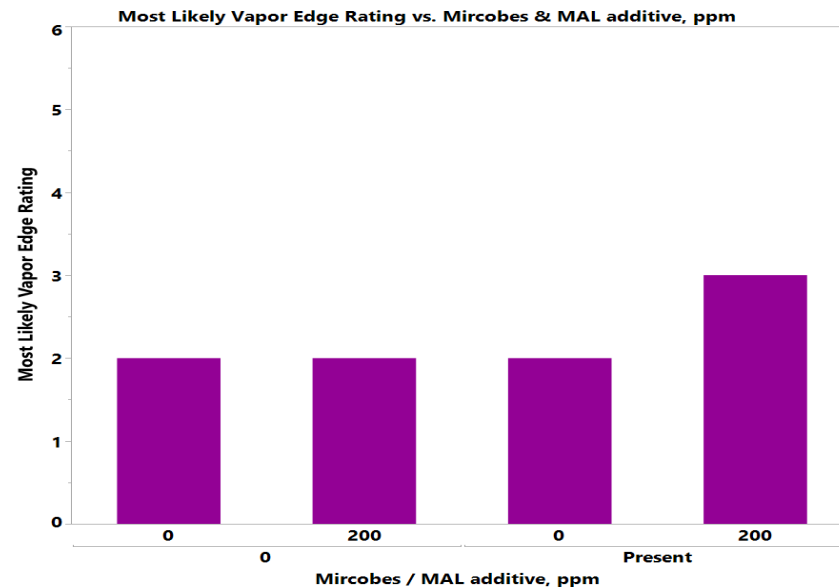
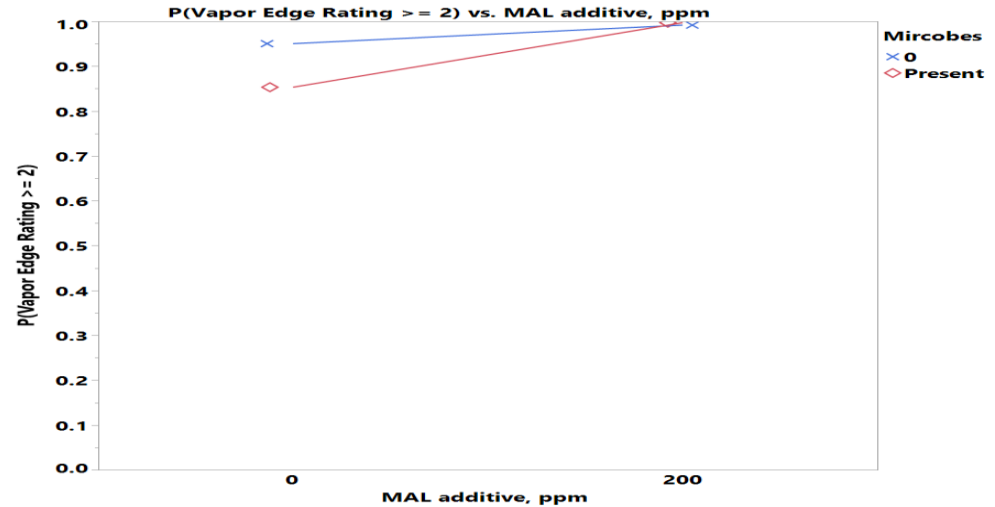


MAL Additive-Microbes Interaction Effect

- 200ppm MAL additive has **higher** probability of high corrosion severity more significantly with Microbes

	Microbes			
	0		Present	
	MAL additive, ppm		MAL additive, ppm	
	0	200	0	200
VaporEdge12	N	N	N	N
1	18	17	11	4
2	17	20	14	20
3	0	1	1	5

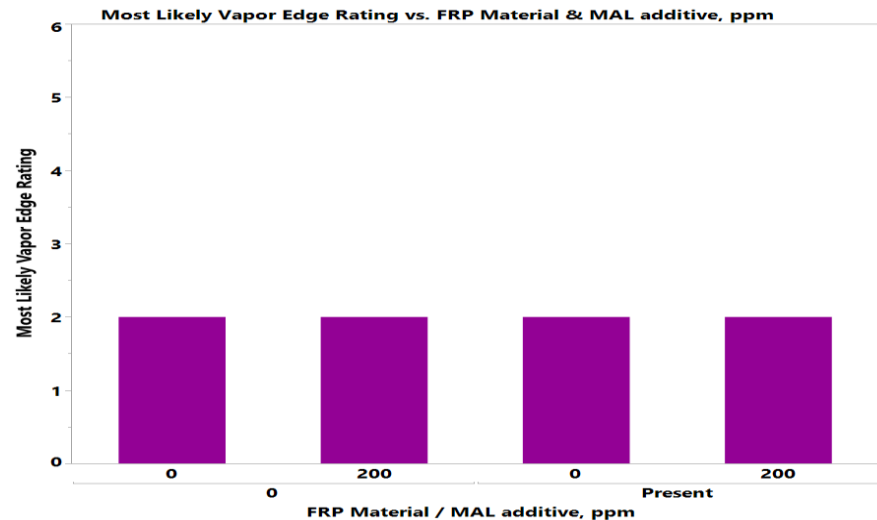
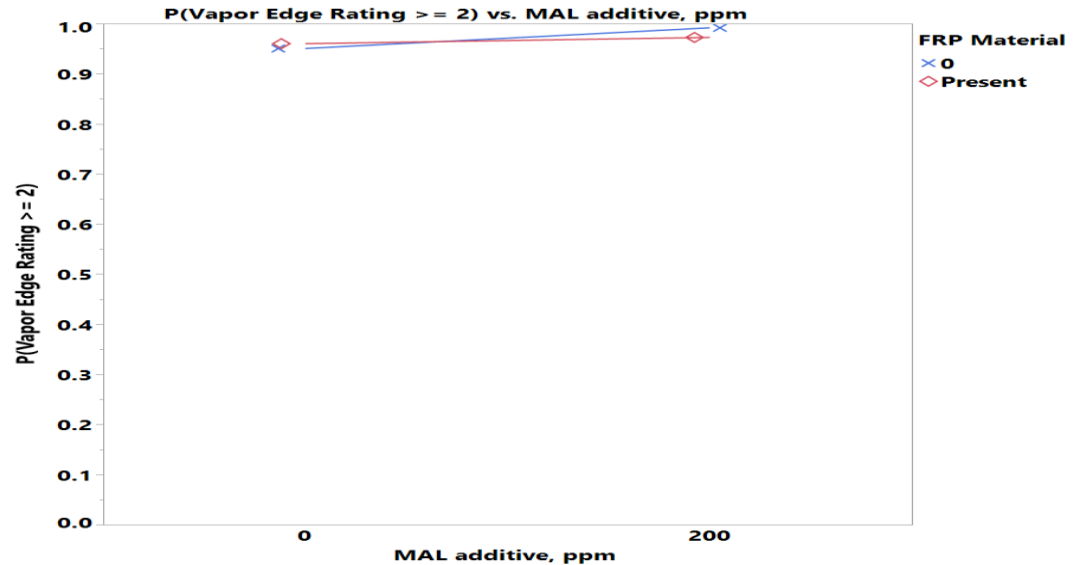
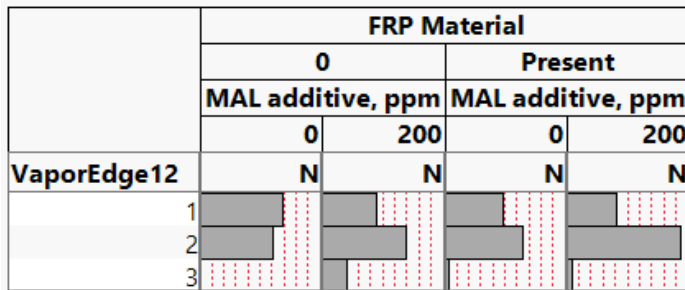
	Microbes			
	0		Present	
	MAL additive, ppm		MAL additive, ppm	
	0	200	0	200
VaporEdge12	N	N	N	N
1				
2				
3				



MAL Additive-FRP Material Interaction Effect

- 200ppm MAL additive has **higher** probability of high corrosion severity than zero MAL additive more significantly without FRP Material

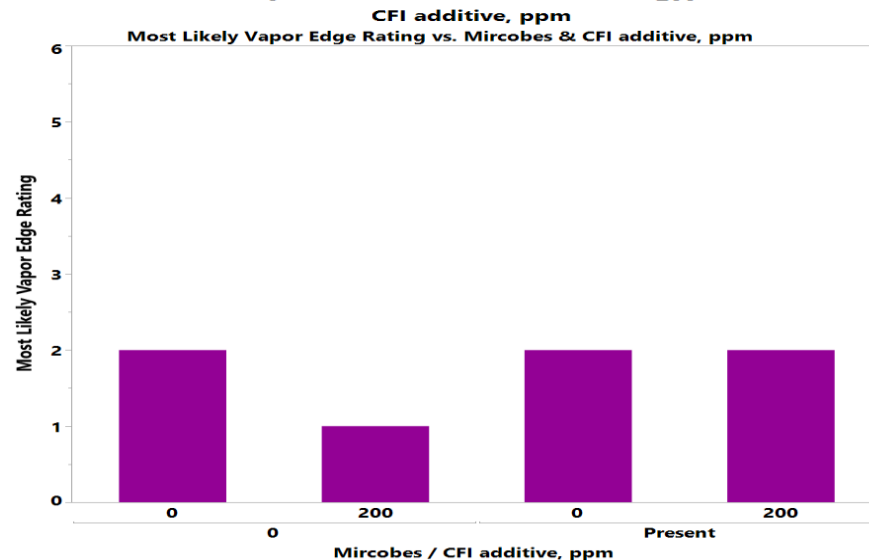
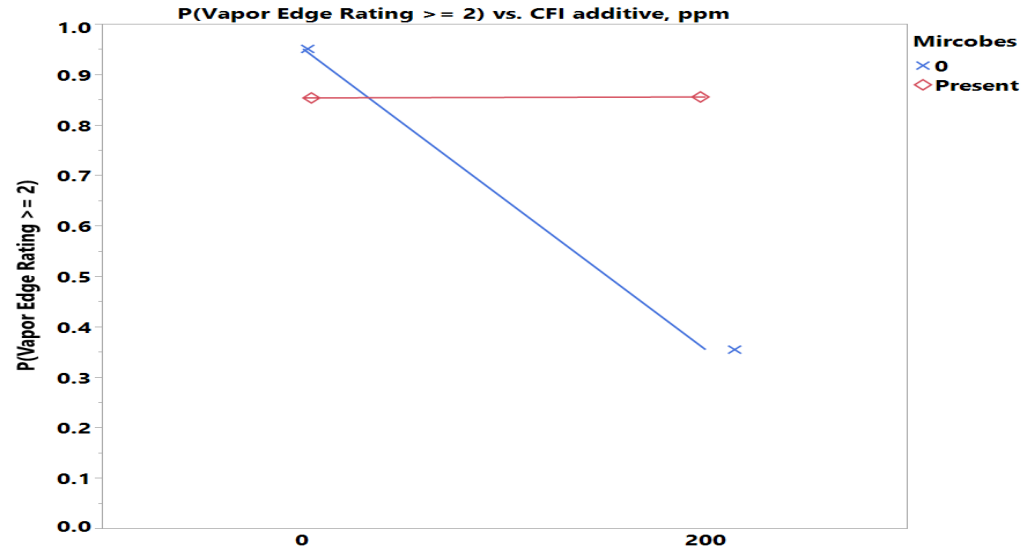
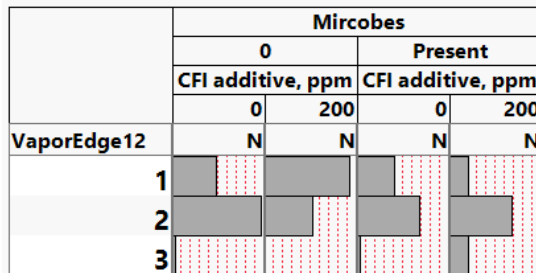
	FRP Material			
	0		Present	
	MAL additive, ppm		MAL additive, ppm	
	0	200	0	200
VaporEdge12	N	N	N	N
1	17	11	12	10
2	15	17	16	23
3	0	5	1	1



CFI Additive-Microbes Interaction Effect

- 200ppm CFI additive has **lower** probability of high corrosion severity than zero CFI additive without Microbes

	Microbes			
	0		Present	
	CFI additive, ppm		CFI additive, ppm	
	0	200	0	200
VaporEdge12	N	N	N	N
1	12	23	10	5
2	24	13	17	17
3	1	0	1	5

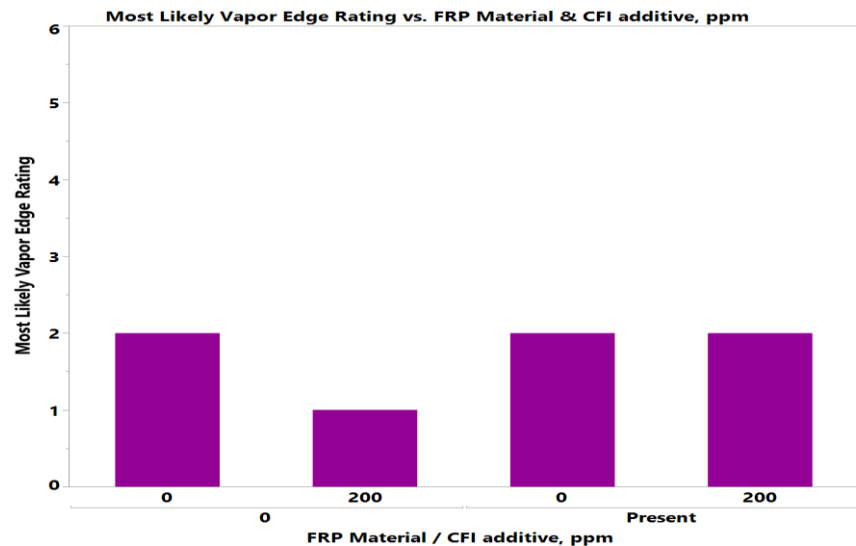
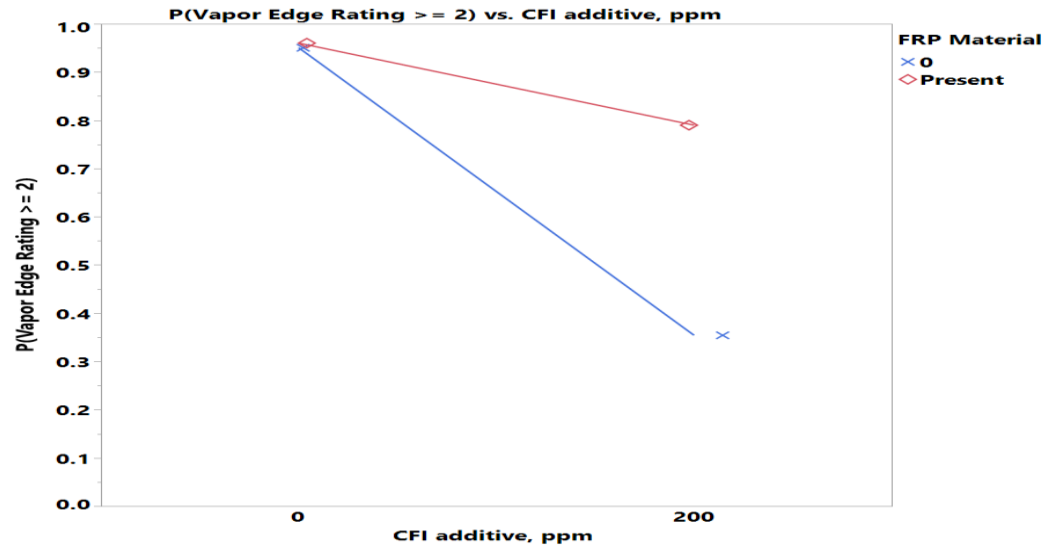


CFI Additive-FRP Material Interaction Effect

- 200ppm CFI additive has **lower** probability of high corrosion severity than zero CFI additive more significantly without FRP Material

		FRP Material			
		0		Present	
		CFI additive, ppm		CFI additive, ppm	
		0	200	0	200
VaporEdge12	N	N	N	N	
1	9	19	13	9	
2	22	10	19	20	
3	1	4	1	1	

		FRP Material			
		0		Present	
		CFI additive, ppm		CFI additive, ppm	
		0	200	0	200
VaporEdge12	N	N	N	N	
1					
2					
3					



Where((Sulfur = LSDF) and (Water = 0) and (Biodiesel = 0) and (Glycerin = 0) and (Ethanol = 0) and (Corrosion Inhibitor = 0) and (MAL Additive = 0) and (Microbes = 0) and (Conductivity Additive = 0))

Ordinal Logistic Regression

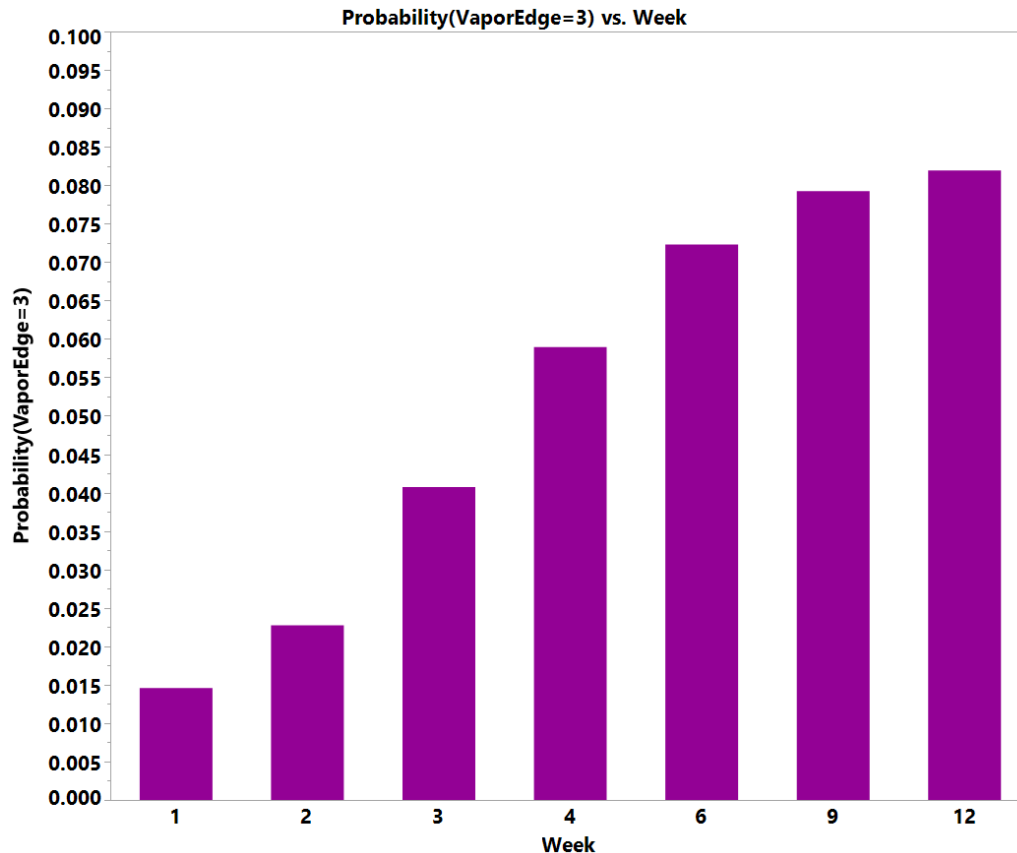
Vapor Edge Phase – All Weeks

Whole Model Test				
Model	-LogLikelihood	DF	ChiSquare	Prob>ChiSq
Difference	162.44801	28	324.896	<.0001*
Full	568.62045			
Reduced	731.06846			
RSquare (U)	0.2222			
AICc	1199.39			
BIC	1341.18			
Observations (or Sum Wgts)	896			
Fit Details				
Measure	Training	Definition		
Entropy RSquare	0.2222	1-Loglike(model)/Loglike(0)		
Generalized RSquare	0.3781	$(1-(L(0)/L(model))^{2/n})/(1-L(0)^{2/n})$		
Mean -Log p	0.6346	$\sum -\log(\rho_{ij})/n$		
RMSE	0.4650	$\sqrt{\sum (y_{ij}-\rho_{ij})^2/n}$		
Mean Abs Dev	0.4060	$\sum y_{ij}-\rho_{ij} /n$		
Misclassification Rate	0.3103	$\sum (\rho_{ij} \neq \rho_{Max})/n$		
N	896	n		
Lack Of Fit				
Source	DF	-LogLikelihood	ChiSquare	
Lack Of Fit	1762	568.62045	1137.241	
Saturated	1790	0.00000		Prob>ChiSq
Fitted	28	568.62045	1.0000	

Parameter Estimates				
Term	Estimate	Std Error	ChiSquare	Prob>ChiSq
Intercept[1]	1.15782947	0.2526043	21.01	<.0001*
Intercept[2]	5.5468444	0.3493852	252.05	<.0001*
Sulfur[LSDf]	-0.6383262	0.1129564	31.93	<.0001*
Biodiesel[0]	-0.1291436	0.0765064	2.85	0.0914
Water[0]	0.13629135	0.1382264	0.97	0.3241
Glycerin[0]	0.23865881	0.0836709	8.14	0.0043*
Ethanol[0]	0.20358976	0.0843159	5.83	0.0158*
Mircobes[0]	0.62828708	0.0873096	51.78	<.0001*
MAL additive[0]	0.39230749	0.0797352	24.21	<.0001*
CFI additive[0]	-0.0169327	0.0770504	0.05	0.8261
Corrosion inhibitor[0]	-0.0517853	0.0762905	0.46	0.4973
Conductivity Additive[0]	-0.1295388	0.0768684	2.84	0.0919
FRP Material[0]	0.17316754	0.0772806	5.02	0.0250*
Sulfur[LSDf]*Water[0]	-0.4890078	0.114043	18.39	<.0001*
Sulfur[LSDf]*Mircobes[0]	0.25706779	0.0842103	9.32	0.0023*
Sulfur[LSDf]*CFI additive[0]	-0.4159405	0.0780175	28.42	<.0001*
Biodiesel[0]*Conductivity Additive[0]	-0.3201543	0.0785148	16.63	<.0001*
Glycerin[0]*Ethanol[0]	-0.2336263	0.0837283	7.79	0.0053*
Glycerin[0]*MAL additive[0]	0.3391564	0.0797866	18.07	<.0001*
Ethanol[0]*Mircobes[0]	-0.4811158	0.0867396	30.77	<.0001*
Mircobes[0]*MAL additive[0]	-0.3786368	0.0798604	22.48	<.0001*
Mircobes[0]*CFI additive[0]	-0.4396931	0.0785528	31.33	<.0001*
MAL additive[0]*FRP Material[0]	0.29914139	0.0774833	14.91	0.0001*
CFI additive[0]*FRP Material[0]	-0.2766314	0.0775437	12.73	0.0004*
Week[2-1]	-0.4528236	0.3052643	2.20	0.1380
Week[3-2]	-0.6022199	0.2887415	4.35	0.0370*
Week[4-3]	-0.388755	0.2781162	1.95	0.1622
Week[6-4]	-0.2180715	0.2745822	0.63	0.4271
Week[9-6]	-0.0992234	0.2735363	0.13	0.7168
Week[12-9]	-0.0363481	0.2732596	0.02	0.8942

Corrosion by Time (Week)

- Significant weekly **increase** in probability of high corrosion severity between weeks 2 and 3.



Where((Sulfur = LSDF) and (Biodiesel = 0) and (Water = 0) and (Glycerin = 0) and (Ethanol = 0) and (Microbes = 0) and (MAL additive = 0) and (CFI additive = 0) and (Corrosion Inhibitor = 0) and (Conductivity Additive = 0) and (FRP Material = 0))

APPENDIX D

Identification of Potential Parameters
Causing Corrosion of Metallic Components
in Diesel Underground Storage Tanks
(CRC Project No. DP-07-16)
Matrix Analysis – Appendix C

Jo Martinez

Staff Statistician, Chevron

October 21, 2019

Agenda

- Matrix Design
- Statistical Method
- Model Result for Aqueous/Fuel Interface

Matrix Design

- **Fractional Factorial Design:** $2^{11-4} = 128$ tests
- **Factors (Levels):**
 - Sulfur (LSDF, ULSD)
 - Biodiesel, % (0, 5)
 - Water (0, Present)
 - Glycerin, ppm (0, 5000)
 - Ethanol, ppm (0, 10000)
 - Microbes (0, Present)
 - Mono Acid Lubricity (MAL) Additive, ppm (0, 200)
 - Cold Flow Improver (CFI) Additive, ppm (0, 200)
 - DSA-type Corrosion Inhibitor, ppm (0, 8-10)
 - Conductivity Additive, ppm (0, 2-3)
 - FRP Material (0, Present)
- **Response:** **Rate of Change Slope (Weeks 1-6)**
- **Objective:** Determine factors affecting Corrosion

Analysis of Variance (ANOVA)

- Modeled 106 Rate of Change Slope data in Aqueous/Fuel interface
 - 22 out of 128 conditions are without Water
- Regressed **Slope data** on:
 - Main effects (10)
 - Two-factor interaction effects (45)
- Stepwise Regression was applied for variable selection

Stepwise Regression

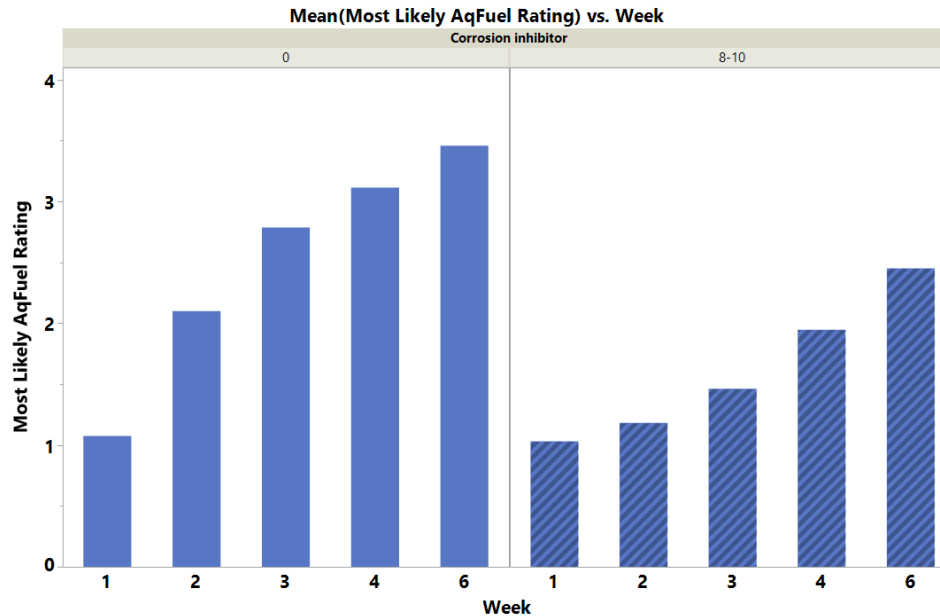
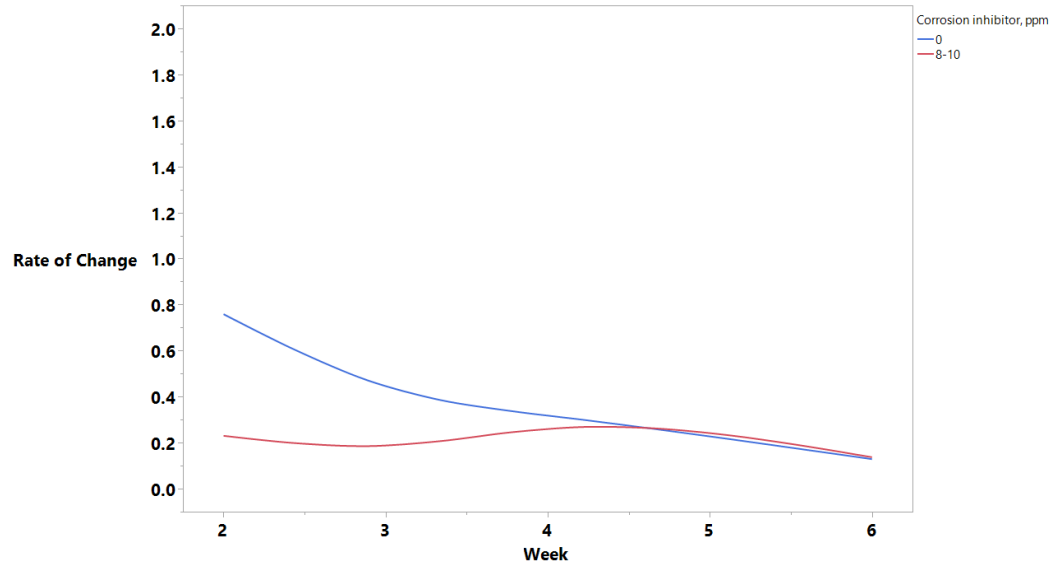
Aqueous/Fuel Phase – Rate of Change Slope

Summary of Fit					
RSquare		0.423355			
RSquare Adj		0.311958			
Root Mean Square Error		0.187089			
Mean of Response		-0.10566			
Observations (or Sum Wgts)		106			

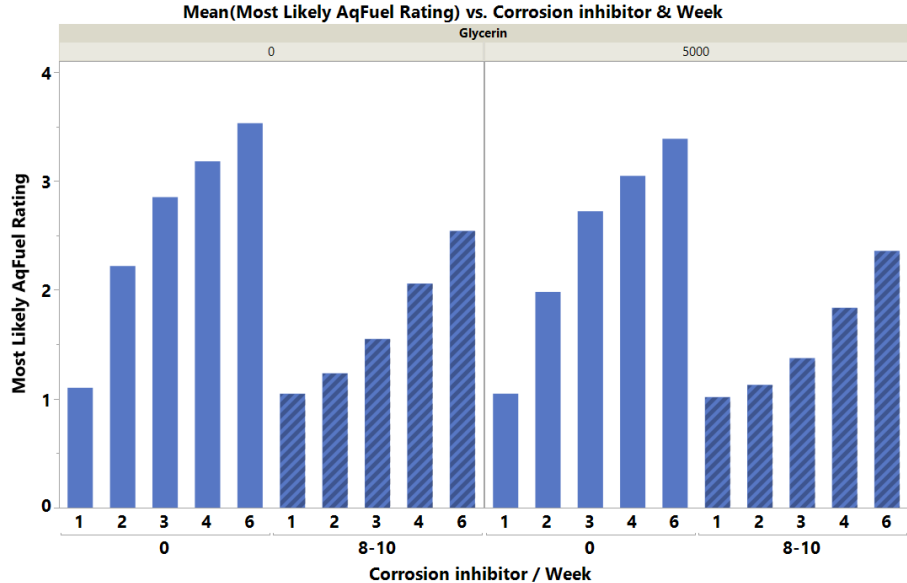
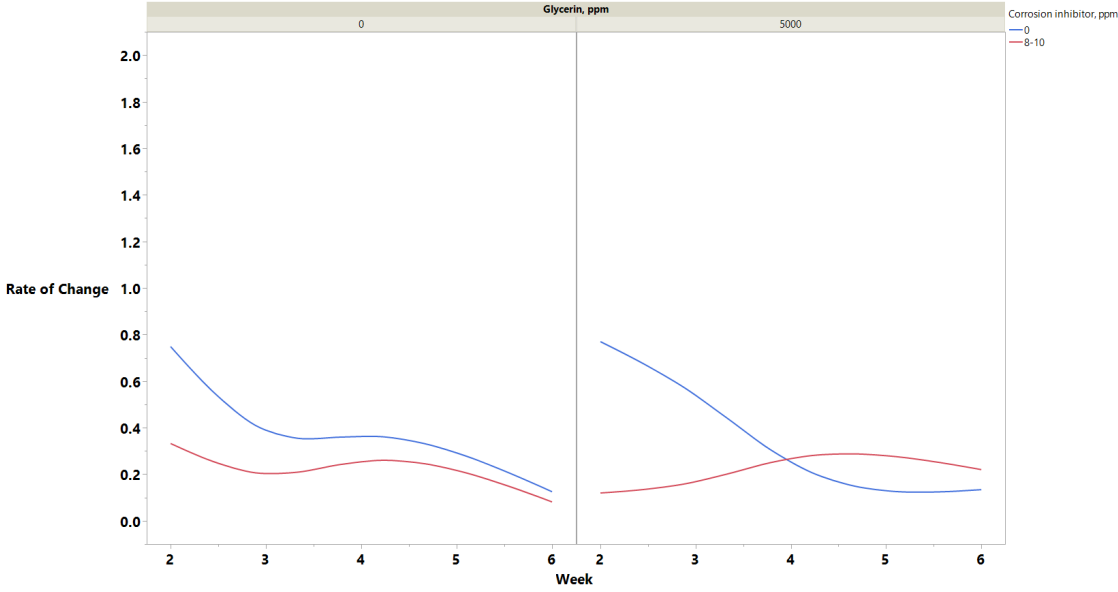
Analysis of Variance					
Source	DF	Sum of Squares	Mean Square	F Ratio	
Model	17	2.2613952	0.133023	3.8004	
Error	88	3.0802086	0.035002		Prob > F
C. Total	105	5.3416038			<.0001*

Effect Tests					
Source	Nparm	DF	Sum of Squares	F Ratio	Prob > F
Sulfur	1	1	0.00174400	0.0498	0.8239
Biodiesel, %	1	1	0.01990307	0.5686	0.4528
Glycerin, ppm	1	1	0.00292692	0.0836	0.7731
Ethanol, ppm	1	1	0.01362735	0.3893	0.5343
Mircobes	1	1	0.01149727	0.3285	0.5680
MAL additive, ppm	1	1	0.00737747	0.2108	0.6473
CFI additive, ppm	1	1	0.03135688	0.8959	0.3465
Corrosion inhibitor, ppm	1	1	0.85373983	24.3909	<.0001*
Conductivity additive, ppm	1	1	0.01238178	0.3537	0.5535
FRP Material	1	1	0.03219900	0.9199	0.3401
Glycerin, ppm*Mircobes	1	1	0.09116429	2.6045	0.1101
Glycerin, ppm*CFI additive, ppm	1	1	0.12600213	3.5998	0.0611
Glycerin, ppm*Corrosion inhibitor, ppm	1	1	0.11361771	3.2460	0.0750
Ethanol, ppm*Conductivity additive, ppm	1	1	0.25933007	7.4089	0.0078*
Mircobes*Corrosion inhibitor, ppm	1	1	0.15633814	4.4665	0.0374*
CFI additive, ppm*Corrosion inhibitor, ppm	1	1	0.25637326	7.3245	0.0082*
CFI additive, ppm*Conductivity additive, ppm	1	1	0.16266061	4.6471	0.0338*

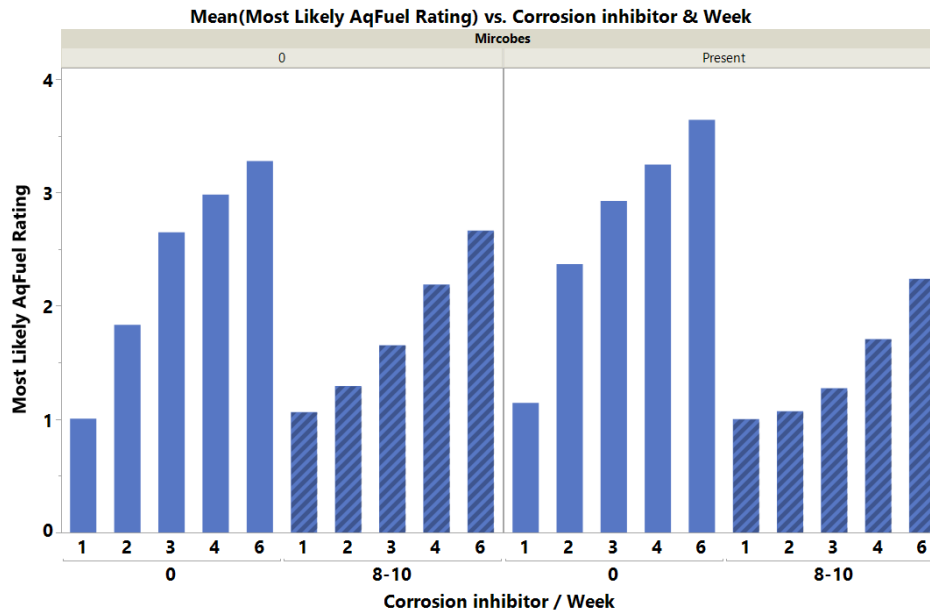
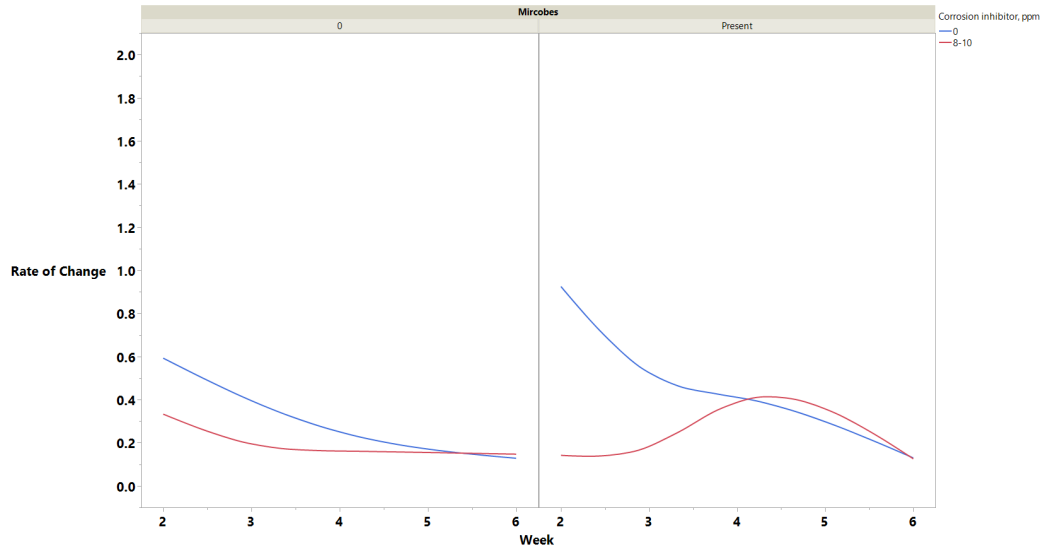
Corrosion Inhibitor Effect – Aq/Fuel Interface



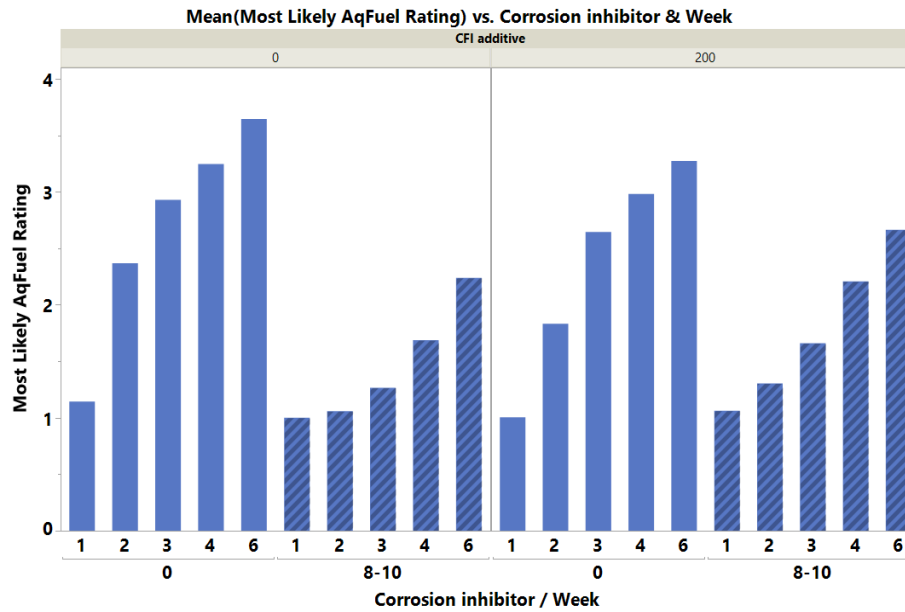
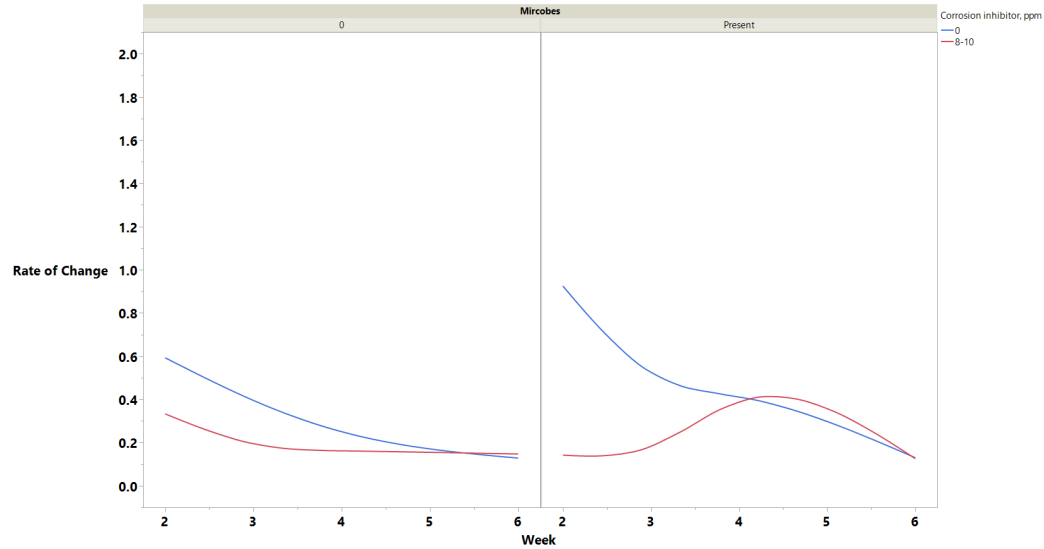
Corrosion Inhibitor-Glycerin Interaction Effect



Corrosion Inhibitor-Microbes Interaction Effect



Corrosion Inhibitor-CFI Additive Interaction Effect



APPENDIX E
Gross Observations of Microcosms

Table E-1. Gross Observations of 128-Jars Set up in the Microcosm Study

		Tot Risk	2				2				31				34				33				2				2				2				2				28													
		Jar #	1				2				3				4				5				6				7				8				9				10													
PARAMETER	CRITERION	Week #	3	4	6	9	12	3	4	6	9	12	3	4	6	9	12	3	4	6	9	12	3	4	6	9	12	3	4	6	9	12	3	4	6	9	12	3	4	6	9	12	3	4	6	9	12	3	4	6	9	12
Fuel phase																																																				
Haze	ASTM < 2	1	1	1	1	1	1	1	1	1	1	1	1	1	1	1	2	1	1	1	2	2	1	1	2	2	2	1	1	1	1	1	1	1	1	1	1	1	1	1	1	1	1	1	1	1	1					
	ASTM 2 to 3	2																																																		
	ASTM > 3	3																																																		
Color	ASTM £ 2	1	1	1	1	1	1	1	1	1	1	1	1	1	1	1	1	1	1	1	1	1	1	1	1	1	1	1	1	1	1	1	1	1	1	1	1	1	1	1	1	1	1	1	1	1	1					
	ASTM 2 to 5	2																																																		
	ASTM > 5	3																																																		
Invert emulsion (rag layer)																																																				
Present	No	0	0	0	0	0	0	0	0	0	0	0	3	3	3	3	3	3	3	3	3	3	3	3	3	3	3	0	0	0	0	0	0	0	0	0	0	0	0	0	0	0	0	0	0	0	0					
	Yes	3																																																		
Thickness	No rag layer	0	0	0	0	0	0	0	0	0	0	0	1	1	1	2	2	1	2	2	2	3	1	1	2	2	3	0	0	0	0	0	0	0	0	0	0	0	0	0	0	0	0	0	0	0	0	0	0	0	0	0
	< 1 mm	1																																																		
	1 to 3 mm	2																																																		
	> 3 mm	3																																																		
Stalagmites/stalagmites	No rag layer	0	0	0	0	0	0	0	0	0	0	0	2	5	5	5	5	2	2	2	2	5	2	2	2	2	2	0	0	0	0	0	0	0	0	0	0	0	0	0	0	0	0	0	0	0	0	0	0	0	0	0
	No	2																																																		
	Yes	5																																																		
Consistency	No rag layer	0	0	0	0	0	0	0	0	0	0	0	1	1	1	1	1	1	1	1	2	5	1	2	5	5	5	0	0	0	0	0	0	0	0	0	0	0	0	0	0	0	0	0	0	0	0	0	0	0	0	0
	Easily disaggregated	1																																																		
	Difficult to disperse	2																																																		
	Membranous pellicle	5																																																		
Water phase																																																				
Adheres to glass	No rag layer	0	0	0	0	0	0	0	0	0	0	0	3	3	3	3	3	1	3	3	3	3	3	3	3	3	3	0	0	0	0	0	0	0	0	0	0	0	0	0	0	0	0	0	0	0	0					
	No	1																																																		
	Yes	3																																																		
Turbidity	Water-white	0	0	0	0	0	0	0	0	0	0	0	4	4	4	4	4	4	4	4	4	4	4	4	4	4	4	0	0	0	0	0	0	0	0	0	0	0	0	0	0	0	0	0	0	0	0					
	Translucent	2																																																		
	Opaque	4																																																		
Color	ASTM £ 2	1	0	0	0	0	0	0	0	0	0	0	1	1	1	1	1	1	1	1	1	1	1	1	2	2	2	0	0	0	0	0	0	0	0	0	0	0	0	0	0	0	0	0	0	0	0					
	ASTM 2 to 5	2																																																		
	ASTM > 5	3																																																		
Sediment	< 25% of sample jar bottom covered	1	0	0	0	0	0	0	0	0	0	0	2	2	3	3	3	1	1	1	2	2	2	3	3	3	3	0	0	0	0	0	0	0	0	0	0	0	0	0	0	0	0	0	0	0	0					
	25 to 75 % bottom covered	2																																																		
	> 75 % of bottom covered	3																																																		
Risk Rating:	Min.	10	2	2	2	2	2	2	2	2	2	2	18	21	22	22	23	15	17	17	20	26	18	20	25	25	25	2	2	2	2	2	2	2	2	2	2	2	2	2	2	2	2	2	2	2	2					
	Max.	40																																																		
Adjusted average:	10 to 15	1	0	0	0	0	0	0	0	0	0	0	3	3	3	3	3	3	3	3	3	3	3	3	3	3	3	0	0	0	0	0	0	0	0	0	0	0	0	0	0	0	0	0	0	0	0	0	0	0	0	0
	16 to 25	3																																																		
	> 25	5																																																		
Overrides:	Subtotal for rag layer > 10	5	0	0	0	0	0	0	0	0	0	0	0	5	5	5	5	0	5	5	5	5	0	5	5	5	5	0	0	0	0	0	0	0	0	0	0	0	0	0	0	0	0	0	0	0	0	0	0	0	5	5
Total Risk			2	2	2	2	2	2	2	2	2	2	21	29	30	30	31	18	25	25	28	34	21	28	33	33	33	2	2	2	2	2	2	2	2	2	2	2	2	2	2	2	2	2	2	2	2	20	20	20	28	28

Table E-1 (continued). Gross Observations of 128-Jars Set up in the Microcosm Study

		Tot Risk	24				12				21				8				14				4				4				4				12				12														
		Jar #	11				12				13				14				15				16				17				18				19				20														
PARAMETER	CRITERION	Week #	3	4	6	9	12	3	4	6	9	12	3	4	6	9	12	3	4	6	9	12	3	4	6	9	12	3	4	6	9	12	3	4	6	9	12	3	4	6	9	12	3	4	6	9	12						
Fuel phase																																																					
Haze	ASTM < 2	1	1	1	1	2	2	1	1	1	1	1	1	1	1	1	2	2	1	1	1	1	1	1	2	3	3	3	1	1	1	1	1	1	1	1	1	1	1	1	1	1	1	1	1	1	1	1					
	ASTM 2 to 3	2																																																			
	ASTM > 3	3																																																			
Color	ASTM E 2	1	1	1	1	1	1	1	1	1	1	1	1	1	1	1	1	1	1	1	1	1	1	1	1	1	1	3	3	3	3	3	3	3	3	3	3	3	3	3	3	3	3	3	3	3	3						
	ASTM 2 to 5	2																																																			
	ASTM > 5	3																																																			
Invert emulsion (rag layer)																																																					
Present	No	0	3	3	3	3	3	0	0	0	0	0	3	3	3	3	3	0	0	0	0	0	0	0	0	0	0	0	0	0	0	0	0	0	0	0	0	0	0	0	0	0	0	0	0	0	0						
	Yes	3																																																			
Thickness	No rag layer	0	1	1	1	1	1	0	0	0	0	0	1	1	1	1	1	0	0	0	0	0	0	0	0	0	0	0	0	0	0	0	0	0	0	0	0	0	0	0	0	0	0	0	0	0	0						
	< 1 mm	1																																																			
	1 to 3 mm	2																																																			
	> 3 mm	3																																																			
Stalagmites/stalagmites	No rag layer	0	2	2	2	2	2	0	0	0	0	0	2	2	2	2	2	0	0	0	0	0	0	0	0	0	0	0	0	0	0	0	0	0	0	0	0	0	0	0	0	0	0	0	0	0	0						
	Yes	5																																																			
Consistency	No rag layer	0	1	1	1	1	1	0	0	0	0	0	1	1	1	1	1	0	0	0	0	0	0	0	0	0	0	0	0	0	0	0	0	0	0	0	0	0	0	0	0	0	0	0	0	0	0						
	Easily disaggregated	1																																																			
	Difficult to disperse	2																																																			
	Membranous pellicle	5																																																			
Water phase																																																					
Adheres to glass	No rag layer	0	3	3	3	3	3	0	0	0	0	0	3	3	3	3	3	0	0	0	0	0	0	0	0	0	0	0	0	0	0	0	0	0	0	0	0	0	0	0	0	0	0	0	0	0	0						
	No	1																																																			
	Yes	3																																																			
Turbidity	Water-white	0	4	4	4	4	4	4	4	4	4	4	2	2	2	4	4	2	2	2	4	4	2	2	4	4	4	0	0	0	0	0	0	0	0	0	0	0	0	0	0	0	4	4	4	4	4	2	4	4	4	4	
	Translucent	2																																																			
	Opaque	4																																																			
Color	ASTM E 2	1	1	1	1	1	2	1	1	1	1	2	2	1	1	1	1	1	1	1	1	1	1	1	1	1	2	2	0	0	0	0	0	0	0	0	0	0	0	0	0	0	0	1	1	1	1	1	1	1	1	1	1
	ASTM 2 to 5	2																																																			
	ASTM > 5	3																																																			
Sediment	< 25% of sample jar bottom covered	1	1	3	3	3	3	1	3	3	3	3	1	1	1	1	1	1	1	1	1	1	1	3	3	3	3	0	0	0	0	0	0	0	0	0	0	0	0	0	0	0	1	1	1	2	2	1	1	2	2	2	
	25 to 75 % bottom covered	2																																																			
	> 75 % of bottom covered	3																																																			
Risk Rating:	Min.	10	17	19	19	20	21	8	10	10	11	11	15	15	15	18	18	6	6	6	8	8	6	9	12	13	13	4	4	4	4	4	4	4	4	4	4	4	4	4	4	4	10	10	10	11	11	8	10	11	11	11	
	Max.	40																																																			
Adjusted average:	10 to 15	1	3	3	3	3	3	1	1	1	1	1	3	3	3	3	3	0	0	0	0	0	1	1	1	1	1	0	0	0	0	0	0	0	0	0	0	0	0	0	0	0	1	1	1	1	1	1	1	1	1	1	
	16 to 25	3																																																			
	> 25	5																																																			
Overrides:	Subtotal for rag layer > 10	5	0	0	0	0	0	0	0	0	0	0	0	0	0	0	0	0	0	0	0	0	0	0	0	0	0	0	0	0	0	0	0	0	0	0	0	0	0	0	0	0	0	0	0	0	0						
Total Risk			20	22	22	23	24	9	11	11	12	12	18	18	18	21	21	6	6	6	8	8	7	10	13	14	14	4	4	4	4	4	4	4	4	4	4	4	4	4	4	4	11	11	11	12	12	9	11	12	12	12	

Table E-1 (continued). Gross Observations of 128-Jars Set up in the Microcosm Study

		Tot Risk	35					18					33					18					20					4					4					34					21					31									
		Jar #	21					22					23					24					25					26					27					28					29					30									
PARAMETER	CRITERION	Week #	3	4	6	9	12	3	4	6	9	12	3	4	6	9	12	3	4	6	9	12	3	4	6	9	12	3	4	6	9	12	3	4	6	9	12	3	4	6	9	12	3	4	6	9	12	3	4	6	9	12	3	4	6	9	12
Fuel phase																																																									
Haze	ASTM < 2	1	1	2	2	2	2	1	1	1	1	1	1	1	1	1	1	1	1	1	1	1	1	1	1	1	1	1	1	1	1	1	1	1	1	1	1	1	1	1	1	1	1	1	1	1	1	1	1	1	1	1					
	ASTM 2 to 3	2																																																							
	ASTM > 3	3																																																							
Color	ASTM E 2	1	3	3	3	3	3	3	3	3	3	3	3	3	3	3	3	3	3	3	3	3	3	3	3	3	3	3	3	3	3	3	3	3	3	3	3	3	3	3	3	3	3	3	3	3	3	3	3	3	3	3					
	ASTM 2 to 5	2																																																							
	ASTM > 5	3																																																							
Invert emulsion (rag layer)																																																									
Present	No	0	3	3	3	3	3	0	0	0	0	3	3	0	0	0	0	3	3	0	0	3	3	3	3	3	3	3	3	3	0	0	0	0	0	0	0	0	0	0	3	3	3	3	3	3	3	3	3	3	0	0	3	3	3		
	Yes	3																																																							
Thickness	No rag layer	0	1	1	2	2	2	0	0	0	0	1	1	0	0	0	0	2	2	0	0	1	1	1	1	1	1	1	1	1	0	0	0	0	0	0	0	0	0	0	1	1	2	2	3	2	2	2	2	2	0	0	1	1	2		
	< 1 mm	1																																																							
	1 to 3 mm	2																																																							
	> 3 mm	3																																																							
Stalagmites/stalagmites	No rag layer	0	2	2	5	5	5	0	0	0	0	2	2	0	0	0	0	5	5	0	0	2	2	2	2	2	2	2	2	2	0	0	0	0	0	0	0	0	0	0	2	2	2	2	5	2	2	2	2	2	0	0	2	5	5		
	No	2																																																							
	Yes	5																																																							
Consistency	No rag layer	0	1	1	2	5	5	5	0	0	1	1	0	0	0	0	5	5	0	0	1	1	1	1	1	1	1	1	1	0	0	0	0	0	0	0	0	0	0	1	1	1	1	5	1	1	1	2	2	0	0	1	1	1			
	Easily disaggregated	1																																																							
	Difficult to disperse	2																																																							
	Membranous pellicle	5																																																							
Water phase																																																									
Adheres to glass	No rag layer	0	1	1	3	3	3	0	0	0	0	1	1	0	0	0	0	1	1	0	0	1	1	1	1	3	3	3	3	3	0	0	0	0	0	0	0	0	0	0	3	3	3	3	3	1	1	1	1	1	0	0	3	3	3		
	No	1																																																							
	Yes	3																																																							
Turbidity	Water-white	0	4	4	4	4	4	4	4	4	4	4	4	4	4	4	4	4	4	4	4	4	2	2	2	2	2	0	0	0	0	0	0	0	0	0	0	4	4	4	4	4	4	4	4	4	4	4	4	4	4	4					
	Translucent	2																																																							
	Opaque	4																																																							
Color	ASTM E 2	1	1	1	1	1	1	1	1	1	1	1	1	1	1	1	1	1	1	1	1	1	1	1	1	1	1	0	0	0	0	0	0	0	0	0	0	1	1	1	1	1	1	1	1	1	1	1	1	1	1	1					
	ASTM 2 to 5	2																																																							
	ASTM > 5	3																																																							
Sediment	< 25% of sample jar bottom covered	1	1	1	1	1	1	1	1	1	1	1	1	1	1	2	2	1	1	1	1	1	1	1	1	1	1	0	0	0	0	0	0	0	0	0	0	1	1	1	1	1	1	1	1	1	1	1	1	2	2	2					
	25 to 75 % bottom covered	2																																																							
	> 75 % of bottom covered	3																																																							
Risk Rating:	Mn.	10	17	18	24	27	27	15	10	10	17	17	10	10	10	25	25	10	10	17	17	17	17	17	17	17	17	4	4	4	4	4	4	4	4	4	4	19	19	19	19	26	17	17	17	18	18	10	10	20	23	23					
	Max.	40																																																							
Adjusted average:	10 to 15	1	3	3	3	3	3	1	1	1	1	1	3	3	3	3	3	1	1	1	1	1	3	3	3	3	3	0	0	0	0	0	0	0	0	0	0	3	3	3	3	3	3	3	3	3	3	3	3	3	3	3					
	16 to 25	3																																																							
	> 25	5																																																							
Overrides:	Subtotal for rag layer > 10	5	0	0	5	5	5	0	0	0	0	0	0	0	0	5	5	0	0	0	0	0	0	0	0	0	0	0	0	0	0	0	0	0	5	5	5	0	0	0	0	0	0	0	0	5	5	0	0	0	5	5					
Total Risk			20	21	32	35	35	16	11	11	18	18	13	13	13	33	33	11	11	18	18	18	20	20	20	20	20	4	4	4	4	4	4	4	4	4	4	22	22	27	27	34	20	20	20	21	21	13	13	23	31	31					

Table E-1 (continued). Gross Observations of 128-Jars Set up in the Microcosm Study

PARAMETER	CRITERION	Tot Risk	34					22					2					11					28					4					29					30					30					27				
		Jar #	31					32					33					34					35					36					37					38					39					40				
		Week #	3	4	6	9	12	3	4	6	9	12	3	4	6	9	12	3	4	6	9	12	3	4	6	9	12	3	4	6	9	12	3	4	6	9	12	3	4	6	9	12	3	4	6	9	12	3	4	6	9	12
Fuel phase																																																				
Haze	ASTM < 2	1	1	1	1	1	1	1	2	2	2	3	1	1	1	1	1	1	1	1	1	1	1	1	1	2	2	1	1	1	1	1	2	2	2	2	2	1	1	1	1	1	1	1	1	2	2	1	1	1	1	1
	ASTM 2 to 3	2																																																		
	ASTM > 3	3																																																		
Color	ASTM 2	1	3	3	3	3	3	3	3	3	3	3	1	1	1	1	1	1	1	1	1	1	1	1	1	1	1	1	1	1	1	1	1	1	1	1	1	1	1	1	1	1	1	1	1	1	1					
	ASTM 2 to 5	2																																																		
	ASTM > 5	3																																																		
Invert emulsion (rag layer)																																																				
Present	No	0	3	3	3	3	3	3	3	3	3	3	0	0	0	0	0	0	0	0	0	0	3	3	3	3	3	0	0	0	0	0	3	3	3	3	3	3	3	3	3	3	3	3	3	3	3					
	Yes	3																																																		
Thickness	No rag layer	0	2	2	2	3	3	1	1	1	1	1	0	0	0	0	0	0	0	0	0	0	2	2	2	2	3	0	0	0	0	0	2	2	2	2	2	1	1	2	2	3	1	1	2	2	2	1	1	1	2	3
	< 1 mm	1																																																		
	1 to 3 mm	2																																																		
	> 3 mm	3																																																		
Stalagmites/stalagmites	No rag layer	0	0	0	0	0	5	2	2	2	2	2	0	0	0	0	0	0	0	0	0	0	2	5	5	5	5	0	0	0	0	0	2	2	2	5	5	2	2	5	5	5	2	5	5	5	5	2	2	2	2	2
	No	2																																																		
	Yes	5																																																		
Consistency	No rag layer	0	1	1	1	1	5	1	1	1	1	1	0	0	0	0	0	0	0	0	0	0	1	1	2	2	2	0	0	0	0	0	1	1	1	2	5	1	1	5	5	5	1	1	1	5	5	1	1	1	1	2
	Easily disaggregated	1																																																		
	Difficult to disperse	2																																																		
	Membranous pellicle	5																																																		
Water phase																																																				
Adheres to glass	No rag layer	0	1	1	1	1	3	1	1	1	1	1	0	0	0	0	0	0	0	0	0	0	3	3	3	3	3	0	0	0	0	0	3	3	3	3	3	3	3	3	3	3	1	1	1	1	1	3	3	3	3	3
	No	1																																																		
	Yes	3																																																		
Turbidity	Water-white	0	4	4	4	4	4	4	4	4	4	4	0	0	0	0	0	4	4	4	4	4																														
	Translucent	2																																																		
	Opaque	4																																																		
Color	ASTM 2	1	1	1	1	1	1	1	1	1	1	1	0	0	0	0	0	1	1	1	1	2	1	1	1	2	2	1	1	1	1	1	1	1	1	1	1	1	1	1	2	2	1	1	1	2	2	1	1	2	2	3
	ASTM 2 to 5	2																																																		
	ASTM > 5	3																																																		
Sediment	< 25% of sample jar bottom covered	1	1	1	1	1	1	1	1	1	1	1	0	0	0	0	0	1	2	2	3	3	2	2	2	2	2	1	1	1	1	1	1	1	1	1	1	2	2	2	2	2	1	1	2	3	3	1	1	2	2	3
	25 to 75 % bottom covered	2																																																		
	> 75 % of bottom covered	3																																																		
Risk Rating:	Min.	10	15	15	15	15	26	17	18	18	18	19	2	2	2	2	2	8	9	9	10	11	14	17	18	20	20	4	4	4	4	4	14	14	14	18	21	14	14	21	22	22	11	14	15	22	22	13	13	15	15	19
	Max.	40																																																		
Adjusted average:	10 to 15	1	3	3	3	3	3	3	3	3	3	3	0	0	0	0	0	0	0	0	0	0	3	3	3	3	3	0	0	0	0	0	3	3	3	3	3	3	3	3	3	3	3	3	3	3	3	3	3	3	3	3
	16 to 25	3																																																		
	> 25	5																																																		
Overrides:	Subtotal for rag layer > 10	5	0	0	0	0	5	0	0	0	0	0	0	0	0	0	0	0	0	0	0	0	5	5	5	5	5	0	0	0	0	0	5	5	5	5	5	0	0	5	5	5	0	5	5	5	5	0	0	0	5	5
Total Risk			18	18	18	18	34	20	21	21	21	22	2	2	2	2	2	8	9	9	10	11	22	25	26	28	28	4	4	4	4	4	22	22	22	26	29	17	17	29	30	30	14	22	23	30	30	16	16	18	23	27

Table E-1 (continued). Gross Observations of 128-Jars Set up in the Microcosm Study

		Tot Risk	25				2				2				16				30				31				28				32				32				4																		
		Jar #	41				42				43				44				45				46				47				48				49				50																		
PARAMETER	CRITERION	Week #	3	4	6	9	12	3	4	6	9	12	3	4	6	9	12	3	4	6	9	12	3	4	6	9	12	3	4	6	9	12	3	4	6	9	12	3	4	6	9	12	3	4	6	9	12										
Fuel phase																																																									
Haze	ASTM < 2	1	1	1	1	1	1	1	1	1	1	1	1	1	1	1	1	1	1	1	1	1	1	1	1	1	1	1	1	1	1	1	1	1	1	1	1	3	3	3	3	3	1	2	2	2	2	1	1	1	1	1					
	ASTM 2 to 3	2																																																							
	ASTM > 3	3																																																							
Color	ASTM £ 2	1	1	1	1	1	1	1	1	1	1	1	1	1	1	1	1	1	1	1	1	1	1	1	1	1	1	1	1	1	1	1	1	1	1	1	1	1	1	1	1	1	1	1	1	1											
	ASTM 2 to 5	2																																																							
	ASTM > 5	3																																																							
Invert emulsion (rag layer)																																																									
Present	No	0	0	0	0	3	3	0	0	0	0	0	0	0	0	0	0	3	3	3	3	3	3	3	3	3	3	3	3	3	3	3	0	0	0	3	3	3	3	3	3	3	3	3	3	3	3										
	Yes	3																																																							
Thickness	No rag layer	0	0	0	0	1	2	0	0	0	0	0	0	0	0	0	0	1	1	1	1	1	2	2	2	2	3	1	2	2	2	2	0	0	0	1	2	1	1	2	2	2	1	2	2	3	3	0	0	0	0	0					
	< 1 mm	1																																																							
	1 to 3 mm	2																																																							
	> 3 mm	3																																																							
Stalagmites/stalagmites	No rag layer	0	0	0	0	2	5	0	0	0	0	0	0	0	0	0	0	2	2	2	2	2	5	5	5	5	5	2	2	5	5	5	0	0	0	5	5	2	2	5	5	5	2	2	5	5	5	0	0	0	0	0					
	Yes	5																																																							
Consistency	No rag layer	0	0	0	0	1	2	0	0	0	0	0	0	0	0	0	0	1	1	1	1	1	1	5	5	5	5	1	1	2	2	5	0	0	0	5	5	5	5	5	5	5	1	5	5	5	5	5	5	5	5	5	0	0	0	0	0
	Easily disaggregated	1																																																							
	Difficult to disperse	2																																																							
	Membranous pellicle	5																																																							
Water phase																																																									
Adheres to glass	No rag layer	0	0	0	0	5	5	0	0	0	0	0	0	0	0	0	0	1	1	1	1	1	3	3	3	3	3	3	3	3	3	3	0	0	0	3	3	3	3	3	3	3	3	3	3	3	3	0	0	0	0	0					
	No	1																																																							
	Yes	3																																																							
Turbidity	Water-white	0																																																							
	Translucent	2																																																							
	Opaque	4																																																							
Color	ASTM £ 2	1	1	1	1	1	1	0	0	0	0	0	0	0	0	0	0	1	1	1	1	1	2	1	1	1	1	1	1	1	2	2	1	1	1	1	1	1	1	1	1	1	1	1	1	2	2	0	0	0	0	0					
	ASTM 2 to 5	2																																																							
	ASTM > 5	3																																																							
Sediment	< 25% of sample jar bottom covered	1	1	1	1	2	2	0	0	0	0	0	0	0	0	0	0	2	2	3	3	3	3	1	2	2	2	3	2	2	2	3	3	3	3	3	3	3	3	3	3	3	2	2	2	3	3	0	0	0	0	0					
	25 to 75 % bottom covered	2																																																							
	> 75 % of bottom covered	3																																																							
Risk Rating:	Min.	10	4	4	4	16	20	2	2	2	2	2	2	2	2	2	2	12	12	13	14	15	16	21	21	21	22	14	14	18	20	23	5	5	5	22	22	21	21	24	24	24	14	19	22	24	24	4	4	4	4	4					
	Max.	40																																																							
Adjusted average:	10 to 15	1	0	0	0	0	0	0	0	0	0	0	0	0	0	0	0	1	1	1	1	1	3	3	3	3	3	3	3	3	3	3	1	1	1	1	1	3	3	3	3	3	3	3	3	3	3	0	0	0	0	0					
	16 to 25	3																																																							
	> 25	5																																																							
Overrides:	Subtotal for rag layer > 10	5	0	0	0	5	5	0	0	0	0	0	0	0	0	0	0	0	0	0	0	0	5	5	5	5	5	0	5	5	5	5	0	0	0	5	5	5	5	5	5	5	0	5	5	5	5	0	0	0	0	0					
Total Risk			4	4	4	21	25	2	2	2	2	2	2	2	2	2	2	13	13	14	15	16	24	29	29	29	30	17	22	26	28	31	6	6	6	28	28	29	29	32	32	32	17	27	30	32	32	4	4	4	4	4					

Table E-1 (continued). Gross Observations of 128-Jars Set up in the Microcosm Study

		Tot Risk	4				6				27				17				6				15				18				30				6				18													
		Jar #	51				52				53				54				55				56				57				58				59				60													
PARAMETER	CRITERION	Week #	3	4	6	9	12	3	4	6	9	12	3	4	6	9	12	3	4	6	9	12	3	4	6	9	12	3	4	6	9	12	3	4	6	9	12	3	4	6	9	12	3	4	6	9	12	3	4	6	9	12
Fuel phase																																																				
Haze	ASTM < 2	1	1	1	1	1	1	1	1	1	1	1	1	2	2	2	3	1	1	1	1	1	1	1	1	1	1	1	1	1	1	1	1	1	1	1	1	1	1	1	1	1	1	2	2	3	3	1	1	1	1	1
	ASTM 2 to 3	2																																																		
	ASTM > 3	3																																																		
Color	ASTM £ 2	1	3	3	3	3	3	3	3	3	3	3	3	3	3	3	3	3	3	3	3	3	3	3	3	3	3	3	3	3	3	3	3	3	3	3	3	3	3	3	3	3	3	3	3	3	3					
	ASTM 2 to 5	2																																																		
	ASTM > 5	3																																																		
Invert emulsion (rag layer)																																																				
Present	No	0	0	0	0	0	0	0	0	0	0	0	3	3	3	3	3	3	3	3	3	3	0	0	0	0	0	0	0	0	3	3	3	3	3	3	3	3	3	3	3	3	0	0	0	0	0	3	3	3	3	3
	Yes	3																																																		
Thickness	No rag layer	0	0	0	0	0	0	0	0	0	0	0	1	1	2	2	2	1	1	1	1	1	0	0	0	0	0	0	0	0	1	1	1	1	1	1	1	1	1	1	2	3	0	0	0	0	0	1	1	1	1	1
	< 1 mm	1																																																		
	1 to 3 mm	2																																																		
	> 3 mm	3																																																		
Stalagmites/stalagmites	No rag layer	0	0	0	0	0	0	0	0	0	0	0	2	2	2	2	2	2	2	2	2	2	0	0	0	0	0	0	0	0	2	2	2	2	2	2	2	2	2	2	2	5	0	0	0	0	0	2	2	2	2	2
	No	2																																																		
	Yes	5																																																		
Consistency	No rag layer	0	0	0	0	0	0	0	0	0	0	0	5	5	5	5	5	1	1	1	1	1	0	0	0	0	0	0	0	0	1	1	1	1	1	1	1	1	1	1	2	5	0	0	0	0	0	1	1	1	1	1
	Easily disaggregated	1																																																		
	Difficult to disperse	2																																																		
	Membranous pellicle	5																																																		
Water phase																																																				
Adheres to glass	No rag layer	0	0	0	0	0	0	0	0	0	0	0	1	1	1	1	1	1	1	1	1	3	0	0	0	0	0	0	0	0	1	1	1	1	1	1	1	1	1	1	1	3	0	0	0	0	0	3	3	3	3	3
	No	1																																																		
	Yes	3																																																		
Turbidity	Water-white	0																																																		
	Translucent	2																																																		
	Opaque	4																																																		
Color	ASTM £ 2	1	0	0	0	0	0	1	1	1	1	1	1	1	1	1	1	1	1	1	1	1	1	1	1	1	1	1	1	1	1	1	1	1	1	1	1	0	0	0	0	0	1	1	1	1	1					
	ASTM 2 to 5	2																																																		
	ASTM > 5	3																																																		
Sediment	< 25% of sample jar bottom covered	1	0	0	0	0	0	1	1	1	1	1	1	1	1	1	1	1	1	1	1	2	1	1	1	1	1	1	1	1	3	3	3	3	3	3	3	1	1	1	1	1	0	0	0	0	0	1	1	1	1	1
	25 to 75 % bottom covered	2																																																		
	> 75 % of bottom covered	3																																																		
Risk Rating:	Min.	10	4	4	4	4	4	6	6	6	6	6	17	18	18	18	19	13	13	13	13	16	6	6	6	6	6	6	6	6	15	15	15	15	15	15	15	13	13	13	14	22	4	5	5	6	6	15	15	15	15	15
	Max.	40																																																		
Adjusted average:	10 to 15	1	0	0	0	0	0	0	0	0	0	0	3	3	3	3	3	1	1	1	1	1	0	0	0	0	0	0	0	0	0	0	3	3	3	3	3	3	3	3	3	3	0	0	0	0	0	3	3	3	3	3
	16 to 25	3																																																		
	> 25	5																																																		
Overrides:	Subtotal for rag layer > 10	5	0	0	0	0	0	0	0	0	0	0	5	5	5	5	5	0	0	0	0	0	0	0	0	0	0	0	0	0	0	0	0	0	0	0	0	0	0	0	0	5	0	0	0	0	0	0	0	0	0	0
Total Risk			4	4	4	4	4	6	6	6	6	6	25	26	26	26	27	14	14	14	14	17	6	6	6	6	6	6	6	6	15	15	18	18	18	18	18	16	16	16	17	30	4	5	5	6	6	18	18	18	18	18

Table E-1 (continued). Gross Observations of 128-Jars Set up in the Microcosm Study

PARAMETER	CRITERION	Tot Risk Jar # Week #	8				26				7				6				2				28				31				23				27				31																		
			61				62				63				64				65				66				67				68				69				70																		
			3	4	6	9	12	3	4	6	9	12	3	4	6	9	12	3	4	6	9	12	3	4	6	9	12	3	4	6	9	12	3	4	6	9	12	3	4	6	9	12	3	4	6	9	12	3	4	6	9	12					
Fuel phase																																																									
Haze	ASTM < 2	1	1	1	1	1	1	1	1	1	1	1	1	1	1	1	1	1	1	1	1	1	1	1	1	1	1	1	1	1	1	1	1	1	1	1	1	1	1	1	1	1	1	1	1	1	1										
	ASTM 2 to 3	2																																																							
	ASTM > 3	3																																																							
Color	ASTM £ 2	1	3	3	3	3	3	3	3	3	3	3	3	3	3	3	3	3	3	1	1	1	1	1	1	1	1	1	1	1	1	1	1	1	1	1	1	1	1	1	2	2	1	1	1	1	1										
	ASTM 2 to 5	2																																																							
	ASTM > 5	3																																																							
Invert emulsion (rag layer)																																																									
Present	No	0	0	0	0	0	0	3	3	3	3	3	3	0	0	0	0	0	0	0	0	0	0	0	0	0	0	3	3	3	3	3	3	3	3	3	3	3	3	3	3	3	3	3	3	3	3										
	Yes	3																																																							
Thickness	No rag layer	0	0	0	0	0	0	1	1	2	2	2	2	0	0	0	0	0	0	0	0	0	0	0	0	0	0	2	2	3	3	3	3	2	2	2	3	3	1	1	2	2	2	2	0	1	1	1	1	1	2	2	2	3	3		
	< 1 mm	1																																																							
	1 to 3 mm	2																																																							
	> 3 mm	3																																																							
Stalagmites/stalagmites	No rag layer	0	0	0	0	0	0	2	2	2	2	5	0	0	0	0	0	0	0	0	0	0	0	0	0	0	2	5	5	5	5	5	2	2	2	5	5	2	2	2	5	5	0	2	2	5	5	2	2	2	5	5					
	No	2																																																							
	Yes	5																																																							
Consistency	No rag layer	0	0	0	0	0	0	1	1	1	1	1	1	0	0	0	0	0	0	0	0	0	0	0	0	0	0	1	2	5	5	5	5	1	1	2	5	5	1	1	2	5	5	0	1	1	2	2	1	1	2	2	5				
	Easily disaggregated	1																																																							
	Difficult to disperse	2																																																							
	Membranous pellicle	5																																																							
Water phase																																																									
Adheres to glass	No rag layer	0	0	0	0	0	0	3	3	3	3	3	3	0	0	0	0	0	0	0	0	0	0	0	0	0	0	3	3	3	3	3	3	3	3	3	3	3	3	3	3	3	3	0	3	3	3	3	3	3	3	3					
	No	1																																																							
	Yes	3																																																							
Turbidity	Water-white	0																																																							
	Translucent	2																																																							
	Opaque	4																																																							
Color	ASTM £ 2	1	1	1	1	1	1	1	1	1	1	1	1	1	1	1	1	1	1	0	0	0	0	0	0	0	0	1	1	1	1	1	1	1	1	1	1	1	1	1	1	1	1	1	1	1	1	2	1	1	1	2	2				
	ASTM 2 to 5	2																																																							
	ASTM > 5	3																																																							
Sediment	< 25% of sample jar bottom covered	1	2	2	2	3	3	1	1	1	1	1	1	1	1	2	2	2	2	1	1	1	1	1	1	1	1	0	0	0	0	0	0	1	1	1	1	1	1	1	1	2	3	3	1	1	1	1	1	1	1	1	1	1			
	25 to 75 % bottom covered	2																																																							
	> 75 % of bottom covered	3																																																							
Risk Rating:	Min.	10	7	7	7	8	8	15	15	15	15	18	6	6	7	7	7	7	6	6	6	6	6	6	6	6	2	2	2	2	2	2	13	17	20	20	20	13	14	16	23	23	13	13	14	17	17	4	14	14	20	21	13	13	15	17	23
	Max.	40																																																							
Adjusted average:	10 to 15	1	0	0	0	0	0	3	3	3	3	3	3	0	0	0	0	0	0	0	0	0	0	0	0	0	0	3	3	3	3	3	3	3	3	3	3	1	1	1	1	1	1	1	1	1	1	1	3	3	3	3	3				
	16 to 25	3																																																							
	> 25	5																																																							
Overrides:	Subtotal for rag layer > 10	5	0	0	0	0	0	0	0	5	5	5	5	0	0	0	0	0	0	0	0	0	0	0	0	0	0	5	5	5	5	5	5	5	5	5	5	0	0	5	5	5	5	0	0	0	5	5	5	5	5	5	5	5	5	5	
Total Risk			7	7	7	8	8	18	18	23	23	26	6	6	7	7	7	6	6	6	6	6	6	6	6	2	2	2	2	2	2	21	25	28	28	28	21	22	24	31	31	14	14	20	23	23	5	15	15	26	27	21	21	23	25	31	

Table E-1 (continued). Gross Observations of 128-Jars Set up in the Microcosm Study

		Tot Risk	21				16				12				31				30				25				24				27				29				30													
		Jar #	71				72				73				74				75				76				77				78				79				80													
PARAMETER	CRITERION	Week #	3	4	6	9	12	3	4	6	9	12	3	4	6	9	12	3	4	6	9	12	3	4	6	9	12	3	4	6	9	12	3	4	6	9	12	3	4	6	9	12	3	4	6	9	12	3	4	6	9	12
Fuel phase																																																				
Haze	ASTM < 2	1	1	1	1	1	1	2	3	3	3	3	1	1	1	1	1	1	1	2	2	2	1	1	1	1	1	1	1	1	1	1	1	1	2	2	2	1	1	1	1	1	1	1	1	1	1	1	1	1	1	1
	ASTM 2 to 3	2																																																		
	ASTM > 3	3																																																		
Color	ASTM £ 2	1	1	1	1	1	1	1	1	1	1	1	1	1	1	1	1	1	1	2	2	2	1	1	1	1	1	1	1	1	1	1	1	1	1	1	1	1	1	1	1	1	1	1	1	1	1					
	ASTM 2 to 5	2																																																		
	ASTM > 5	3																																																		
Invert emulsion (rag layer)																																																				
Present	No	0	0	0	0	3	3	3	3	3	3	3	3	3	3	3	3	0	3	3	3	3	3	3	3	3	3	0	0	0	3	3	3	3	3	3	3	0	0	3	3	3	3	3	3	3	3					
	Yes	3																																																		
Thickness	No rag layer	0	0	0	0	2	2	1	1	1	1	1	2	2	2	2	2	0	1	1	2	2	1	1	1	3	3	0	0	0	2	2	2	2	2	2	3	0	0	2	2	3	1	1	3	3	3	1	1	1	2	3
	< 1 mm	1																																																		
	1 to 3 mm	2																																																		
	> 3 mm	3																																																		
Stalagmites/stalagmites	No rag layer	0	0	0	0	5	5	2	2	2	2	2	2	2	2	2	2	0	2	5	5	5	2	5	5	5	5	0	0	0	2	5	2	2	2	2	2	0	0	5	5	5	2	2	2	2	2					
	No	2																																																		
	Yes	5																																																		
Consistency	No rag layer	0	0	0	0	1	1	1	1	1	1	1	1	1	1	1	1	0	1	2	5	5	1	1	2	2	5	0	0	0	2	5	1	1	1	1	5	0	0	1	5	5	1	1	5	5	5	1	1	1	2	5
	Easily disaggregated	1																																																		
	Difficult to disperse	2																																																		
	Membranous pellicle	5																																																		
Water phase																																																				
Adheres to glass	No rag layer	0	0	0	0	3	3	3	3	3	3	3	1	1	1	1	1	0	1	1	3	3	3	3	3	3	3	0	0	0	1	1	1	1	1	1	1	0	0	1	3	3	1	3	3	3	3	3	3	3	3	3
	No	1																																																		
	Yes	3																																																		
Turbidity	Water-white	0																																																		
	Translucent	2																																																		
	Opaque	4																																																		
Color	ASTM £ 2	1	1	1	1	1	1	1	1	1	1	1	1	1	1	1	1	1	1	1	2	2	1	1	1	1	1	1	1	1	2	3	1	1	1	1	1	1	1	1	2	2	1	1	1	1	1					
	ASTM 2 to 5	2																																																		
	ASTM > 5	3																																																		
Sediment	< 25% of sample jar bottom covered	1	1	1	1	1	1	1	1	1	1	1	1	1	1	1	1	1	1	1	2	2	1	1	1	2	2	1	1	1	2	3	1	1	1	1	1	1	1	1	2	2	1	2	2	3	3	1	1	1	1	1
	25 to 75 % bottom covered	2																																																		
	> 75 % of bottom covered	3																																																		
Risk Rating:	Min.	10	4	4	4	16	16	14	15	15	15	15	11	11	11	11	11	4	11	17	23	23	13	16	17	19	22	4	4	4	13	20	11	12	12	13	18	4	4	14	21	21	11	14	18	21	21	15	15	15	19	22
	Max	40																																																		
Adjusted average:	10 to 15	1	0	0	0	0	0	1	1	1	1	1	1	1	1	1	1	3	3	3	3	3	3	3	3	3	3	0	0	0	0	0	1	1	1	1	1	1	1	1	1	1	3	3	3	3	3	3	3	3	3	3
	16 to 25	3																																																		
	> 25	5																																																		
Overrides:	Subtotal for rag layer > 10	5	0	0	0	5	5	0	0	0	0	0	0	0	0	0	0	0	0	5	5	5	0	5	5	5	5	0	0	0	0	5	0	0	0	0	5	0	0	5	5	5	0	0	5	5	5	0	0	0	5	5
Total Risk			4	4	4	21	21	15	16	16	16	16	12	12	12	12	12	7	14	25	31	31	16	24	25	27	30	4	4	4	13	25	12	13	13	14	24	5	5	20	27	27	14	17	26	29	29	18	18	18	27	30

Table E-1 (continued). Gross Observations of 128-Jars Set up in the Microcosm Study

		Tot Risk	28				9				19				33				16				16				4				4				16				8														
		Jar #	81				82				83				84				85				86				87				88				89				90														
PARAMETER	CRITERION	Week #	3	4	6	9	12	3	4	6	9	12	3	4	6	9	12	3	4	6	9	12	3	4	6	9	12	3	4	6	9	12	3	4	6	9	12	3	4	6	9	12	3	4	6	9	12	3	4	6	9	12	
Fuel phase																																																					
Haze	ASTM < 2	1	1	1	1	1	1	1	2	2	3	3	1	2	3	3	3	1	1	1	1	1	2	2	2	2	2	1	2	2	3	3	1	1	1	1	1	1	1	1	1	1	1	1	1	1	1	1	1	1	1	1	
	ASTM 2 to 3	2																																																			
	ASTM > 3	3																																																			
Color	ASTM £ 2	1	3	3	3	3	3	3	3	3	3	3	3	3	3	3	3	3	3	3	3	3	3	3	3	3	3	3	3	3	3	3	3	3	3	3	3	3	3	3	3	3	3	3	3	3	3						
	ASTM 2 to 5	2																																																			
	ASTM > 5	3																																																			
Invert emulsion (rag layer)																																																					
Present	No	0	0	3	3	3	3	0	0	0	0	0	3	3	3	3	3	0	0	0	3	3	0	0	0	3	3	3	3	3	3	3	0	0	0	0	0	0	0	0	0	0	0	0	3	3	3	0	0	0	0	0	
	Yes	3																																																			
Thickness	No rag layer	0	0	1	2	2	3	0	0	0	0	0	1	1	1	1	2	0	0	0	1	2	2	0	0	0	1	1	1	1	1	1	1	0	0	0	0	0	0	0	0	0	0	0	0	1	1	1	0	0	0	0	0
	< 1 mm	1																																																			
	1 to 3 mm	2																																																			
	> 3 mm	3																																																			
Stalagmites/stalagmites	No rag layer	0	0	2	2	2	5	0	0	0	0	0	2	2	2	2	2	0	0	2	5	5	0	0	0	2	2	2	2	2	2	2	0	0	0	0	0	0	0	0	0	0	0	0	2	2	2	0	0	0	0	0	
	No	2																																																			
	Yes	5																																																			
Consistency	No rag layer	0	0	1	1	2	5	0	0	0	0	0	1	1	1	1	1	0	0	1	5	5	0	0	0	1	1	1	1	1	1	1	0	0	0	0	0	0	0	0	0	0	0	0	1	1	1	0	0	0	0	0	
	Easily disaggregated	1																																																			
	Difficult to disperse	2																																																			
	Membranous pellicle	5																																																			
Water phase																																																					
Adheres to glass	No rag layer	0	0	1	1	1	3	0	0	0	0	0	1	1	1	1	1	0	0	1	3	3	0	0	0	1	1	1	1	1	1	1	0	0	0	0	0	0	0	0	0	0	0	0	1	1	1	0	0	0	0	0	
	No	1																																																			
	Yes	3																																																			
Turbidity	Water-white	0																																																			
	Translucent	2																																																			
	Opaque	4																																																			
Color	ASTM £ 2	1	1	1	1	1	1	1	1	1	1	1	1	1	1	1	1	1	1	1	1	2	1	1	1	1	1	1	1	1	1	1	0	0	0	0	0	0	0	0	0	0	1	1	1	1	1	1	1	1	1	1	
	ASTM 2 to 5	2																																																			
	ASTM > 5	3																																																			
Sediment	< 25% of sample jar bottom covered	1	1	1	1	1	1	2	2	2	2	2	1	1	2	2	2	2	2	2	3	3	1	1	1	2	2	1	1	1	1	1	0	0	0	0	0	0	0	0	0	0	3	3	3	3	3	2	2	3	3	3	
	25 to 75 % bottom covered	2																																																			
	> 75 % of bottom covered	3																																																			
Risk Rating:	Min.	10	6	13	13	14	22	7	8	8	9	9	13	14	16	16	16	7	7	14	24	25	7	7	7	15	15	13	14	14	15	15	4	4	4	4	4	4	4	4	4	4	8	8	15	15	15	7	7	8	8	8	
	Max.	40																																																			
Adjusted average:	10 to 15	1	1	1	1	1	1	0	0	0	0	0	3	3	3	3	3	3	3	3	3	3	1	1	1	1	1	1	1	1	1	1	0	0	0	0	0	0	0	0	0	0	1	1	1	1	1	0	0	0	0	0	
	16 to 25	3																																																			
	> 25	5																																																			
Overrides:	Subtotal for rag layer > 10	5	0	0	0	0	5	0	0	0	0	0	0	0	0	0	0	0	0	0	5	5	0	0	0	0	0	0	0	0	0	0	0	0	0	0	0	0	0	0	0	0	0	0	0	0	0	0	0	0	0	0	
Total Risk			7	14	14	15	28	7	8	8	9	9	16	17	19	19	19	10	10	17	32	33	8	8	8	16	16	14	15	15	16	16	4	4	4	4	4	4	4	4	4	4	9	9	16	16	16	7	7	8	8	8	

Table E-1 (continued). Gross Observations of 128-Jars Set up in the Microcosm Study

		Tot Risk	7				14				14				18				6				16				2				27				8				21													
		Jar #	91				92				93				94				95				96				97				98				99				100													
PARAMETER	CRITERION	Week #	3	4	6	9	12	3	4	6	9	12	3	4	6	9	12	3	4	6	9	12	3	4	6	9	12	3	4	6	9	12	3	4	6	9	12	3	4	6	9	12	3	4	6	9	12					
Fuel phase																																																				
Haze	ASTM < 2	1	1	1	1	1	1	1	1	1	1	1	1	1	1	1	1	1	1	1	1	1	1	1	1	1	1	1	1	1	1	1	1	1	1	1	1	1	1	1	2	2	1	2	2	2	2					
	ASTM 2 to 3	2																																																		
	ASTM > 3	3																																																		
Color	ASTM £ 2	1	3	3	3	3	3	3	3	3	3	3	3	3	3	3	3	3	3	3	3	3	3	3	3	3	3	1	1	1	1	1	1	1	1	1	1	1	1	1	1	1										
	ASTM 2 to 5	2																																																		
	ASTM > 5	3																																																		
Invert emulsion (rag layer)																																																				
Present	No	0	0	0	0	0	0	3	3	3	3	3	3	3	3	3	3	3	3	3	3	3	0	0	0	0	0	3	3	3	3	3	0	0	0	0	0	0	0	3	3	3	0	0	0	0	0					
	Yes	3																																																		
Thickness	No rag layer	0	0	0	0	0	0	1	1	1	1	1	1	1	1	1	1	1	1	1	1	1	0	0	0	0	0	1	1	1	1	1	0	0	0	0	0	0	0	1	2	3	0	0	0	0	0					
	< 1 mm	1																																																		
	1 to 3 mm	2																																																		
Stalagmites/stalagmites	> 3 mm	3																																																		
	No rag layer	0	0	0	0	0	0	2	2	2	2	2	2	2	2	2	2	2	2	2	2	2	0	0	0	0	0	2	2	2	2	2	0	0	0	0	0	0	0	2	5	5	0	0	0	0	0					
	Yes	5																																																		
Consistency	No rag layer	0	0	0	0	0	0	1	1	1	1	1	1	1	1	1	1	1	1	1	1	1	0	0	0	0	0	1	1	1	1	1	0	0	0	0	0	0	0	2	2	5	0	0	0	0	0					
	Easily disaggregated	1																																																		
	Difficult to disperse	2																																																		
	Membranous pellicle	5																																																		
Water phase																																																				
Adheres to glass	No rag layer	0	0	0	0	0	0	1	1	1	1	1	1	1	1	1	1	3	3	3	3	3	0	0	0	0	0	1	1	1	1	1	0	0	0	0	0	0	0	3	3	3	0	0	0	0	0					
	No	1																																																		
	Yes	3																																																		
Turbidity	Water-white	0																																																		
	Translucent	2																																																		
	Opaque	4																																																		
Color	ASTM £ 2	1	1	1	1	1	1	1	1	1	1	1	1	1	1	1	1	1	1	1	1	1	1	1	1	1	1	0	0	0	0	0	1	1	1	1	1	1	1	1	1	2	1	1	1	1	1					
	ASTM 2 to 5	2																																																		
	ASTM > 5	3																																																		
Sediment	< 25% of sample jar bottom covered	1	2	2	2	2	2	1	1	1	1	1	1	1	1	1	1	1	1	1	1	1	1	1	1	1	1	0	0	0	0	0	1	1	2	2	2	3	3	3	3	3	1	1	1	1	1					
	25 to 75 % bottom covered	2																																																		
	> 75 % of bottom covered	3																																																		
Risk Rating:	Min.	10	7	7	7	7	7	13	13	13	13	13	13	13	13	13	13	15	15	15	15	15	6	6	6	6	6	13	13	13	13	15	2	2	2	2	2	4	4	15	18	21	6	6	6	7	8	14	15	15	15	15
	Max.	40																																																		
Adjusted average:	10 to 15	1	0	0	0	0	0	1	1	1	1	1	1	1	1	1	1	3	3	3	3	3	0	0	0	0	0	1	1	1	1	1	0	0	0	0	0	1	1	1	1	1	0	0	0	0	0					
	16 to 25	3																																																		
	> 25	5																																																		
Overrides:	Subtotal for rag layer > 10	5	0	0	0	0	0	0	0	0	0	0	0	0	0	0	0	0	0	0	0	0	0	0	0	0	0	0	0	0	0	0	0	0	5	5	5	0	0	0	0	0	5	5	5	5	5					
Total Risk			7	7	7	7	7	14	14	14	14	14	14	14	14	14	14	18	18	18	18	18	6	6	6	6	6	14	14	14	14	16	2	2	2	2	2	5	5	21	24	27	6	6	6	7	8	20	21	21	21	21

Table E-1 (continued). Gross Observations of 128-Jars Set up in the Microcosm Study

		Tot Risk	27					28					29					6					16					28					30					26					21					23									
		Jar #	101					102					103					104					105					106					107					108					109					110									
PARAMETER	CRITERION	Week #	3	4	6	9	12	3	4	6	9	12	3	4	6	9	12	3	4	6	9	12	3	4	6	9	12	3	4	6	9	12	3	4	6	9	12	3	4	6	9	12	3	4	6	9	12	3	4	6	9	12	3	4	6	9	12
Fuel phase																																																									
Haze	ASTM < 2	1	1	2	2	2	2	1	1	1	1	1	1	1	1	1	1	1	1	1	1	1	1	1	1	1	1	1	1	1	1	1	1	1	1	1	1	1	1	1	1	1	1	1	1	1	1	1	1	1	1	1					
	ASTM 2 to 3	2																																																							
	ASTM > 3	3																																																							
Color	ASTM ε 2	1	1	1	1	1	1	1	1	1	1	1	1	1	1	1	1	1	1	1	1	1	1	1	1	1	1	1	1	1	1	1	1	1	1	1	1	1	1	1	1	1	1	1	1	1	1										
	ASTM 2 to 5	2																																																							
	ASTM > 5	3																																																							
Invert emulsion (rag layer)																																																									
Present	No	0	3	3	3	3	3	3	3	3	3	3	3	3	3	3	3	0	0	0	0	0	3	3	3	3	3	3	3	3	3	3	3	3	3	3	3	0	0	0	0	0	3	3	3	3	3	0	0	3	3	3					
	Yes	3																																																							
Thickness	No rag layer	0	1	1	1	2	3	2	2	3	3	3	1	2	2	2	3	0	0	0	0	0	1	1	1	1	1	1	2	3	3	3	2	2	3	3	3	0	0	0	0	3	1	1	1	2	2	0	0	1	2	2					
	< 1 mm	1																																																							
	1 to 3 mm	2																																																							
	> 3 mm	3																																																							
Stalagmites/stalagmites	No rag layer	0	2	2	2	2	2	2	2	2	5	5	2	2	5	5	5	0	0	0	0	0	2	2	2	2	2	2	2	2	5	5	2	2	2	2	5	0	0	0	0	5	2	2	2	2	2	0	0	2	2	2					
	No	2																																																							
	Yes	5																																																							
Consistency	No rag layer	0	2	2	2	2	5	2	2	5	5	5	1	2	5	5	5	0	0	0	0	0	1	1	1	1	1	1	2	5	5	5	2	2	5	5	5	0	0	0	0	5	1	1	1	1	1	0	0	1	5	5					
	Easily disaggregated	1																																																							
	Difficult to disperse	2																																																							
	Membranous pellicle	5																																																							
Water phase																																																									
Adheres to glass	No rag layer	0	3	3	3	3	3	1	3	3	3	3	3	3	3	3	3	0	0	0	0	0	3	3	3	3	3	3	3	3	3	3	3	3	3	3	3	0	0	0	0	3	1	1	1	3	3	0	0	1	1	1					
	No	1																																																							
	Yes	3																																																							
Turbidity	Water-white	0																																																							
	Translucent	2																																																							
	Opaque	4																																																							
Color	ASTM ε 2	1	1	1	1	1	1	1	1	1	1	1	1	1	1	2	2	1	1	1	1	1	1	1	1	1	1	1	1	1	1	1	1	1	1	1	1	1	1	1	1	1	1	1	1	1	1										
	ASTM 2 to 5	2																																																							
	ASTM > 5	3																																																							
Sediment	< 25% of sample jar bottom covered	1	1	1	1	2	2	1	1	1	1	1	1	1	1	1	1	3	3	3	3	3	2	2	2	2	2	1	1	1	1	1	2	2	3	3	3	2	3	3	3	3	1	1	1	2	2	2	2	2	3	3					
	25 to 75 % bottom covered	2																																																							
	> 75 % of bottom covered	3																																																							
Risk Rating:	Min.	10	14	15	15	16	19	12	14	17	20	20	13	14	20	21	21	6	6	6	6	6	14	14	14	15	15	13	14	17	20	20	15	15	19	19	22	5	6	6	7	21	11	11	11	15	15	5	5	12	17	17					
	Max.	40																																																							
Adjusted average:	10 to 15	1	3	3	3	3	3	3	3	3	3	3	3	3	3	3	3	0	0	0	0	0	1	1	1	1	1	3	3	3	3	3	3	3	3	3	3	0	0	0	0	0	1	1	1	1	1	1	1	1	1	1					
	16 to 25	3																																																							
	> 25	5																																																							
Overrides:	Subtotal for rag layer > 10	5	5	5	5	5	5	0	5	5	5	5	0	5	5	5	5	0	0	0	0	0	0	0	0	0	0	0	5	5	5	5	5	5	5	5	5	0	0	0	0	5	0	0	0	5	5	0	0	0	5	5					
Total Risk			22	23	23	24	27	15	22	25	28	28	16	22	28	29	29	6	6	6	6	6	15	15	15	16	16	16	22	25	28	28	23	23	27	27	30	5	6	6	7	26	12	12	12	21	21	6	6	13	23	23					

Table E-1 (continued). Gross Observations of 128-Jars Set up in the Microcosm Study

		Tot Risk	4					16					6					6					16					9					29					25									
		Jar #	121					122					123					124					125					126					127					128									
PARAMETER	CRITERION	Week #	3	4	6	9	12	3	4	6	9	12	3	4	6	9	12	3	4	6	9	12	3	4	6	9	12	3	4	6	9	12	3	4	6	9	12	3	4	6	9	12	3	4	6	9	12
Fuel phase																																															
Haze	ASTM < 2	1	1	1	1	1	1	1	1	1	1	1	1	1	1	1	1	1	1	1	1	1	1	1	2	3	3	1	2	2	2	2	1	1	1	1	1	1	2	2	3	3					
	ASTM 2 to 3	2																																													
	ASTM > 3	3																																													
Color	ASTM £ 2	1	3	3	3	3	3	3	3	3	3	3	3	3	3	3	3	3	3	3	3	3	3	3	3	3	3	3	3	3	3	3	3	3	3	3	3	3	3	3	3	3					
	ASTM 2 to 5	2																																													
	ASTM > 5	3																																													
Invert emulsion (rag layer)																																															
Present	No	0	0	0	0	0	0	0	0	0	3	3	0	0	0	0	0	0	0	0	0	0	3	3	3	3	3	0	0	0	0	0	0	0	3	3	3	3	3	3	3	3					
	Yes	3																																													
Thickness	No rag layer	0	0	0	0	0	0	0	0	0	1	1	0	0	0	0	0	0	0	0	0	0	1	1	1	1	1	0	0	0	0	0	0	0	1	1	1	1	1	2	2	2					
	< 1 mm	1																																													
	1 to 3 mm	2																																													
	> 3 mm	3																																													
Stalagtites/stalagmites	No rag layer	0	0	0	0	0	0	0	0	0	2	2	0	0	0	0	0	0	0	0	0	0	2	2	2	2	2	0	0	0	0	0	0	0	2	2	2	2	2	2	2	2					
	No	2																																													
	Yes	5																																													
Consistency	No rag layer	0	0	0	0	0	0	0	0	0	1	1	0	0	0	0	0	0	0	0	0	0	1	1	1	1	1	0	0	0	0	0	0	0	1	5	5	1	1	1	1	1					
	Easily disaggregated	1																																													
	Difficult to disperse	2																																													
	Membranous pellicle	5																																													
Water phase																																															
Adheres to glass	No rag layer	0	0	0	0	0	0	0	0	0	1	1	0	0	0	0	0	0	0	0	0	0	1	1	1	1	1	0	0	0	0	0	0	0	3	3	3	3	3	3	3	3					
	No	1																																													
	Yes	3																																													
Turbidity	Water-white	0																																													
	Translucent	2																																													
	Opaque	4																																													
Color	ASTM £ 2	1	0	0	0	0	0	1	1	1	1	1	1	1	1	1	1	1	1	1	1	1	1	1	1	1	1	1	1	1	1	1	1	1	1	1	1	1	1	1	1	1					
	ASTM 2 to 5	2																																													
	ASTM > 5	3																																													
Sediment	< 25% of sample jar bottom covered	1	0	0	0	0	0	2	2	3	3	3	1	1	1	1	1	1	1	1	1	1	1	1	1	1	1	2	2	2	3	3	3	3	3	3	3	1	1	1	1	1					
	covered	1																																													
	25 to 75 % bottom covered	2																																													
	> 75 % of bottom covered	3																																													
Risk Rating:	Min.	10	4	4	4	4	4	7	7	8	15	15	6	6	6	6	6	6	6	6	6	6	13	13	14	15	15	7	8	8	9	9	8	8	17	21	21	15	16	16	17	17					
	Max.	40																																													
Adjusted average:	10 to 15	1	0	0	0	0	0	1	1	1	1	1	0	0	0	0	0	0	0	0	0	0	1	1	1	1	1	0	0	0	0	0	3	3	3	3	3	3	3	3	3	3					
	16 to 25	3																																													
	> 25	5																																													
Overrides:	Subtotal for rag layer > 10	5	0	0	0	0	0	0	0	0	0	0	0	0	0	0	0	0	0	0	0	0	0	0	0	0	0	0	0	0	0	0	0	0	0	5	5	0	0	5	5	5					
Total Risk			4	4	4	4	4	8	8	9	16	16	6	6	6	6	6	6	6	6	6	6	14	14	15	16	16	7	8	8	9	9	11	11	20	29	29	18	19	24	25	25					

APPENDIX F
Coupon Observations

APPENDIX G
GCR Data

Table G-1. Cumulative Average GCR Data per Microcosm

Microcosm #	Avg Perc Weight Loss	Std Perc Weight Loss	Avg GCR	Std GCR
1	-0.082	0.321	-0.138	0.543
2	-0.077	0.477	-0.138	0.867
3	0.775	0.147	1.379	0.258
4	0.343	0.002	0.62	0
5	0.269	0.057	0.406	0.082
6	0.041	0.153	0.069	0.258
7	-0.203	0.152	-0.345	0.258
8	-0.245	0.1	-0.414	0.169
9	-0.244	0.1	-0.414	0.169
10	0.203	0.152	0.29	0.217
11	-0.082	0.208	-0.138	0.352
12	0.082	0.058	0.138	0.097
13	0.205	0.058	0.29	0.082
14	0.081	0.153	0.138	0.258
15	0.326	0.551	0.494	0.833
16	-0.082	0.058	-0.116	0.082
17	0	0.264	0	0.376
18	0.081	0.208	0.116	0.296
19	0.285	0.115	0.406	0.164
20	0.326	0.116	0.464	0.164
21	0.409	0.323	0.689	0.543
22	0.286	0.116	0.406	0.164
23	0	0.1	0	0.142
24	0.041	0.058	0.058	0.081
25	0.286	0.115	0.406	0.164
26	0.164	0.058	0.247	0.087
27	0.082	0.115	0.124	0.175
28	-0.082	0.153	-0.138	0.258
29	0.122	0.264	0.174	0.376
30	-0.082	0.115	-0.124	0.175
31	0.204	0.208	0.29	0.296
32	0.367	0.099	0.62	0.169
33	0.448	0.207	0.679	0.315
34	0.448	0.058	0.679	0.087
35	0.366	0.001	0.522	0
36	0.732	0.1	1.241	0.169
37	0.569	0.25	0.813	0.358
38	0.325	0.114	0.464	0.164
39	0.448	0.208	0.639	0.296
40	0.164	0.153	0.276	0.258

Microcosm #	Avg Perc Weight Loss	Std Perc Weight Loss	Avg GCR	Std GCR
41	0.284	0.229	0.432	0.349
42	-0.001	0.265	0	0.4
43	0	0.1	0	0.151
44	0.98	0.693	1.482	1.048
45	0.08	0.404	0.138	0.682
46	0.366	0.803	0.62	1.351
47	-0.041	0.116	-0.069	0.195
48	0.367	0.459	0.62	0.774
49	0.119	0.753	0.173	1.066
50	0.121	0.263	0.173	0.373
51	-0.13	1.251	-0.185	1.89
52	-0.123	0.437	-0.185	0.66
53	-0.369	0.101	-0.519	0.141
54	0.079	0.707	0.115	1.001
55	0.244	0.36	0.371	0.546
56	0.767	0.671	1.31	1.149
57	-0.287	0.307	-0.483	0.516
58	0.445	0.447	0.639	0.641
59	0	0.173	0	0.262
60	0.326	0.379	0.461	0.534
61	-0.123	0.401	-0.185	0.605
62	0.693	0.152	0.98	0.216
63	-0.37	0.267	-0.556	0.4
64	-0.164	0.232	-0.23	0.326
65	-0.204	0.231	-0.309	0.349
66	0.163	0.115	0.23	0.163
67	0.244	0.263	0.371	0.4
68	0.284	0.664	0.403	0.94
69	-0.082	0.603	-0.124	0.912
70	0.039	0.677	0.058	0.961
71	0.245	0.1	0.371	0.151
72	0.245	0.458	0.346	0.647
73	0	0.1	0	0.141
74	0	0.2	0	0.303
75	-0.246	0.436	-0.346	0.615
76	0.122	0.264	0.207	0.447
77	0.245	0.264	0.346	0.373
78	-0.041	0.253	-0.069	0.425
79	0.082	0.058	0.124	0.087
80	-0.165	0.601	-0.23	0.851

Microcosm #	Avg Perc Weight Loss	Std Perc Weight Loss	Avg GCR	Std GCR
81	0.447	0.349	0.758	0.593
82	0.49	0.264	0.718	0.388
83	0.204	0.417	0.288	0.588
84	0.205	0.209	0.309	0.315
85	0.49	0.1	0.741	0.151
86	0.204	0.116	0.286	0.162
87	0.693	0.35	1.018	0.515
88	0.163	0.058	0.215	0.068
89	0.61	0.172	0.898	0.254
90	0.407	0.305	0.599	0.448
91	0.367	0.2	0.539	0.293
92	0.449	0.153	0.634	0.216
93	0.286	0.153	0.4	0.214
94	0.203	0.152	0.286	0.214
95	0.244	0.2	0.359	0.293
96	0.366	0.098	0.515	0.14
97	0.163	0.058	0.239	0.085
98	0.204	0.208	0.299	0.305
99	0.244	0.199	0.359	0.293
100	0.081	0.058	0.114	0.081
101	-0.123	0.361	-0.173	0.509
102	0	0.265	0	0.447
103	0.122	0.3	0.172	0.42
104	0.026	1.769	0.058	2.489
105	0.571	0.35	0.801	0.492
106	0.365	0.263	0.515	0.371
107	0.366	0.173	0.515	0.243
108	0.283	0.49	0.406	0.701
109	0.322	0.847	0.461	1.2
110	-0.001	0.528	0	0.894
111	0.244	0.263	0.343	0.371
112	0.448	0.208	0.629	0.292
113	0.445	0.66	0.629	0.933
114	0.327	0.058	0.458	0.081
115	0.653	0.153	0.958	0.224
116	0.281	0.733	0.406	1.048
117	0.65	0.303	0.958	0.448
118	0.041	0.464	0.06	0.677
119	0.488	0.263	0.741	0.4
120	-0.369	0.437	-0.522	0.62
121	0.204	0.153	0.29	0.217
122	0.244	0.173	0.348	0.246
123	0.285	0.321	0.419	0.471
124	0.162	0.251	0.276	0.425
125	-0.041	0.058	-0.058	0.082
126	0.122	0.264	0.207	0.447
127	0.122	0.264	0.207	0.447
128	-0.163	0.058	-0.247	0.087

Table G-2. Cumulative Maximum GCR Data per Microcosm. Microcosm # are Rank Ordered and Color Coded Dependent on the Severity of Mass Loss (Red – highest, Green – Lowest)

Microcosm #	Maximum Coupon GCR (Rank Ordered)	GCR Standard Deviation
104	3.135	2.489
44	2.965	1.048
56	2.895	1.149
46	2.275	1.351
113	1.887	0.933
68	1.729	0.94
51	1.668	1.89
3	1.655	0.258
87	1.616	0.515
109	1.556	1.2
15	1.482	0.833
21	1.448	0.543
36	1.448	0.169
48	1.448	0.774
81	1.448	0.593
117	1.437	0.448
58	1.393	0.641
108	1.393	0.701
116	1.393	1.048
49	1.383	1.066
70	1.383	0.961
105	1.373	0.492
119	1.297	0.4
89	1.257	0.254
115	1.257	0.224
110	1.241	0.894
37	1.219	0.358
54	1.210	1.001
60	1.210	0.534
62	1.210	0.216
72	1.210	0.647
33	1.112	0.315
90	1.077	0.448
82	1.077	0.388
123	1.077	0.471
39	1.045	0.296
2	1.034	0.867
45	1.034	0.682
112	1.030	0.292
41	0.927	0.349
55	0.927	0.546
69	0.927	0.912
85	0.927	0.151

Microcosm #	Maximum Coupon GCR (Rank Ordered)	GCR Standard Deviation
91	0.898	0.293
80	0.864	0.851
83	0.864	0.588
92	0.864	0.216
106	0.858	0.371
107	0.858	0.243
32	0.827	0.169
76	0.827	0.447
124	0.827	0.425
34	0.741	0.087
67	0.741	0.4
84	0.741	0.315
98	0.718	0.305
99	0.718	0.293
95	0.718	0.293
29	0.697	0.376
31	0.697	0.296
122	0.697	0.246
20	0.697	0.164
38	0.697	0.164
50	0.691	0.373
77	0.691	0.373
103	0.686	0.42
93	0.686	0.214
96	0.686	0.14
111	0.686	0.371
1	0.620	0.543
126	0.620	0.447
4	0.620	0
40	0.620	0.258
102	0.620	0.447
127	0.620	0.447
61	0.556	0.605
71	0.556	0.151
118	0.539	0.677
19	0.522	0.164
35	0.522	0
5	0.522	0.082
10	0.522	0.217
17	0.522	0.376
18	0.522	0.296
22	0.522	0.164

Microcosm #	Maximum Coupon GCR (Rank Ordered)	GCR Standard Deviation
25	0.522	0.164
121	0.522	0.217
75	0.519	0.615
101	0.519	0.509
86	0.515	0.162
94	0.515	0.214
114	0.515	0.081
6	0.414	0.258
14	0.414	0.258
78	0.414	0.425
26	0.371	0.087
42	0.371	0.4
74	0.371	0.303
27	0.371	0.175
52	0.371	0.66
97	0.359	0.085
13	0.348	0.082
120	0.348	0.62
66	0.346	0.163
88	0.311	0.068
12	0.207	0.097
11	0.207	0.352
28	0.207	0.258
47	0.207	0.195
57	0.207	0.516
59	0.185	0.262
43	0.185	0.151
65	0.185	0.349
79	0.185	0.087
23	0.174	0.142
24	0.173	0.081
73	0.173	0.141
100	0.172	0.081
7	0.000	0.258
16	0.000	0.082
30	0.000	0.175
64	0.000	0.326
125	0.000	0.082

APPENDIX H
cATP Data

Table H-1. cATP Data for Microcosm Samples Collected on Days 0 and 30

Measurement Day	Microcosm #	Matrix	cATP (pg ATP/mL)
0	29	water	3,709
0	29	fuel	1
0	40	water	2
0	40	fuel	0
0	57	water	3
0	57	fuel	0
0	66	water	4,202
0	66	fuel	0
0	77	water	1,046
0	77	fuel	0
0	119	water	2,723
0	119	fuel	0
30	30	water	59,841
30	39	water	34,870
30	35	water	21,475
30	86	water	38,135
30	74	water	7,052
30	4	water	32,528
30	9	water	60,031
30	30	fuel	5
30	3	fuel	17
30	3	interphase	16
30	30	interphase	31
30	39	swab	2,988,928

Table H-2. cATP Data for Microcosm Samples Collected on Day 67

Measurement Day	Microcosm #	Matrix	cATP (pg ATP/mL)
67	3	water	36,676
67	4	water	115,693
67	5	water	15,313
67	11	water	5
67	12	water	10
67	13	water	11,242
67	15	water	6
67	15	fuel	4
67	19	water	15,426
67	21	water	20,985
67	21	fuel	74
67	22	water	12,090
67	22	fuel	15
67	23	water	1,414
67	24	water	35,401
67	24	fuel	48
67	25	water	11,541
67	25	fuel	485
67	29	fuel	223
67	29	water	29,874
67	30	water	45,423
67	30	fuel	6
67	31	fuel	77
67	31	water	22,302
67	32	water	23,383
67	35	water	14,236
67	36	water	3
67	37	water	12,673
67	37	fuel	88
67	38	water	188,757
67	38	fuel	506
67	39	water	7,236
67	39	fuel	156
67	40	water	25,253
67	40	fuel	6
67	41	water	8,184
67	41	fuel	187
67	44	water	37,167
67	44	fuel	1
67	47	fuel	295
67	47	water	20,646
67	48	water	39,705
67	48	fuel	13
67	52	fuel	14
67	52	water	7,247
67	53	fuel	144
67	53	water	100,097
67	54	water	12,902
67	57	water	12,501

Measurement Day	Microcosm #	Matrix	cATP (pg ATP/mL)
67	58	fuel	592
67	58	water	85,535
67	67	water	13,522
67	69	water	288
67	72	water	27,144
67	73	water	21,845
67	74	water	3,497
67	75	water	30,413
67	77	water	9,050
67	79	water	17,816
67	81	water	13,959
67	82	water	7
67	82	fuel	3
67	83	water	3,391
67	83	fuel	909
67	85	water	253
67	85	fuel	172
67	86	water	24,297
67	86	fuel	1,814
67	92	water	5,543
67	92	fuel	648
67	96	water	3,774
67	96	fuel	10
67	100	water	17,476
67	102	water	5,232
67	105	water	42,387
67	106	water	70,434
67	109	water	8,446
67	119	water	12,175
67	123	water	66
67	127	water	16,642

Table H-3. cATP Data for Microcosm Samples Collected on Day 120

Measurement Day	Microcosm #	Matrix	cATP (pg ATP/mL)
120	1	water	1
120	3	water	65,531
120	3	water	61,550
120	3	oil	366
120	4	water	76,039
120	4	water	76,039
120	5	interphase	15,251
120	5	water	67,437
120	10	water	79,520
120	11	water	2
120	11	interphase	1
120	11	bottom sediment	1
120	12	water	3
120	12	bottom sediment	4
120	13	water	1,013
120	14	water	8
120	16	water	2
120	16	water	2
120	21	water	122,608
120	23	water	2,306
120	25	water	7,123
120	25	interphase	7,447
120	28	water	24,855
120	29	water	36,897
120	29	interphase	3,776
120	30	water	66,746
120	31	water	53,093
120	32	water	65,940
120	34	water	99,583
120	34	bottom sediment	1,288,629
120	35	water	15,035
120	36	water	3
120	36	fuel	1
120	37	interphase	145
120	37	water	4,860
120	38	interphase	49,569
120	38	water	199,456
120	39	water	27,296
120	41	water	927
120	41	interphase	679
120	42	water	3
120	44	water	35,060
120	44	interphase	13,953
120	45	oil	478
120	45	oil	464
120	45	interphase	2,462
120	46	water	146,761
120	46	bottom sediment	400,927
120	48	water	1,805

Measurement Day	Microcosm #	Matrix	cATP (pg ATP/mL)
120	48	oil	54
120	48	interphase	6,010
120	49	water	42,843
120	51	oil	0
120	52	water	7,520
120	52	bottom sediment	26,571
120	52	interphase	1,224
120	52	fuel	141
120	70	water	44,278
120	110	bottom sediment	177,507
120	110	interphase	2,844
120	126	water	2,330
120	127	water	33,630
120	127	interphase	64,577
120	47	water	50,113
120	53	water	29,719
120	54	water	86,168
120	55	water	164,978
120	57	bottom sediment	2,429
120	57	interphase	2,626
120	57	water	6,566
120	58	water	18,002
120	60	water	8,939
120	61	water	20,010
120	61	bottom sediment	8,670
120	62	interphase	586
120	62	water	39,284
120	63	bottom sediment	5
120	63	water	2
120	64	water	1,081
120	66	water	137,206
120	67	water	7,592
120	68	water	4,114
120	69	water	90
120	69	bottom sediment	323
120	69	interphase	25
120	71	interphase	2
120	71	bottom sediment	272

Measurement Day	Microcosm #	Matrix	cATP (pg ATP/mL)
120	71	water	263
120	73	water	11,774
120	74	bottom sediment	1,105
120	74	water	2,883
120	74	interphase	6,582
120	75	water	69,665
120	76	bottom sediment	5,073
120	77	bottom sediment	69,327
120	77	interphase	166
120	77	fuel	50
120	77	water	1,452
120	78	water	3,975
120	78	interphase	619
120	80	water	50,457
120	81	water	14,366
120	81	interphase	62,148
120	83	water	6,654
120	84	water	1,153
120	85	water	22
120	89	water	15,318
120	90	bottom sediment	48
120	90	water	32
120	91	water	3
120	91	interphase	1
120	92	water	2,323
120	93	water	38,501
120	95	water	22
120	96	water	606
120	97	fuel	7
120	98	water	4,471
120	98	interphase	3
120	99	water	19
120	100	water	1,298
120	101	water	1,193
120	101	fuel	518
120	101	interphase	50,205
120	103	water	76,615
120	103	interphase	8,610

Measurement Day	Microcosm #	Matrix	cATP (pg ATP/mL)
120	104	water	28
120	105	water	5,464
120	106	water	98,772
120	106	fuel	140
120	107	water	32,992
120	108	water	16
120	109	fuel	19
120	109	water	37,188
120	109	bottom sediment	44,582
120	111	water	10,999
120	112	water	24,254
120	112	interphase	1,629
120	113	water	5,235
120	114	water	1,587
120	115	water	1,139
120	116	water	109,248
120	117	water	25,276
120	118	water	120,471
120	119	water	33,818
120	123	water	451,228
120	124	bottom sediment	16,721
120	124	interphase	68
120	124	water	4,147
120	125	water	8,032
120	128	water	76,182

APPENDIX I
Microscopy Data Whole

Table I - 1. Microcosm Samples Down Selected for Microscopy

Microcosm #	Microscopy Subject	Observations
3	fungal mat	Possible presence of mold (<i>Paracoccidioides</i>) and <i>A. oryzae</i>
28	fungal growth	Possible presence of mold (<i>Paracoccidioides</i>) and <i>A. niger</i> or <i>A. nidulans</i>
32	fungal growth	Possible presence of mold (<i>Paracoccidioides</i>) and <i>A. niger</i> or <i>A. nidulans</i>
36	red-brown spot on fungal mat	Iron sulfate deposit (or some other type of metal)
36	fungal mat	Iron sulfate deposit (or some other type of metal)
40	fungal mat	Iron sulfate deposit (or some other type of metal)
41	fungal mat (black)	possible <i>Conidia</i> and filamentous <i>A. oryzae</i>
41	film at interphase	possible <i>Conidia</i> and filamentous <i>A. oryzae</i>
44	bottom water	metal deposit
44	film at interphase	metal deposit
45	interphase	possible presence of mold (<i>Paracoccidioides</i>) and <i>A. oryzae</i>
46	sample growth where the biofilm splits	possible presence of mold (<i>Paracoccidioides</i>) and <i>A. niger</i> or <i>A. nidulans</i>
47	fungal growth	possible <i>Conidia</i> and filamentous <i>A. oryzae</i>
48	fungal growth	possible <i>Conidia</i> and filamentous <i>A. oryzae</i>
49	fungal growth	possible <i>Conidia</i> and filamentous <i>A. oryzae</i>
56	fungal growth	metal deposit
61	interphase	possible <i>Conidia</i> and filamentous <i>A. oryzae</i>
67	fungal mat	<i>Conidia</i> and germinated <i>Conidia</i> of <i>Aspergillus oryzae</i> RIB40.
70	fungal growth	<i>Conidia</i> and germinated <i>Conidia</i> of <i>Aspergillus oryzae</i> RIB40.
71	bottom residue	metal deposit
74	sediment	metal deposit
76	film at interphase	possible presence of mold (<i>Paracoccidioides</i>) and <i>A. niger</i> or <i>A. nidulans</i>
78	fungal mat	<i>conidia</i> and germinated <i>Conidia</i> of <i>Aspergillus oryzae</i> RIB40.
78	interphase	<i>conidia</i> and germinated <i>Conidia</i> of <i>Aspergillus oryzae</i> RIB40.
79	fungal colonies (20X)	<i>conidia</i> and germinated <i>Conidia</i> of <i>Aspergillus oryzae</i> RIB40.
85	fungal mat	possible presence of mold (<i>Paracoccidioides</i>) and <i>A. niger</i> or <i>A. nidulans</i>
86	film at interphase	<i>conidia</i> and germinated <i>Conidia</i> of <i>Aspergillus oryzae</i> RIB40.
93	fungal growth - needs rinsed	possible <i>Conidia</i> and filamentous <i>A. oryzae</i>
99 -1	bottom water	possible <i>Conidia</i> and filamentous <i>A. oryzae</i>
99 -2	interphase	possible <i>Conidia</i> and filamentous <i>A. oryzae</i>
102	sample of 'fish eyes', wet mass	Possible presence of <i>Aspergillus terreus</i> or <i>fumigates</i> , mold (<i>Paracoccidioides</i>)
109	pellicle	Possible presence of mold (<i>Paracoccidioides</i>)
110	take sample of 'fish eyes', wet mass	Possible presence of <i>Aspergillus terreus</i> or <i>fumigates</i> , mold (<i>Paracoccidioides</i>)
122	fungal growth	Possible presence of <i>Aspergillus terreus</i> or <i>fumigates</i> , mold (<i>Paracoccidioides</i>)
126	fungal mat	Possible presence of <i>Aspergillus niger</i> , <i>A. terreus</i> or <i>fumigates</i> , mold (<i>Paracoccidioides</i>)
127	black growth at interphase	Possible presence of <i>Aspergillus niger</i> , <i>A. terreus</i> or <i>fumigates</i> , mold (<i>Paracoccidioides</i>)

Figure I- 1. Microscopic Images of Selected Microcosm Samples

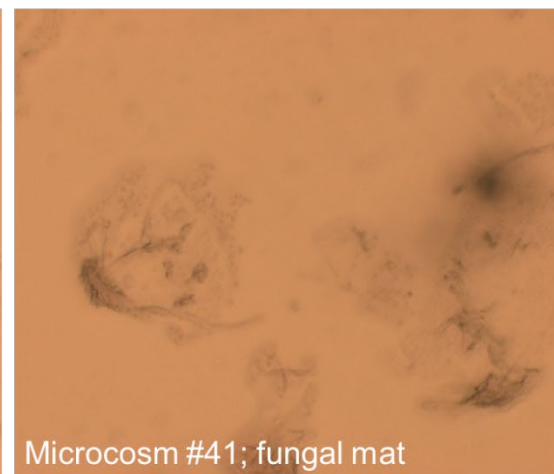
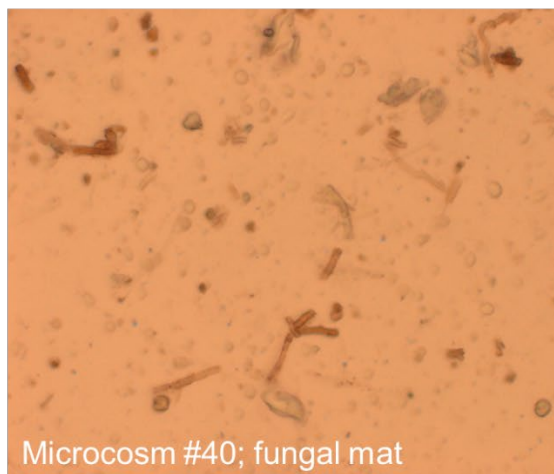
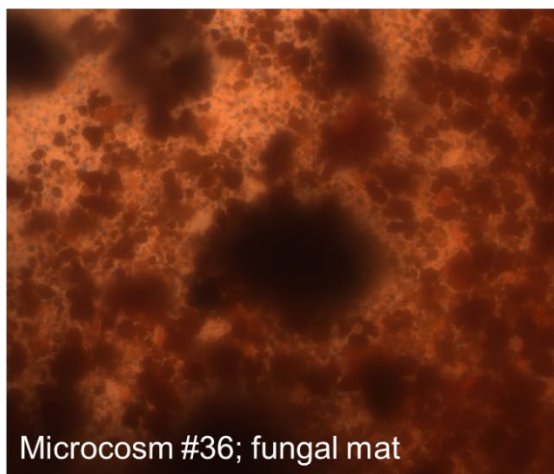
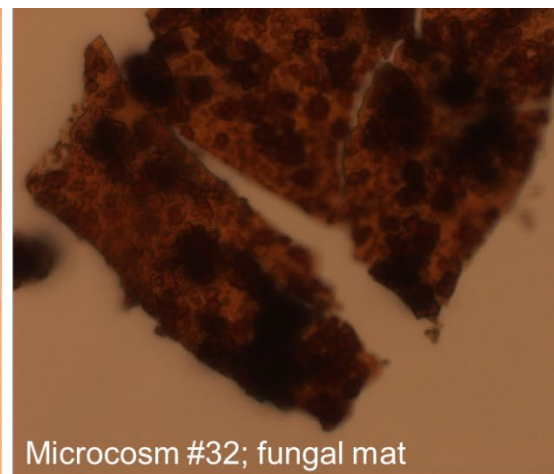
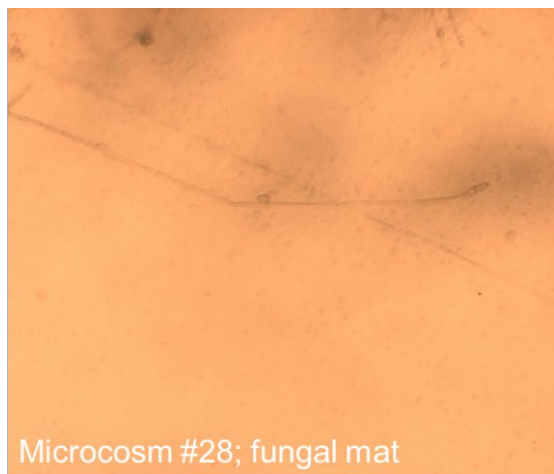
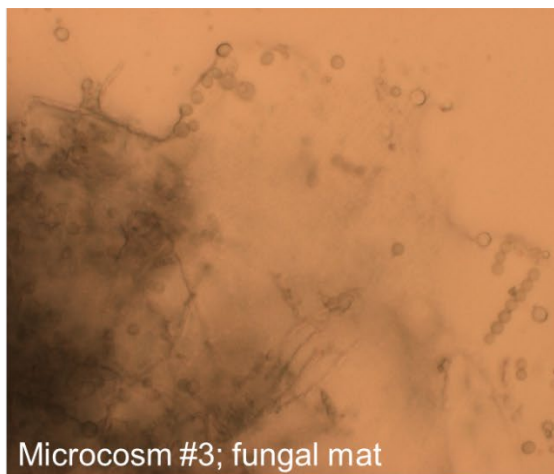


Figure I-1 (continued). Microscopic Images of Selected Microcosm Samples

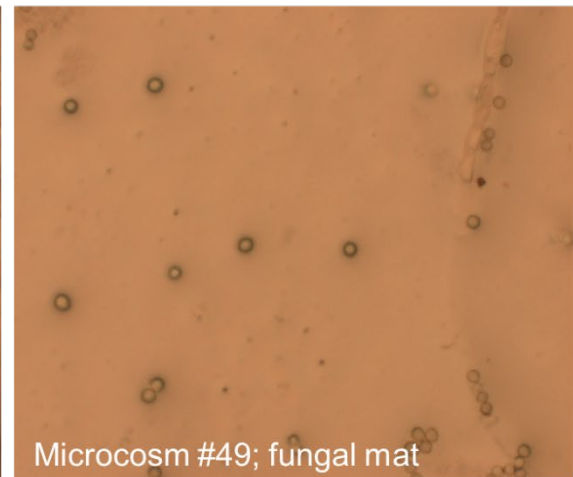
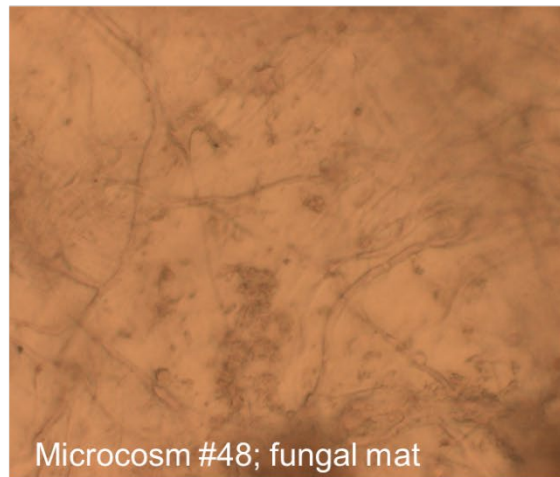
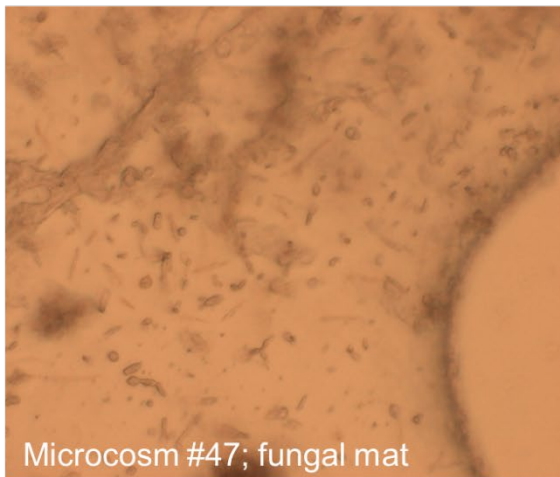
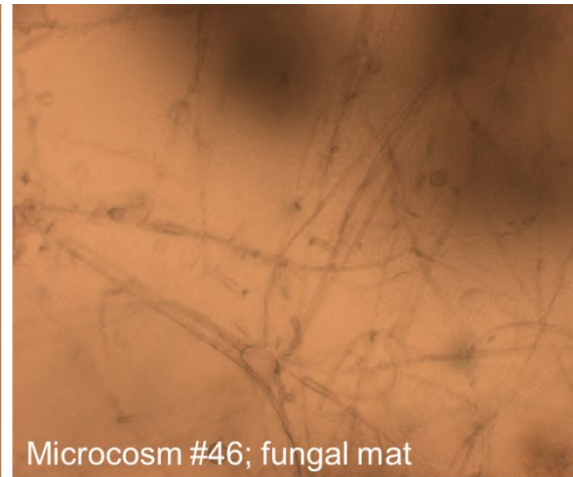
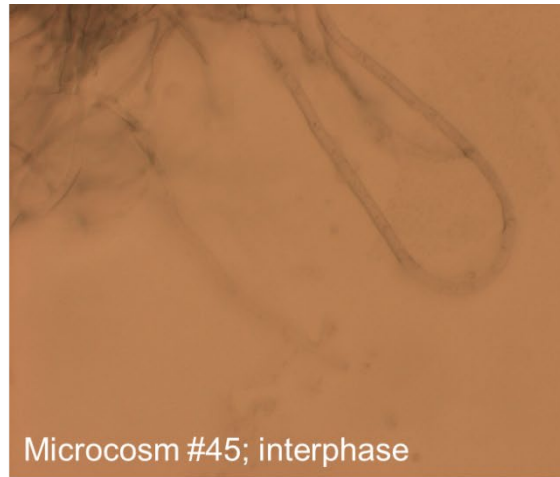
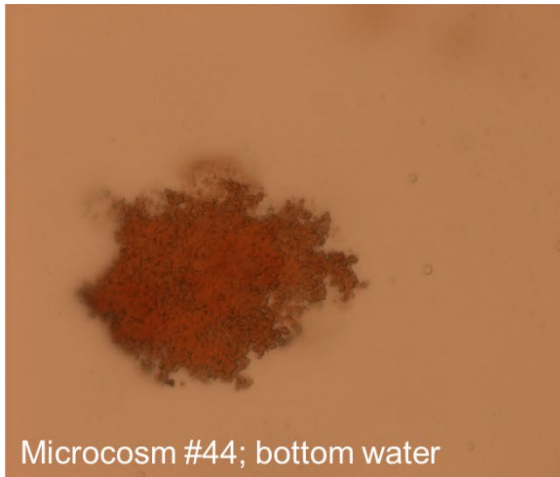


Figure I-1 (continued). Microscopic Images of Selected Microcosm Samples

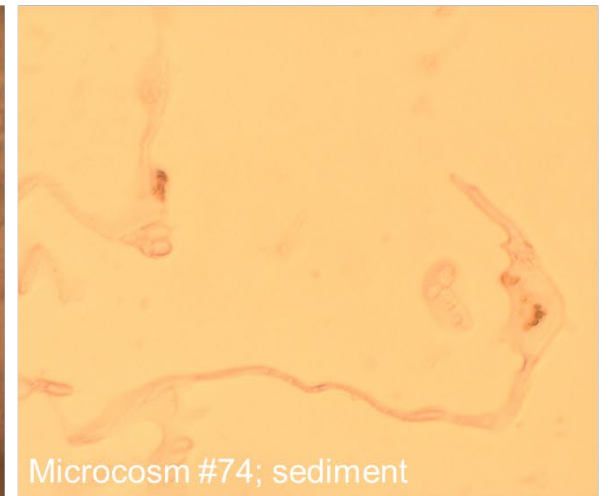
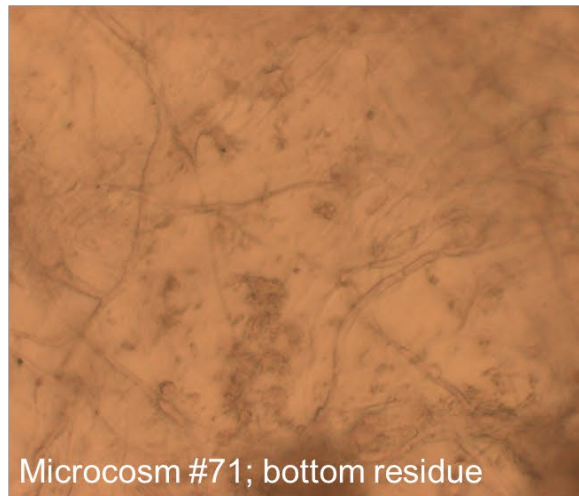
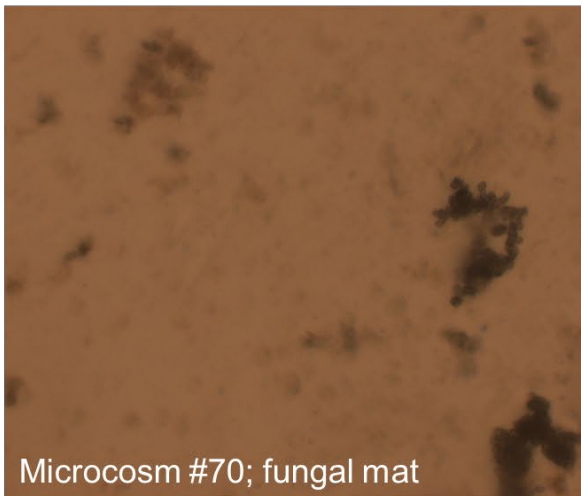
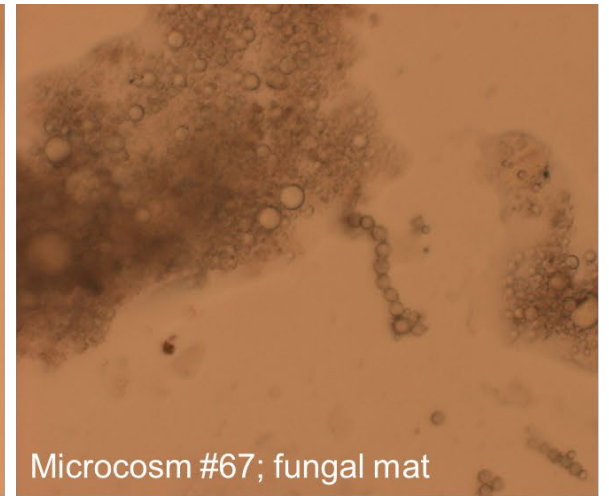
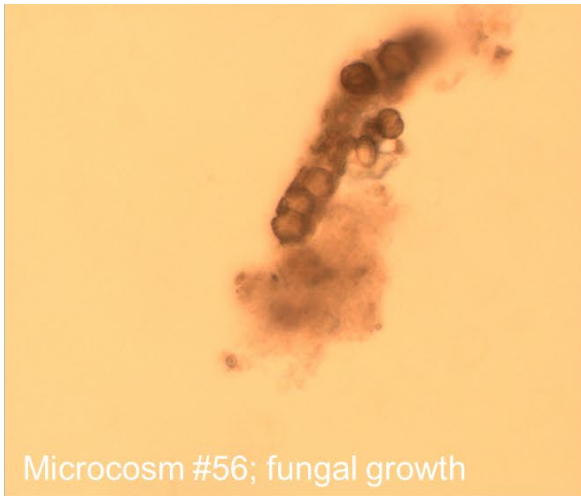


Figure I-1 (continued). Microscopic Images of Selected Microcosm Samples

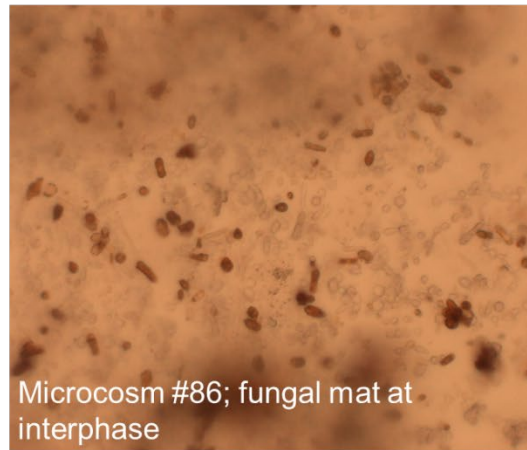
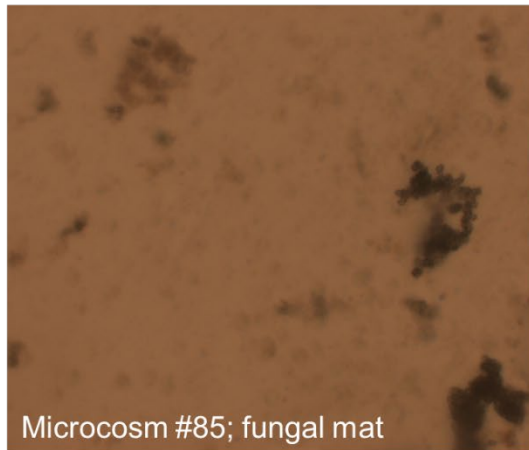
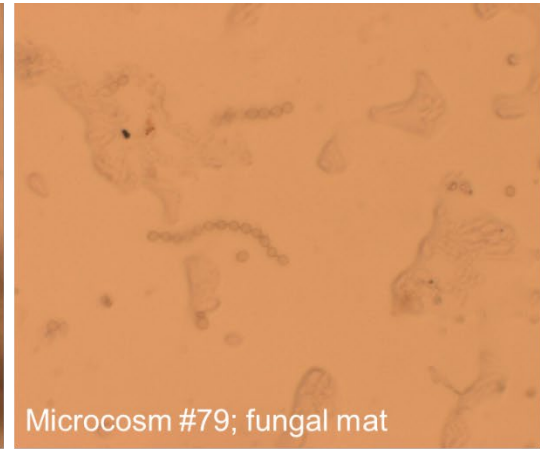
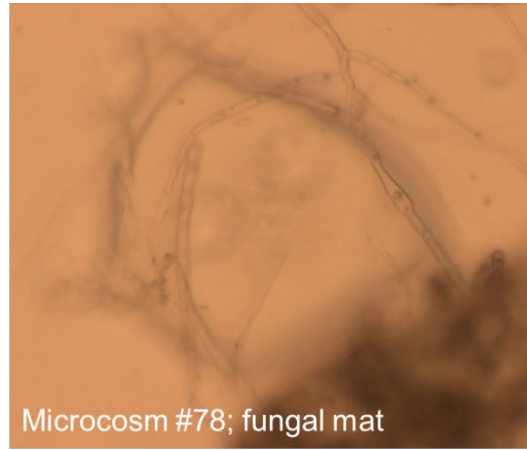
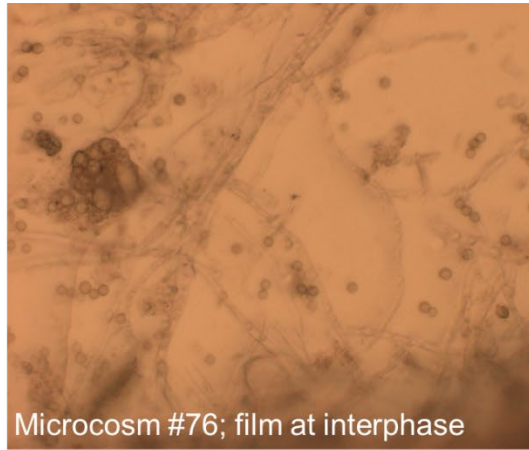


Figure I-1 (continued). Microscopic Images of Selected Microcosm Samples

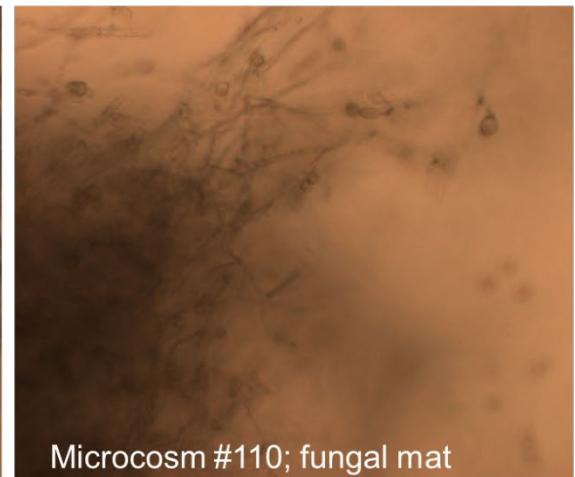
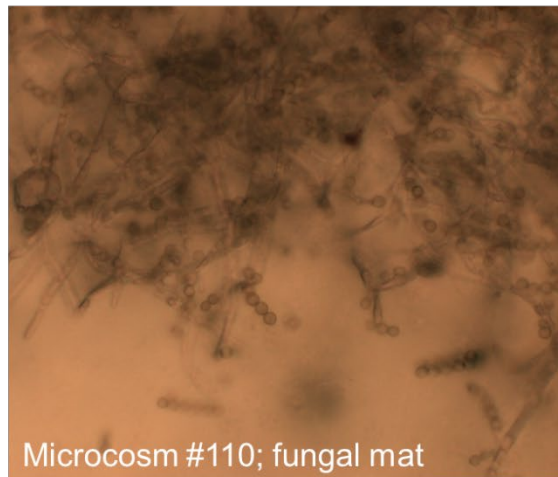
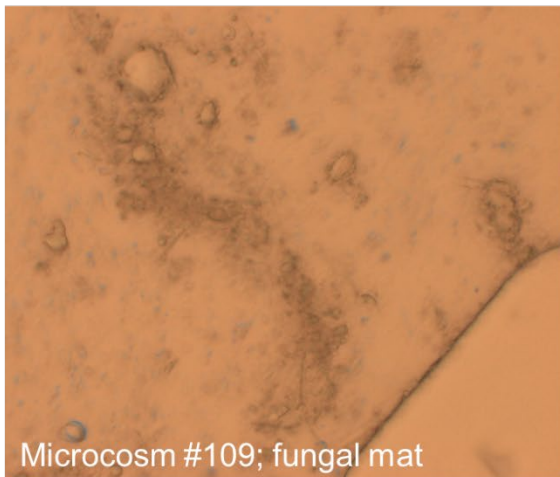
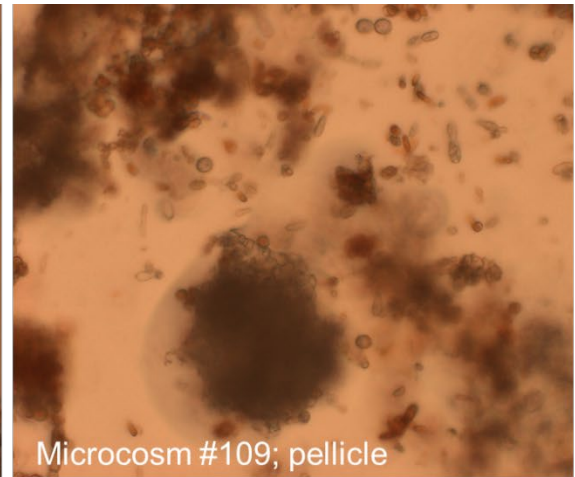
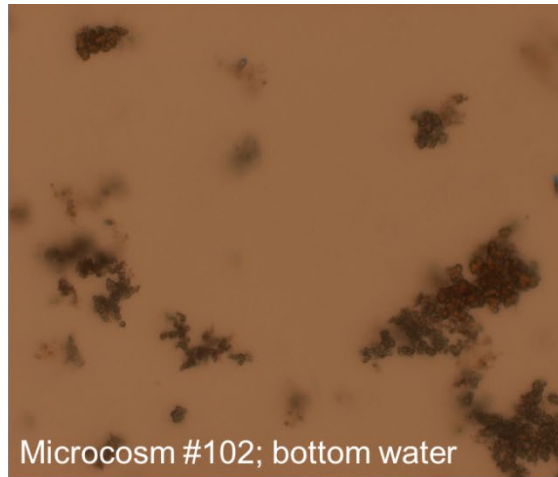
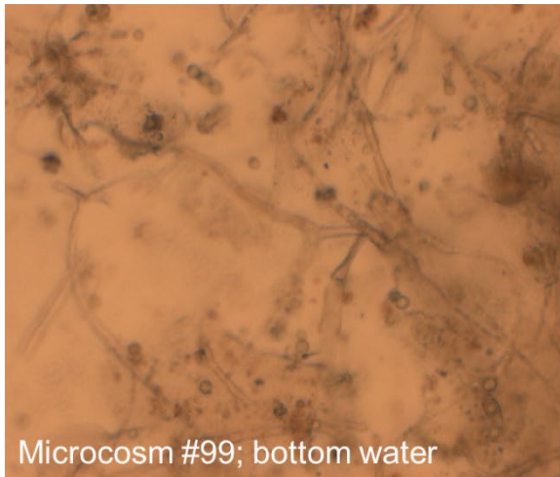
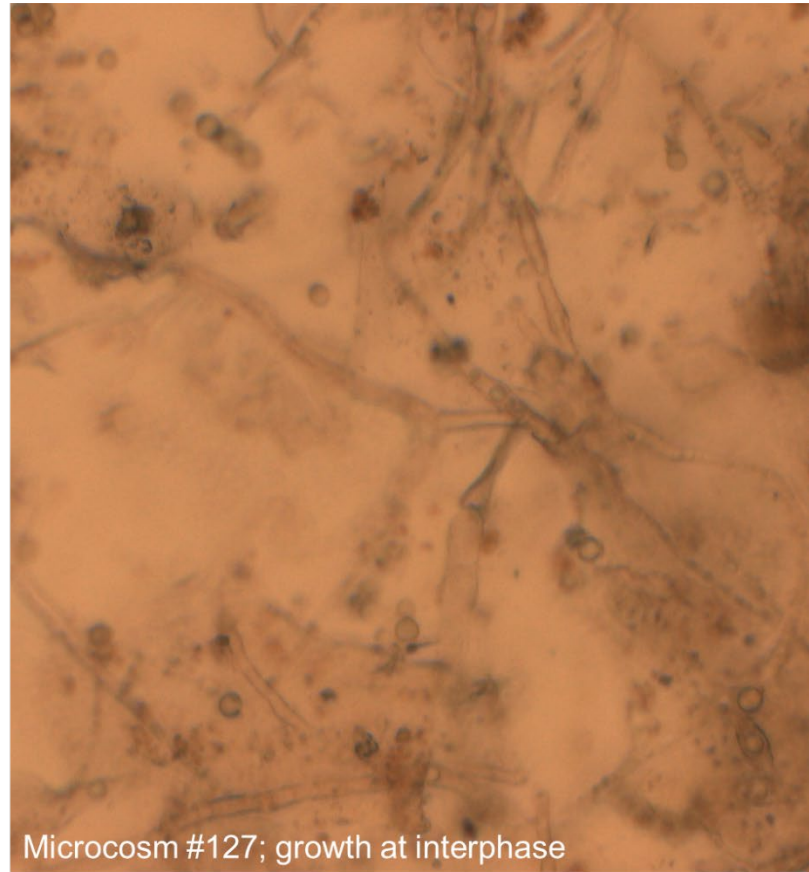
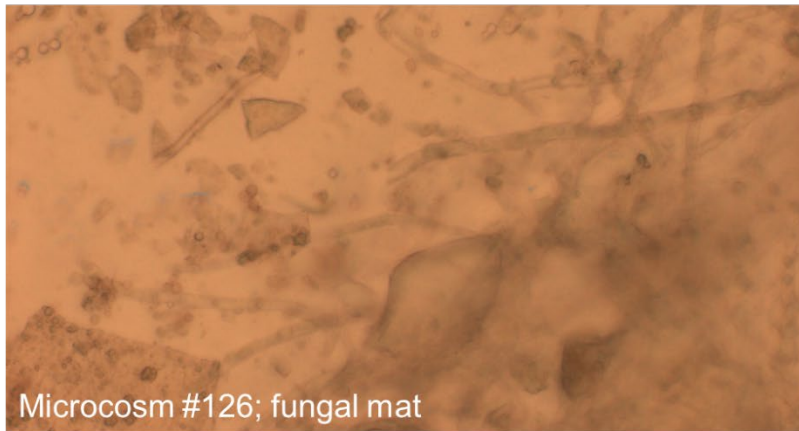
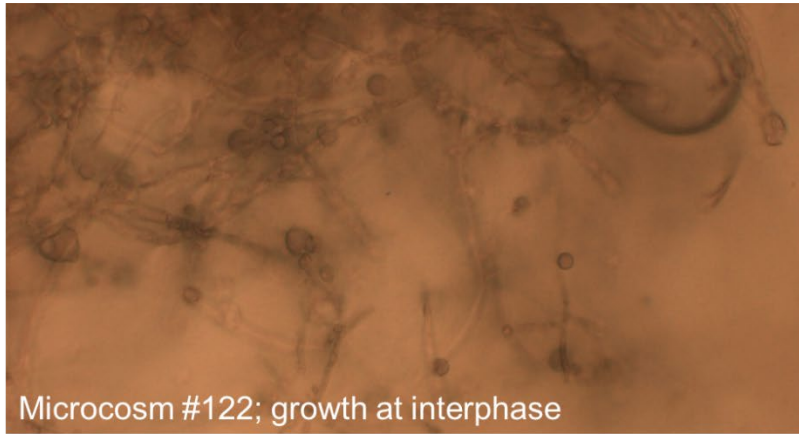


Figure I-1 (continued). Microscopic Images of Selected Microcosm Samples



APPENDIX J
Genomic Data

Table J.1 Genomic Profile UST Bottoms-water Sample I by Whole Genome Sequencing Analysis.

Genus/ species	% Abundance
<i>Pseudomonas</i>	67.44%
<i>aeruginosa</i>	2.33%
<i>aeruginosa</i> BL14	2.33%
<i>aeruginosa</i> BWH051	2.33%
<i>aeruginosa</i> BWH054	2.33%
<i>aeruginosa</i> BWH060	2.33%
<i>aeruginosa</i> BWHP5A012	2.33%
<i>aeruginosa</i> BWHP5A028	2.33%
<i>aeruginosa</i> C52	2.33%
<i>aeruginosa</i> NCAIM	2.33%
<i>aeruginosa</i> PA7	2.33%
<i>aeruginosa</i> PAK	2.33%
<i>aeruginosa</i> PAO1-VE2	2.33%
<i>alcaliphila</i>	2.33%
<i>balearica</i> DSM 6083	2.33%
<i>bauzanensis</i>	2.33%
<i>chlororaphis</i>	2.33%
<i>chlororaphis aureofaciens</i>	2.33%
<i>entomophila</i> L48	2.33%
<i>fluorescens</i>	2.33%
<i>fluorescens</i> R124	2.33%
<i>mendocina</i>	2.33%
<i>monteilii</i> DMS 14164	2.33%
<i>parafulva</i>	2.33%
<i>pseudoalcaligenes</i>	2.33%
<i>putida</i>	2.33%
<i>sp.</i> PAMC 25886	2.33%
<i>sp.</i> URHB0015	2.33%
<i>stutzeri</i>	2.33%
<i>syringae</i> CC1557	2.33%
<i>Rhodoferax</i>	4.65%
<i>ferrireducens</i>	2.33%
<i>ferrireducens</i> T118	2.33%
<i>Acidimicrobium</i>	4.65%
<i>ferrooxidans</i>	2.33%
<i>ferrooxidans</i> DSM 10331	2.33%
<i>Acidiphilium</i>	4.65%
<i>cryptum</i>	2.33%
<i>cryptum</i> JF-5	2.33%

Genus/ species	% Abundance
<i>Rhodopseudomonas</i>	4.65%
<i>palustris</i> BisA53	2.33%
<i>palustris</i> JSC-3b	2.33%
<i>Rhodobacter</i>	4.65%
<i>capsulatus</i>	2.33%
<i>sp.</i> SW2	2.33%
<i>Stenotrophomonas</i>	2.33%
<i>maltophilia</i> K279a	2.33%
<i>Rhodovulum</i>	2.33%
<i>sp.</i> PH10	2.33%
<i>Rhodomicrobium</i>	2.33%
<i>vanniellii</i> ATCC 17100	2.33%
<i>Pseudogulbenkiania</i>	2.33%
<i>sp.</i> MAI-1	2.33%
Grand Total	100.00%

Table J.2 Genomic Profile UST Bottoms-water Sample II by Whole Genome Sequencing Analysis.

Genus/ species	% Abundance
<i>Pseudomonas</i>	35.68%
<i>aeruginosa</i>	0.75%
<i>aeruginosa</i> BL08	0.11%
<i>aeruginosa</i> BWH036	0.11%
<i>aeruginosa</i> BWH051	2.34%
<i>aeruginosa</i> NCAIM B.001380	0.11%
<i>aeruginosa</i> PA7	1.92%
<i>alkylphenolia</i>	0.32%
<i>bauzanensis</i>	0.53%
<i>chlororaphis</i> subsp. <i>aurantiaca</i>	25.56%
<i>chlororaphis</i> subsp. <i>aureofaciens</i> 30-84	0.32%
<i>entomophila</i> L48	0.43%
<i>fluorescens</i>	0.21%
<i>fluorescens</i> R124	0.53%
<i>parafulva</i>	1.28%
<i>sp.</i> PAMC 25886	0.21%
<i>sp.</i> URHB0015	0.53%
<i>sp.</i> UW4	0.11%
<i>sp.</i> WCS374	0.11%
<i>syringae</i> CC1557	0.21%
<i>Acidimicrobium</i>	24.71%
<i>ferrooxidans</i> DSM 10331	24.71%
<i>Rhodobacter</i>	11.40%
<i>capsulatus</i> SB 1003	7.77%
<i>sp.</i> SW2	3.62%
<i>Rhodomicrobium</i>	8.73%
<i>vannielii</i> ATCC 17100	8.73%
<i>Acidiphilium</i>	8.09%
<i>cryptum</i>	4.47%

<i>cryptum JF-5</i>	3.62%
Rhodopseudomonas	3.41%
<i>palustris BisA53</i>	3.09%
<i>palustris JSC-3b</i>	0.32%
Acidimicrobium	3.41%
<i>ferrooxidans</i>	3.41%
Pseudogulbenkiania	1.70%
<i>sp. MAI-1</i>	1.70%
Stenotrophomonas	1.06%
<i>maltophilia K279a</i>	1.06%
Rhodoferax	0.75%
<i>ferrireducens</i>	0.75%
Rhodoferax	0.53%
<i>ferrireducens T118</i>	0.53%
Rhodovulum	0.32%
<i>sp. PH10</i>	0.32%
Bacterium	0.11%
<i>copahuensis</i>	0.11%
Azoarcus sp.	0.11%
<i>BH72</i>	0.11%
Grand Total	100.00%

**Table J.3 Genomic Profile – Secondary LSD Microcosm Used for Challenge Population Cultivation
– Replicate 1**

Genus/ species	% Abundance
<i>Pseudomonas</i>	37.9%
<i>Pseudomonas aeruginosa</i> BL14	0.3%
<i>aeruginosa</i> BWH051	2.0%
<i>aeruginosa</i> BWH054	0.5%
<i>aeruginosa</i> BWH060	0.2%
<i>aeruginosa</i> BWHPA012	0.2%
<i>aeruginosa</i> BWHPA028	0.2%
<i>aeruginosa</i> C23	0.6%
<i>aeruginosa</i> C52	0.2%
<i>aeruginosa</i> NCAIM B.001380	0.6%
<i>aeruginosa</i> PA7	0.5%
<i>aeruginosa</i> PAK	0.2%
<i>aeruginosa</i> PAO1-VE2	0.3%
<i>alcaliphila</i> 34	0.5%
<i>balearica</i> DSM 6083	0.2%
<i>bauzanensis</i>	0.8%
<i>chlororaphis</i> subsp. <i>aurantiaca</i>	23%
30-84	0.5%
<i>entomophila</i> L48	0.3%
<i>fluorescens</i>	0.9%
<i>fluorescens</i> R124	0.3%
<i>mendocina</i>	0.2%
<i>monteilii</i> NBRC 103158 = DSM 14164	0.2%
<i>parafulva</i>	0.6%
<i>pseudoalcaligenes</i>	1.7%
<i>putida</i>	0.3%
PAMC 25886	1.4%
URHB0015	1.1%
<i>stutzeri</i>	0.2%
<i>syringae</i> CC1557	0.2%
<i>Acidimicrobium</i>	28%
<i>ferrooxidans</i> DSM 10331	26%
<i>ferrooxidans</i>	1.4%
<i>Acidiphilium</i>	11.7%
<i>cryptum</i>	9.1%
<i>cryptum</i> JF-5	2.6%
<i>Rhodopseudomonas</i>	3.3%
<i>palustris</i> BisA53	3.2%
<i>palustris</i> JSC-3b	0.2%

Rhodoferax	0.5%
<i>ferrireducens</i>	0.3%
<i>ferrireducens</i> T118	0.2%
<i>Rhodomicrobium vannielii</i> ATCC 17100	9.3%
<i>Rhodobacter capsulatus</i> SB 1003	5.6%
<i>Rhodobacter</i> sp. SW2	2.6%
<i>Pseudogulbenkiania</i> sp. MAI-1	0.3%
<i>Stenotrophomonas maltophilia</i> K279a	0.8%
<i>Rhodovulum</i> sp. PH10	0.3%
unidentified	0.2%
Grand Total	100.0%

**Table J.4 Genomic Profile – Secondary LSD Microcosm Used for Challenge Population Cultivation
– Replicate 2**

Genus/ species	% Abundance
<i>Pseudomonas</i>	35.7%
<i>chlororaphis</i> subsp. <i>aurantiaca</i>	26%
<i>aeruginosa</i> BWH051	2.3%
<i>aeruginosa</i> PA7	1.9%
<i>parafulva</i>	1.3%
<i>aeruginosa</i>	0.7%
<i>aeruginosa</i> BL08	0.1%
<i>aeruginosa</i> BWH036	0.1%
<i>aeruginosa</i> NCAIM B.001380	0.1%
<i>alkylphenolia</i>	0.3%
<i>bauzanensis</i>	0.5%
<i>chlororaphis</i> subsp. <i>aureofaciens</i> 30-84	0.3%
<i>entomophila</i> L48	0.4%
<i>fluorescens</i>	0.2%
<i>fluorescens</i> R124	0.5%
PAMC 25886	0.2%
URHB0015	0.5%
UW4	0.1%
WCS374	0.1%
<i>syringae</i> CC1557	0.2%
<i>Acidimicrobium</i>	28%
<i>ferrooxidans</i> DSM 10331	25%
<i>ferrooxidans</i>	3.4%
<i>Rhodobacter</i>	11.4%
<i>capsulatus</i> SB 1003	7.8%
SW2	3.6%
<i>Acidiphilium</i>	8.1%
<i>cryptum</i>	4.5%
<i>cryptum</i> JF-5	3.6%
<i>Rhodopseudomonas</i>	3.4%
<i>palustris</i> BisA53	3.1%
<i>palustris</i> JSC-3b	0.3%
<i>Rhodoferax</i>	1.3%
<i>ferrireducens</i>	0.7%
<i>ferrireducens</i> T118	0.5%
<i>Rhodomicrobium vannielii</i> ATCC 17100	9%
<i>Stenotrophomonas maltophilia</i> K279a	1%
<i>Pseudogulbenkiania</i> sp. MAI-1	1.7%
<i>Rhodovulum</i> sp. PH10	0.3%
<i>Azoarcus</i> sp. BH72	0.1%

<i>Candidatus acidianus copahuensis</i>	0.1%
Grand Total	100.0%

**Table J.5 Genomic Profile – Secondary LSD Microcosm Used for Challenge Population Cultivation
– Replicate 1 & 2 Combined (Computed Averages)**

Genus/ species	% Abundance		
	DUP #1 ^a	DUP #2	AVG ^b
<i>Pseudomonas</i>			37.2%
<i>aeruginosa</i>	5.5%	5.3%	5.4%
<i>chlororaphis</i>	24%	26%	25%
<i>fluorescens</i>	1.2%	0.7%	1.0%
other spp.	7.3%	4.5%	5.9%
<i>Acidimicrobium ferrooxidans</i>	28%	28%	28%
<i>Acidiphilium cryptum</i>	11.7%	8.1%	9.9%
<i>Rhodopseudomonas palustris</i>	3.3%	3.4%	3.4%
<i>Rhodobacter</i> spp.	11.4%	8.2%	9.8%
<i>Rhodoferax ferrireducens</i>	0.5%	1.3%	0.9%
<i>Rhodomicrobium vannielii</i> ATCC 17100	9.3%	8.7%	9.0%
<i>Pseudogulbenkiania</i> sp. MAI-1	0.3%	BDL	0.2%
<i>Stenotrophomonas maltophilia</i> K279a	0.8%	1.1%	0.9%
<i>Rhodovulum</i> sp. PH10	0.3%	0.3%	0.3%
<i>Pseudogulbenkiania</i> sp. MAI-1	0.3%	1.7%	1.0%
<i>Azoarcus</i> sp. BH72	BDL	0.1%	0.1%
<i>Candidatus acidianus copahuensis</i>	BDL	0.1%	0.1%
unidentified	0.2%	-	0.1%
Grand Total			100%

Notes:

- a) DUP – summarized results from Tables J.3 and J.4. Percentages reflect sums of the total abundance of multiple strains of a given species.
- b) AVG – average OTU abundance. Values in bold font are based on sums of all OTU of the listed genus.

Table J.6 Microbial Diversity in Microcosm # 3 Sample.

Genus and species	% Grand total	Genus and species	% Grand total
Ralstonia sp. 5_2_56FAA	53.20%	Afipia birgiae 34632	0.01%
Paraburkholderia fungorum NBRC 102489	13.19%	Sphingomonas taxi	0.01%
Bradyrhizobium elkanii USDA 76	10.18%	Mesorhizobium loti	0.01%
Sphingomonas sp. RIT328	5.56%	Sphingomonas sp. Root720	0.01%
Mesorhizobium sp. F7	3.81%	Grand Total	100.00%
Caulobacter sp. Root343	2.55%		
Aquabacterium parvum	2.10%		
Novosphingobium nitrogenifigens DSM 19370	1.64%		
Variovorax paradoxus	1.39%		
Paraburkholderia phytofirmans PsJN	1.12%		
Bosea sp. LC85	1.04%		
Mycolicibacterium mucogenicum	0.83%		
Ralstonia solanacearum CMR15	0.66%		
Hammondia hammondi	0.42%		
Methyloversatilis discipulorum	0.35%		
Mesorhizobium japonicum R7A	0.32%		
Methylobacterium radiotolerans JCM 2831	0.23%		
Bradyrhizobium japonicum 22	0.15%		
Bradyrhizobium sp. STM 3843	0.12%		
Reyranelia massiliensis 521	0.12%		
Methylibium petroleiphilum PM1	0.10%		
Blastomonas sp. AAP53	0.10%		
Variovorax paradoxus B4	0.09%		
Bradyrhizobium sp. WSM4349	0.09%		
Pantholops hodgsonii	0.08%		
Sphingopyxis sp. H115	0.08%		
Hyphomicrobium sp. 99	0.06%		
Edaphobacter aggregans DSM 19364	0.06%		
Bosea thiooxidans	0.04%		
Variovorax sp. Root434	0.03%		
Bosea sp. Root381	0.03%		
Bradyrhizobium sp. WSM3983	0.03%		
Leifsonia aquatica H1aii	0.03%		
Leptothrix cholodnii SP-6	0.02%		
Bradyrhizobium japonicum USDA 6	0.01%		
Sphingomonas melonis DAPP-PG 224	0.01%		
Sphingomonas sp. PAMC 26621	0.01%		
Afipia birgiae 34632	0.01%		
Sphingomonas taxi	0.01%		
Mesorhizobium loti	0.01%		
Sphingomonas sp. Root720	0.01%		
Grand Total	100.00%		

Table J.7 Microbial Diversity in Microcosm # 4 Sample.

Genus and species	% Grand total
Lactobacillus paracasei subsp. paracasei 8700:2	68.00%
Bacillus circulans NBRC 13626	31.10%
Lactobacillus paracasei	0.31%
Lactobacillus acidipiscis DSM 15836	0.29%
Lactobacillus rhamnosus LOCK908	0.10%
Aspergillus fischeri NRRL 181	0.09%
Lactobacillus casei BD-II	0.07%
Lactobacillus rhamnosus GG	0.02%
Acinetobacter johnsonii XBB1	0.01%
Grand Total	100.00%

Table J.8 Microbial Diversity in Microcosm # 21 Sample.

Genus and species	% Grand total
Lactobacillus paracasei subsp. paracasei 8700:2	85.76%
Lactobacillus acidipiscis DSM 15836	10.91%
Bacillus circulans NBRC 13626	1.97%
Lactobacillus rhamnosus GG	0.80%
Lactobacillus paracasei	0.27%
Lactobacillus rhamnosus LOCK908	0.18%
Lactobacillus casei BD-II	0.04%
Lactobacillus acidipiscis KCTC 13900	0.02%
Haemophilus parainfluenzae T3T1	0.01%
Porphyromonas sp. KLE 1280	0.01%
Aspergillus fischeri NRRL 181	0.01%
Grand Total	100.00%

Table J.9 Microbial Diversity in Microcosm # 21 Sample.

Genus and species	% Grand total
Lactobacillus acidipiscis DSM 15836	57.42%
Lactobacillus paracasei subsp. paracasei 8700:2	40.79%
Lactobacillus rhamnosus GG	1.01%
Lactobacillus paracasei	0.19%
Bacillus circulans NBRC 13626	0.18%
Lactobacillus rhamnosus LOCK908	0.11%
Porphyromonas sp. KLE 1280	0.08%
Aspergillus fischeri NRRL 181	0.06%
Lactobacillus acidipiscis KCTC 13900	0.06%
Haemophilus parainfluenzae T3T1	0.06%
Lactobacillus casei BD-II	0.04%
Pseudomonas sp. RIT288	0.01%
Grand Total	100.00%

Table J.10 Microbial Diversity in Microcosm # 28 Sample.

Genus and species	% Grand total
Lactobacillus acidipiscis DSM 15836	57.42%
Lactobacillus paracasei subsp. paracasei 8700:2	40.79%
Lactobacillus rhamnosus GG	1.01%
Lactobacillus paracasei	0.19%
Bacillus circulans NBRC 13626	0.18%
Lactobacillus rhamnosus LOCK908	0.11%
Porphyromonas sp. KLE 1280	0.08%
Aspergillus fischeri NRRL 181	0.06%
Lactobacillus acidipiscis KCTC 13900	0.06%
Haemophilus parainfluenzae T3T1	0.06%
Lactobacillus casei BD-II	0.04%
Pseudomonas sp. RIT288	0.01%
Grand Total	100.00%

Table J.11 Microbial Diversity in Microcosm # 32 Sample.

Genus and species	% Grand total
Lactobacillus acidipiscis DSM 15836	96.33%
Lactobacillus paracasei subsp. paracasei 8700:2	3.40%
Lactobacillus acidipiscis KCTC 13900	0.12%
Lactobacillus rhamnosus GG	0.10%
Lactobacillus paracasei	0.02%
Stenotrophomonas maltophilia D457	0.01%
Pseudomonas sp. RIT288	0.01%
Grand Total	100.00%

Table J.12 Microbial Diversity in Microcosm # 36 Sample.

Genus and species	% Grand total
Acinetobacter johnsonii XBB1	37.70%
Pseudomonas sp. RIT288	12.30%
Stenotrophomonas maltophilia D457	11.87%
Acinetobacter lwoffii WJ10621	11.10%
Stenotrophomonas maltophilia	10.68%
Acinetobacter johnsonii SH046	3.30%
Pseudomonas synxantha BG33R	3.09%
Ralstonia sp. NT80	2.18%
Acinetobacter lwoffii NCTC 5866 = CIP 64.10 = NIPH 512	0.96%
Porphyromonas sp. KLE 1280	0.88%
Klebsiella aerogenes EA1509E	0.67%
Pseudomonas fluorescens R124	0.63%
Enterobacter cloacae	0.55%
Pelomonas sp. Root1217	0.50%
Pseudomonas putida H8234	0.48%
Pseudomonas putida HB3267	0.39%
Stenotrophomonas maltophilia MTCC 434	0.37%
Cronobacter turicensis z610	0.27%
Acinetobacter sp. NIPH 1847	0.25%
Acinetobacter sp. CIP 102143	0.19%
Pseudomonas synxantha	0.17%
Acinetobacter johnsonii ANC 3681	0.15%
Enterobacter sp. MGH 22	0.15%
Pseudomonas sp. URMO17WK12:111	0.14%
Prevotella sp. oral taxon 299 str. F0039	0.12%
Ralstonia sp. 5_2_56FAA	0.11%
Enterobacter sp. MGH 24	0.10%
Sphingomonas melonis DAPP-PG 224	0.09%
Prevotella nanceiensis DSM 19126 = JCM 15639	0.08%
Caballeronia zhejiangensis	0.08%
Acinetobacter johnsonii CIP 64.6	0.07%
Pseudomonas chlororaphis	0.06%
Pseudomonas aeruginosa MTB-1	0.06%
Lysinibacillus xylanilyticus	0.04%
Pseudomonas fluorescens NZ007	0.03%
Acinetobacter sp. NIPH 809	0.03%
Stenotrophomonas maltophilia Ab55555	0.03%
Staphylococcus capitis	0.03%
Klebsiella pneumoniae	0.02%
Stenotrophomonas maltophilia NBRC 14161	0.02%
Candidatus Hepatobacter penaei	0.02%
Flavobacterium sp. B17	0.02%
Bacillus coagulans	0.02%
Pseudomonas putida NBRC 14164	0.02%
Pseudomonas sp. S13.1.2	0.01%
Grand Total	100.00%

Table J.13 Microbial Diversity in Microcosm # 40 Sample.

Genus and species	% Grand total
Lactobacillus paracasei subsp. paracasei 8700:2	0.405835305
Acinetobacter johnsonii XBB1	0.223347213
Acinetobacter lwoffii WJ10621	0.076685738
Pseudomonas sp. RIT288	0.071443549
Stenotrophomonas maltophilia D457	0.06290627
Stenotrophomonas maltophilia	0.056256178
Pseudomonas synxantha BG33R	0.017463979
Acinetobacter johnsonii SH046	0.016145943
Ralstonia sp. NT80	0.015337148
Haemophilus parainfluenzae T3T1	0.004942635
Porphyromonas sp. KLE 1280	0.004822814
Acinetobacter lwoffii NCTC 5866 = CIP 64.10 = NIPH 512	0.004553216
Enterobacter cloacae	0.004313573
Cronobacter turicensis z610	0.004043974
Klebsiella aerogenes EA1509E	0.003834287
Pseudomonas fluorescens R124	0.003774376
Acinetobacter sp. NIPH 1847	0.002815804
Lactobacillus paracasei	0.002276608
Enterobacter sp. MGH 24	0.001947099
Pseudomonas putida H8234	0.001677501
Pseudomonas putida HB3267	0.001527724
Gemella sanguinis M325	0.001407902
Pelomonas sp. Root1217	0.001168259
Mycobacterium simiae ATCC 25275 = DSM 44165	0.001078393
Ralstonia sp. 5_2_56FAA	0.000958572
Acinetobacter sp. CIP 102143	0.00083875
Mycobacterium intracellulare subsp. yongonense 05-1390	0.000808795
Haemophilus influenzae KR494	0.000718929
Streptococcus sp. F0441	0.000688973
Acinetobacter ursingii DSM 16037 = CIP 107286	0.000659018
Sphingomonas melonis DAPP-PG 224	0.000659018
Lactobacillus rhamnosus LOCK908	0.000599107
Paraprevotella clara YIT 11840	0.000569152
Stenotrophomonas maltophilia MTCC 434	0.000509241
Acinetobacter johnsonii CIP 64.6	0.000479286
Lactococcus lactis subsp. lactis KLDS 4.0325	0.000479286
Enterobacter sp. MGH 22	0.00044933
Caballeronia zhejiangensis	0.000329509
Pseudomonas synxantha	0.000239643
Sphingobacterium sp. Ag1	0.000239643
Pseudomonas sp. URMO17WK12:I11	0.000209688
Lactobacillus casei BD-II	0.000209688
Acinetobacter johnsonii ANC 3681	0.000209688
Rhizobium sp. IRBG74	0.000149777
Pseudomonas aeruginosa MTB-1	0.000149777
Acinetobacter sp. NIPH 809	0.000119821
Pseudomonas chlororaphis	0.000119821
Grand Total	100.00%

Table J.14 Microbial Diversity in Microcosm # 45A Sample.

Genus and species	% Grand total
Massilia sp. WG5	99.86%
Massilia sp. 9096	0.10%
Porphyromonas sp. KLE 1280	0.02%
Acinetobacter johnsonii XBB1	0.02%
Streptococcus sp. F0441	0.01%
Grand Total	100.00%

Table J.15 Microbial Diversity in Microcosm # 45B Sample.

Genus and species	% Grand total
Massilia sp. WG5	99.77%
Massilia sp. 9096	0.12%
Acinetobacter johnsonii XBB1	0.06%
Stenotrophomonas maltophilia	0.01%
Pseudomonas sp. RIT288	0.01%
Lactobacillus paracasei subsp. paracasei 8700:2	0.01%
Acinetobacter lwoffii WJ10621	0.01%
Grand Total	100.00%

Table J.16 Microbial Diversity in Microcosm # 46 Sample.

Genus and species	% Grand total
Lactobacillus acidipiscis DSM 15836	55.21%
Lactobacillus paracasei subsp. paracasei 8700:2	43.49%
Lactobacillus rhamnosus GG	0.78%
Lactobacillus paracasei	0.16%
Lactobacillus rhamnosus LOCK908	0.15%
Lactobacillus acidipiscis KCTC 13900	0.08%
Bacillus circulans NBRC 13626	0.08%
Lactobacillus casei BD-II	0.04%
Grand Total	100.00%

Table J.17 Microbial Diversity in Microcosm # 47 Sample.

Genus and species	% Grand total
Lactobacillus acidipiscis DSM 15836	81.16%
Methylobacterium radiotolerans JCM 2831	18.70%
Lactobacillus acidipiscis KCTC 13900	0.09%
Acinetobacter johnsonii XBB1	0.02%
Mesorhizobium sp. F7	0.02%
Grand Total	100.00%

Table J.18 Microbial Diversity in Microcosm # 48 Sample.

Genus and species	% Grand total
Lactobacillus acidipiscis DSM 15836	52.37%
Lactobacillus paracasei subsp. paracasei 8700:2	29.96%
Bacillus circulans NBRC 13626	10.55%
Oerskovia sp. Root918	6.13%
Lactobacillus rhamnosus GG	0.51%
Lactobacillus paracasei	0.13%
Lactobacillus acidipiscis KCTC 13900	0.09%
Lactobacillus rhamnosus LOCK908	0.05%
Lactobacillus casei BD-II	0.05%
Acinetobacter johnsonii XBB1	0.05%
Pseudomonas sp. RIT288	0.03%
Stenotrophomonas maltophilia	0.02%
Pseudomonas synxantha BG33R	0.02%
Aspergillus fischeri NRRL 181	0.02%
Acinetobacter lwoffii WJ10621	0.02%
Stenotrophomonas maltophilia D457	0.01%
Mycobacteroides abscessus subsp. bolletii 50594	0.01%
Grand Total	100.00%

Table J.19 Microbial Diversity in Microcosm # 56 Sample.

Genus and species	% Grand total
Methylobacterium sp. 77	72.30%
Methylobacterium radiotolerans JCM 2831	27.56%
Methylobacterium sp. Leaf91	0.08%
Acinetobacter johnsonii XBB1	0.04%
Stenotrophomonas maltophilia D457	0.01%
Methylobacterium sp. Leaf361	0.01%
Grand Total	100.00%

Table J.20 Microbial Diversity in Microcosm # 57 Sample.

Genus and species	% Grand total
Pseudomonas fulva	99.59%
Pseudomonas putida H8234	0.20%
Pseudomonas fluorescens R124	0.17%
Caballeronia zhejiangensis	0.02%
Pseudomonas helleri	0.02%
Grand Total	100.00%

Table J.21 Microbial Diversity in Microcosm #78 Sample.

Genus and species	% Grand total
Lactobacillus acidipiscis DSM 15836	60.95%
Mesorhizobium sp. F7	18.75%
Methylobacterium radiotolerans JCM 2831	12.14%
Sphingomonas sp. Mn802worker	5.72%
Aureimonas sp. AU20	1.20%
Methylobacterium sp. AMS5	0.36%
Ensifer sp. BR816	0.24%
Methylobacterium sp. 77	0.19%
Methylobacterium sp. Leaf361	0.17%
Mesorhizobium loti	0.16%
Lactobacillus acidipiscis KCTC 13900	0.06%
Methylobacterium sp. Leaf469	0.06%
(blank)	0.00%
Grand Total	100.00%

Table J.22 Microbial Diversity in Microcosm #81A Sample.

Genus and species	% Grand total
Lactobacillus paracasei subsp. paracasei 8700:2	71.69%
Lactobacillus acidipiscis DSM 15836	21.61%
Bacillus circulans NBRC 13626	5.66%
Lactobacillus rhamnosus GG	0.44%
Lactobacillus paracasei	0.34%
Lactobacillus rhamnosus LOCK908	0.12%
Aspergillus fischeri NRRL 181	0.07%
Lactobacillus casei BD-II	0.03%
Lactobacillus acidipiscis KCTC 13900	0.02%
Porphyromonas sp. KLE 1280	0.02%
Grand Total	100.00%

Table J.23 Microbial Diversity in Microcosm #81B Sample.

Genus and species	% Grand total
Lactobacillus paracasei subsp. paracasei 8700:2	76.20%
Lactobacillus acidipiscis DSM 15836	17.68%
Bacillus circulans NBRC 13626	5.06%
Lactobacillus rhamnosus GG	0.46%
Lactobacillus paracasei	0.34%
Lactobacillus rhamnosus LOCK908	0.09%
Lactobacillus casei BD-II	0.06%
Acinetobacter johnsonii XBB1	0.03%
Streptococcus sp. F0441	0.02%
Aspergillus fischeri NRRL 181	0.02%
Lactobacillus acidipiscis KCTC 13900	0.01%
Streptococcus cristatus ATCC 51100	0.01%
Porphyromonas sp. KLE 1280	0.01%
Lactococcus lactis subsp. lactis KLDS 4.0325	0.01%
Grand Total	100.00%

Table J.24 Microbial Diversity in Microcosm #102 Sample.

Genus and species	% Grand total
Pseudomonas sp. HPB0071	85.03%
Pseudomonas luteola XLDN4-9	14.76%
Methylobacterium radiotolerans JCM 2831	0.20%
Lactobacillus paracasei subsp. paracasei 8700:2	0.01%
Grand Total	100.00%

Table J.25 Microbial Diversity in Microcosm #110 Sample.

Genus and species	% Grand total
Stenotrophomonas maltophilia K279a	65.51%
Pseudomonas moraviensis R28-S	27.10%
Pseudomonas fluorescens	5.78%
Pseudomonas fluorescens R124	0.85%
Pseudomonas putida GB-1	0.43%
Pseudomonas aeruginosa BWH051	0.20%
Pseudomonas parafulva NBRC 16636 = DSM 17004	0.12%
Pseudomonas fluorescens A506	0.01%
Grand Total	100.00%

Table J.26 Microbial Diversity in Microcosm #126 Sample.

Genus and species	% Grand total
Pseudomonas sp. HPB0071	36.19%
Acinetobacter johnsonii XBB1	21.56%
Pseudomonas sp. RIT288	8.60%
Stenotrophomonas maltophilia	6.42%
Pseudomonas luteola XLDN4-9	6.22%
Stenotrophomonas maltophilia D457	5.60%
Acinetobacter lwoffii WJ10621	5.60%
Acinetobacter johnsonii SH046	1.80%
Pseudomonas synxantha BG33R	1.38%
Ralstonia sp. NT80	1.32%
Pseudomonas monteilii	0.93%
Acinetobacter lwoffii NCTC 5866 = CIP 64.10 = NIPH 512	0.90%
Klebsiella aerogenes EA1509E	0.80%
Cronobacter turicensis z610	0.37%
Pelomonas sp. Root1217	0.34%
Acinetobacter sp. CIP 102143	0.23%
Pseudomonas putida H8234	0.20%
Pseudomonas synxantha	0.17%
Enterobacter cloacae	0.14%
Porphyromonas sp. KLE 1280	0.12%
Hammondia hammondi	0.11%
Pseudomonas fluorescens R124	0.11%
Flavobacterium sp. B17	0.10%
Pseudomonas sp. URMO17WK12:I11	0.09%
Ralstonia sp. 5_2_56FAA	0.08%
Acinetobacter johnsonii CIP 64.6	0.08%
Acinetobacter sp. CIP 102637	0.07%
Pseudomonas sp. S13.1.2	0.07%
Pseudomonas putida HB3267	0.07%
Oerskovia turbata	0.06%
Acinetobacter johnsonii ANC 3681	0.06%
Enterobacter sp. MGH 22	0.03%
Pseudomonas chlororaphis	0.03%
Sphingomonas melonis DAPP-PG 224	0.03%
Pseudomonas sp. NBRC 111130	0.03%
Caballeronia zhejiangensis	0.02%
Cutibacterium acnes HL096PA1	0.02%
Stenotrophomonas maltophilia Ab55555	0.02%
Grand Total	100.00%

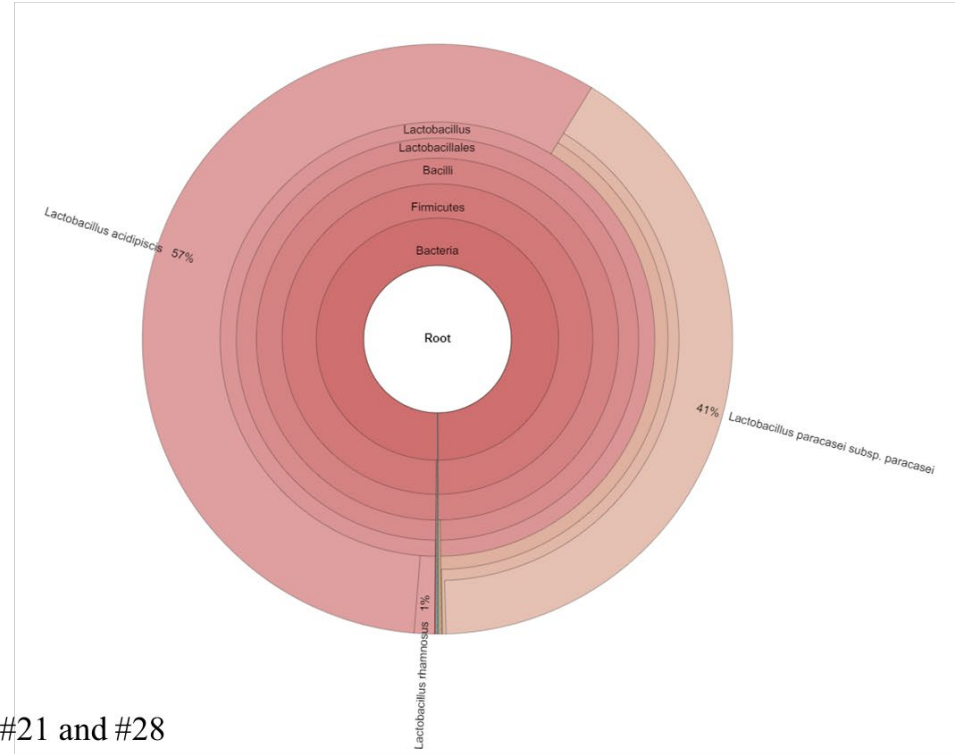
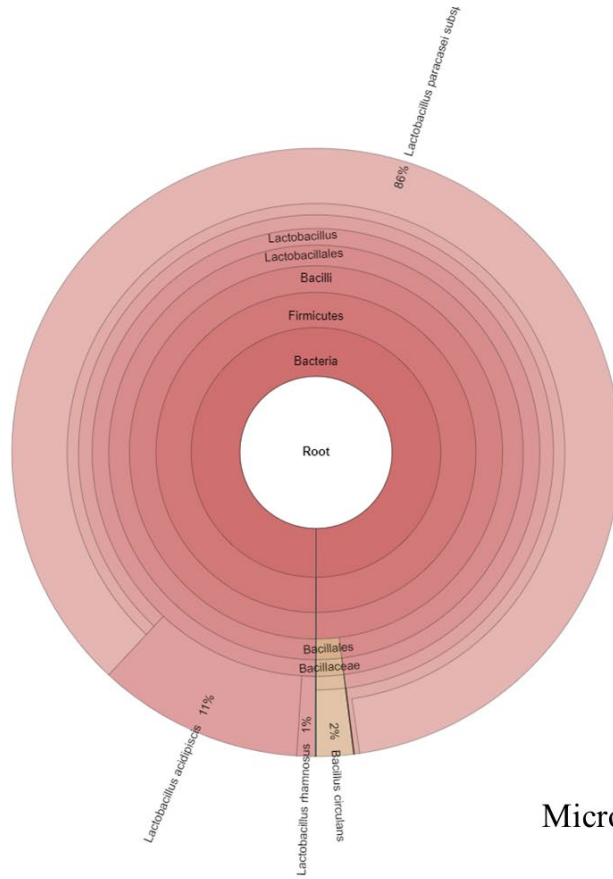
Table J.27 Microbial Diversity in Microcosm #127 Sample.

Genus and species	% Grand total
Lactobacillus paracasei subsp. paracasei 8700:2	87.74%
Acinetobacter johnsonii XBB1	4.33%
Pseudomonas sp. RIT288	1.44%
Acinetobacter lwoffii WJ10621	1.43%
Stenotrophomonas maltophilia D457	1.41%
Stenotrophomonas maltophilia	1.31%
Lactobacillus paracasei	0.43%
Pseudomonas synxantha BG33R	0.34%
Acinetobacter johnsonii SH046	0.20%
Ralstonia sp. NT80	0.18%
Lactobacillus casei BD-II	0.15%
Pseudomonas fluorescens R124	0.14%
Cronobacter turicensis z610	0.12%
Lactobacillus rhamnosus LOCK908	0.11%
Acinetobacter lwoffii NCTC 5866 = CIP 64.10 = NIPH 512	0.10%
Enterobacter cloacae	0.09%
Veillonella dispar ATCC 17748	0.06%
Penicillium solitum	0.06%
Klebsiella aerogenes EA1509E	0.04%
Acinetobacter sp. NIPH 1847	0.04%
Mesorhizobium sp. F7	0.04%
Sphingomonas melonis DAPP-PG 224	0.04%
Pseudomonas putida H8234	0.03%
Enterobacter sp. MGH 24	0.03%
Enterobacter sp. MGH 22	0.03%
Acinetobacter johnsonii CIP 64.6	0.02%
Pelomonas sp. Root1217	0.02%
Cutibacterium acnes HL096PA1	0.02%
Lactobacillus acidipiscis DSM 15836	0.02%
Acinetobacter ursingii DSM 16037 = CIP 107286	0.02%
Ralstonia sp. 5_2_56FAA	0.01%
Acinetobacter sp. CIP 102143	0.01%
Grand Total	100.00%

Table J.28 Summary of Microbial Diversity for All Microcosm Samples

Microcosm	3	4	21	28	32	36	40	45A	45B	46	47	48	56	57	76	78	81A	81B	102	110	126	127	
Microbial Challenge	-	+	+	+	+	-	-	-	-	+	-	+	-	-	-	-	+	+	-	-	-	-	
Genus and Species (OTU)	Abundance (%)																						
Acinetobacter						0.47	0.37															0.30	0.05
Acinetobacter johnsonii	0.01					41.22	24.01	0.02	0.06		0.02	0.05	0.04					0.03				23.50	4.55
Acinetobacter lwoffii						12.06	8.13		0.01			0.02										6.50	1.53
Acinetobacter ursingii							0.07																0.02
Afipia birgiae	0.01																						
Aquabacterium parvum	2.10																						
Aspergillus fischeri		0.09	0.01	0.06								0.02						0.07	0.02				
Aureimonas																	1.20						
Bacillus circulans		31.10	1.97	0.18						0.08		10.55						5.66	5.06				
Bacillus coagulans						0.02																	
Blastomonas	0.10																						
Bosea	1.07																						
Bosea thiooxidans	0.04																						
Bradyrhizobium	0.24																						
Bradyrhizobium elkanii	10.18																						
Bradyrhizobium japonicum	0.16																						
Caballeronia zhejiangensis						0.08	0.03							0.02								0.02	
Candidatus Hepatobacter penaei						0.02																	
Caulobacter	2.55																						
Cronobacter turicensis						0.27	0.40															0.37	0.12
Cutibacterium acnes																						0.02	0.02
Edaphobacter aggregans	0.06																						
Ensifer																	0.24						
Enterobacter						0.25	0.23															0.03	0.06
Enterobacter cloacae						0.55	0.43															0.14	0.09
Flavobacterium						0.02																0.10	
Gemella sanguinis							0.14																
Haemophilus influenzae							0.07																
Haemophilus parainfluenzae			0.01	0.06			0.49																
Hammondia hammondi	0.42																					0.11	
Hypomicrobium	0.06																						
Klebsiella aerogenes						0.67	0.38															0.80	0.04
Klebsiella pneumoniae						0.02																	
Lactobacillus acidipiscis	0.29	10.93	57.48	96.45						55.29	81.25	52.46				61.01	21.63	17.69				0.02	
Lactobacillus casei	0.07	0.04	0.04				0.02			0.04	0.05	0.05					0.03	0.06				0.15	
Lactobacillus paracasei	68.31	86.03	40.98	3.42			40.60		0.01	43.65	30.09						72.03	76.54	0.01			88.17	
Lactobacillus rhamnosus	0.12	0.98	1.12	0.10			0.06			0.93	0.56						0.56	0.55				0.11	
Lactococcus lactis							0.05															0.01	
Leifsonia aquatica	0.03																						
Leptothrix cholodnii	0.02																						
Lysinibacillus xylanilyticus						0.04																	
Massilia								99.96	99.89														
Mesorhizobium	3.81										0.02							18.75				0.04	
Mesorhizobium japonicum	0.32																						
Mesorhizobium loti	0.01																	0.16					
Methylobium petroleiphilum	0.10																						
Methylobacterium													72.39				0.78						
Methylobacterium radiotolerans	0.23									18.70			27.56				12.14		0.20				
Methyloversatilis discipulorum	0.35																						
Mycobacterium intracellulare							0.08																
Mycobacterium simiae							0.11																
Mycobacteroides abscessus												0.01											
Mycobacterium mucogenicum	0.83																						
Novosphingobium nitrogenifigens	1.64																						
Oerskovia												6.13											
Oerskovia turbata																						0.06	
Pantholops hodgsonii	0.08																						
Paraburkholderia fungorum	13.19																						
Paraburkholderia phytofirmans	1.12																						
Paraprevotella clara							0.06																
Pelomonas						0.50	0.12															0.34	0.02
Penicillium solitum																							0.06
Porphyromonas		0.01	0.08			0.88	0.48	0.02									0.02	0.01				0.12	
Prevotella						0.12																	
Prevotella nanceiensis						0.08																	
Pseudomonas			0.01	0.01		12.45	7.16		0.01			0.03			100.00				85.03		44.98	1.44	
Pseudomonas aeruginosa						0.06	0.01													0.20			
Pseudomonas chlororaphis						0.06	0.01															0.03	
Pseudomonas fluorescens						0.66	0.38													6.64	0.11	0.14	
Pseudomonas fulva														0.17									
Pseudomonas helleri														99.59									
Pseudomonas luteola														0.02									
Pseudomonas monteilii																			14.76			6.22	
Pseudomonas moraviensis																						0.93	
Pseudomonas parafulva																					27.10		
Pseudomonas putida						0.89	0.32								0.20					0.12			
Pseudomonas synxantha						3.26	1.77					0.02								0.43	0.27	0.03	
Ralstonia	53.20					2.29	1.63															1.55	0.34
Ralstonia solanacearum	0.66																					1.40	0.19
Reyranella massiliensis	0.12																						
Rhizobium							0.01																
Sphingobacterium							0.02																
Sphingomonas	5.58																5.72						
Sphingomonas melonis	0.01					0.09	0.07															0.03	0.04
Sphingomonas taxi	0.01																						
Sphingopyxis	0.08																						
Staphylococcus capitis							0.03																
Stenotrophomonas maltophilia				0.01		22.97	11.97		0.01			0.03	0.01								65.51	12.04	2.72
Streptococcus							0.07	0.01															
Streptococcus cristatus																					0.02		
Variovorax	0.03																				0.01		
Variovorax paradoxus	1.48																						
Veillonella dispar																							0.06
Grand Total	99.89	99.99	99.98	100.01	99.99	100.03	99.75	100.01	99.99	99.99	99.99	100.02	100.00	100.00	100.00	100.00	100.00	100.00	100.00	100.00	99.97	100.01	

Figure J.2 Krona Plot of Metagenomic Sequencing Results of Microcosms #21 and #28.



Microcosm #21 and #28

Figure J.4 Krona Plot of Metagenomic Sequencing Results of Microcosms #40.

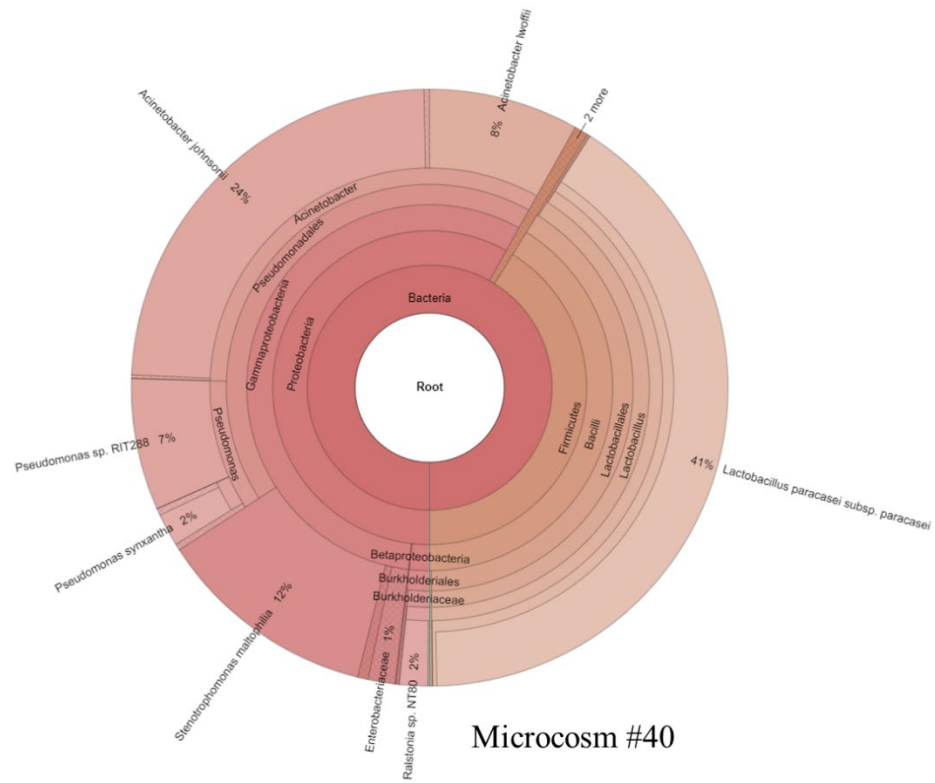


Figure J.5 Krona Plot of Metagenomic Sequencing Results of Microcosms #45A and #45B.

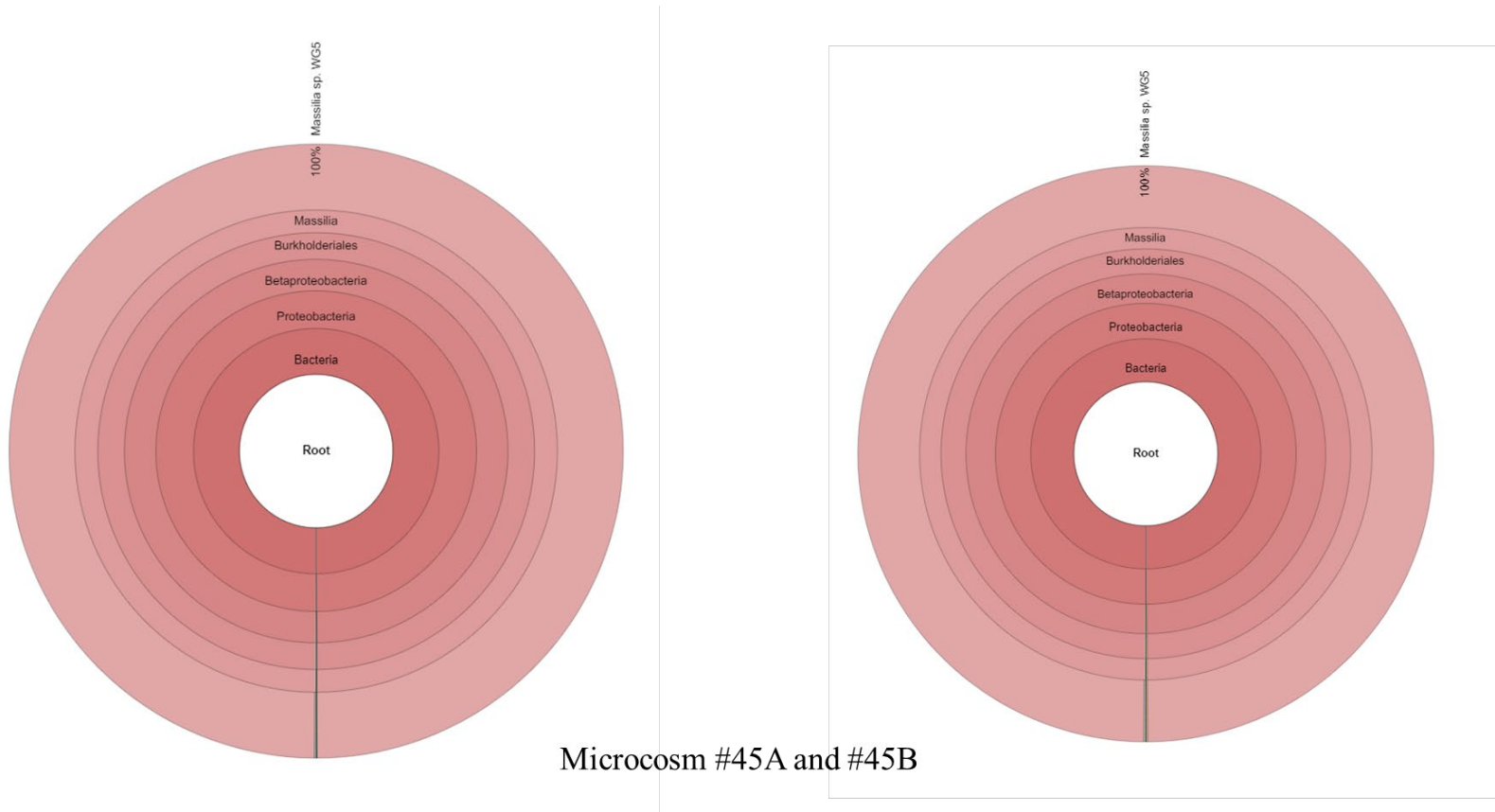


Figure J.6 Krona Plot of Metagenomic Sequencing Results of Microcosms #46 and #47.

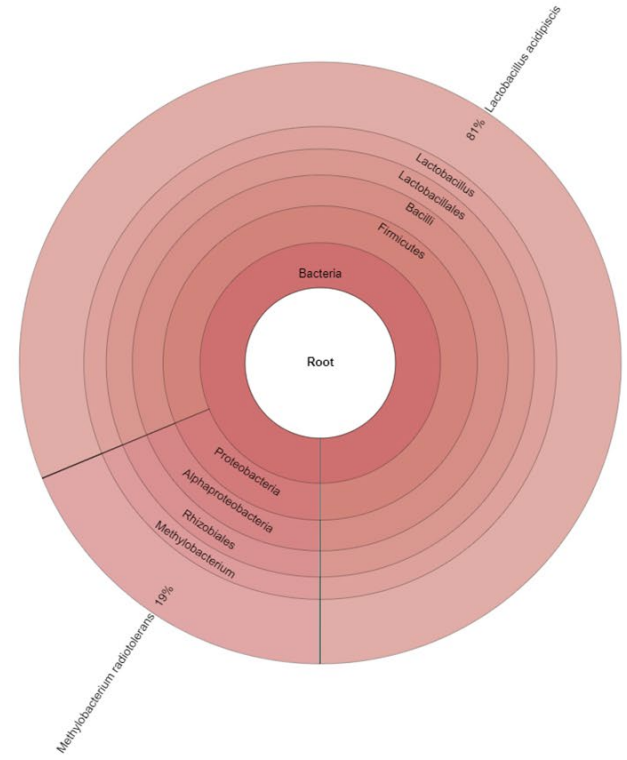
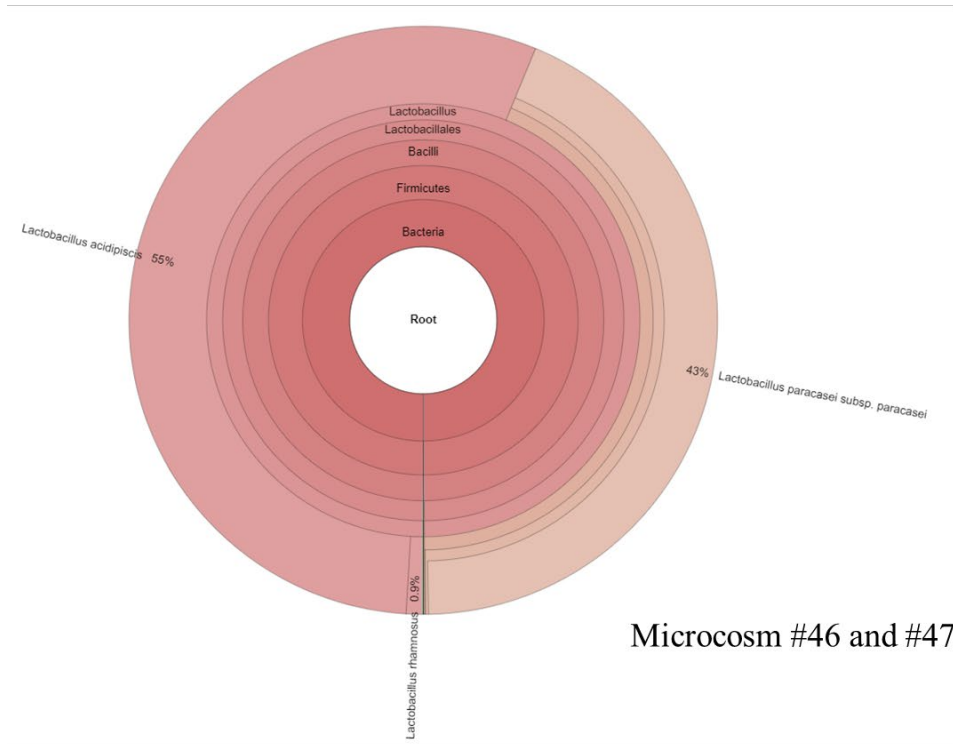
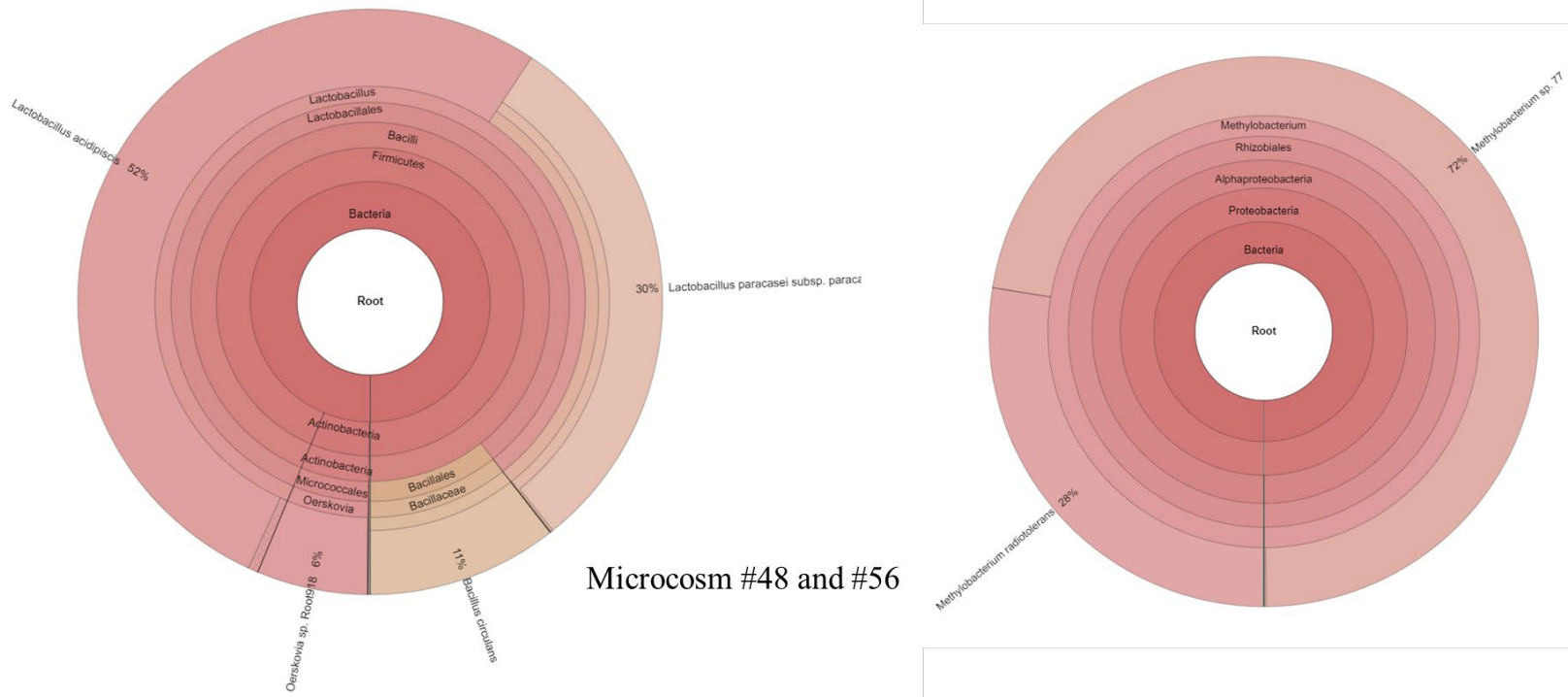


Figure J.7 Krona Plot of Metagenomic Sequencing Results of Microcosms #48 and #56.



Microcosm #48 and #56

Figure J.8 Krona Plot of Metagenomic Sequencing Results of Microcosms #57 and #78.

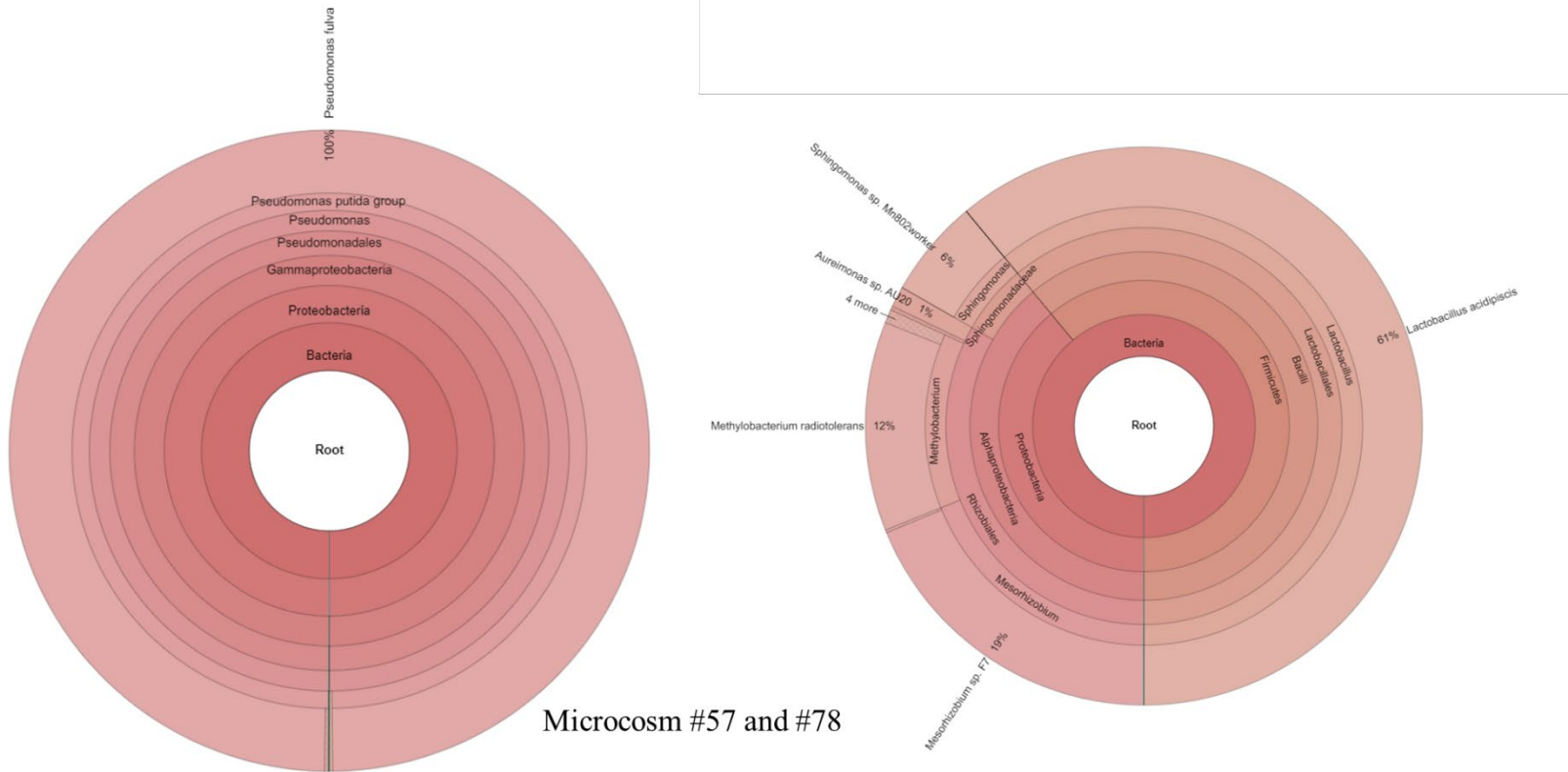
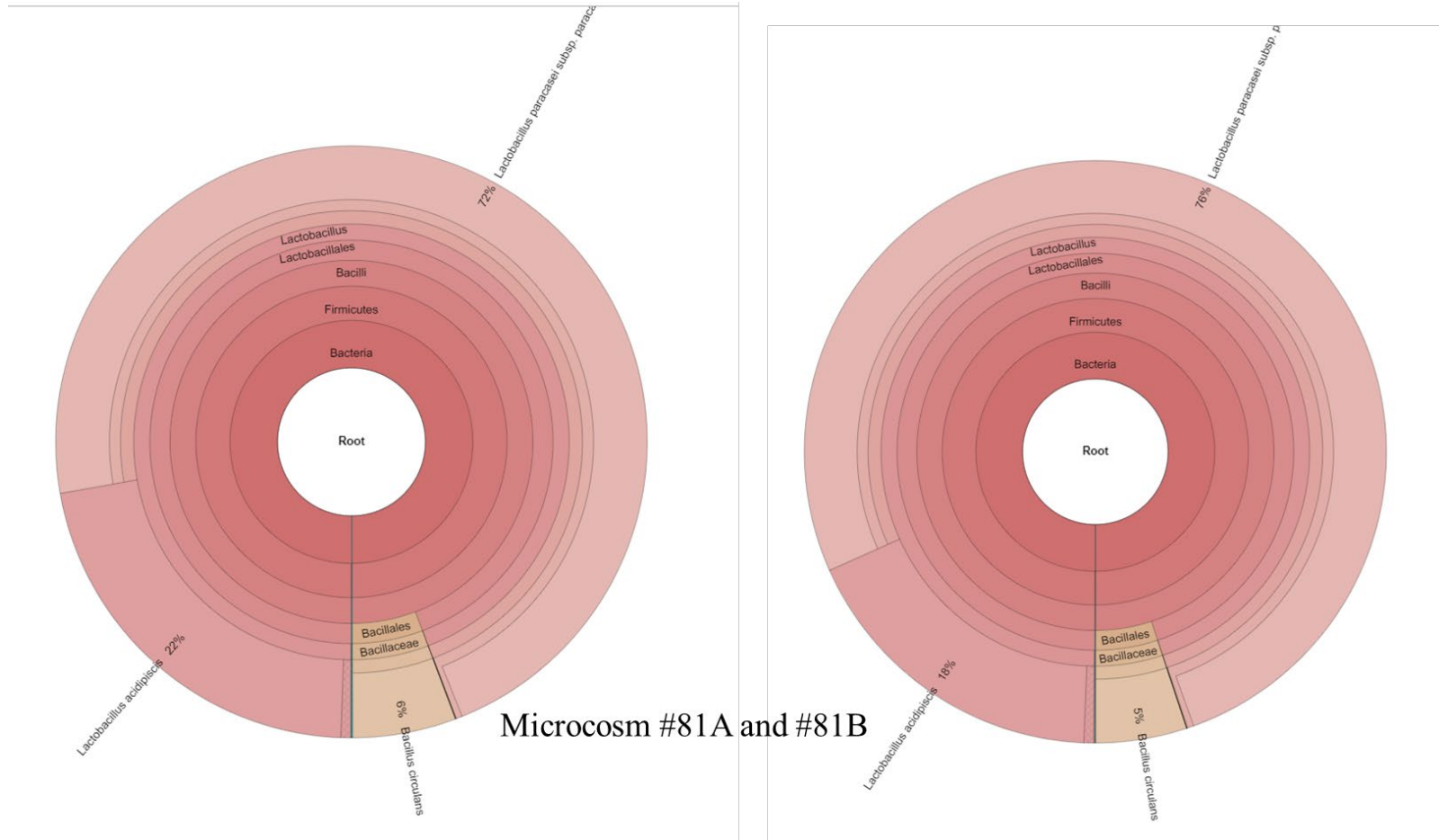


Figure J.9 Krona Plot of Metagenomic Sequencing Results of Microcosms #81A and #81B.



Microcosm #81A and #81B

Figure J.10 Krona Plot of Metagenomic Sequencing Results of Microcosms #102 and #110.

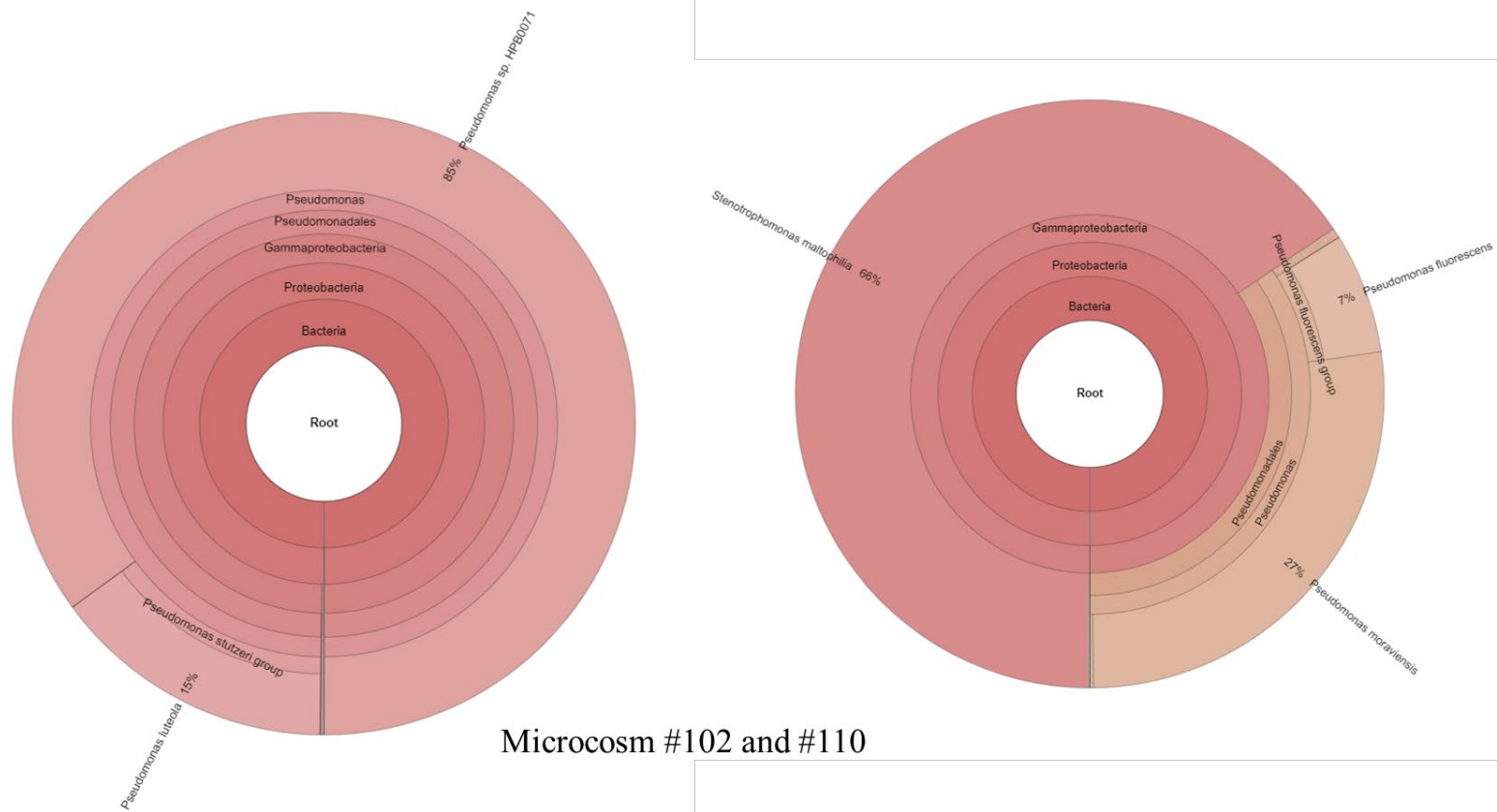
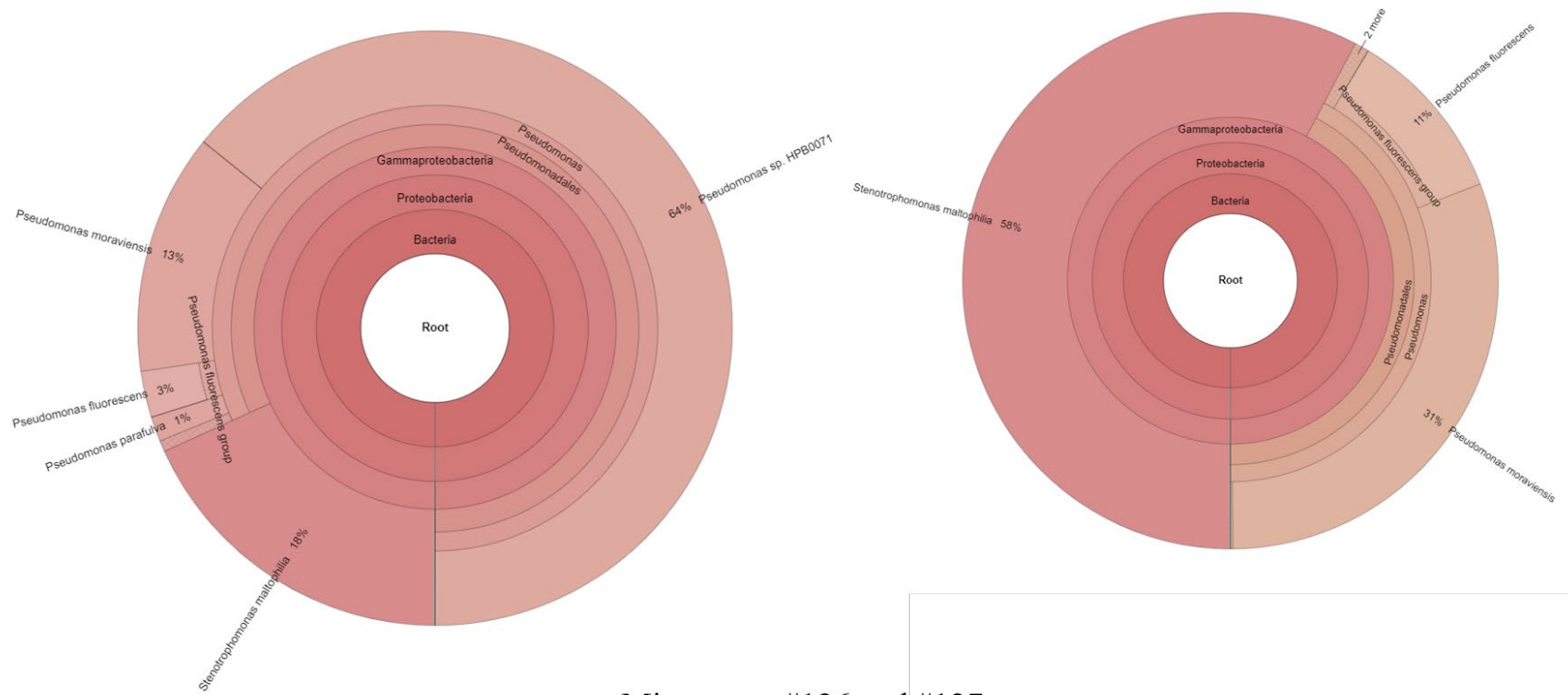


Figure J.11 Krona Plot of Metagenomic Sequencing Results of Microcosms #126 and #127.



Microcosm #126 and #127

APPENDIX K
Chemical Analyses

Table K-1 . Calibration Curve Concentrations for Volatile Acids, Methanol, and Ethanol Quantification

			C7	C6	C5	C4	C3	C2	C1
	Molecular Weight	ug/mL Stock	0.5829	0.4998	0.4164	0.333	0.2499	0.166	0.0833
Acetic acid	60.02113	600.2113	349.8632	299.9856	249.928	199.8704	149.9928	99.63508	49.9976
Propionic acid	74.036781	732.9641	427.2448	366.3355	305.2063	244.0771	183.1677	121.672	61.05591
2-methyl propanoic acid	88.052429	880.5243	513.2576	440.086	366.6503	293.2146	220.043	146.167	73.34767
Butanoic acid	88.052429	871.7190	508.125	435.6852	362.9838	290.2824	217.8426	144.7054	72.6142
3-methyl butanoic acid	102.13	1011.0870	589.3626	505.3413	421.0166	336.692	252.6706	167.8404	84.22355
Pentanoic acid	102.068077	1020.6808	594.9548	510.1362	425.0115	339.8867	255.0681	169.433	85.02271
4-methyl pentanoic acid	116.16	1197.6096	698.0866	598.5653	498.6846	398.804	299.2826	198.8032	99.76088
Hexanoic acid	116.16	1153.4688	672.357	576.5037	480.3044	384.1051	288.2519	191.4758	96.08395
Heptanoic acid	130.09938	1281.4789	746.974	640.4832	533.6078	426.7325	320.2416	212.7255	106.7472
Ethanol				102.7	63.2	31.6	15.8	7.9	3.95
Methanol				102.7	63.2	31.6	15.8	7.9	3.95

Table K-2 . Analysis of Composition and Concentration of Organic Acids in Samples Collected at Day 0 and Day 60 in the Fuel Phase the Microcosm Experiment

Sample and Time Point	29F D_0	40F D_0	57F D_0	66F D_0	77F D_0	119F D_0	15F D_60	21F D_60	24F D_60	37F D_60	39F D_60	40F D_60	44F D_60	48F D_60	53F D_60	83F D_60	85F D_60	86F D_60	96F D_60
Analyte (ug/mL)																			
Acetic Acid C-2	0.00	0.00	0.00	0.00	0.00	0.00	0.00	0.00	0.00	0.00	0.00	0.00	0.00	trace	0.00	0.00	0.00	trace	trace
Methanol **linear curve used**	trace	trace	0.00	trace	trace	trace	trace	trace	trace	18.80	18.70	15.03	25.23	9.57	10.28	10.85	22.97	18.72	17.62
Ethanol **linear curve used**	trace	trace	trace	trace	trace	trace	trace	0.00	trace	0.00	0.00	trace	0.00	0.00	0.00	trace	0.00	trace	0.28
Propionic Acid C-3	0.00	0.00	0.00	0.00	0.00	0.00	0.00	0.00	0.00	0.00	0.00	0.00	0.00	0.00	0.00	0.00	0.00	trace	0.00
Isobutyric Acid	0.00	0.00	0.00	0.00	0.00	0.00	0.00	0.00	0.00	0.00	0.00	0.00	0.00	0.00	0.00	0.00	0.00	0.00	0.00
Butanoic Acid C-4	0.00	0.00	0.00	0.00	0.00	0.00	0.00	0.00	0.00	0.00	0.00	0.00	0.00	0.00	0.00	0.00	0.00	0.00	0.00
3-methyl butanoic acid	0.00	0.00	0.00	0.00	0.00	0.00	0.00	0.00	0.00	0.00	0.00	0.00	0.00	0.00	0.00	0.00	0.00	0.00	0.00
Pentanoic Acid C-5	0.00	0.00	0.00	0.00	0.00	0.00	0.00	0.00	0.00	0.00	0.00	0.00	0.00	0.00	0.00	0.00	0.00	0.00	0.00
4-methyl pentanoic acid	0.00	0.00	0.00	0.00	0.00	0.00	0.00	0.00	0.00	0.00	0.00	0.00	0.00	0.00	0.00	0.00	0.00	0.00	0.00
Hexanoic Acid C-6	0.00	0.00	0.00	0.00	0.00	0.00	0.00	0.00	0.00	0.00	0.00	0.00	0.00	0.00	0.00	0.00	0.00	0.00	0.00
Heptanoic Acid	0.00	0.00	0.00	0.00	0.00	0.00	0.00	0.00	0.00	0.00	0.00	0.00	0.00	0.00	0.00	0.00	0.00	0.00	0.00
Glycerol mg/mL	0.00	0.00	0.00	0.00	0.00	0.00	0.00	0.00	0.00	0.00	0.00	0.00	0.00	0.00	0.00	0.00	0.00	0.00	0.00
<i>trace indicates below the curve but response greater 3/1 S/N</i>																			
Analytes of Interest Present in Samples																			
ethyl acetate										X		X				X		X	X
2-methyl-propyl ester													X						
8,11-octadecadienoic acid, methyl ester	X				X								X						X
octadecanoic acid methyl ester													X	X					
15-methyl heptadecanoic, methyl ester	X																		X
docosanoic acid methyl ester	X						X						X	X					X
tetracosanoic methyl ester	X																		
hexadecanoic acid methyl ester							X						X	X					
10,13-octadecadienoic acid methyl ester							X												
9,13-octadecadienoic acid methyl ester														X					
11-octadecanoic acid methyl ester														X					
14-methyl-pentadecanoic acid methyl ester																			X
eicosane	X		X	X	X		X			X	X	X		X	X	X		X	X
docosane	X		X	X	X	X	X	X		X	X	X	X	X	X	X			X
nonacosane														X					
octacosane	X																X	X	
heptacosane	X		X					X					X			X			
tricosane	X		X			X	X	X	X	X	X	X	X	X	X	X		X	
tetracosane	X		X		X	X		X	X	X		X			X		X	X	X
hexacosane	X		X	X			X	X		X			X	X	X				
campesterol	X																		
stigmasterol	X																		
.gamma.sitosterol	X																		
2,6,10,14-tetramethyl octadecane	X																		
nonahexcontanoic acid		X																	
undecane					X												X		X
dodecane					X											X	X	X	
tridecane					X		X		X							X	X	X	
tetradecane			X	X								X		X	X	X	X	X	X
pentadecane					X			X	X		X	X	X	X	X	X		X	X
octadecane			X	X				X	X	X	X	X	X	X	X	X			X
hexadecane				X	X	X	X	X	X	X		X		X	X	X			X
heptadecane				X	X	X	X	X	X	X	X	X	X	X	X	X	X	X	X
heneicosane				X				X		X	X				X				
pentatriacontane					X														
nonadecane	X		X		X	X		X	X	X	X	X	X	X	X	X		X	X
hentriacontane					X	X		X											
2-methyl nonodecane							X												
7,9-dimethyl hexadecane									X										
cyclododecyl isothiocyanate																	X		

Table K-3 . Analysis of Composition and Concentration of Organic Acids in Samples Collected on Day 0 in the Water Phase of the Microcosm Experiment

Sample	29W D_0	40W D_0	59W D_0	66W D_0	77W D_0	119W D_0
Analyte (ug/mL)						
Acetic Acid C-2	0.00	0.00	0.00	0.00	69.61	361.02
Methanol <i>**linear curve used***</i>	1.54	1.85	1.52	1.53	1.65	2.36
Ethanol <i>**linear curve used**</i>	0.93	0.93	0.93	0.93	0.93	0.93
Propionic Acid C-3	0.00	0.00	0.00	0.00	0.00	0.00
Isobutyric Acid	0.00	0.00	0.00	0.00	0.00	0.00
Butanoic Acid C-4	0.00	0.00	0.00	0.00	0.00	0.00
3-methyl butanoic acid	0.00	0.00	0.00	0.00	0.00	0.00
Pentanoic Acid C-5	0.00	0.00	0.00	0.00	0.00	0.00
4-methyl pentanoic acid	0.00	0.00	0.00	0.00	0.00	0.00
Hexanoic Acid C-6	0.00	0.00	0.00	0.00	0.00	0.00
Heptanoic Acid	0.00	0.00	0.00	0.00	0.00	0.00
Glycerol mg/ml	0.00	58.51	223.32	0.00	0.00	236.76
<i>for volatile acids, trace indicates below the curve, but is a hit</i>						

Table K-4 . Analysis of Composition and Concentration of Organic Acids in Samples Collected on Day 30 in the Water Phase of the Microcosm Experiment

Sample	3W D_30	4W D_30	30W D_30	35 D_30	39W D_30	74 D_30	86W D_30
Analyte (ug/mL)							
Acetic Acid C-2	0.00	0.00	0.00	0.00	0.00	0.00	503.13
Methanol <i>**linear curve used***</i>	1.52	1.52	1.52	1.55	1.52	1.52	1.69
Ethanol <i>**linear curve used**</i>	0.93	0.93	0.93	0.93	0.93	0.93	0.93
Propionic Acid C-3	0.00	0.00	0.00	0.00	33.43	0.00	0.00
Isobutyric Acid	0.00	0.00	0.00	0.00	1673.21	0.00	0.00
Butanoic Acid C-4	0.00	0.00	0.00	0.00	0.00	0.00	0.00
3-methyl butanoic acid	0.00	0.00	0.00	0.00	0.00	0.00	0.00
Pentanoic Acid C-5	0.00	0.00	0.00	0.00	0.00	0.00	0.00
4-methyl pentanoic acid	0.00	0.00	0.00	0.00	0.00	0.00	0.00
Hexanoic Acid C-6	0.00	0.00	0.00	0.00	0.00	0.00	0.00
Heptanoic Acid	0.00	0.00	0.00	0.00	0.00	0.00	0.00
Glycerol mg/ml	0.00	0.00	65.34	0.00	119.53	0.00	44.77
<i>for volatile acids, trace indicates below the curve, but is a hit</i>							

Table K-7. Fuel Layer Analytical Samples Collected on Day 90 in the Microcosm Experiment

Fuel Layer Analytical Results												
Microcosm #	Contains Biodiesel	ASTM D4176 Haze Rating	Surfactants By D7261	Water Sep by D7451				GCMS of Fuel Layer				
				Aqueous Vol, ml	Fuel App	Fuel-Water Sep	Interface	LMA	FAME	Glycerin	Ethanol	Other
82	N	6	0	26	2	3	2	ND	ND	ND	ND	
1	N	1	94	19	3	3	1B	ND	ND	ND	ND	
91	Y	5	0	8	6	3	4	ND	Y	ND	ND	
11	Y	2	0	8	6	3	3	ND	Y	ND	ND	
123	Y	2	0	5	6	2	4	ND	Y	ND	ND	
6	Y	1	0	<5	6	3	4	ND	Y	ND	ND	
17	N	1	0	7.5	6	3	4	ND	ND	ND	ND	
52	N	1	0	9	5	3	2	ND	ND	ND	ND	
3	N	1	96	9.5	2	2	1B	ND	ND	ND	ND	
99	N	1	69	9.5	3	2	1B	ND	ND	ND	ND	
4	N	1	92	9.5	2	2	1B	ND	ND	ND	ND	
35	N	1	97	9.5	2	2	1B	ND	ND	ND	ND	
53	N	1	45	10	5	3	3	ND	ND	ND	ND	
54	N	1	43	9.5	5	3	3	ND	ND	ND	ND	
10	Y	1	0	8.5	2	3	3	ND	Y	ND	ND	
106	N	1	54	9	3	2	2	ND	Y	ND	ND	
29	N	1	0	7.5	6	3	4	ND	Y	ND	ND	
37	N	1	93	10	3	3	2	ND	ND	ND	ND	
100	N	1	52	8.5	3	2	4	ND	ND	ND	ND	
83	N	1	0	8.5	6	3	3	ND	ND	ND	ND	
5	N	1	81	10	2	2	2	ND	ND	ND	ND	
103	N	1	75	9	2	2	3	ND	ND	ND	ND	
58	N	2	0	9	5	3	3	ND	ND	ND	ND	
116	N	1	54	10.5	5	3	3	ND	ND	ND	ND	
64	Y	1	0	9	5	2	3	ND	Y	ND	ND	
96	Y	1	0	7	6	3	4	ND	Y	ND	ND	
111	Y	1	61	8	4	3	4	ND	Y	ND	ND	
128	Y	2	0	8.5	6	2	3	ND	Y	ND	ND	

ATTACHMENT 1

Passman *et al.*

**IASH 2019, the 16TH INTERNATIONAL CONFERENCE ON
STABILITY, HANDLING AND USE OF LIQUID FUELS
Long Beach, California USA
08-12 September 2019**

**THE RELATIONSHIP BETWEEN PLANKTONIC AND SESSILE MICROBIAL
POPULATION ADENOSINE TRIPHOSPHATE BIOBURDENS IN DIESEL FUEL
MICROCOSMS**

Frederick J. Passman, PhD¹, Jordan Schmidt, PhD², Russell P. Lewis³, and Perry Christian. PhD³

¹ *Biodeterioration Control Associates, Inc., PO Box 3659, Princeton NJ, 08540-3659, USA*
fredp@biodeterioration-control.com

² *LuminUltra Technologies, Ltd., 520 King Street, Fredericton, NB, E3B 6G3, Canada,*
jordan.schmidt@luminultra.com

³ *Marathon Petroleum Company, LP, 11631 US Route 23, Catlettsburg, KY, 41129, USA,*
rplewis@marathonpetroleum.com, pachristian@marathonpetroleum.com

ABSTRACT

Fluid samples drawn from the fuel, interface and water phases of fuel over water microcosms were tested for cellular Adenosine triphosphate (cATP). Additionally, surface swab samples from steel corrosion coupon surfaces exposed to each of these three phases were collected and tested for total ATP (tATP). Relationships between planktonic and sessile population ATP concentrations were determined, as were relationships among ATP bioburdens in each of the three listed microcosm phases.

This paper describes the relationship between planktonic and biofilm population ATP bioburdens in: 1) the bottoms-water, 2) interface, 3) fuel phases, and 4) biofilms of the tested steel coupons; the relationships among planktonic ATP-bioburdens in each fluid phase and the relationship among biofilm bioburdens on each corrosion coupon zone.

INTRODUCTION

Fuel and fuel system biodeterioration are well documented phenomena. Since Miyoshi's (1895) seminal paper describing microbial contaminants in gasoline, thousands of research papers have addressed various aspects of fuel and fuel system biodeterioration (Passman, 2012). As the use of fatty acid methyl ester (FAME) blend stocks blended with ultra-low-sulfur diesel (LSD) has increased internationally, interest in biodiesel biodeterioration has grown proportionately. Soriano and her coworkers (2015) reported that population densities, taxonomic diversity, and the relative abundance of the bacterial taxa present also varied among fuels – depending on FAME source and concentration. Subsequently, Bückner *et al.* (2018) determined that biodiesel

blend biodeterioration rates varied depending on the source of FAME used and the FAME concentration in B5 to B50 blends.

In the U.S. since 2007, an increased incidence of component corrosion in retail fuel dispensing systems has been reported. In response to these reports, the Clean Diesel Fuel Alliance (CDFA) – a consortium of industry stakeholders – and the U.S. EPA, each sponsored field studies to investigate the phenomenon. The CDFA study (Battelle, 2012) included onsite observations and laboratory testing of samples from twelve fuel retail sites. The investigators posed three hypotheses that they hoped to test:

- i. Aerobic and/or anaerobic microbes are producing byproducts that are establishing a corrosive environment in ULSD systems;*
- ii. Aggressive chemical specie(s) (e.g., acetic acid) present in ULSD systems is(are) facilitating aggressive corrosion; and*
- iii. Additives in the fuel are contributing to the corrosive environment in ULSD systems.*

Given the small sample size, the study's conclusions were equivocal. None of the theories could either be dismissed or validated. The U.S. EPA study included 40 retail sites. One noteworthy outcome was that although 83 % of the underground storage tank (UST) systems inspected were found to have moderate to heavy corrosion only 23 % of site owners were aware of any damage (US EPA, 2016). As with the 2012 study the results did not support any unequivocal conclusions but suggested that biodeterioration was a likely contributing factor. Both studies were limited by the sample size. In the U.S. there are more than 800,000 UST. A representative study would include at least 80,000 UST – a prohibitively expensive undertaking. There is no general consensus on the cost impact of post-2007 retail fuel system. Consequently, there is no economic basis for assessing the potential return on investment for a full root cause analysis effort.

In 2016, members of the Coordinating Research Council, Inc. (CRC) Fuel Corrosivity Panel agreed that instead of attempting a third survey, a multivariate laboratory study would provide a basis for assessing the primary factors contributing to fuel system corrosion. A 128-microcosm laboratory study was commissioned as CRC Project DP-07-16-1. The project's final report is still pending, so its details are not provided in this paper. Instead, the focus is on adenosine triphosphate (ATP) test results.

The use of ATP to assess fuel and fuel-associated bioburdens has been reported at previous conferences (Passman *et al.*, 2003, Passman and Eachus, 2007, Passman *et al.*, 2007, Passman, 2009, and Passman *et al.*, 2014). Because of its speed, accuracy, ease of use, and small specimen volume required, ASTM D7687 (ASTM, 2017) was used as the primary parameter for monitoring bioburdens in the CRC study microcosm fuels and bottoms-waters. A related ATP

test method was used to assess biofilm population densities of microcosm corrosion coupons. This paper reports the fluid and surface ATP bioburdens.

EXPERIMENTAL

Test Plan

Members of the CRC Fuel Corrosivity Panel designed a 128-microcosm test plan that included the following variables:

- Fuel grade – LSD; ULSD, 500 mL
- FAME – none or 5 % by volume
- Ethanol – none or 10,000 mg L⁻¹
- Glycerin – none or 5,000 mg L⁻¹
- Free water – none or 250 mL
- Monoacid lubricity additive – none or 200 mg L⁻¹
- Cold flow improver – none or 200 mg L⁻¹
- Corrosion inhibitor – none or 8 to 10 mg L⁻¹
- Conductivity additive – none or 2 to 3 mg L⁻¹
- Microbial inoculum – added or not

Half of the microcosms contained a 250 mL aqueous phase. Additionally, half contained low sulfur diesel (LSD) and half contained ultra-low-sulfur diesel (ULSD). Of the 64 water-containing microcosms, 32 were inoculated and the balance were not. Similarly, the test plan design included various individual and multiple additive combinations.

All microcosms included four carbon steel corrosion coupons (figure 1). Polymeric resin coupons were suspended into a subset of microcosms. All microcosms were stored in the dark, in fume hoods, at laboratory room temperature (20±2 °C).



Fig 1. LSD over Bushnell-Hass microcosm.

Inoculum

An inoculum was prepared from UST samples. Initially primary microcosms of either LSD or ULSD over Bushnell-Hass medium (Bushnell and Hass, 1941) were inoculated with bottoms-

water samples from microbially contaminated ULSD UST. Once the aqueous-phase ATP-bioburdens were $>4\text{Log}_{10} \text{ pg mL}^{-1}$, they were pooled and used to inoculate secondary fuel over Bushnell-Hass medium microcosms. At the beginning of microcosm studies (T_0), challenged test microcosms were inoculated with 1 ml of secondary bottoms-water in which the ATP-bioburden was $4.5\pm 0.5\text{Log}_{10} \text{ pg mL}^{-1}$.

ATP Testing

Bottoms-water and fuel phase sample cellular ATP concentrations ([cATP]) were determined by ASTM D7687 (ASTM, 2017). The method was modified in that 5 mL fuel and 1 mL aqueous specimens were tested instead of the 20 mL fuel and 5 mL water specimens prescribed in D7687. Briefly, the specimen was filtered through a $0.7 \mu\text{m}$ glass fiber filter to capture cells. Interferences were then washed away using a proprietary rinsing agent (LumiClean™, LuminUltra Technologies, Ltd, Fredericton, NB, Canada) and air-dried using a 60 mL syringe. The washed and dried cells were then lysed using 1.0 mL of a proprietary lysing agent (UltraLyse™ 7, LuminUltra Technologies, Ltd, Fredericton, NB, Canada) and flushed into 9.0 mL of a proprietary buffer (UltraLute™ LuminUltra Technologies, Ltd, Fredericton, NB, Canada). The diluted ATP-extract was then mixed with an equal volume of Luciferin-Luciferase reagent in a cuvette which was then placed into a luminometer. Luminescence was recorded as relative light units (RLU). Test specimen RLU were converted to [cATP] by comparing the results with those obtained from a 1 ng mL^{-1} ATP reference standard (UltraCheck™ 1, LuminUltra Technologies, Ltd, Fredericton, NB, Canada). To facilitate data interpretation pg mL^{-1} values were transformed to $\text{Log}_{10} \text{ pg mL}^{-1}$.

Surface (biofilm) was tested using 1 cm x 1 cm swab samples. After sample collection, swabs were immersed into 2.0 mL of UltraLyse™ 7, vortexed for 30 sec and permitted to stand for 5 min. After the 5 min extraction period, 1.0 mL of UltraLyse™ 7 was transferred to 9.0 of UltraLute™ buffer. Luminescence was tested in accordance with ASTM D7687 and RLU were normalized to total ATP concentration ([tATP]) in pg cm^{-2} . As for fluid specimens, [tATP] values were transformed to $\text{Log}_{10} \text{ pg g}^{-1}$.

Statistical Analysis

All statistics were computed using the Microsoft® (registered trademark of Microsoft Corp., Redmond, WA) Excel Analysis ToolPak Add-in.

RESULTS AND DISCUSSION

Test Method Precision

Eight samples were tested in triplicate to assess [cATP] test method repeatability. The data, shown in Table 1, indicated that the repeatability standard deviation – s_r - for ASTM D7687 testing was $0.17 \text{ Log}_{10} \text{ pg mL}^{-1}$ (CV = 6 %). Due to limited sample availability, [tATP] repeatability testing was not performed. Previous evaluations indicated that the s_r for [tATP]

was approximately $0.5 \text{ Log}_{10} \text{ pg cm}^{-2}$ – reflecting the combined effect of the variability of biomass capture during swabbing, ATP extraction from swabs, and heterogeneous bioburden distribution on surfaces (Passman, unpublished).

Table 1. ASTM D7687 repeatability evaluation, microcosm, CRC study microcosms.

SAMPLE	1	2	3	AVG	s
A	1.43	1.45	1.44	1.44	0.01
B	2.45	2.45	2.44	2.45	0.00
C	3.23	3.24	3.25	3.24	0.01
D	4.23	4.26	4.25	4.25	0.01
E	1.65	1.69	1.71	1.68	0.03
F	2.82	2.80	2.85	2.82	0.02
G	3.98	4.02	4.00	4.00	0.02
H	3.05	3.07	3.10	3.07	0.02
Grand Mean				2.87	
s_r				0.17	

After this repeatability precision evaluation was completed, no other ATP tests were performed in replicate. In this paper, [cATP] results are implied to be $X \pm 0.17 \text{ Log}_{10} \text{ pg mL}^{-1}$ (where $X = \text{Log}_{10} [\text{cATP}]$) and [tATP] results are implied to be $Y \pm 0.17 \text{ Log}_{10} \text{ pg cm}^{-2}$ (where $Y = \text{Log}_{10} [\text{tATP}]$).

Inoculation with Challenge Population – Impact

Substantial cATP-bioburdens – ranging from $0.2 \text{ Log}_{10} \text{ pg mL}^{-1}$ to $5.7 \text{ Log}_{10} \text{ pg mL}^{-1}$ – developed in the unchallenged microcosms (Table 2). One-way analysis of variance (ANOVA) was computed to determine whether intentional inoculation impacted week-12 aqueous-phase bioburdens. The summary statistics, shown in Table 3, indicate that the bioburdens in challenged microcosms were ultimately greater than those in unchallenged microcosms. As will be discussed below, aqueous-phase bioburdens were affected by the microcosms’ chemical composition.

It is noteworthy that although the minimum and maximum ATP-bioburdens in challenged and unchallenged microcosms were comparable, the variability among unchallenged microcosms was much greater than that among challenged ones. The source of microbial contamination in the unchallenged microcosms was not investigated. The Bushnell-Haas medium was sterile when it was dispensed. Although microcosm jars were kept closed during incubation, they were not handled aseptically during set up or periodic coupon removal for inspection. Consequently, laboratory air could have been the contamination source. More likely, dormant bioburdens were

present in the LSD and ULSD fuels or the fuel additives used in the microcosm study. The T_0 fuel-phase bioburdens in LSD and ULSD were both $<1.0 \text{ pg mL}^{-1}$. Moreover, bioburden distribution in fuels is heterogeneous (Passman, 2018). This also could have accounted for the variability in ATP-bioburdens among unchallenged microcosms.

Table 2. Summary statistics – aqueous-phase cATP-bioburdens in challenged and unchallenged microcosms.

Statistic	Microbial Challenge	
	Unchallenged	Challenged
Avg	3	4.2
s	1.73	0.71
Median	3.6	4.5
Min	0.2	0.7
Max	5.7	5.3

Table 3. One-way ANOVA impact of inoculating microcosms with intentional challenge population.

SUMMARY

<i>Groups</i>	<i>Count</i>	<i>Sum</i>	<i>Average</i>	<i>Variance</i>
Unchallenged	20	61	3.0	2.99
Challenged	26	110	4.2	0.51

ANOVA

<i>Source of Variation</i>	<i>SS</i>	<i>df</i>	<i>MS</i>	<i>F</i>	<i>P-value</i>	<i>F crit</i>
Challenge (+ or -)	16.3	1	16.3	10.3	0.0025	4.06
Within Groups	69.6	44	1.6			
Total	85.9	45				

ATP-bioburden in microcosm phases

Figure 2 provides a profile of planktonic ATP-bioburden as a function of distance from the microcosm's bottom. Historically, culture-test based fuel system bioburden profiles have shown relative bioburdens as interface > sediment layer > aqueous-phase >> fuel-phase (Passman, 2012). Despite considerable variability among microcosms, the relative concentrations of [cATP] were: aqueous-phase ($4 \pm 1.3 \text{ Log}_{10} \text{ pg mL}^{-1}$) > sediment layer ($3 \pm 2 \text{ Log}_{10} \text{ pg mL}^{-1}$) \approx

interface ($3 \pm 1.4 \text{ Log}_{10} \text{ pg mL}^{-1}$) > fuel-phase ($2 \pm 0.5 \text{ Log}_{10} \text{ pg mL}^{-1}$). The number of aqueous-phase, sediment layer, interface, and fuel-phase specimens tested were: 43, 20, 7, and 7, respectively. The small number of sediment and fuel samples could have impacted the apparent relative bioburden results. Additionally, the substantial variability of sediment ATP-bioburden most likely reflected the heterogeneous distribution of sediment in jar bottoms (figure 3). The data on which figure 2 is based are provided in Supplemental Table S-1.

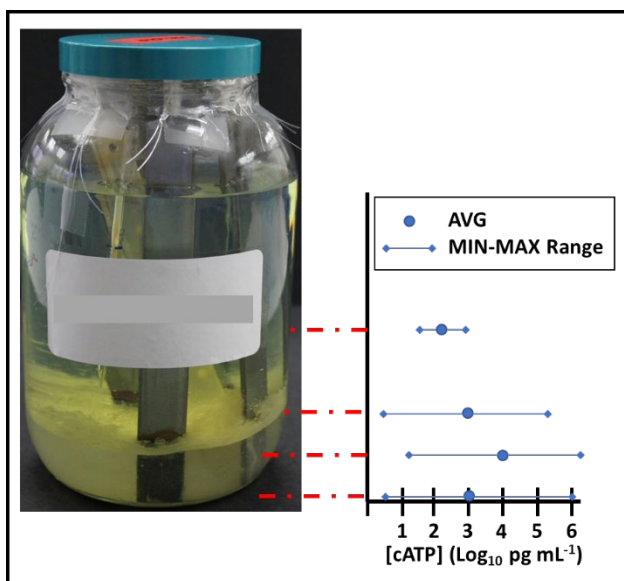


Fig 2. Fuel microcosm ATP=bioburden profile.



Fig 3. Microcosm jar, bottom-view at T₁₂ weeks.

Surface bioburdens were determined as $\text{Log}_{10} [\text{tATP}]$ from 1 cm^2 areas at the aqueous-phase (bottom 1 cm), interface-zone (~2 cm above the coupon's bottom), fuel-phase (9 cm to 10 cm above the coupon's bottom), and in the vapor-phase zone (13 cm to 15 cm above the coupon's bottom). Relative surface bioburdens (figure 4) were: fuel-phase ($4 \pm 1.2 \text{ Log}_{10} \text{ pg cm}^{-2}$) >

aqueous-phase ($3 \pm 1.0 \text{ Log}_{10} \text{ pg cm}^{-2}$) \gg interface-zone ($1 \pm 1.4 \text{ Log}_{10} \text{ pg cm}^{-2}$) \approx vapor-phase ($0.9 \pm 0.20 \text{ Log}_{10} \text{ pg cm}^{-2}$). The low interface-zone ATP bioburden was surprising. The gross appearance of this zone (figure 4) suggested that the ATP-bioburden would have been substantially greater than in the other three zones. Also surprising were the high surface bioburdens recovered from fuel-phase swab samples. However, these results are consistent with moderate to severe corrosion damage (putatively MIC) frequently observed on UST turbine risers (U.S. EPA, 2016). The data on which figure 3 is based are provided in Supplemental Table S-2. The relationship between planktonic and sessile (biofilm) ATP bioburdens will be addressed below.

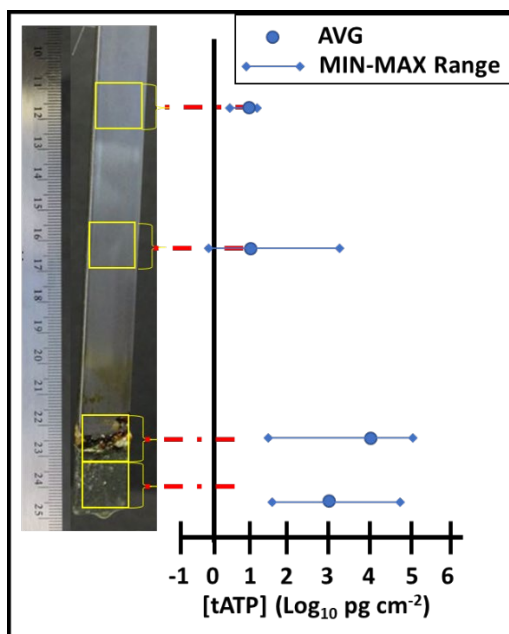


Fig 4. Fuel microcosm corrosion coupon ATP bioburden profile.

Relationship between ATP concentrations in different microcosm phases

Having determined that ATP-bioburdens differed among microcosm phases, the next step was to examine the relationships between bioburdens in adjacent phases. Correlation coefficients were computed for all interfaces for which there were ≥ 4 data pairs (i.e., $n \geq 4$). The results are summarized in Table 4.

The computations indicated that there were significant correlations between five carbon steel coupon phase-pairs:

- Aqueous-phase and sediment [cATP]
- Aqueous-phase and interface [cATP]
- Interface and fuel-phase [cATP]
- Aqueous-phase and interface [tATP]
- Aqueous-phase [cATP] and [tATP]

There we not enough data pairs to permit evaluation of correlations between fuel-phase or interface [cATP] and [tATP]. Similarly, because of the limited number of data pairs, P-values for the following phase-pairs were equivocal (i.e., $0.4 \leq P \leq 0.6$):

- Carbon steel coupon aqueous-phase & fuel [tATP]
- Epoxy resin coupon aqueous-phase & interface [tATP]
- Carbon steel coupon interface [cATP] and [tATP]

Table 4. ATP-bioburden correlations between phase pairs in fuel over water microcosms.

Interface	Slope	Intercept	r^2	r^2_{crit}	n	P
Planktonic ([cATP])						
Aqueous-phase & Sediment	1.1	-0.3	0.95	0.9	4	0.03
Aqueous-phase & Interface	0.76	0.1	0.45	0.18	21	0.0009
Aqueous-phase & Fuel	0.33	0.7	0.38	0.45	9	0.08
Interface & Fuel	0.54	0.28	0.75	0.56	7	0.01
Sessile ([tATP])						
<i>Carbon steel coupons</i>						
Aqueous-phase & Interface	1.0	-0.5	0.61	0.21	18	0.0001
Aqueous-phase & Fuel	0.63	-0.73	0.37	0.36	11	0.05
<i>Epoxy resin coupons</i>						
Aqueous-phase & Interface	0.64	-0.66	0.34	0.3	13	0.04
<i>Carbon steel & epoxy resin coupons</i>						
Aqueous-phase	0.5	1.32	0.34	0.65	6	0.23
Sessile - Planktonic						
Aqueous-phase	0.6	1.28	0.69	0.1	39	<0.0000
Interface	0.62	1.49	0.52	0.56	7	0.06

Relationship between microcosm chemistry and [cATP]

The presence of an intentional aqueous-phase was one of the controlled variables in the microcosm test array. The [cATP] in the one water-free microcosm (B0 ULSD) tested was $0.09 \text{ Log}_{10} \text{ pg mL}^{-1}$ (1.2 pg mL^{-1}). As reported above, the fuel-phase [cATP] in the microcosms with an aqueous zone was $2.0 \pm 0.49 \text{ Log}_{10} \text{ pg mL}^{-1}$ (minimum and maximum [cATP]_s = 19 pg mL^{-1} and 510 pg mL^{-1} , respectively). Despite insufficient data to determine the impact of water statistically, it was clear that the development of substantial bioburdens was water-dependent.

One-way ANOVA statistics were computed for each of the other controlled variables and [cATP]. The results, summarized in Table 5 indicate that, except for water, neither fuel

chemistry nor the presence of epoxy resin coupons had significant effects on aqueous-phase, ATP-bioburdens.

Table 5. One-way ANOVA summary: controlled variables versus microcosm aqueous-phase [cATP].

Statistic	Sulfur		Biodiesel (%)		Glycerin (ppm)		Ethanol (ppm)		Microbes	
	LSD	ULSD	B0	B5	+ ^a	-	+ ^b	-	+ ^c	-
AVG	4.2	4.4	3.9	3.5	4.2	4.5	4.5	4.2	4.5	4.1
s	0.77	0.69	0.98	1.48	0.86	0.54	0.54	0.95	0.66	0.75
F	0.69		0.02		0.42		0.84		1.58	
P	0.42		0.90		0.52		0.37		0.22	
F-crit	4.38		4.35		4.38		4.38		4.38	

Stat	MAL ^d		CI ^f		Conductivity Additive		FRP Material		
	+ ^e	-	-	+ ^g	-	+ ^h	-	+	-
AVG	4.5	4.3	0.7	4.3	4.4	4.3	4.5	4.4	4.3
s	0.79	0.70	0.18	0.69	0.83	0.66	0.81	0.84	0.59
F	0.65		0.001		0.36		0.01		
P	0.43		0.97		0.56		0.93		
F-crit	4.38		4.38		4.38		4.41		

Notes: a) Glycerin +: 5,000 ppm

b) Ethanol +: 10,000 ppm

c) Microbes +: Challenged

d) MAL – mon-acid lubricity additive

e) MAL +: 200 ppm

f) CI – corrosion inhibitor

g) CI +: 8ppm to 10 ppm

h) Conductivity additive +: 2 ppm to 3 ppm

CONCLUSIONS

The ATP-bioburden testing reported in this paper was done as an ancillary effort to CRC Project DP-07-16-1. Consequently, the relationships between [cATP] and [tATP] and other microcosm parameters was not fully considered. Moreover, the number of specimens tested were insufficient to support unequivocal conclusions for several of the relationships reported herein. Notwithstanding these limitations, it was possible to draw several conclusions from the ATP data. Although the conclusion was not novel, the results left no doubt that the presence of water is the primary factor determining whether microbial proliferation will occur in fuels, fuel-associated waters, or fuel system surfaces. Also, it was most likely that dormant microbes transported in the fuels used for the study were able to proliferate in the microcosms that had an aqueous-phase. Unchallenged microcosms developed substantial ATP-bioburdens in and on all microcosm phases.

Unexpectedly, although aqueous-phase [cATP]s were predictive of interface [cATP]s, and interface [cATP]s were predictive of fuel-phase [cATP]s, aqueous-phase [cATP]s were not predictive of fuel-phase [cATP]s. This absence of a significant correlation could have been an artifact of the small sample size, but merits further investigation. In contrast to this non-correlation, in each microcosm phase, the correlation of [cATP] to [tATP] was strong – planktonic bioburdens predicted biofilm bioburdens.

ACKNOWLEDGEMENTS

Much of the microcosm work was performed by Battelle Memorial Institute staff members. The authors are grateful for the work performed primarily by Dr. Bryan Gemler and Dr. Kate Kucharzyk. The authors also appreciate the hospitality provided by the Battelle team, permitting us to visit and perform tests in their laboratory.

CRC's support of Passman's travel to Battelle and the non-project work completed by the authors is also gratefully acknowledged.

The authors also acknowledged LuminUltra Technologies, Ltd, Fredericton, NB Canada, for their generous contribution of ATP test reagents and supplies used outside the scope of Project DP-07-16-1.

The authors also acknowledge the support of Marathon Petroleum Company, LCC, Research and Development Center, Catlettsburg, TN for their support of ancillary sampling and testing in support of this investigation.

REFERENCES

ASTM, 2017. D7687-17, Standard Test Method for Measurement of Cellular Adenosine Triphosphate in Fuel and Fuel-associated Water With Sample Concentration by Filtration, ASTM International, West Conshohocken, PA, 2017, www.astm.org, DOI: 10.1520/D7687-17.

Battelle, 2012. Corrosion in systems storing and dispensing ultra low sulfur diesel (ULSD), hypotheses investigation. Study No 10001550, Battelle Memorial Institute, Columbus, OH. 36 pp.

Bücker, F., de Moura, T.M., da Cunha, M.E., de Quadros, P.D., Beker, S.A., Cazarolli, J.C., Caramão, E.B., Frazzon, A.P.G., and Bento, F.M., 2018. Evaluation of the deteriogenic microbial community using qPCR, n-alkanes and FAMES biodegradation in diesel, biodiesel and blends (B5, B10, and B50) during storage. *Fuel* 233:911-917, <https://doi.org/10.1016/j.fuel.2017.11.076>

Bushnell, L.D. and Hass, H.F., 1941. The utilization of certain hydrocarbons by microorganisms. *J. Bacteriology* 41(5): 653-673.

Miyoshi, M., 1895. Die durchbohrung von membranen durch pilzfäden. *Jahrbücher für wissenschaftliche Botanik* 28, 269e289.

Passman, F. J., Loomis, L. and Sloyer, J., 2003. Non-conventional methods for estimating fuel system bioburdens rapidly.” In: R. E. Morris. Ed. *Proceedings of the 8th International Conference on the Stability and Handling of Liquid Fuels*; 14-19 September 2003, Steamboat Springs, CO.

Passman, F. J. and Eachus, A. C., 2007. Adenosine triphosphate as a rapid measure of microbial contamination in fuel systems. In: Bartz, W. J. Ed. “ *Fuels 2007 – 6th International Colloquium.*” Technische Akademie Esslingen, Ostfildern, Germany. pp: 689-695.

Passman, F. J., English, E. Lindhardt, C., 2007. Using adenosine triphosphate concentration as a measure of fuel treatment microbicide performance. In: R. E. Morris. Ed. *Proceedings of the 10th International Conference on the Stability and Handling of Liquid Fuels*; 7-11 October, 2007, Tucson, Arizona.

Passman, F. J., 2009. Using adenosine triphosphate to quantify bioburdens in various liquid fuels.” *7th International Fuels Colloquium.*” Technische Akademie Esslingen, Ostfildern, Germany. On CD.

Passman, F. J., 2012. Microbial contamination control in fuels and fuel systems since 1980 – A Review. *International Biodeterioration & Biodegradation* 81(1): 87-104, <http://dx.doi.org/10.1016/j.ibiod.2012.08.002>

Passman, F. J., Duguay, J., Maradukhel, G., and Merks, M., 2014. Adenosine triphosphate testing – recent advances in the differentiation between bacterial and fungal contamination and detection of dormant microbes in fuel and fuel associated water samples. In: R. E. Morris. Ed. *Proceedings of the 13th International Symposium on the Stability and Handling of Liquid Fuels*; 06-10 October 2013, Rhodes, Greece. <http://iash.omnibooksonline.com/>

Passman, F. J., 2018. Chapter 8 – Sampling. *In*: S. J. Rand and A. W. Verstuyft, Eds. ASTM Manual 1 – Significance of Tests for Petroleum Products–9th Edition, ASTM International, West Conshohocken, pp: 119-142. ISBN 978-0-8031-7108-4.

Soriano, A. U., Martins, L.F., Ventura, E.S.A, de Landa F.H.T.G., Valoni, E.A. , Faria, F.R.D., Ferreira, R.F., Faller, M.C.K., Valério, R.R., Leite, D.C.A., do Carmo, F.L., and Peixoto, R., 2015. Microbiological aspects of biodiesel and biodiesel/diesel blends biodeterioration. *International Biodeterioration & Biodegradation* 99(1): 102-114, <http://dx.doi.org/10.1016/j.ibiod.2014.11.014>

U.S. EPA, 2016. Investigation of corrosion-influencing factors in underground storage tanks with diesel service. EPA 510-R-16-001, U.S. Environmental Protection Agency Office of Underground Storage Tanks, Washington, DC., 61 pp.

Supplemental Tables

Table S-1. [cATP] ($\text{Log}_{10} \text{ pg mL}^{-1}$) in different phases of fuel over water microcosms.

Fuel Grade	Aqueous-phase		Interface		Fuel-phase		Sediment	
	AVG	s	AVG	s	AVG	s	AVG	s
ALL	4	1.3	3	1.4	2	0.5	3	2.0
LSD	4	1.3	3	0.9	2	0.3	3	1.5
BO LSD	4	1.1	3	0.6	2	N.C. ^a	4	0.7
B5 LSD	4	1.1	3	0.6	2	N.C.	4	0.7
ULSD	4	1.3	3	1.5	2	0.5	4	2.6
B0 ULSD	4	0.9	3	1.8	3	0.0	6	0.0
B5 ULSD	4	1.5	3	1.2	2	0.5	2	2.3

Note: a – N.C. – not computed (AVG is result from one specimen).

Table S-2. [tATP] ($\text{Log}_{10} \text{ pg cm}^{-2}$) in different phases of fuel over water microcosms.

Fuel Grade	Bottom		Interface		Fuel-phase		Vapor-phase	
	AVG	s	AVG	s	AVG	s	AVG	s
ALL	3.4	0.95	1	1.4	4	1.2	0.9	0.21
LSD	3	1.0	1	1.6	4	1.4	1.0	N.C.
BO LSD	3.6	0.97	2	1.6	4.5	0.63	1.0	N.C.
B5 LSD	3	1.0	-0.2	N.C. ^a	3	1.9	N.C.	N.C.
ULSD	3.5	0.92	1	1.3	4	1.1	0.7	N.C.
B0 ULSD	3.7	0.84	0.9	1.1	4	1.5	N.C.	N.C.
B5 ULSD	3.3	0.98	2	1.6	3.7	0.64	0.7	N.C.

Note: a – N.C. – not computed (AVG is result from one specimen).